Loughborough University

Loughborough University
Institutional Repository

Spine modelling for lifting

This item was submitted to Loughborough University's Institutional Repository by the/an author.

Additional Information:

- Doctoral Thesis. Submitted in partial fulfillment of the requirements for the award of Doctor of Philosophy of Loughborough University.

Metadata Record: https://dspace.lboro.ac.uk/2134/8065

Publisher: © Senay Mihcin

Please cite the published version.

Loughborough University

This item is held in Loughborough University's Institutional Repository (https://dspace.lboro.ac.uk/) and was harvested from the British Library's EThOS service (http://www.ethos.bl.uk/). It is made available under the following Creative Commons Licence conditions.

creative commons

COMMONS DEED

Attribution-NonCommercial-NoDerivs 2.5

You are free:

- to copy, distribute, display, and perform the work

Under the following conditions:

Attribution. You must attribute the work in the manner specified by the author or licensor.

Noncommercial. You may not use this work for commercial purposes.

No Derivative Works. You may not alter, transform, or build upon this work.

- For any reuse or distribution, you must make clear to others the license terms of this work.
- Any of these conditions can be waived if you get permission from the copyright holder.

Your fair use and other rights are in no way affected by the above.

This is a human-readable summary of the Legal Code (the full license).

Disclaimer

For the full text of this licence, please go to:
http://creativecommons.org/licenses/by-nc-nd/2.5/

Spine Modelling for Lifting

by

Senay Mihcin, BSc, MSc, MSc

A Doctoral Thesis

Submitted in partial fulfilment of the requirements
for the award of
Doctor of Philosophy of Loughborough University
October, 2007

© *by* Senay Mihcin (2007)

PAGE NUMBERING AS ORIGINAL

ABSTRACT

Mathematical modelling is widely used in the field of biomechanics. The traditional approach to investigate spine related injuries is to check the strength of the components of the spine. Spinal stability approach focuses on the force polygons formed by the body weight, muscle forces, ligament forces and external load. This force polygon is expected to stay within the boundaries of the spine to ensure stability. Proving the possibility of one force polygon within the spine boundaries proves the stability of the spine.

This study focuses on the full curvature of the spine for spinal stability investigations in a lifting activity. An experiment has been designed to investigate the postural differences in males and females by measuring the full spinal curvature with a skin surface device. Distributed body weight force, with increased detail of muscle and ligament forces acting on the spine have been modelled by writing a code in Visual Basic, while lifting a load from the boot of a car in the sagittal plane. This model is flexible enough to reflect changes in body weight parameter.

Results show that there is a difference between male and female postures during the full span of lifting activities. Application of individual muscle forces provides greater control of stability at each vertebral level. By considering the elongation of the ligaments and the force requirements of the muscle groups, it is possible to diagnose soft tissue failure. The differences in posture result in different moment arms for muscles and ligaments causing different loading on the spine. Most critical postures have been identified as the fully flexed postures with external load acting on the spine. Conceptual design ideas have been proposed to assist lifting a load from the boot of a car to eliminate the excessive flexion and loading on the spine.

Key Words: Spine Modelling, Thrustline Theory, Posture Analysis, Stability Analysis, Back Pain, Lifting.

ACKNOWLEDGEMENTS

The following thesis, while an individual work, benefited from the insights and direction of several people.

I would like to express my gratitude to my supervisor, Dr. B. Serpil Acar, whose expertise, understanding, and patience, added considerably to my graduate experience. I appreciate her vast knowledge and skill in many areas and her assistance in my writing reports.

I would like to thank to my director of research Prof Paul Chung for taking time out from his busy schedule.

I would like to thank to EPSRC and IMCRC who exemplify the high quality scholarship to which I aspire and to each individual who provided insights that guided and challenged my thinking, substantially improving the finished product in the group of Biomechanics and Injury Prevention.

In addition to the technical and instrumental assistance that I mentioned above, I received equally important assistance from family and friends providing on-going support throughout the thesis.

Thanks for all those who added meaning on the way.

To My Mother
And
To my Father
With love and respect

TABLE OF CONTENTS

1 Introduction 1
1.1 Research Outline 3
1.2 Research Aim 4
1.3 Thesis Overview 4
2 Literature Review 6
2.1 Vertebral Column Bone Structure 6
2.1.1 Cervical Spine 7
2.1.2 Thoracic Spine 8
2.1.3 Lumbar Spine 8
2.1.4 Sacrum 9
2.1.5 The coccyx 9
2.2 Intervertabral Discs 9
2.3 Muscles of the Vertebral Column 11
2.4 Ligaments of Spine 13
2.4.1 Ligaments at Cervical Region 14
2.4.2 Ligaments at Lumbar Region 15
2.5 LBP: Sources 16
2.6 LBP: Causes 17
2.7 Lifting 19
2.7.1 The loads acting on the spine and their affect 20
2.7.1.1 Compressive forces 20
2.7.1.2 Shear forces 21
2.7.1.3 Tensile Forces 22
2.7.1.4 Combined loading 22
2.7.2 Methods of estimating and measuring the loads on spinal column 22
2.8 Mechanical Factors Causing LBP 25
2.8.1 The magnitude of the weight lifted 25
2.8.2 The influence of Horizontal Moment Arm 27
2.8.3 Effect of Speed in Lifting 27
2.8.4 Effect of Dynamic loading in Lifting 28
2.8.5 Effect of Posture and Lifting Technique 29
2.9 Biomechanical models with a focus on mechanical factors 32
2.10 Models in Literature 33
2.10.1 Beam Model 33
2.10.2 Lever Model 35
2.10.3 Arch Model 36
2.10.4 Thrustline Model 40
2.10.5 Discrete Modelling 42
2.11 Discussion 45
2.11.1 Biomechanical factors in lifting 45
2.11.2 Biomechanical Models 47
2.12 Conclusion 49
3 Advanced Thrustline Theory & Development of the model in VB 51
3.1 Theory of the Model 51
3.2 Construction of the Model in Visual Basic 56
3.2.1 Assigning of values to type Vertebrae and Force 56
3.2.2 Assigning of values to type Vertebrae 62
3.2.3 Assigning of values to type Force 62

3.2.4 Inclusion of external forces 64
3.2.5 Loading of Posture Data into the Code 65
3.2.6 Calculation of coordinates for vertebrae corners, geometric and mass centres 66
3.2.7 Projection of forces into the components 67
3.2.8 Calculation of Reaction Forces 72
3.2.9 Drawing of Force H1 73
3.2.10 Calculation of reaction force R2 74
3.2.11 Calculation of R1 74
3.2.12 Drawing of force R1 74
3.2.13 Drawing of force R2 74
3.2.14 Drawing of force H2 75
3.2.15 Calculation of Thrustline coordinates 75
3.2.16 Calculation of the joint reaction forces 76
3.2.17 Calculations for Lever Theory 77
3.2.18 Parameterisation of the model 78
3.3 Running the Code 78
3.4 Visual Aspects of the program 82
3.5 Conclusion 83
4 Modelling of Muscles and Ligaments in Thrustline Theory 85
4.1 Muscle attachment points and morphology 85
4.1.1 Sub occipital Muscles 89
4.1.2 Deep Back Muscles 91
4.1.3 Lumbar Musculature 114
4.2 Discussion 118
4.3 Physiology of Ligaments 120
4.3.1 Ligaments at Cervical Region in the model 120
4.3.2 Ligaments at Lumbar Region in the model 125
4.3.3 Ligaments for the full spine in the model 127
4.4 Discussion 129
5 Body Contour in a lifting activity 134
5.1 Need for the Experiment 134
5.2 Design process of the experiment 135
5.2.1 Background information and feasibility study on measurement devices 136
5.2.1.1 Radiography 137
5.2.1.2 Skin Surface Devices 138
5.2.1.3 Arcometer 138
5.2.1.4 Skin surface markers 140
5.2.1.5 Computerized motion analysis systems 142
5.2.1.6 Flexicurve 143
5.2.1.7 Inclinometers and goniometers 144
5.2.1.8 Spinal Mouse 145
5.2.2 Conclusion 147
5.3 The Experiment 148
5.3.1 Controlled parameters 148
5.3.2 Fixed parameters 149
5.4 Methodology 150
5.4.1 Theory 150
5.4.2 Measurements 150

5.5 Data Analysis 153
5.6 Results 154
5.7 Discussion 165
5.8 Conclusion 167
6 Stability analysis of the spine with thrustline theory 168
6.1 Stability Analysis 168
6.1.1 Body Weight Forces with Postures in Lifting 168
6.1.2 External Load with Postures in Lifting 174
6.1.3 Discussions on the Effect of Body Weight & External Forces 181
6.2 Grouping of Muscles with Respect to Their Effect on Thrustline 182
6.2.1 Discussions on the Effect of Muscle Groups on Thrustline 188
6.3 Muscle groups with body weight forces and external load 194
6.4 Body weight, muscle groups, ligaments with an external load for postures in lifting 205
6.5 Conclusion 212
7 Evaluation of the Model and Conceptual Designs 213
7.1 Single Equivalent Muscle Model 213
7.2 Distributed Loading versus Point Force Loading 215
7.2.1 Effects of distributed body weight force on thrustline curvature 216
7.3 Discussion 226
7.3.1 The effects of distributed body weight forces on predicted joint reactions 227
7.3.2 Compressive Force at Intervertebral Level 227
7.3.3 Shear Force at Intervertebral Level 231
7.4 Comparison of the Model 236
7.4.1 Structure 236
7.4.2 Compatibility of the Results 236
7.5 Discussion 239
7.6 Conceptual design suggestions for lifting 239
7.6.1 Conceptual Designs 240
7.6.1.1 Alternative 1 240
7.6.1.2 Alternative 2 243
7.6.1.3 Alternative 3 244
7.7 Evaluation of the Conceptual Design Alternatives 244
8 Conclusions and Recommendations 246
8.1 Model Development 246
8.2 Contribution to the knowledge 247
8.3 Future Work 250
REFERENCES 252
APPENDIX 1 276
APPENDIX 2 276
APPENDIX 3 278
APPENDIX 4 285
APPENDIX 5 289
APPENDIX 6 292

LIST OF FIGURES

Figure 2- 1 Vertebral Column with lateral and posterior view 7
Figure 2- 2 Lateral Aspect of Lumbar Spine 9
Figure 2-3 Horizontal section of a disc(Rosse and Gaddum-Rosse, 1997) 10
Figure 2- 4 Concentric bands of annular fibres(Rosse and Gaddum-Rosse, 1997)..... 10
Figure 2- 5 Mean of Disc Compression Failures by Age (Adapted from Evans, 1959, and Sonada,1962)..... 10
Figure 2- 6 The ligaments of the spine shown on functional spinal unit (FSU)..... 13
Figure 2- 7 The model types and methods for measuring loads on spine..... 24
Figure 2- 8 Shape of the thoraco-lumbar spine projected on the sagittal plane (Meakin et al., 1996) 33
Figure 2- 9 Beams in mode 1 and mode 2 (Meakin et al., 1996)..... 34
Figure 2- 10 The straight rigid bar carrying compressive load P is concentrically loaded 34
Figure 2- 11 Description of the concept of lever model 36
Figure 2- 12 Vector representations of forces acting on an arch 37
Figure 2- 13 Funicular polygon of APQRB..... 37
Figure 2- 14 Stable Arch (Heyman, 1982)..... 38
Figure 2- 15 Thrustline of an arch with forces of a) Hmin b) Hmax c) Hcollapse..... 39
Figure 2- 16 Loading system of the spine (Acar and Grilli, 2002)..... 41
Figure 2- 17 The method of representing a given musculoskeletal structure by a discrete-parameter type mathematical model 42
Figure 3-1Forces acting on the spine, reference line and thrustline 53
Figure 3-2 Illustration of the location of the y coordinates of the thrustline is equal to the y coordinates of the forces acting on the spine 54
Figure 3-3 Illustration of the first coordinates of the thrustline, dy1, and X1 55
Figure 3- 4 Illustration of the Form 1 which is the main screen that appears when the code is run 58
Figure 3- 5 Illustration of the Form 2 which displays and stores the data related to forces acting on spine..... 59
Figure 3- 6 Illustration of the Form 3 which displays and stores the data related to vertebrae..... 59
Figure 3- 7 Illustration of the Form 4 which displays and stores the data related to muscle forces. 60
Figure 3- 8 Illustration of the Form5 which displays and stores the data related muscle fascicle start and end indexes..... 61
Figure 3- 9 Illustration of the Form 6 which displays and stores the data related to ligament forces..... 62
Figure 3- 10 Vertebrae with global angle 65
Figure 3- 11 Representation of Vertebrae with the corners 66
Figure 3- 12 Fully Flexed posture reference line angle equal to 0°..... 67
Figure 3- 13 Force acting with an angle of 270 degree 67
Figure 3-14 Similarity of triangles to calculate the distances of the forces acting on the spine. 68
Figure 3- 15 Illustration of the axis and zones..... 70
Figure 3- 16 Representation of joints..... 76
Figure 3-17. The boxes from the user interface of the program. 78
Figure 3- 18 Open dialog box for CSV files and the open button for the opening the dialog box in the program. 79

Figure 3- 19 Drawing window mode. 79
Figure 3- 20 Check boxes for muscle and ligaments. 79
Figure 3- 21 Muscle and ligament groups selection lists on the user interface. 80
Figure 3- 22 Open box for selecting erect posture vertebrae coordinates to calculate ligament forces. 80
Figure 3- 23 List of muscles and ligaments selected on the list box. 81
Figure 3- 24 Click boxes to add and remove external force. 81
Figure 3- 25 Main user interface of the program. 82
Figure 4- 1 Muscle force relation with muscle length (Lieber & Bodine-Fowler, 1993) 86
Figure 4- 2 Muscle force relation depending on the level of activation. (Winter, 1990) 86
Figure 4- 3 Inferior surface of the right half of the base of the skull showing points of attachment of muscle groups with insertions on the skull from Gary (1980)..... 89
Figure 4- 4 An anatomical drawing of the suboccipital muscles and their attachments to the skull and vertebrae (Basmajian, 1921)..... 89
Figure 4- 5 An anatomical drawing of the longus capitis and their attachments (Basmajian, 1921). 91
Figure 4- 6 Anatomical drawing of the muscle longus colli superior, inferior oblique and vertical portions (Basmajian, 1921). 92
Figure 4- 7 Anatomical drawings of the Scalenus muscles showing points of attachment to the ribs and cervical vertebra. From left to right, Scalenus Anterior, Scalenus Medius, Scalenus Posterior (Basmajian, 1921). 93
Figure 4- 8 Transverse plane of thoracic Iliocostalis lumborum (Basmajian, 1921) 98
Figure 4- 9 Lumbar fascicles of the iliocostalis lumborum (Basmajian, 1921)..... 98
Figure 4- 10 A sketch of lumbar vertebra tilted in the sagittal plane on which coordinate axes have been superimposed to demonstrate the sagittal, coronal, transverse planes of the vertebra Macintosh and Bogduk, 1991. 100
Figure 4- 11 The point 0 marks the origin of an obliquely oriented fascicle with an insertion at I acting on the vertebra (Macintosh and Bogduk, 1991)..... 101
Figure 4- 12 Anatomical drawing of the Splenius capitis and cervicis showing the points of attachment to the head and spine. Splenius muscle is represented by 5 muscle elements on each side of the neck (Basmajian, 1921). 104
Figure 4- 13 Anatomical drawing of Semispinalis Capitis showing origins and insertions of the muscle (Basmajian, 1921). 105
Figure 4- 14 An anatomical drawing of the Semispinalis Cervicis and Thoracis (Basmajian, 1921). 106
Figure 4- 15 An anatomical drawing of the upper section of the Trapezius muscle, showing attachments to the spine, skull and scapula (Basmajian, 1921). 110
Figure 4- 16 Anatomical drawing of levator scapulae (Basmajian, 1921). 112
Figure 4- 17 Force versus elongation graphs of the ALL in C2-C5 , C5-T1 (a), (b) respectively. Force versus elongation graphs of the PLL in C2-C5 , C5-T1 (c), (d) respectively. Force versus elongation graphs of the LF in C2-C5 , C5-T1 (e), (f) respectively. (Yoganandan et al, 2000)..... 122
Figure 4- 18 Force versus elongation graphs of the ALL, PLL, and LF in C2-C5 (a), (b), (c) respectively. Force versus elongation graphs of the ALL, PLL, LF in C5-T1 (d), (e), (f) respectively (Yogonandan et al, 1998). 123
Figure 4- 19 Force versus elongation graphs of the ALL, PLL, and LF in C2-C5 (a), (b), (c) respectively. Force versus elongation graphs of the ALL, PLL, LF in C5-T1 (d), (e), (f) respectively. Yoganandan et al, 2001 124

Figure 4- 20 Force versus elongation graphs of the ALL in T12-L2, L2-L4, and L4-S1. (a), (b), (c)..... 126
Figure 4- 21 Force versus elongation graphs of the PLL in T12-L2, L2-L4, and L4-S1. (a), (b), (c)..... 126
Figure 4- 22 Force versus elongation graphs of the LF in T12-L2, L2-L4, and L4-S1. (a), (b), (c)..... 127
Figure4- 23 Three distinct portions of a load deformation curve for the ligaments under loading applied at a slow rate (1mm/min) reported by Chazal et al (1985) 132
Figure 5- 1Conceptual design of the experiment..... 136
Figure 5- 2 Arcometer..... 139
Figure 5- 3 The physical shape of the spinal mouse with the base unit (Spinal Mouse Manual, 2000)..... 145
Figure 5- 4 Spinal curvature produced by the spinal mouse software (Spinal Mouse Manual, 2000)..... 145
Figure 5- 5 Spinal Mouse Intervertebral Angles..... 146
Figure 5-6. Geometrical distances of the object and the subject at the start of the experiment and (α) is the reference line angle between the horizontal and the line connecting L5 to T1..... 149
Figure 5- 7 A subject showing intermediate postures from fully flexed (P1) to fully erect (P10) posture..... 152
Figure 5- 8 The mean difference between X coordinates of the genders for the full spine with a highlight on different significance (p) values..... 155
Figure 5- 9 The mean difference between Y coordinates of the genders for the full spine with a highlight on different significance (p) values..... 155
Figure 5- 10 The average coordinates of postures of females and males for the interval of (- 5° to 0°)..... 156
Figure 5- 11 The average coordinates of postures of females and males for the interval of (0° to 5°)..... 157
Figure 5- 12 The average coordinates of postures of females and males for the interval of (5° to 10°)..... 157
Figure 5- 13 The average coordinates of postures of females and males for the interval of (10° to 15°)..... 158
Figure 5- 14 The average coordinates of postures of females and males for the interval of (15° to 20°)..... 158
Figure 5- 15 The average coordinates of postures of females and males for the interval of (20° to 25°)..... 159
Figure 5- 16 The average coordinates of postures of females and males for the interval of (25° to 30°)..... 159
Figure 5- 17 The average coordinates of postures of females and males for the interval of (30° to 35°)..... 160
Figure 5- 18 The average coordinates of postures of females and males for the interval of (35° to 40°)..... 160
Figure 5- 19 The average coordinates of postures of females and males for the interval of (40° to 45°)..... 161
Figure 5- 20. The average coordinates of postures of females and males for the interval of (45° to 50°)..... 161
Figure 5- 21 The average coordinates of postures of females and males for the interval of (50° to 55°)..... 162
Figure 5- 22 The average coordinates of postures of females and males for the interval of (55° to 60°)..... 162

Figure 5- 23. The average coordinates of postures of females and males for the interval of (60° to 65°) 163
Figure 5- 24. The average coordinates of postures of females and males for the interval of (65° to 70°) 163
Figure 5- 25 The average coordinates of postures of females and males for the interval of (70° to 75°) 164
Figure 5- 26 The average coordinates of postures of females and males for the interval of (75° to 80°) 164
Figure 5- 27. The average coordinates of postures of females and males for the interval of (80° to 85°) 165
Figure 5- 28 The average coordinates of postures of females and males for the interval of (85° to 90 165
Figure 6- 1 Male and female thrustline with Body Weight force (0° to 5°) interval of reference line angle. 169
Figure 6- 2 Male and female thrustline with Body Weight force (5° to 10°) interval of reference line angle. 169
Figure 6- 3 Male and female thrustline with Body Weight force (15° to 20°) interval of reference line angle. 170
Figure 6- 4 Male and female thrustline with Body Weight force (25° to 30°) interval of reference line angle 170
Figure 6- 5 Male and female thrustline with Body Weight force (40° to 45°) interval of reference line angle 170
Figure 6- 6 Male and female thrustline with Body Weight force (80° to 85°) interval of reference line angle. 170
Figure 6- 7 Male and female thrustline with Body Weight force (85° to 90°) interval of reference line angle. 171
Figure 6- 8 Shear forces for males and females at L5/S1 172
Figure 6- 9 Compressive forces for males and females at L5/S1 172
Figure 6- 10 Shear forces for males and females at superior surface of C1 173
Figure 6- 11 Compressive forces for males and females at superior surface of C1 173
Figure 6- 12 Male and female thrustline with Body Weight and External Load of 900N (0° to 5°) interval of reference line angle. 174
Figure 6- 13 Male and female thrustline with Body Weight and External Load of 900N (5° to 10°) interval of reference line angle. 175
Figure 6- 14 Male and female thrustline with Body Weight and External Load of 900N (10° to 15°) interval of reference line angle. 176
Figure 6- 15 Male and female thrustline with Body Weight and External Load of 900N (20° to 25°) interval of reference line angle. 177
Figure 6- 16 Male and female thrustline with Body Weight and External Load of 900N (80° to 85°) interval of reference line angle. 178
Figure 6- 17 Male and female thrustline with Body Weight and External Load of 900N (85° to 90°) interval of reference line angle. 178
Figure 6- 18 Shear forces for males and females at L5/S1 with external loading 179
Figure 6- 19 Compressive forces for males and females at L5/S1 with external loading 179
Figure 6- 20 Shear forces for males and females at superior surface of C1 with external loading 180
Figure 6- 21 Compressive forces for males and females at superior surface of C1 with external loading 180

Figure 6- 22 a) Illustration of force pair acting on the spine above and below the superior surface of C1 189
Figure 6- 23 Illustration of an increase in the direction of lumbar and cervical muscle forces in the negative perpendicular direction relative to the reference line due to the flexion. 191
Figure 6- 24 Male and female thrustline with Body Weight and External Load of 900N (0° to 5°) interval of reference line angle. 194
Figure 6- 25 Male and female thrustline with Body Weight and External Load of 900N (5° to 10°) interval of reference line angle. 195
Figure 6- 26 Male and female thrustline with Body Weight and External Load of 900N (10° to 15°) interval of reference line angle. 195
Figure 6- 27 Male and female thrustline with Body Weight and External Load of 900N (15° to 20°) interval of reference line angle. 196
Figure 6- 28 Male and female thrustline with Body Weight and External Load of 900N (20° to 25°) interval of reference line angle. 196
Figure 6- 29 Male and female thrustline with Body Weight and External Load of 900N (25° to 30°) interval of reference line angle. 196
Figure 6- 30 Male and female thrustline with Body Weight and External Load of 900N (30° to 35°) interval of reference line angle. 197
Figure 6- 31 Male and female thrustline with Body Weight and External Load of 900N (35° to 40°) interval of reference line angle. 197
Figure 6- 32 Male and female thrustline with Body Weight and External Load of 900N (40° to 45°) interval of reference line angle. 197
Figure 6- 33 Male and female thrustline with Body Weight and External Load of 900N (45° to 50°) interval of reference line angle. 198
Figure 6- 34 Male and female thrustline with Body Weight and External Load of 900N (50° to 55°) interval of reference line angle. 199
Figure 6- 35 Male and female thrustline with Body Weight and External Load of 900N (55° to 60°) interval of reference line angle. 199
Figure 6- 36 Male and female thrustline with Body Weight and External Load of 900N (60° to 65°) interval of reference line angle. 200
Figure 6- 37 Male and female thrustline with Body Weight and External Load of 900N (65° to 70°) interval of reference line angle. 200
Figure 6- 38 Male and female thrustline with Body Weight and External Load of 900N (70° to 75°) interval of reference line angle. 201
Figure 6- 39 Male and female thrustline with Body Weight and External Load of 900N (75° to 80°) interval of reference line angle. 201
Figure 6- 40 Male and female thrustline with Body Weight and External Load of 900N (80° to 85°) interval of reference line angle. 201
Figure 6- 41 Male and female thrustline with Body Weight and External Load of 900N (85° to 90°) interval of reference line angle. 202
Figure 6- 42 Shear forces for males and females at L5/S1 with external loading, body weight forces and muscle groups acting on the spine. 202
Figure 6- 43 Compressive force H1 for males and females at L5/S1 with external loading, body weight forces and muscle groups acting on the spine. 203
Figure 6- 44 Shear force R2 for males and females at superior surface of C1 with external loading, body weight forces and muscle groups acting on the spine. 203
Figure 6- 45 Compressive force H2 for males and females at C1 with external loading, body weight forces and muscle groups acting on the spine. 204

Figure 6- 46 Male and female thrustline with Body Weight and External Load of 900N (0° to 5°) 206
Figure 6- 47 Male and female thrustline with Body Weight and External Load of 900N (5° to 10°) 207
Figure 6- 48 Male and female thrustline with Body Weight and External Load of 900N (10° to 15°) 207
Figure 6- 49 Male and female thrustline with Body Weight and External Load of 900N (15° to 20°) 207
Figure 6- 50 Male and female thrustline with Body Weight and External Load of 900N (20° to 25°) 207
Figure 6- 51 Male and female thrustline with Body Weight and External Load of 900N (25° to 30°) 208
Figure 6- 52 Male and female thrustline with Body Weight and External Load of 900N (30° to 35°) 208
Figure 6- 53 Male and female thrustline with Body Weight and External Load of 900N (35° to 40°) 208
Figure 6- 54 Male and female thrustline with Body Weight and External Load of 900N (40° to 45°) 209
Figure 6- 55 Male and female thrustline with Body Weight and External Load of 900N (45° to 50°) 209
Figure 6- 56 Male and female thrustline with Body Weight and External Load of 900N (50° to 55°) 209
Figure 6- 57 Male and female thrustline with Body Weight and External Load of 900N (55° to 60°) 210
Figure 6- 58 Male and female thrustline with Body Weight and External Load of 900N (60° to 65°) 210
Figure 6- 59 Male and female thrustline with Body Weight and External Load of 900N (65° to 70°) 210
Figure 6- 60 Male and female thrustline with Body Weight and External Load of 900N (70° to 75°) 210
Figure 6- 61 Male and female thrustline with Body Weight and External Load of 900N (75° to 80°) 211
Figure 6- 62 Male and female thrustline with Body Weight and External Load of 900N (80° to 85°) 211
Figure 6- 63Male and female thrustline with Body Weight and External Load of 900N (85° to 90°) 211
Figure 7- 1Moment imposed male and females with respect to the pivot point L5 214
Figure 7- 2 Force carried by single muscle according to the SEM model imposed on male and females for the full lifting activity..... 214
Figure 7- 3 Moment imposed male and females with respect to the pivot point L5 ... 215
Figure 7- 4Force carried by single muscle according to the SEM model imposed on male and females for the external load of 900 N in a full lifting activity..... 215
Figure 7- 5Thrustline for males for the interval of 0-5 degrees of reference line angle with distributed body weight force and point force 217
Figure 7- 6 Thrustline for females for the interval of 0-5 degrees of reference line angle with distributed body weight force and point force 217
Figure 7- 7Thrustline for males for the interval of 45-50 degrees of reference line angle with distributed body weight force and point force 218
Figure 7- 8 Thrustline for females for the interval of 45-50 degrees of reference line angle with distributed body weight force and point force 218

Figure 7- 9 Thrustline for males for the interval of 85-90 degrees of reference line angle with distributed body weight force and point force 219
Figure 7- 10 Thrustline for females for the interval of 85-90 degrees of reference line angle with distributed body weight force and point force. 219
Figure 7- 11 Shear force for males at L5/S1 with distributed force and point force approach. 220
Figure 7- 12 Shear force for females at L5/S1 with distributed bodyweight force and point force approach. 220
Figure 7- 13 Shear force for males at superior surface of C1 with distributed bodyweight force and point force approach..... 221
Figure 7- 14 Shear force for females at superior surface of C1 with distributed bodyweight force and point force approach..... 221
Figure 7- 15 Compressive force for males at L5/S1 with distributed bodyweight force and point force approach..... 222
Figure 7- 16 Compressive force for females at L5/S1 with distributed bodyweight force and point force approach..... 222
Figure 7- 17 Compressive force at superior surface of C1 for males with distributed bodyweight force and point force approach..... 223
Figure 7- 18 Compressive force at superior surface of C1 for females with distributed bodyweight force and point force approach..... 223
Figure 7- 19 Thrustline for males for the interval of 0-5 degrees of reference line angle external loading with distributed body weight force and point force. 224
Figure 7- 20 Thrustline for females for the interval of 0-5 degrees of reference line angle external loading with distributed body weight force and point force. 224
Figure 7- 21Thrustline for males for the interval of 45-50 degrees of reference line angle external loading with distributed body weight force and point force. 225
Figure 7- 22 Thrustline for females for the interval of 45-50 degrees of reference line angle external loading with distributed body weight force and point force. 225
Figure 7- 23 Thrustline for males for the interval of 85-90 degrees of reference line angle external loading with distributed body weight force and point force. 226
Figure 7- 24 Thrustline for females for the interval of 85-90 degrees of reference line angle external loading with distributed body weight force and point force. 226
Figure 7- 25 Compression values at each inter-vertebral level for a distributed bodyweight loading pattern for the various postures for males. 228
Figure 7- 26 Compression values at each intervertabral level for a point force loading pattern for the various postures for males. 228
Figure 7- 27 Compression values at each intervertabral level for a distributed bodyweight loading pattern for the various postures for females 229
Figure 7- 28 Compression values at each intervertabral level for a point force bodyweight loading pattern for the various postures for females. 229
Figure 7- 29 Compression values at each intervertabral level for a point force bodyweight loading pattern for the various postures for males. 230
Figure 7- 30 Compression values at each intervertabral level for point force bodyweight loading pattern for the various postures for females 230
Figure 7- 31 Shear force values at each intervertebral level for distributed bodyweight loading pattern for the various postures for males. 231
Figure 7- 32 Shear force values at each intervertebral level for a distributed bodyweight loading pattern for the various postures for females 232
Figure 7- 33 Shear force values at each intervertebral level for a point force bodyweight loading pattern for the various postures for males. 233

Figure 7- 34 Shear force values at each intervertebral level for a point force bodyweight loading pattern for the various postures for females..... 233
Figure 7- 35 Shear force values at each intervertebral level for point force bodyweight loading pattern with external load for the various postures for males with external load. 234
Figure 7- 36Shear force values at each intervertebral level for point force bodyweight loading pattern for the various postures for females with external load..... 234
Figure 7- 37 Scissor lift..... 240
Figure 7- 38 Conceptual design alternative scissor lift mounted in a car boot..... 241
Figure 7- 39 Rack and pinion..... 241
Figure 7- 40 Conceptual design alternative for a load to be lifted into a boot space... 242
Figure 7- 41 Piston-rope-clips and an inclined surface for cars having a higher boot. 243
Figure 7- 42 Rotary arm which can be mounted on the tow bar of the car during lifting. 244
Figure A.3.1 Vertebral Body with front and side views..... 278
Figure A.3.2 Vertebral body top view (McGill, 2002)..... 279
Figure A.3.3 Figure Vertebral body posterior view (McGill, 2002) 279
Figure A.3.4 Vertebral connection points (McGill, 2002)..... 280
Figure A.3. 5 Sagittal views with the dimensions shown..... 280
Figure A.3. 6 Sagittal views with top view for transverse process..... 281
Figure A.3. 7 Sagittal views with top view for transverse process..... 282
Figure A.3. 8 Sagittal views with side view for mamillary process 283
Figure A.6.1 Force provided by lumbar ligament groups of ALL for all of the intervals. 292
Figure A.6.2 Force provided by lumbar ligament groups of PLL for all of the intervals. 292
Figure A.6. 3 Force provided by lumbar ligament groups of, LF for all of the intervals. 293

LIST OF TABLES

Table 2- 1The list of the ligaments of the spine..... 14
Table 2- 2 The data collected experimentally by Ruff (1950). The percentage of the body weight carried by each vertebrae and the breaking strength in compression for the thoracolumbar region..... 21
Table 3- 1 A sample representation of the force components with their relative x and relative y values for a posture of reference line angle of 90.47 degrees..... 72
Table 3- 2 Joint reaction forces for a sample flex posture..... 76
Table 4- 1 Origin and insertion points of the suboccipital muscles..... 90
Table 4- 2 Morphometric parameters of the Suboccipital muscles, taken from Kamibayashi and Richmond (1998) connection points from Vasavada et al, (1998).. 90
Table 4- 3 Origin and insertion points of the longis capitis..... 91
Table 4- 4 Morphometric parameters of the Longus Capitis..... 91
Table 4- 5 Origin and insertion points of longis colli..... 92
Table 4-6 Morphometric parameters of the longis colli..... 93
Table 4- 7 Origin and insertion points of Scalenus muscles..... 93
Table 4- 8 Morphometric parameters of Scalenus anterior, medius and posterior..... 94
Table 4- 9 Origin and insertion points of longissimus cervices..... 94
Table 4- 10 Morphometric parameters of Longissimus Cervicis..... 94
Table 4- 11 Origin and insertion points of longissimus capitis..... 94
Table 4- 12 Morphometric parameters of Longissimus Capitis..... 95
Table 4- 13 Origin and insertion points of spinalis thoracis..... 95
Table 4- 14 Morphometric parameters of Spinalis thoracis..... 96
Table 4- 15 Origin and insertion points of spinalis cervicis..... 96
Table 4- 16 Morphometric parameters of Spinalis cervicis..... 96
Table 4- 17 Origin and insertion points of iliocostalis cervicis..... 97
Table 4- 18 Morphometric parameters of iliocostalis cervicis..... 97
Table 4-19 Points of attachments of the erector spinae muscle..... 99
Table 4- 20 Morphometric parameters of iliocostalis lumborum pars thoracis..... 99
Table 4- 21 Morphometric parameters of iliocostalis lumborum pars lumborum..... 99
Table 4- 22 Morphometric parameters of longissimus thoracis pars thoracis..... 100
Table 4- 23 Morphometric parameters of iliocostalis lumborum pars lumborum..... 100
Table 4- 24 Fasiscle by origin for the longissimus thoracis pars thoracis and iliocostalis lumborum pars thoracis..... 102
Table 4- 25 Fascicle orientation in lateral and sagittal planes for longissimus thoracis pars lumborum..... 102
Table 4- 26 Fascicle orientation in lateral and sagittal planes for iliocostalis thoracis pars lumborum..... 103
Table 4- 27 Fascicle orientation in lateral planes and magnitude of force in sagittal plane for iliocostalis thoracis pars lumborum..... 103
Table 4- 28 Fascicle orientation in lateral planes and magnitude of force in sagittal plane for iliocostalis lumborum pars lumborum..... 103
Table 4- 29 Points of attachments of the Splenius Capitis and Splenius Cervicis..... 104
Table 4- 30 Morphometric parameters of Splenius Capitis and Cervicis..... 104
Table 4- 31 Morphometric parameters of Semispinalis Capitis..... 105
Table 4- 32 Morphometric parameters of Semispinalis Cervicis..... 106
Table 4- 33 Points of attachments of the semispinalis thoracis..... 107
Table 4- 34 Morphometric parameters of Semispinalis Thoracis..... 107
Table 4- 35 Morphometric parameters of Cervical Multifidus..... 108

Table 4- 36 Morphometric parameters of Thoracic Multifidus 108
Table 4- 37 Morphometric parameters of Lumbar Multifidus (Macintosh and Bogduk , 1986). 109
Table 4- 38 Morphometric parameters of Trapezius. 112
Table 4- 39 Points of attachments of levator scapulae 113
Table 4- 40 Morphometric parameters of the Levator Scapulae. 113
Table 4- 41 Points of attachments of latissimus dorsi 113
Table 4- 42 Morphometric parameters of Latissimus dorsi..... 113
Table 4- 43 Points of attachments of quadratus lumborum 114
Table 4- 44 Morphometric parameters of Quadratus Lumborum..... 115
Table 4- 45 Morphometric parameters of Psoas Major. (Bogduk et al, 1991)..... 116
Table 4- 46 Points of attachment of rectus abdominis (Stokes and Gardner-Morse, 1999) 116
Table 4- 47 Points of attachment of internal oblique (Stokes and Gardner-Morse, 1999) 117
Table 4- 48 Morphometric parameters of internal oblique (Stokes and Gardner-Morse, 1999) 117
Table 4- 49 Points of attachment of external oblique (Stokes and Gardner-Morse , 1999) 118
Table 4- 50 Morphometric parameters of external oblique (Stokes and Gardner-Morse , 1999) 118
Table 4- 51 Equations of stiffness calculated for ALL, PLL and LF for the C2-C5, and C5, T1 sub regions separately by using the graphs above (Yoganandan et al, 2000). 122
Table 4- 52 Equations of stiffness calculated for ALL, PLL and LF for the C2-C5, and C5, T1 sub regions separately by using the graphs above (Yogonandan et al, 1998). 123
Table 4- 53 Equations of stiffness calculated for ALL, PLL and LF for the C2-C5, and C5, T1 sub regions separately by using the graphs above Yoganandan et al, 2001.... 124
Table 4- 54 Equations of stiffness calculated for ALL, PLL and LF for the T12-L2, L2-L4, and L4-S1 sub regions separately by using the graphs above. 127
Table 4- 55 The result of experiments from the study of Myklebust et al, 1988. Force versus deflection values in mm for ALL, PLL and FL..... 128
Table 4- 56 Equations of stiffness calculated for ALL, PLL and LF for the C2-C5, and C5, T1 sub regions separately by using the graphs above. (Yoganandan et al, 2000). 130
Table 4- 57 Equations of stiffness calculated for ALL, PLL and LF for the C2-C5, and C5, T1 sub regions separately by using the graphs above (Yoganandan et al, 1998). 130
Table 4- 58 Equations of stiffness calculated for ALL, PLL and LF for the C2-C5, and C5, T1 sub regions separately by using the graphs above (Yoganandan et al, 2001). 130
Table 5- 1Example output from the Spinal Mouse software 146
Table 5- 2 Demographic characteristics of the experiment subjects. 151
Table 5- 3 The angle of line α connecting the lower L5 and upper C1 measured shown from horizontal as shown in Figure above. P1 is the fully flexed posture.P10 is the fully erect posture. 152
Table A1 Percentage of body weight carried by each vertebral level 276
Table A2. Coordinate and size values for male's 0 to 5 degrees of reference line angle of interval 277
Table A.6.1 Connection points to atlas and axis for suboccipital muscles..... 284
Table A.6.2 Calculated x and y coordinates for muscle attachment points to the skul284
Table A5 Interval of reference angle and the active muscle groups for each interval. 289

CHAPTER 1

1 Introduction

Back pain is defined by The International Association for the Study of Pain Subcommittee on taxonomy (IASP,1979), as "An unpleasant sensory and emotional experience associated with actual or potential tissue damage, or described in terms of such damage" (White and Gordon, 1982; Frank *et al.*,1996). Troup *et al.* (1983), define the problem of low back pain as a symptom with various pathologies, diagnoses, etiologies and medical management techniques.

Low Back Pain (LBP) is one of the most widespread ailments having a huge effect on society by causing the suffering of great deal of the population. It is estimated that in industrialised countries, up to 80% of the population experience back pain at some stage in their life. During any one year, up to half of adult population (15%-49%) have back pain (Burton *et al*, 2006, Palmer *et al*, 2000). Nearly 5 million working days were lost as a result of back pain in 2003-04 in the UK. Back pain is the second most common reason for long term sickness in much of the UK. In manual labour jobs, back pain is the number one reason (Department for Work and Pensions, 2002.).

According to the statistics conducted by the back care organisation, nearly half of the adult population in the UK (49%) reports that they had low back pain lasting for at least 24 hours in the year 2000. Ten years ago, this was only the one third of the population. The increasing trend of LBP shows that the potential future of the problem are more serious and the prevalence of the problem implies that there are a large number of unknowns in injury mechanism and back pain.

With the complex mechanism of pain, back pain is a matter of investigation for many researchers. Usually the direct mechanism of pain is not very obvious. While Low Back Pain (LBP) is perceived as idiopathic, its development is attributed to a combination of multi-factors like mechanical, chemical, biological, infectious, genetic, psychological, and degenerative origins (Vernon-Roberts, 1988). However, the prevalence of low back

pain shows that there are still lots of unknowns to be investigated and the mechanism of back pain have not been understood well enough to produce preventive methods.

LBP is mostly associated with activities like basic manual material-handling activities and lifting (Snook *et al.*, 1978; Cady *et al.*, 1979.; U.S. Bureau of Labor Statistics, 1982). Despite the advancements in technology, most of the population still has to lift objects on many occasions. This is valid for people who have to perform lifting activities as a requirement of their work like manual handling workers, health care personnel, gardeners, house wives, retailers or anyone loading and unloading the boots of their car might be under risk.

The biomechanical risk factors of LBP related with lifting are usually the weight lifted, task asymmetry, lift rate, weight position, lower origin heights, reach distances and previous back pain history (Davis and Marras, 2003; Marras *et al.*, 2004). In order to minimize the effect of risk factors associated with lifting, "proper" lifting methods have been introduced (Snook, 1988). However, it is usually very difficult to measure the effect of "proper lifting" techniques. Investigations for proper lifting methods are usually based on the subjective measures like energy expenditure, minimum overall effort, local effort, maximum stability and biomechanical analysis (Dysart and Woldstad, 1996). In these approaches, the conditions in lifting activities are likely to change from one experiment to the other making it more difficult to compare the results.

On the other hand, there are several approaches for understanding the mechanism of back pain. Biomechanical modelling is one of the options to predict the loads on spine. In biomechanical modelling approach, the studies conducted in literature usually focus on the L5/S1 joint of the spine or the partial regions of the spine (Chaffin, 1969). Nevertheless, in a typical lifting activity it is not only the vertebrae but also the muscles and ligaments play the main role (Bogduk *et al.*, 1992; Stokes and Gardner-Morse, 1995). The spine is a full structure and is considered as a whole starting from the cervical to the lumbar spine while understanding the mechanism of injury. The contribution of each muscle and ligament groups may play critical role in terms of stability of the full spine.

The posture of the body during the whole span of a lifting activity plays a role in distribution of the magnitude and direction of the loads acting on each vertebra. Little is known about the possible body postures during lifting activities. There is no study to-date to differentiate the postural differences between male and female spine for lifting activities. No data is available comparing the full spine coordinates of different genders. A model including the full curvature of the spine with the real life data focusing on postural differences of genders while the body weight, muscle and ligament groups act on the spine for lifting activities, has never been used to understand the mechanism of injury.

A full mathematical model of the spine is developed to investigate spinal stability. The thrustline theory, which is used in checking the stability of the structures in the field of construction engineering, is used for checking the stability of the human spine. Thrustlines are generated by the resultant compressive force vectors. The stability decision is based on whether the thrustline curvature is within the spine boundaries. This study has representation of the postures taken from experiments of lifting an object from the boot of a car. The experiments have been conducted over 20 males and 19 females. The spinal curvature of each experimental subject is recorded with a skin surface device. Generic male and female posture data is produced by using the results of the measurements while they lift an object from the boot of a car. The postures are fed into a computational model coded in Visual Basic which includes comprehensive muscle and ligament attachments for investigating spinal stability.

1.1 Research Outline

The rationale behind this research is the mathematical model of the full spine which can help explain the mechanisms of back pain and increase the understanding of back injury during lifting activities. Investigation into intervertebral joints and into the cases of instability of the spine leads to a better understanding of its mechanics with the medical views on the resources for low back pain. This is accomplished by investigating whether the mechanism of injury is due to the development of compressive or shear forces beyond physiological limits or due to the failure of transmission of compressive forces within the physical boundaries of the spine leading to instability of the spine.

1.2 Research Aim

The objective of this research is to create a detailed two-dimensional model of the full human spine that can simulate the behaviour of a spine while lifting an object from the boot of a car. The postures which are at risk of instability are to be identified.

1.3 Thesis Overview

Chapter 2 gives information about the spine including vertebra, muscles and ligaments. Sources and causes of back pain are explained. The types of possible loads on the spine, during lifting activities and evaluation of the methods used for understanding the mechanism of the back pain is discussed and effects of mechanical factors on back pain is provided. A summary of existing spine models developed for understanding the back pain is provided. Early models are reviewed and compared with thrustline theory. The reasons applying this theory are explained.

The development of a mathematical model of the full human spine by using thrustline theory is described in Chapter 3. The mathematical details are supplied. The details of the structure of the code developed in Visual Basic Language are provided.

In Chapter 4, the information about the muscle and ligament groups which have been used in the model for simulating the lifting activity is introduced with the representation of connection points and force estimations with the collected data available from literature.

In Chapter 5, data collection tools for the spine coordinates are introduced. Information about the experiment for the collection of different postures while lifting an object from the boot of a car is provided. The method used for analysing the data and the results are explained.

In Chapter 6, the stability analysis have been conducted on the spine have been explained in four different conditions for both genders; first with body weight only acting the spine; second the body weight and external load acting on the spine, third the body weight, external load and muscle forces, fourth the body weight, external load,

muscle and ligament forces on spinal stability with different loading combinations are provided.

In Chapter 7, the distributed and point force body weight loading approaches are compared in terms of their effect on interpretation of stability by using thrustline theory. The intervertebral joint reaction forces are evaluated to check if there is a structural failure of the vertebrae. Depending on the results of the stability analysis, three conceptual design alternatives are provided.

Chapter 8 concludes this thesis bringing together the findings of this research and outlines the limitations of the model. Further possible enhancements to the model are described as well as future applications and developments that may aid in a better understanding of back pain for lifting activities.

CHAPTER 2

2 Literature Review

In this chapter, information about the spine and the soft tissues i.e. muscle and ligament groups supporting the spine are provided. The role of the ligaments and their structure is provided in detail. Back pain related to lifting activities is focused on. Common causes and sources of back pain are provided. Lifting activities and its relation to back pain is explained. The loads imposed on the spine; compressive, shear, tensile and combined loading are defined. The methods for estimating these forces are introduced and the detailed comparison of these methods were given. The mechanical factors which affect the stress imposed on the spine during a lifting activity are introduced. The way that they contribute to the LBP is explained in detail. The need for biomechanical models is explained. The biomechanical models available in literature are explained in detail and the model which is used in this research is compared with them. Detailed information about the thrustline theory is also given with all justification for the use of this theory.

2.1 Vertebral Column Bone Structure

The vertebral column, which is one of the most vital parts of our body, consists of 24 separate bony vertebrae with five fused vertebrae forming the sacrum and 4 fused vertebrae forming the coccyx.

The functions of the vertebral column can be mainly grouped into 3

-It supports the human body in the upright posture.

-It allows movement and locomotion

-It protects the spinal cord

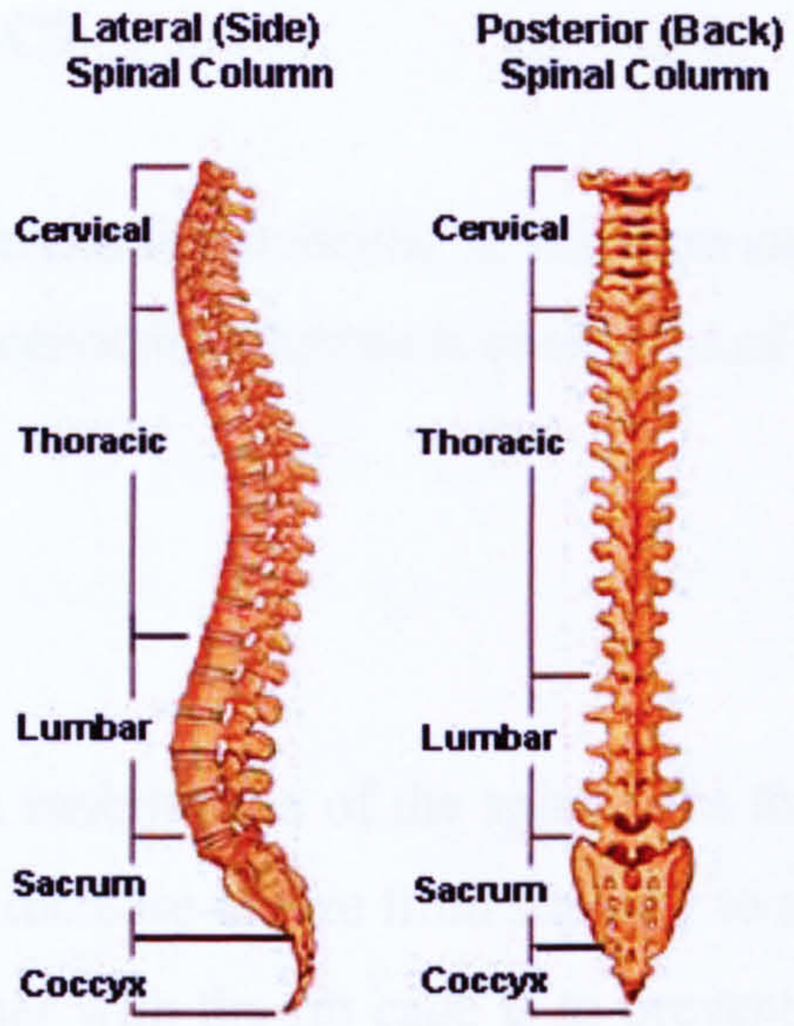


Figure 2- 1 Vertebral Column with lateral and posterior view

From the side view, the vertebral column has 5 curves in the upright posture: two cervical, and one each thoracic, lumbar and sacral. These curves help to dissipate vertical compressive forces by distributing the cumulative force not only as a compressive force but resulting in some shear force. They provide the spine with an important shock absorbing capacity. The compressive forces are absorbed by the ligaments of the spine (Oliver and Middleditch, 1991).

2.1.1 Cervical Spine

There are two curves in the cervical spine. This region is divided into 2 called upper and lower segments at the second cervical vertebra. Occiput, atlas and axis form the primary upper cervical curve.

Upper Cervical Spine: The atlas is the first cervical vertebra; this vertebra doesn't have a body, but consists of two lateral masses that are joined together by an interior or posterior arch.

The axis is the second vertebrae on the upper cervical vertebra with a function of a pivot around which the atlas and the head rotate. Cervical vertebrae bear the least weight, and their bodies are relatively small and thin.

Lower Cervical Spine C2-C7

The 2nd to the 7th cervical vertebrae are similar in structure and form the lower cervical part of the spine. A typical cervical vertebrae is composed of an anterior body and posterior arch

2.1.2 Thoracic Spine

Thoracic region is the least mobile area of the spine. The thoracic vertebrae are larger than cervical vertebrae and increase in size from superior to inferior. The basic function of the thoracic spine together with the rib cage is to prevent compression of the heart, lungs and major vessels. Protection of these structures causes loss of mobility. The rib cage has an energy absorbing capacity, so that the load bearing capacity in this part is increased. Although the rib cage contributes to the stiffness of the thoracic spine, the most restricting elements are the intervertebral disc (Van De Graaff and Fox, 1995).

The thoracic disk height is less than the lumbar disk height. A larger disc height tends to decrease stiffness, whereas a larger cross-sectional area increases it. Flexibility of the thoracic and lumbar discs is the same in flexion; extension, and lateral flexion. This might be due to the effect of greater cross-sectional area of the lumbar discs is neutralized by the shorter height of the thoracic disc (Oliver and Middleditch, 1991).

2.1.3 Lumbar Spine

The lumbar vertebral column comprises five vertebrae and the intervertebral discs. From sagittal side, the lumbar column has a curve that is concave posteriorly. This curve is known as the lumbar lordosis. The degree of curvature of the lumbar lordosis varies between individuals and in each individual it alters in different postures and positions. Gender, age, prolonged static standing position, compression and footwear are the factors affecting the lumbar lordosis (Oliver and Middleditch, 1991).

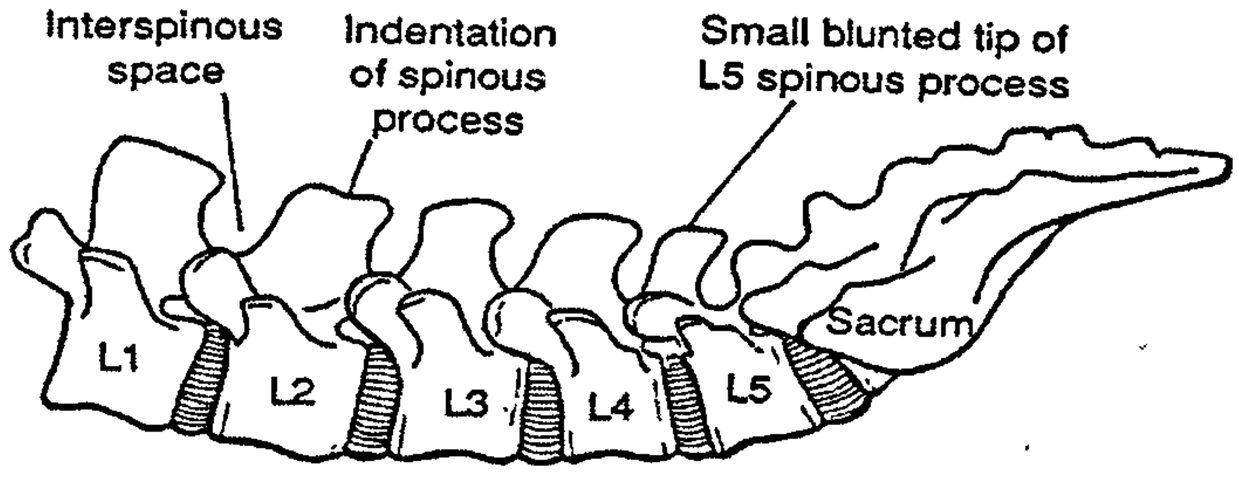


Figure 2- 2 Lateral Aspect of Lumbar Spine (Rosse and Gaddum-Rosse, 1997)

The fifth lumbar is the largest and heaviest of all the vertebrae. The height of its body is greater anteriorly than posteriorly. This causes a lumbo sacral angle. This angle is created by the change in the spinal curvature between the lumbar and sacral regions of the spine (Rosse and Gaddum-Rosse, 1997) .

2.1.4 Sacrum

Sacrum is formed by fusion of five sacral vertebrae. Sacrum transmits the weight of the body to hipbones by sacrum. The sacroiliac joint can play an important in non-specific low back pain.

2.1.5 The coccyx

The last four vertebrae, the final three of them are fused together. The last three coccygeal segments don't look like the vertebrae but they are remains of the vertebral bodies (Rosse and Gaddum-Rosse, 1997) .

2.2 Intervertabral Discs

Main function of the intervertebral discs is to restrain the movements at the inter-body joints and act as the main component in the transmission of loads from one vertebral body to the next. In the vertebral column they are positioned between each vertebra. However, there is no disk between the atlas and axis. The L5 disk is between the fifth lumbar vertebrae and the sacrum. The two basic components of the disc are the annulus fibrous (outer part) and the nucleus pulpous (inner part). Annulus Fibrosus: The annulus fibrosus is composed of densely packed collagen fibres in the outer and fibro-cartilage in the more central part of the ring. Concentric layers encapsulate the nucleus pulpous and proteoglycan gel binding the collagen fibres and lamellae firmly attached together to prevent them from buckling. It has a laminated structure. This laminated

structure is essential for biomechanical properties of the fibres and functions of the discs: It permits angular movements (flexion-extension, lateral flexion) provides stability against shear and torsion (Rosse and Gaddum-Rosse, 1997) .

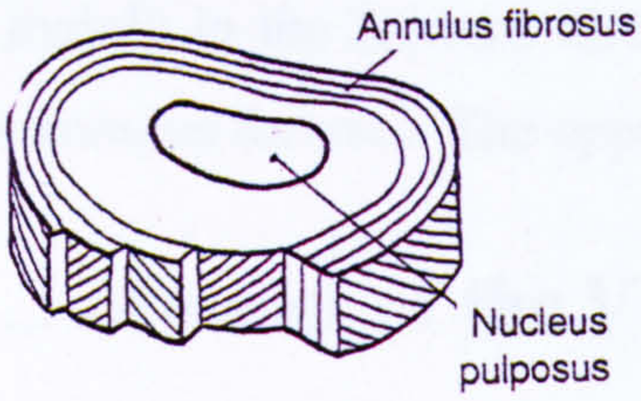


Figure 2-3 Horizontal section of a disc

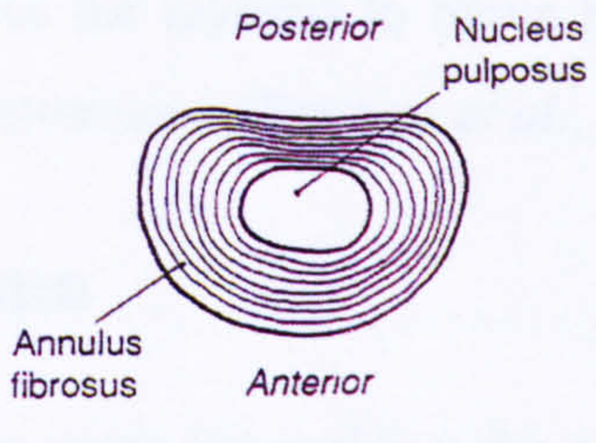


Figure 2- 4 Concentric bands of annular fibres (Rosse and Gaddum-Rosse, 1997).

The nucleus pulpous is a semi fluid gel. It forms the 40-60 % of the disc. It can be easily deformed under pressure without reduction in volume. This enables it to accommodate to movement and to transmit some of the compressive load from one vertebra to the next (Oliver and Middleditch, 1991).

Vertebral End Plates: Thin end plates separate discs from their adjacent vertebral bodies. End plates also play role related to the nutrition of the discs and a mechanical role in preventing the nucleus bulging into the vertebral body. Under high compressive loading, they fail. These failure values depend on the age. Below in Figure 2.5 the mean values of the compressive failure force values for the L5/S1 is given with respect to age. As the age grows the failure values decrease. This is mainly due to the intervertebral endplates ossify with age and lose their energy absorbing properties.

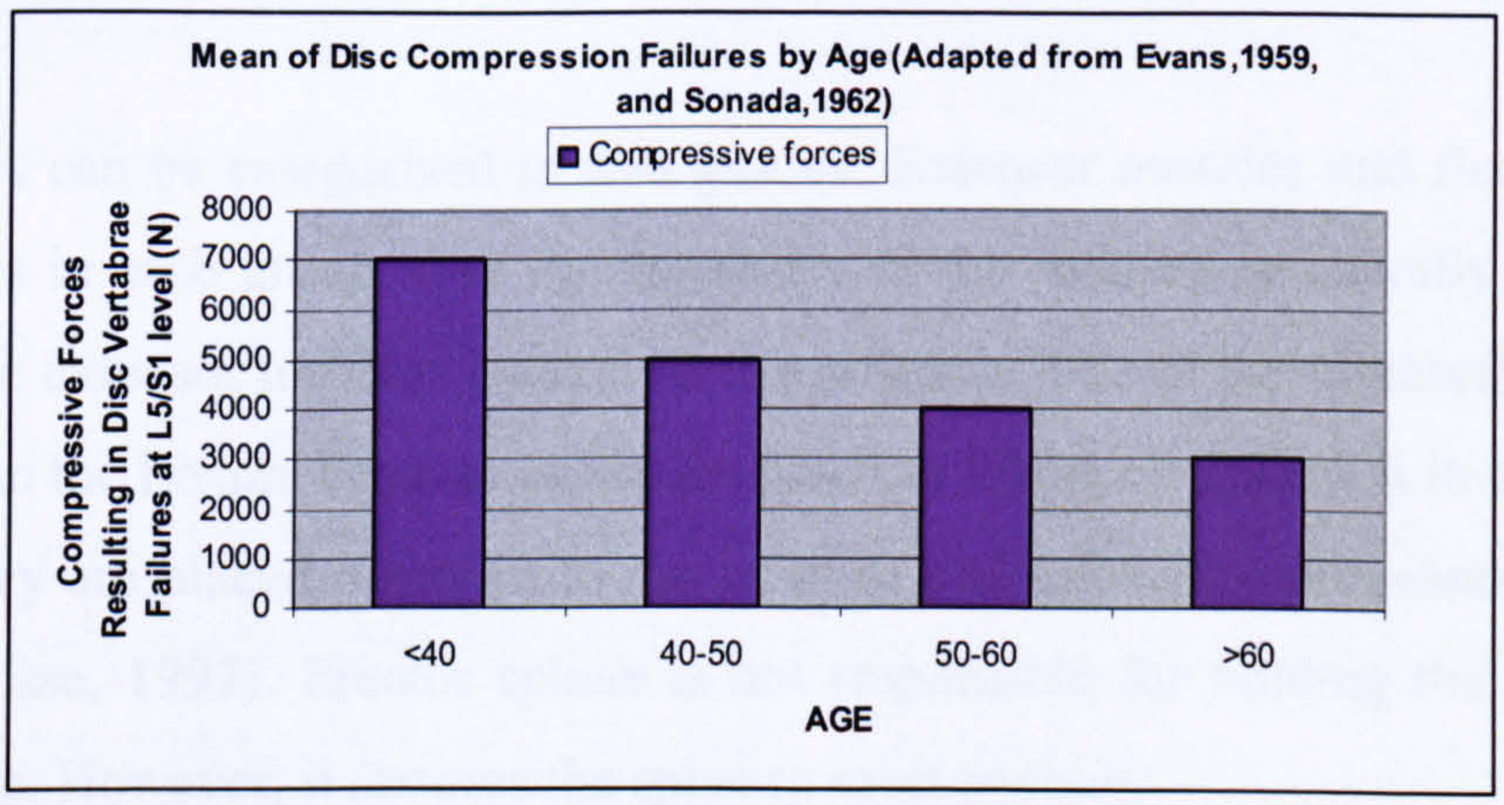


Figure 2- 5 Mean of Disc Compression Failures by Age (Adapted from Evans, 1959, and Sonada,1962)

The disc height is the thickest in the lumbar region, thinnest in the upper thoracic region. Disc height varies with respect to age, congenital anomalies, pathology, and

diurnal variation (Oliver and Middleditch, 1991). Intradiscal pressure is applied even in the free form so it is pre-stressed. The loading varies depending on the position of the body, or the position of the load, flexion of the body. During compression displacement is mainly in the forward direction. Flexion causes the nucleus to move backward and the annulus forward. The opposite occurs during extension (Rannou *et al.*, 2001).

2.3 Muscles of the Vertebral Column

Soft tissues like muscles ligaments and tendons; work for making the spinal column stable. These tissues act like ropes in tension to stabilise the spine. Muscles can shorten or lengthen for a better stabilisation of any posture. Spinal muscles also play an important role in shock-absorbing mechanisms, which help to relieve the spine of large loads.

The role of the muscles is to exert active forces. Muscles usually work in groups. These groups are named according to their function. When muscles act to initiate and maintain a movement, they are classified as prime movers or agonists. Muscles, which work to oppose the movement, are called antagonists. Both agonists and antagonists may contract together to hold a joint in one position to fix the joint. The degree of freedom of spine is determined by the position of the joints in the vertebral arch. The control and the strength of these movements depend on the muscles. Muscles are essential for the stability of the spine, for neutralizing or controlling the effects of the gravity.

The muscles can be categorized in two groups: Extensor muscles and flexor muscles. The muscles in each group have the capability of the rotating or laterally bending the column. The extensor muscles located on the posterior side of the vertebral column are stronger than the flexors because extension (such as lifting an object) is in opposition to gravity. They are placed posterior to the laminae and transverse processes (Rosse and Gaddum-Rosse, 1997). Erector spinae is not responsible for holding the spine in the erect posture. However, it restores the spine to erect posture.

Posterior spine muscles are usually covered by other muscles that do not belong to the spinal extensors. The deepest muscles are usually the shortest and extend not farther

than the next vertebrae. More superficial ones cover the whole vertebrae. Individual muscles insert by multiple tendinous slips. They cross each other at different layers establishing a system of layers. This maintains the stability of the spine.

Cervical Muscles: Cervical region is the most mobile in the spine. The neck muscles have important function of balancing the head on the neck.

Muscles, which flex the neck: These muscles are the most active muscle groups acting in sagittal plane. Longus colli and scalenus anterior are in this group.

Muscles, which flex the head and the neck: Longus Capitis flexes the head on the neck and the upper cervical spine.

Muscles, which flex the head on the neck: Rectus capitis anterior is the short muscle lying deep to longus capitis. Its main function is flexing the head on the neck.

Muscles, which extend the spine in the sagittal plane: Longissimus thoracis pars thoracis and lumborum, Iliocostalis lumborum pars, Lumborum (Lumbar iliocostalis), Spinalis and semispinalis thoracis, Longissimus cervicis, Lumbar multifidus, Splenius cervicis, Spinalis cervicis, Iliocostalis cervicis, lumbar muscles

Muscles which produce flexion of the trunk: Psoas major: Long deep muscle situated on the lateral aspect of the lumbar spine and the pelvic brim.

Obliquus externus abdominis: It is the most superficial of the abdominal muscles.

Obliquus internus abdominis: It lies deep to the obliquus externus abdominis.

Rectus abdominis: It is a long muscle running vertically on the front of the abdomen.

The last three muscles are the abdominal muscles.

Muscles which produce extension of the trunk: Quadratus lumborum, Multifidus, Semispinalis, Erector spinae.

If there happens any injury to the one of the muscle groups, movement of the muscle groups change with respect to that. Although the roles of the muscles are known, it is difficult to know which muscle is active in any posture. Although EMG studies are for checking muscle activity, they are not efficient to provide information if they are 100% active. Because of deep muscles lying under superficial muscles, it is possible to get cross talks in the measurements. On the other EMG studies are used to validate muscle models in the field of biomechanics due to the fact that they give some information on the level of muscle activation.

2.4 Ligaments of Spine

Ligaments are soft collagenous tissues. They play a significant role in musculoskeletal biomechanics. Ligaments are fibrous bands or sheets of connective tissue linking two or more bones, cartilages, or structures together. One or more ligaments provide stability to a joint during rest and movement by preventing excessive motion. The ligaments usually provide passive resistance at the joints. The moments resulting from ligament resistance are small when compared with the muscle contraction. However, ligaments are elastic and pre-tensioned, implying that their fatigue characteristics are unlike those of the muscles (White and Panjabi, 1979). Due to this property, they are expected to reduce the trunk muscle contractions.

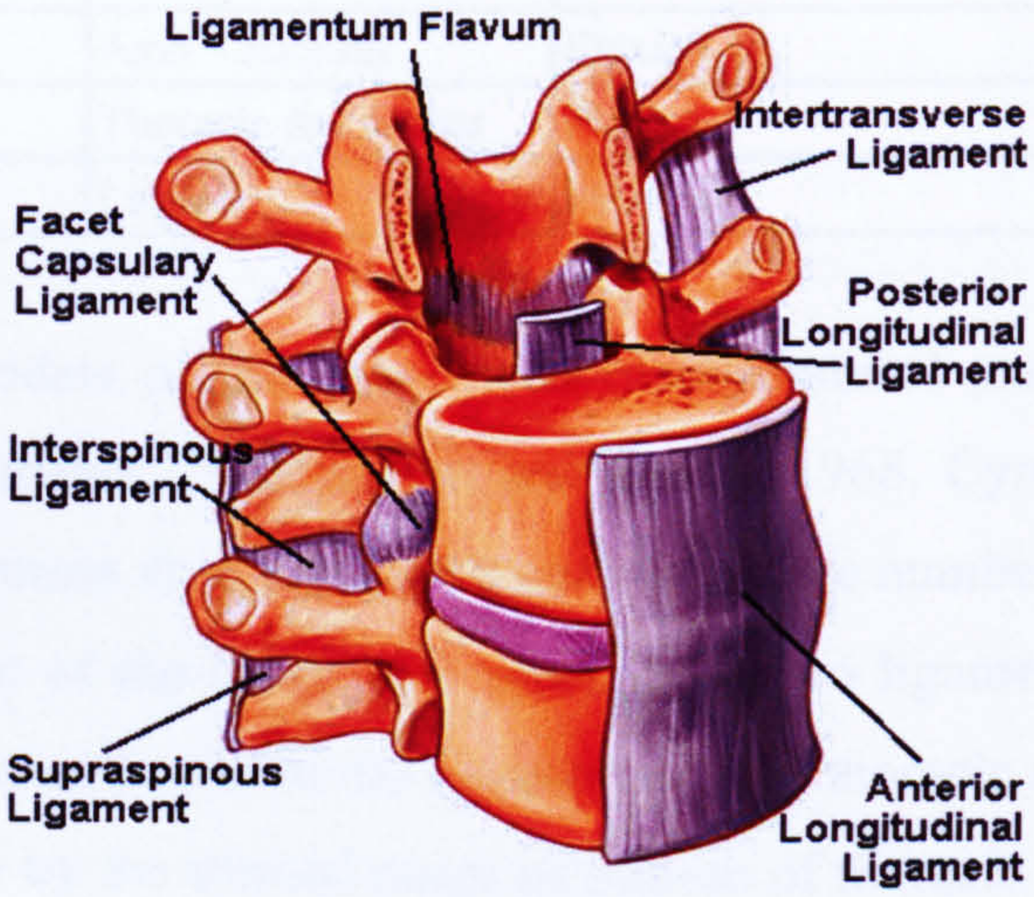


Figure 2- 6 The ligaments of the spine shown on functional spinal unit (FSU)

In the spine, ligaments help to provide structural stability. There are two primary ligament systems in the spine, the intrasegmental and intersegmental systems. The intrasegmental system holds individual vertebrae together. The intrasegmental system includes the ligamentum flavumn, interspinous and intertransverse ligaments. The intersegmental system holds many vertebrae together. The intersegmental system includes the anterior and posterior longitudinal ligaments, and the supraspinous ligaments

One of the principal clinical considerations in acute and chronic structural disorders of the spine is to establish the stability of the spinal column and preserve the functional integrity of the spinal column. Stability of the spine depends on the integrity of all constituents, including the spinal ligaments. Knowledge of the strength of spinal

ligaments may help the estimation of damage and stability of the spine. Information concerning the properties of the spinal ligaments is expected to enable improved mathematical models of spinal structures.

Table 2- 1The list of the ligaments of the spine

Ligament	Spinal Region	Function
Alar	Axis – skull	Head rotation & lateral flexion
Anterior Atlantoaxial	Axis & Atlas	Extension
Posterior Atlantoaxial	Axis & Atlas	Flexion
Ligamentum Nuchae	Cervical	Flexion
Anterior Longitudinal	Axis – Sacrum	Extension & reinforces front of annulus fibrosis
Posterior Longitudinal	Axis – Sacrum	Flexion & reinforces back of annulus fibrosis
Ligamentum Flavum	Axis – Sacrum	Flexion
Supraspinous	Thoracic & Lumbar	Flexion
Interspinous	Lumbar	Flexion

The mathematical models of the spine need biomechanical parameters and material properties of the ligaments. (Nuchamson and Evans, 1968, Cyron and Hutton, 1981, Panjabi et al, 1982, Dumas et al, 1987). There is extensive number of studies conducted on the cervical region of the spine, and some related to ligaments of lumbar region. However, the information based on the ligaments of the thoracic region is very limited. This can be explained by the limited range of motion of thoracic region by articulating facets and the ribs with low flexibility; for this reason the need for modelling of the ligaments in thoracic region is considered to be negligible when compared to lumbar and cervical injuries of the spine. The detailed information about the structure of the ligaments used in the model is explained with respect to the regions in chapter 4.

2.4.1 Ligaments at Cervical Region

Anterior Longitudinal Ligament (ALL): The anterior longitudinal ligaments of the cervical vertebral column are defined by fibres that attach to anterior surfaces of the vertebral bodies. This ligament is comprised of 4 layers of fibres. The first layer consists of fibres that longitudinally cross several segments, attached to the central areas of the anterior surface of the vertebral bodies. Rostrally, they are attached to the anterior tubercle of the atlas. The fibres of the second layer are also longitudinal but are shorter than the superficial fibbers. The third layer consists of even shorter longitudinal

fibres. The forth layer forms a thin curtain layer over each intervertebral discs (S. Mercer et al., 1999) .

Posterior Longitudinal Ligament (PLL): Posterior longitudinal ligament covers the entire floor of the cervical vertebral canal and consists of distinct superficial, intermediate and deep layers. The superficial layer contains 2 elements:

1. Central longitudinally directed fibres that span a variable number of segments, lateral extension that sweep out from the central band to cross and intervertebral disc and attach to the base of the pedicle one or two segments below. Centrally, all fibres of the superficial layer are attached to the central posterior surfaces of the vertebral bodies to which they are attached. The intermediate layer of the posterior longitudinal ligament consist of longitudinal fibres that span only one intervertebral disc. These fibres, restricted to a position close to the median plane, are attached to the posterior surfaces of the adjacent vertebral bodies' just caudially or cranially to the tubercles on the posterior surfaces of the vertebral bodies. Deep layer of the posterior longitudinal ligaments consist of short fibres that span each intervertebral disc. These fibres arise from the posterior surface of the upper vertebra just above its inferior border and passed inferiorly and somewhat laterally to reach the vertebra below. The deep layer is considered to be a component of the posterior longitudinal ligament rather than a component of the annulus fibrous because its fibres are attached to the posterior surfaces of the vertebral bodies rather than to their inferior and superior surfaces or edges.(S. Mercer et al., 1999)

2.4.2 Ligaments at Lumbar Region

Ligamentum Flavum (LF): The ligamenta flava shows no regular surface structure when examined by reflected light microscopy. A simple structural model for ligamentum flavum consists of densely packed elastic fibres. The fibrils become more highly oriented as the ligament stretches. Collagen fibril reorientation accounts for the increasing stiffness of ligamentum flavum with increasing strain. The structure of ligamenta flava allows them to resist extreme flexion of the spine. Ligamenta flava are unlikely to be damaged at the strains attained during normal flexion. (D.W.L Hukins et al., 1990)

Longitudinal ligaments: Reflected light microscopy of both anterior and posterior longitudinal ligaments shows that they have a wavy appearance when they are excised from the bone. The longitudinal ligaments contain very few elastic fibres. It is suggested that the presence of a small number of these low stiffness fibres in a relatively stiff ligament which contains high proportion of stiff collagen fibres enables the ligament to withstand sudden loading. The mechanical properties of longitudinal ligaments depend on the rate at which they are loaded, they are viscoelastic. In the model used here, the viscoelastic properties of the ligaments were excluded, due to the nature of the static model. The ALL resists bending of the spine, posterior ligament resists flexion and the anterior ligament resist extension.(D.W.L Hukins et al., 1990)

2.5 LBP: Sources

Priest and Hoggart, 2002 define the simple back pain as mechanical pain either increasing or decreasing in magnitude depending on the way the back moves (Priest and Hoggart, 2002). Despite its simple definition, the source of back pain is usually unpredictable.

Any kind of anatomical structure in the body might be the source of the pain, facets, ligaments, joints, intervertebral discs, vertebrae, nerve root sleeves and muscles. Usually the intervertebral disk is shown as a source of pain by many researchers. Annular tears and reduction in disc height are associated with a history of low back pain in many patients (Videman *et al.*, 2003).

Pain is usually felt when the nerves are compressed or distorted by damage to the intervertebral discs. Nerve damage is also known to cause chronic back pain. However, it is usually difficult to give precise diagnosis of back pain. That strains and sprains have never been anatomically characterised shows how difficult it is to give a precise diagnosis for LBP. Bulging disks and spinal stenosis can be diagnosed only in very small percent of patients of back pain as herniated disk occur in 20-70% percent of the people without back pain (Deyo and Weinstein, 2001).

2.6 LBP: Causes

With complex mechanisms of pain, back pain is a matter of investigation for many researchers. Usually the direct mechanism of pain is not very obvious. LBP is perceived as idiopathic. Its development is attributed to combination of multi-factors like mechanical, chemical, biological, infectious, genetic, physiological and degenerative origins (Vernon-Roberts, 1988).

According to the Bureau of Labour Statistics, approximately one-third of cases in 1997 involving days away from work were the results of injuries involving, lifting, pushing, pulling, holding, carrying, or turning objects or repetitive motion (Bureau of Labour Statistics, 1999). The prevalence rates of back pain among manual material handlers are also very high (Snook, 1978). Especially, lifting is observed to be a high risk factor for LBP (van Dieen *et al.*, 2002). The nurses, who do lifting while serving to patients, experience serious back injuries and occupational back pain than most other professions (Smedley *et al.*, 1997). Even in a standardized lifting task, there is a substantial variance in spinal loading within and between the subjects (Granata *et al.*, 1999; van Dieen *et al.*, 2001; van Dieen *et al.*, 2002). Development of LBP starts gradually at the beginning without any specific accident or any unusual activity and becomes more obvious in later parts (Hall *et al.*, 1998). The biomechanical risk factors of LBP related with lifting are usually an increase in the amount of the load to be lifted, an increase in the lift speed, task asymmetry, lift rate, decrease in the initial height of the load to be lifted, reach distances and previous back pain history (Davis and Marras, 2003).

Leboeuf-Yde points out that there is a strong relationship between hard work, genetics and LBP (Leboeuf-Yde, 2004). Moreover, Battié *et al* state that genetics is more important than occupational factors in disc degeneration and LBP has a tendency to run in families (Battié *et al.*, 1995). Similar to Battié *et al*, Adams *et al.* also point out patient's personal characteristics is more important than exposure to the labour (Adams *et al.*, 1999). Reduced lumbar lordosis, long back, increased physiological distress and previous non-serious LBP were consistent predictors of serious first time LBP. Al-Eisa *et al.*, show that fluctuating asymmetry (FA) in body dimensions has high relevance with LBP(Al-Eisa *et al.*, 2003). Leg length discrepancy and skeletal asymmetry is also associated with LBP (Friberg, 1983; Lee, 1989).

Intervertebral disks are among the earliest parts of the body to change, disks degenerate with age and tears develop in the annulus of the disk causing pain. Although LBP is common also among the young, its nature is different. For young people, it is mostly acute and short for elderly people, it is long term. The nature of back pain shows differences with respect to age (Snook, 2004).

These findings imply that while searching for the correct lifting techniques in order to prevent from LBP and understanding the mechanisms of back pain, it is necessary to include personal factors. Genetics and personal factors play an important role in the development of LBP, so the models based on the average properties of the people might not produce very realistic results. Neglecting the personal parameters might cause quite misleading results for the individual under consideration.

Several attempts have been made to rationalize the manual material handling tasks, using different approaches like physiological, psychophysical and biomechanical. Physiological approach asses the stress imposed on the cardio-respiratory system. Mostly the oxygen, demand of work is determined and generally if it is less than a third of the individual's aerobic capacity, the task is considered acceptable for an 8 hour of work. But this approach works well for frequently performed tasks. Psychophysical approach establishes lifting weights that are acceptable to the individual. This approach assumes that both physiological and biomechanical stresses are present in a manual material handling. The contribution of each varies but both stresses can be integrated under the measure of the perceived stress. Using perceived stress that can be sustained individuals determine the maximum weight they agree to lift occasionally or frequently. This approach has a very subjective nature. There is a reasonable agreement that subject's perceived workloads are also compatible with the physiological approach. Biomechanical approach focuses on the mechanical stresses imposed on the spinal column for a given task condition (weight, load, size etc). This stress is compared with the stress tolerance limit of the spine in order to determine if the task is within the acceptable range. However, limitations exist with the biomechanical approach, primarily on the efficacy of the biomechanical models.

The biomechanical models are the least subjective in nature and can be used as a good tool to investigate the causes of back pain and back injuries. It is possible to improve

the assumptions in each model and look at the effect of different parameters unlikely to the other two approaches. The biomechanical models are expected to give more reasoning for understanding the causes of back injuries whereas the other two approaches are more likely to be used for setting some limits as evaluation criteria on subjective level without producing the explanation of the injury.

2.7 Lifting

Lifting can be defined as a task of handling an object from its original location while overcoming the gravity forces acting both on the object and the body itself in the vertical direction by means of the muscles lying along the spine carrying it for a while before placing it to final position. Although the task is quite simple, due to the complexity of the structure playing in a typical lifting activity, the results of a possible injury occurring during lifting can be quite severe. Gracovetsky, 1986 draws attention to the amazing structure of human spine by comparing its load carrying capacity with that of a gorilla. While man can lift about 3.3 times of his body weight a gorilla can afford to lift only a little more than half of his body weight. (Gracovetsky, 1986). This proves that human spine has its uniqueness in its own structure and the causes of injury need to be understood properly.

In a typical lifting activity, the trunk and the load result in a forward torque in sagittal plane. This torque lowers the trunk. The back muscles produce counteracting torque in the opposite direction to keep the body in equilibrium. These muscles are attached to the spine and they exert high compressive forces on the spine. The most significant amount of the compressive forces on the intervertebral discs is produced by the back muscles. Even in the upright posture without any load there is always a compression force due to the body's own weight (Jager and Luttmann, 1989).

The mechanical load on the spine during symmetric lifting consists of 3 components; compressive, tensile and shear loading. These loads have been found out to have the potential to cause injury in a typical lifting activity. (McGill and Norman, 1985; Gracovetsky, 1986; Bush-Joseph *et al.*, 1988; Snook and Ciriello, 1991; Gagnon and Gagnon, 1992; Marras *et al.*, 1993; Chaffin and Page, 1994; Gallagher *et al.*, 1994; van Dieen *et al.*, 1999).

2.7.1 The loads acting on the spine and their affect

In a typical lifting activity, compressive, shear and tensile forces act on the spine. Information for each type of loading is provided briefly.

2.7.1.1 Compressive forces

In a typical lifting activity, compressive forces are applied to the spine by muscles while producing counteracting torques to keep the body in equilibrium. This might cause micro fractures of the vertebral endplates resulting in pain. A chance of injury is more likely if the micro damage accumulates more rapidly than can be repaired (Jager and Luttmann, 1992; Rannou *et al.*, 2001; Burgess-Limerick, 2003). The compressive forces exert high pressure to nucleus pulpous and cause intervertebral discs to prolapse into the vertebra (Hansson and Roos, 1981; Adams and Hutton, 1982; Brinckmann *et al.*, 1989; Adams *et al.*, "b", 1994). In extremely flexed postures, due to large bending moment arm, the ligaments of the neural arch can be sprained resulting in pain (Adams *et al.*, 1980). On vitro studies conducted by Adams *et al,* the compressive strength of lumbar spine is observed to be depended on posture (Adams *et al.*,1994 (a)). It is suggested that lumbar spine should be flexed by 80% to achieve an optimum compressive strength and even distribution of compressive and tensile stresses in the annulus fibrous. Under pure compression only the vertebral body gets damaged (Liu *et al.*, 1983; Brinckmann *et al.*, 1988).

The compressive strength of the lumbar spine appears to be the only strength that is widely used in biomechanical analysis and prediction. The models are used to predict compressive forces in simulated modes. The ultimate compression of the lumbar spine is affected by the personal and physical factors, including spinal level and type of specimen. There is a great deal of variability in compressive strength values. Jager and Luttman, and Geniady et all integrated the results of several studies to predict the compressive strength of the lumbar spine. According to Jager and Luttman, the lumbar spine fails at compression of 5700±2600 N and for females, the failure occurs at a compression of 3900N±1500 N. Genaidy et al, found that the compressive strength of lumbar motion segments averaged 7915±2545 N for males and 6638±1213 N for females in the 20-29 years age group. For people over 60 years, the compressive values were 4392±1169 N and 3336±897 N for females and males respectively.

Bone injury (end plate fracture) is far from the common cause of most back pain. However, extensive research is conducted into disc compression as it is thought to be largely responsible for vertebral end-plate fracture, disc herniation and resulting nerve root irritation. Back compression is argued to be a good predictor of low-back and other (Herrin, 1986) overexertion injuries. Due to clinical interest in this area data exists on the compressive strength of the lumbar vertebral bodies and intervertebral discs. In Table 2.2, the data collected experimentally by Ruff (1950) is supplied. It gives information about the percentage of the body weight carried by each vertebrae and the breaking strength in compression for the thoracolumbar region based on Ruff's experiments.

Table 2- 2 The data collected experimentally by Ruff (1950). The percentage of the body weight carried by each vertebrae and the breaking strength in compression for the thoracolumbar region

Vertebrae	% of Body Weight Carried	Mass carried by 72.7 kg man	Breaking strength in compression (N)
T1	9	6.5	1605
T2	12	8.7	2140
T3	15	10.9	2675
T4	18	13.1	3211
T5	21	15.2	3746
T6	25	18.1	4459
T7	29	21	5173
T8	33	23.9	5864
T9	37	37	6657
T10	40	40	7277
T11	44	44	7580
T12	47	47	7835
L1	50	50	7932
L2	53	53	8584
L3	56	56	9636
L4	58	58	9667
L5	60	60	10550

In addition to this, there are two commonly accepted tolerance limits for compression (Davis and Marras,2000(a)) one with 3400 N where some people have endplate micro fractures and the other 6400 N where 50 % of workers would be expected to have endplate micro-fractures (NIOSH, 1981). These limits can be reached in a typical lifting activity (Davis and Marras, 2000(a))

2.7.1.2 Shear forces

Due to gravity acting on the body and the muscular forces, the forward shear forces occur. Jager and Luttmann found out that for all of the different postures and loads,

they tested; the shear forces were below the compressive forces (Jager and Luttmann, 1989). The muscle forces lying along the spine are capable of applying more compressive forces than shear forces in a typical lifting activity. On the other hand, Cyron and Hutton state that shear forces can cause damage to the neural arch and to the facet joints (Cyron and Hutton, 1978). Shear tolerance limits are not well defined. McGill estimated that shear tolerance limits both lateral and A-P shear are to be around 1000 N in that case there is an increased possibility of tears in annulus fibrosis (McGill, 1997).

2.7.1.3 Tensile Forces

While lifting a heavy load, high tensile forces are imposed on the erector spinae muscles. In full flexions, the elongation of passive tissues is observed indicating that they help exerting extensor moments.(Dolan and Adams, 1993; Toussaint *et al.*, 1995). Tensile forces are applied on the posterior spinal ligaments and intervertebral disc with possible damages when the limits of these structures are exceeded (Adams and Hutton, 1982; Adams *et al.*," 1994).

2.7.1.4 Combined loading

Combination of compression, shear and bending can be exerted to a spine during a lifting activity. Combination loads might result in higher probabilities of LBD (Shirazi-Adl, 1991). Combinations of flexion and bending have been observed to cause strains on postero-lateral region of the disc by (Adams and Hutton, 1985; Gordon *et al.*, 1991). Combined loading have been observed to cause shear stresses causing circumferential and radial tears in the annulus (Goel *et al.*, 1995). In order to understand the mechanism of injury during a lifting activity, the magnitude of each type of the load acting on the spine should be known. Once the loading on the spine with a specific posture is known, injury analysis can be conducted depending on the information about the strength of structures which are already available in the literature.

2.7.2 Methods of estimating and measuring the loads on spinal column

In order to decide on loading conditions which may give possible damage to a spine during a lifting activity, determination of spinal stress and establishment of suitable criteria for the assessment of the determined stress are essential. However, the forces

acting on the spine are usually dependent on each other. Formation of models is one of the options to predict the loads on spine. The other method is to measure these forces directly during a lifting activity. Possible and most widely used measurement methods are: EMG; measurement of activity of trunk muscles (Chaffin and Anderson, 1984) measurement of disk pressures intra-discal pressure (IDP) (Nachemson, 1981); intra-abdominal pressure (IAP) (Anderson, 1982; Davis, 1985).There are some advantages and disadvantages related with direct measurement depending on the method of the measurement

Advantages of measurement methods:

- They are comparatively practical. For example, EGM systems are portable and suitable for use in work place (Dolan *et al.*, 2001) and IDP is the most direct way of getting the pressure magnitude on discs (Nachemson and Morris, 1964). It is possible to measure antagonistic muscle forces which cannot be detected by linked segment models (Dolan *et al.*, 2001).
- They give information about each subject; they are subject-specific in nature.

Disadvantages of measurement methods:

- They can be invasive in nature and impractical to apply and limited in data. For example, although IDP is one of the better ways to get information about the compressive forces acting on the spine. The pressure measured is obtained from one point of the disk (Nachemson and Morris, 1964). It is not possible to know exact value pressure at every point of the disc.
- The measured parameters can be highly depended on each other. For example, the relationship between, IAP and IDP depends on the posture and difficult to know (Schultz and Andersson, 1981).
- Although EMG amplitude appears to be an indication of muscle force activation, it does not give the exact amount of the force that muscles exert. In nature, EMG data is noisy (Dolan *et al.*, 2001). EMG-force relationship is influenced by muscle length and velocity of contraction (Dolan and Adams, 1993; Dolan *et al.*, 2001) .
- It is difficult to get deep muscle signals and possible to get mostly superficial muscles activations with surface EMG (Dolan *et al.*, 2001).

The other method is to establish biomechanical models:

Biomechanical models can be broken into four groups

1. Linked segment model (LSM).
2. EMG based incorporated kinematics data models.
3. Optimization
4. Single equivalent muscle model (SEM) (Hsiang *et al.*, 1997; Brown and Potvin, 2004).

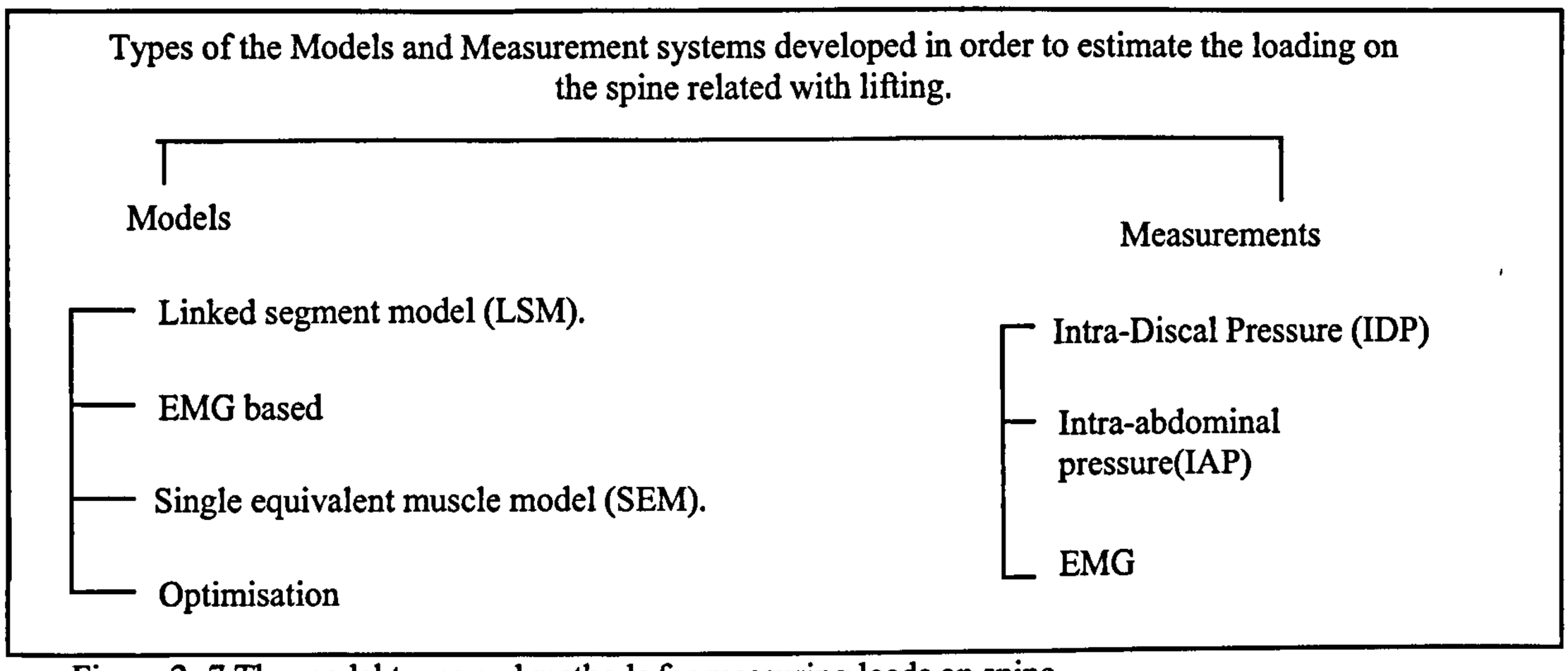


Figure 2- 7 The model types and methods for measuring loads on spine

The figure provides the visualisation for model types and methods for measuring loads on spine is given in Figure 2.7.

Disadvantages of the models:

- In the link segment models, usually the number of the joints does not allow the representation of the curved structure of the spine in a typical lifting activity. The influence of vertebral arch during the transmission of force within the spine can not be quantified.
- In the link segment models, the links are usually assumed to be homogenous structures; however, in reality, there is a huge variety in the skeletal and muscular structure of the human body. The structure of the bone is not same at every point or the cross sectional area or strength of the muscle is same at each point along the muscle.
- The biomechanical models are usually based on anthropometric data (the length of the body segments or the position of the muscles). These measurements are not valid for each individual. The difference in muscular structure affects the level of the accuracy of the calculated values very much (Jager and Luttmann, 1989).
- EMG based models are advantageous with their capability to predict pure antagonist muscle activation (Dolan *et al.*, 2001; Brown and Potvin, 2004). Net

moment can be estimated using EMG data and a model incorporating kinematic data (van Dieen and Kingma, 1999). However, in spinal system active and passive structures apply moments to the system; EMG-based models might produce results where static equilibrium is not achieved for all 3 axes. To overcome this problem optimization models are used (Brown and Potvin, 2004). Muscle forces can be estimated from the net moments by using single equivalent muscle model (SEM). Using net moments as a starting point, forces acting on the spine can be calculated using a model of the trunk musculature. Major factors are the changes with trunk flexion and of the moment arms of the muscles and of the orientation of the muscles with respect to the spine (van Dieen and Kingma, 1999).

2.8 Mechanical Factors Causing LBP

With the help of the models and measurements, it is possible to investigate how each factor; the weight of the load, the position of the load, the technique, speed, repetition and the acceleration of the lifting, effects the load imposed on the spinal column. Different approaches for investigating the effects of these parameters are given below.

2.8.1 The magnitude of the weight lifted

The weight lifted imposes a force on the spine and its substructures like discs, muscles and ligaments. Extensive efforts have been made to establish acceptable lifting limits for eliminating the risks associated with LBP (Chaffin and Park, 1973; Snook *et al.*, 1978; NIOSH, 1981; Kroemer, 1983; Ayoub, 1992).

There are two approaches in determining the maximum allowable weight to be lifted (MAWL) : the psychophysical approach and biomechanical approach (Jorgensen *et al.*, 1999). The psychophysical approach is based on the perception of the effort of the participants for lifting the MAWL without overexertion (Snook, 1978). Drury and Pfeil,1975 had a predicted weight that can be lifted with 5 factors of multiplication ie: gender, age, height of lift, percentile value, awkwardness of the object, based on a weight that can be lifted under optimal conditions (Drury and Pfeil, 1975). The results of the psychophysical studies were incorporated into the equations developed for assessing the risk of LBP. The base weight was in 40.9 kg and 23 kg in year 1981 and

1991 respectively (NIOSH, 1981; Waters *et al.*, 1993). The lifting equation established by the NIOSH is restrictive as it applies to the 99% of the male population and 75% of the female population. Stambough *et al* ,1995 developed the lifting equation with more parameters such as body weight, task duration, and lifting frequency, horizontal and vertical distance of the load, coupling factor, heat stress and age group multiplier (Stambough *et al.*, 1995). However, the effectiveness of psychophysical approach has not been evaluated a lot (Herrin *et al.*, 1986). Thompson and Chaffin,1993 showed that back stress is not very well perceived by the individuals indicating that the result of psychophysical approach is questionable (Thompson and Chaffin, 1993).

On the other hand, the biomechanical approach, takes into account the spinal loading and trunk kinematics. The biomechanical models are good at predicting the structural failure. With the increasing weights, extensor moment on the spine increases. This is confirmed by the studies of (Buseck *et al.*, 1988; Schipplein *et al.*, 1990; Potvin *et al.*, 1991; Lavender *et al.*, 2003) . Weights are observed to affect trunk kinematics (Ferguson *et al.*, 1992; Allread *et al.*, 1996).

With very heavy weights, 3D spinal loads (Chaffin and Park, 1973; Freivalds *et al.*, 1984; Marras and Sommerich, , 1991a, b, 1991; Kumar, 1994; Granata and Marras, , 1995a, b 1995) , extensor moments and peak bending torque (Dolan *et al.*, 1994) were observed to increase with higher muscle activity. (Marras and Mirka, 1990a, b1992; Dolan and Adams, 1993; Marras and Mirka, 1993). As the weight increased, static compression A-P shear force values increase uniformly. Increases in box weight reduce bending and trunk velocity in the sagittal and lateral planes. (Freivalds *et al.*, 1984). With the rate of carriage and distance of carriage, reductions were observed in maximum weight. (Morrissey and Liou, 1988).

In this research, it is also desired to investigate the effect of magnitude of load on spinal stability. However, the model which is used in this research is static. The combination of the velocity parameter is excluded; however, affect of moment arm can be incorporated.

2.8.2 The influence of Horizontal Moment Arm

The distance between the centre of the load and the spine play role on the moments imposed on spinal column (Schipplein *et al.*, 1995). Increases in horizontal moment arm significantly increase the estimated spinal compression. The influence of horizontal distance (Chaffin and Page, 1994) and the importance of the combination of weight and moment arm distance have been demonstrated by Marras *et al.*, 1993; Marras *et al.*, 1995; Lavender *et al.*, 2003). Extensor moment and bending torque is observed to increase with increasing distance of the load (Dolan *et al.* 1994). The arm positions which allow load manipulation close to the body lead to the lower lumbar stress than those held away from the body (Jager and Luttmann, 1989).With lower weight and higher moment arms, it is possible to see no changes in spinal load.

The holding places of the load affect the loads on the spine. Freivalds *et al* observed that boxes with handles result in higher L5/S1 compressive forces than for boxes without handles (Freivalds *et al.*, 1984). Lifting larger boxes didn't compensate the reduced box weights in order to maintain uniform L5/S1 compressive forces. Morrissey and Liou, showed the usage of container handles leading to lower MAW than without handles (Morrissey and Liou, 1988). Larger box sizes and handles cause the load to be positioned away from the body increasing horizontal distance. Large moment arms increase L5/S1 compressive forces.

The horizontal length of the moment arm during a lifting activity changes quiet much: For this reason, it could be a good idea to see how the change of the moment arm affects the spinal stability.

2.8.3 Effect of Speed in Lifting

Lifting is a dynamic activity. Bush-Joseph et all, 1988 investigated the effect of lifting speed on lumbo-sacral moment with 3 different methods of lifting, leg lifting, back lifting, kinetic lifting. As a result of increased sagittal trunk velocity muscle coactivity and spinal loads are observed to increase. The peak flexion, extension moment at the L5-S1 region of the spine is observed to increase linearly with increasing lifting speed (Bush-Joseph *et al.*, 1988; Marras and Mirka, 1990a, b1992a, b1993). With faster

speed, forward bending moment and the compression on L5/S1 is observed to increase (Hall, 1985; Buseck *et al.*, 1988; De Looze *et al.*, 1994; Lavender *et al.*, 2003). However, Dolan et all, 1994, didn't observe an increase in bending torque with increase in speed. This result shows that excessive speed of lifting should be avoided in order to prevent from high loads on the spine (Bush-Joseph *et al.*, 1988). Although it is advised to avoid from high speeds, there is not much known about the limit of how slowly lifting should be performed. Despite the fact that lifting faster tends to reduce the work the body has to do, with slower lifts the work and moment related whole body stress measures increase. Lifting too slowly might cause difficulty for a person to finish the lift at the later stage when the load is far away from the body and begins to lose its momentum. The body is under great stress due to slow motion and large moment arm between the load and the body (Lin *et al.*, 1999). This shows that there is a disadvantage for slow motion. The biomechanical disadvantages and advantages of the slow lifting need further investigation for a better understanding of optimum lifting speed.

With the model used in this research and in the experiment designed for the analysis, the lifting speed was very slow. Due to the static nature of the model, high speed loading was avoided. The measurement method requires slow lifting speed rather than fast. The postures used in this research are the result of extremely slow speed lifting which is a reason for using static modelling.

2.8.4 Effect of Dynamic loading in Lifting

Most of the lifting movements have inertial components. Dynamic effects due to initial moments of inertia, acceleration and deceleration patterns tend to increase compressive forces on L5/S1. In a simulated jerky lift, the resultant maximum value on spine is approximately twice as high as those without an initial jerk (Freivalds *et al.*, 1984).

However, there are few dynamic studies investigating the effect of dynamic forces. (Kumar and Davis, 1983; Leskinen *et al.*, 1983; Freivalds *et al.*, 1984; Jager and Luttmann, 1989). There is a difference between static and dynamically calculated lumbar moments. With the increase in the mass of the load, the difference between

dynamic and static modes of calculation is observed to increase. It is explained by the force= mass*acceleration. (Jager and Luttmann, 1989).

Static models under-predict the compressive values up-to 60% or 90% and shear values by 150% to 230% depending on the weight, as they are done by zeroing the accelerations of the load and body segments (Davis and Marras, 2000). When the inertial forces of the load itself and the load weight are incorporated into an otherwise static model (quasi-static model) the moments exceed fully dynamic model by 25% (McGill and Norman, 1985).

Leskinen *et al., 1983* finds out that the forces for dynamic biomechanical model are 33 % higher than the static model (Leskinen *et al.*, 1983). Trunk moments were underestimated by 20% and 30% when dynamics of lifting are ignored (McGill and Norman, 1985).These results show that trunk kinematics and muscle coactivity should be considered when estimating spinal loads. Sudden loading causes spinal instability leading to back pain (Lavender *et al.*, 1993).

Although the literature review related to acceleration of the lifting activity says that the dynamic forces acting on the spine is quite high when compared to static loading, in order to record the posture data with the resources available, it was not possible to collect dynamic postures. For this reason, as an initial start the model in this research is based on static assumptions. It is still possible to incorporate the acceleration affect to the model for quasi-static modelling. By assuming a moderate level of acceleration during lifting, it is possible to get the simulation results for quasi-static modelling. However, the results are expected to be affected by the assumptions made because the postures used in the model are still supposed to be static postures rather dynamic.

2.8.5 Effect of Posture and Lifting Technique

Lifting technique can be defined as the posture adopted just before the load is lifted. The posture represents a fundamental influencing variable for lumbar stress. Jager and Luttmann showed that lower torque and compressive force values result for postures with slight trunk inclination than in cases where trunk is steeply inclined (Jager and Luttmann, 1989). Burgess-Limerick also supports the idea by stating that extreme

lumbar flexion should be avoided (Burgess-Limerick, 2003). In extreme lumbar vertebral flexions, no erector spinae muscle activity is observed (McGill and Kippers, 1994). It is the para-vertebral ligaments, interspinous ligaments, posterior fibres of annulus fibrosus and passive elements of the musculotendinous tissues working in extreme flexion (Adams and Dolan, 1995; Dolan and Adams, 2001).

For a body to adopt while lifting an object there are two extreme postures: Stoop, where the knee joints are fully extended and hip joints and vertebral column are flexed. Squat lifting, where the vertebral column is kept erect and knee joints are kept flexed as much as possible. Although squat is believed to be a superior technique, there is no evidence supporting this technique (Burgess-Limerick, 2003). The advantages and disadvantages of these two postures are given below. The postures which can not be classified as either squat or stoop are called as self selected body postures; the details about these postures are also provided.

Squat Posture

Advantages of the squat lifting

- The stress is distributed well due to lordotic posture.
- Squat lift is only beneficial when the load is too close to the body (Leskinen *et al.*, 1983).
- Lower lumbar shear force (Straker, 2003).
- Less lumbar passive tissue stress (Straker, 2003) .

Disadvantages of squat lifting:

- The increase in potential energy is greater than stoop lifting.
- The vertical displacement of a larger proportion of body weight results in greater forces at the feet (Leskinen *et al.*, 1983) .
- Peak moments are marginally higher (van Dieen *et al.*, 1994).
- MAW for squat lifting is less than semi-squat and stoop lifting (Straker, 2003) .
- Compression forces are higher mean (Leskinen *et al.*, 1983) .
- Stability is reduced. It is possible to get unexpected perturbations. The loss of contact from the ground is possible (NIOSH, 1981) .
- Energy expenditure is greater, because of the vertical displacement of a greater portion of the body weight (Straker, 2003).

- It is not a natural body posture.
- Higher perceived exertion than stoop lifting (Garg and Moore, 1992)

Stoop Posture

Advantages of stoop lifting

- It is a more natural posture than squat with low energy expenditure, heart rate and ventilation (Burgess-Limerick, 2003; Straker, 2003) .
- The advantage of lowering the centre of gravity resulting in less work performed (Burgess-Limerick, 2003) .
- Peak extensor moment is reduced when compared to squat lifting (Dolan et al, 1993).
- MAW is higher (Burgess-Limerick, 2003; Straker, 2003) .
- The maximum oxygen consumption is less (Hagen *et al.*, 1993) .

Disadvantages of stoop lifting

- The trunk is flexed too much. Increased sagittal flexion is expected to increase spinal loads by either increasing trunk moment or muscle activity. Estimated peak lumbar moments for stoop lifts are 5% greater than squat lifting (Potvin *et al.*, 1991, Marras and Mirka, 1992,Dolan *et al.*," 1994)))
- Lifting heavy weights with a flexed lumbar spine is hazardous. Excessive flexion can sprain the ligaments of the neural arch which is possible during stoop technique. (Adams *et al.*, 1980). Stoop result in 75% more stress on passive tissues which is explained by 15% increase in peak lumbar flexion (Dolan *et al.*" 1994)
- The higher level of compression .The load on the L5/S1 is increased. The horizontal moment arm between the body and the load is increased (Leskinen *et al.*, 1983).
- The estimates of shear forces for stoop lifting are found to be 180% greater than for squat lifting (Potvin *et al.*, 1991) .

Self selected body posture

Self selected body posture can be described as something between squat and stoop (Burgess-Limerick *et al.*, 1995; Burgess-Limerick, 2003). Semi-squat posture has some advantages. One of the geometrical advantageous of this lifting style is that knee and

lumbar joint extremes are avoided. It is a more natural way of lifting rather pure squat and stoop (Straker, 2003). Greater lumbar compression force is on the trunk kinetic lift (Leskinen *et al.*, 1983). Freestyle lifting has higher oxygen consumption than stoop and less than squat (Kumar, 1984). The increase of peak flexion, extension moments occurring at the L5-S1 level of the spine was greatest for back lifts but occurred with other two lifting techniques as well (Bush-Joseph *et al.*, 1988) . Greater MAW than squat and stoop lifting.(Straker, 2003)

Between the introduced lifting techniques, in this research stoop type of lifting is simulated. Due to the nature of the lifting load from the boot of a car, it is not possible to expect squat lifting method although it is generally considered as safer. The selection of stoop lifting during unloading of the car gives us a reasoning to investigate the high loading on the L5/S1 region as much as investigating the spinal stability.

2.9 Biomechanical models with a focus on mechanical factors

The modelling of the spine is very crucial as it leads to the better understanding of the way the spine functions mechanically. Understanding of the mechanical behaviour of the spine is a prerequisite to describe potentially damaging postures. So that it is possible to make predictions about the results of an activity or assessment of performance and risk.

The results of such an assessment might be applied to any area. The design of new work situations or set of instructions during material handling or designing a new equipment for the loading and unloading of a baggage from the boot of a car are possible applications for biomechanical models. Modelling of the spine is also practical; it is not usually possible to measure the effects of manual work in industry. This is particularly true when a new work situation is being developed. If manual activity can be simulated then it may be possible to predict the consequences of the activity.

The basic limitation with the modelling is the availability of the data at hand. As long as the data is provided, it is possible to do an analysis of any posture during lifting activities. As the posture changes, the role of each muscle is expected to change. The

other basic difficulty lying behind modelling is the validation of the models. Usually the validation of the model is experimental. It might be difficult to match with the each value of the parameters of the experimental subject while verifying the model which is developed for average human population.

In literature, there are models developed for the lumbar or thoracolumbar spine. The model that is developed for this research is going to be a unique as it covers the whole spine and inspects the effect of each posture by taking snapshots at each different time interval of a lifting activity considering the body weight and effects of muscle and ligament forces at each snapshot. However, it is useful to look at the other models in order to understand the benefits of the new model over the existing models. Extended summaries of these models are given in the following section.

2.10 Models in Literature

The models in literature are explained below with their superiorities and shortcomings

2.10.1 Beam Model

Simple beam models define the spine as a straight slender elastic beam and Euler's theory of elastic buckling is used for this analysis. It is developed as a model for the curvature and flexion of the lumbar spine. This model establishes an analogy between the shape of the thoroco-lumbar spine and Euler column buckled in the second mode when it is viewed in the sagittal plane. Mode 2 is the optimum mode for the extra load carrying capability of the spine without switching to the stooped posture. Flexion of the spine is considered as the mode 1 of Euler buckling column (Meakin *et al.*, 1996).

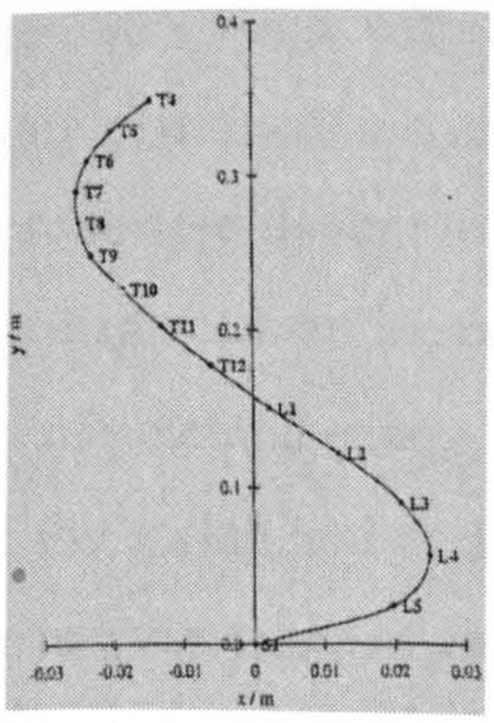


Figure 2- 8 Shape of the thoraco-lumbar spine projected on the sagittal plane (Meakin et al., 1996)

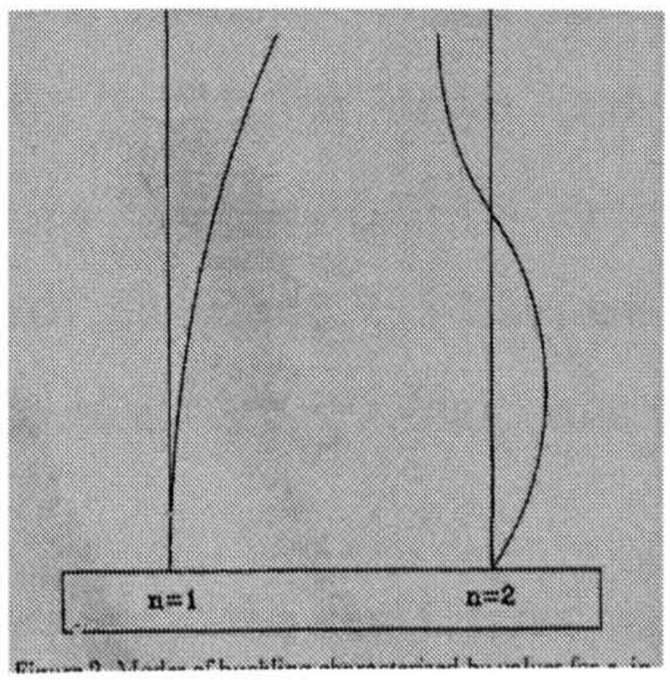


Figure 2- 9 Beams in mode 1 and mode 2 (Meakin et al., 1996)

Meakin et al (1996) classified the compression members in four groups (Meakin *et al.*, 1996):

1. Long columns with central loading.
2. Intermediate-length columns with central loading
3. Columns with eccentric loading
4. Struts or short columns with eccentric loading

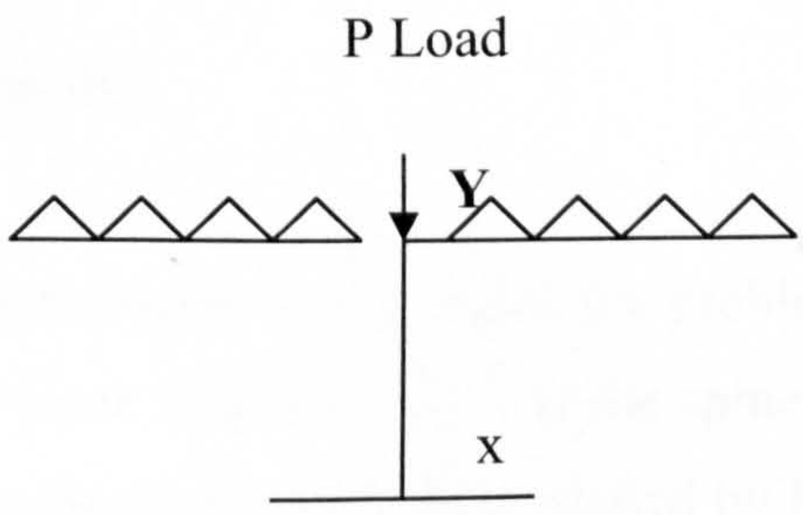


Figure 2- 10 The straight rigid bar carrying compressive load P is concentrically loaded

The bar is held vertically by a pair of springs with a combined spring with a spring constant of K. For a light load, any perturbation creating a displacement of the bar to the right or left causes the spring to restore the bar to the vertical. At high loading, the spring is unable to correct and the displacement increases. For a small displacement of θ, the load P is lowered and a loss of potential energy of the load Ep is calculated. This is equated to the strain energy of the spring and critical loading is found. $P_{crit} = k*l$. The failure to carry the load is due to a condition of elastic instability.

Long Columns with Central Loading: When force is applied to the rounded-end columns, moment equation is written down and differential equation is solved. Deflection of the curve is calculated. $Y=A*\sin\pi*X/L$ which indicates that the deflection of the curve is half sine curve. Critical load occurs when n=1. For values of n greater than 1 result in deflection curves, which cross the axis at points of inflection.

$P_{cr}/A= \pi^2E/ (l/k)^2$, where (l/k) is the slenderness ratio, this is the critical load where stability is likely to occur. The critical load depends on the modulus of elasticity and slenderness ratio. Critical loads are likely to occur depending on the end conditions.

However, this model considers the spine as a fully determined model and does not give any information about the forces acting on the spine by the muscles and ligaments. This model takes into account the modulus elasticity of the spine different from thrustline theory which is used in this research. Thrustline theory assumes that the spine is rigid with infinite modules of elasticity. It is difficult to assign a modulus of elasticity for the full spine, considering all the complicated structure of the disks, vertebrae, nerves, veins, muscles and ligaments.

2.10.2 Lever Model

The models, which are developed to investigate the problems of low back pain usually, represent the spine as a lever. Models based on the spine behaving like a lever have a common assumption that bending moments produced by lifting a weight in front of the body are balanced directly by a moment generated by the erector spinae muscles. The sum of the forward bending moments produced by the weight of the trunk, plus any extra load being carried is equal to the erector spinae muscle tension multiplied by the perpendicular distance of this muscle from the pivot. This pivot is usually taken to be the lumbo-sacral joint (L5/S1 or L4/L5). The compressive force on this joint is the sum of the erector spinae muscle force and the components of the other loads in that direction. In this model, as the lever arm of the spinae muscles is small the force on this muscle is estimated to be very high. The estimated force on these muscles is believed to be unrealistic; in addition to that, the magnitude of the forces on the sacrum is extremely high.

The muscles follow the curvature in many postures and it is very difficult to fully straighten out the spine. Forces acting around the curved structure are difficult to analyse. The lever model fails to include the curved structure of the human spine. However, the compressive forces in spine must follow the curvature of the spine in all postures. For these reasons, the lever model is believed to be too simple and falls behind in explaining the complex structure of the spine, like disks, muscles and ligaments. Usually the force necessary to counteract the moment produced by the load imposed on the spine is assumed to be carried by a single equivalent muscle force. This approach oversimplifies the muscle structure when compared to the complicated muscle structure of the real human spine.

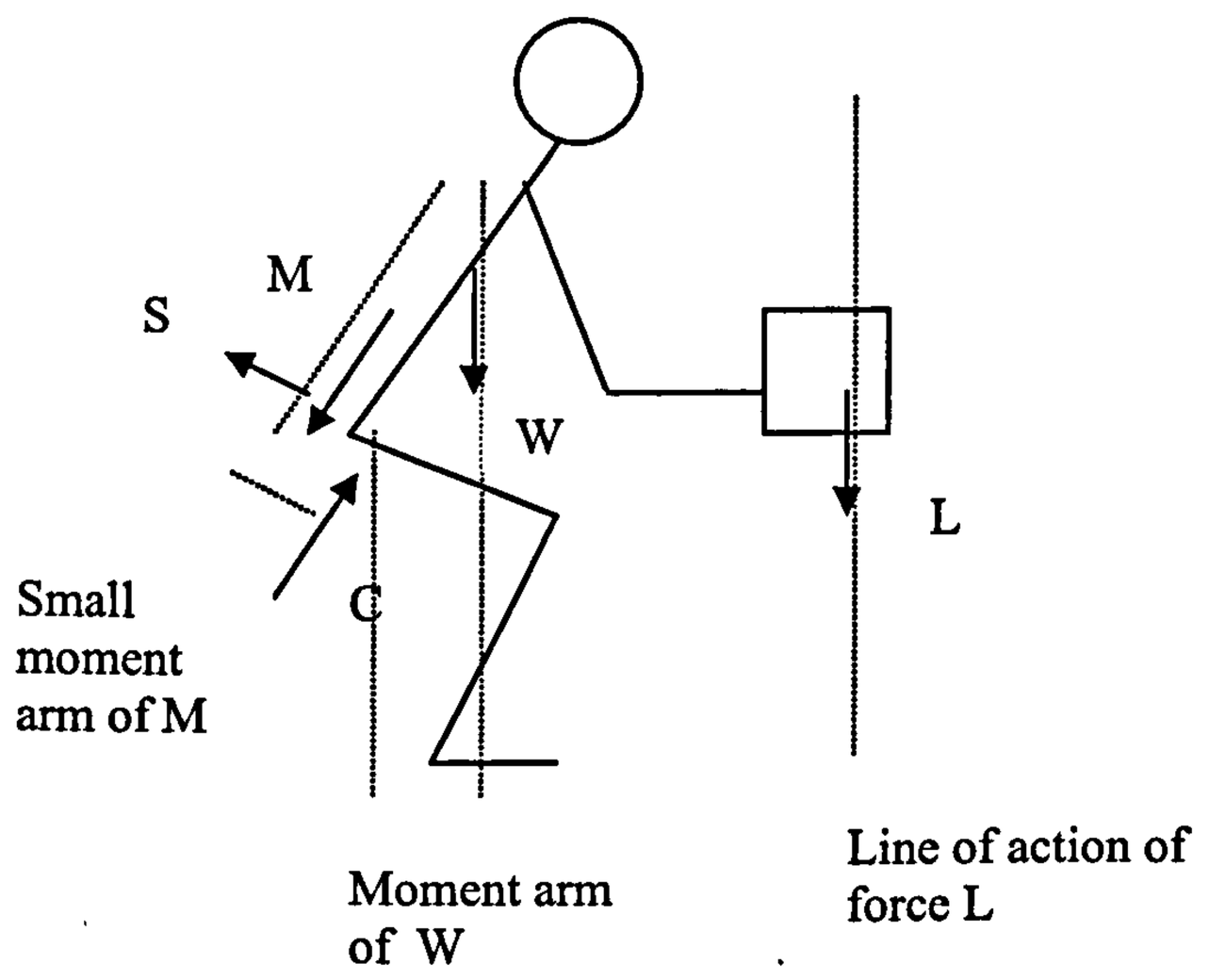


Figure 2- 11 Description of the concept of lever model

2.10.3 Arch Model

The basic difference of an arch model from a lever model is that it treats the spine as a curved structure. Unlike the lever model, it needs an external support. Stability is provided for an arch by compressive forces along it and does not need external moments like it is in masonry arches. Stability of a masonry arch is related with its shape rather than the strength of the material. The geometry of the arch is related with the shape of the arch. The best shape of the arch and the thickness of the arch are among the questions to be investigated for the stability of it.

If the shape and the thickness of an arch are given, just like as if the dimensions and the posture of a spine are given, then the stability of an arch while carrying these loads can be investigated. The loads are mainly due to the self-weight of the arch and the weight of the traffic imposed on the bridge, which is similar to the weight of the body and the loads lifted by the person.

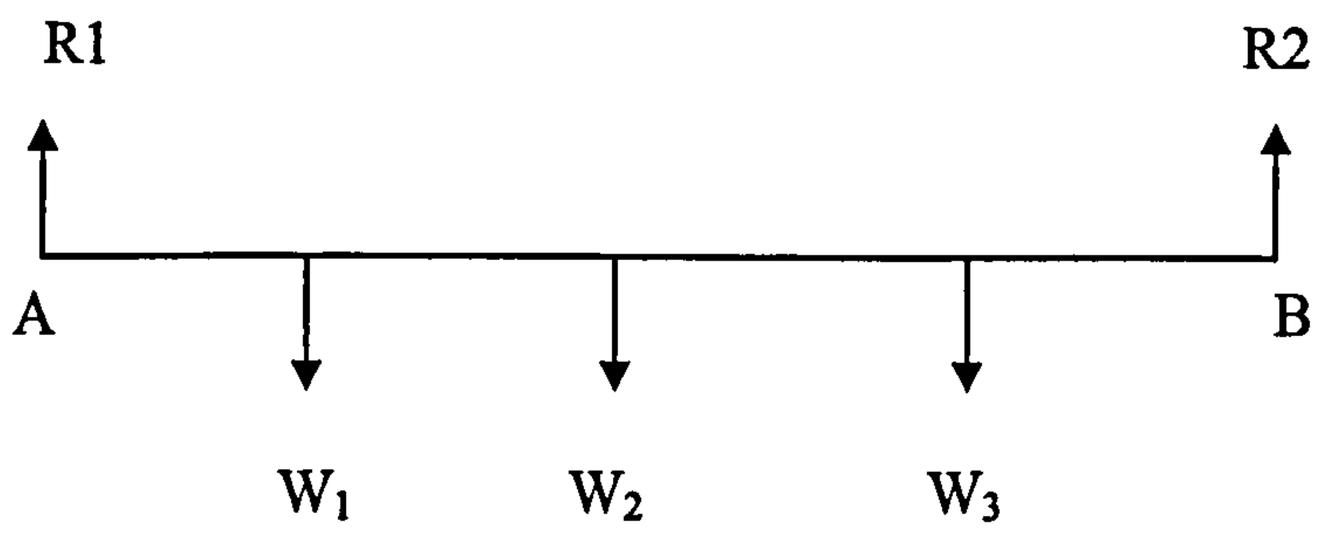


Figure 2- 12 Vector representations of forces acting on an arch

The forces acting on the arch is drawn as shown on the figure above. The equations of equilibrium are written assuming that the whole system is in equilibrium. So the reaction forces R1 and R2 can be calculated. If H is assumed to be known, then the triangle of the forces gives the inclination of the AP portion of the string.

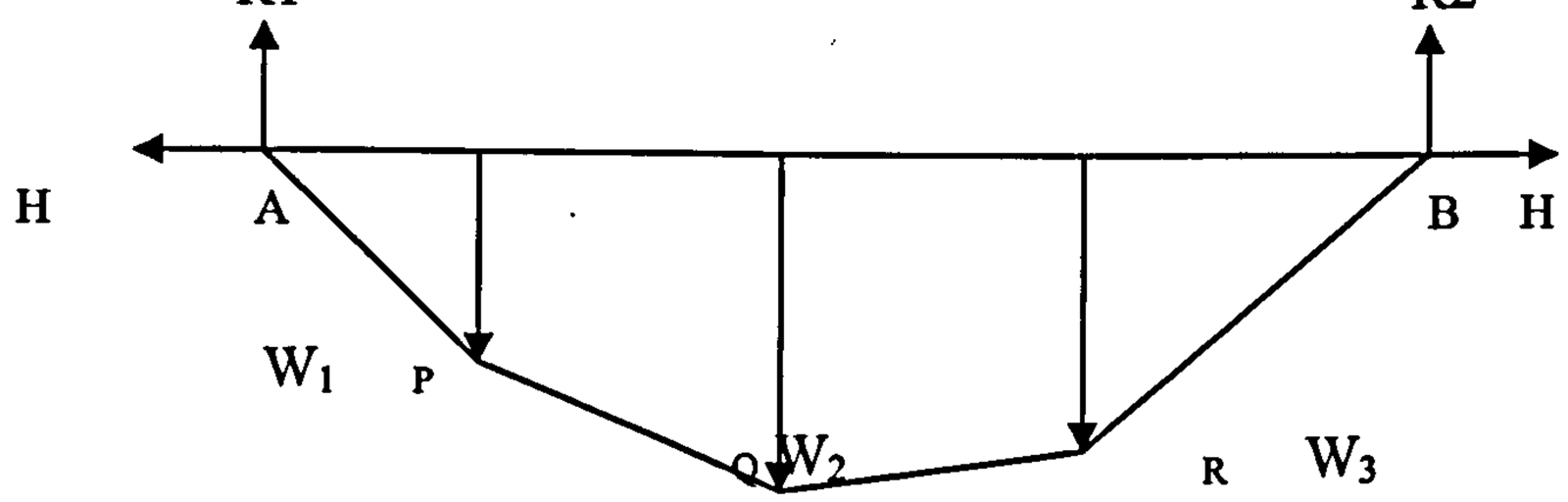


Figure 2- 13 Funicular polygon of APQRB

The funicular polygon of APQRB is the line of thrust in an arch which carries the loads W_1, W_2, W_3. The thickness of the voussoirs surrounding the line of thrust is supposed to be thick enough to include the compressive line of thrust. It is possible to start with an arbitrary origin point for drawing the funicular polygon, so that it is possible to find the real deviation of the funicular polygon. However, it is impossible to locate its exact location.

The funicular polygon represents the line of thrust. If the arch is cut at any point, along the joint between two voussoirs, equilibrium is maintained. Thrust is not transmitted normal to the abutting faces of the voussoir. There is also a tangential component which

is neglected. It is assumed that slip does not occur. Shear forces are not transmitted, only the normal component of the compressive force is transmitted.

A point load is applied at the centre of the pile of the slabs, which are on the top of each other without connected mortar and surmounted by a rigid slab. These slabs compress equally. When application point of the load is changed, distribution of stress is like in elastic stress distribution. The distribution is linear. However, when the load is in the limit of the middle third rule, then they are unable to transmit tensile stress. The slabs tend to separate. If the thrust line of the funicular polygon is outside the limit of middle third rule application point, then, masonry arch can be expected to collapse but this ratio is for rectangular shapes. It is different for every different shape. However, if it is ensured that the line of force polygon lines within the middle third rule region, then the structure is expected to be safe (Heyman, 1982).

Adopting plastic theory to the arch provides a set of criteria that can be adopted to determine stability and the state of stress of such a structure. Plasticity theory is concerned with safe limits and determining nominal values for the state of stress. By considering the spine as an arch, plasticity theory can be used to analyse the static behaviour of the structure. However there are 3 assumptions to be made.

1. No tensile force can be transmitted by the arch.
2. The arch has an infinite compressive strength.
3. Sliding failure cannot occur.

For a given posture of the spine subject to a given pattern of loading, a line of thrust can be calculated. It describes one possible way in which compressive forces can be transmitted through the spine. If this line of thrust satisfies the equilibrium condition, the yield condition, then the safe theorem of plastic theory validates that the structure is stable.

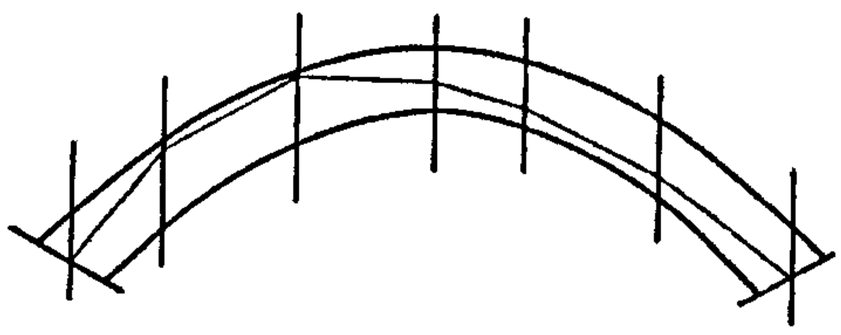


Figure 2- 14 Stable Arch (Heyman, 1982)

Constructing a thrust line in equilibrium with all the loads satisfy the equilibrium condition. The yield condition demands that the line of trust lies everywhere within the cross-section of the arch. The thrust line calculated does not have to be the line along which forces are actually transmitted in the arch. One thrustline exists along which the spine could transmit the load is a sufficient condition for safety. If the horizontal thrust H is outside the limits then four hinges forms

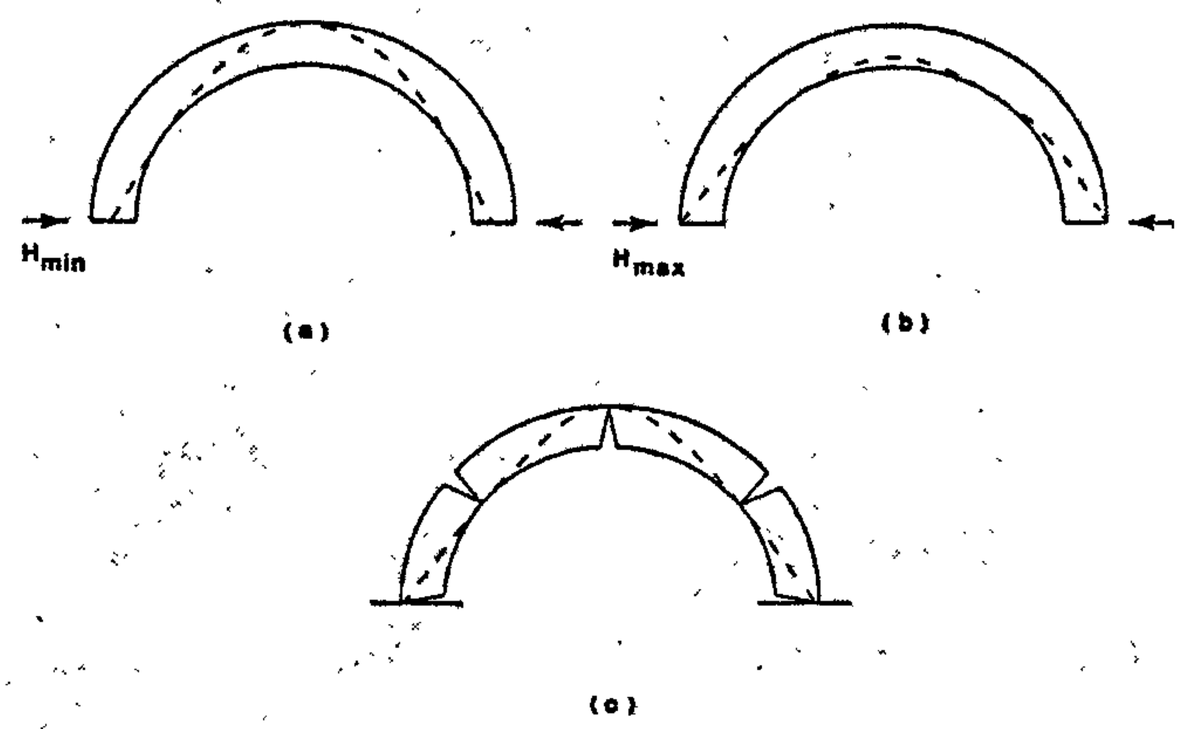


Figure 2- 15 Thrustline of an arch with forces of a) Hmin b) Hmax c) Hcollapse

The stability of the arch is determined by its being thick enough to contain thrustline. Increasing the tension in the string reduces its curvature. The flatter the arch the greater the horizontal thrust that is required to maintain its stability.

In the normal erect position the lumbar spine is convex (anteriorly), however when flexed it changes into concave. Abutment is provided by the sacrum. The reaction is generated by some combination of body weight, muscular and ligamentous forces. Aspden (1989) , divided the body weight into 2. First the head and shoulders acting at T2 and the second trunk weight acting at T12. Intra abdominal pressure was obtained from published measurements for the posture and the loading analysed. An analysis was made for 3 different regimes of posture and the load. In the first two, intra-discal pressures were calculated at different values of intra-abdominal pressure. The third was the reanalysis of a rather extreme situation to justify the beneficial effects of intra-abdominal pressure.

With respect to the result of that study, intra-discal pressure was found to be increasing with intra-abdominal pressure in the upright posture. It was due to the longitudinal

component of the abdominal muscle force. If the lumbar lordosis functioned as an arch, the increased intra-discal pressure in the upright solution was a natural result. Due to the nature of the flat arch, lumbar spine was very stable. However, if the lumbar lordosis disappeared, then the stability would be removed.

Plasticity theory showed that the lumbar lordosis and intra-abdominal pressure had to exist together to strengthen the spine. Increasing the pressure in the absence of lumbar lordosis was dangerous. The plastic analysis of a near maximum loading of the trunk showed that stability of the spine was critically dependent on its shape and intra abdominal pressure.

The arch model provided a significant role for the curvature of the spine when compared to the lever model as the calculated forces showed significant reductions in the amount of the muscle forces and the loads on the intervertebral joints. The model is more useful when compared to the lever model as it provides a graphical representation of the state of the stability of the spine.

2.10.4 Thrustline Model

In thrustline model spine is assumed as rigid. In rigid models, the deformation is small relative to overall motion. Each segment has a mass located at its centre of gravity. The location of a segment's centre of mass is fixed during any movement. In these models gravitational forces act downward through centre of mass of each segment.

The arch model has some advantages when compared to the lever model; however, it neglects the concept of distributed body weight. The forces acting on the spine are body weight, external loads, and individual muscle and ligament groups. Type of the curvature, direction, magnitude of the applied forces and the activation of different muscle groups for different postures change the position of the thrustlines. The level of activation of the muscle group varies according to the force required for the stability of the spine for the given posture. If the muscles are not strong enough to provide the required force, this may cause instability.

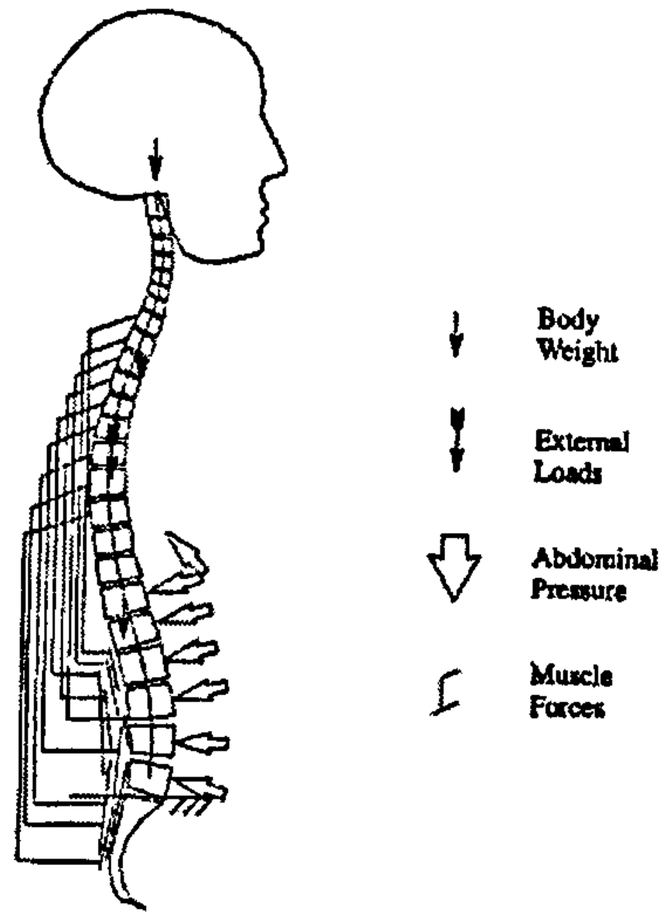


Figure 2- 16 Loading system of the spine (Acar and Grilli, 2002).

Distributed body weight forces must be matched by the consideration of the muscle force distribution along the spine, so that it is possible to search for the direction of the muscle forces and the impact of these forces. The magnitude of the muscle forces depend on the points of attachments and the curvature of the spine. The direction of the muscles around the spine changes so that they can adjust themselves to keep the thrust line within the limits of the spine.

Spine is a redundant mechanism, that is, the number of the unknowns for equilibrium is more than the number of equations. To solve this problem a reduction method is applied. The number of unknowns is reduced until the number of unknowns is equal to the number equations. Optimisation is the other method for solving an infinite number of thrust lines existing in a statically indeterminate structure. It involves the best thrustline closest to the centre-line of an arch. If the best fitting trustline among all thrust lines can be found but if it is not located within the core of the complete arch of the spine then the spine fails. To find the best fitting thrustline, the best position for the pole O of the force polygon formed by compressive forces in 2D should be solved by using optimisation method (Case *et al.*, 1999).

Acar and Grilli used thrustline concept to develop functions to calculate the mass and eccentricity of the upper body acting at each spinal level (Acar and Grilli, 2002). The trunk was sliced by imaginary horizontal planes at each vertebral level of the thoraco-lumbar spine with a gravity force acting on it. The arms were considered parallel to the line of gravity in every posture and their weights were assumed to be 18 N acting on

T2, T3 and T4 combined with the weight of the each slice. In computer based modelling application of ADAMS, simulation of the configuration was performed and three different positions representing various degrees of flexion were presented; erect, slightly flexed, fully flexed. The point of force application relative to each vertebral body centre remained fixed for each posture. The line of action of the force altered consequently. The moment arm of each force was changed from posture to posture. The moment of arm of each force relative to the L5/S1 joint increased from the erect posture to the position of near full flexion.

Thrustline theory is improved in the way it approaches a solution to the problem of spinal stability and contributes to the understanding of back injuries related with lifting. Muscles, ligaments can be inspected in detail for their role in spinal stability. The joint reaction forces can be used to investigate the damage at end plates of the vertebrae. The discs can also be investigated with the joint reaction forces. The level of the detail when compared to the other methods justifies the use of thrustline theory in this thesis.

2.10.5 Discrete Modelling

Mathematical modelling of a spine was developed for a three-dimensional force analysis by Belytschko *et al.*, (1973). The model was in 3D for inspecting force deformation in non-linear terms. The vertebrae were idealized as rigid bodies while the discs, ligaments, and connective tissues were represented by deformable elements. The model assumed N rigid bodies connected by n deformable elements. Deformable bodies connected intervertebral discs. Each deformable element had axial, torsional, bending and shear resistance in any combinations. Thus, it was possible to include the non-linearity of the biological tissues.

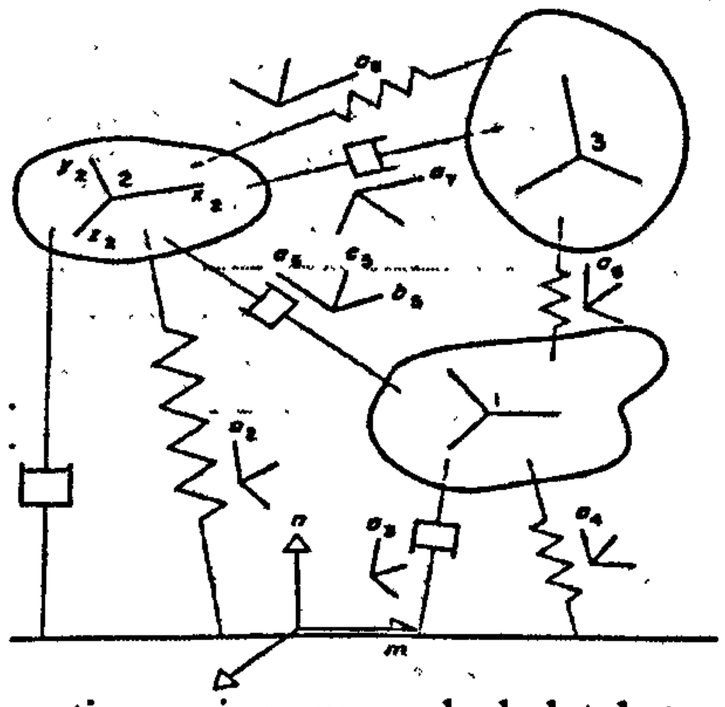


Figure 2- 17 The method of representing a given musculoskeletal structure by a discrete-parameter type mathematical model

The analysis was based on the stiffness method of structural analysis. The non-linearity of the system was treated by a procedure of incremental linearization combined with equilibrium checks. The external forces were applied in small increments and the solution for each increment was obtained by solving linear equations approximating non-linear behaviour. Next each increment was checked and corrective forces were introduced.

One point on each rigid body is designated as a base point called primary node. The points where deformable elements were connected to rigid bodies were called the secondary nodes. Two types of deformable elements were used axial or spring elements offering resistance only in tension or in compression and beam elements with bending, torsion, shear and axial stiffness. In matrix structural analysis, work was defined by incremental displacement multiplied by force. The equilibrium of forces was checked with the equilibrium of internal and external forces. The external load applied in increments was solved for each node for equilibrium. In the beginning, total stiffness was computed on the basis of the current configuration. Equation was solved for the incremental displacements and new configuration was established. The resulting internal forces were found. In their research three problems were investigated:

1. The response of the spine to lateral loads.
2. Stability of the spine under compressive loading.
3. Behaviour of a mildly scoliotic vertebral volume when subjected to traction.

Their research was unique as it introduced numerous elements rather than one element. It explained the constraints due to the orientation of the facets. It was possible to inspect various material parameters, the changes of spinal behaviour with age, the affects of arthrodesis and the alterations of internal forces in scoliotic spines and the response of forces exerted by braces.

A method by Panjabi was also presented for constructing discrete parameter type 3-D mathematical models and governing equations of motion of the spine structure Panjabi, (1973). He separated the mathematical models into two. In continuum models, spine was considered as a rod having infinite degrees of freedom. It was too different from the real spine structure because of its limitations taking into account important

anatomic features. In discrete parameter type models spine was considered as a structure formed by various anatomic elements like vertebrae, ligaments, muscles, articulating facets by mass-less springs and dashpots. This idea was closer to the real structure.

In Panjabi's model, basic procedure was to formulate a set of equations of motion representing the mechanical behaviour of the model to external loads and displacements. Each rigid body had 6 degree of freedom with each connecting element (spring and dashpot), 21 coefficients of stiffness and damping.

The model may consist of any number of bodies, springs, dashpots connected to each other in any manner required to form an anatomically true model. The bodies are 3-D rigid bodies and having all the possible 6-degree of freedom of motion. They may be of any size, shape and orientation. The springs are mass less and each may have all of the possible 21 spring stiffness coefficients. The end conditions may be any combination of fixed, hinged and ball joints. The dashpots, similar to springs are mass less and each may have all of the twenty-one damping coefficients. The dashpots and springs may be connected in any combination, in parallel to form-Kelvin Viscoelastic solids or in a parallel-series combination to form the 3-parameter solids. The system may have any initial configuration. External loads, static and dynamic consisting of force and torque vectors may be applied singularly or simultaneously to number of bodies. Matrix methods are used to make the method versatile and suitable for computer use.

Every method had some limitations to relax some underlying problems: For example: Displacements are small. Bodies are rigid. Spring and dashpots are mass-less and linear. The conclusion of this study was that spine cannot be investigated separately. Muscles, joints, ligaments, ribs should also be integrated into the system. Although the 3 D models are accepted to be superior over 2D, for an activity like lifting where the initial movements are usually in 2D, a 3D model can be considered as a complex solution.

In a recent study, software called AnyBody is used in the field of biomechanics. It is a tool for analyzing the musculoskeletal system of humans or animals. It computes muscle forces, joint reactions, metabolism, mechanical work, efficiency for given

movements. Any property of the AnyBody model is parametric and the system can be used for optimization which means that AnyBody can determine movement patterns, working positions, anthropometric data, boundary conditions (Rasmussen *et al.* 2002)

The other recently developed software is called Jack. Jack is a human modeling and simulation software that helps organizations in various industries improve the ergonomics of product designs and refine workplace tasks. Jack enables virtual environment building and virtual human creation. In this virtual enviorment, it is possible to define the human size, shape and position, for specifically assigned tasks where analysis is conducted for assessing the human performance (Burnette 1998).

The code developed in this thesis with the computational modelling approach can be incorporated into these programs. This might give a deeper insight in terms of understanding the mechanisms of injury in a more applied field.

2.11 Discussion

Discussions on biomechanical factors in lifting and biomechanical models are provided below.

2.11.1 Biomechanical factors in lifting

Multiple biomechanical factors play an important role in lifting related injuries and low back pain. In order to avoid from risky situations, it may be good to know how the spine and the whole body behaves in extreme conditions of these parameters, like excessive acceleration, excessive loading, and excessive flexion of the spine. One of the possible methods, in order to determine boundary conditions for the safe region, is either modelling or measurements.

One of the limitations of modelling is that there is a huge variety in the skeletal and muscular structure of the human body. This property of human body prevents from inclusion of all the details in a single biomechanical model (Jager and Luttmann, 1989). However, they still add great information to the understanding of the injury mechanisms.

The models are based on average tolerance limits of the populations. The tolerance limits of the body can be different for each individual; depending on the gender, body dimensions, age and so on. For example, the cross sectional area of their muscles is different from men (Marras and Davis 2000). The best approach for this problem would be parameterization of the properties for each individual to the model. With the thrustline theory which is used in this thesis, it is possible to include the effect of body dimensions in a parametric way and parameterize the muscle parts also depending on the data available in literature.

On the general review, it can be observed that the evaluation of the models and the experiments are mostly based on the forces acting on the L5/S1 region. However, the spine is a complete structure and should be considered as a whole. A model considering all of these forces acting on the full spine would provide better information about the stability of the spine for risky situations. The thrustline theory which is used in this thesis focuses on the full spine rather than only L5/S1 region.

The evaluation of the lifting techniques is very sensitive to the model developed. The assumptions made while modelling should be considered in order to prevent from missing out the important inputs for modelling. Any model focused on only one effect of the biomechanical factors would be inefficient. It is the combination of the magnitude of the weight, the posture of the body. For example, the study of MacKinnon and Li, 1998 show that the kinematics of the lumbar spine are effected by increases in mass lifting than by the kinematics of the load. The higher biomechanical risk is associated with lifts of greater loads, subjects are observed to alter their lifting techniques in order to compensate high load masses. (MacKinnon and Li, 1998). This shows that the combination of all these factors determine the nature of the lifting activity and these parameters should be considered while developing any biomechanical model and designing any lifting related experiments.

Even the initial height of the load has an important role in spinal loading. The peak moments are greater when lifting from lower heights. NIOSH guidelines are observed not to take into account the initial height of the load acting on the spine (Lavender *et al.*, 2003). Lavender et all, observed that NIOSH model under estimates the increases in spine loading associated with lower heights.

Each parameter i.e; the load magnitude, initial height of the load, the height and the weight of the person, play important roles in the kinematics of lifting. For this purpose, in a research for lifting activities, all these parameters should be considered and the way the body interacts with them should be observed to understand the nature of the lifting.

2.11.2 Biomechanical Models

With the inspection of the models available in literature, it is seen that there are many different approaches while modelling the spine. Each modelling has its own pros and cons.

The beam model is based on the analogy of the beams and spine and also its elasticity. However, it is very difficult to explain the different postures of the body which might be seen in a typical lifting activity. The beam models limit themselves with the thoracolumbar region only, whereas the neck region is also as important as the others. As the spine is a complete structure, the results without including the neck region can be quite misleading.

The lever model is based on the equation of equilibrium around a rotation point; however this model neglects the curvature of the spine and results in very highly unrealistic muscle values due to the short arm of force. Although the lever model when compared to the beam model can include the full spine, it still fails to include the curvature of the spine. The Arch model solves the curvature of the spine problem but neglects the distributed loading pattern.

The thrustline model includes the body weight, muscle and ligament forces. With this model, it is possible to investigate the role of each part in spinal stability in a lifting activity. Although the thrustline theory answers the questions related to spine, a more realistic approach would be to model the whole body including legs and arms, as they all play role in a typical lifting activity depending on the style of the lifting chosen by the person. In this thesis, lifting a load from the boot of a car is focused on. While lifting a load from the boot of a car, normally stoop lifting is used due to the height of the boot. The spine is flexed with knees normally in a straight posture. As mentioned in Chapter 2, the most vulnerable part in stoop lifting is the lumbar region, whereas for

squat lifting it is mostly the lower extremes of the body like the knees, hamstrings and quadriceps. However, stoop lifting does not involve these injuries but the spine related injuries and pain. For this purpose, it is reasonable to focus mostly on the full spine rather than the whole body with the lower extremities.

The other 3-D discrete models have some advantages by including all the structures muscles, vertebrae and ligament. However, it is very difficult to know the stiffness and damping coefficients of the structures as they change properties depending on the loading conditions and posture of the body. Moreover, as it is the coherence of the whole system, it is unpredictable how all the parts work together with different properties. There are still unknowns in terms of the interaction of the muscles when they transmit load in an actual mechanism.

Lifting a load from the boot of a car takes place in the sagittal plane. 3 D model would be a good option if the lateral bending and twisting motions of the spine was going to be investigated. However, only the sagittal plane flexion is focused on this research. The thrustline theory is based on the analogy between the bridges and their loading which takes place in 2 D plane.

Considering all the modelling approaches, in order to simulate a lifting activity, it is decided to use the advanced thrust line theory with modified end point reaction forces approach. This enables us to investigate the effect of load magnitude, and body posture at the same time. With the end point reaction forces calculated for each frozen frame in a lifting activity it is possible to look at the loading at the L5/S1 region. The joint reaction forces and their magnitudes can also be calculated with this theory. With the visual aspects of evaluating spinal stability by looking at the position of the thrustlines within the spine, thrustline model provides practicality.

The steps during the development of the modelling of the thrustline theory in Visual Basic are explained in detail in chapter 3.

2.12 Conclusion

LBP is a big industrial problem (low back injury claims account for 40-50 % of compensation claims in some industries) but it is not only caused by lifting. The personal risk factors for back pain are physique, anthropometry, strength (static and dynamic endurance), physical fitness, health history, spinal abnormalities, spinal mobility, age, gender , psychophysical factors, motivation, training. Environmental or outside risk factors are the posture, handling techniques, confined environments, spatial restraints, load characteristics (weight, size, shape, handles and other couplings), duration and repetition. Any research focused on the investigation of LBP should consider these parameters.

The studies based on biomechanical approach prove that the loads which are safe by psychophysical approach exceed the limits of strength of body structure. This shows that biomechanical models are good at predicting the injuries. For this purpose a biomechanical model is used in this study.

The disk between L5/S1 has the potential to incur the greatest moment and is one of the most vulnerable tissues to force-induced injuries. Between 85-95% of all disk herniation occur relatively equally at the L4/L5 and L5/S1 regions. For this purpose stoop type lifting is considered in this study rather than squat which does not put much on the L5/S1 region.

In a computer environment, due to the flexibility of the software, it is possible to simulate all the factors and find out the forces acting on the body. However, the models in a computer environment have some defects. In a link segment model (LSM), the links are assumed to be homogenous; however, in reality their structural properties changes significantly On the other hand, even in measurements, there are a large number of assumptions in terms of the data filtered or how the EMG values are considered. With mathematical models it is possible to make use of the parameterisation of the variables, so that the effect of each variable can be seen easily and tedious, repetitive calculations can be prevented. Any kind of alteration is possible

due to the high flexibility of parameterisation. For this reason, mathematical modelling of the spine by using thrustline theory is decided on.

In addition to this, through the construction of the biomechanical models, it is possible to use cadaver failure data to predict the risk of injury to a person performing a specified task. As a result, it is better to make use of the computer environment for a better simulation of lifting activities, considering the combination of all the factors. It is possible to include the load magnitude and the body posture.

CHAPTER 3

3 Advanced Thrustline Theory & Development of the model in VB

In this chapter, the mathematical background behind the thrustline theory is explained in detail. The code developed for advanced thrustline theory in Visual Basic for full spine for lifting activities is given in detail. The implementation of theory into the code is explained. The parametric and constant variables of the model are provided. The visual aids while using the code are provided. Retrieval of the data files and implementing the muscle and ligament groups while running the code for simulations are provided with illustrations of screen shots of the code.

3.1 Theory of the Model

Stability is an important issue for structures.Timoshenko (1965), worked on force polygons for the stability of structures especially in civil engineering related topics where arc like bridges were under investigation. Later on, Aspden investigated the lumbar spine stability with the similar analogy as it was in the bridges with Timoshenko. Although it is a pragmatic approach to investigate the lumbar spine, spine is a full structure and instability in one of the regions affects the other regions as well.
In the advanced thrustline model, the spine is assumed to be completely rigid which has an infinite modulus of elasticity. The applied forces; are the body weight forces, muscle and ligaments forces and external loading.

The conditions of equilibrium for any system of forces in a plane are a closed polygon of forces and a vanishing resultant couple. From the conditions of a closed polygon of forces acting on a 2D surface of the spine, the algebraic sums of projections of the given forces on any pair of orthogonal axes are taken as zero. From the condition of a vanishing resultant couple, the algebraic sum of the moments of the given forces with respect to any centre in their plane is taken as zero (Timoshenko, 1965). These conditions are expressed analytically as follows:

$$\sum Fx_i = 0 \quad (1)$$

$$\sum Fy_i = 0 \quad (2)$$

$$\sum M_i = 0 \quad (3)$$

Where;

Fx_i is the x component of the force acting on the spine in sagittal plane.

Fy_i is the y component of the force acting on the spine in sagittal plane.

M_i is the moment component perpendicular to the x and y axis.

Once the equations of equilibrium (Eq1, 2, 3) are satisfied, for any posture of the spine subject to a given loading, it is possible to calculate the line of thrust. The line of thrust determines the possible pathway for the transmission of compressive forces. Instability occurs if the thrustline lies outside the physical boundaries of the spine. This means that the spine is incapable of transmitting compressive forces and this becomes instable. The equilibrium does not guarantee the stability; a structure might be in equilibrium but might be still unstable. Satisfying the condition of equilibrium means that the equations 1, 2, 3 are solvable for the unknowns in the systems. For our case they are the reaction forces acting on the spine. By drawing the vector polygon formed by the reaction forces and the forces acting on the spine by muscles, ligaments and external forces. The stability of the spine is checked. It is the geometric positioning of the force polygon, in other words, the thrustline, which determines the stability, not the equilibrium of the forces (Timoshenko, 1965).

In order to apply the theory of thrustline, the reaction forces at the end points of the spine should be calculated. These reaction forces are located at the inferior central point of the L5 and at the superior centre point of the C1. The line connecting these points is defined as reference line. Although there are only 3 equations of equilibrium, the number of the unknowns in this case is four:

R1: Reaction force at the inferior centre of the L5 perpendicular to reference line.

H1: Reaction force at the inferior centre of the L5 parallel to reference line.

R2: Reaction force at the superior centre of the C1 perpendicular to reference line.

H2: Reaction force at the superior centre of the C1 parallel to reference line.

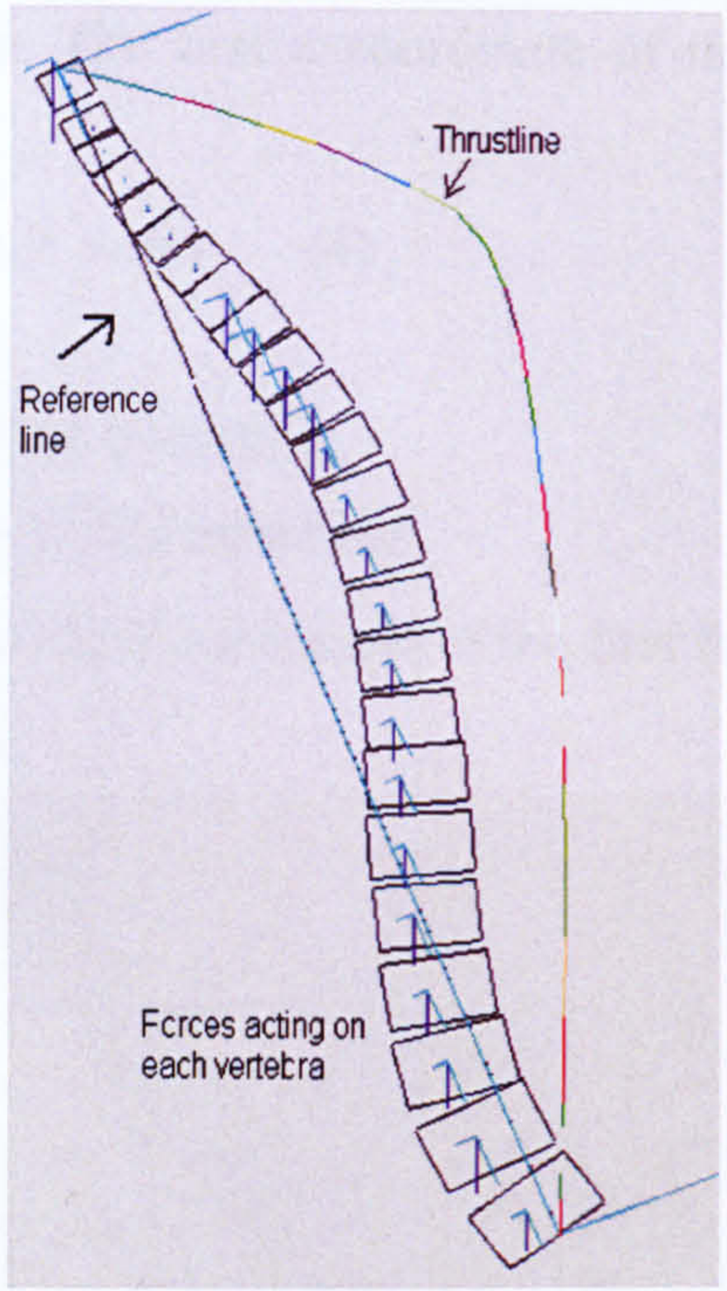


Figure 3-1Forces acting on the spine, reference line and thrustline

In order to solve the problem of indeterminacy due the number of unknowns, the weight of the head with the muscle forces acting above C1 is assumed to act as force H1 thereby making the number of unknowns and the equations equal to each other. The weight of head is assumed to be 6.2% of the total body weight. As an average person who has a total body weight of 71.76 kg the weight of head is calculated as 4.44 kg acting 0.45 cm anterior to and 4.55 cm superior top surface centre of C1. For people who have a different body weight this values are rescaled for each person to implement the real weight of body. The rest of the segmental weights of the body are scaled also for each person to implement the real weight of their body. By applying the Equations (1), (2), (3) with the distributed body weight of the spine, we get the numerical values for the reaction forces of R1, R2, and H1.

After the reaction forces at the end points of the spine are calculated, the next step is the construction of the funicular polygon. It is possible to draw the thrustlines (funicular polygon) either using an analytical method or graphical method. Here, we followed the analytical method by constraining the start and end coordinates of the thrustline coinciding with the start and end points of the vertebrae mainly inferior centre of L5 and superior centre of C1. To build the thrustline, it is necessary to find out the x and y

coordinates of the thrustline. The first x coordinate of the thrustline is calculated by Equation 4.

$$\tan\theta_i = R1/H1 \quad X_1 = \tan\theta_i \times dy1 \qquad (4)$$

Where,

$\tan\theta_1$ is the initial slope of the thrustline.

X_1 is the initial X coordinate of the thrustline.

$dy1$ is the distance between the y coordinate of the first force on spine and the inferior centre of L5 along the y axis.

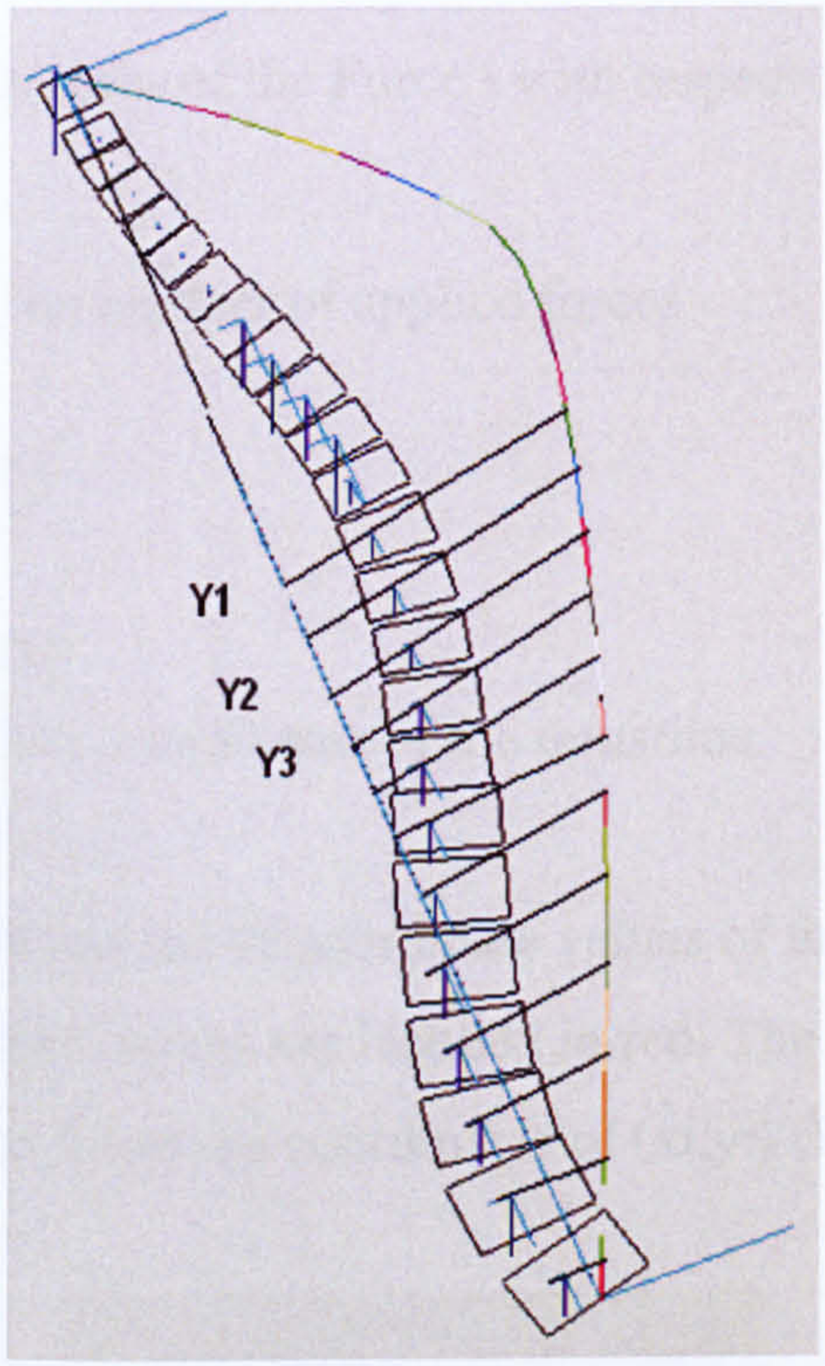


Figure 3-2 Illustration of the location of the y coordinates of the thrustline is equal to the y coordinates of the forces acting on the spine

The y coordinate of the thrustline is equal to the y coordinate of the force acting on the vertebrae which is along the axis parallel to the reference line as shown in Figure 3.2. For the next coordinate, it is necessary to find out the new tangent angle of the force vectors. This is calculated by the Eq. 6, the new value of the x coordinate is added to previous one (Eq.7). This procedure is repeated until all the forces acting on the spine are accounted for. As we have set the constraint of aligning the start and end points of the thrustline with the spine the shifting of the coordinates is necessary. This is accomplished by Eq.8

I=1 to 24 for each vertebrae

$$dy_i = y_i - y_{i-1} \qquad (5)$$

Y_i is the coordinate of the each force acting on the spine. Equation 5 is used to calculate the distance between the y coordinates of the sequential forces

$$\tan\theta_i = \left(R1 + \sum_{k=1}^{i-1} Fr_k\right) / \left(H1 + \sum_{k=1}^{i-1} Fh_k\right) \qquad (6)$$

Where,

$\tan\theta$, is the slope of thrustline at segment i of the thrustline

Fr_i is the perpendicular component of the Force i with respect to the reference line acting on the spine.

Fh_i, is the horizontal component of the Force i with respect to the reference line acting on the spine.

For i =2 to n+1 where n is the number of applied forces

$$x_i' = x_i + (-Xn/Yn) \times y_i \quad (7)$$

$$x_i = x_{(i-1)} + \tan\theta_i \times dy_i \quad (8)$$

Where X_n and Y_n are the final coordinates of the thrustline.

The following figure shows one set of coordinate values of thrustline where a force acts on the thrustline. The reaction forces are labelled in red. The angle θ refers to the angle of the thrustline section which has the coordinates of (xi,yi) (Figure 3.3).

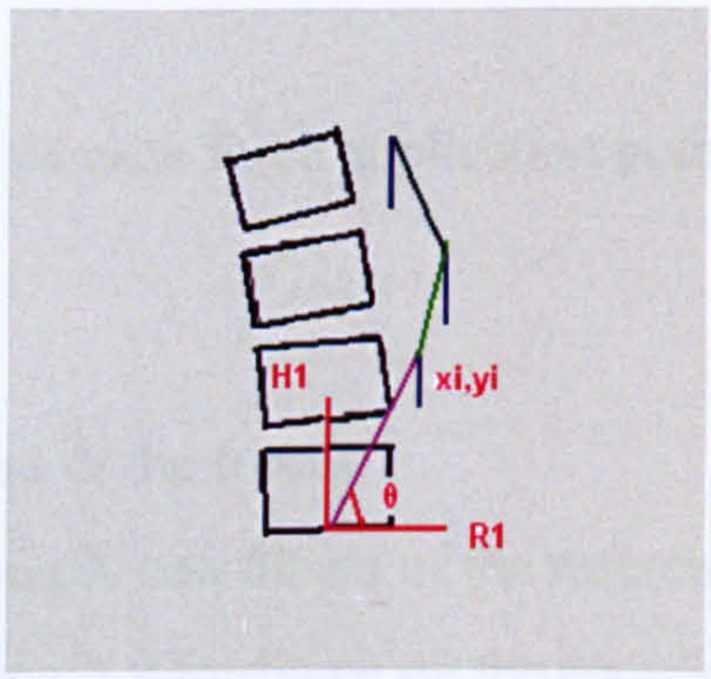


Figure 3-3 Illustration of the first coordinates of the thrustline, dy1, and X1

After drawing the thrustline, the stability analysis by checking out if the thrustline stays within the physical boundaries of the spine is performed. The more the deviation of the thrustline from the spine, the more unstable the spine becomes.

3.2 Construction of the Model in Visual Basic

In this model each vertebrae composing the spine has common properties. Each force has some common properties too. For this purpose, two types have been defined; one is ***Vertebrae***, the other is ***Force***. The properties need to be defined for each type. For vertebra, these are:

- X coordinate of inferior centre of vertebrae,
- Y coordinate of inferior centre of vertebrae,
- Relative orientation of the vertebrae,
- Thickness and height of the vertebrae, which is used to draw each vertebra as a rectangular box.
- Centre of gravity of the horizontal slice,
- Joint centres

The type ***Vertebrae*** contains a second type which is called ***Dimension*** and enables to define the four corners for each vertebra.

Forces acting on the spine have some specific properties which need to be defined. These are as follows:

- X and Y coordinates of each force application point
- Magnitude of force
- Angle of force
- Fx and Fy component of the forces
- Relative distance along X coordinate of the reference line
- Relative distance along Y coordinate on the coordinate system
- X and Y coordinates of the thrustline for each force

3.2.1 Assigning of values to type Vertebrae and Force

In order to load all the data related to each vertebra and the forces acting on spine, five forms are created. These are in tabular form. To deal with tabular data there is a control

which is called the Microsoft FlexGrid (MSFlexGrid) in Visual Basic. To use the MsFlexGrid in the application, the MSFlxGrd.ocx file is added.

MsFlexGrid displays and operates on tabular data. It allows complete flexibility to sort, merge, and format tables containing strings. It displays read only data. It is possible to specify the current cell in code, or the user can change it at run time using the mouse or the arrow keys. This property makes it possible to add external forces to the program whenever it is needed at run time. The Text property references the contents of the current cell. The Cols property is used to set the number of the columns in a table. The Rows property is used to set the number of rows in MSFlexGrid.

In order to store the data related with vertebrae and body weight forces, muscle force and ligament forces, MSFlexgrid were used in five different forms. They are named as Form2, Form3, Form4 and Form5. Form1 is the main screen when the user runs the code this is the property of multiple document interface in VB (Figure 3.4). More detailed information about Form1 is provided later.

Form2 displays all the active force data acting on the spine. Initially, it is only the body weight forces acting on the spine when the code runs. However, during the running of the code, depending on the muscle and ligament groups selected by the user new force groups are added (Figure 3.3). The headings for each colon are recorded to Form2 with the property of Textmatrix. Textmatrix property Returns or sets the text contents of an arbitrary cell. Its usage is:

```
MSFlexgrid.Textmatrix(Rownumber, Coloumn Number) = Set value
```

The information listed on Form2 about the forces is as follows: The index, point of application of force in rectangular coordinate system (X and Y), angle of each vertebra with respect to the vertebra below, magnitude of force, relative X, relative Y values representing the magnitude of distances of force values from the reference line, thrustline x and y coordinates, X and Y components of forces, X and Y pixel values. To store this information, the number of the rows is assigned to 26 for Form2. The body weight of each vertebra (from 1 to 24) plus weight of head plus the row for headline add up to 26 rows (Figure 3.5). For body weights the index number is also entered to the fifth column. So that it is possible to determine which force is the body weight and

which force is the external force. External forces acting on the spine are not assigned an index number. The index number for the external forces is zero.

For vertebrae related data Form3 is generated Figure (3.6). The column headings are named as follows; X and Y geometric centres of each vertebra, gravity centres, relative angle for each vertebrae, global angle, the radius, the height, X offset for centre of gravity, weight, and coordinates of four corners of each vertebrae are named as X1, Y1, X2, Y2, X3, Y3, X4, Y4, superior coordinates of each vertebral joint, force components of joint reaction forces parallel to joint axis (shear forces) as Fx and perpendicular (compression forces) to joint axis as y components as Fy , magnitude of joint reaction forces and the angle of joint reaction forces. As center of gravity of the vertebrae are unknown before the loading of data from the excel files, the zero values are assigned to Form2 for these values. The weight of head is assigned to 25th row with 270 degrees of direction.

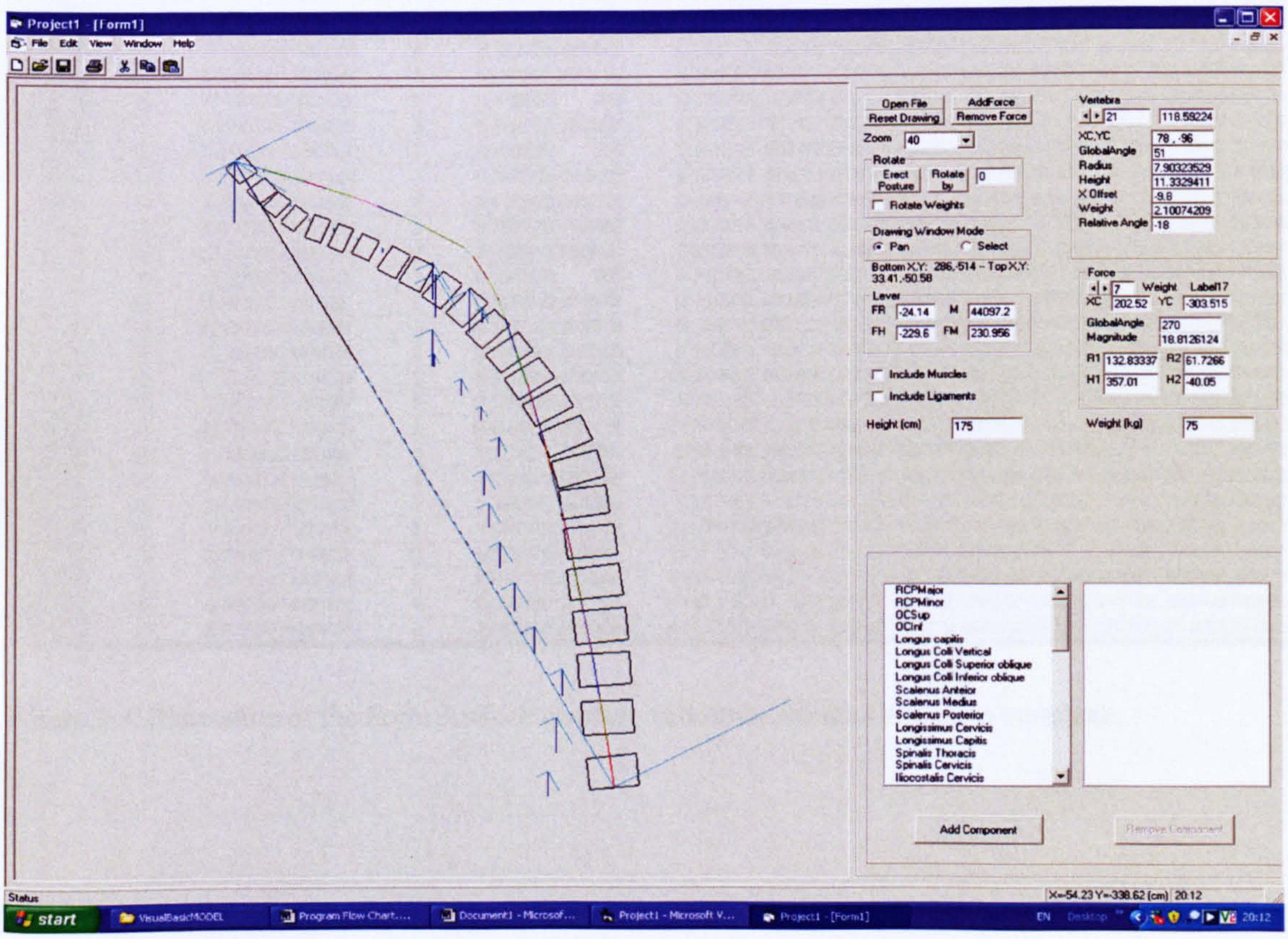


Figure 3- 4 Illustration of the Form 1 which is the main screen that appears when the code is run

Project1 - [Form2]

File Edit

index	XC	YC	Angle	Magnitude (I		Relative X	Relative Y	Thrust X	Thrust Y	FX	FY	X_Pixels	Y_Pixels		
	0186622906	3708564112	270	1812612475	1	1791807971	3103487305	281.17	-481.23	-9	-16.52	7974.255	11475.78		
	3059958279	3729939411	270	2862868275	2	2190082372	4967333604	275.94	-447.47	-12.5	-22.94	8100.421	10576.69		
	4778989022	3817420146	270	5775785775	3	3277039075	3467113458	270.93	-417.43	-9.5	-17.44	8186.644	9786.549		
	7446940464	7638345324	270	5775785775	4	7244464698	0509977444	264.1	-378.89	-9.5	-17.44	7768.485	9056		
	3282312953	3179437972	270	4804862325	5	3739565884	5730422247	257.25	-342.71	-10.5	-19.27	7469.582	8313.695		
	0578006112	3575738225	270	5775785775	6	5218328493	3480406912	250.68	-310.51	-9.5	-17.44	7248.73	7622.418		
	5521837014	5682930956	270	1812612475	7	4243767163	3435986309	244.14	-280.83	-9	-16.52	7083.302	6958.736		
	2432505323	3368931982	270	1812612475	8	3820260324	3953765472	238.68	-257.84	-9	-16.52	7008.592	6410.621		
	3071095852	5147294981	270	5320324155	9	3432836074	0206602989	234.44	-241.42	-7	-12.85	7232.344	5863.756		
	5249014393	0299562237	270	5145162025	10	0687749879	3363362762	227.53	-216.5	-5	-9.18	6965.955	5358.313		
	1267438381	0143003108	270	2.54174165	11	7268956873	3826906278	220.52	-192.56	-6	-11.01	6661.788	4894.503		
	4997636797	2750269322	270	5145162025	12	3330777157	3759994846	212.69	-167.53	-5	-9.18	6250.23	4454.344		
	0761154147	5376502234	270	.496597003	14	0223795575	4487080354	208.09	-153.74	-5.5	-10.09	6974.009	3690.337		
	1913936205	3944814893	270	1891944825	13	1011539026	7250108483	207.37	-151.71	-13.5	-24.78	6223.398	4044.362		
	5279837826	3907348387	270	3949950775	15	3782957573	3606233855	201.83	-139.05	-15.51	-28.45	6775.052	3388.296		
	3086535282	0746052538	270	3949950775	16	5279772543	5797209751	191.12	-120.88	-15.51	-28.45	6268.898	3119.58		
	3250907022	0354969782	270	1891944825	17	7520759043	3744417833	185.22	-114.36	-13.5	-24.78	6232.03	2918.853		
	1094593339	1566784843	270	3696869375	18	5976033859	4361052453	159.4	-99.14	-1.96	-3.6	5482.197	2663.05		
	2753062541	3055367634	270	2022220525	19	2353351015	3001569585	143.87	-91.15	-1.11	-2.04	5098.489	2499.108		
	3882528718	3334517375	270	1759183163	20	2866736954	1404773123	128.59	-83.95	-1.32	-2.42	4740.08	2342.304		
	3178440267	3836797207	270	0074209425	21	4323284248	5750320622	111.87	-76.91	-1.01	-1.84	4381.429	2171.403		
	0930549876	3857799682	270	3907242825	22	3254486639	5346975049	93.34	-69.82	-0.77	-1.4	4097.628	1936.295		
	4496293051	0078351287	270	3907242825	23	2748415342	2032518557	79.68	-65	-0.77	-1.4	4003.81	1709.094		
	4418799674	4705789947	270	3907242825	24	5220092661	4867627573	52.98	-56.36	-0.77	-1.4	3694.477	1351.623		
	3837599348	3411579894	270	45.610614	25	0	7999496477	33.39	-50.59	-21.83	-40.05	3247.85	1222.085		

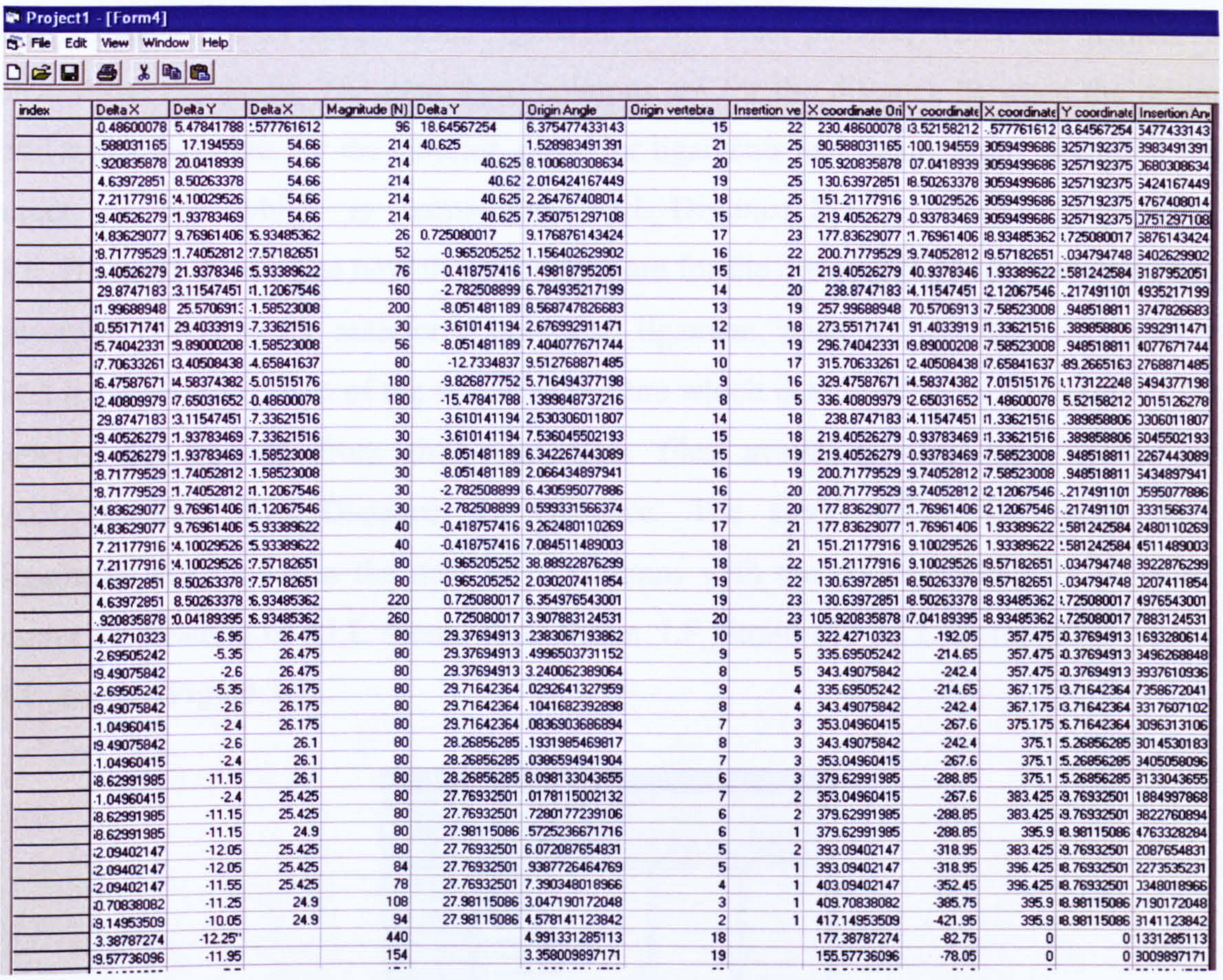
Figure 3- 5 Illustration of the Form 2 which displays and stores the data related to forces acting on spine.

Project1 - [Form3]

File Edit View Window Help

Vert #	X_Center	Y_Center	XG	YG	Relative Ang	Global Angle	Radius	Heigth	X_Offset	Weight	X1	Y1	X2	Y2	X3	Y3	X4	Y4
1	371	471	2560664966	7446192607	-6	18	3529411765	2941176471	43	1812612475	3333447403	3519035944	4666552597	0480964056	3787882529	3404816196	0454777336	344288808
2	358	432	3569125679	3062786635	-3	15	2941176471	2352941177	34	2862868275	3868401117	1186997488	5131598883	3813002512	5269850241	3938575782	3006652476	331257075
3	349	397	3057416329	1403193431	-1	14	3470588235	23.66	28	5775785775	5169375269	4689155956	3830624731	3310844044	3945457389	3117230907	2284207928	749554281
4	341	364	3698508879	3374507285	2	16	3529411765	3588235294	44	5775785775	4657214167	1589384367	3342785833	3410615633	5739803591	7159630203	3054231924	333839893
5	331	331	3443206911	3004097837	2	18	1764705882	23.66	53	4804862325	2598514859	2078974965	7401485141	7921025035	3042867341	7592922071	0123989706	308717063
6	321	300	1093775725	3790714455	-1	17	7647058824	4705882353	60	5775785775	2365682215	3897263911	7634317785	5102736089	2785307293	3684164999	5258443736	347869282
7	312	270	3320618506	3831398485	1	18	4705882353	7058823529	63	1812612475	7156735766	4479076597	2843264234	3520923403	3484501246	7183720372	3797972777	514187356
8	304	245	5115861979	7470225835	6	24	3588235294	1764705882	62	1812612475	3894016652	3650433735	3105983348	1349566265	1337707306	5290017934	3125740611	359088540
9	293	220	3519865976	3854942857	10	34	3235294118	4705882353	44	5320324155	3518301998	3522495065	4481698002	3477504935	3521429953	7187390648	3558033949	323238077
10	278	199	1919586956	4984656036	7	41	5294117647	18.59	44	5145162025	1045395052	3735637131	3954604948	1264362869	3279377886	2612940762	4884568963	732568338
11	261	180	3310283262	3841076351	2	43	1764705882	3411764706	45	2.54174165	3531355824	1327303683	3468644176	3672696317	1089210599	5354849018	3151922348	300945638
12	243	162	4347001074	4369465081	2	45	3823529412	3470588235	50	.496597003	5375782223	4658946615	4624217777	5341053385	3318219326	4079983546	4069784371	339787677
13	226	145	1529212983	4059888388	5	50	1176470588	7058823529	37	5145162025	3836118544	3860883027	3163881456	5139116973	5222307422	4258893749	1989454451	198065980
14	209	131	3888259286	3137490228	5	55	3411764706	7058823529	-10.5	3949950775	3042290485	3601089351	4957709515	4398910649	2734228087	7148715209	2818809057	335089391
15	190	119	1681021884	3104785077	5	60	4705882353	3470588235	-18	1891944825	3289267025	3861922936	3710732975	3138077064	4072776743	5347647218	2651310793	260714930
16	172	108	3899714456	1193144483	9	69	4705882353	2352941176	-12.4	3949950775	2421276976	3369626138	7578723024	5303738624	3378151936	3166628282	4220705889	575591510
17	153	102	4129780985	3605814946	1	70	5882352941	3588235294	-26	1891944825	3944925918	3153498685	3055074082	3846501315	7314636053	3861761391	3204487889	745614983
18	134	95	4108525119	3163296712	4	74	3823529412	7058823529	-11.6	3696869375	3290182693	7107560781	1709817307	2892439219	3926867545	5250985614	3507232932	740220123
19	116	90	3916474756	2450101856	3	77	3823529412	3823529412	-11	2022220525	1470888847	3124052299	3529111153	3875947701	1362060666	3776151413	7330383836	402425601
20	101	87	3034155184	1254811134	-3	74	5294117647	3411764706	-10.5	1759183163	3829922745	3919844035	2417007725	3080155965	4853180942	3589778232	3513026432	342946630
21	86	83	5796702559	3765857709	-12	62	3529411765	3411764706	-9.8	0074209425	5734331205	1519674836	3265668795	3480325164	3199719975	3797479345	2668382384	583682901
22	72	75	2957195983	3096671289	-8	54	1764705882	7647058824	-9.1	3907242825	2578282078	2229977816	7421717922	7770022184	3336109888	5963364761	3492674044	342332039
23	62	68	3925783197	4678116696	-4	50	1764705882	5294117647	-14.9	3907242825	7613740035	3089060163	2386259965	3910939837	2237826359	3267173228	7465306429	344529355
24	47	56	4529749843	4628596187	0	50	7058823529	7647058824	-14.9	3907242825	3633548238	3930646822	3366451762	3069353178	3425951448	3326545553	2693047924	318783919

Figure 3- 6 Illustration of the Form 3 which displays and stores the data related to vertebrae.



index	Delta X	Delta Y	Delta X	Magnitude (N)	Delta Y	Origin Angle	Origin vertebra	Insertion ve	X coordinate Ori	Y coordinate	X coordinate	Y coordinate	Insertion An
	0.48600078	5.47841788	:.577761612	96	18.64567254	6.375477433143	15	22	230.48600078	13.52158212	-.577761612	13.64567254	5477433143
	.588031165	17.194559	54.66	214	40.625	1.528983491391	21	25	90.588031165	-100.194559	3059499686	3257192375	3983491391
	.920835878	20.0418939	54.66	214	40.625	8.100680308634	20	25	105.920835878	07.0418939	3059499686	3257192375	0680308634
	4.63972851	8.50263378	54.66	214	40.62	2.016424167449	19	25	130.63972851	18.50263378	3059499686	3257192375	5424167449
	7.21177916	:4.10029526	54.66	214	40.625	2.264767408014	18	25	151.21177916	9.10029526	3059499686	3257192375	4767408014
	:9.40526279	:1.93783469	54.66	214	40.625	7.350751297108	15	25	219.40526279	-0.93783469	3059499686	3257192375	0751297108
	:4.83629077	9.76961406	:6.93485362	26	0.725080017	9.176876143424	17	23	177.83629077	:1.76961406	18.93485362	1.725080017	5876143424
	:8.71779529	:1.74052812	:7.57182651	52	-0.965205252	1.156402629902	16	22	200.71779529	:9.74052812	19.57182651	-.034794748	5402629902
	:9.40526279	21.9378346	:5.93389622	76	-0.418757416	1.498187952051	15	21	219.40526279	40.9378346	1.93389622	:.581242584	3187952051
	29.8747183	:3.11547451	:1.12067546	160	-2.782508899	6.784935217199	14	20	238.8747183	:4.11547451	:2.12067546	-.217491101	4935217199
	:1.99688948	25.5706913	-1.58523008	200	-8.051481189	8.568747826683	13	19	257.99688948	70.5706913	:7.58523008	.948518811	3747826683
	:0.55171741	29.4033919	-7.33621516	30	-3.610141194	2.676992911471	12	18	273.55171741	91.4033919	:1.33621516	.389858806	5992911471
	:5.74042331	:9.89000208	-1.58523008	56	-8.051481189	7.404077671744	11	19	296.74042331	19.89000208	:7.58523008	.948518811	4077671744
	:7.70633261	:3.40508438	-4.65841637	80	-12.7334837	9.512768871485	10	17	315.70633261	:2.40508438	:7.65841637	-89.2665163	2768871485
	:6.47587671	:4.58374382	-5.01515176	180	-9.826877752	5.716494377198	9	16	329.47587671	:4.58374382	7.01515176	:.173122248	5494377198
	:2.40809979	:7.65031652	-0.48600078	180	-15.47841788	.1399848737216	8	5	336.40809979	:2.65031652	:1.48600078	5.52158212	0015126278
	29.8747183	:3.11547451	-7.33621516	30	-3.610141194	2.530306011807	14	18	238.8747183	:4.11547451	:1.33621516	.389858806	0306011807
	:9.40526279	:1.93783469	-7.33621516	30	-3.610141194	7.536045502193	15	18	219.40526279	-0.93783469	:1.33621516	.389858806	5045502193
	:9.40526279	:1.93783469	-1.58523008	30	-8.051481189	6.342267443089	15	19	219.40526279	-0.93783469	:7.58523008	.948518811	2267443089
	:8.71779529	:1.74052812	-1.58523008	30	-8.051481189	2.066434897941	16	19	200.71779529	:9.74052812	:7.58523008	.948518811	5434897941
	:8.71779529	:1.74052812	:1.12067546	30	-2.782508899	6.430595077886	16	20	200.71779529	:9.74052812	:2.12067546	-.217491101	0595077886
	:4.83629077	9.76961406	:1.12067546	30	-2.782508899	0.599331566374	17	20	177.83629077	:1.76961406	:2.12067546	-.217491101	3331566374
	:4.83629077	9.76961406	:5.93389622	40	-0.418757416	9.262480110269	17	21	177.83629077	:1.76961406	1.93389622	:.581242584	2480110269
	7.21177916	:4.10029526	:5.93389622	40	-0.418757416	7.084511489003	18	21	151.21177916	9.10029526	1.93389622	:.581242584	4511489003
	7.21177916	:4.10029526	:7.57182651	80	-0.965205252	38.88922876299	18	22	151.21177916	9.10029526	19.57182651	-.034794748	3922876299
	4.63972851	8.50263378	:7.57182651	80	-0.965205252	2.030207411854	19	22	130.63972851	18.50263378	19.57182651	-.034794748	0207411854
	4.63972851	8.50263378	:6.93485362	220	0.725080017	6.354976543001	19	23	130.63972851	18.50263378	18.93485362	1.725080017	4976543001
	.920835878	:0.04189395	:6.93485362	260	0.725080017	3.907883124531	20	23	105.920835878	17.04189395	18.93485362	1.725080017	7883124531
	4.42710323	-6.95	26.475	80	29.37694913	.2383067193862	10	5	322.42710323	-192.05	357.475	20.37694913	1693280614
	2.69505242	-5.35	26.475	80	29.37694913	.4996503731152	9	5	335.69505242	-214.65	357.475	20.37694913	3496268848
	:9.49075842	-2.6	26.475	80	29.37694913	3.240062389064	8	5	343.49075842	-242.4	357.475	20.37694913	3937610936
	2.69505242	-5.35	26.175	80	29.71642364	.0292641327959	9	4	335.69505242	-214.65	367.175	13.71642364	7358672041
	:9.49075842	-2.6	26.175	80	29.71642364	.1041682392898	8	4	343.49075842	-242.4	367.175	13.71642364	3317607102
	1.04960415	-2.4	26.175	80	29.71642364	.0836903686894	7	3	353.04960415	-267.6	375.175	16.71642364	3096313106
	:9.49075842	-2.6	26.1	80	28.26856285	.1931985469817	8	3	343.49075842	-242.4	375.1	15.26856285	3014530183
	1.04960415	-2.4	26.1	80	28.26856285	.0386594941904	7	3	353.04960415	-267.6	375.1	15.26856285	3405058096
	:8.62991985	-11.15	26.1	80	28.26856285	8.098133043655	6	3	379.62991985	-288.85	375.1	15.26856285	3133043655
	1.04960415	-2.4	25.425	80	27.76932501	.0178115002132	7	2	353.04960415	-267.6	383.425	19.76932501	1884997868
	:8.62991985	-11.15	25.425	80	27.76932501	.7280177239106	6	2	379.62991985	-288.85	383.425	19.76932501	3822760894
	:8.62991985	-11.15	24.9	80	27.98115086	.5725236671716	6	1	379.62991985	-288.85	395.9	18.98115086	4763328284
	:2.09402147	-12.05	25.425	80	27.76932501	6.072087654831	5	2	393.09402147	-318.95	383.425	19.76932501	2087654831
	:2.09402147	-12.05	25.425	84	27.76932501	.9387726464769	5	1	393.09402147	-318.95	396.425	18.76932501	2273535231
	:2.09402147	-11.55	25.425	78	27.76932501	7.390348018966	4	1	403.09402147	-352.45	396.425	18.76932501	0348018966
	:0.70838082	-11.25	24.9	108	27.98115086	3.047190172048	3	1	409.70838082	-385.75	395.9	18.98115086	7190172048
	:9.14953509	-10.05	24.9	94	27.98115086	4.578141123842	2	1	417.14953509	-421.95	395.9	18.98115086	3141123842
	:3.38787274	-12.25"		440		4.991331285113	18		177.38787274	-82.75	0	0	1331285113
	:9.57736096	-11.95		154		3.358009897171	19		155.57736096	-78.05	0	0	3009897171

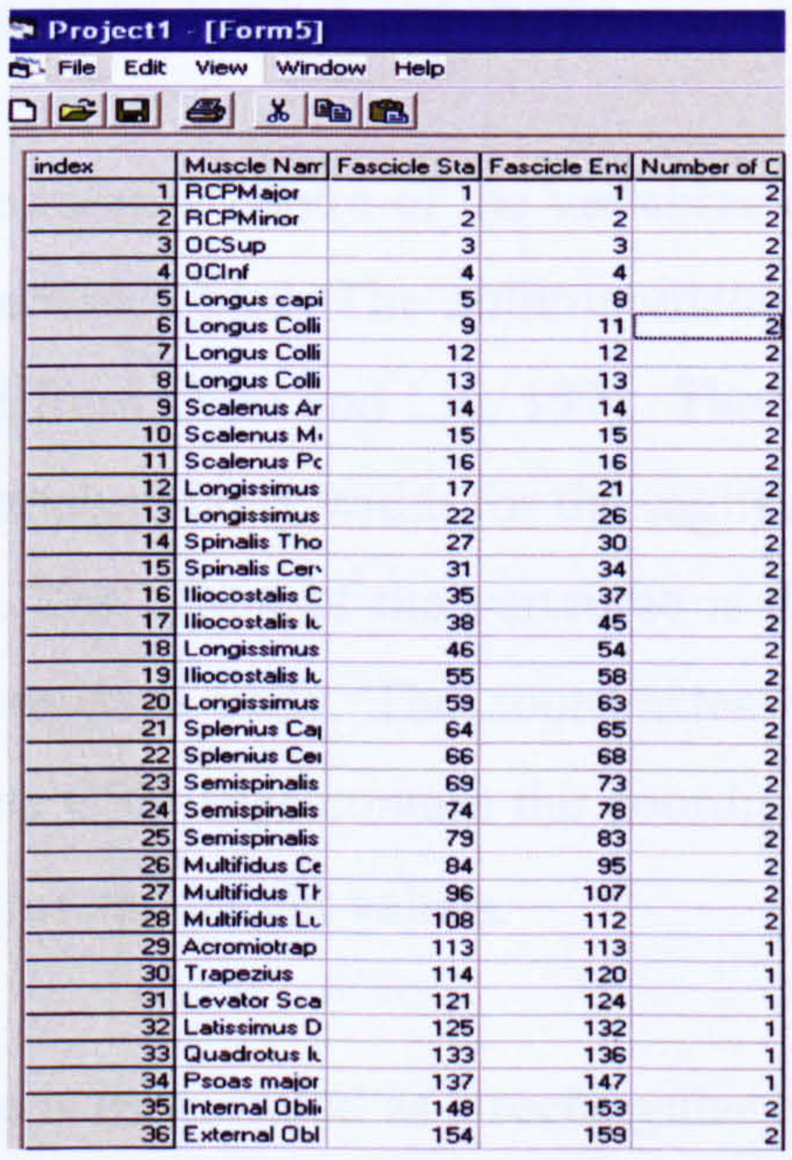
Figure 3- 7 Illustration of the Form 4 which displays and stores the data related to muscle forces.

Form4 is created for displaying the muscle forces (Figure 3.7). The column headings are recorded as follows, index, ΔX, ΔY values for the origin part of the muscle, ΔX, ΔY for the insertion part of the muscle, Origin Angle, Magnitude (N), Origin vertebra, Insertion Vertebra, X and Y of the coordinate Origin, X and Y coordinate of the Insertion, Insertion Angle of the muscle force.

Form5 is created to serve as an address book during the execution of the program at run time (Figure 3.8). The code retrieves the name of the muscles start and end index of the fascicles from this table. The connection number of the muscle is also retrieved from this form. The number of connection points can be either 2 or 1. If it is one, then it means, the muscle is connected to the outside limbs.

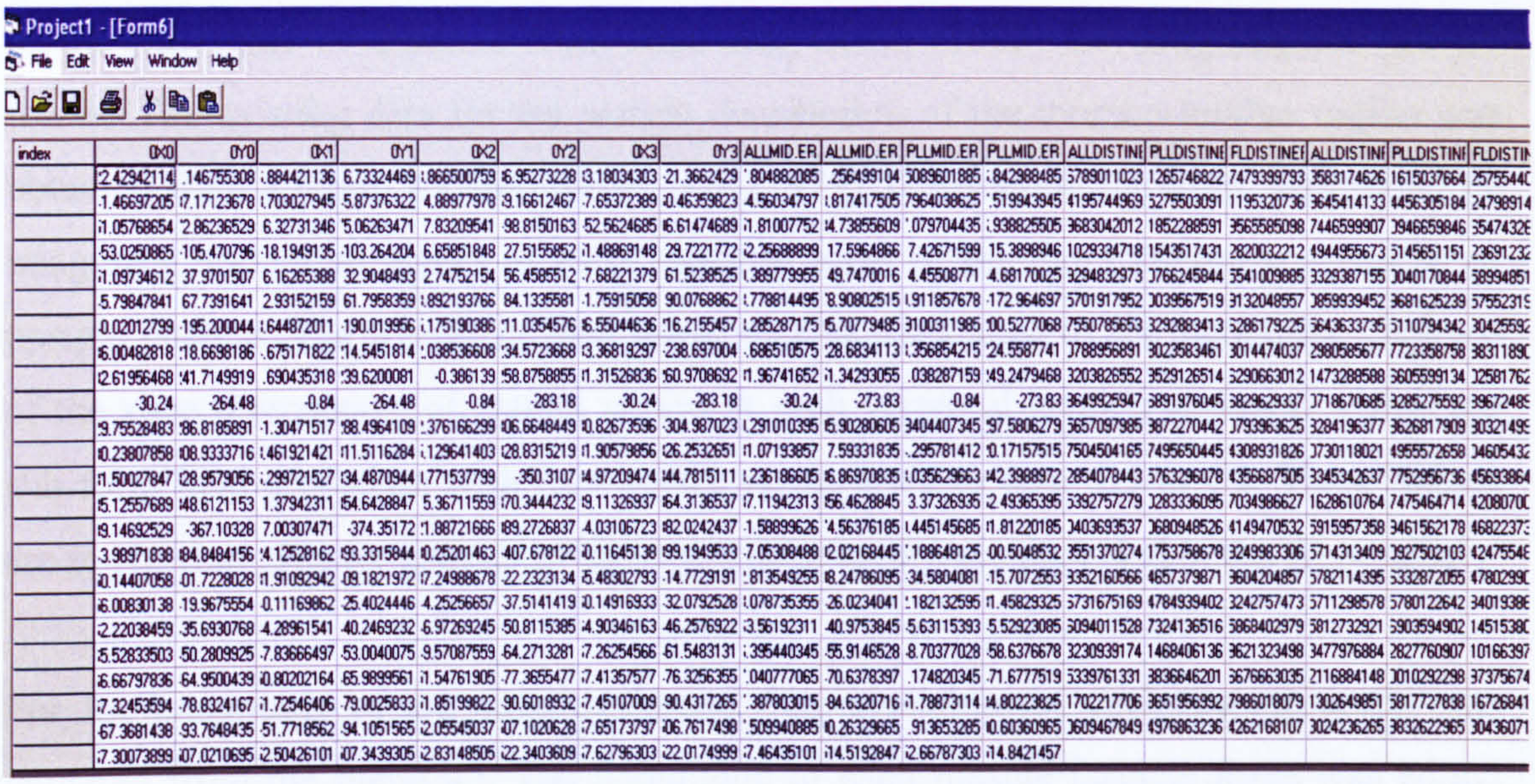
Form6 is created for ligament forces. The first 8 columns are assigned for the corner coordinates of each vertebra which are named as X0, Y0, X1, Y1, X2, Y2, X3, Y3. The next 2 columns are for the x and y coordinates of the connection points of the anterior longitudinal ligament which are named as ALLMidx, ALLMidy. The next 2 columns

are for the posterior longitudinal ligament in the erect posture, which are named as PLLMidx, PLLMidy. The next three columns are for the distance between the origin and insertion points for the anterior, posterior ligaments and ligamentum flavum in the erect posture which is named as ALL_Distance_Erect, PLL_Distance_Erect, LF_Distance_Erect. The next three columns are for the distance between the origin and insertion points of the anterior longitudinal ligament, posterior longitudinal ligament and ligamentum flavum of the specified posture which is to be inspected when the user selects the posture from the excel data files available which are named as ALL_Distance, PLL_Distance, LF_Distance. The strain values for these three ligaments are shown in the next three columns with the corresponding force values under the heading of ALL Strain, PLL_Strain, LF_Strain and ALL_Force, PLL_Force, LF_Force (Figure 3.9).



index	Muscle Nam	Fascicle Sta	Fascicle End	Number of C
1	RCPMajor	1	1	2
2	RCPMinor	2	2	2
3	OCSup	3	3	2
4	OCInf	4	4	2
5	Longus capi	5	8	2
6	Longus Colli	9	11	2
7	Longus Colli	12	12	2
8	Longus Colli	13	13	2
9	Scalenus Ar	14	14	2
10	Scalenus M	15	15	2
11	Scalenus Pc	16	16	2
12	Longissimus	17	21	2
13	Longissimus	22	26	2
14	Spinalis Tho	27	30	2
15	Spinalis Cer	31	34	2
16	Iliocostalis C	35	37	2
17	Iliocostalis lu	38	45	2
18	Longissimus	46	54	2
19	Iliocostalis lu	55	58	2
20	Longissimus	59	63	2
21	Splenius Cap	64	65	2
22	Splenius Cer	66	68	2
23	Semispinalis	69	73	2
24	Semispinalis	74	78	2
25	Semispinalis	79	83	2
26	Multifidus Ce	84	95	2
27	Multifidus Th	96	107	2
28	Multifidus Lu	108	112	2
29	Acromiotrap	113	113	1
30	Trapezius	114	120	1
31	Levator Sca	121	124	1
32	Latissimus D	125	132	1
33	Quadrotus lu	133	136	1
34	Psoas major	137	147	1
35	Internal Obli	148	153	2
36	External Obl	154	159	2

Figure 3- 8 Illustration of the Form5 which displays and stores the data related muscle fascicle start and end indexes



index	0X0	0Y0	0X1	0Y1	0X2	0Y2	0X3	0Y3	ALLMID.ER	ALLMID.ER	PLLMID.ER	PLLMID.ER	ALLDISTINE	PLLDISTINE	FLDISTINEI	ALLDISTINI	PLLDISTINI	FLDISTIN
	2.42942114	.146755308	.884421136	6.73324469	.866500759	6.95273228	3.18034303	-21.3662429	'.804882085	.256499104	3089601885	.842988485	5789011023	1265746822	7479399793	3583174626	1615037664	25755440
	-1.46697205	7.17123678	.703027945	-5.87376322	4.88977978	-9.16612467	-7.65372389	-0.46359823	-4.56034797	.817417505	7964038625	'.519943945	4195744969	5275503091	1195320736	3645414133	4456305184	24798914
	1.05768654	'2.86236529	6.32731346	'5.06263471	7.83209541	-98.8150163	-52.5624685	6.61474689	1.81007752	4.73855609	'.079704435	.938825505	3683042012	1852288591	3565585098	7446599907	3946659846	35474326
	-53.0250865	-105.470796	-18.1949135	-103.264204	6.65851848	27.5155852	1.48869148	29.7221772	-2.25688899	17.5964866	7.42671599	15.3898946	1029334718	1543517431	2820032212	4944955673	5145651151	23691232
	1.09734612	37.9701507	6.16265388	32.9048493	2.74752154	56.4585512	-7.68221379	61.5238525	.389779955	49.7470016	4.45508771	-4.68170025	3294832973	0766245844	3541009885	3329387155	3040170844	38994851
	-5.79847841	67.7391641	2.93152159	61.7958359	.892193766	84.1335581	-1.75915058	90.0768862	.778814495	'8.90802515	.911857678	-172.964697	5701917952	3039567519	3132048557	3859939452	3681625239	37552319
	-0.02012799	-195.200044	.644872011	-190.019956	.175190386	11.0354576	6.55044636	16.2155457	.285287175	5.70779485	3100311985	100.5277068	7550785653	3292883413	3286179225	3643633735	3110794342	30425932
	6.00482818	18.6698186	-.675171822	14.5451814	.038536608	34.5723668	3.36819297	-238.697004	-.686510575	28.6834113	.356854215	24.5587741	0788956891	3023583461	3014474037	2980585677	7723358758	38311890
	2.61956468	41.7149919	.690435318	39.6200081	-0.386139	58.8758855	1.31526836	60.9708692	1.96741652	1.34293055	.038287159	49.2479468	3203826552	3529126514	3290663012	1473288588	3605599134	32581762
	-30.24	-264.48	-0.84	-264.48	-0.84	-283.18	-30.24	-283.18	-30.24	-273.83	-0.84	-273.83	3649925947	3891976045	3829629337	0718670685	3285275592	39672485
	9.75528483	86.8185891	-1.30471517	88.4964109	.376166299	06.6648449	0.82673596	-304.987023	.291010395	5.90280605	3404407345	97.5806279	3657097985	3872270442	0793963625	3284196377	3626817909	30321495
	0.23807858	08.9333716	.461921421	11.5116284	.129641403	28.8315219	1.90579856	26.2532651	1.07193857	7.59331835	-.295781412	0.17157515	7504504165	7495650445	4308931826	0730118021	4955572658	34605432
	1.50027847	28.9579056	.299721527	34.4870944	.771537799	-350.3107	4.97209474	44.7815111	.236186605	6.86970835	.035629663	42.3988972	2854078443	5763296078	4356687505	3345342637	7752956736	45693864
	5.12557689	48.6121153	1.37942311	54.6428847	5.36711559	70.3444232	9.11326937	64.3136537	7.11942313	56.4628845	3.37326935	-2.49365395	5392757279	3283336095	7034986627	1628610764	7475464714	42080700
	9.14692529	-367.10328	7.00307471	-374.35172	1.88721666	89.2726837	4.03106723	82.0242437	-1.58899626	4.56376185	.445145685	11.81220185	3403693537	3680948526	4149470532	3915957358	3461562178	46822373
	3.98971838	84.8484156	4.12528162	93.3315844	0.25201463	407.678122	0.11645138	99.1949533	-7.05308488	2.02168445	'.188648125	00.5048532	3551370274	1753758678	3249983306	5714313409	3927502103	42475548
	0.14407058	01.7228028	1.91092942	09.1821972	7.24988678	22.2323134	5.48302793	14.7729191	.813549255	8.24786095	34.5804081	15.7072553	3352160566	4657379871	3604204857	5782114395	5332872055	47802990
	6.00830138	19.9675554	0.11169862	25.4024446	4.25256657	37.5141419	0.14916933	32.0792528	.078735355	26.0234041	.182132595	1.45829325	5731675169	4784939402	3242757473	5711298578	5780122642	34019386
	2.22038459	35.6930768	4.28961541	40.2469232	6.97269245	50.8115385	4.90346163	46.2576922	3.56192311	40.9753845	5.63115393	5.52923085	3094011528	7324136516	3868402979	3812732921	5903594902	14515380
	5.52833503	50.2809925	7.83666497	53.0040075	9.57087559	64.2713281	7.26254566	61.5483131	.395440345	55.9146528	8.70377028	58.6376678	3230939174	1468406136	3621323498	3477976884	2827760907	10166397
	6.66797836	64.9500439	0.80202164	65.9899561	1.54761905	77.3655477	7.41357577	76.3256355	'.040777065	70.6378397	.174820345	71.6777519	5339761331	3836646201	3676663035	2116884148	3010292298	37375674
	7.32453594	78.8324167	1.72546406	79.0025833	1.85199822	90.6018932	7.45107009	90.4317265	'.387803015	84.6320716	1.78873114	4.80223825	1702217706	3651956992	7986018079	1302649851	5817727838	16726841
	67.3681438	93.7648435	51.7718562	94.1051565	2.05545037	07.1020628	7.65173797	06.7617498	'.509940885	0.26329665	.913653285	0.60360965	3609467849	4976863236	4262168107	3024236265	3832622965	30436071
	7.30073899	07.0210695	2.50426101	07.3439305	2.83148505	22.3403609	7.62796303	22.0174999	7.46435101	14.5192847	2.66787303	14.8421457						

Figure 3- 9 Illustration of the Form 6 which displays and stores the data related to ligament forces

3.2.2 Assigning of values to type Vertebrae

X and Y coordinates of the inferior centre of the vertebrae are recorded into the Excel CSV (comma separated variable) files. The anthropometric data for the thoracic and lumbar region are obtained from Orne and Liu, 1971. The diameter obtained from the paper is converted to the vertebral body width for the sagittal view and these values are recorded into the csv files. The origin of the vertebrae is defined as the centre of the inferior end plate of the vertebral body. The coordinates of these points were taken from Farnsworth, 2007. The CSV files contain the coordinates, relative orientation of each 24 vertebrae, their radius and height values.

In the model each vertebrae is represented as a rectangular box and drawn by using the coordinates of the four corners. The joint coordinates are located as the superior surface of each vertebra and they are calculated by using the corner coordinates of each vertebra. The drawing of the spine is explained in a separate section later in this chapter.

3.2.3 Assigning of values to type Force

For assigning the value of each force acting on the spine the magnitude of the force is hard coded. The type of the forces acting on the spine can be grouped as gravity forces acting on the spine, muscle force and ligament forces. The weight distribution pattern

of the full spine is obtained from Acar and Grilli, (2002) for assigning the gravity forces. The existing data for the weight distribution of the thoraco-lumbar region was obtained from a report by Takashima *et al.*(1979), considering the trunk was sliced by imaginary horizontal planes at each vertebral level of the thoraco-lumbar spine in an upright posture. The weight of each trunk slice was assumed to act though the centroid of the slice. Percentage of weight values at each vertebral level is assigned within the sub-form load procedure with their offset values starting from L5 to C1. These values are in Newton. The magnitude of the percentage values are provided in the Appendix1.

For the magnitude of the muscles forces, data available for each muscle group was gathered from the literature. The magnitude of each muscle fascicle force was edited into the code. The detailed information about the muscle forces are provided in chapter 4. For ligament forces, the force calculation produced by the ligaments is different from the muscles.

For the angle of the force, the direction for the gravity forces is assigned as 270 degrees from the horizontal. For muscles it is the direction of line connecting the origin and insertion points. For the muscles which have only one connection point, the angle of the muscle is incorporated into the code with data available from literature. For ligaments, the orientation is the angle of the line connecting the origin and the insertion.

All the forces acting on the spine is projected into its components with respect to the coordinate system. In this model a coordinate system is defined with respect to the reference line, the line which connects the bottom surface centre point of the L5 lumbar vertebra and the superior centre of the C1 cervical vertebra forms the Y axis and the line perpendicular to this is X axis (Figure 3.1). The force component parallel to x axis is named as Fr and the force component parallel to y axis is named as Fh.

The x and y coordinates of the forces for body weights are calculated by taking into account the eccentricity values provided in the paper of Acar and Grilli, (2002). The eccentricity values are added to the geometric centre of the vertebrae to calculate coordinates of the application point of the gravity forces. The application points of the muscle forces are calculated by using the information available in literature. The application point for a muscle is calculated as the attachment point of the muscle. The

detailed information about the calculation of coordinates for muscle forces and the application point of ligament forces to the vertebrae are provided in Chapter 4.

The distance of each force applied on spine plays a vital role in thrustline theory. The distance of the force along the Y axis is calculated and the distance along the X axis is calculated and recorded as relative y and relative x distances.

In addition to gravity forces, muscle forces and ligament forces, there is the external force acting on the spine during lifting activity. In order to provide flexibility for the magnitude and orientation of each external force, these forces are not embedded in the code but designed to be interactive depending on the need of the user and can be added while running the code.

3.2.4 Inclusion of external forces

There are two ways of introducing an external force to the system:

The first is by clicking the mouse; it is possible to add external forces to the system. There are two figures used for adding the force, which are made invisible at the start of the code. When the user presses the add force button, the first shape, which is a circle, becomes visible. With the first click the end point of the x and y coordinates of the force is fixed. At this stage, the user is expected to determine the angle and the magnitude of the force acting on the spine by clicking the mouse. The second shape is used for the purpose of determining the direction and the magnitude of the force to be added. As a result in order to add a new force, two clicks are required: First, to specify the position; second to specify the magnitude and the angle. In order to exclude the force, remove force button is clicked. In the code initially, all the Boolean variables are set to false as the program starts running to show there is no external forces applied to the spine.

The other method of introducing the force is manually entering the values in the program. After executing the code with only the gravity forces acting on spine, the user of the programme can go to Form2 on the multiple document interface of the code and

enter the magnitude, direction and application point of the force applied to spine externally.

3.2.5 Loading of Posture Data into the Code

When the user, clicks the open file button, function load data is called in the code. The program line reads the command, *CommonDialog1.ShowOpen* in order to select a file with an extension of CSV. Depending on the selected file, the posture data which is necessary for drawing the spine is loaded to the program.

A sample of the input values is supplied in the Appendix 2 for a fully flexed posture of the one of the subjects.

The arrays are filled with by assigning values to the following parameters:

```
Verts(n).xc, Verts(n).yc, Verts(n).Relative_Angle, Verts(n).Radius, Verts(n).Height
```

Verts(n).xc and Verts(n).yc represent inferior centres of the vertebrae. Verts(n). R is for the width of each vertebra, and Verts(n).Height is the height of each vertebrae. Alpha is the relative angle for each vertebra (Figure 3.10). The angles are the relative angles of vertebrae with respect to the vertebrae below. In order to calculate the global angle it is necessary to add all the angles consecutively.

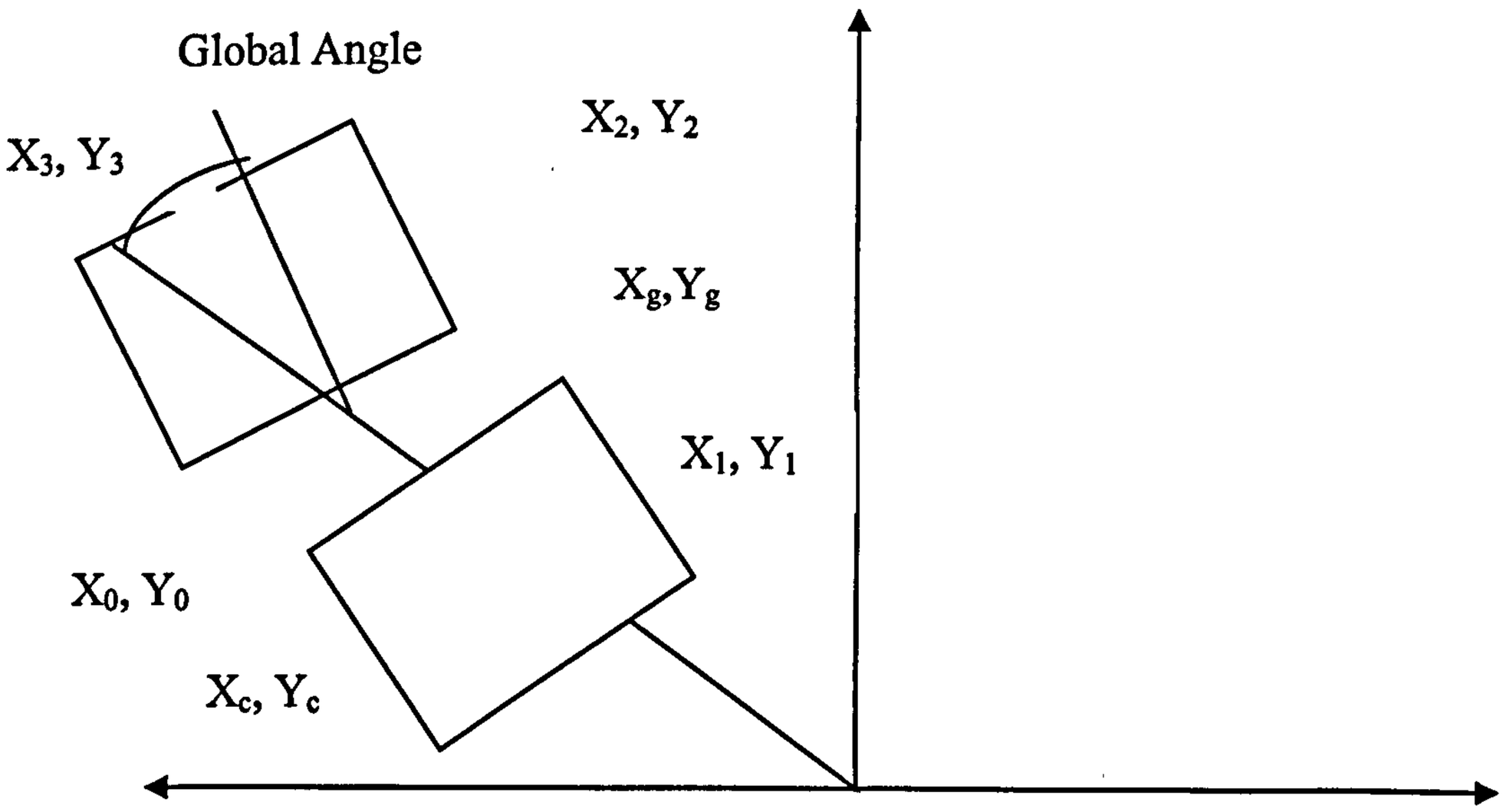


Figure 3- 10 Vertebrae with global angle

3.2.6 Calculation of coordinates for vertebrae corners, geometric and mass centres

To form the anterior posterior shape of each vertebra and the full shape of the spine, the corner coordinates of each vertebra is calculated. Figure 3.11 represents the four corners of the vertebrae. From the input file, the coordinates of the corners for each vertebra are calculated.

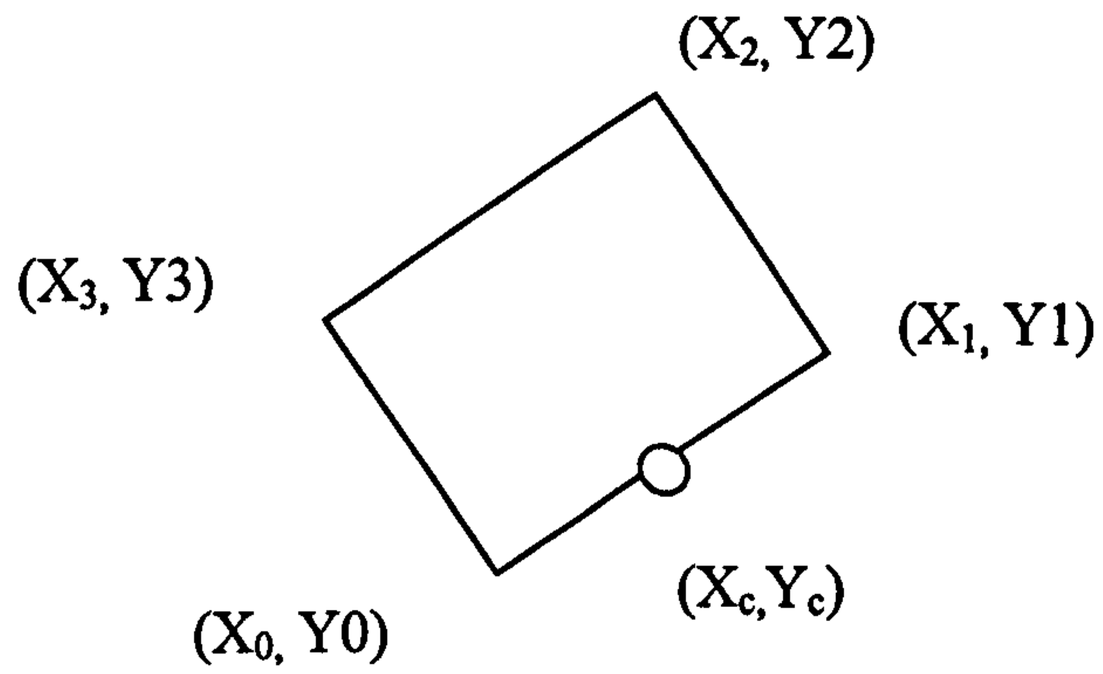


Figure 3- 11 Representation of Vertebrae with the corners

Formulas for calculating the corners of the vertebrae in the anterior posterior view

```
X(0) = Vertebra.Xcentre - Vertebra.Radius * Cos(Global_Angle)          (1)
Y(0) = Vertebra.Ycentre + Vertebra.Radius * Sin(Global_Angle)          (2)
X(1) = Vertabra.Xcentre + Vertebra.Radius * Cos(Global_Angle)          (3)
Y(1) = Vertabra.Ycentre - Vertabra.Radius * Sin(Global_Angle)          (4)
X(2) =Vertebra.X(1) - Vertabra.Height * Sin(Global_Angle)              (5)
Y(2) =Vertabra.Y(1) - Vertabra.Height * Cos(Global_Angle)              (6)
X(3) = Vertabra.X(2) - Vertabra.Radius * 2 * Cos(Global_Angle)         (7)
Y(3) = Vertabra.Y(2) + Vertabra.Radius * 2 * Sin(Global_Angle)         (8)
```

With the offset values already assigned while defining the constants in the code, the following formulation is used for calculating coordinates of centre of gravity.

```
Vert.xG = Vert.xc - VertHeight / 2 * Sin(Global_Angle) - VertX_Offset *
Cos(RotationAngle)
Verts.yG = Vert..yc - Vert.Height / 2 * Cos(Global_Angle) + VertX_Offset *
Sin(RotationAngle)
```

Where x centre and y centre are the inferior centre coordinates of each vertebra.

In order to calculate the joint centre points of each vertebra the superior corner coordinates are added and divided into 2. The y coordinate of the top joint is multiplied by minus value before recorded.

Formulation for calculating the joint centres:

```
Verts(Index).xj = (Verts(Index).r.X(3) + Verts(Index).r.X(2)) / 2
Verts(Index).yj = -(Verts(Index).r.Y(3) + Verts(Index).r.Y(2)) / 2
```

3.2.7 Projection of forces into the components

The subroutine Form2.UpdateForces calculates the h and r components of the forces with respect to the reference line. The reference angle is defined as the angle between the reference line and the horizontal axis. Initially, the reference line angle is defined as zero. In a posture with the reference line angle aligned with the horizontal, reference line angle is zero. For the upright postures, the reference line angle makes an angle of 90 degrees with the horizontal.

This is represented in the following Figure 3.12:

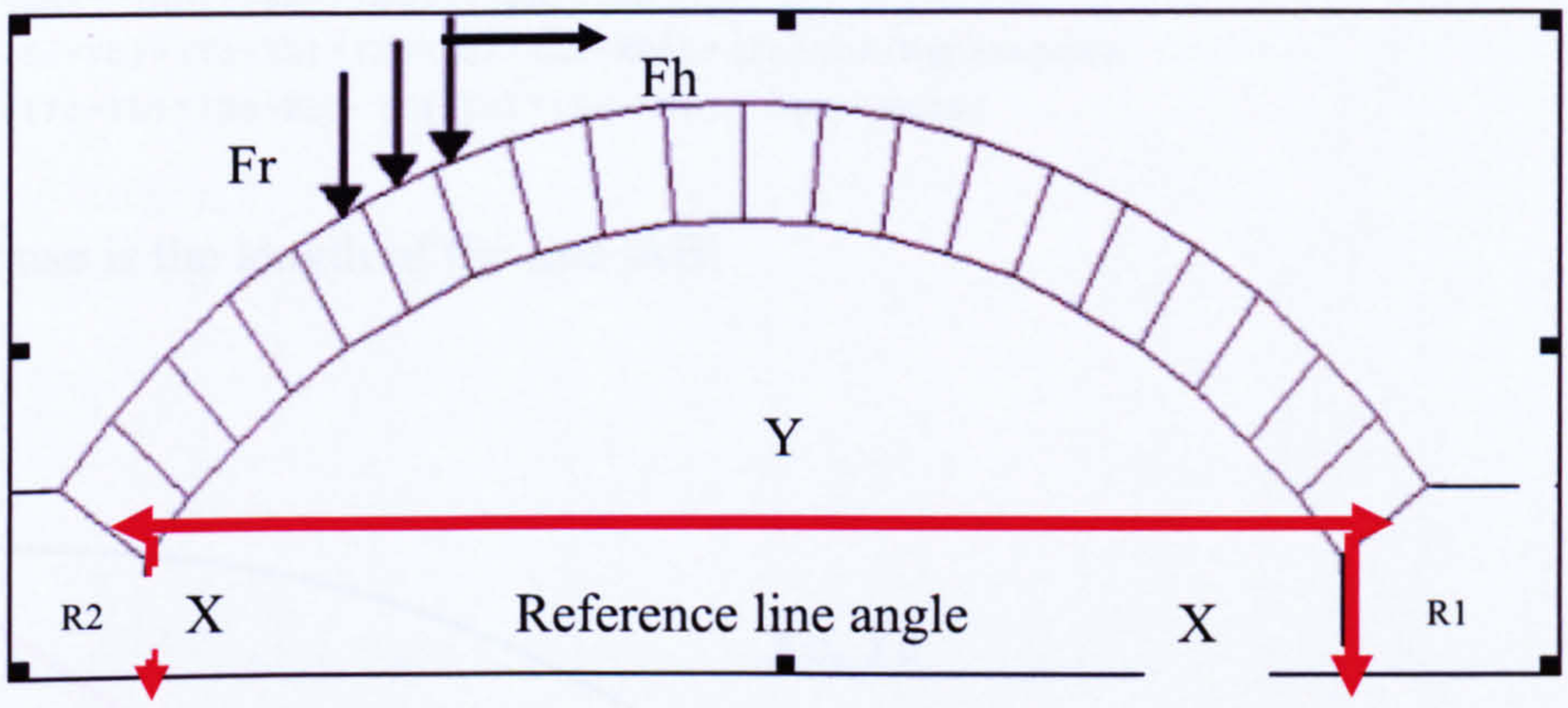


Figure 3- 12 Fully Flexed posture reference line angle equal to 0°.

Reference line angle in this posture is 0. The force angle is 270 degrees. F component of force parallel to the reference line is called Fh and perpendicular force component to reference line is called Fr

Fr is assigned to column 10 of Form2 with the following formula

```
Fr = Force magnitude* Sin (Reference Line Angle -Force Angle)
```

Fh is assigned to column 11 of Form 2 with the following formula

```
Fh= Force magnitude*Cos (Reference Line Angle -Force Angle)
```

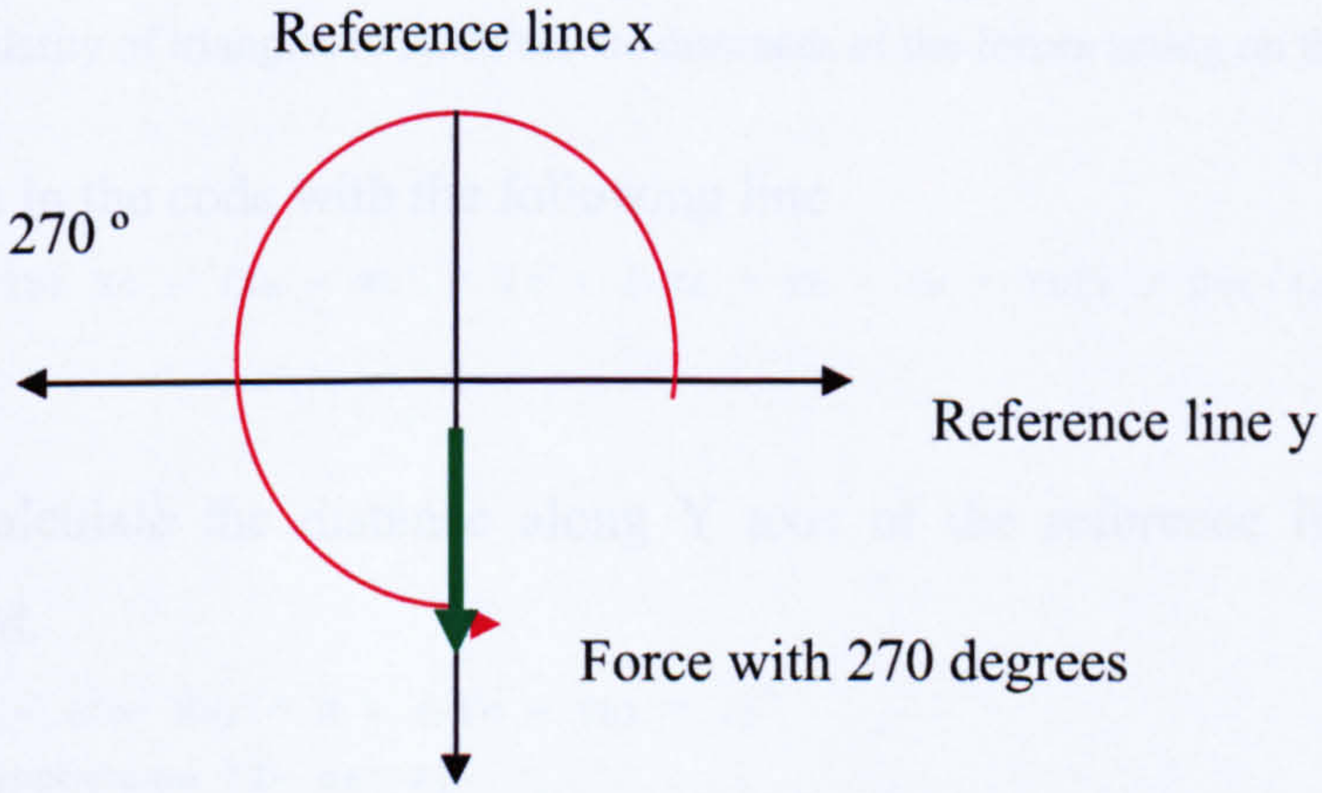


Figure 3- 13 Force acting with an angle of 270 degree

```
Fr=Force magnitude* Sin (0-270)          Fh=Force magnitude*Cos (0-270)
Fr=Force magnitude.                              Fh=0
```

In order to calculate the vertical distances along the X and Y axis of the reference line, similarity between the triangles in the figure below is used.

```
|EB|/|BD|=|EF|/|AD|
|EF|=|AD|*|EB|/|BD|
|CF|=|CE|-|EF|
|CF|=|CE|- |AD|*|EB|/|BD|
dx: It is the vertical distance of a force along the X axis of the reference line
and it can be expressed as ;
dx=|CF|*|DB|/|AB|
dx=[|CE|- |AD|*|EB|/|BD|]*|DB|/|AB|
dx=[(Yc-Yb)-(Ya-Yb)*(Xc-Xb)/(Xa-Xb)]*(Xa-Xb)/Hypotenuse
dx =[(Yc-Yb)*(Xa-Xb)-(Ya-Yb)*(Xc-Xb)]/ Hypotenuse
```

Hypotenuse is the length of the line |AB|

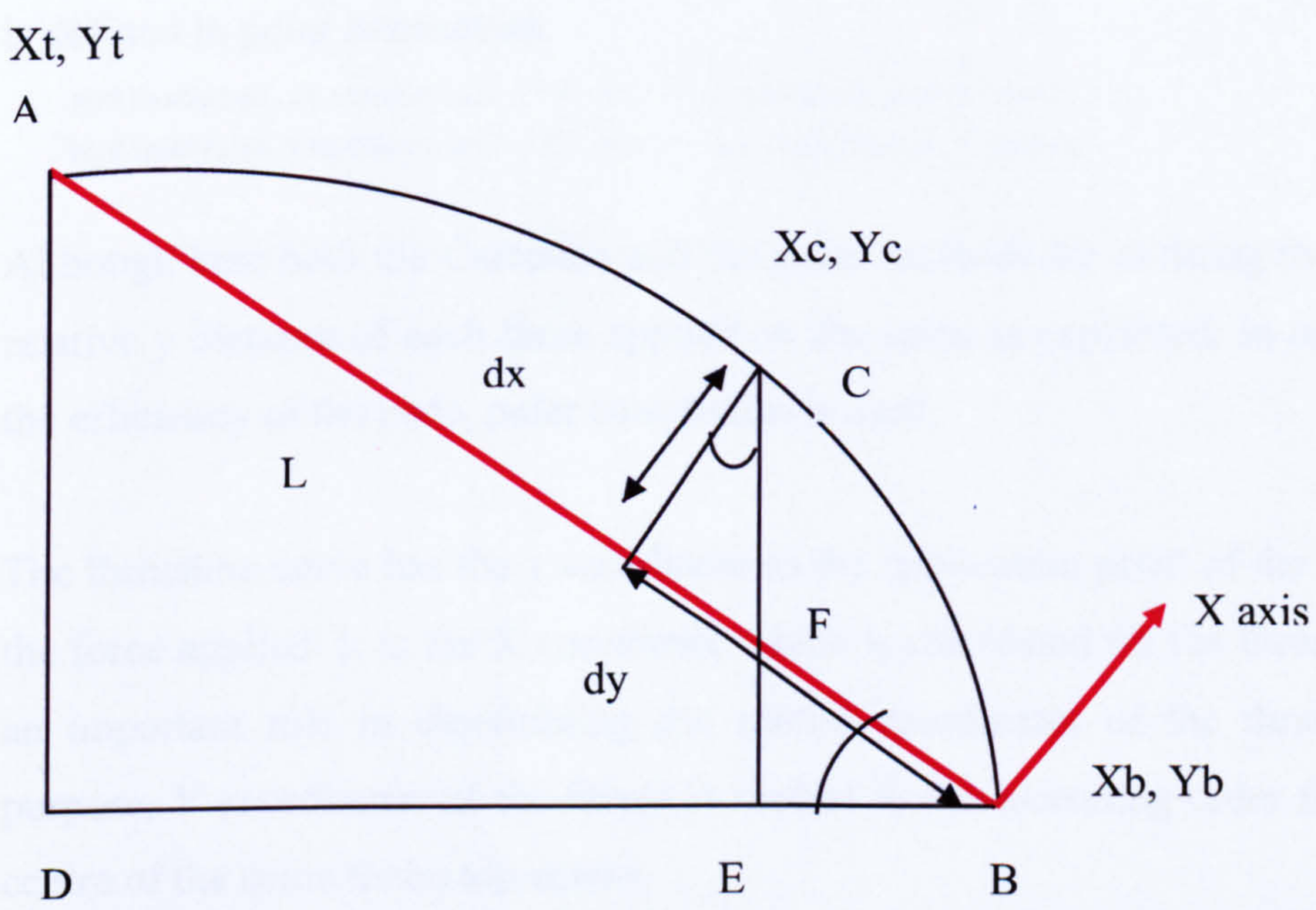


Figure 3-14 Similarity of triangles to calculate the distances of the forces acting on the spine.

This is written in the code with the following line

```
dx =  -((Ya - Yb) Xc + (Xa - Xb) * Yc + (-Xa * Yb + Xa * Yb)) / Sqr((Xa - Xb) ^ 2 + (Ya
- Yb) ^ 2)
```

In order to calculate the distance along Y axis of the reference line the following formula is used.

```
Hypotenuse = (Xc- Xa) ^ 2 + (-Yc - Yb) ^ 2)
dY = Sqr(Hypotenuse ^2- dx^ 2)
```

The 6th and 7th columns are assigned to relative X and Y distances of the forces from the inferior central point of L5 along the axis connecting the superior central point of C1 and inferior central points of the spine in Form2.

The second way to calculate the distance of each force with respect to the axis of reference line is to find the distance of each force from the bottom coordinates of the spine is using polar coordinate system. For this reason (r, θ) is defined

R = ((X coordinate of inferior surface of the L5 – X coordinate of the force) ^ 2 + (Y coordinate of inferior surface of the L5 centre + Y coordinate of the force) ^ 2) ^1/2

R is equivalent to the length of line |CB| connecting points C and B.

```
Angle(θ) = Find_Angle(Xb, Xcoordinateof the force, YB, Ycoordinateof the force)
```

Find_Angle function is defined to calculate the angle of line CB.

With the command lines below the x and y distances relative to the inferior centre at L5 is defined in polar convention.

```
MSFlexGrid1.TextMatrix(i, 6) = r * Sin(AxisAngle - ang1)
MSFlexGrid1.TextMatrix(i, 7) = r * Cos(AxisAngle - ang1)
```

Although here both the Cartesian and the polar methods for defining the relative x and relative y distance of each force applied on the spine is explained. In order to improve the efficiency of the code, polar convention is used.

The thrustline curve has the y coordinate as the application point of the y coordinate of the force applied. It is the X coordinate which is calculated for the thrustline and plays an important role in determining the spatial coordinates of the thrustline. For this purpose, Y coordinates of the forces is ranked in the ascending order from the bottom centre of the spine to the top centre.

```
Form2.MSFlexGrid1.Col = 7 (Gives the coloumn number for the relative y distance)
Form2.MSFlexGrid1.Sort = flexSortNumericAscending
```

FlexSortNumericAscending is used to convert the strings into numbers. The command lines above are used to sort the distances with respect to the ascending distance from the bottom point of the spine. This process is vital when the muscle and ligament forces are added in addition to the gravity forces. With only gravity forces they are already in the in the ascending order, but with the addition of other forces, the order of the forces is changed and they need to be arranged with respect to their distance from the bottom of the spine.

With the chosen posture data, the coordinate values of the inferior centre of L5 and superior centre of C1 is calculated after the corner coordinates of each vertebra is calculated, hence, the angle of reference line is determined. In order to avoid from any zone related mistakes, the following algorithm is used and the formulas corresponding are used to calculate the angle of the axis line.

```
If x2 > x1 Then
        If y2 > y1 Then '    ZONE 1 (+,+)    (Fig.4.14)
        FindAngle = -Atn((y2 - y1) / (x2 - x1)
        Else If  y2 < y1 Then 'ZONE 4 (+,-) (Fig 4.14)
        FindAngle = Atn((y1 - y2) / (x2 - x1))
        Else
        FindAngle = 0         (ON THE +X AXIS )      (Fig 4.14)
End If
Else   If x2 < x1 Then
          If y2 > y1 Then 'ZONE 2 (-,+)          (Fig 4.14)
          FindAngle = Atn((y2 - y1) / (x1 - x2)) +   π
          ElseIf y2 < y1 Then 'ZONE 3 (-,-)      (Fig 4.14)
          FindAngle = Atn((x1 - x2) / (y1 - y2)) + π / 2
Else
FindAngle = π    ' ON THE -X AXIS           (Fig 4.14)
End If
Else
If y2 < y1 Then 'ON THE -Y AXIS             (Fig 4.14)
FindAngle = π / 2
ElseIf y2 > y1 Then 'ON THE +Y AXIS     (Fig 4.14)
FindAngle = - π / 2
Else     ' ON THE ORIGIN (0,0)                    (Fig 4.14)
FindAngle = 0
```

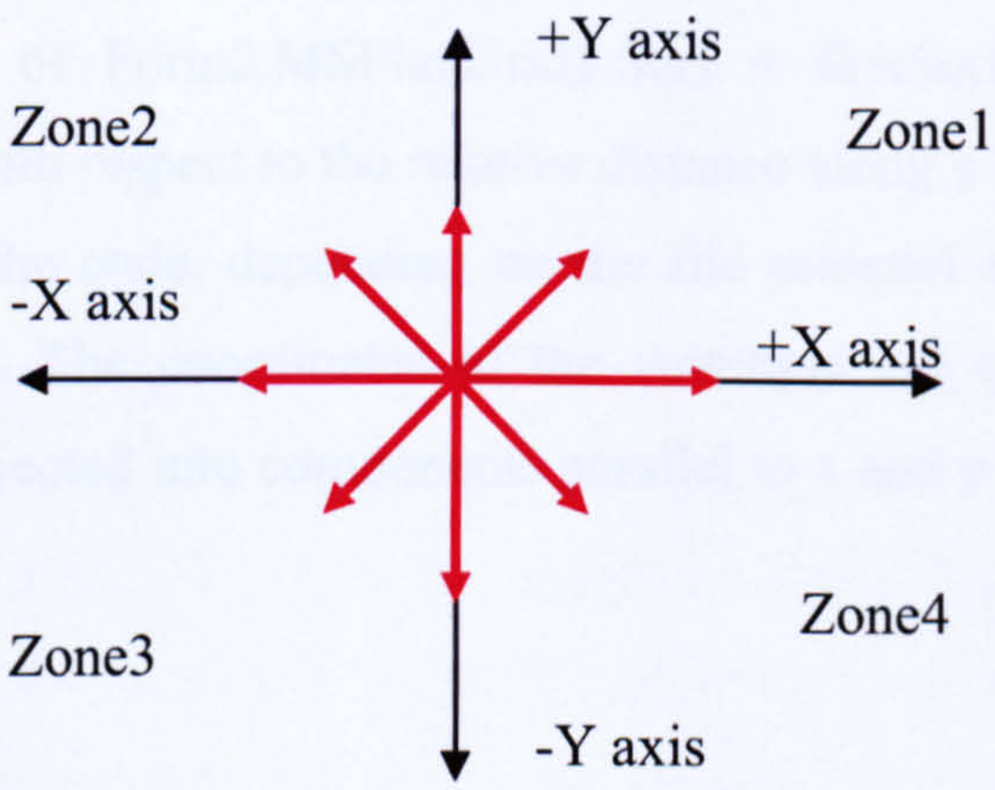


Figure 3- 15 Illustration of the axis and zones

The coordinates of all the weights are calculated and recorded. The weight of head has a special condition. The offset values for weight of head are:
x=0.45 and y=4.55 in global coordinates.

The magnitude of the vector of the head offset values is:

```
h = Sqr(HeadXOffset ^ 2 + HeadYOffset ^ 2)
h= (0.45^2+4.55^2)^0.5
h=4.57 cm
```

The angle that position of head makes with the vertical line in the global coordinate system is determined by the formula:

Head_X_Offset/ Head_Y_Offset = 0.45/4.55=5.66 degrees =0.098rad

Global coordinates of the head is calculated by the following command lines:

```
Relative_y = h * Sin(AxisAngle + headangle)=4.547
Relative_x = h * Cos(AxisAngle + headangle)=-0.48
X = TopX + Relative_x
Y = TopY - Relative_y
```

The coordinates (X, Y) of the head are the coordinates of the head for a chosen posture. With the geometric data obtained the force data needs to be updated. As the orientation of the spine is now known, the force components parallel and perpendicular to the axis line are calculated for each force acting on the spine. For example, with a reference line angle of 90.47 degrees and with the force angle of 270 degrees with body weights, the following force components are calculated.

```
Fr = Force magnitude* Sin (Reference line Angle -Force Angle)
Fh=18*sin (90.47-270)
Fr=-0.15 N.
Fh= Force magnitude*Cos (Reference line Angle -Force Angle)
FY=18*cos(90.47-270)
FY= -17.99 N
```

With the command of Form2.MSFlexGrid1.Sort = flexSortNumericAscending the forces are arranged with respect to the relative distance along y axis.

Up to this stage, in the code, depending on the file selected all the geometric data is filled into the forms. The coordinates of the vertebrae are calculated and the body weight forces are projected into components parallel to x and y axis along the reference line.

Table 3- 1 A sample representation of the force components with their relative x and relative y values for a posture of reference line angle of 90.47 degrees.

Force Number	Fx	Fy	Relative X	Relative Y
1	-0.15	-18	-10.1	12.74
2	-0.21	-25	-21.46	48.22
3	-0.16	-19	-24.33	80.67
4	-0.16	-19	-23.71	110.93
5	-0.17	-21	-18.89	141.53
6	-0.16	-19	-12.31	170.05
7	-0.15	-18	-5.41	196.8
8	-0.15	-18	0.15	219.45
9	-0.12	-14	6.47	243.11
10	-0.08	-10	9.24	266.22
11	-0.1	-12	10.47	289.52
12	-0.09	-11	10.4	312.32
13	-0.08	-10	10.76	333.9
14	-0.26	-31	13.04	354.1
15	-0.22	-27	10.-55	373.87
16	-0.26	-31	5.17	392.9
17	-0.22	-27	1.31	410.48
18	-0.03	-3.92	-4.22	427.14
19	-0.02	-2.22	-6.76	442.92
20	-0.02	-2.64	-7.36	457.38
21	-0.02	-2.01	-6.32	471.97
22	-0.01	-1.53	-4.32	485.31
23	-0.01	-1.53	-1.95	496.8
24	-0.01	-1.53	0.51	515.65
25	-0.28	-34.33	0	527.65

3.2.8 Calculation of Reaction Forces

The reaction forces at the superior centre of the C1 are named as H2 and R2. H2 is the force component parallel to reference line which is called the compression force and R2 is the force perpendicular to the reference line which is called the shear force.

The access to the force information is possible by a function called FindForce. All the force components parallel to the reference line are named as Fy and perpendicular to the reference line are named as Fx .H2.Fx is always 0 by definition as H2 is parallel to the reference line and H2.Fx is the component perpendicular to the reference line. H2.Fy is the component parallel to the reference line. It is the value to be calculated. H2 relative X value is assigned to 0 as it is already on the reference line. H2 relative y value is assigned to the length of the reference line. It is along the y axis with the relative distance of equivalent to arch length.

In a typical moment calculation: $M = \vec{r} X \vec{F}$

$\vec{r} = (r_x, r_y)$ and $\vec{F} = (F_x, F_y)$

$$M = r_x * f_y - f_x * r_y$$

The contribution of each force to the moment value around the L5/S1 region is calculated. After running the program line by line starting from the first force to the final force acting on the spine are added to find out:

TotalFy values: Paralel to the reference line

TotalFx values: Perpendicular the reference line

The final force value is the weight of the head which has the index number of 25 when the code is run for the body weights only. H2.magnitude is equalised to y component of the 25^{th} force. H2.Fy is equalised to H2.magnitude. The magnitude of R2 is equalised to the horizontal x component of the head weight.

The angle for the force H2 is determined by the equation:

```
H2.angle = Reference Line Angle * 180 / π + (Sgn(H2.Magnitude) - 1) * 90
For example with a reference line angle of 1.579
H2.angle=1.579*180/3.14+ (-1-1)*90
H2.angle=-89.52°
```

By applying the equations of equilibrium

$$\sum Fx_i = 0 \quad \sum Fy_i = 0 \quad \sum M_i = 0$$

With the Total Fx, Total Fy and Total moment values acting on the spine

On the Y axis

$$H1 + H2 + \sum Fy = 0$$

H2 value is already assumed. H1 value is calculated. The angle for the reaction force H1 is calculated by the following equation.

```
H1.angle = AxisAngle * 180 / π + (Sgn (H1.Magnitude) - 1) * 90
H1.Angle=1.579*180/ π + (1-1)*90
H1.Angle=90.47
```

3.2.9 Drawing of Force H1

To draw any force vector, start and initial coordinates of a force is calculated. The first coordinate for H1 is inferior centre of the spine. The end point for the H1 is calculated as follows:

```
x2 = x1 + |(H1.Magnitude) * Cos(H1.angle)|
y2 = y1 - |(H1.Magnitude) * Sin(H1.angle)|
```

Where x1 and y1 are the start coordinates of H1 which are inferior centre point of L5. X2 and y2 are the final coordinates of the force vector.

3.2.10 Calculation of reaction force R2

The horizontal component of the head which is R2.fx also causes a moment; it is also included in the calculation.

$M = -r2_x * D \vec{k}$, $\sum Mz = 0$,

$-r2*D + \sum Mbybodyweight = 0$ $\qquad$ $r2 = \sum Mbybodyweight / D$

Where; r2 is the horizontal component of the head force and D is the distance from the inferior central point of L5 to superior central point of C1.

3.2.11 Calculation of R1

R1+R2+FX=0

$$Xi = X(i-1) + \left(R1 + \sum_{k=1}^{i-1} Frk\right) / \left(H1 + \sum_{k=1}^{i-1} Fhk\right)$$

Solving out the equation, R1 is calculated as:

R1=-(R2+FX)

3.2.12 Drawing of force R1

Start point is the inferior central point of L5 and End Point is calculated with the following equations.

```
X2 = x1 + R1 * Cos(R1.angle )
Y2 = y1 - R1 * Sin(R1. angle )
```

Where X2 and Y2 are the end point of force vector R1

3.2.13 Drawing of force R2

Start Point is the superior central point of C1 and end point is calculated as :

```
X2 = x1 + R2 * Cos (R2.angle)
Y2= -y2 +R2*sin (R2.angle)
```

3.2.14 Drawing of force H2

Start point is the lower end coordinates of L5 and End Point is calculated with the following equations.

End Point coordinates are

```
x2 = x1 + H2 * Cos(H2.angle)
y2= -y2-H2*sin(H2.angle)
```

3.2.15 Calculation of Thrustline coordinates

In order to calculate the coordinates of the thrustline, the slope of the first segment of the thrustline is calculated.

$\mathrm{Tan}(\theta) = \mathrm{R1}/\mathrm{H1}$

First x coordinate is calculated by the following equation

$$x1 = R1 / H1 * dy1$$

dy1 is calculated as

dy1=| Y coordinate of inferior centre point of L5–Y coordinate of the 1st force applied|

The other coordinates of the thrustline are calculated with the following method.

$$Slope = \left(R1 + \sum_{k=1}^{i-1} Frk\right) / \left(H1 + \sum_{k=1}^{i-1} Fhk\right)$$

i is the number of the forces acting on the spine.

Fr is the force components acting perpendicular to the reference line

Fh is the force components acting parallel to the reference line

New divisor for the angle is calculated by:

```
hrem = hrem + Fy .component of each force
rrem = rrem  +  Fx. component of each force
```

hrem and rrem are the remaining force values to be added.

The code checks for the repeated force values having the same relative y coordinate and add them to count as one force. The procedure is repeated for each force value acting on the spine. The x coordinate of the thrustline coincides with the top coordinate of the structure. To shift the x coordinates of the thrustline while y values remain the same, the following formula is used:

$$x_i' = x_i + (-Xn / Yn) * y_i$$

Where *Xn* and *Yn* is the final top coordinates of the thrustline.

3.2.16 Calculation of the joint reaction forces

Each force acting on the spine is projected into components as parallel and perpendicular to the reference line in the code. In order to calculate the forces acting on each joint axis, all the forces up to each joint axis are added as Fr and Fh components. To calculate the magnitude of the forces acting on the joint axis, Pythagoras theory is applied to all the force components up to the joint axis for each joint. It is assumed that each joint follows the same line direction as the axis of the vertebrae above. The global angle for each vertebra is calculated while the data is read from the excel files. After the magnitude and the direction of the forces acting on a joint is calculated, the forces acting on each joint are projected to components as parallel and perpendicular to the joint axis as shear forces and compressive forces respectively. Table 3.2

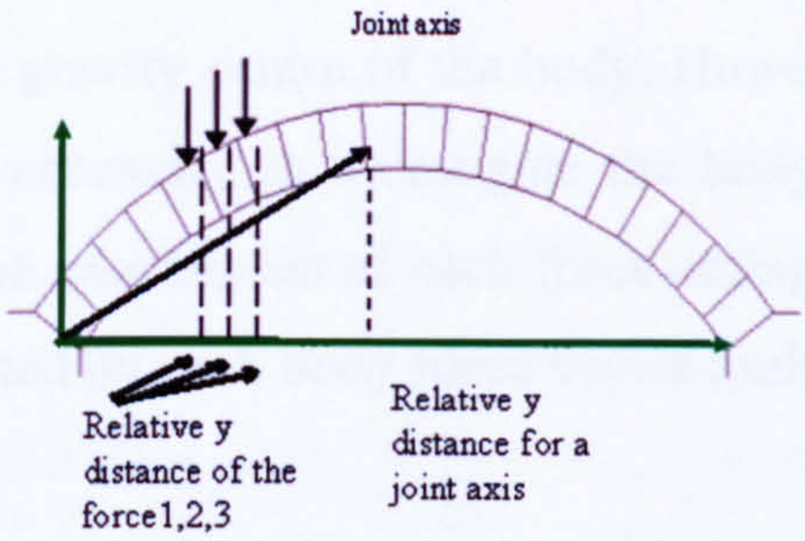


Figure 3- 16 Representation of joints

Table 3- 2 Joint reaction forces for a sample flex posture

Joint	Fx (N)	Fy (N)	Magnitude (N)
L5-L4	329.7241	-149.444	362.0105293
L4-L3	331.5391	-60.4837	337.0110198
L3-L2	317.9879	3.875812	318.0115381
L2-L1	295.5398	45.43681	299.0122079
L1-T12	269.9973	66.27772	278.0131292
T12-T11	249.1698	70.73033	259.014223
T11-T10	232.9036	62.00318	241.0155056
T10-T9	217.3211	50.08151	223.0170961
T9-T8	206.422	32.8444	209.0186273
T8-T7	198.2351	17.65675	199.0198402
T7-T6	186.889	7.039336	187.0215565
T6-T5	175.9831	3.766734	176.0233647
T5-T4	165.2033	-16.5003	166.0252342
T4-T3	134.1878	-15.0877	135.0333125
T3-T2	106.3924	-18.8221	108.0444718
T2-T1	74.35168	-20.2806	77.06798683
T1-C7	49.05234	-10.255	50.11285446
C7-C6	45.8126	-5.99877	46.20367546
C6-C5	43.98073	-0.94526	43.99088984
C5-C4	41.1285	4.371659	41.360188
C4-C3	38.4509	8.403589	39.35850878
C3-C2	36.45229	10.13492	37.83498374
C2-C1	35.4146	8.022941	36.31200595

3.2.17 Calculations for Lever Theory

In the lever theory, the spine is assumed to bending about at a fixed point, namely the sacrum. The flexion moments produced by the body weight and loads being lifted acting anterior to the spine are calculated. The model determines the extension moments required to produce predominantly by the posterior muscles. So that flexion and extension moments are in equilibrium. These moments are generally considered about the lower lumbar levels, in this case at L5/S1 region at which the moments and loads are predicted to be greatest.

Equilibrium of the structure is ensured when both the forces and the moments acting on it are in equilibrium. In literature lever theory is usually simplified by assuming only one body force acts at the gravity centre of the body. However, in order to reach more realistic conclusions it is necessary to investigate the body with the distributed body forces. In this program, the coordinates of each force acting on the body is known. To calculate the moment created by each body force vector multiplication which is;

$\vec{M} = \vec{r} * \vec{f}$ is applied.

Where

$\vec{r}$: is the distance from the lower centre of the L5/S1 joint to the application point of the force.

$\vec{f}$: is the force acting at the gravity centre of the body.

The magnitude of the distance is calculated by the Pythagoras theorem.

The angle is calculated with respect to the global coordinate system. The x and y components of the distances are calculated by the following equations.

```
ry = r * Sin(angl)
rx = r * Cos(angl)
```

The angles of the forces are in global coordinate system. The components are inserted into the following matrix and the resulting equation is applied.

$\vec{M} = r_x * f_y - f_x * r_y$

All the x and y components of the forces acting on the spine are added in the global coordinate system. In order to calculate the compressive and shear forces acting on the lower centre of L5 the force components are projected to the coordinate axis of the vertebrae L5. This is accomplished by the following formula

```
Magnitude of the force acting on lower L5 = Sqr((totalFy) ^ 2 + (totalFx) ^ 2)
totalFx = Magnitude * Sin(Global angle of the L5- Global Angle of the resultant
Force)
totalFy = Magnitude* Cos(Global angle of the L5 - Global Angle of the resultant
Force )
```

The magnitude of the moment acting on the L5/S1 increases with more flexed postures. This trend should be investigated from erect postures to fully flexed postures.

3.2.18 Parameterisation of the model

The radius and thickness parameters representing the geometrical shape of the spine are recorded into the CSV files are the same for each person. However, not everybody has the same dimensions of vertebra. For small stature people's vertebrae are expected to be smaller than people who have a larger stature. For this purpose, the data recorded in CSV files are scaled for each person. The user of the program is expected to enter the value of the height and weight of the person before the selecting the desired posture file of the person which is produced by using the spinal mouse. With this approach, the people who are short and thin are represented as having smaller vertebral dimensions when compared to the tall and big bodies. The units are cm for height and kg for weight.

3.3 Running the Code

The steps for a user to simulate a lifting activity by using thrustline model developed in Visual Basic, the steps that should be followed by the user are:

1. Enter the weight and height of the person whose spinal stability to be investigated. (Figure 3.17)



Figure 3-17. The boxes from the user interface of the program.

2. Click the open file button, select the file for the person saved as CSV files by using the spinal mouse and processed in java code before by the researchers (Figure 3.18).

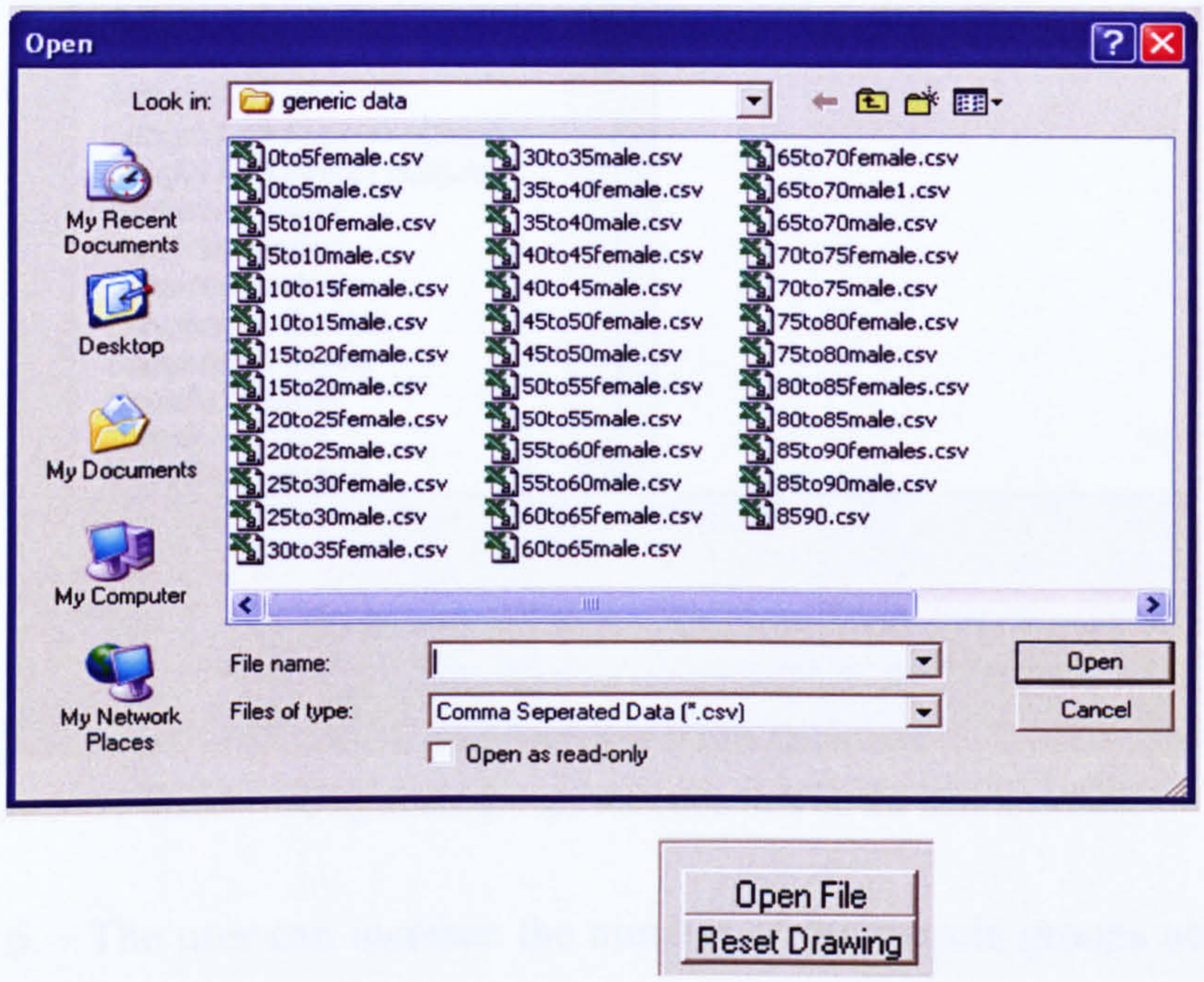


Figure 3- 18 Open dialog box for CSV files and the open button for the opening the dialog box in the program.

3. Check the spinal curvature drawn on the screen if it is visible fully. If not, drag it to the centre by pan option. (Figure 3.19)



Figure 3- 19 Drawing window mode.

4. To evaluate the affect of each muscle for on spinal stability, the user should check the add muscle forces box. (Figure 3.20)

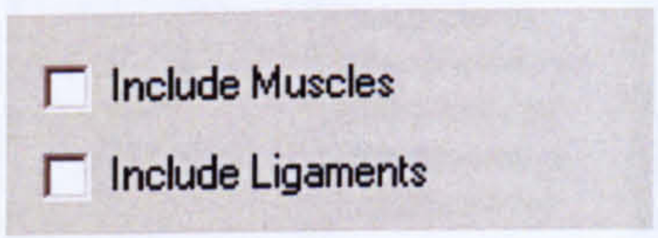


Figure 3- 20 Check boxes for muscle and ligaments.

5. The user adds the muscles groups which are expected to act on the spine for the inspected posture from the list of the muscle group by highlighting the muscle name and pressing the add button, the desired muscle group appears in a box called selected muscle and ligament groups (Figure 3.21).

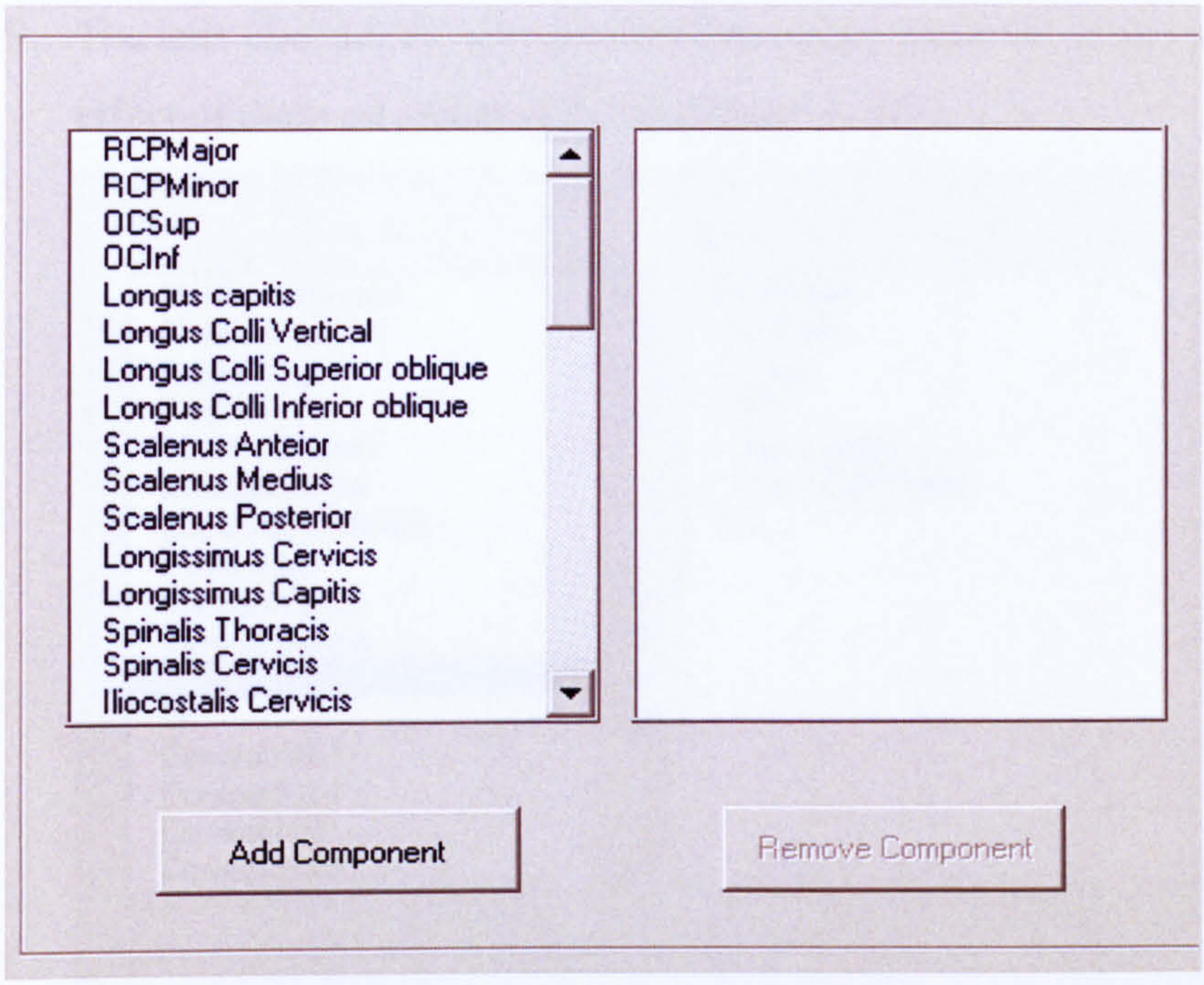


Figure 3- 21 Muscle and ligament groups selection lists on the user interface.

6. The user can increase the number of the muscle groups acting on the spine by pressing Add Component button (Figure 3.21).
7. To include the ligament forces acting on the spine, the user selects the option for ligaments (Figure 3.20).
8. Open file menu appears with the corner coordinates of an erect posture in a CSV file. The user of the program loads the CSV file (Figure 3.22)

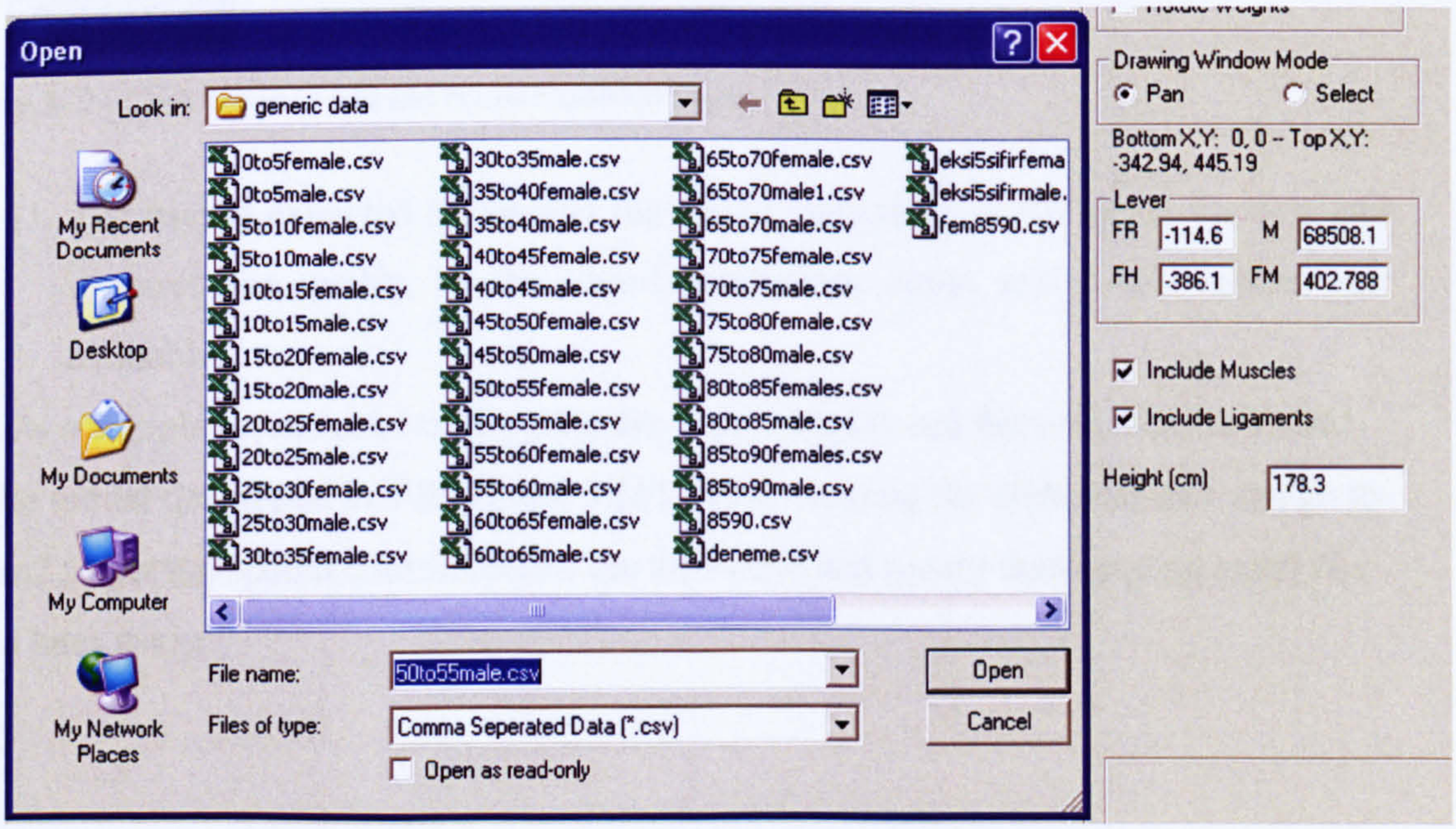


Figure 3- 22 Open box for selecting erect posture vertebrae coordinates to calculate ligament forces.

9. The user chooses the group of the ligaments which he or she wants to see the effect of them on spinal stability (Figure 3.23).

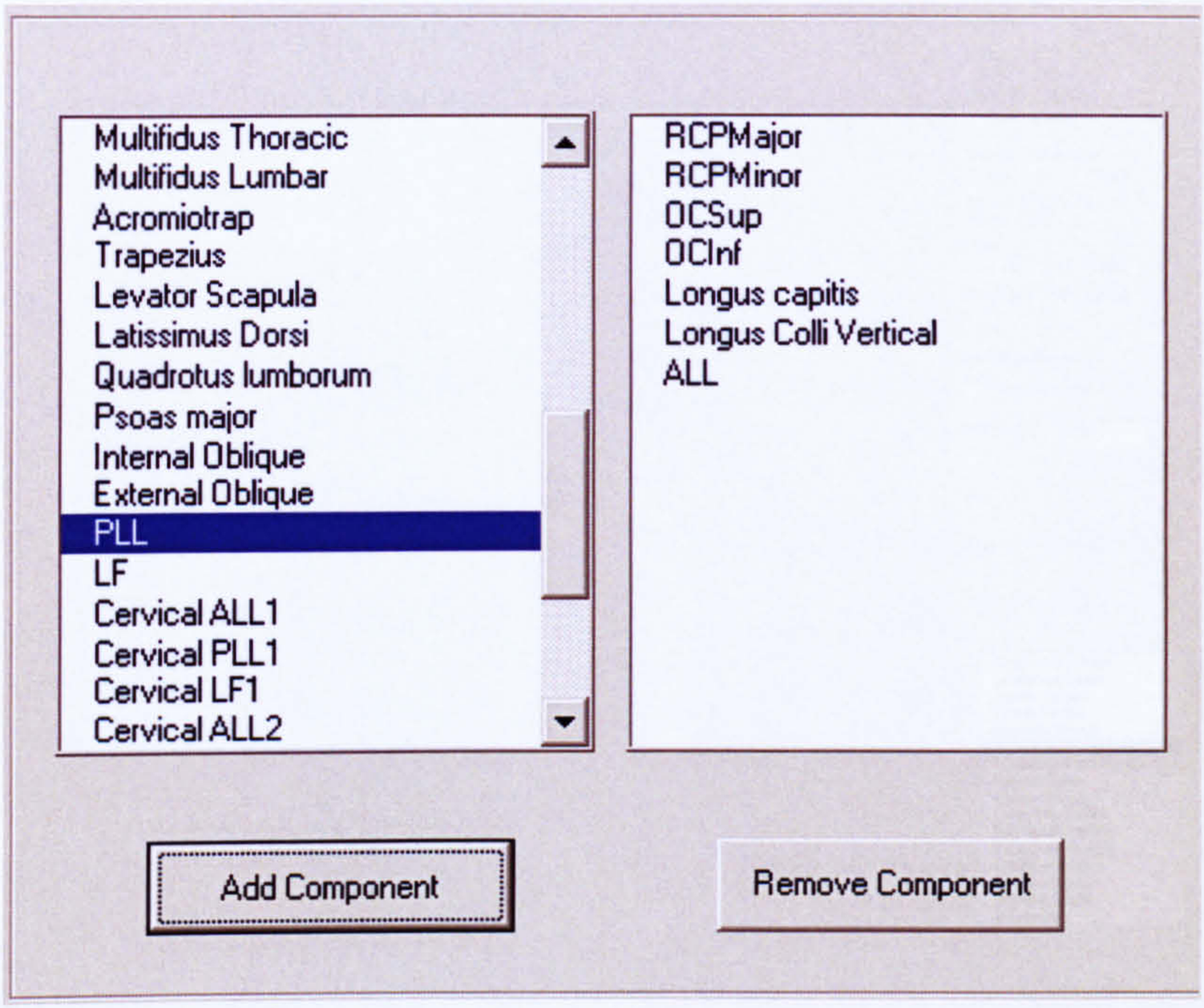


Figure 3- 23 List of muscles and ligaments selected on the list box.

10. To add any external forces the user can either click on the add force button (Figure 3.24) or directly enter the force values with the angle, magnitude and coordinates acting on the spine into Form2.



Figure 3- 24 Click boxes to add and remove external force.

11. The user is expected to conduct the visual inspection of the spine. To help and improve the quality of the visual inspection, zoom and rotate options are available.

Below a sample screen print of the program is provided to see the main screen, Form1 of the model developed in VB (Figure 3.25). After running the code, the user can go to Form2 to get the spatial coordinates of the thrustline and record them into an excel file for a later usage.

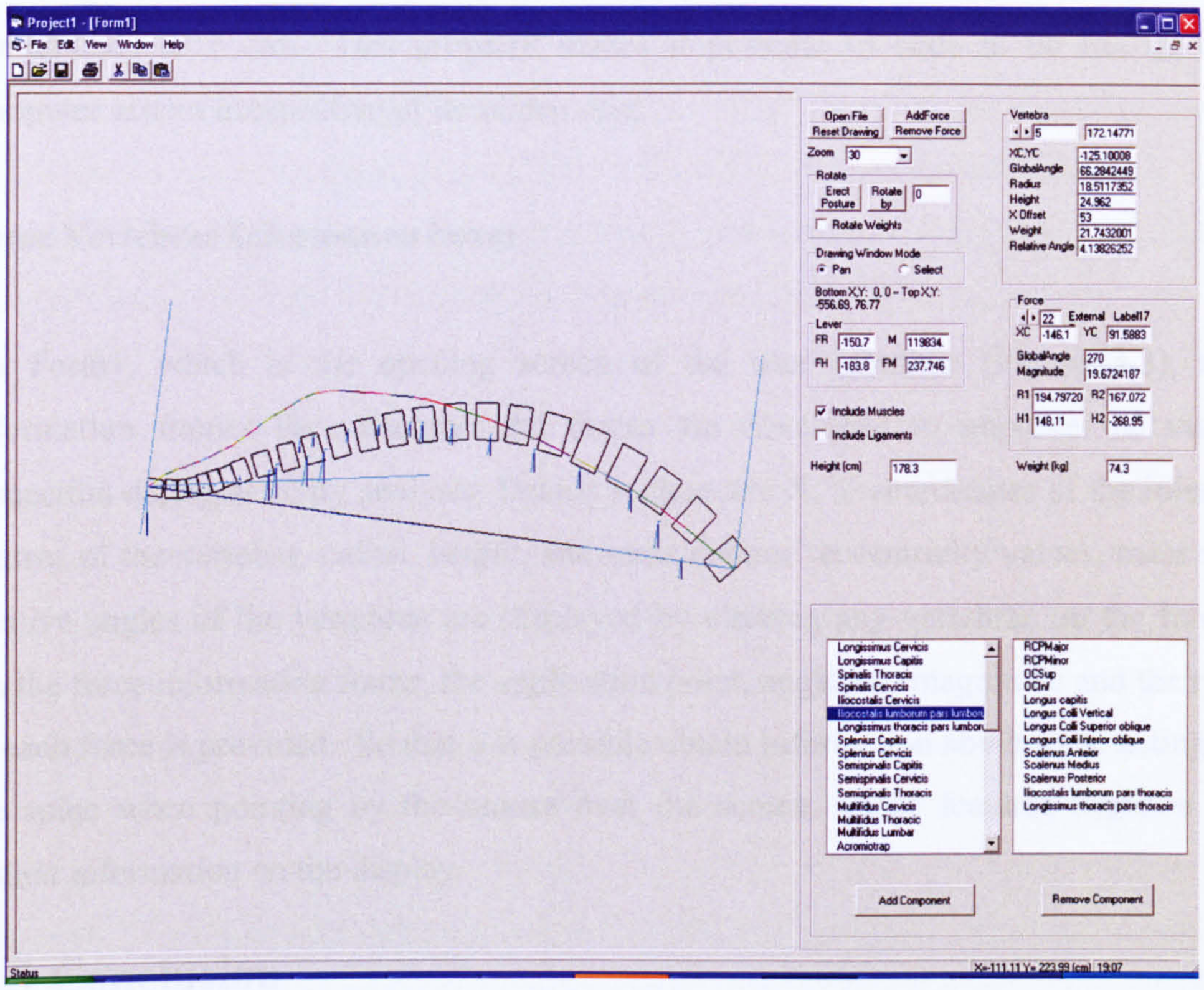


Figure 3- 25 Main user interface of the program.

3.4 Visual Aspects of the program

Zooming

In order to improve the visual inspection of the program the zoom property is added to the program. Although the zoom ratio can be changed depending on the user requests, it is possible to see the drawn figure from 10 % of it to 200% of its real size. The zoom values are recorded to the zoom box in the sub form load procedure.

Scaling

The initial scales are assigned to the value of 1. For drawing scale, 1cm corresponds to 100*Draw Scale twips. Twips are screen-independent units to ensure that the proportion of screen elements is the same on all display systems. A twip is defined as being 1/1440 of an inch, (http://www.applecore99.com). For force values 1 N

corresponds to 1 cm. This property makes it possible to code to be run on any computer screen irrespective of its screen size.

Force Vertebrae Information boxes

On Form1, which is the opening screen of the user interface (Figure 3.3), two information frames for vertebrae and forces are developed to improve the visual inspection during stability analysis. Details such as the X, Y coordinates of the inferior centres of the vertebra, radius, height, and mass centres' eccentricity values, mass and relative angles of the vertebrae are displayed by clicking any vertebrae on the frame. On the force information frame, the application point, angle and magnitude and the type of each force is provided. So that it is possible obtain information about force acting on the spine when pointing by the mouse over the screen. These features improve the instant information on the display.

3.5 Conclusion

In this chapter, how the program is structured and run is explained however, how the muscle and ligament force calculation are estimated is not explained. The detailed information about the thrustline theory is provided, the way how the code was implemented to develop the visual basic model is explained in detail. The forms used in the code and the screen shots of the code are presented.

A parametric model is developed. The individual parameters for each person used in the model are the body weight forces and spine dimensions depending on the weight and height of each individual. The magnitude of the muscle and ligament forces could not be parameterised mainly because of the muscles and ligaments data. The model is designed to include muscle and ligament parameterisation when consistent data is available in the future.

It is observed that the use of MSFlexGrid increases the efficiency of the program. All the calculated data is stored in the cells of the MSFlexGrid. So that all the calculated muscle force values and ligament forces are stored in separate forms within the multiple document interface of the code. While applying thrustline theory it is very important to

sort the forces in the ascending order along the reference line axis and to check if there are forces with the same coordinates. With the use of MSFlexGrid, the command "sort" the forces are reordered depending on their y coordinates along the reference line. This is considered as an important advantage for the implementation of the thrustline theory. The run time of the code is negligible with these improved properties.

One of the other important gains of the way program built is the flexibility of addition of muscle and ligament forces. It is possible to combine any kind of muscle group and ligaments depending on the selection of the user. There is no limitation in the number of the muscle and ligament groups which can be selected to acting on the spine.

The results which are the coordinates of the thrustline and the Fr, Fx components of the forces acting on the spine with the joint reaction forces are stored in the forms by use of MSFlexgrid. This enables user to transfer the results into other office programs like Microsoft Excel. Considering the properties of the user interface, the visual inspection of the thrustline is improved for stability analysis.

CHAPTER 4

4 Modelling of Muscles and Ligaments in Thrustline Theory

In this chapter, the muscles used in the model are given in detail. Their cross sectional areas, attachment points and force producing capacities are tabulated to add in the thrustline model developed in Visual Basic. The connection points of the ligaments and the force produced by ligaments are explained and the way they are included in the code is provided.

4.1 Muscle attachment points and morphology

The muscles play an important role in stabilizing the spine. The accuracy, with which the forces exerted by the muscles can be modelled, depends on how accurately the muscle is depicted in relation to the vertebrae. The attachment points of muscles are very crucial for the biomechanical model to represent realistic results. The literature review is conducted for this purpose very carefully to represent the correct attachment points of the fascicles of each muscle unit.

While investigating the spinal loading, it is necessary to estimate the force exerted by the muscles. Since the muscles are multi-segmental, the number of fascicles acting on a given segment must be known. For any obliquely oriented fascicle, its action is distributed proportionally in different directions, so to determine its action in any chosen plane of movements; its three-dimensional orientation must be known. Muscle's maximum force generation potential is proportional to its size: either its cross sectional area, or in the case of an irregularly shaped or fusiform muscle, its physiological cross sectional (PCSA), which is defined in cadaver studies as the muscle volume divided by its length (Brand *et al.* 1986; Bogduk *et al.* 1992).

One of the methods for collecting data for the muscle cross sectional area is MRI. In MRI scan planes are perpendicular to the scan table, the raw cross sectional areas (CSA) derived directly from MRI is usually the over estimates of the true CSA as the direction of most muscles are not perpendicular to the scan plane (McGill *et al.* 1993). McGill at all, used a correction method for this purpose, while calculating this, they took the dot product of the unit vectors using muscle fibre angles determined from different literature sources (McGill *et al.* 1993). The resulting corrected CSA at each vertebral level correspond to the anatomical cross sectional area (ACSA). The PCSA, which is necessary to estimate the force producing capability of the muscle, is defined as the maximum CSA that "cuts" all fibres at right angles (Narici,1999).

The largest ACSA for each muscle is defined as the estimate of the PCSA (Marras,et al., 2001). Active muscle force is proportional to number of active actin/myosin binding sites. The number of sites available for actin/myosin binding depends on the muscle's length. As the muscle shortens, the increasing overlap of actin and myosin chains leaves relatively few additional binding sites. As the muscle is elongated, decreasing overlap of actin and myosin chains provides relatively few binding sites. The greatest number of actin-myosin binding sites are available when the muscle fiber is at an intermediate length (Lieber & Bodine-Fowler, 1993, Smith, Weiss, & Lehmkuhl, 1996).Therefore, the active length-tension curve is dome-shaped (Figure 4.1).

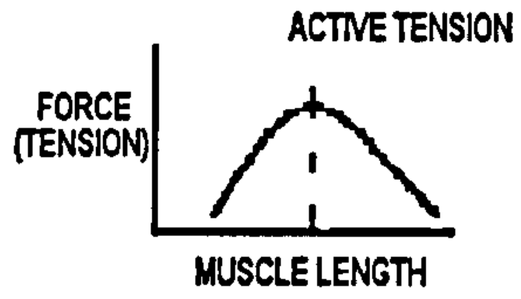


Figure 4- 1 Muscle force relation with muscle length (Lieber & Bodine-Fowler, 1993)

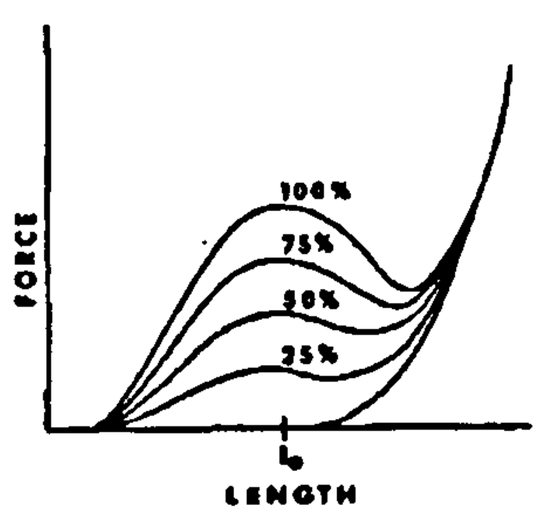


Figure 4- 2 Muscle force relation depending on the level of activation. (Winter, 1990)

The curve's amplitude (the height of the dome) varies with the amount of active force that the muscle's motor units generate resulting in redundancy in muscle force calculations (Figure 4.2) It is possible to expect any percentage of muscle activation during a lifting activity. This brings out the problem of redundancy the number of equations is less than the number of unknows. For this reasons, the muscles are assumed to be activated 100% in this model. It is not possible to measure the percentage of the amount of active force that the muscle's motor units generate resulting in muscle force calculations. In addition to that, the active length tension curve is theoretical and it is not possible to measure directly. For this reason, in this model while modelling the muscles the length parameter is kept out of scope. The maximum muscle force is produced is assumed to act on the spine is assumed in this model.

In order to calculate the full load bearing capacity of the spine, for each muscle group an indication of maximum muscle force is necessary. The relation between the maximum force (N) generated by the muscle and PCSA is as follows:

$$F=PCSA*k$$

Where k is the force coefficient indicating the maximum muscle force generated per unit of cross sectional area. The value for k in literature has varied from 30-100 N/cm^2 (McGill *et al.* 1987). With this method it is possible to estimate every muscle force of which cross sectional area is known. The data represented in literature is usually for the whole muscles on the right and left sides of the body or average. Assuming sagittal symmetry, the total muscle area in this plane is therefore twice the nominal value. However, as this model is in two dimensions, the force component of the muscles only in sagittal plane should be used in calculations. There is a possibility that the force components of the muscles act in a direction perpendicular to the paper surface to cancel each other. However, due to limited data available for the fascicle orientations, only the muscles whose both sagittal and lateral plane angles are known is calculated for sagittal plane components. The force values of the other muscles are assumed as if they are already in the sagittal plane. With this approach, the magnitude of the force that can be produced by the muscle groups can be more than the muscle can produce in the sagittal plane. For the muscles whose total cross sectional area is given in literature,

the procedure for calculation of the force magnitude applied by each fascicle is as follows:

1. Calculate the maximum force applied by the muscle group by using the F=PCSA*k

2. Divide the calculated force value into the number of fascicles.

If the cross sectional area of the each fascicle is known, then the force applied by each fascicle can be calculated directly by F=PCSA*k.

To see the effect of each muscle force, it is better to group muscles. Deep muscles of the back are expected to play an important role in the fine tuning of the spine. Because of short moment arms, they cause a little change in the position of the thrustlines. The superficial muscles are expected to change the position of the thrustlines more when compared to deep muscle groups.

A large number of the muscle groups of the neck make attachment to the skull. The positions of these attachments are important. In the cervical region the main areas of the muscle attachment are the tip of the spinous process, the tip of the transverse process and the anterior tubercle of the transverse process. Muscles attaching to the anterior tubercle are positioned laterally at a distance of two thirds of the transverse process width in line with the anterior edge of the vertebral body.

The approximations for the calculations of the attachment points with respect to the lower centre of each vertebra are embedded in the program. The approximations and the formulation of the muscle attachment and ligament attachment points are explained in Appendix 3. The data used in the formulations are obtained from Ceran, (2006).

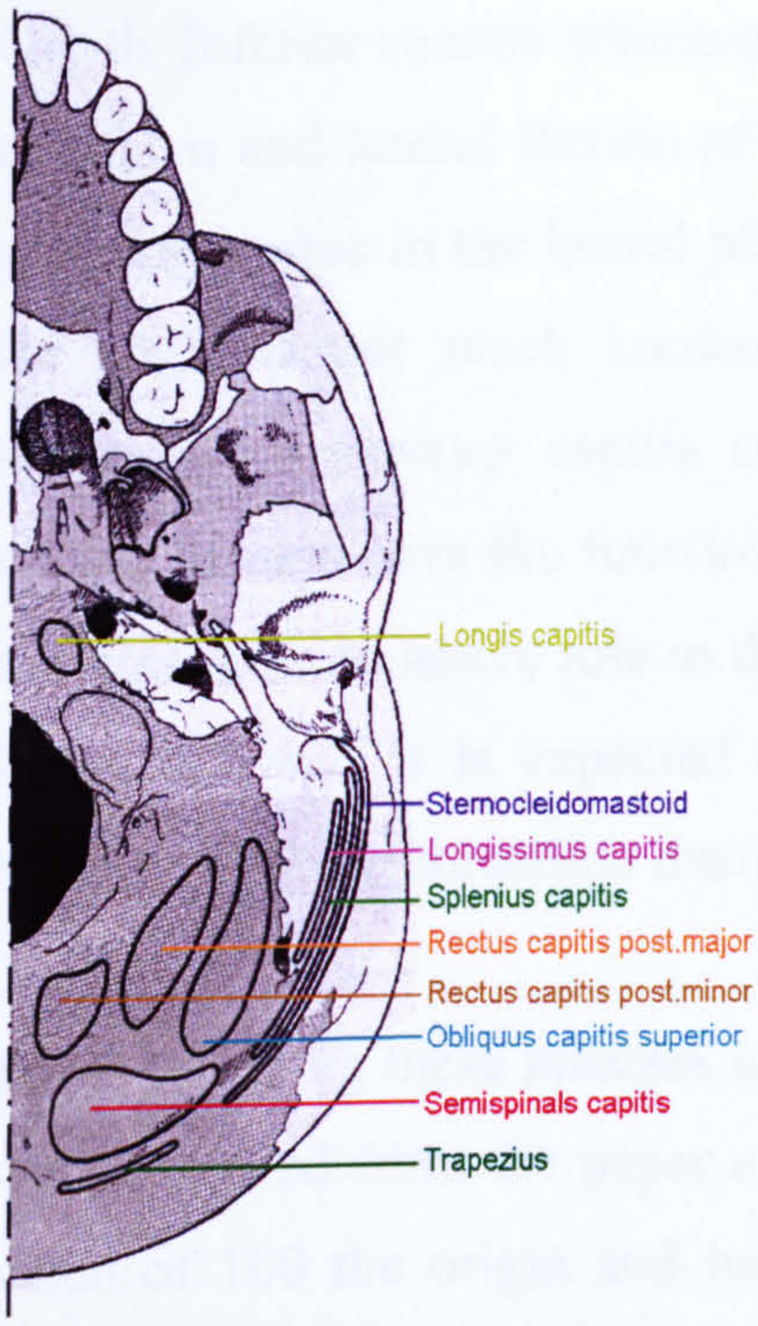


Figure 4- 3 Inferior surface of the right half of the base of the skull showing points of attachment of muscle groups with insertions on the skull from Gary (1980).

4.1.1 Sub occipital Muscles

Both rectus capitis posterior major and minor have simple structures. Obliquus capitis inferior is oriented nearly perpendicular to the rectus muscles from the spinous process of the axis to the transverse process of the atlas. Obliquus capitis superior has a more complex structure (Kamibayashi and Richmand, 1998). The suboccipital muscles of the cervical spine play a role in fine-tuning the movements of the head

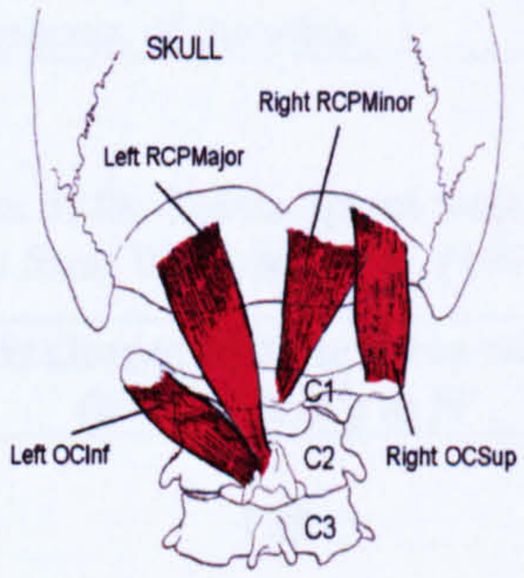


Figure 4- 4 An anatomical drawing of the suboccipital muscles and their attachments to the skull and vertebrae (Basmajian, 1921).

Action of the rectus capitis posterior minor is extending the head at the neck. Rectus capitis posterior major extends the head and rotates it to the same side. Obliquus

Capitis Inferior rotates atlanto-axial joint. Obliquus capitis superior is thought to help extension and lateral flexion of the head at the neck. The obliquus muscles should be applying torque in the lateral plane with a little contribution in sagittal plane, however the angle is not much known. Rectus Capitis major and minor, obliquus capitis superior, longissimus capitis and semispinalis capitis are synergist muscles. These muscle groups have the function of flexion mostly in general. It is expected that these muscles have an active role in the postures when the head and neck is straightened in a lifting activity. It is expected to see the effect of these muscles groups on spinal stability by using thrustline theory in the model.

For introducing these muscles into the model, the cross sectional areas of the muscles were obtained from the paper of Kamibayashi and Richmond (1998) and with the K value of 100 the origin and insertion points of these muscles are given in the table below

Table 4- 1 Origin and insertion points of the suboccipital muscles

Parts	**Origin**	**Insertion**
Rectus Capitis Posterior Major	The spinous process of the axis	Lateral part of the inferior nuchal line of the occipital bone.
Rectus Capitis Posterior Minor	The tubercle on the posterior arch of the atlas.	The medial part of the inferior nuchal line of the occipital bone and the surface between it and the foramen magnum
Obliquus Capitis Inferior	Spinous process of the axis	Transverse process of the atlas (Gurumoorthy and Twomey, 2000).
Obliquus Capitis Superior	The superior aspect of the transverse process of the atlas	Lateral third of the inferior nuchal line

Table 4- 2 Morphometric parameters of the Suboccipital muscles, taken from Kamibayashi and Richmond (1998) connection points from Vasavada et al, (1998).

Muscle Name	**Muscle PCSA (cm^2)**	**Maximum Muscle force with ($k=100N/cm^2$) in N**	**Origin**	**Insertion**
RCPMajor Fascicle 1	0.89	178	C2	C0
RCPMinor Fascicle 1	0.49	98	C1	C0
OCSup Fascicle 1	0.94	188	C1	C0
OCInf Fascicle 1	1.23	246	C2	C1

4.1.2 Deep Back Muscles

Longus Capitis

Longus capitis is one of three deep pre-vertebral muscles of the neck. It arises from the anterior tubercles of the transverse processes of the third to sixth cervical vertebrae (Warfel, 1985).

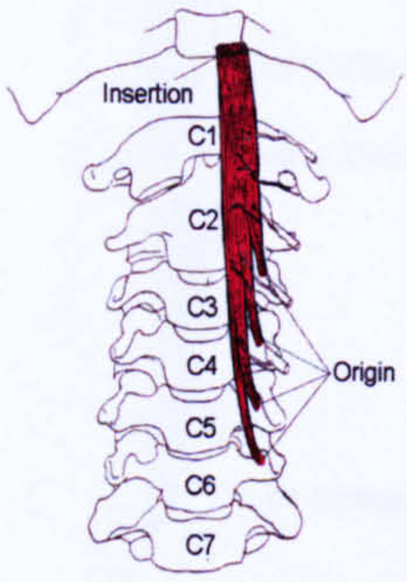


Figure 4- 5 An anatomical drawing of the longus capitis and their attachments (Basmajian, 1921).

From these origins, it converges superomedially to insert into the anterior and basilar surface of the occipital bone (Gurumoorthy and Twomey, 2000). This muscle when acting bilaterally, flexes the head and neck. Morphometric parameters are reported by Kamibayashi and Richmond (1998). Longis capitis is thought to have 4 fascicles. Longus capitis, longus colli, scalenous group muscles are the synergist muscles.

Table 4- 3 Origin and insertion points of the longis capitis

Muscle Name	**Origin**	**Insertion**
Longis Capitis	Tubercles of transverse process of 3^{rd}, 4^{th}, 5^{th}, 6^{th} cervical vertebrae.	Inferior surface of basilar part of occipital bone

Table 4- 4 Morphometric parameters of the Longus Capitis

Muscle Name	**Muscle PCSA (cm^2)**	**Maximum Muscle force with ($k=100N/cm^2$) in N**	**Origin**	**Insertion**
Longus capitis				
Fascicle 1	0.23	46	C3	C0
Fascicle 2	0.23	46	C4	C0
Fascicle 3	0.23	46	C5	C0
Fascicle 4	0.23	46	C6	C0

Longus Colli

Longus colli is the longest and most medial of the pre-vertebral muscles. It arises from the anterior bodies of the T1 to T3 vertebrae anterior tubercles of the transverse

processes of C3 to C7 vertebrae. It inserts into the: anterior tubercle of the atlas vertebral bodies of C2 to C4 It consists of three portions, the superior oblique, the inferior oblique and the vertical portion. The longus colli is thought to flex the cervical spine (Warfel, 1985). Longus capitis, longus colli, scalenous group muscles and sternocleidmasteoid muscles are synergist muscles.

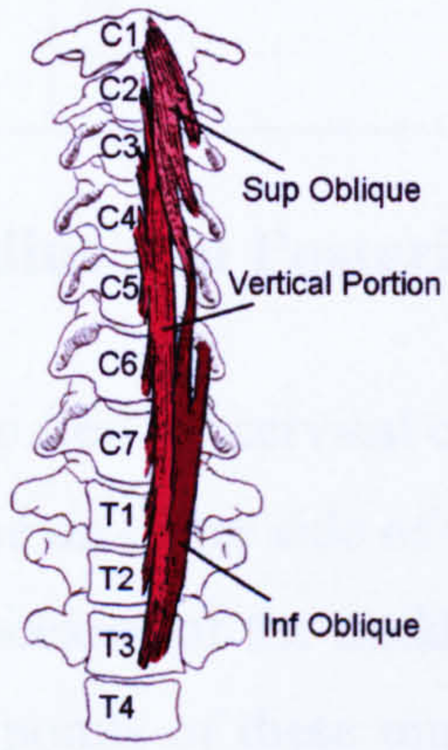


Figure 4- 6 Anatomical drawing of the muscle longus colli superior, inferior oblique and vertical portions (Basmajian, 1921).

Table 4- 5 Origin and insertion points of longis colli

Parts	**Origin**	**Insertion**
Vertical portion	First 3 thoracic and last 3 cervical vertebrae (C5-T3)	Tubercles of transverse process of 3rd, 4th, 5th, 6th cervical vertebrae
Inferior oblique portion	From the bodies of 1st 3 thoracic vertebrae	Anterior tubercles of the transverse processes of the fifth and sixth cervical vertebrae.
Superior oblique portion	transverse processes of 3 rd, 4th, 5th cervical vertebrae	Tubercle on the anterior arch of the atlas.

In the model the longus colli is divided into a total of 5 individual muscle elements, 3 to represent the vertical portion and one each to represent the superior and inferior oblique portions. The vertical portion has a single origin on T1 which is the central vertebrae between C5 and T3 with the three elements inserting onto C2, C3 and C4 respectively. No measured morphometric data for the longus colli could be obtained from the literature so the values were estimated based on other researchers work (Vasavada et al., 1998).

Table 4-6 Morphometric parameters of the longis colli

Muscle Name	Muscle PCSA (cm^2)	Maximum Muscle force with ($k=100N/cm^2$) in N	Origin	Insertion
Longus Colli				
Vertical				
Fascicle 1	0.4	80	T1	C4
Fascicle 2	0.4	80	T1	C3
Fascicle 3	0.4	80	T1	C2
Superior Oblique	0.4	80	C5	C1
Inferior Oblique	0.4	80	T1	C5

Scalenus: Anterior, Medius and Posterior

The Scalenus muscles serve to flex the cervical column when contracted symmetrically. The three Scalenus muscles lie on either side of the anterior aspect of the cervical spine connecting the transverse processes of the middle and lower vertebrae to the first and second ribs. The connection points of these muscles to the first rib and second rib is assumed as the connection points of the ribs to the vertebrae in the model (Warfel, 1985).

Table 4- 7 Origin and insertion points of Scalenus muscles

Parts	Origin	Insertion
Scalenus Anterior	The transverse processes of C3 through C6.	The scalene tubercle of the first rib
Scalenus Medius	the transverse processes of C2 through C7	Posterior aspect of the first rib
Scalenus Posterior	Three tendinous slips onto the transverse processes of C4-C6.	Superior border and lateral aspect of the second rib

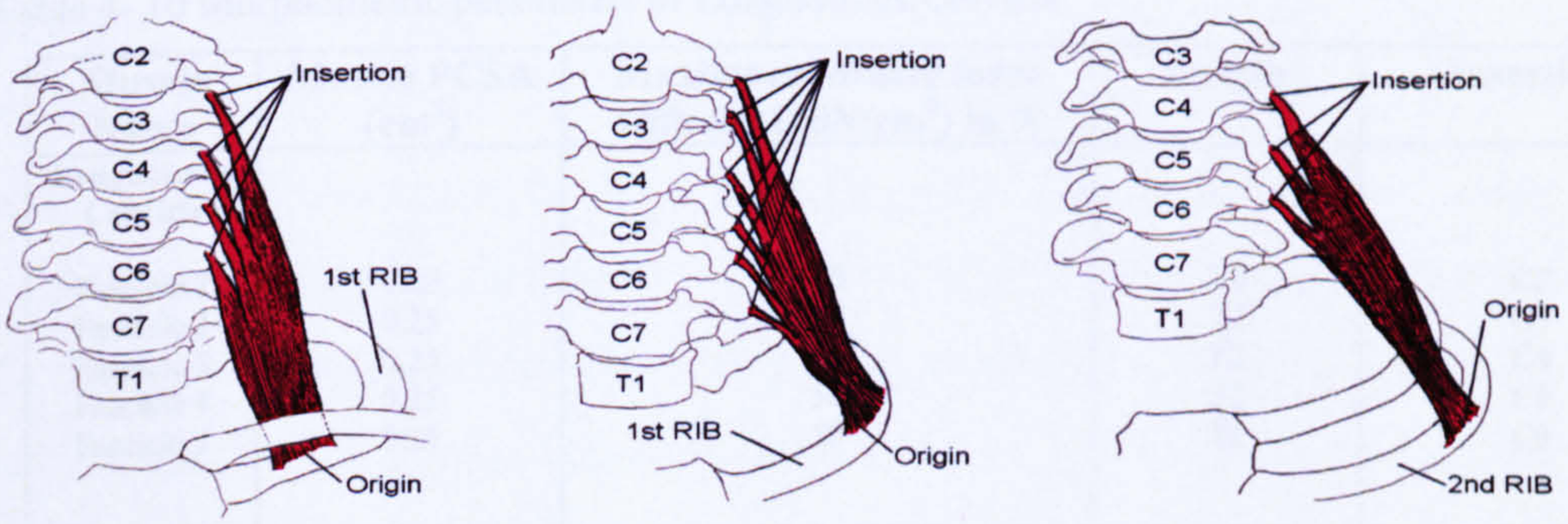


Figure 4- 7 Anatomical drawings of the Scalenus muscles showing points of attachment to the ribs and cervical vertebra. From left to right, Scalenus Anterior, Scalenus Medius, Scalenus Posterior (Basmajian, 1921).

The morphometric parameters of the muscle elements are obtained from Kamibayashi and Richmond (1998).

Table 4- 8 Morphometric parameters of Scalenus anterior, medius and posterior

Muscle Name	Muscle PCSA (cm^2)	Maximum Muscle force with ($k=100N/cm^2$) in N	Origin	Insertion
Scalenus Anterior	1.26	252	C4	1st Rib
Medius	2.00	400	C3	1st Rib
Posterior	1.61	322	C5	2nd Rib

Longissimus cervicis

Together with the Longissimus Capitis, the Longissimus Cervicis aids in producing extension, lateral flexion and rotation of the cervical column. Longissimus Cervicis has five muscle fascicles on each side of the neck originating from the approximate position of the transverse process of T2. Due to very little data on the morphometric parameters of the longissimus cervicis, they have been estimated based on the other similar muscles of the neck. Semispinalis capitis, semispinallis cervicis, illiocostalis cervicis, longissimus capitis, spinalis cervicis are synergist muscle groups (Warfel, 1985).

Table 4- 9 Origin and insertion points of longissimus cervices

Parts	Origin	Insertion
Longissimus Cervicis	Transverse process of upper 4 or 5 thoracic vertebrae.	The transverse processes of C2 to C6

Table 4- 10 Morphometric parameters of Longissimus Cervicis

Muscle Name	Muscle PCSA (cm^2)	Maximum Muscle force with ($k=100N/cm^2$) in N	Origin	Insertion
Longissimus Cervicis				
Fascicle 1	0.25	50	T2	C2
Fascicle 2	0.25	50	T2	C3
Fascicle 3	0.25	50	T2	C4
Fascicle 4	0.25	50	T2	C5
Fascicle 5	0.25	50	T2	C6

Longissimus capitis

The Longissimus Capitis lies between the Longissimus Cervicis and the semispinalis capitis. Together with the Longissimus Cervicis the Longissimus Capitis aids in producing extension, lateral flexion of the cervical column (Warfel, 1985).

Table 4- 11 Origin and insertion points of longissimus capitis

Parts	Origin	Insertion
Longissimus Capitis	The transverse processes of the upper 4 or 5 thoracic and from the articular processes of the lower 3 or 4 cervical vertebrae	The posterior margin of the mastoid processes on the skull

Longissimus Capitis has 5 individual muscle elements on each side of the neck. The first four elements have origins on the transverse processes of C4-C7 respectively. All five muscle elements share the same insertion point positioned on the skull (C0) at the location of the mastoid process. Very little data is available on the morphometric parameters of the Longissimus muscles so here they have been estimated based on other similar muscles of the neck. Semispinalis capitis, spinalis capitis, Longissimus cervicis are the synergist muscles.

Table 4- 12 Morphometric parameters of Longissimus Capitis

Muscle Name	Muscle PCSA (cm^2)	Maximum Muscle force with ($k=100N/cm^2$) in N	Origin	Insertion
Longissimus Capitis				
Fascicle 1	0.16	32	C4	C0
Fascicle 2	0.16	32	C5	C0
Fascicle 3	0.16	32	C6	C0
Fascicle 4	0.16	32	C7	C0
Fascicle 5	0.16	32	T2	C0

Spinalis thoracis

Spinalis thoracis lies posterior to semispinalis thoracis, and medial to longissimus thoracis, which blends with it. Spinalis thoracis stabilises adjoining vertebrae, and controls their movement during movement of the whole vertebral column. This allows more effective action of the long back muscles. This muscle when acting bilaterally helps extension and hyperextension of the spine. The synergist muscles are semispinalis thoracis, longissimus thoracis, semispinalis thoracis, iliocostalis thoracis, lumborum, and longissimus thoracis. The cross sectional area of this muscle is obtained from the studies of Delp et al., (2001).

Table 4- 13 Origin and insertion points of spinalis thoracis

Parts	Origin	Insertion
Spinalis thoracis	Spinous process of eleventh thoracic to second lumbar vertebral spines.	Spinous process of the upper four to eight thoracic vertebrae

Table 4- 14 Morphometric parameters of Spinalis thoracis

Muscle Name	Muscle PCSA (cm^2)	Maximum Muscle force with ($k=100N/cm^2$) in N	Origin	Insertion
Spinalis thoracis				
Fascicle 1	0..2	40	T11	T4
Fascicle 2	0.2	40	T12	T5
Fascicle 3	0.2	40	L1	T6
Fascicle 4	0.2	40	L2	T7

Spinalis Cervicis

Spinalis cervicis is often absent, when it present, it originates from the lower part of ligamentum nuchae and the spine of seventh cervical vertebra (and occasionally first and second thoracic vertebra). Spinalis cervicis inserts into spine of axis (and occasionally first and second cervical vertebra). Spinalis cervicis stabilises adjoining vertebrae, and controls their movement during movement of the whole vertebral column. This allows more effective action of the long back muscles. It provides extension of vertebral column and maintenance of erect posture. Due to very little data on the morphometric parameters of the spinalis cervicis, they have been estimated based on other similar muscles of the thoracic. The synergist muscle groups are Longissimus cervicis, Semispinalis cervicis, Longissimus cervicis, splenius cervicis, iliocostalis cervicis (Warfel, 1985).

Table 4- 15 Origin and insertion points of spinalis cervicis

Parts	Origin	Insertion
Spinalis cervicis	Spinous processes of C6-T2	Spinous processes of C2 (and possibly extend to C3 or C4)

Table 4- 16 Morphometric parameters of Spinalis cervicis

Muscle Name	Muscle PCSA (cm^2)	Maximum Muscle force with ($k=100N/cm^2$) in N	Origin	Insertion
Spinalis cervicis	0.05	10	C6	C2
Fascicle 1	0.05	10	C7	C2
Fascicle 2	0.05	10	T1	C2
Fascicle 3	0.05	10	T2	C3
Fascicle 4				

Iliocostalis cervicis

Iliocostalis cervicis is one of three parts of the iliocostalis muscle. It originates on angles of third to sixth ribs, medial to tendons of iliocostalis thoracis. It inserts into posterior tubercles of transverse processes of fourth, fifth and sixth cervical vertebra.

Iliocostalis cervicis extends the vertebral column (Warfel, 1985). Data related to iliocostalis cervicis muscles cross sectional area is not available in literature, so PCSA assumptions are based on the similar muscle groups.

Table 4- 17 Origin and insertion points of iliocostalis cervicis

Parts	**Origin**	**Insertion**
Iliocostalis cervicis	Angles of third to sixth ribs	Posterior tubercles of transverse processes of fourth, fifth and sixth cervical vertebra

Table 4- 18 Morphometric parameters of iliocostalis cervicis

Muscle Name	**Muscle PCSA (cm^2)**	**Maximum Muscle force with ($k=100N/cm^2$) in N**	**Origin**	**Insertion**
Iliocostalis cervicis				
Fascicle 1	0.05	10	3rd rib	C4
Fascicle 2	0.05	10	4th rib	C5
Fascicle 3	0.05	10	5th rib	C6

Erector Spinae Muscle

Erector spinae is the largest muscle in the lumbar region. The erector spinae plays a critical role in the stability of the lumbar spine. Erector spinae is described as a common muscle mass arising in the lumbosacral region from the erector spinae aponeurosis and inserts into the lumbar and thoracic transverse processes and the ribs . Intact lumbar erector spinae consists of two muscles; each with thoracic and lumbar parts as Iliocostalis lumborum and Longsissimus thoracis. These four components are clearly defined by their different and constant attachment points (Bogduk ,1992 (a)).

Longissimus thoracis pars thoracis

Iliocostalis lumborum pars thoracis

Longissimus thoracis pars lumborum

Iliocostalis lumborum pars lumborum

The four divisions of the lumbar erector spinae have distinctly different segmental attachments and different individual actions on the lumbar vertebrae. The two thoracic divisions arise from the thoracic transverse process, ribs and form the erector spinae aponeurosis in the lumbar region (Bogduk,1992).The two lumbar divisions arise in a segmental fashion from accessory and transverse processes of the lumbar vertebrae and

insert directly into the ilium without contributing to the erector spinae aponeurosis (Bogduk,1992). Iliocostalis lumborum is composed of 8 or 9 small fascicles, arising from the lower 8 or 9 ribs at their angle. The lumbar fibres of iliocostalis lumborum consisted of 4 large fascicles arising from the first 4 lumbar vertebrae. Each fascicle attached rostally to the lateral one quarter of the transverse process and to the adjacent surface of surface of the middle layer of thoracolumbar fasica. Caudally, each fascicle has a direct attachment to the iliac rest (Bogduk, 1992).

Thoracic components of longissimus thoracis is consisted of two series of fascicles, arising from the thoracic transverse process or ribs. Fascicles arising from transverse processes were represented at each thoracic level; those arising from the ribs are represented below T3 and T4. From first to ninth thoracic level attach in the vicinity of the L1 spinous process and those from successively lower levels attach to successively lower spinous processes until the tendon from the 9^{th} thoracic level reaches the S4 spinous process (Bogduk, 1992). The tendons from the 10^{th} to 12^{th} thoracic levels assume a more vertical course and insert along line (Bogduk, 1992). Lateral to the multifidus; five fascicles arising from the accessory and transverse processes of the lumbar vertebrae and inserting into the ilium form the longissimus thoracis pars lumborum (Bogduk,1992).

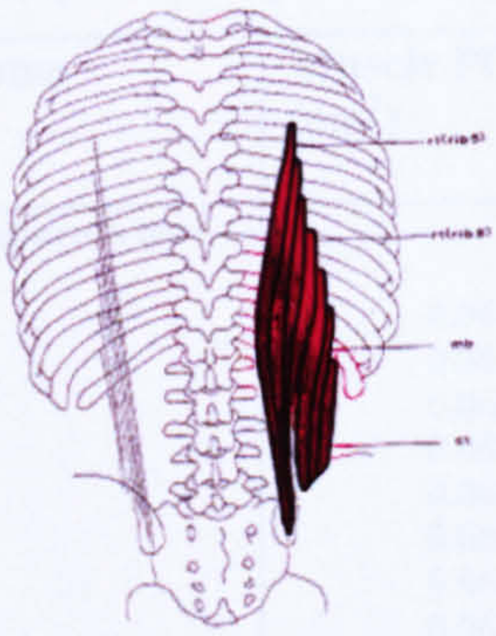


Figure 4- 8 Transverse plane of thoracic Iliocostalis lumborum (Basmajian, 1921)

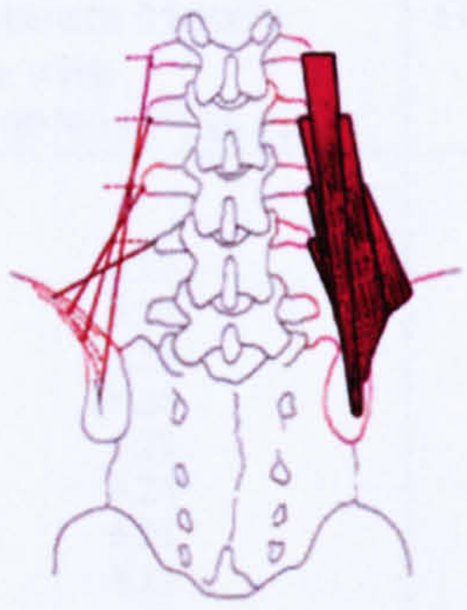


Figure 4- 9 Lumbar fascicles of the iliocostalis lumborum (Basmajian, 1921).

Although there is detailed research about the morphology of the erector spinae muscles especially in the study of the Macintosh and Bogduk (1991), there is no detailed data about the cross sectional areas of the erector spinae muscles. Gary Yamaguchi *et al.* (1990), a number of studies about morphological data are compiled in tables, categorized by region and by muscle from which the cross sectional areas of the muscles are obtained for most of the muscles.

Table 4-19 Points of attachments of the erector spinae muscle

Muscle name	**No of Fascicles**	**Origin**	**Insertion**
Iliocostalis lumborum pars thoracis	8	8^{th} or 9^{th} Rib and from T5 to T12	Iliac crest
Iliocostalis lumborum pars lumborum	4	One quarter of the transverse processes of lumbar vertebrae from L1 to L4	Iliac crest 5 cm laterally
Longissimus thoracis pars thoracis	9	Transverse processes of thoracic region T1-T9	Fascicles before T6 attach to lumbar spinous process. L1-S4 spinous processes
Longissimus thoracis pars lumborum	5	Transverse and Accessory processes of L1 to L5	Ilium

The information for the erector spinae muscles in the following table is from the research of Reid, J.G. and Costigan P.A., (1985). Cross-sectional areas and average volumes for erector spinae muscles were calculated based on computer tomography scans of 28 living subjects (16 normal males and 12 normal females). Transverse (coronal) scans were taken at 0.5 to 2.0 cm intervals between the xiphoid process and the symphysis pubis. The PCSA values are listed in the table below.

Table 4- 20 Morphometric parameters of iliocostalis lumborum pars thoracis

Muscle Name	**Muscle PCSA (cm^2)**	**Maximum Muscle force with ($k=100N/cm^2$) in N**	**Origin**	**Insertion**
Iliocostalis lumborum pars thoracis				
Fascicle 1	0.0625	6.25	T5	L5
Fascicle 2	0.0625	6.25	T6	L5
Fascicle 3	0.0625	6.25	T7	L5
Fascicle 4	0.0625	6.25	T8	L5
Fascicle 5	0.0625	6.25	T9	L5
Fascicle 6	0.0625	6.25	T10	L5
Fascicle 7	0.0625	6.25	T11	L5
Fascicle 8	0.0625	6.25	T12	L5

Table 4- 21 Morphometric parameters of iliocostalis lumborum pars lumborum

Muscle Name	**Muscle PCSA (cm^2)**	**Maximum Muscle force with ($k=100N/cm^2$) in N**	**Origin**	**Insertion**
Iliocostalis lumborum pars lumborum				
Fascicle 1	0.25	25	L1	L5
Fascicle 2	0.25	25	L2	L5
Fascicle3	0.25	25	L3	L5
Fascicle 4	0.25	25	L4	L5

Table 4- 22 Morphometric parameters of longissimus thoracis pars thoracis

Muscle Name	Muscle PCSA (cm^2)	Maximum Muscle force with ($k=100N/cm^2$) in N	Origin	Insertion
Longissimus thoracis pars thoracis				
Fascicle 1	0.11	11	T1	L1
Fascicle 2	0.11	11	T2	L1
Fascicle 3	0.11	11	T3	L1
Fascicle 4	0.11	11	T4	L1
Fascicle 5	0.11	11	T5	L1
Fascicle 6	0.11	11	T6	L1
Fascicle 7	0.11	11	T7	T12
Fascicle 8	0.11	11	T8	S1
Fascicle 9	0.11	11	T9	S2

Table 4- 23 Morphometric parameters of iliocostalis lumborum pars lumborum

Muscle Name	Muscle PCSA (cm^2)	Maximum Muscle force with ($k=100N/cm^2$) in N	Origin	Insertion
Longissimus thoracis pars lumborum				
Fascicle 1	0.1	10	L1	L5
Fascicle 2	0.1	10	L2	L5
Fascicle3	0.1	10	L3	L5
Fascicle 4	0.1	10	L4	L5
Fascicle 5	0.1	10	L5	L5

The orientation of the muscle forces is important as the components of the forces change the path of the thrustline however, in literature most of the studies are not detailed enough. Macintosh and Bogduk, (1991) searched for the orientation of the fascicles of the erector spinae muscles.

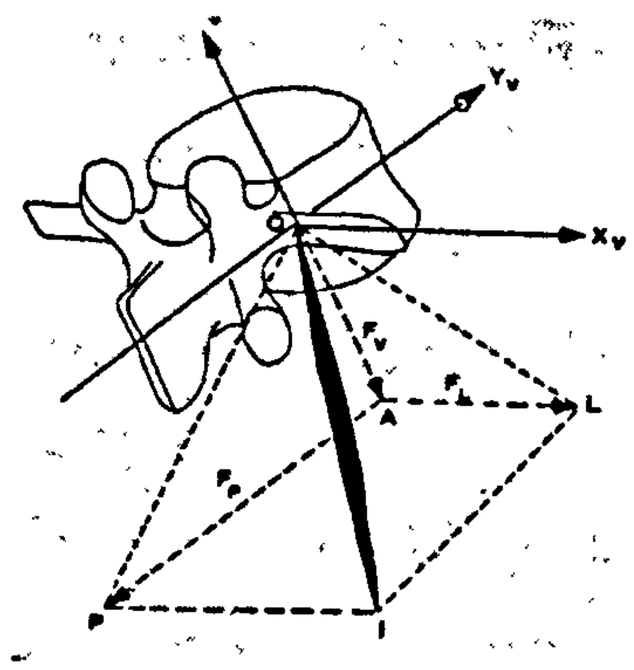


Figure 4- 10 A sketch of lumbar vertebra tilted in the sagittal plane on which coordinate axes have been superimposed to demonstrate the sagittal, coronal, transverse planes of the vertebra Macintosh and Bogduk, 1991.

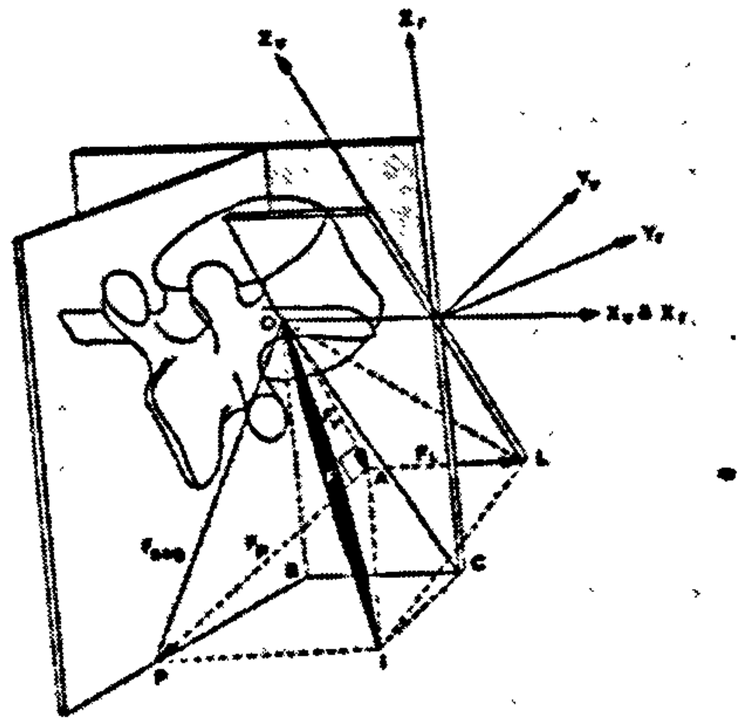


Figure 4- 11 The point 0 marks the origin of an obliquely oriented fascicle with an insertion at I acting on the vertebra (Macintosh and Bogduk, 1991)

The lines OA, AL, and AP depict longitudinal, lateral and posterior vectors of any force exerted by the fascicle along longitudinal, transverse and posterior axes of the vertebrae. In the thrustline model longitudinal and posterior force components are needed. Fp and Fv forces should be calculated for this purpose.

OP is the projected length of the fascicle. OA and AP can be constructed. The angle OAP is a right angle.

Angle POA = λ

Angle POI=μ

OP=OIcos μ

OP is the force component in the sagittal plane which is the force to be used in our model. In order to obtain absolute magnitude of force acting on this plane the estimated force value should be multiplied by the cos(μ). In the research of Macintosh and Bogduk (1991), lateral radiographs showed that fascicles of the longissimus thoracis pars thoracic and iliocostalis lumborum pars thoracis show a general counter of the thoracic vertebral column. Thus, their lateral angle is zero, indicating that they already apply a force only in the sagittal plane. The angle POA that they are making with the centre of the origion of the vertebral plane is given in the table below. In our code the angles of each vertebrae relative to the global coordinate system is already known, to calculate the angles of fascicles at the attachment points it is necessary to add the angles that the fascicles have with the centre of each vertebrae.

Table 4- 24 Fasiscle by origin for the longissimus thoracis pars thoracis and iliocostalis lumborum pars thoracis

Longissimus thoracis pars thoracis	Angle with the centre of vertebrae	Iliocostalis lumborum pars thoracis	Angle with the centre of vertebrae
T1	6	T5	7
T2	6	T6	8
T3	5	T7	8
T4	5	T8	8
T5	5	T9	8
T6	7	T10	9
T7	7	T11	8
T8	7	T12	4
T9	7		

Ilicostalis lumborum pars lumborum has four fascicles arising from L1-L4 transverse processes. For the longissimus thoracis pars lumborum five fascicles from the lumbar accessory and transverse processes insert into the posterior superior iliac. As seen in the tables below the fascicles show obliquity in the lateral plane. To calculate the force component in sagittal plane we need to have dot product with the force vector, after the multiplication we have the force in the sagittal plane. The orientation of the fascicle should be added to vertebral global angle in the code. For the forces transmitted in the iliocostalis lumborum pars thoracis and longissimus thoracis pars thoracis, the force calculated is already in the sagittal plane. Therefore there is no need to have a cross multiplication with cos0. However, the sagittal orientation of the fascicles is given with respect to the vertebrae centre. Their orientation changes with respect to the posture and needs to be embedded in the program for automation purposes. The magnitude of the force needs to be multiplied by two as the body is symmetric around the vertebra so that the values of force in the fascicles of the iliocostalis lumborum pars thoracis and longissimus thoracis pars thoracis is 12.5 N and 22 N respectively.

Table 4- 25 Fascicle orientation in lateral and sagittal planes for longissimus thoracis pars lumborum

Fasiscle by origin for the Longissimus thoracis pars lumborum	Angle with the centre of vertebrae	
	Lateral Angle	Sagittal Plane Angle
L1	20	4
L2	26	5
L3	33	9
L4	40	14
L5	46	27

Table 4- 26 Fascicle orientation in lateral and sagittal planes for iliocostalis thoracis pars lumborum

Fasiscle by origin for the Illiocostalis lumborum pars lumborum	Angle with the centre of vertebrae	
	Lateral Angle	Sagittal Plane Angle
L1	20	3
L2	24	5
L3	30	5
L4	38	15

For the Iliocostalis lumborum pars lumborum and longissimus thoracis pars lumborum, it is necessary to find out the magnitude of the force in the sagittal plane. Once the magnitude of the sagittal plane force is know, the angle of the fascicles needs to be calculated, the orientation of the vertebrae centres are added to the sagittal plane angle for global angle calculation of the fascicles.

Table 4- 27 Fascicle orientation in lateral planes and magnitude of force in sagittal plane for iliocostalis thoracis pars lumborum

Longissimus thoracis pars lumborum	Angle with the centre of vertebrae	Magnitude of Force component in the sagittal plane (N)	Resultant force in the sagittal plane (N)
L1	20	9.40	18.80
L2	26	8.99	17.98
L3	33	8.399	16.77
L4	40	7.66	15.32
L5	46	6.94	13.89

Table 4- 28 Fascicle orientation in lateral planes and magnitude of force in sagittal plane for iliocostalis lumborum pars lumborum

Illiocostalis lumborum pars lumborum	Angle with the centre of vertebrae	Magnitude of Force component in the sagittal plane (N)	Resultant force in the sagittal plane (N)
L1	20	23.49	46.98
L2	24	22.84	45.68
L3	30	21.65	43.30
L4	38	19.70	39.40

Splenius Muscles

Splenius: Capitis and Cervicis

The Splenius muscle is at the back of the neck and upper part of the thoracic region. It arises as a single muscle from the last cervical vertebrae C7 and the upper six thoracic vertebrae (T1-T6). From this origin the muscle precedes into two sections, the Splenius

capitis and the Splenius cervicis. This muscle works in conjunction with the semispinalis capitis to extend the head (Gurumoorthy and Twomey, 2000).

Table 4- 29 Points of attachments of the Splenius Capitis and Splenius Cervicis

Parts	Origin	Insertion
Splenius Capitis	The spinous processes of C7 and T2	The superior nuchal line and mastoid process.
Splenius Cervicis	The spinous process of T3	The posterior tubercles of the transverse processes of the upper three cervical vertebrae (C1-C3).

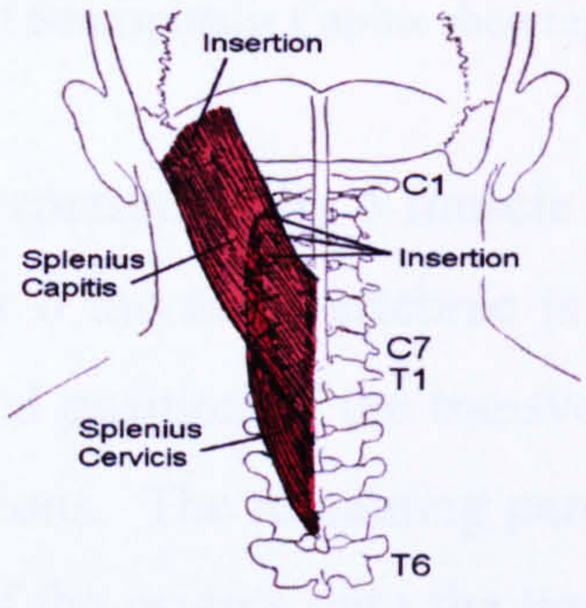


Figure 4- 12 Anatomical drawing of the Splenius capitis and cervicis showing the points of attachment to the head and spine. Splenius muscle is represented by 5 muscle elements on each side of the neck (Basmajian, 1921).

Table 4- 30 Morphometric parameters of Splenius Capitis and Cervicis

Muscle Name	Muscle PCSA (cm^2)	Maximum Muscle force with ($k=100N/cm^2$) in N	Origin	Insertion
Splenius Capitis				
Fascicle 1	1.57	314	T2	C0
Fascicle 2	1.57	314	C7	C0
Splenius Cervicis				
Fascicle 1	0.48	96	T3	C1
Fascicle 2	0.48	96	T3	C2
Fascicle 3	0.48	96	T3	C3

Transversospinal Muscles

Semispinalis Capitis

The size and length of this muscle make it one of the strongest muscles among the post-vertebral group of neck muscles. It has origins on the articular processes of the 4^{th} to 6^{th} cervical vertebrae as well as to the transverse processes of the upper 6 thoracic

vertebrae and the 7th cervical vertebra. Acting together with the semispinalis capitis muscles produces extension in the atlanto-occipital joints.

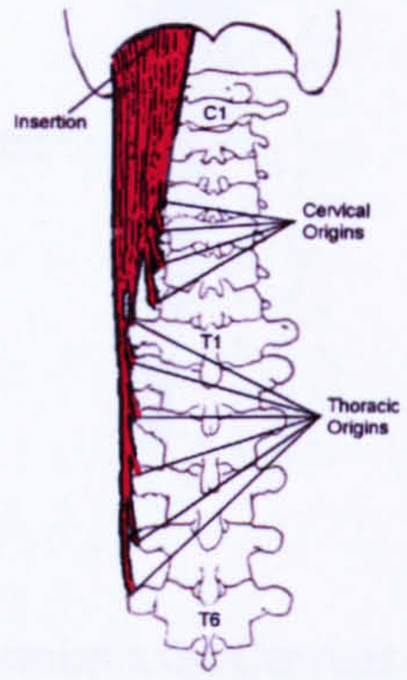


Figure 4- 13 Anatomical drawing of Semispinalis Capitis showing origins and insertions of the muscle (Basmajian, 1921).

The Semispinalis Capitis is represented by 5 muscle elements. The section of muscle that has origins on the upper 6 thoracic vertebrae is represented by a single element with an origin at the estimated position of the transverse process of T3 based on van-Lopik, (2004) thesis assumptions. The remaining part of the muscle is divided up into four elements one for each of the origins onto the transverse processes of C4-C7. The morphometric parameters of the semispinalis capitis muscle elements are shown in table Kamibayashi and Richmond (1998).

Table 4- 31 Morphometric parameters of Semispinalis Capitis

Muscle Name	Muscle PCSA (cm^2)	Maximum Muscle force with (k=100N/cm2) in N	Origin	Insertion
Semispinalis Capitis				
Fascicle1	1.07	214	C4	C0
Fascicle 2	1.07	214	C5	C0
Fascicle 3	1.07	214	C6	C0
Fascicle 4	1.07	214	C7	C0
Fascicle 5	1.07	214	T3	C0

Semispinalis Cervicis

The semispinalis cervicis arises from the transverse processes of the upper 5 thoracic vertebrae and inserts onto the spinous processes of C2 through C6. The semispinalis thoracis has origins on the transverse processes on the lower thoracic vertebrae and insert onto the spinous processes of the first 4 thoracic vertebrae and onto the last 2 cervical vertebrae.

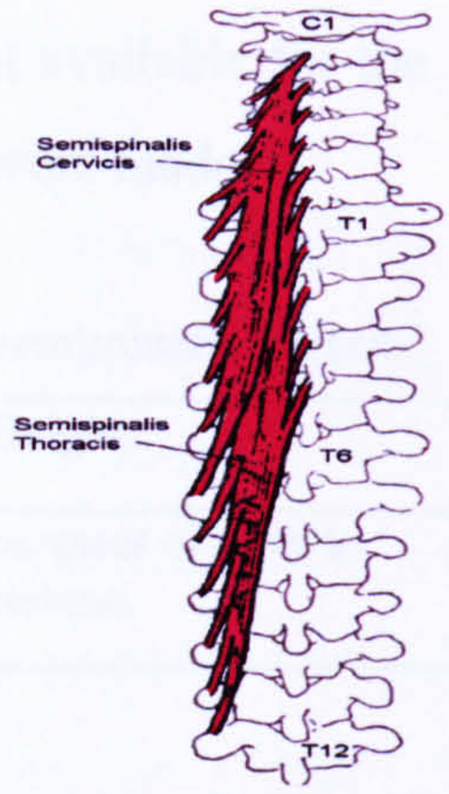


Figure 4- 14 An anatomical drawing of the Semispinalis Cervicis and Thoracis (Basmajian, 1921).

In the model this muscle group is divided into 6 muscle elements on each side of the neck. The first element has its origin on the transverse process of T1 and ascends to insert onto the spinous process of C2, the remaining elements each have origin on the transverse processes of the next thoracic vertebrae down inserting on the spinous process of the 5th vertebrae superior to the vertebrae of origin, i.e. T1 goes to C2, T2 goes to C3, T3 goes to C4 and so on. The position of the transverse processes of the thoracic vertebrae below the level of T1 are estimated from anatomical drawings and quantitative data found in the literature (Adam-Rouilly, 1992; Panjabi et al., 1991) The morphometric values used for the muscle elements can be seen in the table.

Table 4- 32 Morphometric parameters of Semispinalis Cervicis.

Muscle Name	**Muscle PCSA (cm^2)**	**Maximum Muscle force with (k=100N/cm2) in N**	**Origin**	**Insertion**
Semispinalis Cervicis				
Fascicle1	0.13	26	T1	C2
Fascicle 2	0.26	52	T2	C3
Fascicle 3	0.38	76	T3	C4
Fascicle 4	0.80	160	T4	C5
Fascicle 5	1.00	200	T5	C6

Semispinalis thoracis

Semispinalis thoracis consists of thin fasiculi between long tendons. Semispinalis thoracis originates from the transverse processes of the sixth to tenth thoracic vertebrae. Semispinalis thoracis inserts onto the spines of the superior four thoracic and inferior two cervical vertebrae. Semispinalis thoracis extends the thoracic and cervical vertebral

column. Data in literature was not available for the PCSA of this muscle; adjustments with respect to the other muscles were made.

Table 4- 33 Points of attachments of the semispinalis thoracis

Parts	Origin	Insertion
Semispinalis thoracis	The transverse processes of sixth to tenth thoracic vertebrae.	superior four thoracic and inferior two cervical vertebrae

Table 4- 34 Morphometric parameters of Semispinalis Thoracis.

Muscle Name	Muscle PCSA (cm^2)	Maximum Muscle force with (k=100N/cm2) in N	Origin	Insertion
Semispinalis Thoracis				
Fascicle1	0.15	30	T6	C7
Fascicle 2	0.28	56	T7	C6
Fascicle 3	0.40	80	T8	T1
Fascicle 4	0.90	180	T9	T2
Fascicle 5	1.00	200	T10	T3

Multifidus

Multifidus originates on the posterior sacrum from the fourth sacral foramen, from the aponeurosis of erector spinae, the posterior superior iliac spine and dorsal sacro-iliac ligaments, from all lumbar mamillary processes, all thoracic transverse processes and the articular processes of the lower four vertebrae. For this purpose it is best to divide the multifidus with respect to regions, cervical, thoracic, and lumbar. Multifidus inserts into the length of the spine of the vertebrae above. The deepest fibres insert into the vertebrae directly above. The intermediate fibres insert into the second or third vertebrae above. The superficial fibres insert into the third or fourth vertebrae above. Multifidus stabilises adjoining vertebrae, and controls their movement during movement of the whole vertebral column. This allows more effective action of the long back muscles. In theory it can also extend, laterally flex and rotate the vertebral column. In the cervical and thoracic region muscle they arise from the articular and transverse processes of the vertebrae, insert into the spinous process of the second, third and forth vertebrae above as well as connecting two adjacent vertebrae (Gray, 1980). The role of the Multifidus is thought to be in aiding extension, lateral flexion and rotation of the spinal column.

Cervical Multifidus

In the model, the first segment that makes attachment to the cervical spine has its origin on the transverse processes of T4 and inserts into the spinous process of C7. The next takes its origin on the transverse processes of T3 and splits to insert onto the spinous processes of C7 and C6; this is represented by two muscle elements in the model. From T2 transverse process two elements insert into C6 and C5 spinous processes. This pattern continues as far as C5 where one element with origin on the articular process ascends obliquely inwards and upward to insert onto the spinous process of C2. In total there are 12 muscle elements representing the Multifidus muscle group on each side of the neck, the origin and insertion of each can be seen in table 4.35. There was no morphometric data available for the Multifidus muscle so the values were estimated based on other similar sized muscles in the neck and on other researches decisions.

Table 4- 35 Morphometric parameters of Cervical Multifidus

Muscle Name	Muscle PCSA (cm^2)	Maximum Muscle force with (k=100N/cm2) in N	Origin	Insertion
Multifidus				
Fascicle 1	0.15	30	T4 transverse process	C7 spinous process
Fascicle 2	0.15	30	T3 transverse process	C7 spinous process
Fascicle 3	0.15	30	T3 transverse process	C6 spinous process
Fascicle 4	0.15	30	T2 transverse process	C6 spinous process
Fascicle 5	0.15	30	T2 transverse process	C5 spinous process
Fascicle 6	0.15	30	T1 transverse process	C5 spinous process
Fascicle 7	0.20	40	T1 transverse process	C4 spinous process
Fascicle 8	0.20	40	C7 transverse process	C4 spinous process
Fascicle 9	0.40	80	C7 transverse process	C3 spinous process
Fascicle 10	0.40	80	C6 transverse process	C3 spinous process
Fascicle 11	1.10	220	C6 transverse process	C2 spinous process
Fascicle 12	1.30	260	C5 articular process	C2 spinous process

Thoracic Multifidus

Table 4- 36 Morphometric parameters of Thoracic Multifidus

Muscle Name	Muscle PCSA (cm^2)	Maximum Muscle force with (k=100N/cm^2)in N	Origin	Insertion
Thoracic Multifidus				
Fascicle1	0.4	80	T8 spinous process	L1 mamillary process
Fascicle2	0.4	80	T9 spinous process	L1 mamillary process
Fascicle3	0.4	80	T10 spinous process	L1 mamillary process
Fascicle4	0.4	80	T9 spinous process	L2 mamillary process
Fascicle5	0.4	80	T10 spinous process	L2 mamillary process
Fascicle6	0.4	80	T11 spinous process	L2 mamillary process
Fascicle7	0.4	80	T10 spinous process	L3 mamillary process
Fascicle8	0.4	80	T11 spinous process	L3 mamillary process
Fascicle9	0.4	80	T12 spinous process	L3 mamillary process
Fascicle10	0.4	80	T11 spinous process	L4 mamillary process
Fascicle11	0.4	80	T12 spinous process	L4 mamillary process
Fascicle12	0.4	80	T12 spinous process	L5 mamillary process

Lumbar Multifidus

The principal fascicles of the lumbar multifidus arise from the lateral surface of the caudal edge of the spinous process by way of common tendon from the tubercle of the spinous process. The caudal attachments of these fascicles are to mamillary processes and to certain areas on the iliac crests and dorsal surface of the sacrum (Macintosh and Bogduk , 1986).

Multifidus is believed to function as a stabilizer during rotation. Oblique abdominal muscles are believed to produce axial rotation. However, because of their orientation, they must produce flexion moment. Rotation by the abdominal muscles occurs at the cost of concomitant anterior sagittal rotation (flexion). This unwanted by product could be balanced by contraction of the erector spinae, since both the erector spinae and oblique abdominals are active in rotation. In addition to the erector spinae, the lumbar multifidus, through its downward vector, can act directly on the lumbar vertebral column and produce anti-flexion (extension) moment needed to balance the anterior sagittal ration generated by contraction of the internal and external abdominal muscles.

Table 4- 37 Morphometric parameters of Lumbar Multifidus (Macintosh and Bogduk , 1986).

Muscle Name	Muscle PCSA (cm^2)	Maximum Muscle force with (k=100N/cm^2)in N	Sagittal angle In Degrees	Lateral Angle In Degrees	Origin	Insertion
Lumbar Multifidus						
Fascicle 1	0.40	80	14.8	86.8	L1 spinous process	L4 mamillary process
Fascicle 2	0.42	84	15	85.4	L1 spinous process	L5 mamillary process
Fascicle 3	0.39	78	18.8	85.8	L2 spinous process	L5 mamillary process
Fascicle 4	0.54	108	23.2	88.4	L3 spinous process	L5 mamillary process
Fascicle 5	0.47	94	15.6	93.6	L4 spinous process	L5 mamillary process

Regardless of any action that it may have on the vertebrae to which it is attached, the lumbar multifidus is capable of producing compressive forces on vertebrae interposed between the attachments of any of its fascicles. It lies behind the lumbar lordosis; it is expected to act as a bowstring. The bowstring effect occurs when tension is produced by muscles can no longer be translated into tension along the anterior longitudinal ligament and anterior portions of the discs of interposed vertebrae and the posterior portions of the interposed discs would be compressed.

Superficial Back Musculature

Trapezius

The trapezius is a very powerful muscle that aids in stabilising the head and cervical column. When the trapezius muscles on both sides of the neck contract simultaneously they extend the cervical spine. (Kapandji, 1974). It starts from the inner third of the superior curved line of the occipital bone, from the spinous processes of all the cervical vertebrae spinous processes (C1-T12) and those of all the dorsal vertebrae (Gray, 1980). The upper section of the trapezius known as the clavotrapezius, with origins above the level of C7, inserts onto the clavicle. The individual muscle fascicles to posterior border of the distal third of the clavicle bone, such that the fascicle from the superior nuchal line assumes the most anterior and medial attachment, followed in sequence by the fascicle from the spinous processes of the descending vertebrae, with the fibres from C6 inserting into the distal corner of the clavicle as far as the acromioclavicular joint (Johnson *et al.* 1994). The middle part of the trapezius (lower part in model), also known as the acromiotapezius, with origin on the C7 spinous process inserts on to the scapula on the inner border of the acromion. It elevates scapula and retracts scapula.

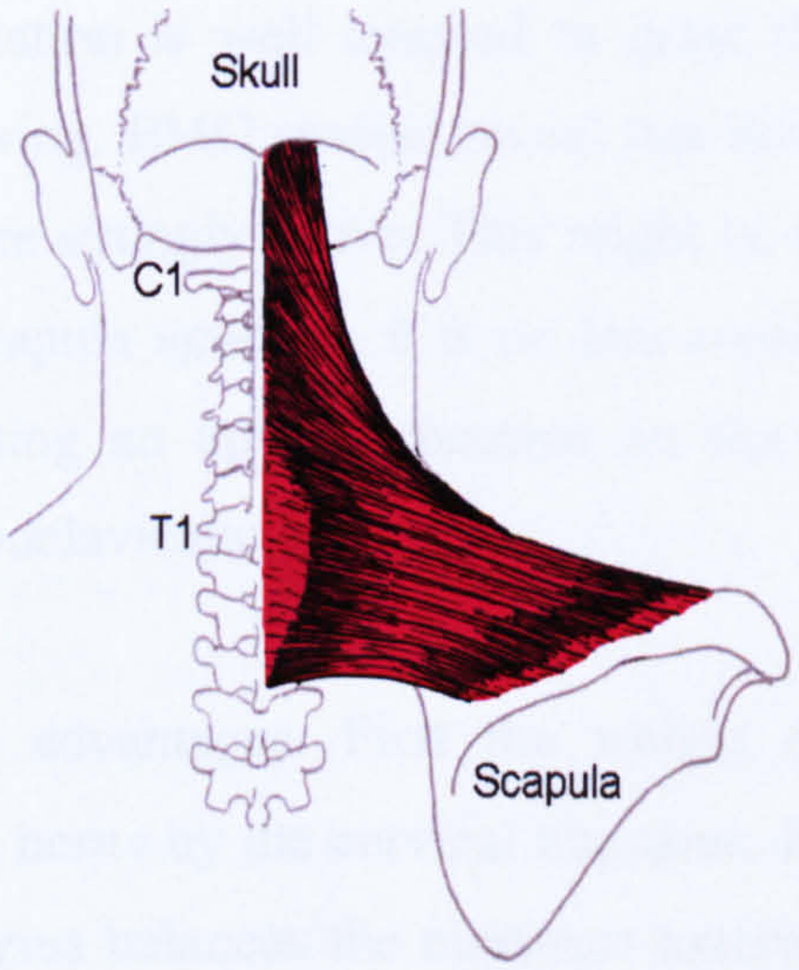


Figure 4- 15 An anatomical drawing of the upper section of the Trapezius muscle, showing attachments to the spine, skull and scapula (Basmajian, 1921).

The fibers from the superior nuchal line assume any major degree of downward orientation. The other fibres of the nuchal portion of trapezius pass more transversely to

the clavicle. The fascicles from C7 to T1 are almost transverse in orientation with the scapula in neutral portion.

The nuchal portion of trapezius is not disposed to elevate the scapula. Only the fibers from the superior nuchal line might be accorded some capacity to apply vertical forces to the clavicle. Its fibres act on the clavicle and not on the scapula. When they reach the scapula, the fibres approach the clavicle in almost a horizontal plane. Whatever, upward inclination they might have would be dissipated in the cervical fascia before the fibres reach the clavicle.

The transverse orientation of the nuchal fibres of the trapezius and those from C7 and T1 spinous processes dictates that in the horizontal plane action of the upper and middle trapezius is to draw clavicle, acromion, and spine of the scapula backward and medially. This action would be aided by thoracic fibres which individually and collectively have a transverse orientation in addition to their upward orientation

The nuchal fibers of trapezius have no direct action on the scapula because they attach to the clavicle. But they can move the scapula indirectly through the acromioclavivular joint. Their transverse orientation is well situated to draw the clavicle and scapula backwards in pulling and rowing. EMG studies reveal that during the elevation of the scapula the upper trapezius are strongly active. This might be interpreted as indicating that the trapezius pulls the scapula upwards, it is no less consistent with the trapezius achieving elevation by exerting an upward moment on the clavicle at the cost of compression loads at the sternoclavicular joint.

This mechanism offers two advantages. First the weight of the upper limp and anyweight carried by it is not borne by the cervical trapezius. Because of its transverse orientation the cervical trapezius balances the moments exterted by this load. But the vertical force exerted by the weight is transferred to the sternoclavicular joint. Consequently, the trapezius does not need to be anchored to the cervical vertebrae, which explains why the ligamentum nuchae does not attach to the C2-C6 spinous process. To balance moments, all that trapezius requires is an attachment site that resists lateral displacement, this is provided by the superficial funicular portion of the ligamentum nuchae.

The second advantage of this mechanism is that it avoids compressive loads exerted on the cervical spine by the upper limb. The strongest fascicles of trapezius arise from C6 and C7 but are basically transverse in orientation and would contribute little compressive load to the neck. The only compressive loads exerted by trapezius would be those resulting from the obliquity of its uppermost fibres, but those with the greatest obliquity and hence the greatest capacities to exert compressive loads also happen to be the smallest component of trapezius.

In essence by exerting only transverse loads on the ligamentum nuchae, the cervical trapezius spares the cervical spine from compressive loads and transfers the weight of the upper limb and any loads carried by it to the sternoclavicular joint. In the model the trapezius muscle is split into 8 separate muscle elements. Johnson *et al.* (1994) reported the PCSA values.

Table 4- 38 Morphometric parameters of Trapezius.

Muscle Name	Muscle PCSA (cm^2)	Maximum Muscle force with ($k=100N/cm^2$) in N	Origin	Insertion
Trapezius Acromiotrap Fascicle 1	2.20	440	C7spinous process	Scapula
Clavotrap				
Fascicle 1	0.77	154	C6spinous process	Clavicle
Fascicle 2	0.77	154	C5spinous process	Clavicle
Fascicle 3	0.77	154	C4spinous process	Clavicle
Fascicle 4	0.23	46	C3spinous process	Clavicle
Fascicle 5	0.23	46	C2spinous process	Clavicle
Fascicle 6	0.23	46	C1spinous process	Clavicle
Fascicle 7	0.30	60	C0spinous process	Clavicle

Levator Scapulae

The Levator Scapulae is situated at the back and side of the neck. Symmetrical contraction of the Levator Scapulae can assist in extension of the cervical spine

The Levator Scapulae is represented by four muscle fascicles. They have a single insertion positioned relative to T1 at the approximate location of the superior angle of the spine of the scapula estimated from anatomical drawings and descriptions (Adams-Rouilly, 1992; Gray, 1980.).

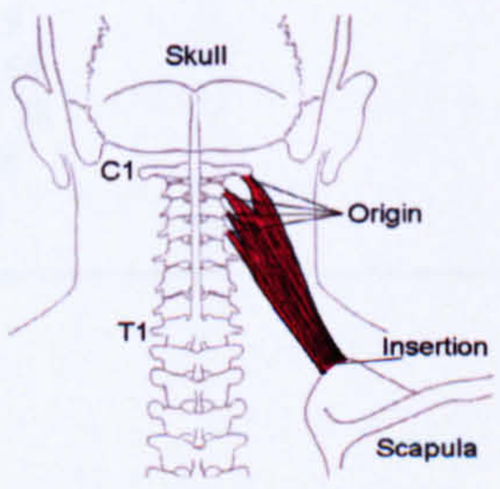


Figure 4- 16 Anatomical drawing of levator scapulae (Basmajian, 1921).

Table 4- 39 Points of attachments of levator scapulae

Parts	Origin	Insertion
Levator scapulae	The transverse processes of the upper four cervical vertebrae, C1-C4.	The superior border of the medial scapula

Table 4- 40 Morphometric parameters of the Levator Scapulae.

Muscle Name	Muscle PCSA (cm^2)	Maximum Muscle force with ($k=100N/cm^2$) in N	Origin	Insertion
Levator Scapulae				
Fascicle 1	0.56	112	C1 transverse process	Scapula
Fascicle 2	0.56	112	C2 transverse process	Scapula
Fascicle 3	0.56	112	C3 transverse process	Scapula
Fascicle 4	0.56	112	C4 transverse process	Scapula

Latissimus dorsi

It originates from the spinous process of T7-L5, upper sacral segments, iliac crest and lower 3 or 4 ribs. It inserts into lateral lip of the intertubercular groove of humerus. It is thought to help adduction, and medial rotation of humerus, extension from flexed position and downward rotation of scapula. The morphometric parameters of latissimus dorsi were obtained from Marras *et al,* (2001) by magnetic resonance imaging scans.

Table 4- 41 Points of attachments of latissimus dorsi

Parts	Origin	Insertion
Latissimus dorsi	Spinous process of T7-L5, upper sacral segments, iliac crest and lower 3 or 4 ribs	Lateral lip of the intertubercular groove of humerus

Table 4- 42 Morphometric parameters of Latissimus dorsi

Muscle Name	Muscle PCSA (cm^2)	Maximum Muscle force with ($k=100N/cm^2$) in N	Origin	Insertion
Latissimus dorsi				
Fascicle 1	13.5	27	T8	Humerus
Fascicle 2	11.51	23	T9	Humerus
Fascicle 3	9.77	18.54	T10	Humerus
Fascicle 4	8.45	16.9	T11	Humerus
Fascicle 5	7.34	14.68	T12	Humerus
Fascicle 6	5.39	10. 78	L1	Humerus
Fascicle 7	3.44	6.88	L2	Humerus
Fascicle 8	1.45	2.9	L3	Humerus

4.1.3 Lumbar Musculature

In a quantitative anatomy of the lumbar musculature study, Stokes and Morse, (1999) represent the oblique abdominal muscles by broad curved sheets of muscles divided into a set of 6 component parts, each represented by a single vector with individualised activation. The geometry is assumed to be symmetrical about the mid-sagittal plane. In their study transverses muscle was neglected because it is the smallest of the abdominal muscles, and its line of action is much curved. For all these reasons, transversus muscle is also excluded in this work also. The total PCSA between the six component vectors, the points of intersection of the six vectors with each image section were located. The normals to the lines passing through these points were calculated. Their intersections with the inside and outside outlines of the corresponding muscle were determined. These normal lines subdivided the total area into a set of partial areas. The effective PCSA of each of the six muscle components was obtained as its partial volume divided by the length of the respective vector (Stokes and Morse, 1999).

Quadratus Lumborum

Quadratus lumborum is one of the muscles of the posterior abdominal wall. One each side, it originates from the inferior border of the twelfth rib. Descending and broadening, it inserts into the transverse processes of the first to fourth lumbar vertebrae, posterior third of iliac crest, iliolumbar ligament in continuity with the iliac crest. Quadratus lumborum has the function of extension of the lumbar vertebral column upon bilateral contraction (Stokes and Morse, 1999).

Table 4- 43 Points of attachments of quadratus lumborum

Parts	Origin	Insertion
Quadratus lumborum	Posterior part of iliac crest	Transverse process of upper 4 lumbar vertebrae

The morphometric parameters of quadratus lumborum were obtained from Marras *et al,* (2001) by magnetic resonance imaging scans.

Table 4- 44 Morphometric parameters of Quadratus Lumborum

Muscle Name	Muscle PCSA (cm^2)	Maximum Muscle force with (k=100N/cm2) in N	Origin	Insertion
Quadratus lumborum				
Fascicle1	2.5	500	L1	Iliac crest
Fascicle 2	3.04	608	L2	Iliac crest
Fascicle 3	5.2	504	L3	Iliac crest
Fascicle 4	3.56	702	L4	Iliac crest

Psoas Major

The psoas major is well known as a flexor of the hip. Psoas arises from lumbar spine. Electromyography studies show that the psoas is active during upright standing and during forward bending and lifting. Psoas major might function as a stabilizer. Others have proposed that psoas controls the lumbar lordosis and balances the bodyweight in relaxed upright standing.

By inspection, it is a homogenous muscle with a continuous attachment to the vertebral column at one end, tapering to a single, round tendon at the other end. By dissection, it consists of a series of overlapping segmental fascicles. Each fascicle consists of bundles of fleshly fibres that arise from a discrete area on the lumbar vertebral column centred on either an intervertebral disc or a transverse process. Five fascicles arise from the T12-L1 to L4-L5 discs and five fascicles arise from the L1- L5 transverse process. Additionally a fascicle arises from transverse processes. At each segmental level, those fascicles centre on the intervertebral discs and arise from the posterior seven-eights or so of the lateral surface of the discs and from the lateral surface of the vertebral bodies immediately above and below the disc. Those fascicles from the L1-L2 to L4-L5 discs centre just posterior to midpoint of the disc. The fascicles from the L3 to L5 transverse process occupy the medial three-quarters or so of the anterior surface of the transverse process while the fascicles from L2 to L1 occupied only the medial one quarter of the transverse process (Bogduk et al, 1991).

From above downwards the fascicles assume a progressively less steep orientation with respect to the long axis of the vertebral column in anterior posterior and lateral projection (Bogduk et al, 1991).

Table 4- 45 Morphometric parameters of Psoas Major. (Bogduk et al, 1991)

Muscle Name	Muscle PCSA (cm^2)	Maximum Muscle force with ($k=100N/cm^2$)in N	Origin	Insertion
Psoas major				
Fascicle 1	2.11	420	L1 vertebral body	Femur
Fascicle 2	0.61	120	L1 transverse process	Femur
Fascicle 3	2.11	420	L1-L2 inter-vertebral disk	Femur
Fascicle 4	1.01	200	L2 transverse process	Femur
Fascicle 5	1.61	320	L2-L3 intervertabral disk	Femur
Fascicle 6	1.73	340	L3 transverse process	Femur
Fascicle 7	1.91	360	L3-L4 intervertabral disk	Femur
Fascicle 8	1.2	240	L4 transverse process	Femur
Fascicle 9	1.19	220	L4-L5 intervertabral disk	Femur
Fascicle 10	0.36	60	L5 transverse process	Femur
Fascicle 11	0.79	140	L5 vertebral body	Femur

Rectus abdominis

Rectus means straight, rectus muscles are parallel muscles whose fibers generally run along the long axis of the body. The rectus abdominis is positioned vertically at the front of the abdomen. It attaches from the symphasis pubis and pubic crest and runs to the xiphoid process and 5, 6, 7^{th} ribs, being broader superiorly. Of the three noticeable tendinous intersections of this muscle, one is level with the umbilicus; one is midway between the two. Each rectus muscle is enclosed within a fiborous sheath changes at a level midway between the pubic symphasis and the umbilicus. It compresses the abdomen, supports abdominal viscera, active in forced expiration, and flexes pelvis and vertebral column. Rectus abdomen PCSA was calculated as 0.0567 cm^2

Table 4- 46 Points of attachment of rectus abdominis (Stokes and Gardner-Morse, 1999)

Parts	Origin	Insertion
Rectus abdominis	Medial tendon from pubic symphysis, lateral tendon from crest of pubis.	Anterior surface of xiphoid process and surface of costal cartilages of 5^{th}, 6^{th} and 7^{th} ribs.

Obliquus internus abdominis

Obliquus internus abdominis lies beneath the obliquus externus abdominis, and is less bulky. Obliquus internus abdominis originates from the lateral two-thirds of the grooved upper surface of the inguinal ligament, the anterior two-thirds of the intermediate line of the ventral segment of the iliac crest, and from the thoracolumbar fascia. Obliquus internus abdominis' posterior fibres insert into the inferior borders and

tips of the lower three or four ribs and their cartilages, being continuous with the intercostales interni. The upper fibres form a short, free super medial border. The upper fibres attach to the cartilages of the seventh, eighth and ninth ribs. The intermediate fibres diverge and end as an aponeurosis. The upper two-thirds splits at the lateral border of the rectus abdominus into two laminae, and pass around it, re-joining in the linea alba. The lowest fibres, from the inguinal ligament, arch downward and medially across the spermatic cord in the male and round ligament of the uterus in the female. They then become tendinous and insert into the aponeurosis of the transversus abdominus to the crest and medial part of the pecten pubis, forming the conjoint ligament (falx inguinalis).Obliquus internus abdominus flexes the lumbar vertebral column.

Obliquus internus abdominus rotates the lumbar vertebral column to the ipsilateral side.

Table 4- 47 Points of attachment of internal oblique (Stokes and Gardner-Morse, 1999)

Parts	Origin	Insertion
Internal oblique	Upper surface of the inguinal ligament, the anterior two-thirds of the intermediate line of the ventral segment of the iliac crest, and from the thoracolumbar fascia	Obliquus internus abdominis' posterior fibres insert into the inferior borders and tips of the lower three or four ribs and their cartilages

Table 4- 48 Morphometric parameters of internal oblique (Stokes and Gardner-Morse, 1999)

Muscle Name	Muscle PCSA (cm^2)	Maximum Muscle force with (k=100N/cm2) in N
Internal oblique		
Fascicle1	0. 0185	2.7
Fascicle 2	0. 0224	4.48
Fascicle 3	0. 0226	4.52
Fascicle 4	0.0267	3.34
Fascicle 5	0.0235	4.7
Fascicle 6	0.0207	4.14

The external oblique

It is positioned on the anterolateral aspect of the abdomen, with its fibers running downward and medially. It attaches from the outer borders of the lower eight ribs and then passes toward the midline. The muscle interdigitates with the serratus anterior and latissimus dorsi. The lateral fibres are almost vertical and attach to the iliac crest, while the medial fibers attach into the rectus sheath. The lower border of the muscle aponeurosis passes between the pubic tubercle and the anterior superior iliac spine to form the inguinal ligament.

Table 4- 49 Points of attachment of external oblique (Stokes and Gardner-Morse , 1999)

Parts	Origin	Insertion
External oblique	the outer borders of the lower eight ribs and then passes toward the midline.	The lateral fibres are almost vertical and attach to the iliac crest, while the medial fibers attach into the rectus sheath

Table 4- 50 Morphometric parameters of external oblique (Stokes and Gardner-Morse , 1999)

Muscle Name	Muscle PCSA (cm^2)	Maximum Muscle force with (k=100N/cm2) in N
External oblique		
Fascicle1	0. 0196	2.92
Fascicle 2	0. 0232	4.64
Fascicle 3	0. 0243	4.83
Fascicle 4	0.0234	4.68
Fascicle 5	0.0273	5.46
Fascicle 6	0.0397	5.94

4.2 Discussion

One of the basic assumptions in the model is that the PCSA's of the muscles do not change with the posture. The values used in the tables above are the results from medical imaging studies mostly. Because of the constraints due to the physical design of computerized tomography, and magnetic resonance imaging equipment, the PCSA values from subjects are obtained when the subjects are oriented in a supine or prone posture.

Many manual material handling activities like lifting involves the flexion of torso, some evidence suggest that torso flexion alters the muscle geometry of the lumbar back muscles (Tvait et al., 1994). Tvait et al. (1994), utilizing MRI reported that the CSA of the lumbar erector mass from subjects in a supine posture decreased when the subjects voluntarily decreased their lumbar curvature. However, they did not quantify the lumbar curvature that corresponded to the change in the CSA, nor could they investigate the effect of torso flexion and the impact on lumbar muscle CSA due to the physical design of the MRI. For this purpose, in a research conducted by Jorgensen et al (1999), where the maximum CSA of the muscle in the lumbar spine and at which postures occurs is investigated, they used MRI scans of people at the angles of neutral, 15, 30 and 45 of torso flexion. This flexion angle is defined by a line angle connecting the S1 and C7. The axial scans were located thorough each of the five lumbar intervertebral disc spaces for each of the four torso flexion angles and oriented parallel

to each intervertebral discs. For the fascicle orientation of the intermediate postures, the sagittal plane fascicle orientation was assumed by a linear relationship. They observed that the maximum lumbar back muscle ACSA occurred in the neutral posture, between the L3/L4 and L4/L5 level. However, these values did not vary significantly as a function of sagittal plane torso posture. The areas of L4/L5 and L5/S1 intervertebral levels decreased by different percentages as the torso moved from neutral to 45 degrees of flexion in the sagittal plane, suggesting that the lengthening of the lumbar back muscles may not be uniform throughout the muscle during torso flexion. These results indicate that the change in the cross sectional areas of the muscles with do not change significantly with the torso flexion (Jorgensen et al, 1999).

This research uses muscle data in the neutral position having the greatest cross sectional area. As the decrease of PCSA trend in the muscles is unknown, it is not appropriate to include the change of area with torso flexion. Although with the flexion of the spine, the muscle cross section area thereby the force exerted by the muscles decreases, the change in the force magnitude is unlikely to change the results significantly.

The other assumption related to cross sectional areas used for the muscles is that there is no difference between the genders both the females and males have the same cross sectional area. It is possible to expect variations in muscle size and direction of the muscles (females have wider pelvis). The differences from males with respect to muscle size may alter the magnitude of the loading and the loading paths on the spine. However, there is very limited study in literature to represent the differences between genders covering all the muscles. Marras et al, 2001 investigated the muscle cross sectional area differences with respect to genders. But the muscles inspected in their research involved only lattissimus dorsi, erector spinae, external oblique, internal oblique, and quadrotus lumborum. As the number of the muscle groups introduced is more than 30 in this thesis. The level of the detail for the fascicles of each muscle group is not comparable with the level of the detail with the study of Marrras et al, 2001. For this purpose the same cross sectional area for both males and females is used in this thesis, although the males show higher cross sectional area in general. However, to analyse this effect, the code written can be changed to introduce the muscles in the same way as Marras et al defined and investigate the gender differences for the specific muscle groups that they introduced in their study.

4.3 Physiology of Ligaments

Ligaments differ from the other soft tissues of the spine in that they are required to be stretched before they produce a force and they buckle under compression (A.A White III & M.M Panjabi, 1990.). Some ligaments are capable of resisting tensile force in a range of directions due to their fibre arrangement and orientation. In particular, the stiffness of a ligament depends on the direction in which its collagen fibrils are oriented. A ligament has only appreciable stiffness if its collagen fibrils are strained when the tissue is stretched. The restoring stress in the strained fibrils then balances the applied tensile stress so that they reinforce the tissue. A range of techniques is used to investigate ligament composition and structure. Several of these techniques have been applied to ligaments while they have been subjected to controlled strains (D.W.L Hukins et al., 1990).

Mechanical tests allow the stress associated with the applied strains to be measured. Tissue strains are defined by posture and can be determined by measuring their lengths without knowing the forces exerted by the musculature. From their positions in the spine, that the anterior longitudinal ligament is stretched during extension and that flexion stretches the posterior ligament and ligamenta flava. Given the position of the flexion axis, geometry dictates that during flexion the degree of stretching is in the following order:

Stretching of posterior longitudinal ligaments< Stretching of ligamentum flavumn (D.W.L Hukins et al., 1990).

These expectations are confirmed by measurements of ligament lengths in cadaveric specimens during controlled bending (D.W.L Hukins et al., 1990). These results are obtained from ligaments in segments of lumbar spine removed from cadavers. However, frozen tissues fail at an earlier rate due to formation of ice crystals, so these results are not the same as the fresh cadavers.

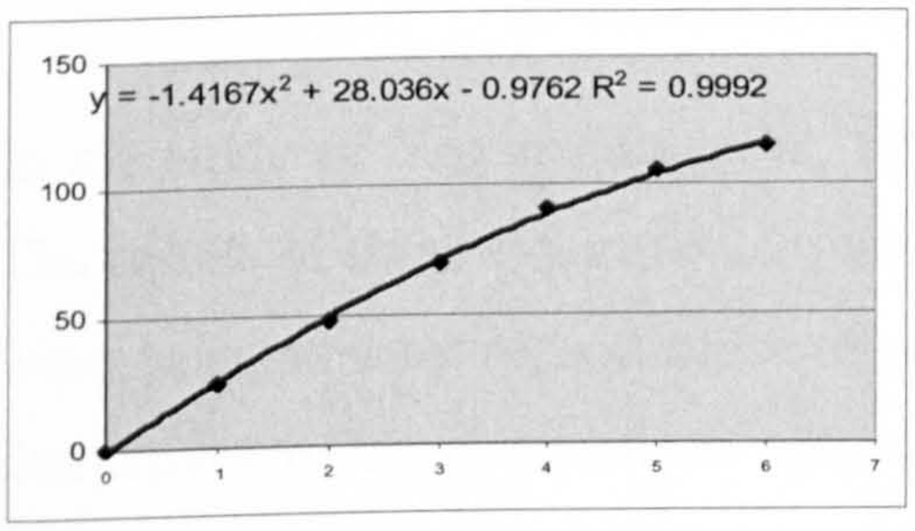
4.3.1 Ligaments at Cervical Region in the model

It is observed that there are plenty of studies to investigate the properties of ligaments especially in the cervical region. For this purpose, it is considered to include the results

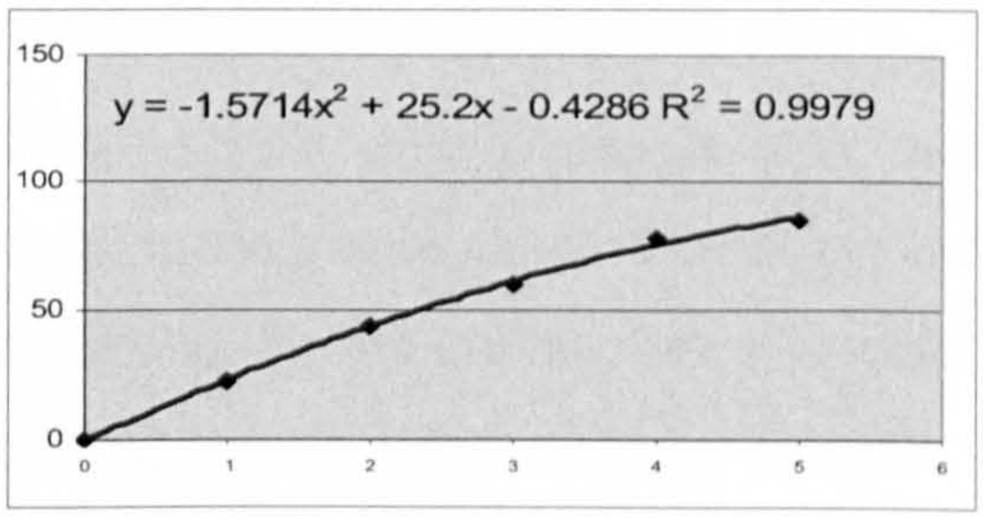
of as many studies as possible to investigate the effect of different ligament force on spinal stability with different experiment results.

Yoganandan et al, 2000 defined the anterior and posterior longitudinal ligaments from the mid-height of the inferior vertebral body to the mid-height of the superior body and ligamentum flavum from the superior points of attachment to the corresponding inferior points of attachment. Ligaments were treated on an individual type and level by level basis, they were grouped into 3 equal regions with 2 sequential motion segments in each group (middle and lower cervical spine categories; C2-C5 and C5-T1)

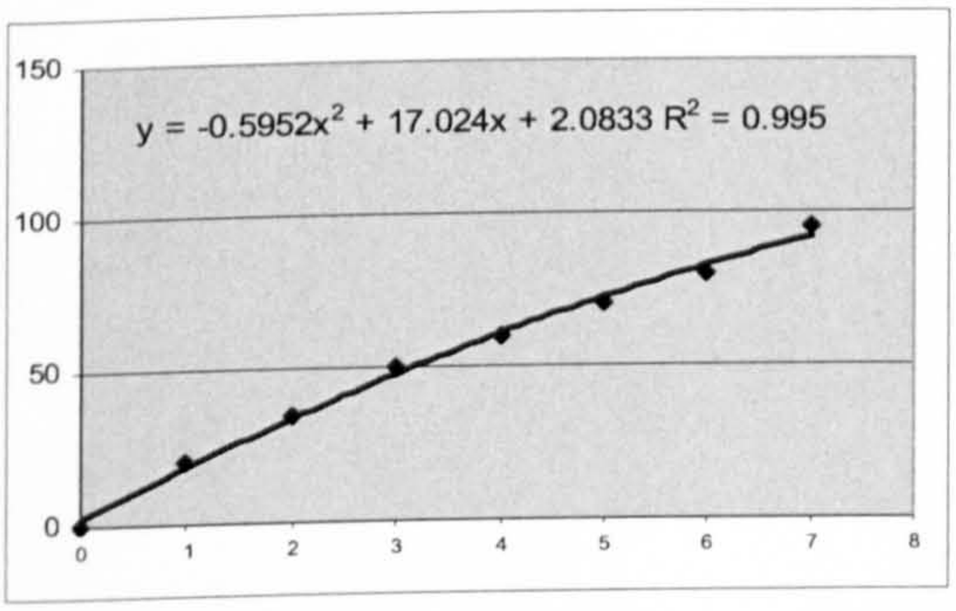
Discrepancies between the methods used in literature stem from the methodology used and biological variations. In the following graphs, force deflection curves of ALL, PLL and LF were provided from the studies of Yoganandan et al, 2000. The equations for the curves were calculated by using the curve fitting methods in excel. The derivatives of the curves with respect to elongation were calculated to find out the stiffness, the equations for stiffness were given in tabular form.



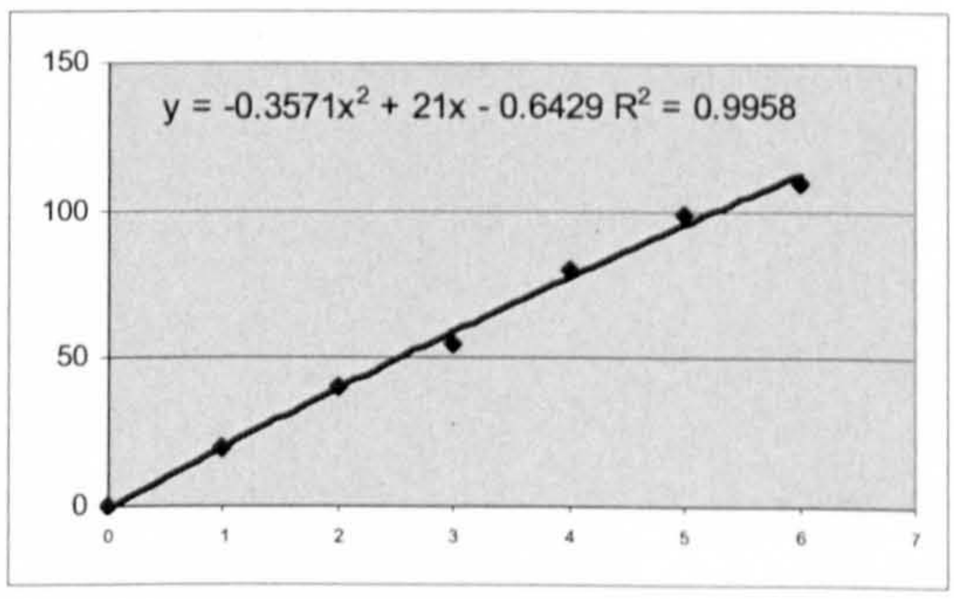
a)



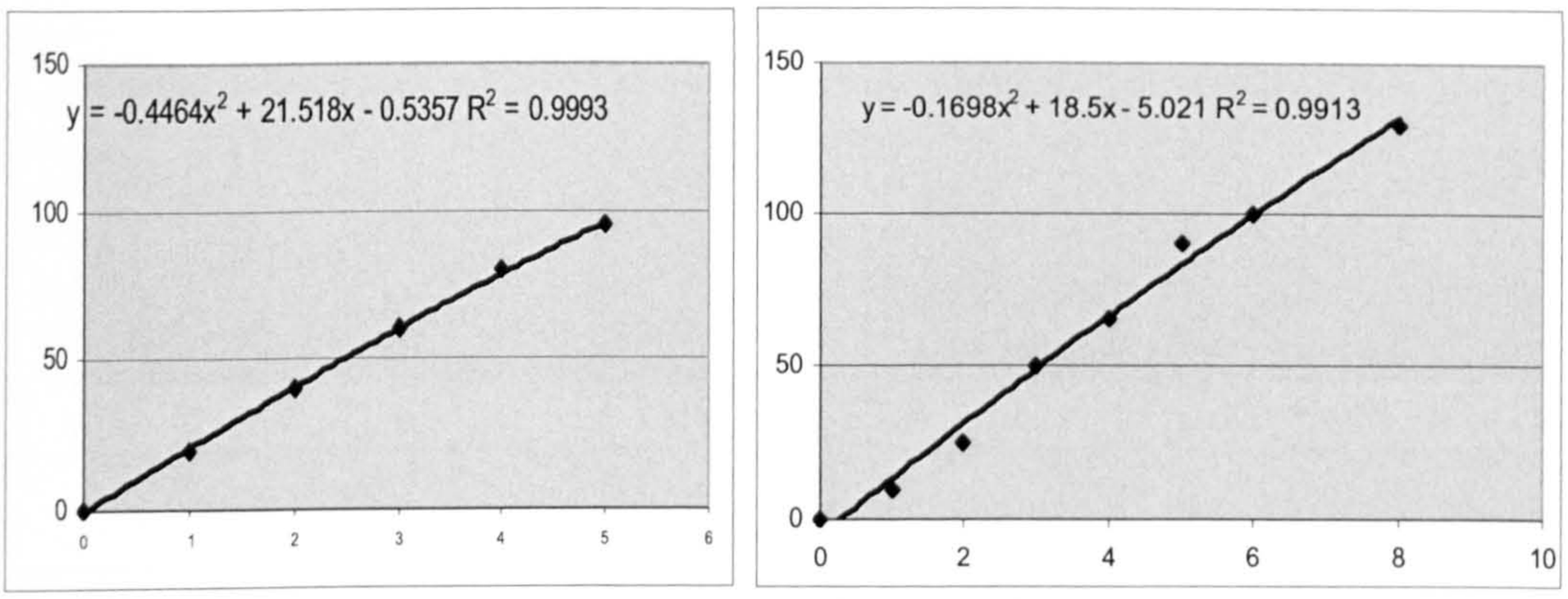
b)



c)



d)



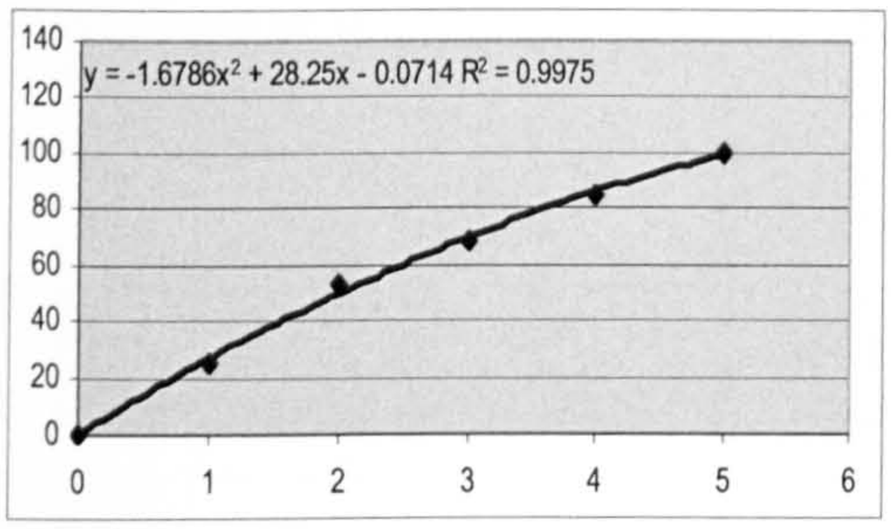
e) f)

Figure 4- 17 Force versus elongation graphs of the ALL in C2-C5 , C5-T1 (a), (b) respectively. Force versus elongation graphs of the PLL in C2-C5 , C5-T1 (c), (d) respectively. Force versus elongation graphs of the LF in C2-C5 , C5-T1 (e), (f) respectively. (Yoganandan et al, 2000)

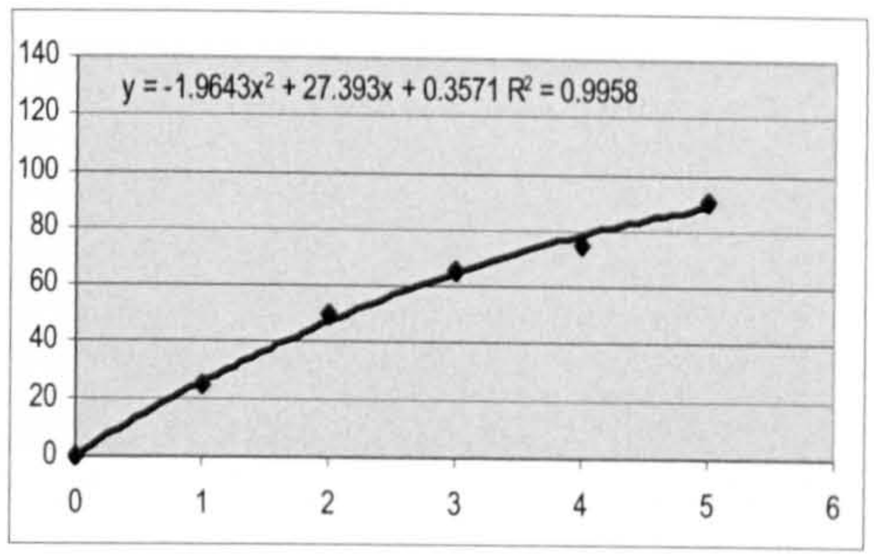
Table 4- 51 Equations of stiffness calculated for ALL, PLL and LF for the C2-C5, and C5, T1 sub regions separately by using the graphs above (Yoganandan et al, 2000).

Type	Region	Stiffness
ALL	C2-C5	"-2.8334x+28.036"
ALL	C5-T1	"-0.714X+21"
PLL	C2-C5	"-3.1428x+25.2"
PLL	C5-T1	"-0.8928x+21.518"
LF	C2-C5	"-1.1904X+17.024"
LF	C5-T1	"-0.3396x+18.5"

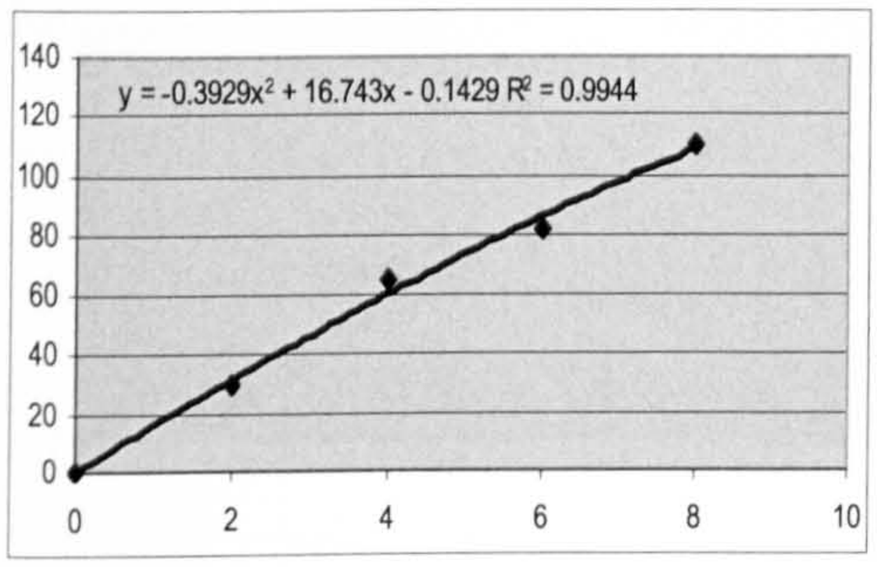
In the study of Yoganandan et al, 1998 the cervical spine ligaments were measured. The results of these experiments were drawn in the graphs shown below, the equations were calculated by second order of polynomials for the curves drawn in excel. The derivatives of these equations were calculated to find out stiffness formulas of the ligaments.



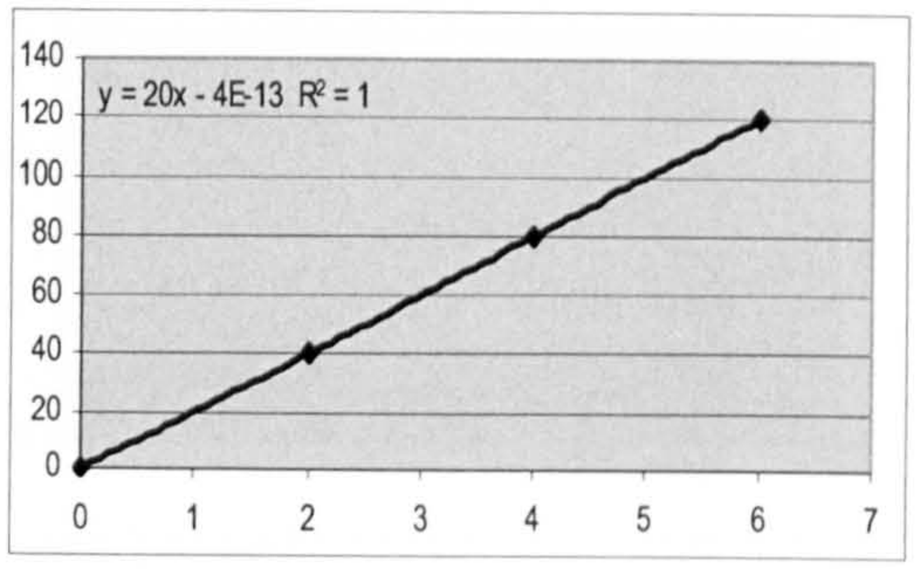
a)



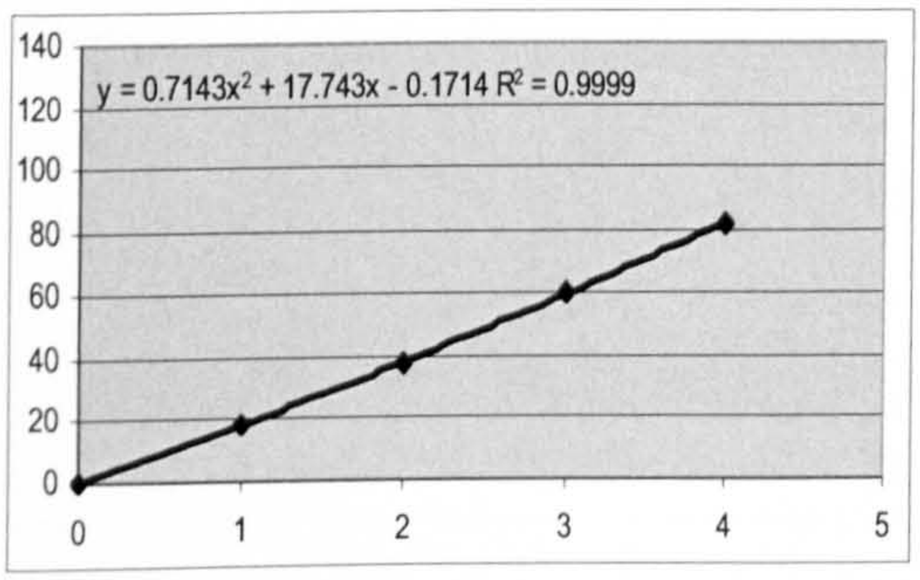
b)



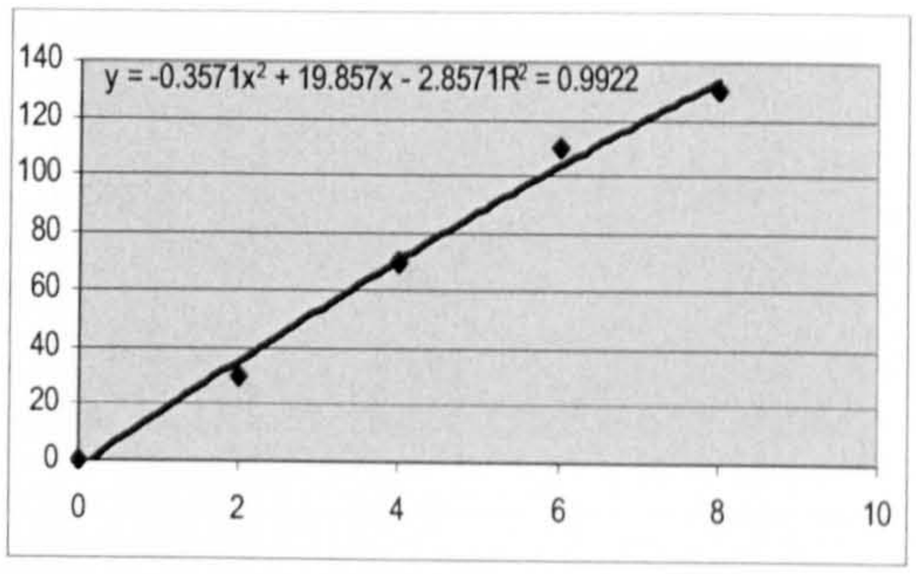
c)



d)



e)



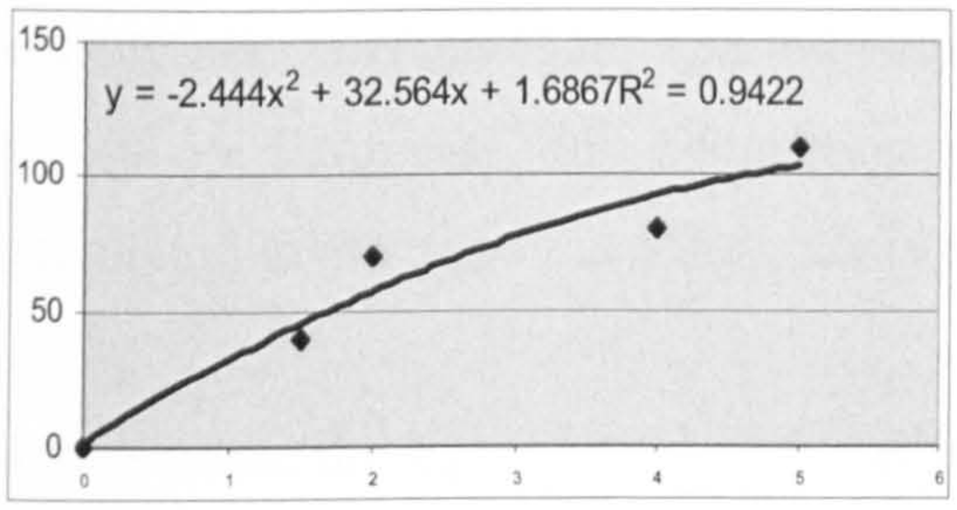
f)

Figure 4- 18 Force versus elongation graphs of the ALL, PLL, and LF in C2-C5 (a), (b), (c) respectively. Force versus elongation graphs of the ALL, PLL, LF in C5-T1 (d), (e), (f) respectively (Yogonandan et al, 1998).

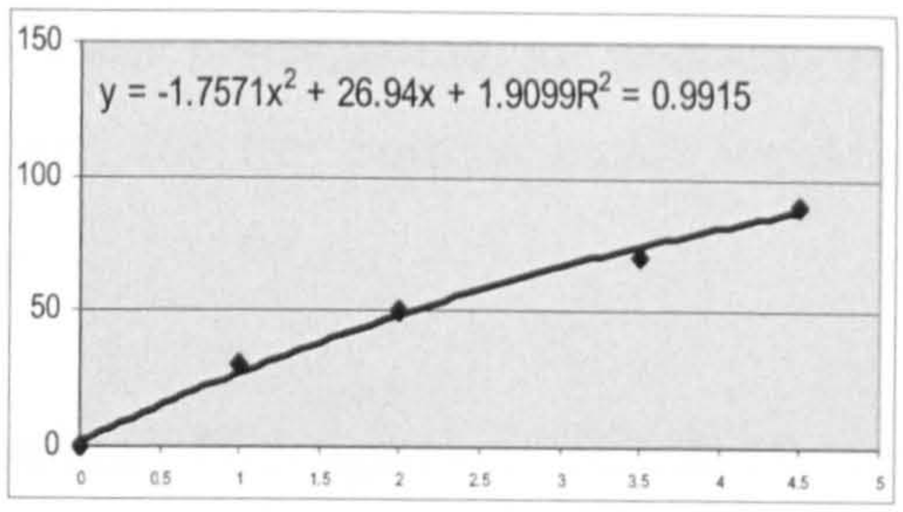
Table 4- 52 Equations of stiffness calculated for ALL, PLL and LF for the C2-C5, and C5, T1 sub regions separately by using the graphs above (Yogonandan et al, 1998).

Region	Stiffness
ALL mid cervical	"-3.352X+28.5"
ALL lower cervical	"20"
PLL mid cervical	"-3.93X+27.393"
PLL lower cervical	"1.43x+17.743"
LF midcervical	"-0.786X+16.743"
LF lower cervical	"-0.714X+19.857"

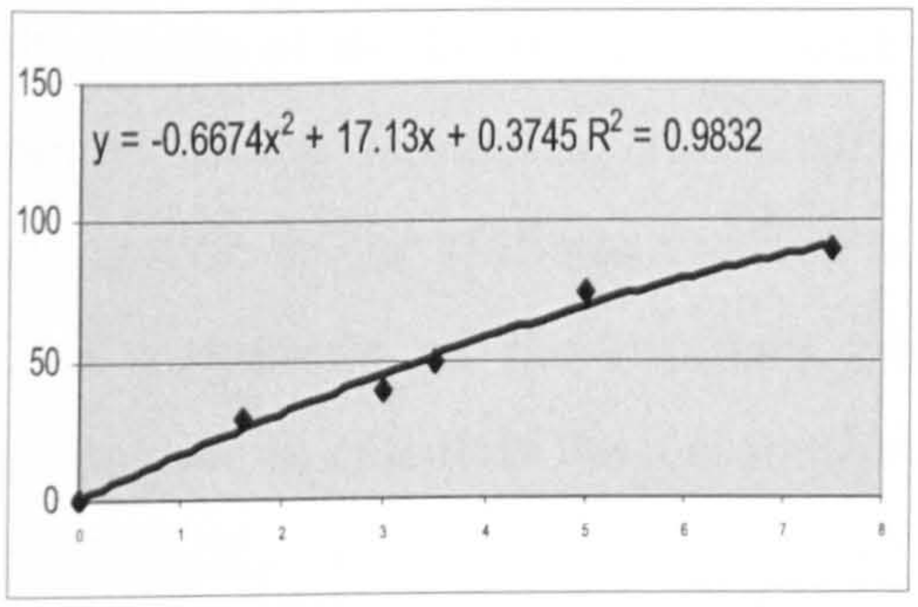
In the study of Yoganandan et al, 2001 the cervical ligaments of the spine have been tested the experiment results with the formulas of the fitted curves and the equations of the stiffness are given below.



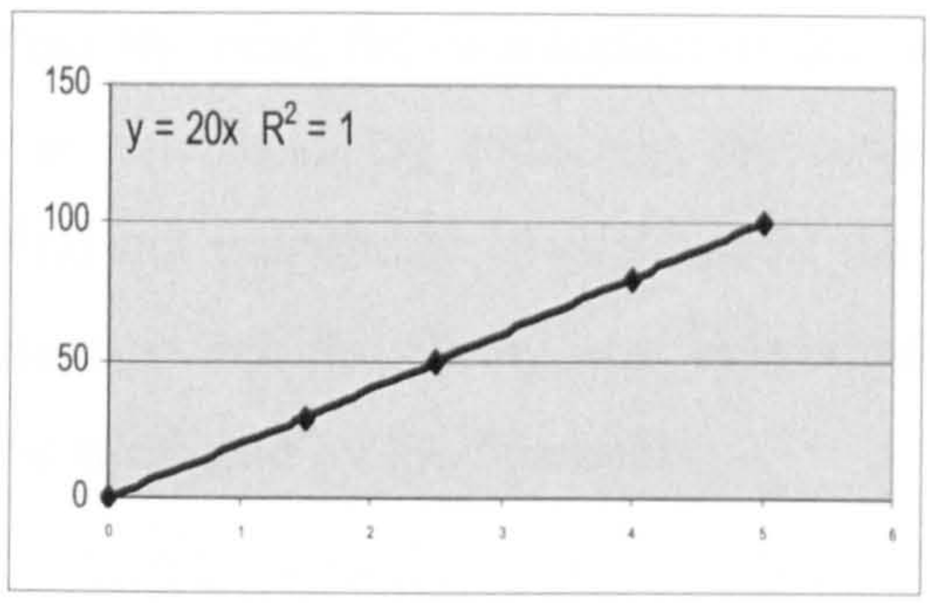
a)



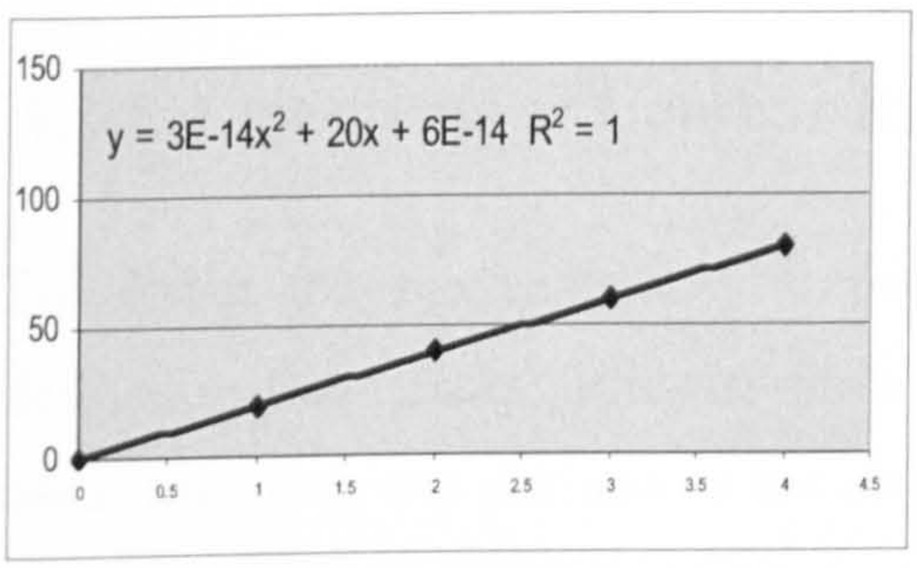
b)



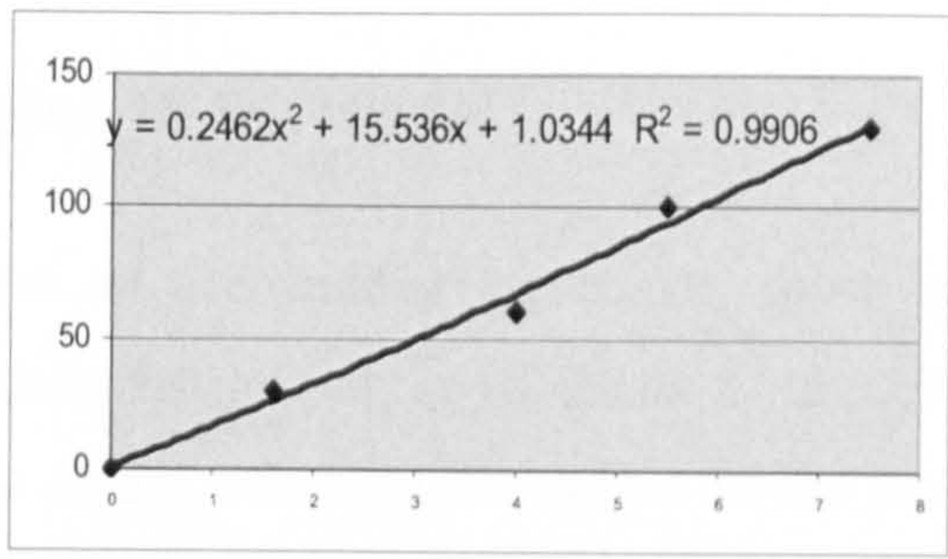
c)



d)



e)



f)

Figure 4- 19 Force versus elongation graphs of the ALL, PLL, and LF in C2-C5 (a), (b), (c) respectively. Force versus elongation graphs of the ALL, PLL, LF in C5-T1 (d), (e), (f) respectively. Yoganandan et al, 2001

Table 4- 53 Equations of stiffness calculated for ALL, PLL and LF for the C2-C5, and C5, T1 sub regions separately by using the graphs above Yoganandan et al, 2001.

Type	Region	Stiffness
ALL	C2-C5	"-4.88x+32.564"
ALL	C5-T1	"20"
PLL	C2-C5	"-3.514x+26.94"
PLL	C5-T1	"20"
FL	C2-C5	"-1.3348x+17.13
FL	C5-T1	"0.4924x+15.536"

In the model the erect posture is assumed to have zero tension. The coordinates of the connection points of the ligaments in the erect posture are recorded into the CSV files. When the user selects the option to include ligament forces, the main dialog box appears for the user to upload the CSV file recorded with the erect posture ligament

connection coordinates for that individual under investigation. To calculate the applied forces by ligaments, the connection points for the posture under investigation is calculated in the code when the code is run.

To calculate the ligament force, the elongation of the ligaments between two postures, i.e. the erect posture and the posture under investigation, is calculated by subtracting the length of the ligaments from each other by using the coordinates of the connection points of the ligaments. The stiffness is calculated by replacing the magnitude of elongation to the stiffness function to find out magnitude of stiffness at that posture. The magnitude of the resultant stiffness is multiplied by the magnitude of the elongation to calculate the real force value produced by the ligaments.

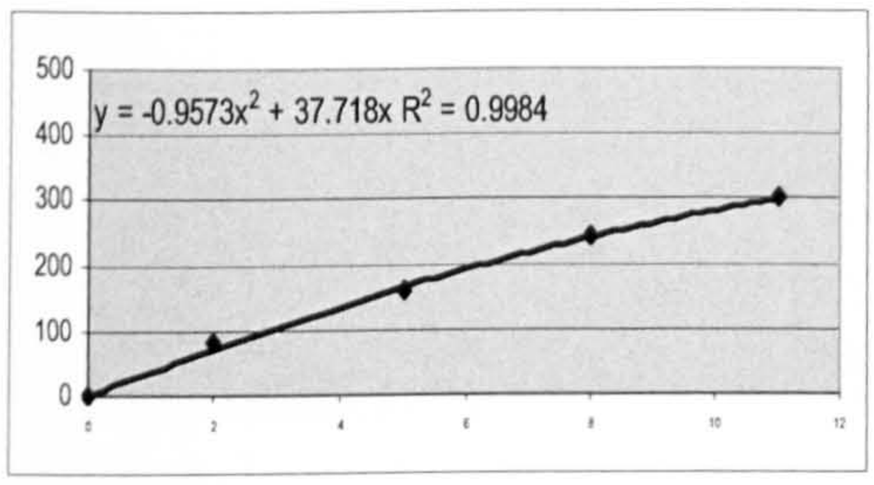
$F=K(x).\ X.$

Where; K(x) is the stiffness value and X is the elongation of the ligament at that point.

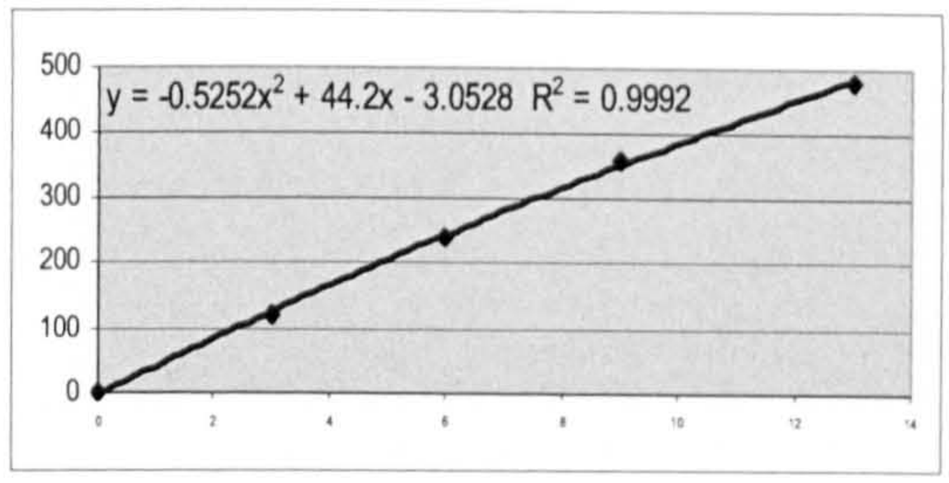
4.3.2 Ligaments at Lumbar Region in the model

To obtain the biomechanical properties of the lumbar ligaments, force time and deflection time traces from the force–deformation curves of Pintar et al., 1992 were used. Stiffness was defined as the slope of the least-squares fit line in the most linear portion of the force deformation curve. To determine the original length of each ligament, they used the sagittal anatomic sections. The ALL, PLL were defined from the mid-height of the inferior vertebral body to the mid height of the superior vertebral body. The LF was derived from their superior points of attachment to their inferior points of attachment.

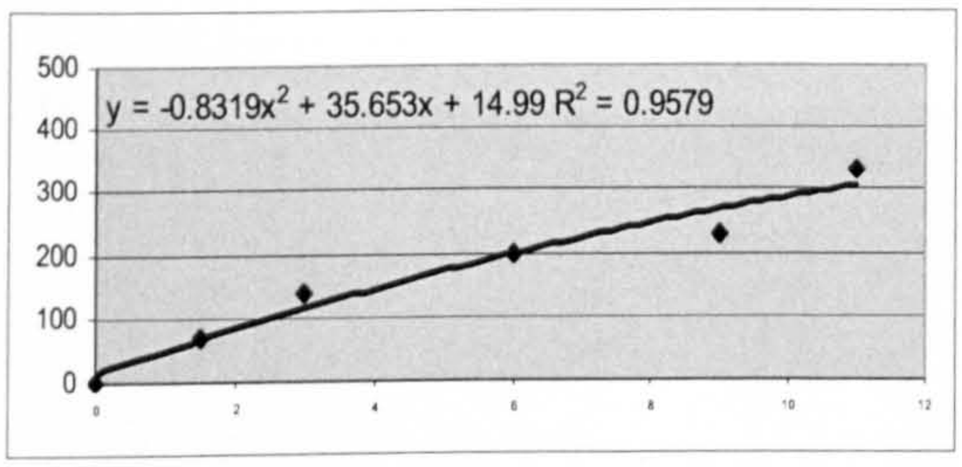
The mean force deformation curves for each ligament at each lumbar level from T12 to S1 were determined. Force-time and deformation-time traces were normalized with respect to their corresponding failure force and failure deformation value for each specimen. The curves were grouped by spinal level and ligament type. In the figures below force elongation graphs of the T12-L2, L2-L4, L4-S1 of the ALL, PLL and LF for each ligament tested in the experiments of Pintar, et al 1992 were drawn.



a)



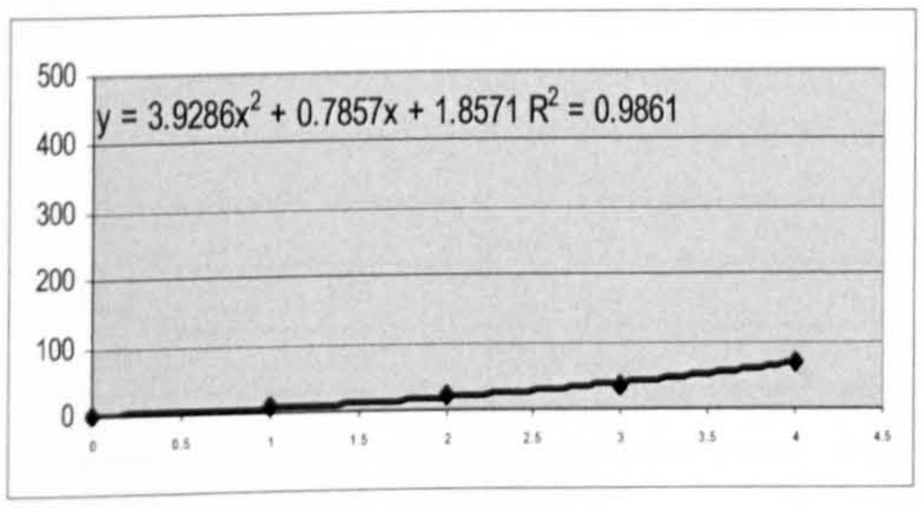
b)



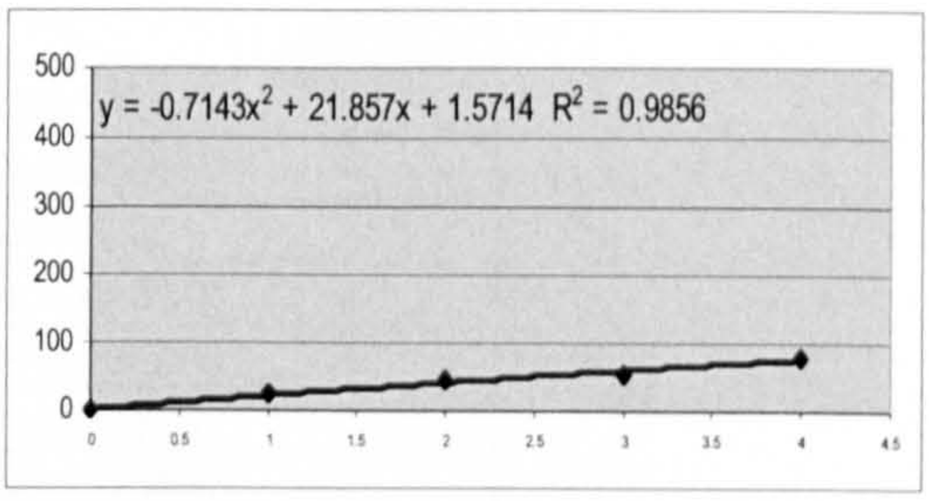
c)

Figure 4- 20 Force versus elongation graphs of the ALL in T12-L2, L2-L4, and L4-S1. (a), (b), (c).

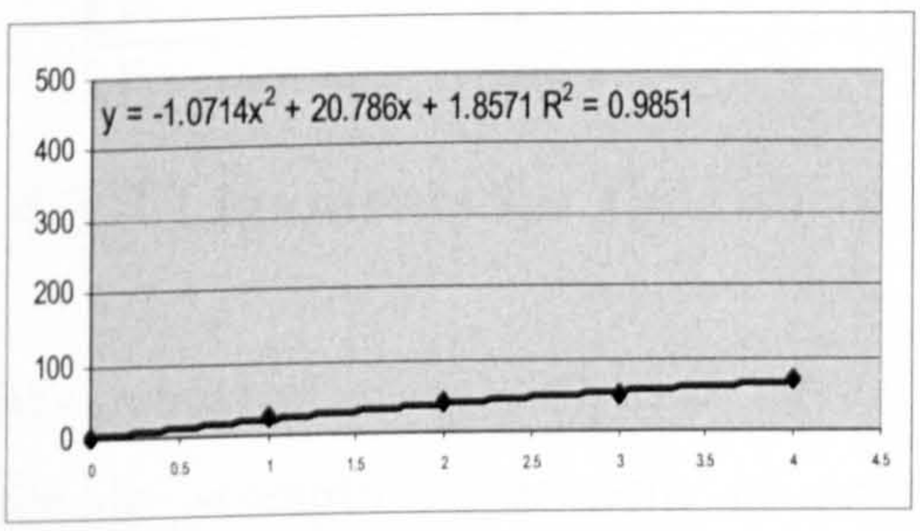
These forces versus deformation graphs are entered into excel and derivatives at these points are calculated to calculate the stiffness values. Failure stress and strain data can be used to check if the ligament force value is exceeded in the model.



a)

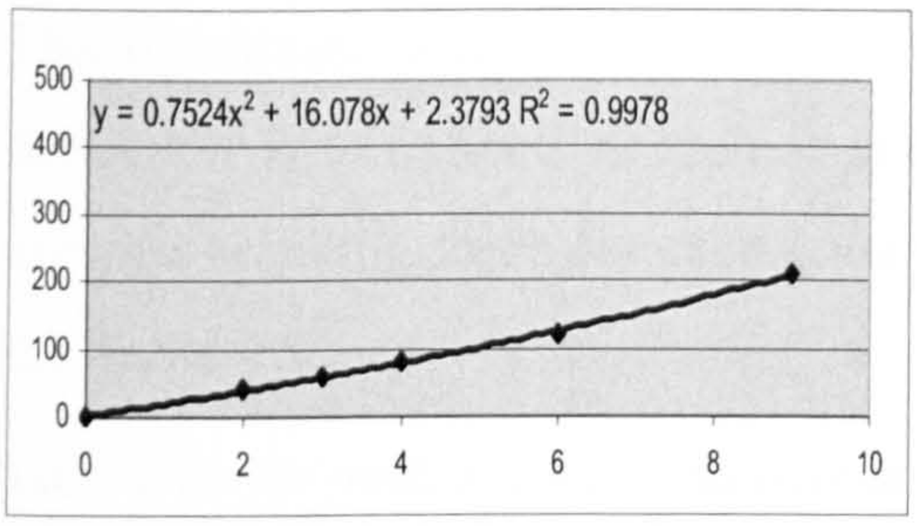


b)

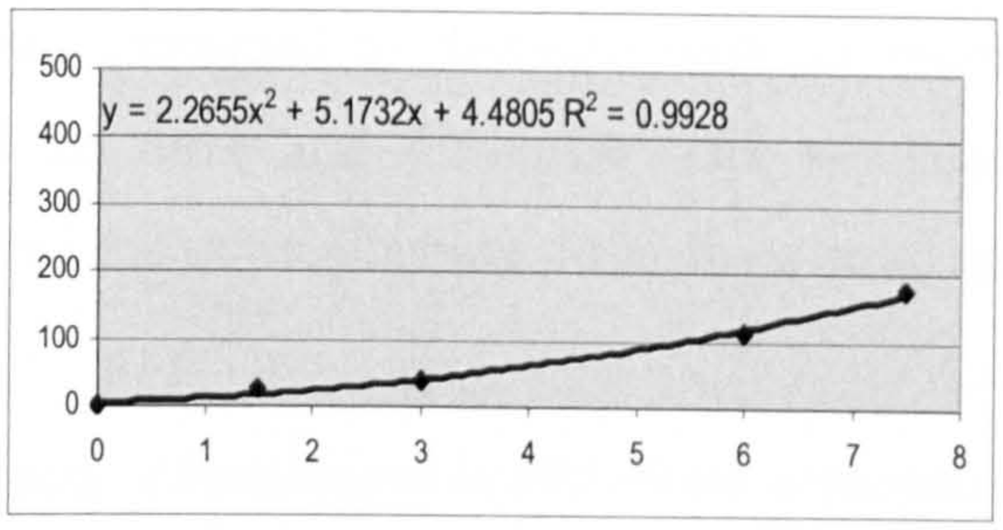


c)

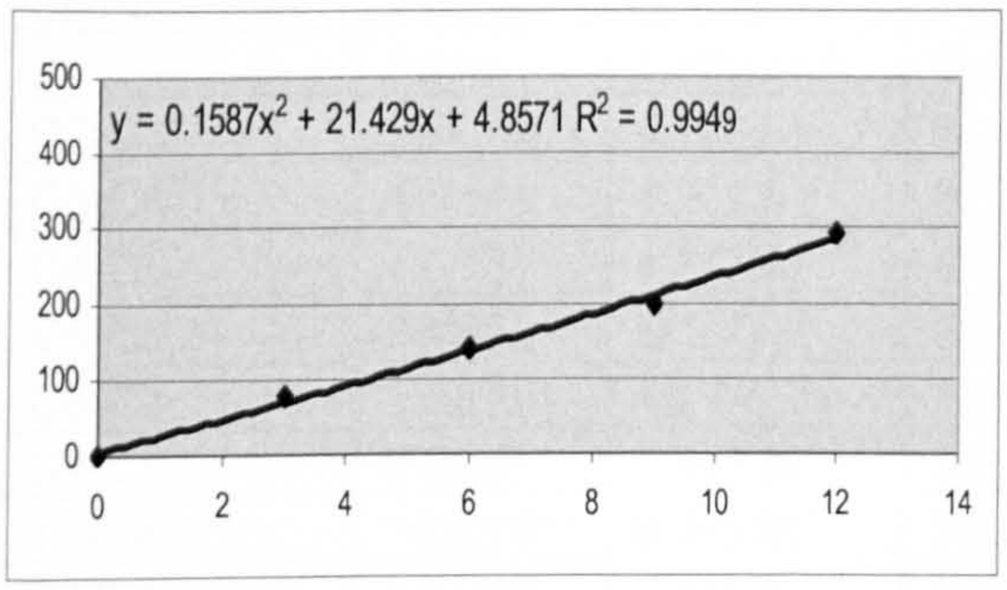
Figure 4- 21 Force versus elongation graphs of the PLL in T12-L2, L2-L4, and L4-S1. (a), (b), (c).



a)



b)



c)

Figure 4- 22 Force versus elongation graphs of the LF in T12-L2, L2-L4, and L4-S1. (a), (b), (c).

Table 4- 54 Equations of stiffness calculated for ALL, PLL and LF for the T12-L2, L2-L4, and L4-S1 sub regions separately by using the graphs above.

Type	Region	Stiffness
ALL	T12-L2	"-1.76x+36.587"
ALL	L2-L4	"-1.05x+44.2"
ALL	L4S1	"-1.68x+35.653"
PLL	T12-L2	"7.84x+0.7857"
PLL	L2-L4	"-1.42x+21.857"
PLL	L4S1	"-2.14X+20.786"
LF	T12-L2	"1.55x+16.078"
LF	L2-L4	"4.54X+5.1732"
LF	L4S1	"0.32X+21.429"

4.3.3 Ligaments for the full spine in the model

Myklebust et al, (1988) used ligaments from 41 fresh human male cadavers in the tensile strength experiment of spinal ligaments. The ligaments were tested by sectioning all elements. The force and deformation at failure level were shown for each ligament as a function of spinal level. They fixed the vertebral bodies above and below the ligament under study in a frame. The apparatus was aligned to pull each ligament in direct axial tension at a constant rate of 1cm per second. They obtained the plots from force versus time and time curves.

The force-deflection curves exhibited a sigmoid shape with an initial concave upward section followed by a region of decreasing stiffness and terminated by an abrupt drop.

The maximum point at which the load continued to decrease with an increase in deflection was defined as failure and the force and deflection were tabulated. The average breaking force for each level and the corresponding deflections were given in the Table 4.55.

Table 4- 55 The result of experiments from the study of Myklebust et al, 1988. Force versus deflection values in mm for ALL, PLL and FL

Spinal Level	Anterior Longitidunal		Posterior Longitudinal		Ligamentum Flavum	
	Force	Deflection	Force	Deflection	Force	Deflection
C2-C3	207(98)	8.7(3.8)	84(81)	9.6(9.3)	86(61)	5.8(0.8)
C3-C4	47(14)	4.2(1.8)	82(66)	7.4(7.1)	75(8)	3.7(1.5)
C4-C5	47(13)	4.8(2.9)	47(11)	3.4(1.4)	56(17)	12.8(7.3)
C5-C6	89(67)	5(1.7)	85(50)	4.8(2)	89(48)	8(4.4.)
C6-C7	176(25)	13.7(5.7)	102(29)	5(1.6)	160(38)	7.7(0.4)
C7-T1	97(28)	7.6(3.8)	95(23)	6.4(1.6)	221(67)	9.9(6.0)
T1-T2	182(101)	6.3(5.9)	86(53)	3.6(1.6)	135(84)	6.4(5.5)
T2-T3	123(48)	7.3(1.4)	116(85)	3.2(1.8)	144(21)	10.4(1.1)
T3-T4	154(43)	7.5(4.8)	67(20)	3.9(1.2)	161(67)	6.3(2.2)
T4-T5	169(46)	6.9(2.9)	99(9)	3.7(0.5)	182(23)	9.1(3.5)
T5-T6	284(25)	10.6(3.0)	82(7)	7.3(6.9)	128(46)	6.3(2.2)
T6-T7	332(58)	7.6(2.2)	138(123)	5.7(1.7)	281(115)	10.2(0.2)
T7-T8	213(58)	17.7(6.8)	74(59)	3.6(2.0)	221(79)	10.4(5.1)
T8-T9	332(53)	13.2(1.7)	76(45)	3(2.3)	200(55)	6.7(3.1)
T9-T10	213(58)	14.2(4.9)	75(18)	4.7(3.1)	221(119)	10.3(4.4)
T10-T11	332(53)	11.6(4.0)	118(116)	5.9(3.0)	265(25)	11(6.3)
T11-T12	281(88)	13.7(3.6)	116(38)	3.3(1.6)	282(57)	10.1(2.3)
T12-L1	276(81)	12.7(9.1)	66(32)	4.8(4.0)	278(134)	9.2(1.8)
L1-L2	341(72)	11.5(12.1)	91(46)	5.2(3.1)	215(72)	12.1(1)
L2-L3	504(218)	15.7(7.0)	160(82)	4.2(0.1)	133(41)	4.5(1.3)
L3-L4	676(359)	20.4(3.5)	38(15)	7(3.2)	251(176)	12.2(3.6)
L4-L5	606(191)	14.9(7.2)	53(7)	4.3 (2.1)	334(158)	14.5(3.4)
L5-S1	209(196)	13.4(9.3)	108(53)	4.7(3.1)	287(47)	11.9(3.4)

ALL was found out to be the strongest at the high cervical level and lower thoracic and lumbar regions with the highest average force value of 676 N at the lumbar levels. They observed that the ligaments on the convex side of the spinal curvature tend to be relatively stronger. The increase in strength were observed at the thoraco-lumbar and cervico-thoracic junctions.

The tabulated data was adopted into our thrustline model to represent the full ligament model connected to the spine. For this purpose the force deflection curve was assumed to be linear. The elongation of the ligaments between the erect posture and the posture under investigation was calculated. The relationship between force and elongation was assumed to be linear.

4.4 Discussion

In order to investigate the role of spinal ligaments and to model them to simulate spine behaviour, quantifying their material properties (stiffness, force-deflection) and their geometrical positioning is important. Three different models of cervical region ligaments from the studies of the researchers, one set of ligaments of lumbar region and full set spinal ligaments were introduced in this chapter. Based on a morphologic study (Hukins et al, 1990), only the anterior and posterior longitudinal and the ligamentum flavumn ligaments were considered to be capable of generating significant force. The ligaments as explained in the sections of this chapter is grouped into sub-regions in literature and investigated differently by different researchers. In these studies, with regard to the definition of the specific ligament for measuring geometry like length, an approach parallel to and consistent with the mathematical models is observed. For example, for the anterior and posterior longitudinal ligaments, because of their continuous nature in the human spinal column, they are treated to span from mid-height of caudal vertebral body to mid-height of adjacent cephalad body at the specific vertebral level. This approach allows for a continuous ligament when full spine model is constructed. Ligamentum flavumn span the superior and inferior points of attachment of the two vertebrae. From mathematical modelling viewpoint, fundamental properties such as stiffness or elastic modulus, a function of stress and strain are required. Experiments conducted for this purpose, in literature, include ligament test in situ bone-ligament- bone preparations.

The calculated stiffness functions from the experiments were tabulated for each subgroup, for a better comparison these tables have been listed below (Table 4.55, 4.56, 4.57). There are some slight variations in the stiffness functions of these ligaments. There might be several reasons for these differentiations:

There might be anatomical and morphological variances evident in several of the ligaments. This is expected to cause difficulty in determining the actual attachment points of the ligament causing different results. In addition to this, due to the differences of the procedures applied in the experiments these stiffness functions might vary slightly for each experiment. The loading rate in force-deformation experiments might cause differences due to the viscoelastic nature of the ligaments. Although it is

observed that most of the experiments have been conducted in a quasi static manner, the little variations in the application speed of the force might produce these slightly different results. In most of the studies, it is observed that the failure force, stiffness and energy have all been reported to increase with rate of loading. For example, with increase in loading rate from 1.0 to 2.5 cm/s, the tensile failure load, stiffness and energy for the anterior longitudinal ligament and ligamentum flavumn of the cervical spine increased by a factor of 2-4 (Yoganandan et al, 2001).

Table 4- 56 Equations of stiffness calculated for ALL, PLL and LF for the C2-C5, and C5, T1 sub regions separately by using the graphs above. (Yoganandan et al, 2000).

Type	Region	Stiffness
ALL	C2-C5	"-2.8334x+28.036"
ALL	C5-T1	"-0.714X+21"
PLL	C2-C5	"-3.1428x+25.2"
PLL	C5-T1	"-0.8928x+21.518"
LF	C2-C5	"-1.1904X+17.024"
LF	C5-T1	"-0.3396x+18.5"

Table 4- 57 Equations of stiffness calculated for ALL, PLL and LF for the C2-C5, and C5, T1 sub regions separately by using the graphs above (Yoganandan et al, 1998).

Type	Region	Stiffness
ALL	C2-C5	"-3.352X+28.5"
ALL	C5-T1	"20"
PLL	C2-C5	"-3.93X+27.393"
PLL	C5-T1	"1.43+17.743"
LF	C2-C5	"-0.786X+16.743"
LF	C5-T1	"-0.714X+19.857"

Table 4- 58 Equations of stiffness calculated for ALL, PLL and LF for the C2-C5, and C5, T1 sub regions separately by using the graphs above (Yoganandan et al, 2001).

Type	Region	Stiffness
ALL	C2-C5	"-4.88x+32.564"
ALL	C5-T1	"20"
PLL	C2-C5	"-3.514x+26.94"
PLL	C5-T1	"20"
FL	C2-C5	"-1.3348x+17.13
FL	C5-T1	"0.4924x+15.536"

Although there have been some differences in the cervical stiffness functions, the validity of the data should be appreciated. In previous researchers studies, because of lack of data earlier researchers adopted data from lumbar spine Jager et al, 1994 and lower extremity ligaments Nitsche et al, 1996. In general by looking at the stiffness

functions, the stiffness values are higher in the mid-cervical region compared to the lower region for the anterior and posterior longitudinal ligaments.

In literature, general approach is to calculate the stiffness function where the slope of the curve is steepest. However, in this model, more accurate stiffness function is calculated and the elongation value is inserted into this function to find out the exact stiffness value applied by ligament in that posture. This provides more detailed information about the stiffness values for different postures with the data collected for the intervals of a lifting activity.

Modelling approach

By using the connection coordinates of the ligaments in the erect posture, the length of the ligaments in the erect posture is calculated. The length of the ligament in the posture that is under investigation is also calculated by using the connection coordinates of the ligaments in that posture. Elongation in ligaments is calculated by subtracting the length of the ligament from the posture under investigation than that of the fully erect posture. This value is multiplied by the value calculated from the stiffness function.

For linear approach, only single number representing the linear stiffness is necessary and sufficient (Kumaresan et al, 1997, Yoganandan et al, 1996). This approach is shown to be efficacious at low-magnitude loading (e.g. 0.5 N m flexion-extension moment) to capture the spinal behaviour (Yoganandan et al, 2001). In contrast, at higher levels of pure moment, it is necessary to incorporate non-linear force-deflection/stress-strain responses in order to determine realistic spine behaviours (Kumaresan et al, 1999, Kumaresan et al, 2000). In this model, in order to eliminate the debate over the magnitude of the moment to decide whether a nonlinear or linear stiffness value to use, it is decided to calculate the magnitude of stiffness by using the stiffness function.

One of the important issues in ligament modelling is the effect of ligament pre-stress on the internal and external biomechanical responses of the spine. From functional and anatomical perspectives, ligaments have varying levels of pre-stress. For example, the ligamentum flavumn has more pre-stress than the anterior longitudinal ligament

(Chazal et al, 1985). However, in order to simplify the model it is assumed that in the erect posture the ligaments have no pre-stress in our model.

The modelling of ligaments was also used in the thesis of S. L. Grilli, (1997) for investigating spinal stability for four postures. The modelling of ligaments is different from that of previous researcher. Grilli calculated the ligament force as multiplication of stress with the cross sectional area. However, the cross sectional area of the ligaments were only available for the lumbar region. The rest of the spinal ligament values were only estimation based on the available lumbar region data.

For the stress values, Grilli used the experimental data of Chazal et al, 1985 where the loading of 1mm/min is applied to ligaments. The resulting load deformation curves had a sigmoid shape with 3 distinct portions: OA, AB, BC as shown below. In order to calculate the force, the strain of the ligaments between the fully flexed and fully erect postures were estimated and the corresponding stress values at the A, B, and C levels were reported in her thesis. The force values were calculated by multiplying the stress values obtained at points A, B, C. However, due to the lack of real data for the strain levels of the ligaments in her thesis for the force estimation resulted in poor estimation of ligament forces.

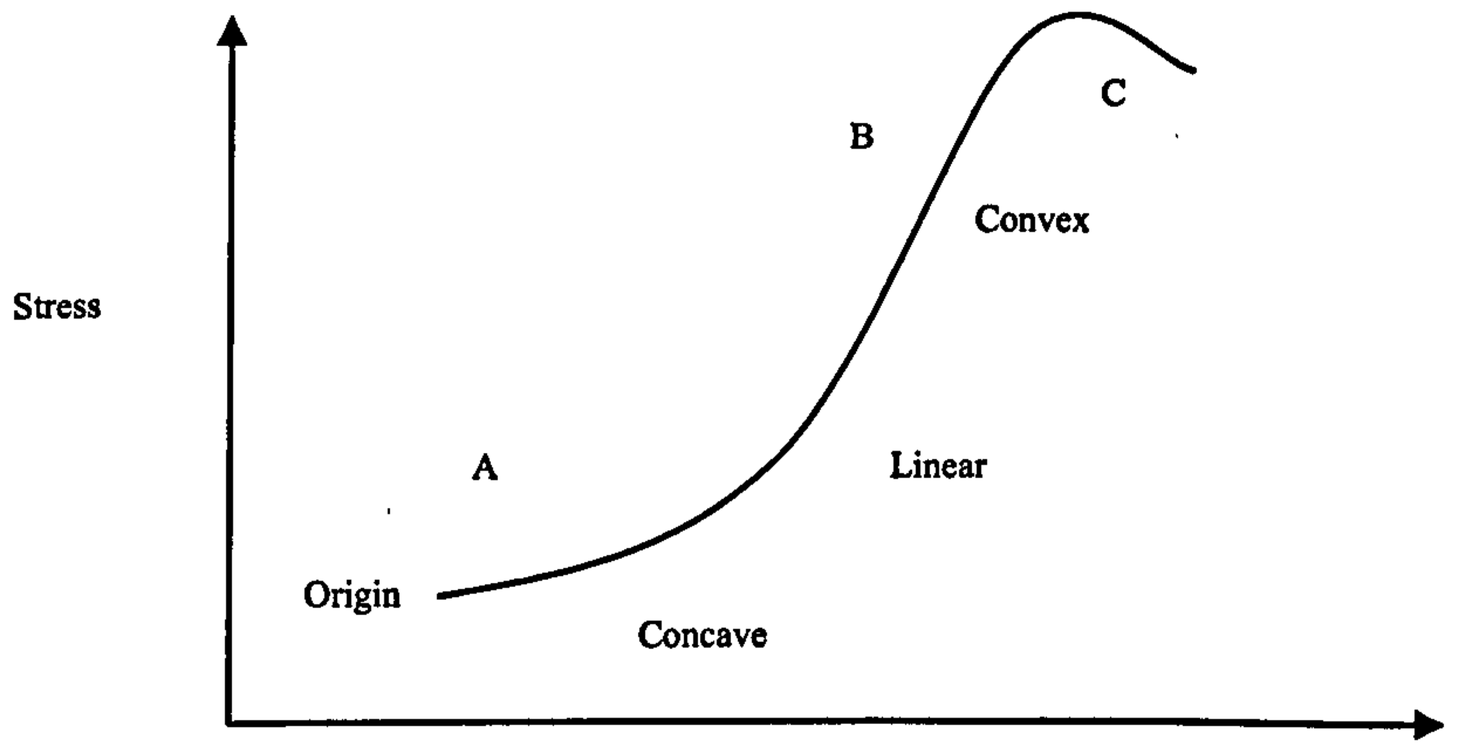


Figure4- 23 Three distinct portions of a load deformation curve for the ligaments under loading applied at a slow rate (1mm/min) reported by Chazal et al (1985)

The superiority of using stiffness functions with respect to strain values for each different posture realise on the continuity of these stiffness functions, unlike her three point force estimation results for the postures, this approach produces unique results specific to the investigated postures only. The other superiority of this method is that it

does not rely on the cross sectional area data for ligaments. This eliminates the dependency of results to the other variable in force calculation which increases the reliability of the results in this approach.

In this thesis, stability of a spine is focused rather than the tissue injury. However, with the known coordinates of the ligaments it was possible to calculate their strain values based on the erect posture. Load produced by these sub-structures are calculated by using the real strain data and the stiffness functions from the experiments. Control functions were developed to check if the failure of a ligament was attained based on the force values in the experiments where the failure occurred. So that a possible ligament failure can also be suggested for a specific posture if the calculated force value exceeds the force value where the ligaments failed in the experiments. However, there might be slight differences in reality with this approach, the experiments were conducted in frozen specimens, and the tissue structure is expected to be less flexible, resulting in an early failure unlike the in vivo situations where ligaments are at body temperature.

The mechanical role of the lumbar posterior ligaments during lifting tasks remains controversial. Cholewicki and McGill, 1991 investigated the ligament contribution in resisting trunk flexion moment during extremely heavy lifts performed by national class power lifters. The ligaments were observed not to strain sufficiently to resist the extremely heavy load placed on the lumbar spine, suggesting that it is not their primary role to assist the musculature, but limit range of motion. They found out that the ligament resistance was insignificant contribution when compared to the total moment. These findings are consistent with those of Hukins et al (1990) who examined the posterior lumbar ligament structure and Hindle et al (1990). Each of the investigators concluded that resisting the forward flexion moment is not a primary role of these ligaments. Muscles rather than ligaments are exposed to heavy loading during lifting and subject to greater level of injury. However, whatever the level of risk for injury, because ligaments apply load on spine, the effect of them on spinal stability with thrustline approach should be investigated. The detailed results related to the contribution of muscles and ligaments to stability are provided in Chapter 6.

CHAPTER 5

5 Body Contour in a lifting activity

In this chapter, the main focus is to understand how the contour of the spine changes during a lifting activity. The thrustline theory focuses on the extremities of the spinal column. By checking if the thrustline stays within the internal region of the spine, the stability of the spine can be decided on. For this purpose, it is very important to investigate about how the curvature of the spine changes during a lifting activity. This information is expected to guide researchers with the new sets of ideas for producing new design criteria for the design of a new lifting device to assist people in their lifting activities.

For this purpose, a literature review is conducted to decide on which measurement devices to use for data collection. With the feasibility analysis, a measurement device called spinal mouse, is chosen. An experiment is designed for unloading an object from the boot of a car to collect data for the changes of the contour of the spine during the full span of the lifting activity. The results and conclusions are provided in this chapter.

5.1 Need for the Experiment

Due to the complex nature of the human spine, it is difficult to estimate the exact posture of a body at any time. (Ayoub, 1992) developed a simulation model for the lifting activities. In his study, he used the minimization of the total muscular effort by assuming that the whole body is composed of 5 links only. Using the optimisation concepts, lifting

is assumed to be performed in such a way that it minimizes a non-linear objective function (1).

$$\int_{t=0}^{T} \sum_{i=1}^{5} (M_i(t)) / S_i(t))^2 \, dt \quad (1)$$

Where S_i is the moment strength of each joint, M_i is the reactive moment at each joint and T is the time to perform the lifting activity. His results represent the whole body posture as 5 rigid links. Although the study gives some information about the lifting motion pattern of a body, it does not give any information in the desired level of detail for each vertebra. In literature, there is no study to estimate the exact orientation of each vertebra in human spine with respect to each other and their coordinate values. In order to analyse the combination of posture with the changing roles of muscles and ligaments and to understand the mechanism of an injury for a lifting activity, lifting posture data in the level of vertebra for full span of lifting activity is needed.

Pure mathematical models which are not supported by real data are highly conceptual and unlikely to produce realistic results. Experimental methods are known to produce more realistic results in the investigation of injury mechanisms. In addition to this, the difference between the spinal contours of the genders is investigated. This investigation is expected to produce some useful results for the parametric modelling of the thrustline for investigating the spinal stability for understanding injury mechanisms and leading design criteria for a device which assist people in their lifting activities.

5.2 Design process of the experiment

Before designing the experiments, the parameters which are considered to have an effect on the spinal contour and the range of motion of the spine have been examined. The experiment is considered for analysing the spinal posture starting from L5 to C1 for different postures while lifting an object from the boot of a car. The contour of the spine is recorded as well as the spinal length; height and the gender of the subject in the designed experiment.

The control parameter is the gender of the subjects. Spinal curvature is the dependent parameter.

List of fixed parameters in the experiment are as follows:

1. The object to be lifted
2. The horizontal and vertical distance of the object.
3. Back pain history of the subject

The experiment is to lift an object from the boot of a car in the sagittal plane and record the spinal curvature data of the subjects in each phase of the lifting activity starting from fully flexed posture to fully erect posture with the object at hand in the final posture. For a better understanding of the experiment steps a conceptual drawings of the experiment are shown in Figure 5.1. For this purpose a reliable measurement method had to be chosen which would not interfere with the natural flow of the lifting activity with the desired level of accuracy for this experiment. In section 5.2.1 the background information about all the possible measurement devices considered for the experiment is supplied. The detailed in formation about the constants and parameters of the experiment is going to be provided in section 5.3.1.

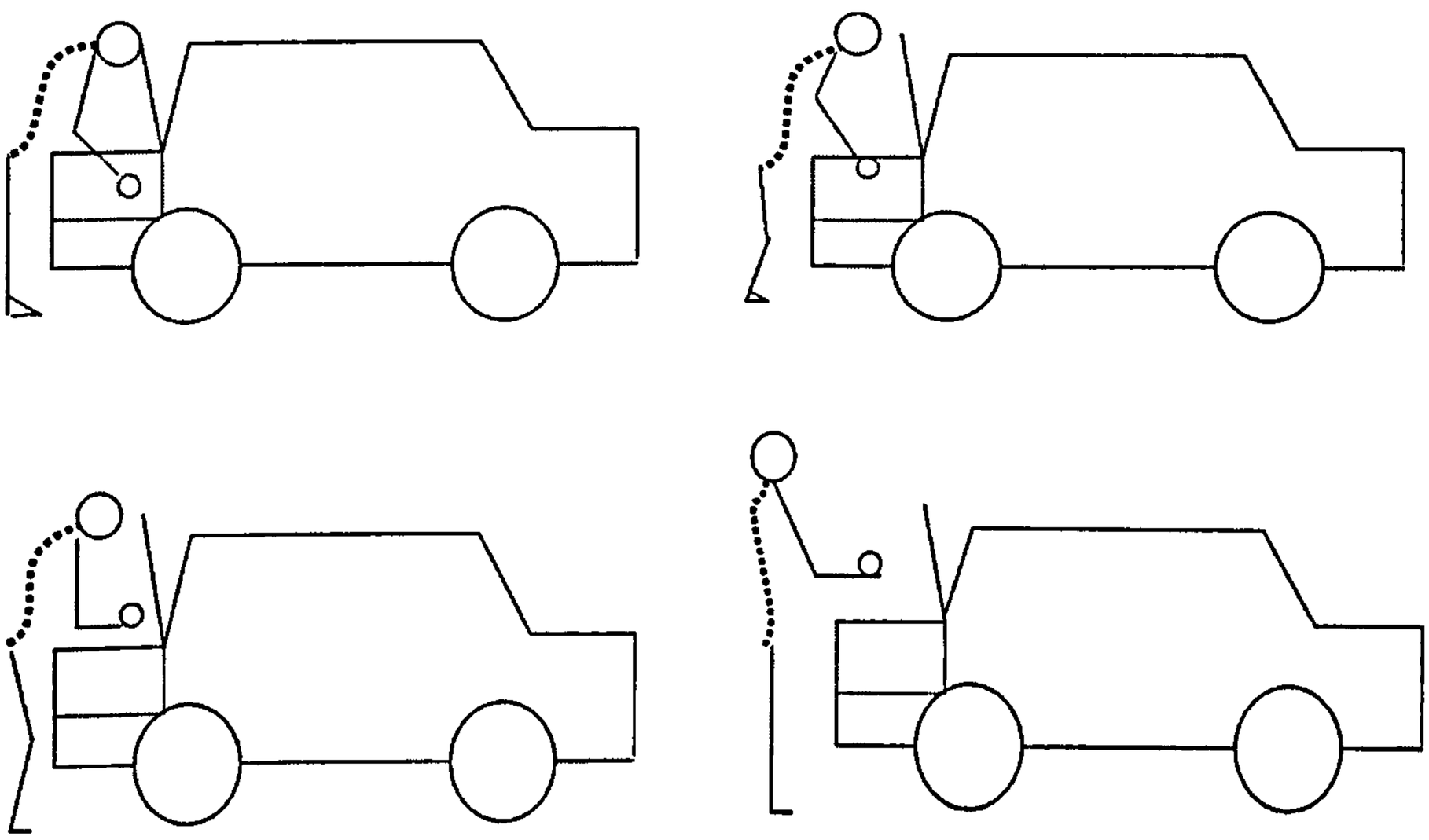


Figure 5- 1Conceptual design of the experiment

5.2.1 Background information and feasibility study on measurement devices

The main objective of the experiment is to gain insight about the contour change of the full spinal curvature. The exact orientation and the space coordinates of each vertebra are calculated by using the spinal curvature obtained from the experiment. It was aimed to implement the shape of the spine in thrustline theory for stability analysis. The main criteria while deciding on the measurement equipment to be used is to keep the natural flow of a lifting activity. Non-invasive methods are preferred over invasive methods. Non-invasive methods cause no harm to the body of the experiment subjects and are

easier to get permissions for conducting the experiment. Radiography, skin surface devices, spinal mouse, arcometer, skin surface makers, computerized motion analysis systems, flexicurve, inclinometers and goniometers are considered as the possible options for conducting the experiment in this research. Feasibility study is conducted to get information about the usage, applications, advantages and disadvantages of each device for a better decision of the measurement equipment.

5.2.1.1 Radiography

Biplanar radiography, is one of the methods for measuring spinal movements between individual vertebrae (McGill 2002). X-rays allow the radiographer to see the vertebrae and the arrangement without having to invade the person being examined, the non-invasive X-rays use ionizing radiation which requires licensed technicians. Any technique that subjects the patient to X-ray radiation is harmful and is not advisable especially if the experiment subject is pregnant. It is not ethical to ask anyone to have multiple X-rays during a lifting activity for the experimental purposes.

Even if radiographic measures of range of motion are commonly considered to represent the ideal, no study has ever demonstrated acceptable reliability for X ray measures of spinal range of motion. A number of studies have examined the error associated with repeated measurement of vertebral angles on a given set of radiographic films and found that the error can sometimes be significant. But, this represent only one likely source of error associated with the whole procedure. In addition to the interpretation and measurement of the final X-ray films, the measurement error can also arise as a result of differences in patient position during imaging, image quality, and patient's performance. X-ray technique itself has not been shown to be reliable then its application can hardly be considered to be a gold standard (Mannion *et al.* 2004), for the experiment we designed where reliability is strongly desired.

As a result, due to safety concerns and need for a licensed technicians and in addition to vulnerability of the method to measurement errors due to image quality and evolution, the radiography method is decided as the not best method for collecting data for this experiment.

5.2.1.2 Skin Surface Devices

Increased awareness of the risks and dangers of exposure to radiation associated with repeated radiographic assessment of spinal curvature led to increased number of attempts to develop skin surface devices. A number of devices employing different methods/techniques of measurement are currently available for the non-invasive assessment of spinal movements- ranging from the simple tape measure to computerized motion analysis systems including kyphometers, goniometers, inclinometers, and flexicurves. To asses the curvature of the spine and observe the spinal range of motion, the skin surface techniques are used mostly by researchers. The magnitude of the curvature and the extent of the range of motion are easier to detect with skin surface devices. The basic advantages of the skin surface measurement techniques are as follows:

- Less expensive to use
- Smaller in size
- Portable
- Does not need highly skilled technicians
- The measurements are quicker

One of the disadvantages of external skin surface devices is the external obstructions such as tumours and fat-tissue can impair the results. Skin surface techniques are a desirable method of measuring the curvature of the human spine. As well as being non-invasive, they prevent the people being exposed to the radiation. The skin-surface measurements by definition follow the line of posterior elements and not that of the vertebral bodies (as in X-ray measures). The varying distribution of subcutaneous tissue, overlying the spine, in the lumbar region towards the sacrum, it would not necessarily be expected that the absolute curves can be comparable to those measured radiographically. However, all of these measurements are believed to produce a quantified description of the shape of the lumbar spine or the total movement allowed during a task, forward bending (Mannion, Knecht et al. 2004).

5.2.1.3 Arcometer

Arcometer is one of the other possible devices for obtaining the contour of the back. The arcometer is a device used for measuring the angle of curvature. It was created at

the Engineering Faculty at Udine University, Italy. Flavio D'Osualdo *et al.* (1997), compared measurements of the degree of kyphosis between the arcometer and radiographs in addition to inter and intra-rater testing. In their study, the arcometer was applied on spinous processes at any two sites between T1 and T12, including all the more evident kyphotic portions. Correlation index between radiographs and clinical measurements is estimated to be good (0.98).

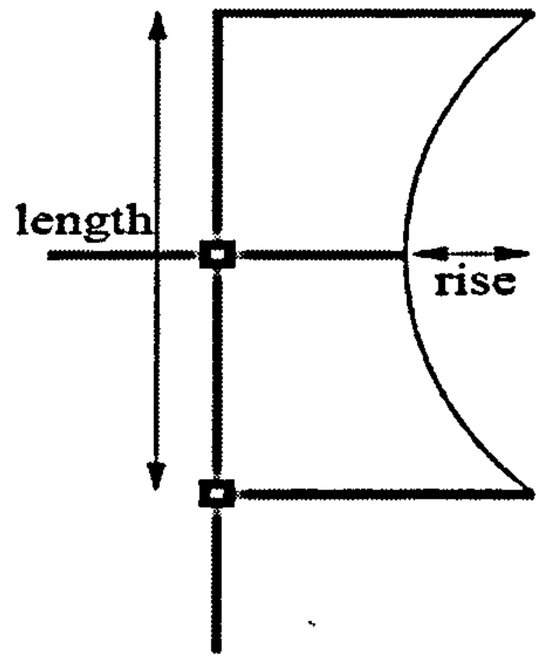


Figure 5- 2 Arcometer

The arcometer is a tool of a long, millimetre-scaled bar and three smaller, perpendicular bars. The first perpendicular bar is fixed at one end. The second movable on a single axis and at the other end the third perpendicular bar is movable on both axes .The instrument can provide the length of the cord and the rise of the kyphosis arc. Through a trigonometric formula the circumference of the radius and the arch of the underlying angle can be determined; the latter corresponds to Cobb's angle. With a double-entry table (x=rise, y=chord) one can calculate the value of the radius and of the circumference and the angle underlying the arch. The main problem of this device is the variability caused by the observer due to the location of the instrument, the end vertebrae chosen, the pressure exerted on the skin, the correct positioning of the bars and scale reading errors.

When performing the measurements, the pad at the base of the central rod is placed on the most posterior part of the kyphotic curve. The top horizontal rod is fixed and placed at the apex of the kyphotic curve. The vertical bar is also millimeter scaled and the bottom horizontal rod can be moved along it so that its pad is at the base of the kyphotic curve. The reading on the vertical bar is the chord length and the reading on the central horizontal bar is the arc rise corresponding to the x and y values as mentioned above.

In our experiment, finding the exact location of lumbar and thoracic regions at each measurement which is repeated at least 10 times is considered to produce unreliable results. The subject is supposed to hold on the posture for specific intervals of lifting activity. This is expected to create positioning and reading errors for the start and end points of each region. Recording the x and y values manually is also considered as very tedious work considering the number of the measurements and subjects. After the radius and the arch of the underlying angle determined, it is still necessary to calculate the coordinates of the vertebral bodies and no relative angle information is provided by arcometer. Although the accuracy is in millimeters level while reading the scale, there is possibility of scale reading error and the subject might cause changes in his or her posture. The peak point of the curvature might change due to the posture change during the measurement resulting in measurement errors.

Due to the reasons mentioned above, although this method is not as harm full as radiography, it is still not a reliable method considering the number of the measurements and the time allocated for an accurate measurement of the spine during a lifting activity.

5.2.1.4 Skin surface markers

Skin surface markers come in varying shapes and sizes. For sagittal profile measurements, where angles are being measured, a lightweight rod with two pieces of radiographic/reflective tape around it is used so that an angle to the horizontal/vertical can be calculated (Martin Descarreaux *et al.* 2003; Y-L Chen *et al.* 1997). The markers are usually placed perpendicularly to the surface of the skin (Chen and Y-H Lee 1997) although not all studies make it clear that this is the case (Martin Descarreaux, et al. 2003). If only positional data is required, spherical markers can be attached to the skin (Y-H Lee *et al.* 1995). For lateral positional measurements a circular piece of radiographic/reflective material is generally used (Michel A. Leroux *et al.* 2000). This is attached to the skin purely to note the position of the marked point relative to other marked points. The position and orientation of the markers are usually recorded using photography or videography. In comparison studies radiographic tape/markers are used as they show up on X-rays so that it can be seen where the markers were placed relative to the vertebrae (Martin Descarreaux, Jean-Sebastien Blouin et al. 2003).

Michael A Leroux *et al,* (2000) performed the non-invasive stereo video graphic estimations of the sagittal plane curves of the spine for the postural geometry evaluation of the Ideopathic Scoliosis (IS) patients. The main objective of their study is to evaluate the accuracy of non-invasive anthropometric approach for the estimation of sagittal spine curvatures in scoliotic patients. Postural geometry evaluation was performed with the subject standing in the foot template with the arms slightly abducted to ensure the visibility of all skin landmarks. The anthropometric estimation of the sagittal curves of the spine is based on the detection of spinous process and the calculation of their position. The landmarks were detected by palpation and identified with a circular reflective marker. In this study the spatial coordinates of the spinous process of T1, T3, T5, T7, T9, T11, L1, L3, L5 and S1 were obtained using a video based system. The position of the T2 and T12 were linearly interpolated. Anthropometric kyphosis (Ka) and lordosis (La) were calculated using the X and Z coordinates as input in a trigonometric equation. Anthropometric kyphosis Ka and lordosis were developed to match the conventional radiologic parameters and to describe the relationship between back surface and spine geometry. Radiologic kyphosis and lordosis were developed to match the conventional radiologic parameters and to describe the relationships between back surface and spine geometry. Radiologic kyphosis and lordosis were considered as the standard measurement even if a ±5 degree error is generally accepted. The correlation coefficients demonstrate a strong relationship between both approaches for kyphosis and lordosis. (r=0.89 and r=0.84) The advantage of the model and the technique represented in their study depends on its non-invasive aspect, the time needed for evaluation and its integration in a complete postural evaluation.

For this research, in the experiment designed, the basic problem for using skin surface markers would be the expertise knowledge. There is also possibility of the movement of the skin when the patients perform the lifting activity which might cause misleading results. Because of the nature of the lifting activity, the subjects are moving their arms with respect to their body, which might cause skin surface markers to be out of side when recording them with the camera. Due to these kinds of risks this method is considered not suitable for this experiment. Although it could have been possible to collect more posture data because of the continuous recording of the motion by a camera, still because of the reasons mentioned above, the reliability of the of the data is

questioned. For these reasons, this method is considered as inappropriate to use in this experiment.

5.2.1.5 Computerized motion analysis systems

The computerized motion analysis systems use various movement sensors affixed to the skin surface at positions believed to correspond to the underlying vertebrae, as determined by palpation and skin marking. The curvature and range of motion of a given section of the whole spine can be measured with them. These computerised motion analysis devices offer the additional advantage of being able to monitor and record continuously the changing curvature of the spine, thereby allowing both the pattern and extent of movement to be assessed not only during range of motion testing but also during the performance of given activities.

In general, most of these motion analysis devices have been shown to be reliable. However, they also have certain drawbacks. Palpation of the precise land marks for placement of the sensors as well as the preparation of the skin for their firm attachment can both be time-consuming. Inaccuracies in the angles measured can arise not only as a result of skin movement unrelated to underlying vertebral movement but also if true contact, complete apposition between the sensors and the skin is not maintained throughout the testing procedure. Thus, the firm and stable attachment of the measuring device to the individual's back plays a crucial role in obtaining reliable measures. In the case of devices that are attached to the patient by means of straps or belts, slippage may be a problem if considerable movement occurs between standing and end ranges of motion; with sensors that are attached to the skin with adhesive/sticky tape, problems may arise if the contact between the sensors and the skin deteriorates, for example if the patient begins to sweat.

Despite the faster transfer rate of coordinate data to the computer via the cables connected to the sensors than the method of calculating the coordinates by the help of skin surface markers, computerized motion systems are very expensive to use for this experiment. They are mostly preferred when there is a need to calculate velocity, acceleration data for dynamic models. The model in this thesis is a static one which asks for the positions of the vertebrae. A suggestion of usage of computerized motion

system for this experiment would be too costly and would be more appropriate for 3 D models.

5.2.1.6 Flexicurve

Several articles detail how the flexicurve can be used to measure spinal curvature (Caine *et al.* 1996, Hart *et al.* 1986; K. Malcolm Tillotson *et al.* 1991.; Hinman 2004). The flexicurve is a flexible piece of coated metal. To use it, an examiner would press it paravertebrally against the patient's back so as to mould it to the same curvature. When this is achieved, the curve is carefully removed and placed on a piece of paper where it is traced. In some tests the patient's skin is palpitated and marked and then the corresponding point on the flexicurve is also marked so that some reference points, usually the spinous processes, are gained. Although cheap, simple to use and free from side effects, the flexicurve does have problems. The flexicurve can lose some of its shape when being transferred from the patient's back to the paper for tracing. Also, when molding the flexicurve onto to the patient's back the force required may alter the patient's posture. Caine, McConnell et al. (1996) looked at ways of improving the measurements taken using a flexicurve and suggested mounting it to a rigid frame at three points so that:

- The flexicurve does not change its shape when being transferred from the patient's back onto the paper for tracing. When the flexicurve is molded into shape the paper used for tracing is attached to the frame alongside the flexicurve, so that the flexicurve is not moved at all.

- The pressure, which is required to mould the flexicurve into the shape of patients' spines, does not cause the patient to change their posture, thus causing the wrong posture to be measured. By having the flexicurve suspended, less pressure needs to be exerted, reducing the possibility of changing the patient's posture. A compacted foam lining is fixed to the flexicurve which also apparently reduces the pressure required.

- The frame is attached by an adjustable means to a stadiometer (an instrument used for measuring the standing or sitting height of a patient). When the patient is first measured the reading of where the frame is on the stadiometer is taken. In subsequent

measurements of the same patient, the frame is moved to the same position. This reduces the chance of placing the flexicurve in a different position each time a patient is measured.

Although these improvements produce more reliable results than most other similar studies, the portability of the flexicurve is compromised.

The data analysis from flexicurve measurements is rather cumbersome for use in practice. This is a big concern in the experiment designed for this research. The flexible ruler is determined to be a reliable and valid measurement technique for the shape of the lumbar spine and may prove helpful in quantifying the lumbar postures. However, this research is for full spine and asks for the full spine curvature. This might cause complications in preserving the shape of the flexicurve for the full spine. Considering the fact that during the experiment continuous motion of the subjects is required, usage of flexicurve would be asking for many breaks for data to be transferred, causing the subject to hold on for longer periods of time destroying the nature of the continuous motion.

5.2.1.7 Inclinometers and goniometers

There are devices used to measure the angle to the vertical when placed on an object. Elaine Thomas *et al.* (1998) used an inclinometer to measure spinal extension. This measurement requires that markings are made on the patient at 5cm below the lumbosacral junction and at 10cm above the lumbosacral junction. These markings are made with the patient standing fully erect. The patient then leans back as far as possible (extension) and the inclinometer is used to measure the angular difference between the two markers. This measurement technique is often used in diagnosing patients with limited ranges of motion. They found that there was a strong association between their spinal extension measurements and the Schober test. K. Malcolm Tillotson *et al.* (1991) used an inclinometer to measure flexed and extended postures to compare with flexicurve measurements. In their study, measurements were taken with the inclinometer over the T12 spinous process and over the sacral crest at the S2 level in both the flexed and extended postures. They found that inclinometer measurements are not the same with flexicurve measurements. Kyphometers, goniometes and dual

inclometers have the disadvantage that only one global region of the spine can be monitored at a time (e.g. thoracic or lumbar spine or sacral tilt). Because of this, for full spine measurements which are desired in this study, these devices are not preferred.

5.2.1.8 Spinal Mouse

The Spinal Mouse works by using two inclinometers arranged in orthogonal planes and an accelerometer (Figure 5.3). The combination of the two inclinometers in perpendicular planes allows the device to measure the angle to the vertical whether measuring in the sagittal or lateral planes. The accelerometer allows the device to measure the distance that the wheels of the Spinal Mouse have travelled over the patient's skin. This data is then sent to a computer via a serial port to provide a digital representation of the skin surface curve of the human spine. The hardware appears to measure correctly and accurately and it is quoted that its angular measurement accuracy is 0.1 and distance measurement accuracy is 1 mm.

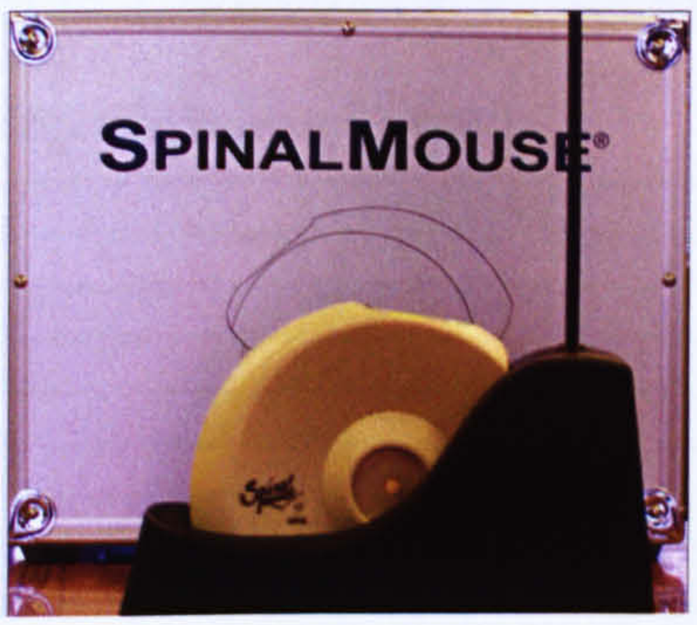


Figure 5- 3 The physical shape of the spinal mouse with the base unit (Spinal Mouse Manual, 2000).

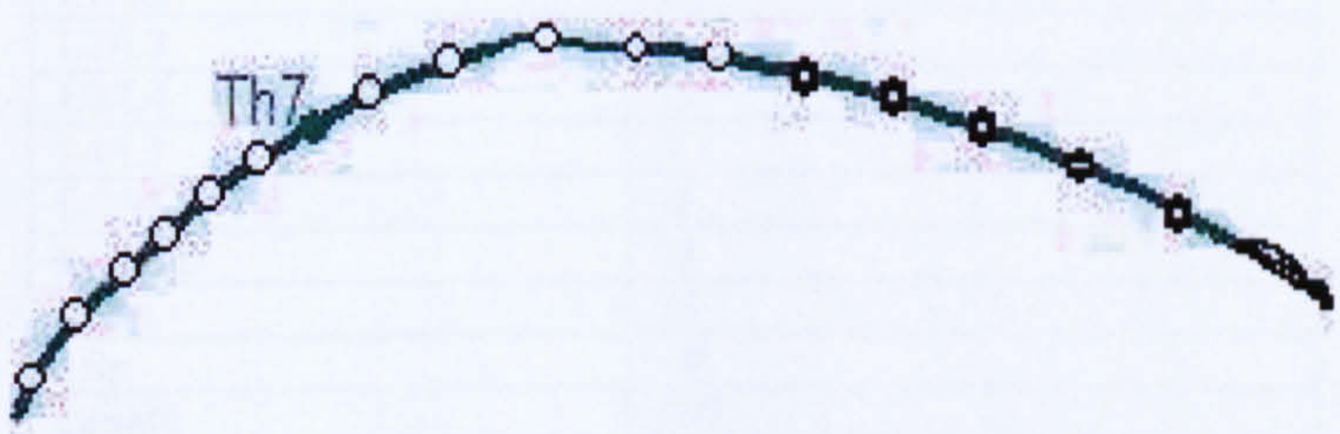


Figure 5- 4 Spinal curvature produced by the spinal mouse software (Spinal Mouse Manual, 2000).

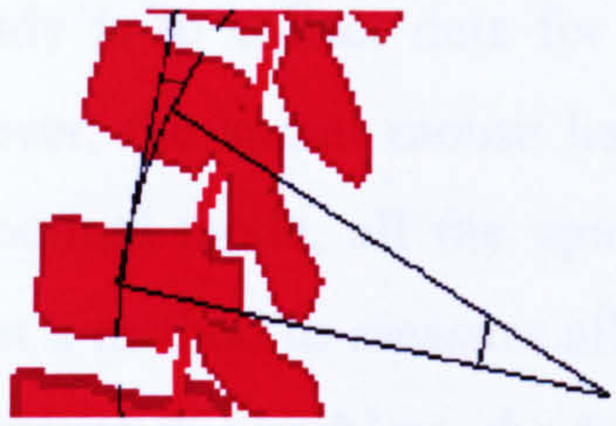


Figure 5- 5 Spinal Mouse Intervertebral Angles

Using the angle and the distance travelled, the SM software can construct line segments at the recorded angle for the recorded distance continuously. SM software provides set of line segments to form the spinal curve (Figure 5.4). The intervertebral angle is the difference between the orientations of two adjacent vertebrae to the vertical (Figure 5.5). Once all 17 intervertebral angles (T1/T2–L5/S1) are calculated by the software of the Spinal Mouse, the thoracic and lumbar spine section angles are also supplied in the Spinal Mouse software's results table (Table 6.1). According to the manual this is done simply by adding the intervertebral angles for Th1/2 to Th11/12 for the thoracic section of the spine and by adding Th12/L1 to L5/S1 for the lumbar spine section.

Table 5- 1Example output from the Spinal Mouse software

Segment	Flex Posture
Th1/2	5
Th2/3	-10
Th3/4	-5
Th4/5	0
Th5/6	-1
Th6/7	0
Th7/8	2
Th8/9	3
Th9/10	4
Th10/11	9
Th11/12	13
Th12/L1	11
L1/L2	10
L2/L3	8
L3/L4	11
L4/L5	7
L5/S1	-2
Sac/Hip	35
ThSp	36
LSp	-48
Length	489

Flex - the intervertebral angles of the subject in a flexion posture

Sac-Hip is the sacral hip angle to the vertical

ThSp - the overall change in the angle of the thoracic section

LSp - the overall change in angle of the lumbar section

Length - the length of the curve of the spine

The main objective in our study is to collect data for the full intervertebral angles starting from C1 to L5. However, the spinal mouse has some major defects in this respect. For example, in the normal mode, all the spinal measurements have to be between C7 and S1; there is not a method to measure all of the spinal column starting from C1 to S1. In order to overcome this problem, the free mode was used. In the free mode, the software draws the contour followed by the device as in the normal mode; however, no intervertebral angles are calculated. Instead, the free mode allows the user to select up to 22 points; at each point the software calculates the distance from the previous point and the angle of the tangent at that point. However, there are 24 vertebrae between C1 and S1. In order to collect the full spine data, a combination of the two modes is considered to be a good solution with the help of additional software for generating full spinal curvature data. This additional software is developed by the research student for Human Spinal Curvature Thesis (Farnsworth 2007).

The Spinal Mouse with a higher measuring accuracy than many other methods can prove to be a reliable method for analyzing surface curvatures. Spinal mouse gives us valuable information which enables us to produce coordinate data to draw the full spinal curvature.

5.2.2 Conclusion

In summary, considering the advantages and disadvantages of measurement options listed above, the spinal mouse was chosen to be used in the experiments. The main criterion for the selection of the spinal mouse is the accuracy. No previous expertise knowledge to obtain the data is necessary while doing the measurements. The measurement time is very short. Although the device in the normal mode can only measure the thoracic and lumbar regions, with the help of the free mode the full curvature of the spine can be traced. By developing special software for coordinates, the two measurements for the same posture are expected to be overlapped so that the cervical region could be added to the top of the thoracic part to obtain the full spine data with the additional software.

5.3 The Experiment

The parameters are explained in detail in this section.

5.3.1 Controlled parameters

Gender: There is not much information about the posture differences of genders during the full lifting activity. Study of Pearsall and Reid (1992), focuses on erect postures, however, none so far have investigated the postures that both females and males had so far. Although the fundamental units of the spine are the same for each gender, ie, both genders have the vertebrae, muscles, ligaments and disks; however typical anthropometric differences between the genders such as height and weight may play a role in the body postures of each gender. Gender is taken as a major parameter in this experiment. The main purpose of this experiment is to investigate whether the difference in gender results in different spinal postures. With different posture patterns for each gender, it is expected to have different loading patterns for both males and females. Any differences between the contour of the male and female bodies may provide important data and information for LBP investigations in the future.

Dependent Parameter

Spinal curvature The spinal curvature is determined by the relative orientation and the positions of the vertebrae which form the spinal column with the combined effect of the muscles and ligaments. The relative orientation and positions of the vertebrae affect the role of the muscles and ligaments causing a new load distribution while the different role of the muscles and ligaments also creates a change in the spinal curvature. For these reasons, the spinal curvature at each phase of the lifting activity was measured in this experiment. The surface length of the spine was computed by the Spinal Mouse from the distance that it has travelled from C7 to L5 over the skin of the back. This value is used to calculate the co-ordinates of the vertebral bodies forming the spinal curves. The number of the spinal curvatures to be recorded during the lifting activity is defined to be 10 as minimum.

5.3.2 Fixed parameters

The weight of the object to be lifted: The aim of the experiment is to investigate the geometric positioning of each vertebra during a lifting activity. The ergonomics studies show that magnitude of the object and the shape of the object plays role in a lifting technique. A simple rectangular cartoon box with negligible weight is asked to be lifted by holding from the gaps positioned on each side of it. With a heavier weight, it is possible to expect changes in the posture of the subject and this change is expected to be relevant to the strength of the subjects. In order to eliminate this factor, a standard box with a negligible weight is chosen.

The horizontal and vertical distance of the object from the subject: The relative height of the person with respect to the height of the object plays an important role by affecting the final the curvature of the spine attained by the body, thereby effecting the load distribution on the body. Before starting the spinal curvature measurements, the initial height of the object is recorded and this is kept as constant for each experimental subject during the start of the experiment. The initial position of the object was 52 cm above the ground due to the height of the boot of the car used in the experiment. The horizontal distance from the subject also plays a crucial role while the subject reaches to the object affecting the flexion and the moment arm of the load. For this purpose, the location of the object was kept constant and the horizontal distance between the load and the subjects was kept as 25 cm by marking the standing point on the floor before starting the experiment (Figure 5.6).



Figure 5-6. Geometrical distances of the object and the subject at the start of the experiment and (α) is the reference line angle between the horizontal and the line connecting L5 to T1.

Back pain history of the subject: For this study, we chose the subjects who had healthy spines. A subject who experienced simple back pain sometime in their life was acceptable as long as they were not currently suffering from any form of back pain, as this might influence their posture.

5.4 Methodology

5.4.1 Theory

The thrustline theory is applied in two dimensions. In order to implement different body postures into this theory, the full lifting activity is supposed to remain in sagittal plane only. Pure sagittal lifting is meant to be pure flexion. The subjects are required to perform the lifting activity in an extremely slow way. The reason for this research is to investigate how the spine (starting from neck to hips) changes its position during a lifting activity. In order to simulate the real lifting activity, it is necessary to take as many measurements as possible while lifting an object from the boot of a car to detect the possible changes in the postures of the subjects. The number of the measurements is minimum 10 for each subject. The measurements are supposed to start from the cervical spine and end at the sacrum. As the spinal mouse – in normal mode - can only measure the angles from T1/2 to L5/S1, the measurements are in two parts; the first part in free mode - and the second part is in normal mode to measure. In free mode, the measurements started from C1 and finished at L5. In normal mode, the measurements started at T1 and finished at L5. With these measurements the spinal curvature is recorded and the relative angle of each vertebra with respect to each other is produced in the result table of the spinal mouse by the Spinal Mouse Software.

5.4.2 Measurements

Loughborough University ethical advisory committee approval was obtained for the experiment and each volunteer read and signed the participation document before they started the experiment 20 males and 19 females volunteered for the experiment. The average height of the males measured in the experiment is 178.3 (5.6) cm and average weight of 74.3 (12.8) kg. The average height of the females measured in the experiment is 164.3 (4.3) cm, and the average weight of 52 (11.2) kg. Age groups are similar with

the average age of 27 (3.4) years old for males and 25 (10) for females. None of the volunteers had back pain history.

Table 5- 2 Demographic characteristics of the experiment subjects.

Male			
	Height	Weight	Age
Max	190.5	112	36
Min	169	55.5	23
Range	21.5	56.5	13
Average	178.34	74.29	26.95
Std	5.6	12.8	3.4

Female			
	Height	Weight	Age
Max	171.3	86.7	58
Min	156	47.3	24
Range	15.3	39.4	34
Average	164.30	52.00	25.00
Std	4.3	11.2	10.9

Spinal Mouse is guided along the midline of the spine, starting at the spinous process of C7 and finishing at the top of the anal crease for the normal mode and for the free mode starting from the occipital bone, finishing at the top of the anal crease. These landmarks are firstly determined by palpation and marked on the contour of the spine. Distance and angle measures are communicated from the device to a base station positioned approximately 1-2 meters away and interfaced to a laptop. Data is sampled at every 1.3 mm as the mouse is rolled along the spine, giving a sampling frequency of approximately 150 Hz. This information is used to calculate the relative positions of the sacrum and vertebral bodies of the sacrum and vertebral bodies of the underlying bony spinal column.

Spinal Mouse measurement requires the tracking of the spine so extremely thin clothes are asked to be worn. The participants are asked to wear flat or nearly flat shoes. The participants are asked to use their both hands to eliminate the affect of asymmetric loading. During the experiment the postures are first described and demonstrated by the research student and practiced once by volunteers.

The distance of the volunteers from the boot of the car is held constant by 10 cm to provide the consistency and the distance from the boot of the car to the load position is kept as 25 cm at initial position (Figure 5.6). During the lifting activity, the volunteers are not allowed to lean against the car. The parameters are recorded by the spinal mouse in each position are the individual motion segment angles from T1-2 to though

L5-S1 angle and spine curvature length for the normal mode. First the normal mode measurements are conducted from T1 to L5, and then the free mode measurement is conducted starting from C1 to L5 without the subject changing his or her posture between these two measurements. With the help of these parameters, further data analyses are conducted. This is explained in section 5.4.

First posture: Maximum extension is required, legs straight, arms extended to hold the load which is placed in the boot of a car; trunk is extended as much as possible.

Final posture: Standing upright, knees straight arms extended holding the load.

A photo of the subject is taken while a measurement using spinal mouse is conducted for each posture. The photos of the one of the experiment subject are as follows, describing the full set of measurements conducted for the full span of a lifting activity.

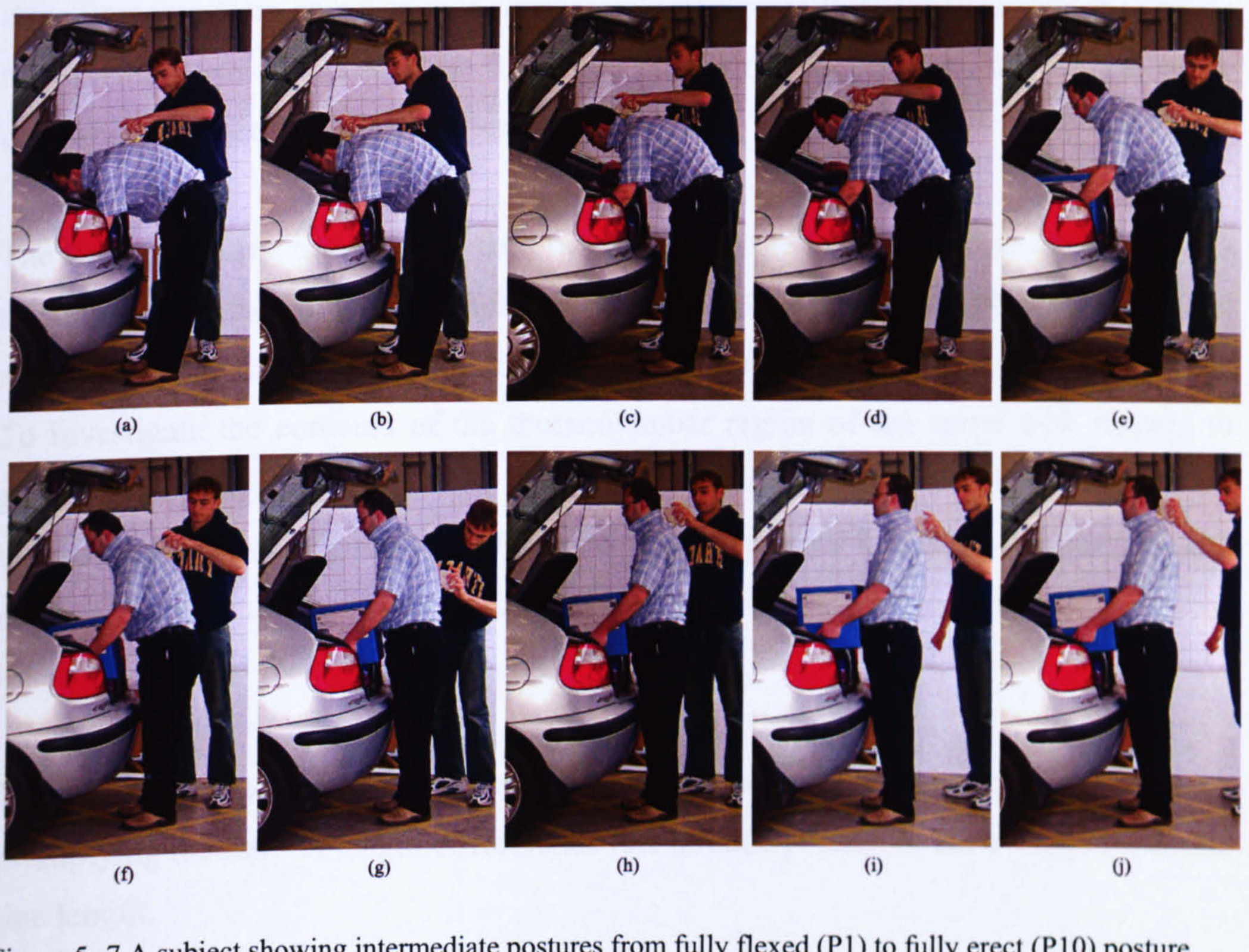


Figure 5- 7 A subject showing intermediate postures from fully flexed (P1) to fully erect (P10) posture.

Table 5- 3 The angle of line α connecting the lower L5 and upper C1 measured shown from horizontal as shown in Figure above. P1 is the fully flexed posture P10 is the fully erect posture.

Postures	P1	P2	P3	P4	P5	P6	P7	P8	P9	P10
α	1	3	10	21	27	41	53	68	75	85

5.5 Data Analysis

The experiment data needed pre-processing. The files containing all the posture data of the 39 experimental subjects are recorded in the software of the spinal mouse. The files containing all the posture data for each of the 39 subjects were recorded in the software of the Spinal Mouse. The measurements from the Spinal Mouse only provide the length of the curvature and the relative angles of each vertebra with respect to each other for thoracolumbar region. The x and y coordinates of spinal segments are calculated in the sagittal plane with the code developed in Java (J.M.Farnsworth, 2007). The software calculating the x and y coordinates of the thoracolumbar region is run for 39 people for all the postures produced by them. To produce the full spine data, free mode measurements from spinal mouse software is transferred to excel files. The free mode measurement which includes the full spine data is overlapped with the normal mode data which contain only Thoracolumbar Spine data.

The Reference Line is defined as the line connecting the lower end plate of vertebra L5 and superior surface of C1. The Reference Line Angle (α), defined as the angle that the reference line makes with the horizontal for each posture, is calculated for each posture. To investigate the contours of the thoracolumbar region of the spine with respect to gender during sagittal plane lifting activity, the data from the Java code are transferred into the excel files and grouped with respect to the reference line angle in intervals of 5 degrees. In order to make comparisons between the postures, the length of the reference line is normalized for both genders.

The x and y values of each vertebra coordinates for each posture are normalized by multiplying the ratio of length of reference line of each posture to the average reference line length.

$$(x_n, y_n) = (x_{original}, y_{original}) * (Length_{(average\ reference\ line)} / Length_{(reference\ line)}) \quad (1)$$

where;

(x_n, y_n) are the new coordiante values

$(x_{original}, y_{original})$ are the measured raw coordiante values

$Length_{(reference\ line)}$ is the length of the reference line in the specified interval

$Length_{(average\ reference\ line)}$ is the average length of the reference line.

All the posture data for 39 people were clustered with respect to the reference line angle with 5 degrees of interval. The postures for females and males are investigated separately. The postures within the same cluster of reference line angle are drawn in excel graphs. The results of the analyses for investigating the body posture is provided in section 6.7

5.6 Results

For thrustline theory, the reaction forces at the end points are calculated with respect to the coordinate frame which connects the lower endplate of the lumbar L5 and the upper surface of the cervical C1 which forms the y coordinate and the line perpendicular to this line as x axis. For this purpose orientation of reference line is very important as it determines the magnitude of the shear and compressive forces in this region. All the postures obtained for females and males are grouped with respect to the angle of the reference line. Student's t tests for independent samples is used to compare the mean values of x and y coordinates of each vertebra from C1 to L5 for both genders for 19 intervals of reference line angle with 5 degrees of increment starting from (-5° to 0°) to (85° to 90°). The results showing the differences of the mean values of X and Y coordinates with the magnitude of the significance factor for each gender based on the Student's t test are provided in Figure 5.8 and 5.9

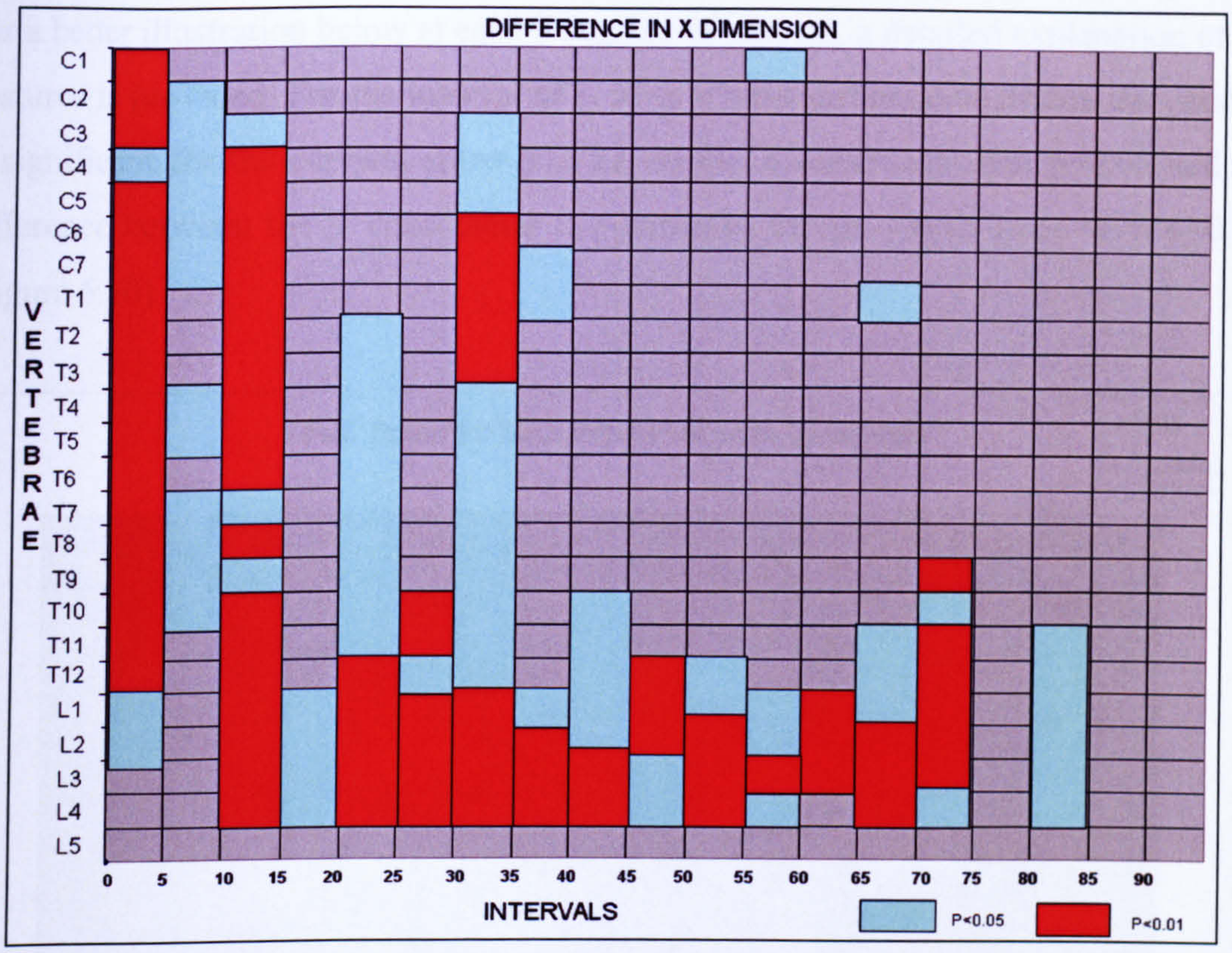


Figure 5- 8 The mean difference between X coordinates of the genders for the full spine with a highlight on different significance (p) values.

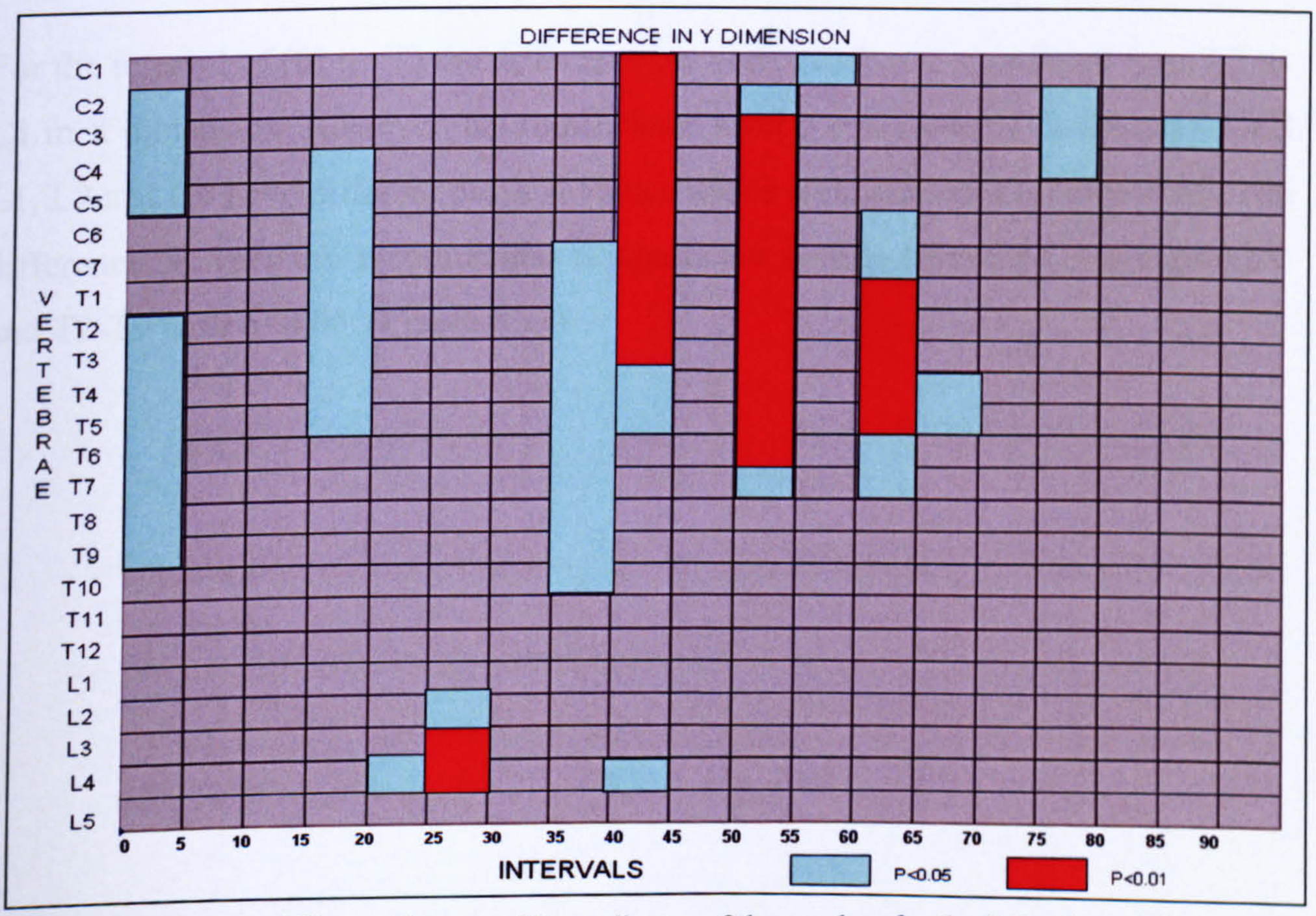


Figure 5- 9 The mean difference between Y coordinates of the genders for the full spine with a highlight on different significance (p) values.

For a better illustration below at each 5 degrees of interval, a detailed explanation of the postures is provided. For the interval of (- 5° to 0°) the difference between the genders is significant for the cervical spine (C2-T2) in the X dimension with $p<0.05$ and the difference between the Y coordinates is significant for the whole spine with $p<0.01$. (Figure 5.10)

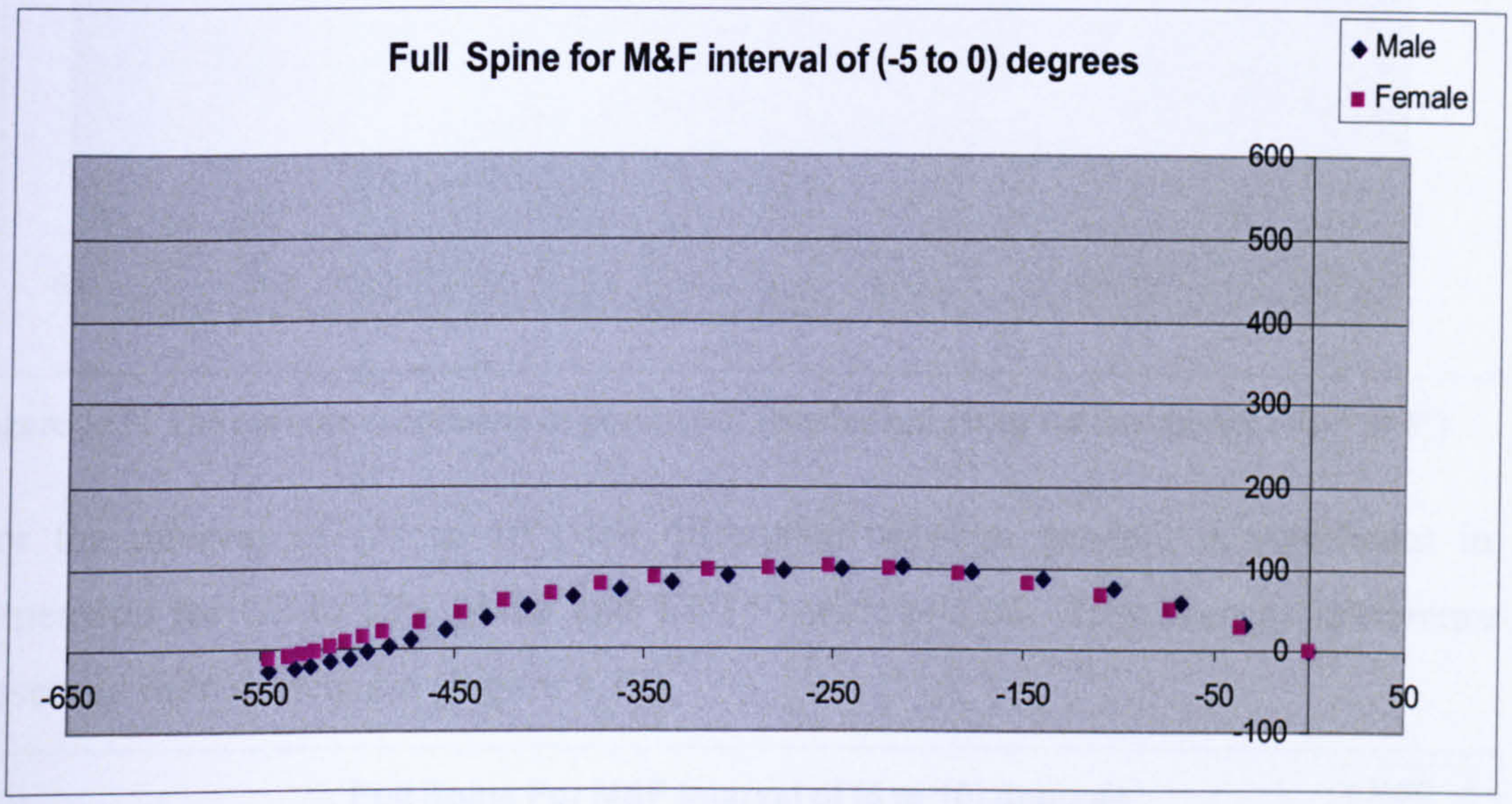


Figure 5- 10 The average coordinates of postures of females and males for the interval of (- 5° to 0°)

For the interval of (0° to 5°) the difference between genders is significant from L2 to C1 in X dimension. However, the significance level is $p<0.01$ for T12-C5 and C1-C3. L1, L2 and C4 have different mean X values with a significance level of $p<0.05$. The difference between the Y coordinates is significant starting from C2-C5 with $p<0.05$ and T2-T9 with $p<0.05$. (Figure 5.11)

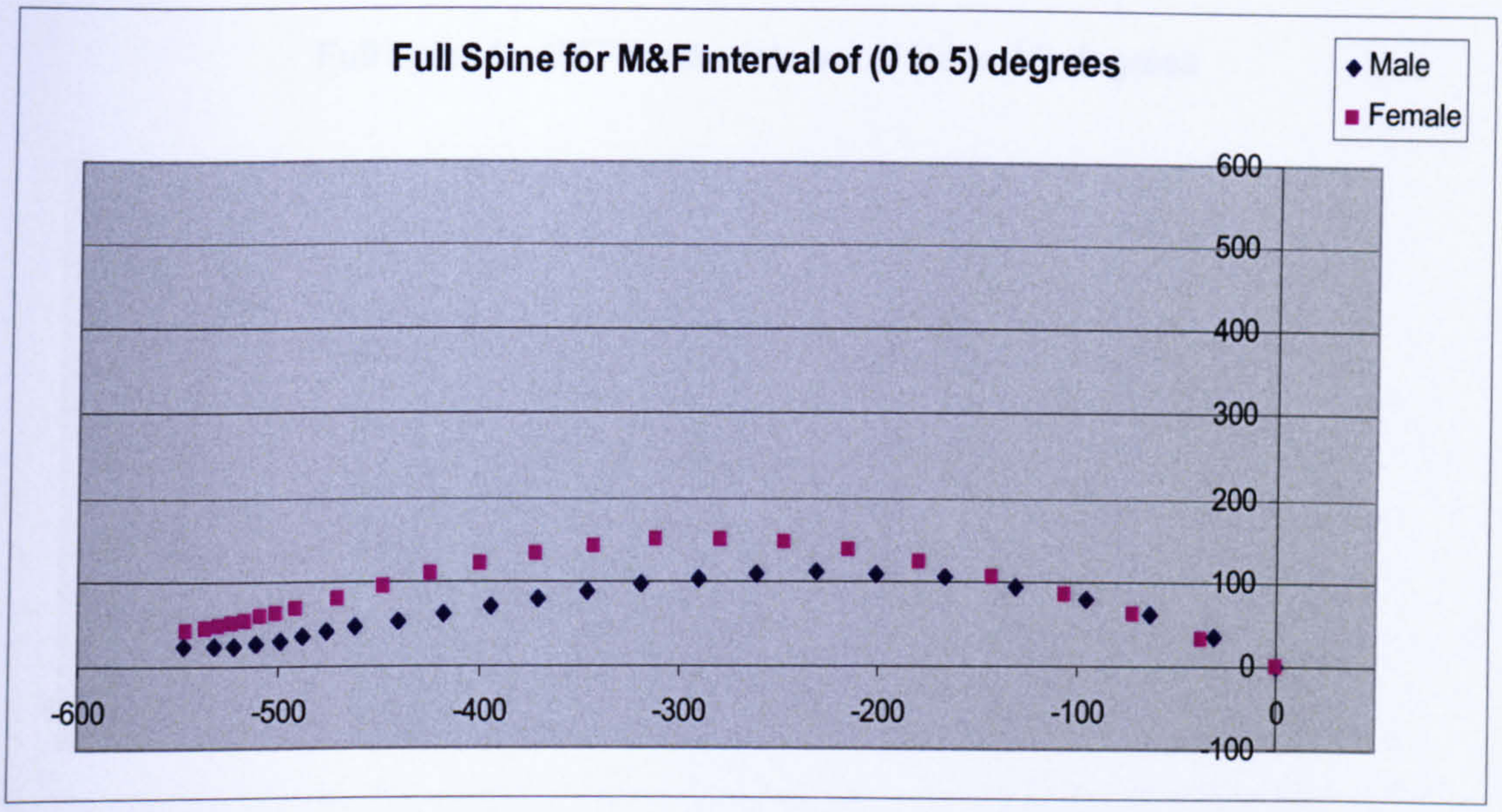


Figure 5- 11 The average coordinates of postures of females and males for the interval of (0° to 5°)

For the interval of (5° to 10°) the difference between genders is significant in X dimension for C2 to C7, T4-T5 and T7-T10 with $p<0.05$. However, no difference is observed in Y dimension (Figure 5.12).

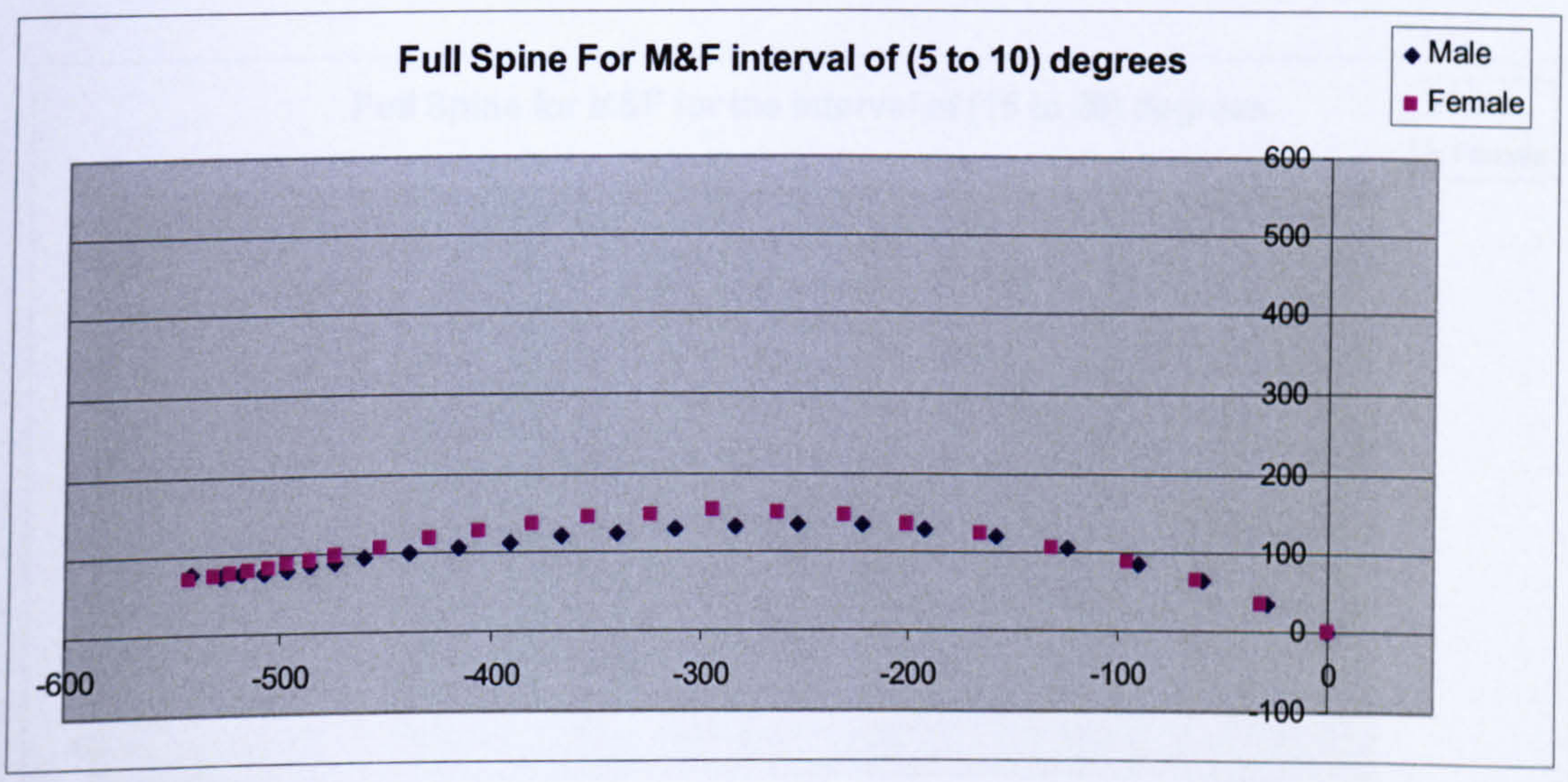


Figure 5- 12 The average coordinates of postures of females and males for the interval of (5° to 10°)

For the interval of (10° to 15°) the difference between genders is significant in X dimension for T7, T9, C3 with $p<0.05$ and for C4-T6, T8, T10-L4 with $p<0.01$. However, no difference is observed in Y dimension (Figure 5.13).

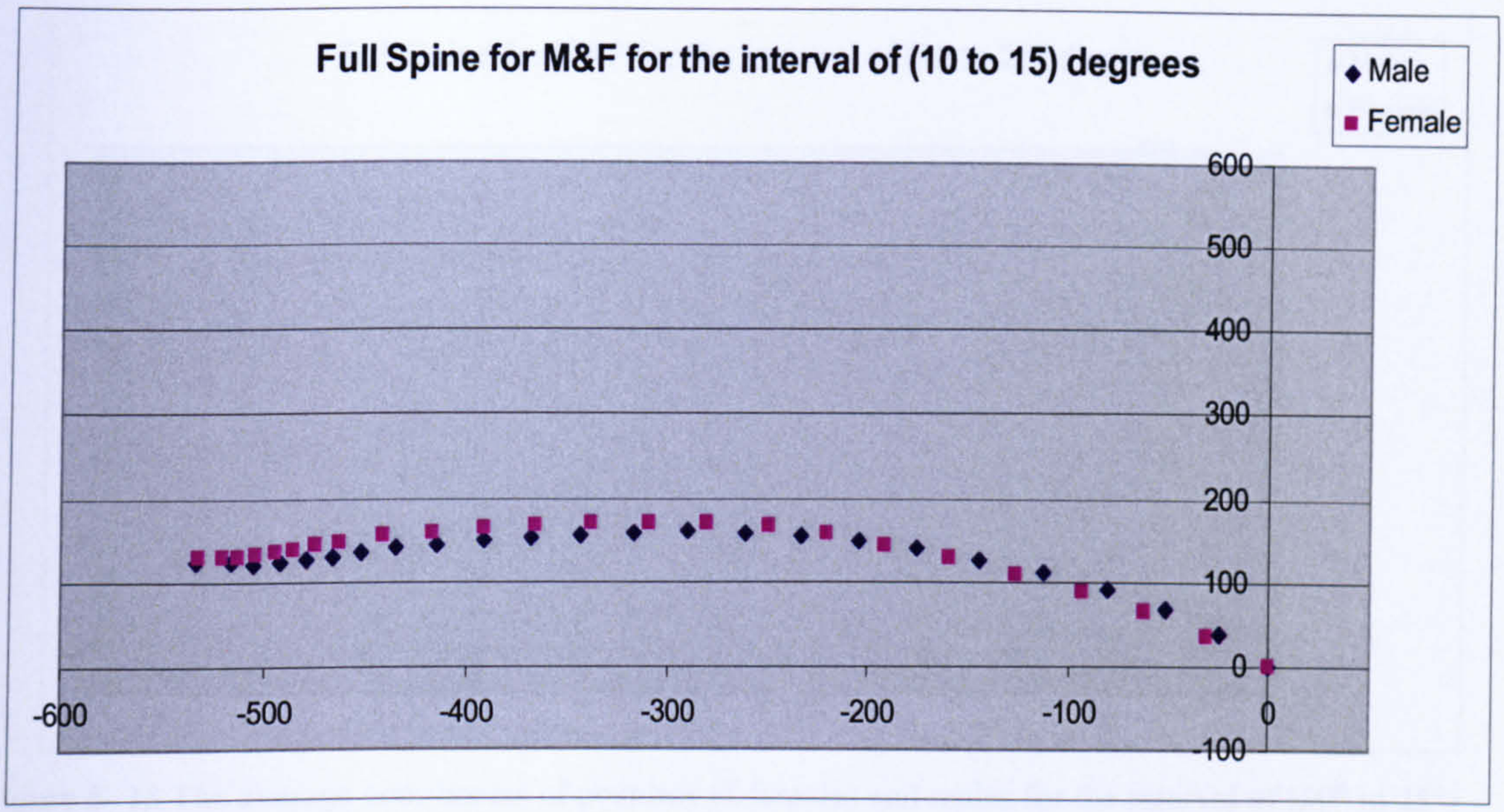


Figure 5- 13 The average coordinates of postures of females and males for the interval of (10° to 15°)

For the interval of (15° to 20°) the difference between genders is significant for L1 to L4 with $p<0.05$ in X dimension. In Y dimension the difference between the mean values of genders is C4-T5 with $p<0.05$ (Figure 5.14).

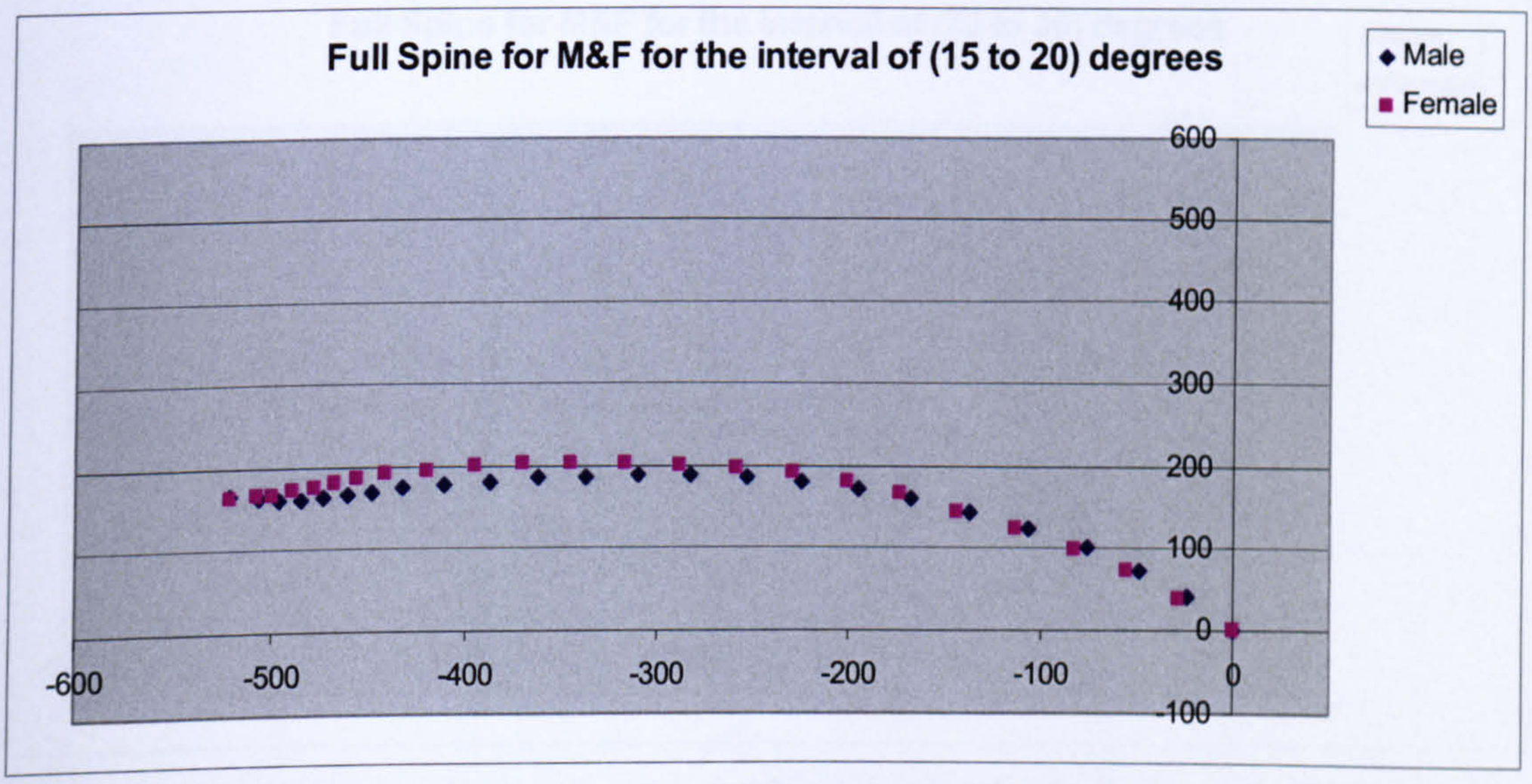


Figure 5- 14 The average coordinates of postures of females and males for the interval of (15° to 20°)

For the interval of (20° to 25°) the difference between the mean values of genders is significant for L4 to T12 with $p<0.01$ and for T11 to T2 with $p<0.05$ in X dimension. In Y dimension the difference between the mean values of genders is for L4 with $p<0.05$ (Figure 5.15).

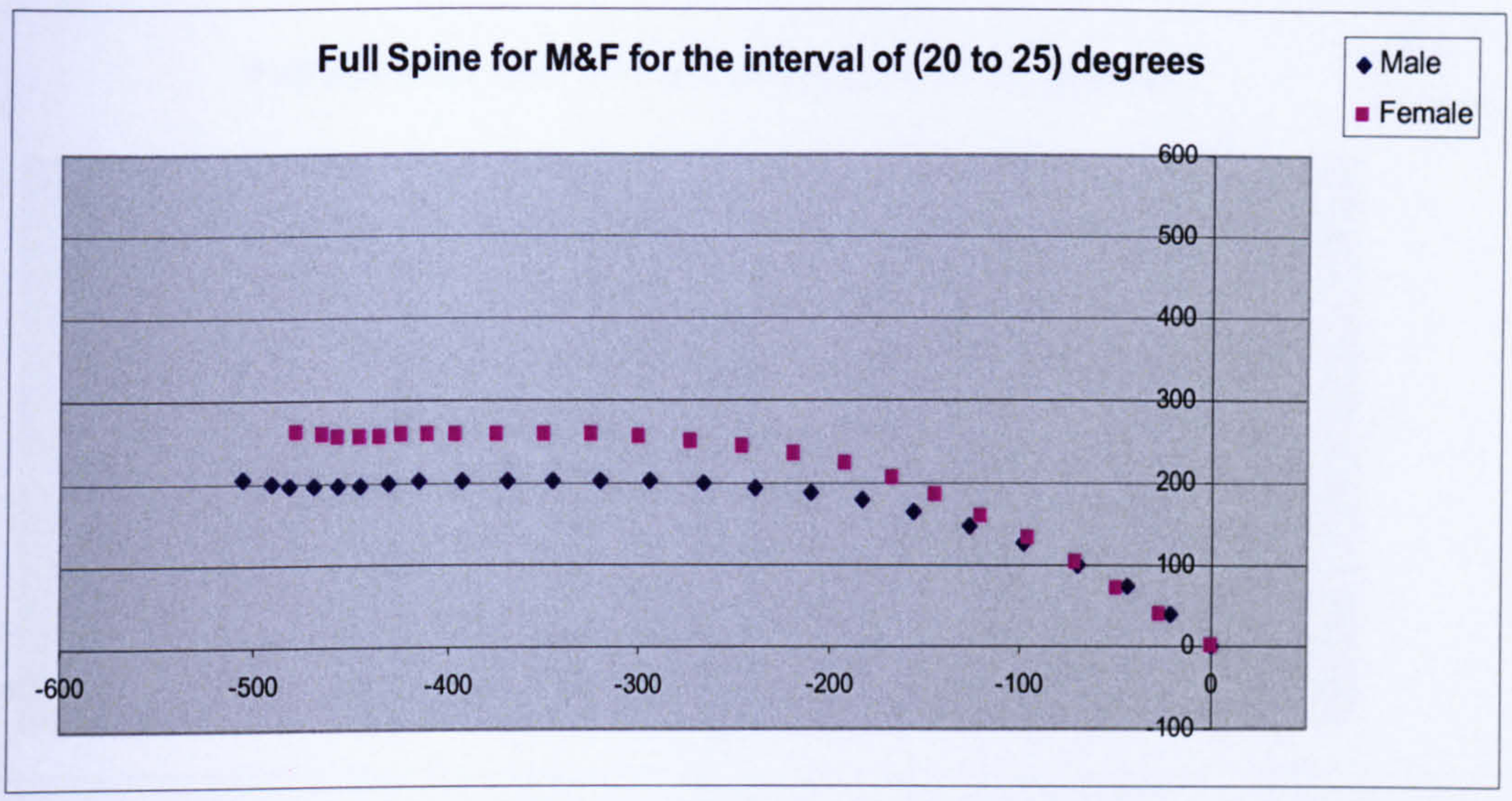


Figure 5- 15 The average coordinates of postures of females and males for the interval of (20° to 25°)

For the interval of (25° to 30°) the difference between genders is significant for L4 to T10 with $p<0.01$ except for T12 where p is <0.05 in X dimension. In Y dimension the difference between the mean values of genders is for L4, L3 with $p<0.01$ and for L2 with $p<0.05$ (Figure 5.16).

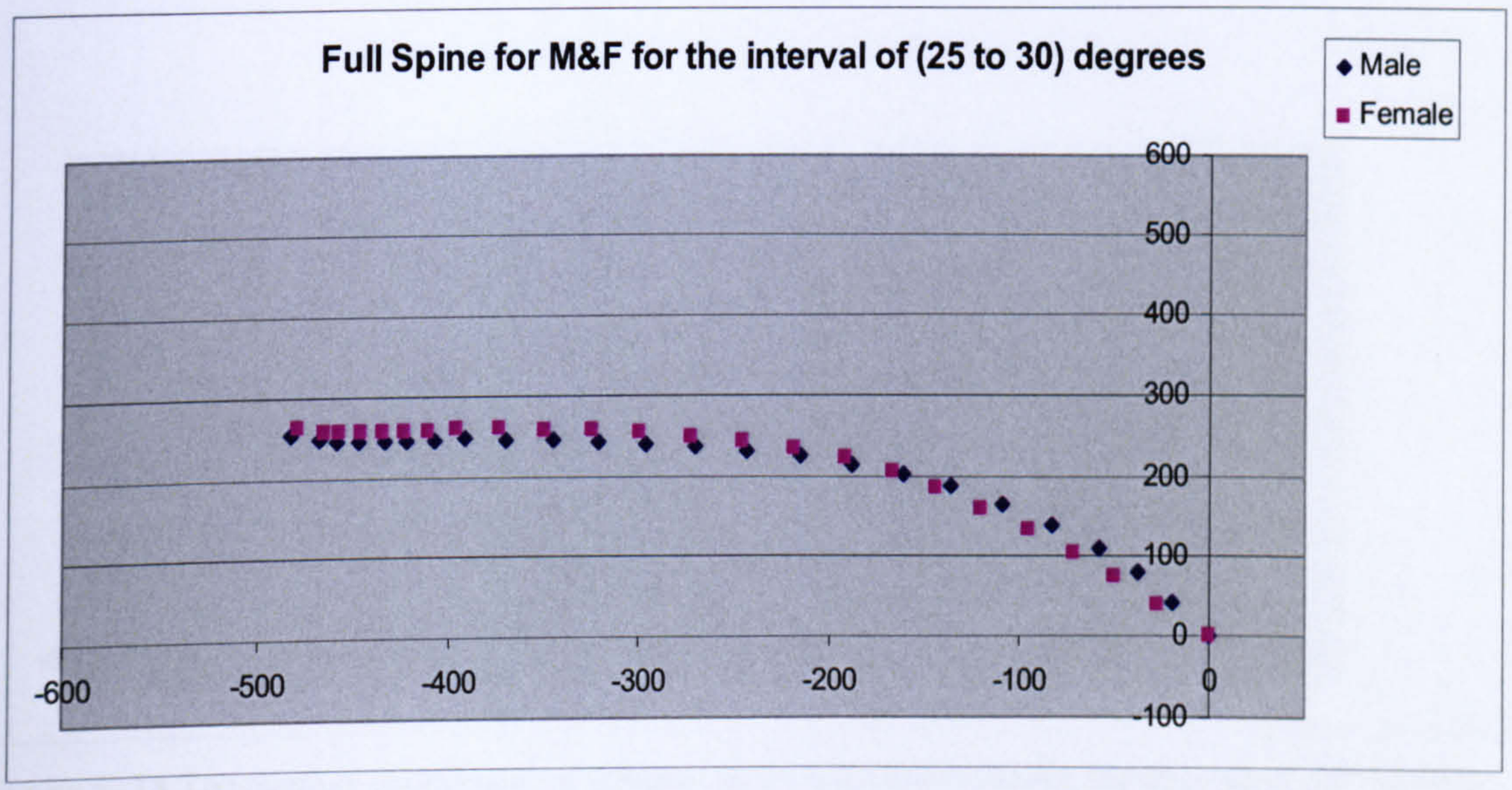


Figure 5- 16 The average coordinates of postures of females and males for the interval of (25° to 30°)

For the interval of (30° to 35°) the difference between genders is significant for Lumbar spine and T3 to C6 with $p<0.01$ and for T12 to T4 and C5 to C3 with $p<0.05$ in X dimension. In Y dimension the difference between the mean values of genders is not significant (Figure 5.17).

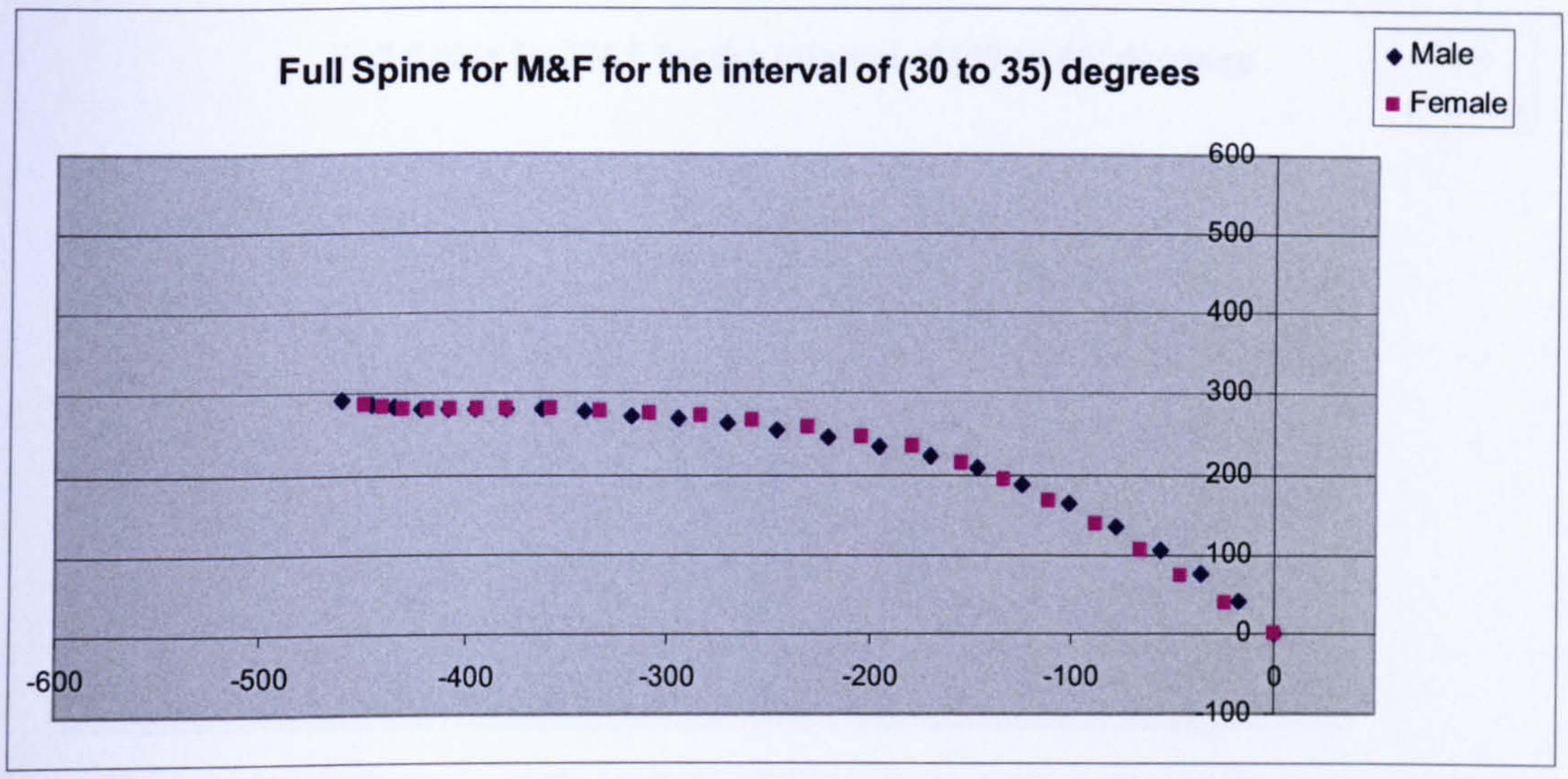


Figure 5- 17 The average coordinates of postures of females and males for the interval of (30° to 35°)

For the interval of (35° to 40°) the difference between genders is significant for L4, L3, L2 with $p<0.01$ and for L1, T12 with $p<0.05$ in X dimension. In Y dimension the difference between the mean values of genders is from T10 to C7 with $p<0.05$ (Fig 5.18).

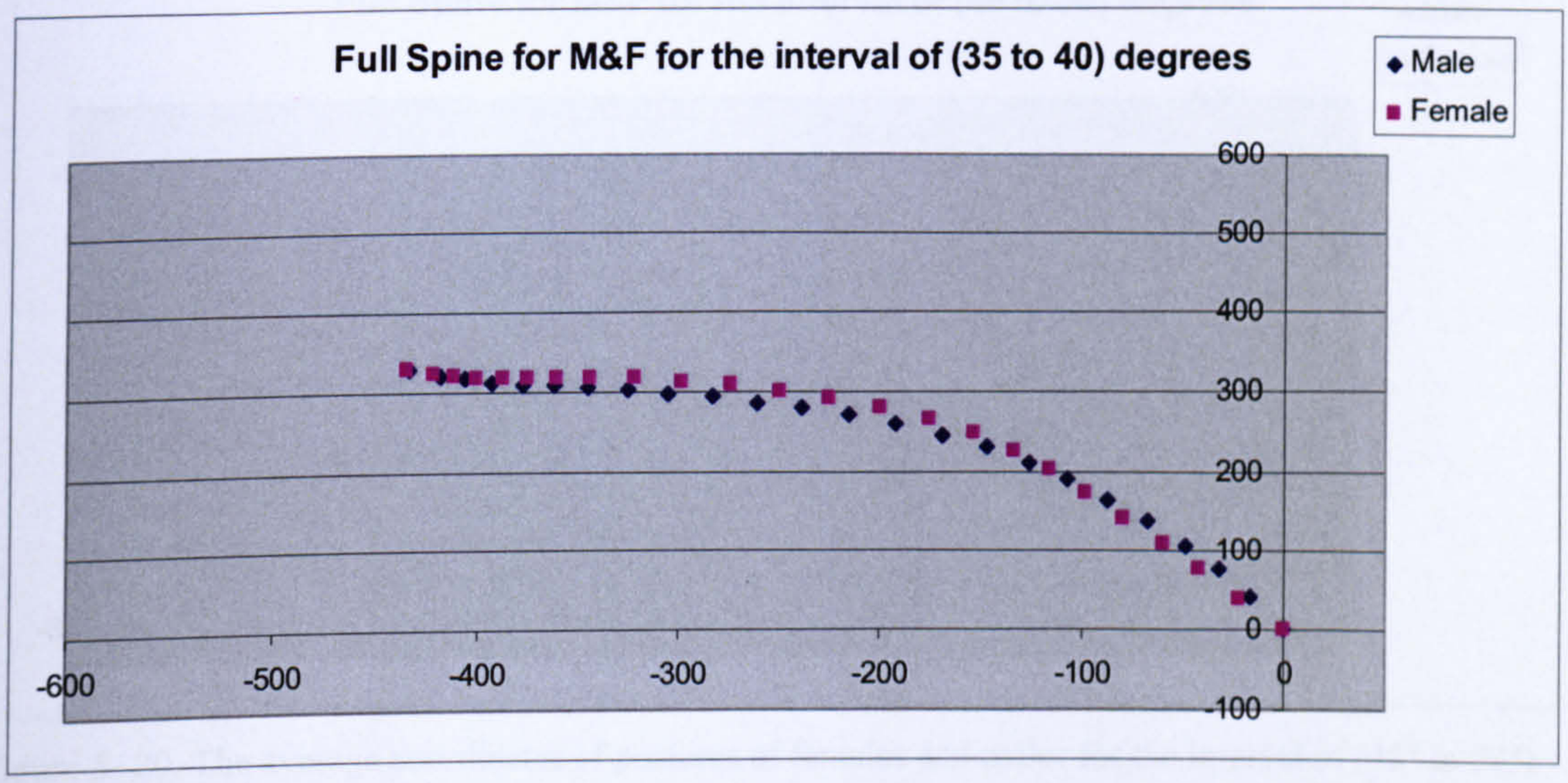


Figure 5- 18 The average coordinates of postures of females and males for the interval of (35° to 40°)

For the interval of (40° to 45°) the difference between genders is significant for L4, L3 with $p<0.01$ and for L2-T10 with $p<0.05$ in X dimension. In Y dimension the difference between the mean values of genders is for L4, T5, T4 with $P<0.05$ and for T3 to C1 with $p<0.01$ (Figure 5.19).

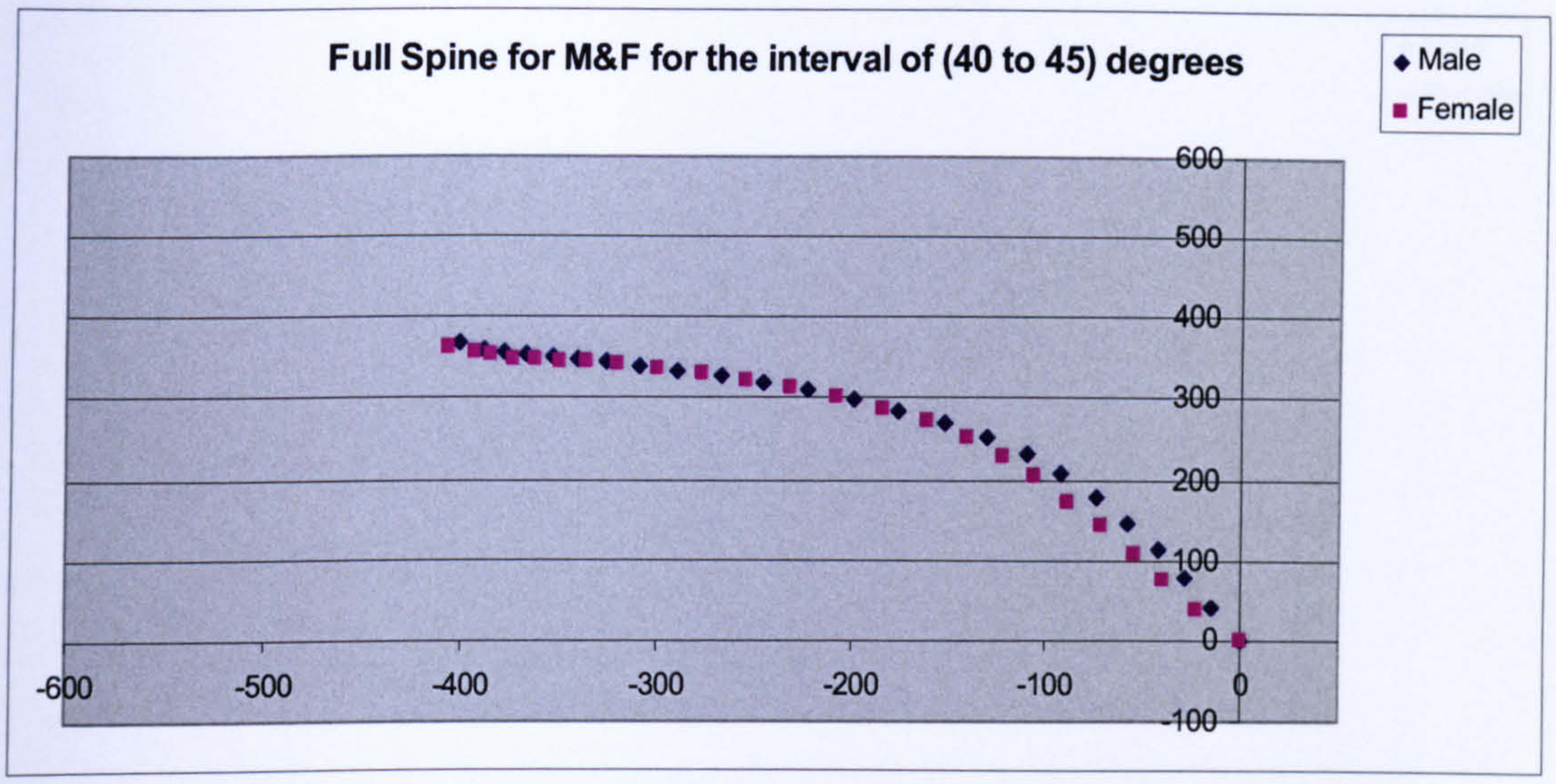


Figure 5- 19 The average coordinates of postures of females and males for the interval of (40° to 45°)

For the interval of (45° to 50°) the difference between genders is significant for L4, L3 with $p<0.05$ and for L2, L1, T12 with $p<0.01$ in X dimension. In Y dimension the difference between the mean values of genders is not significant (Figure 5.20).

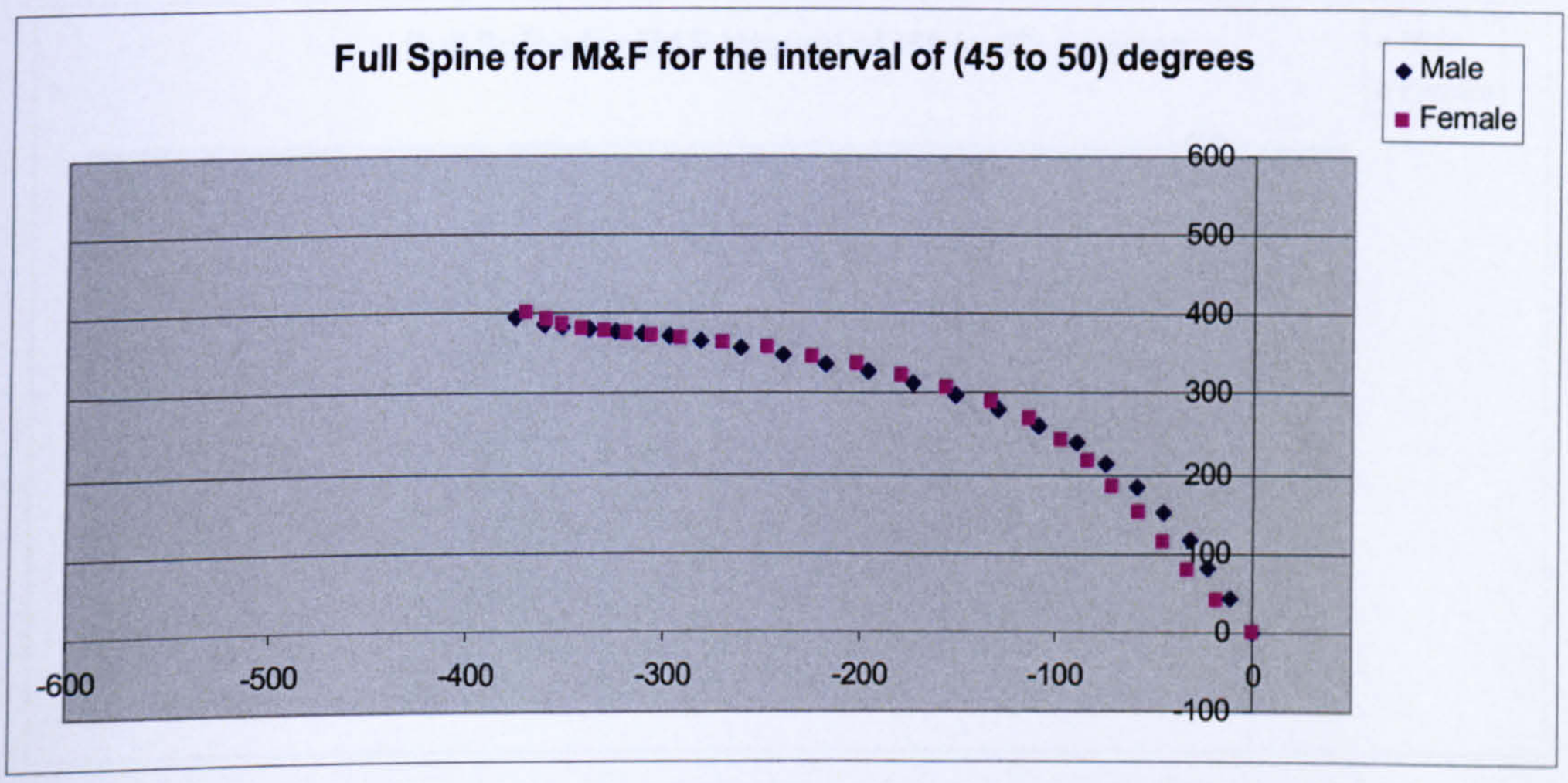


Figure 5- 20. The average coordinates of postures of females and males for the interval of (45° to 50°)

For the interval of (50° to 55°) the difference between genders is significant for L4, L3, L2 with $p<0.01$ and for L1, T12 with $p<0.05$ in X dimension. In Y dimension the difference between the mean values of genders is significant for T6 to C3 with $p<0.01$ and for T7, C2 with $p<0.05$ (Figure 5.21).

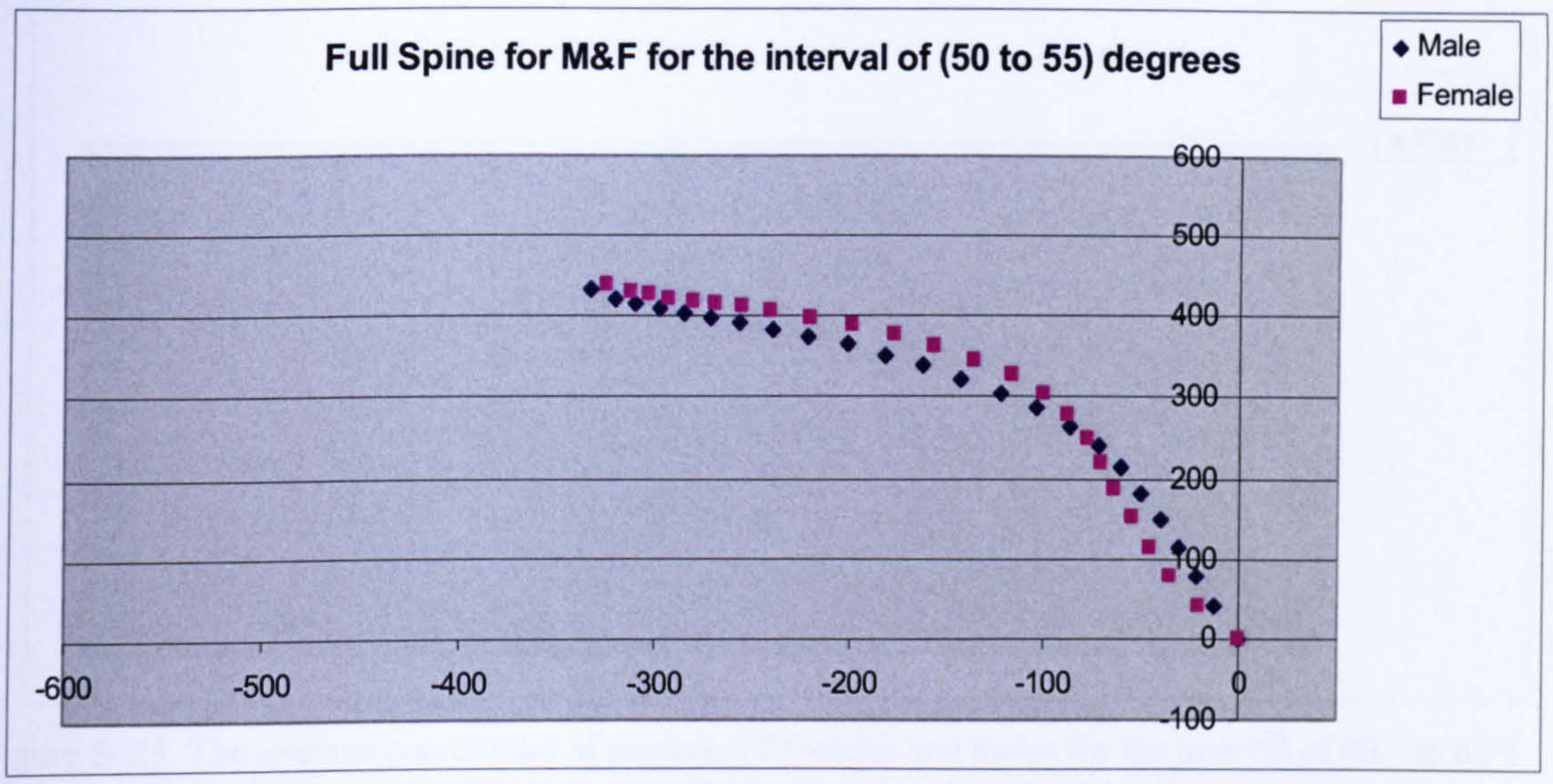


Figure 5- 21 The average coordinates of postures of females and males for the interval of (50° to 55°)

For the interval of (55° to 60°) the difference between genders is significant for L4, L2, L1 with $p<0.01$ and for L3 with $p<0.05$ in X dimension. In Y dimension the difference between the mean values of genders is significant for C1 with $p<0.05$ (Figure 5.22).

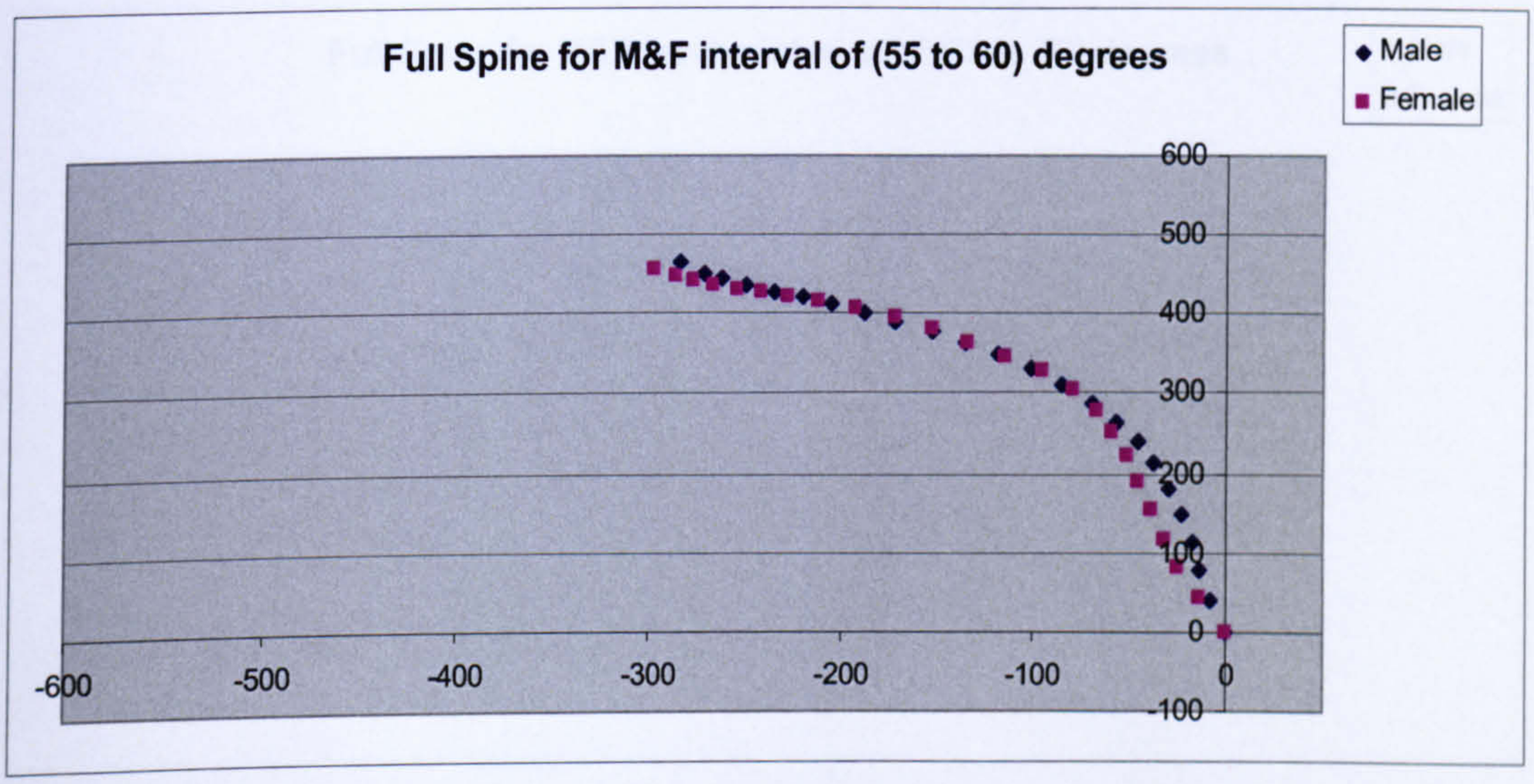


Figure 5- 22 The average coordinates of postures of females and males for the interval of (55° to 60°)

For the interval of (60° to 65°) the difference between genders is significant for L3, L2, L1 with $p<0.01$. In Y dimension the difference between the mean values of genders is significant for T7, T6, C7, C6 with $p<0.05$ and T4-T1 with $p<0.01$ (Figure 5.23).

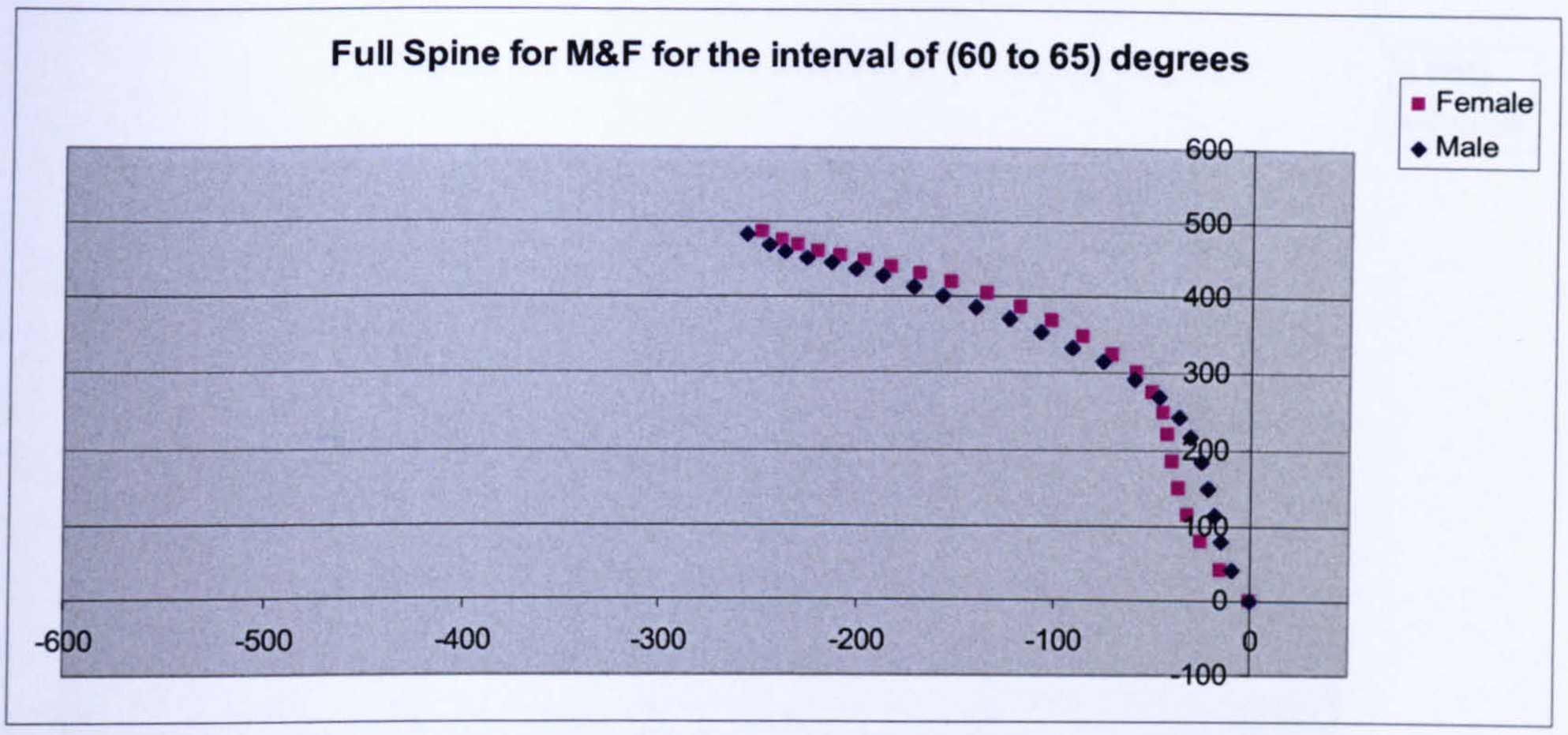


Figure 5- 23. The average coordinates of postures of females and males for the interval of (60° to 65°)

For the interval of (65° to 70°) the difference between genders is significant for L4, L3, L2, with $p<0.01$ and for L1, T12, T11, T1 with $p<0.05$. In Y dimension the difference between the mean values of genders is significant for T5, T4 with $p<0.05$ (Figure 5.24).

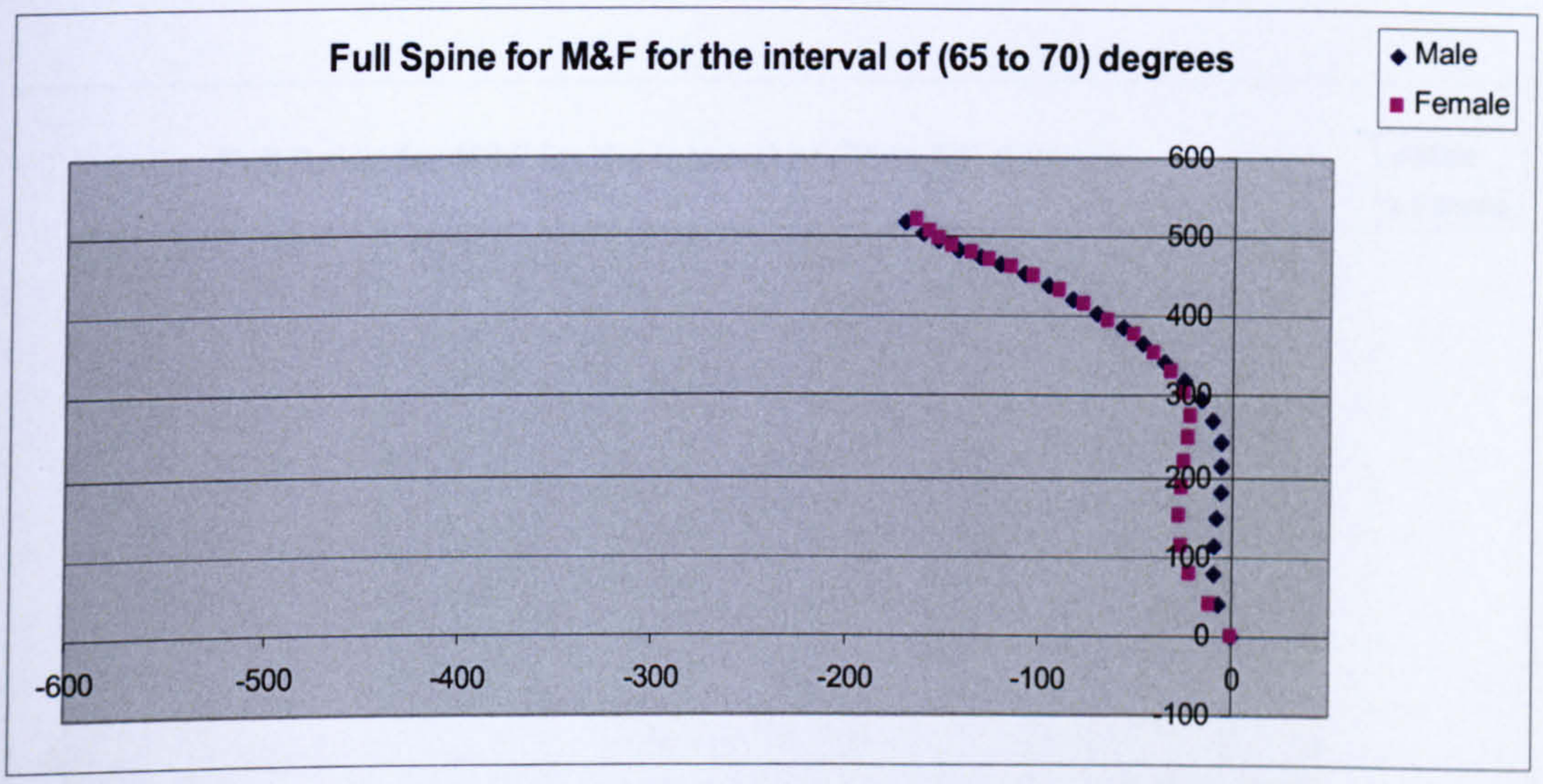


Figure 5- 24. The average coordinates of postures of females and males for the interval of (65° to 70°)

For the interval of (70° to 75°) the difference between genders is significant for L4, T9, with $p<0.05$ and T10-L3 with $p<0.01$ in X dimension. In Y dimension the difference between the mean values of genders is insignificant (Figure 5.25).

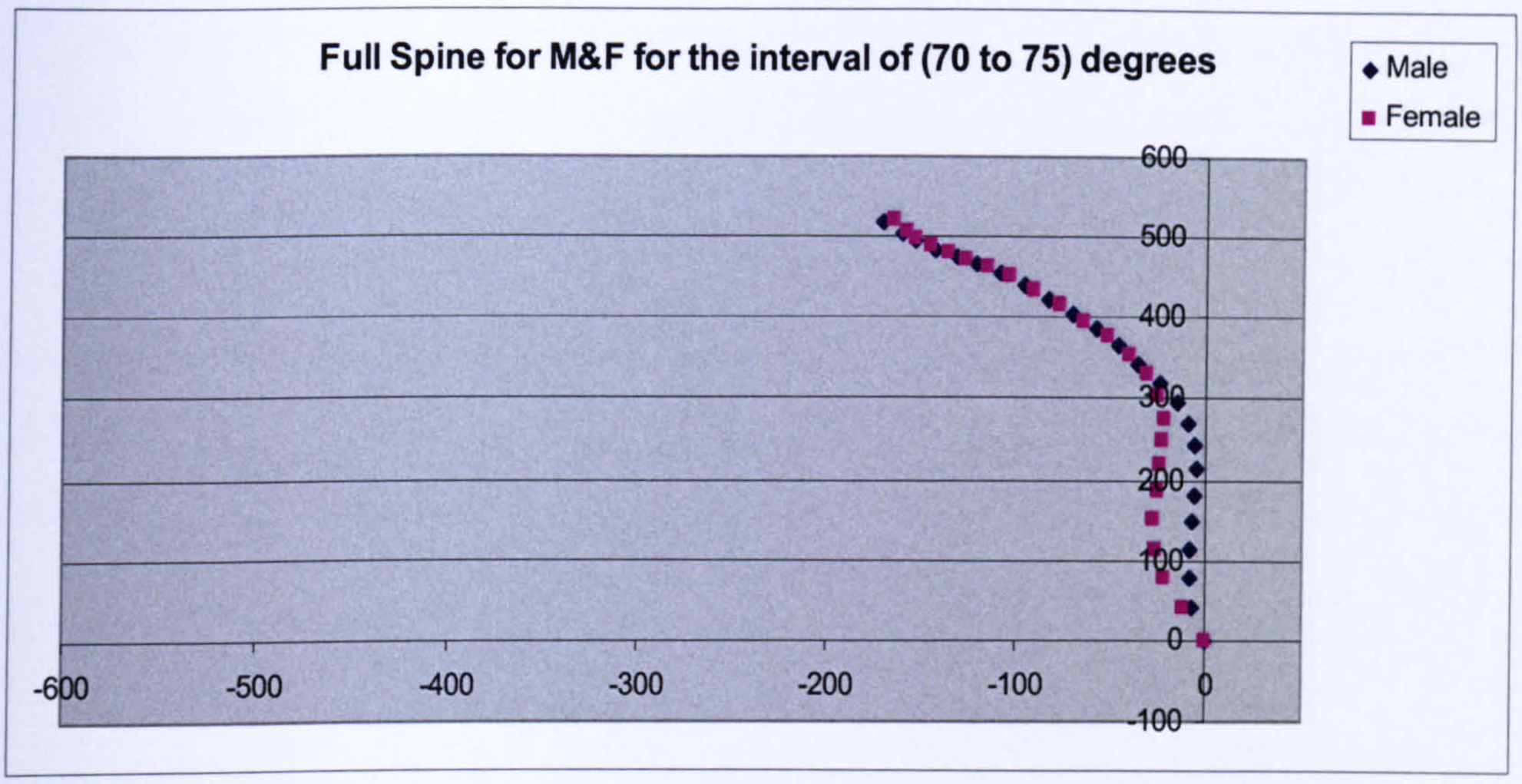


Figure 5- 25 The average coordinates of postures of females and males for the interval of (70° to 75°)

For the interval of (75° to 80°) the difference between genders is insignificant for X dimension and there is significant difference for C2, C3, C4 with $p<0.05$ in Y dimension (Figure 5.26).

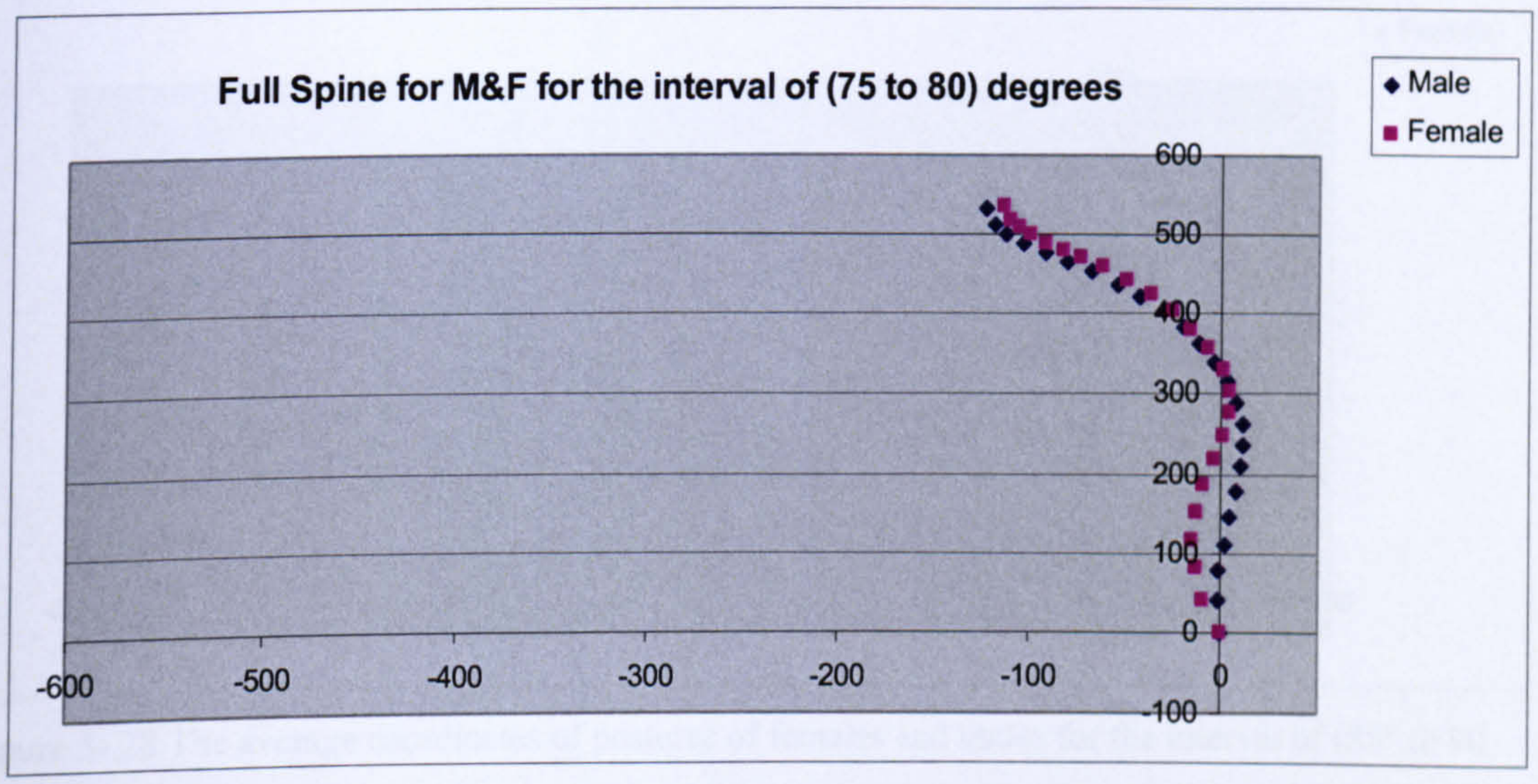


Figure 5- 26 The average coordinates of postures of females and males for the interval of (75° to 80°)

For the interval of (80° to 85°) the difference between genders is significant for L4 to T11 with $p<0.05$ in X dimension and C3 with $p<0.05$ in Y dimensions (Figure 5.27).

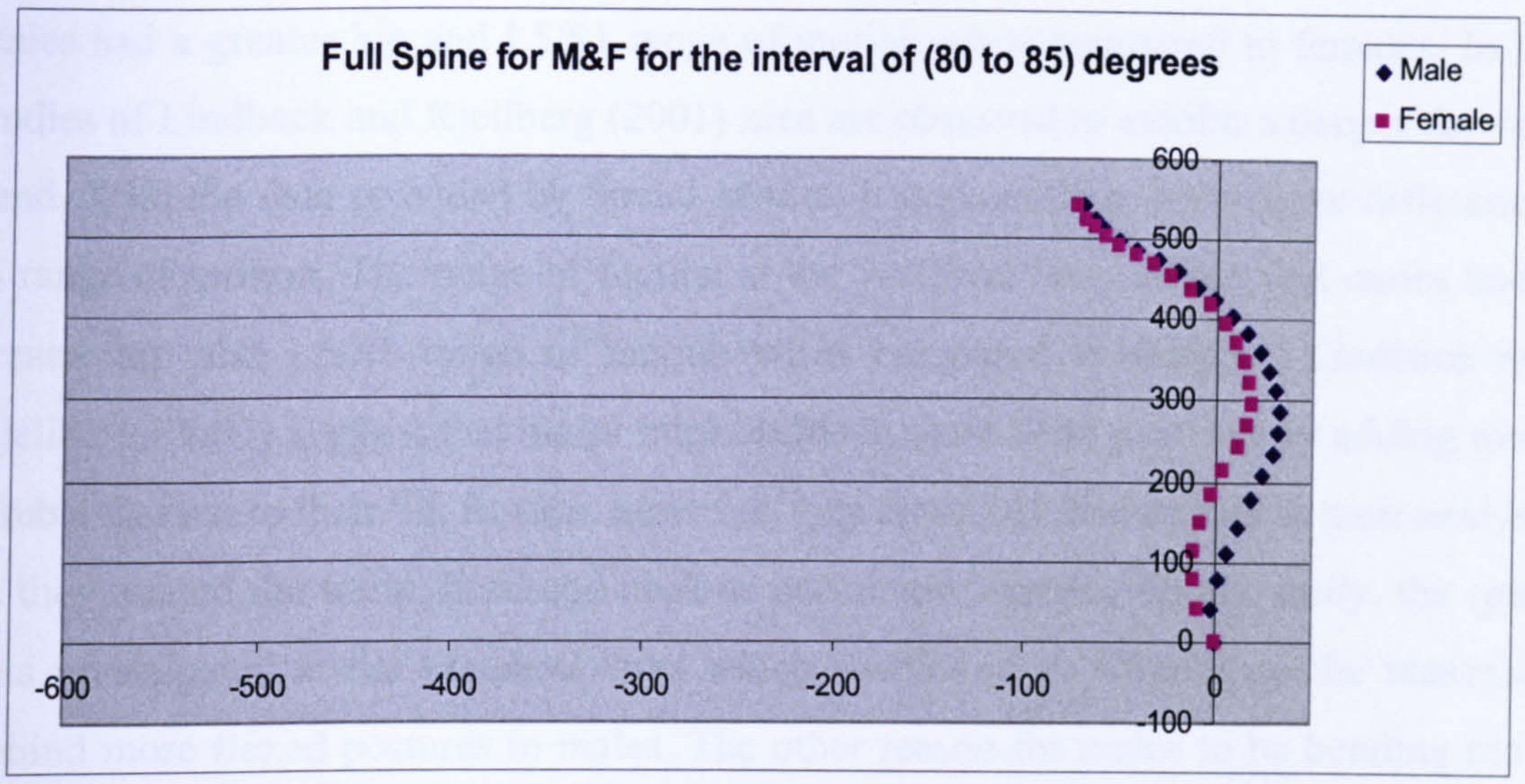


Figure 5- 27. The average coordinates of postures of females and males for the interval of (80° to 85°)

For the interval of (85° to 90°) the difference between genders is insignificant in X and in Y dimensions (Figure 5.27).

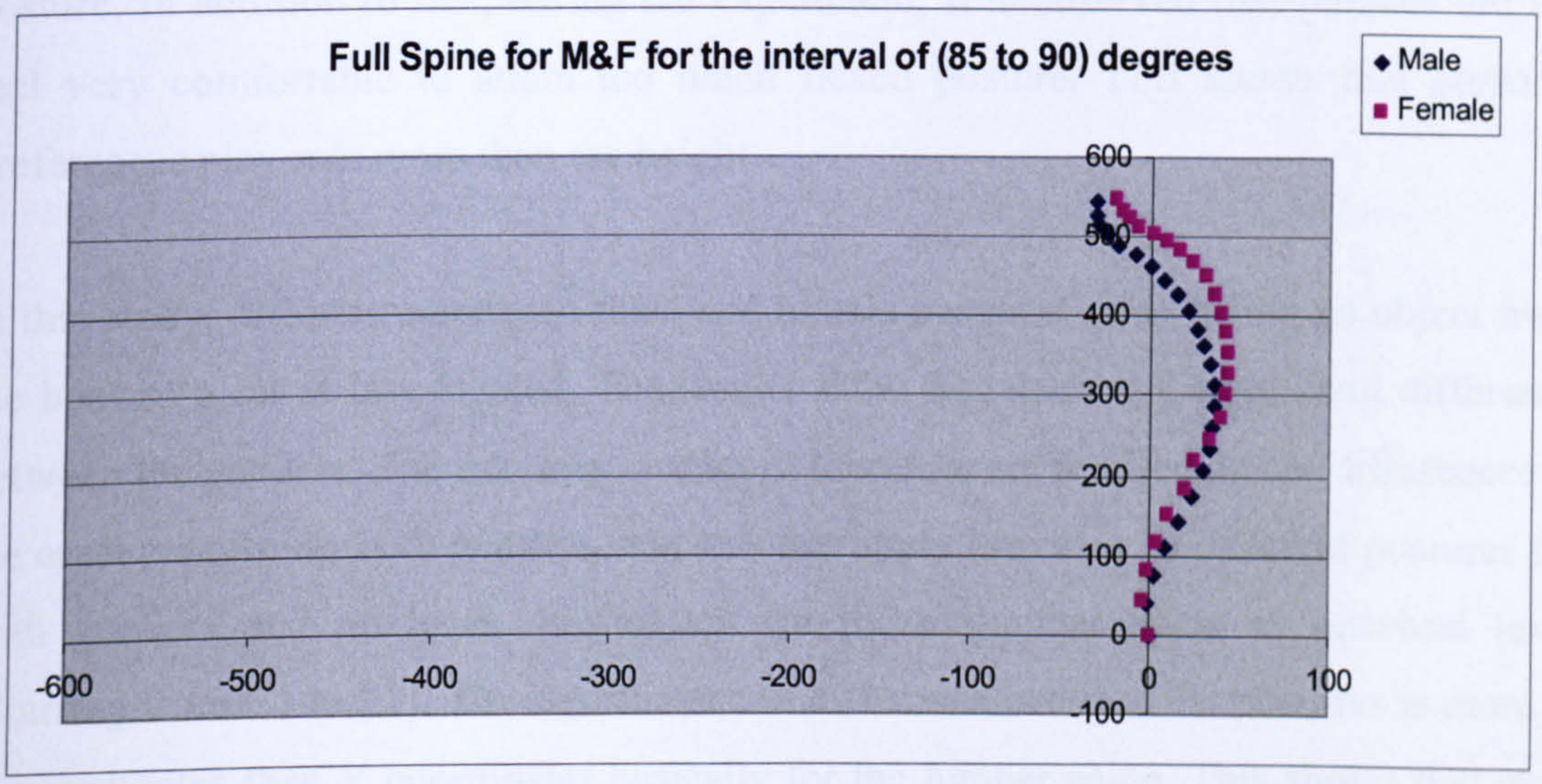


Figure 5- 28 The average coordinates of postures of females and males for the interval of (85° to 90

5.7 Discussion

The analyses show that the first interval of the reference line angle that males had is the interval of (-20° to -15°) and the next is the interval of (-10° to -5°). Whereas, females had their first posture with (-5° to 0°) interval. The more flexed posture of males can be explained by different ranges of motion at the vertebral level when compared to females. With the data provided by the Spinal Mouse, it is possible to investigate differences in range of motion. The range of motion at the vertebral level shows that

males had a greater hip and L5/S1 range of motion when compared to females. In the studies of Lindback and Kjellberg (2001) men are observed to exhibit a deeper forward bend. With the data provided by Spinal Mouse, it is possible to investigate differences in range of motion. The range of motion at the vertebral level shows that males had a greater hip and L5/S1 range of motion when compared to females. Lindback and Kjellberg (2001) suggest that males might achieve more bend postures by adding more lumbar flexion to their hip flexion; however, they could not display this in their analysis as they treated the trunk, head and neck as one single segment. In our study, the spine was investigated at the vertebral level which enables us to investigate the reasoning behind more flexed postures in males. The other reason for males to be bending more than females can be related to the height of the males. However, the authors checked the height of the males who produced the most flexed postures, the height of the males with most flexed postures (182.25 cm) were slightly above than the average male height (178.34 cm). The tallest males were observed not to produce the most flexed posture. In addition to this, during the experiment, it is observed that females did not feel very comfortable to attain too much flexed posture. This shows that personal preferences play role more than the height.

In this study, difference between male and female postures while lifting an object from the boot of a car is investigated. The results show that there is a significant difference between the genders. The previous studies in literature are focused on the differences in the erect posture for both genders, whereas this study provides 19 different postures for both genders and produces information for thoracolumbar spine at vertebral level (Starting from C1 to L5). The significance of difference between the postures is more in X coordinates then Y coordinates basically for the lumbar spine. This shows that each gender have different muscle recruitment patterns affecting the lumbar region. It is possible to expect different loading and different injury scenarios for females and males.

Cholewicki *et al.* (1991), claim that there are advantages in preserving sufficient lordosis when lifting i.e. maximization of muscular contributions to extensor moment support. This lifting technique which avoids posterior ligament recruitment is believed to reduce compressive spine loads. The collective ligamentous tissues possess a shorter moment arm than collective erector spinae muscles and therefore would impose a

higher compressive penalty on the lumbar discs if activated (McGill SM *et al.* 1988). Further, the anterior shear force on a lumbar disc is also reduced if the extensor moment is produced by the musculature (McGill *et al.* 1985;Potvin *et al.* 1991).

In the theory of thrustline, which is used for the investigation of the injury mechanism in this research, the contour of the spine plays an essential role in the investigation of the injury. Such as, if the thrustline stays out of the boundaries of the spine, an injury is likely to be expected. For the researchers who need to use the posture data in their biomechanical models for different genders, the results produced in this experiment provide valuable information.

5.8 Conclusion

The curvature of the spine has an important role as it effects the transmission of the loads within a body. Spinal Mouse was chosen to record the curvature of the spine and relative orientations of the vertebrae because of the accuracy and no previous expert knowledge requirement. The experiments were repeated over 20 male and 19 female volunteers. The coordinates of the spine were calculated based on the spinal mouse measurements with the additional software. The movement of vertebrae is known to be constrained by the facet contacts. In this study facet contact problem is kept out of scope.

The coordinates which were produced as result of this experiment are used to simulate the real lifting activity for understanding the role of muscles and ligaments in order to provide spinal stability and gain more insight for understanding of injury mechanisms. With the final results of the thrustline theory, it is expected to produce new design criteria for the inspection of a device which are used for avoiding injury while unloading from the boot of a car.

This information is valuable as it is the first study conducted in literature so far giving so much detail about the position and orientation of each vertebra in a lifting activity. It is believed that this information can be useful to researchers who need real life data to understand the mechanism of injury during lifting activities.

CHAPTER 6

6 Stability analysis of the spine with thrustline theory

In this chapter, the thrustline theory is applied to the generic female posture and generic male posture produced for each interval of the reference line angle.
The stability analysis is provided for:

a) Body weight for the postures in lifting
b) Body weight with an external load for postures in lifting
c) Body weight, muscle groups with an external load for postures in lifting
d) Body weight, muscle groups, ligaments with an external load for postures in lifting

The reaction forces at the end points of the reference line, at lower end plate of L5 and superior surface of C1 are provided and compared for structural failure.

6.1 Stability Analysis

6.1.1 Body Weight Forces with Postures in Lifting

In order to evaluate stability of the spine for postures in lifting, the postures produced by females and males were analysed separately. For vertebral body dimensions, the average height of males and females are used as a scaling factor. The forces acting on the spine due to the body weight of each gender are considered to be different. For males, average height of 178.3 cm and a weight of 74.3 N, for females the average height of 164.3 cm and weight of 64.3 N from the experimental data are used.
The results show that males and females have different stability patterns for the same interval of degrees of reference line. For the interval of (0 to 5) degrees of reference line angle the position of the thrustline shows the highest instability for both genders among all postures. All the force components acting on the spine act nearly

perpendicular to the reference line resulting in minimum compressive forces. The requirement for the supportive forces is highest for this interval for both genders. The component of gravity forces result in high shear forces which causes deviation of the thrustline from the spine borders. For males, the high magnitude of body weight forces results in higher deviation when compared to females as shown in Figure 6.1.

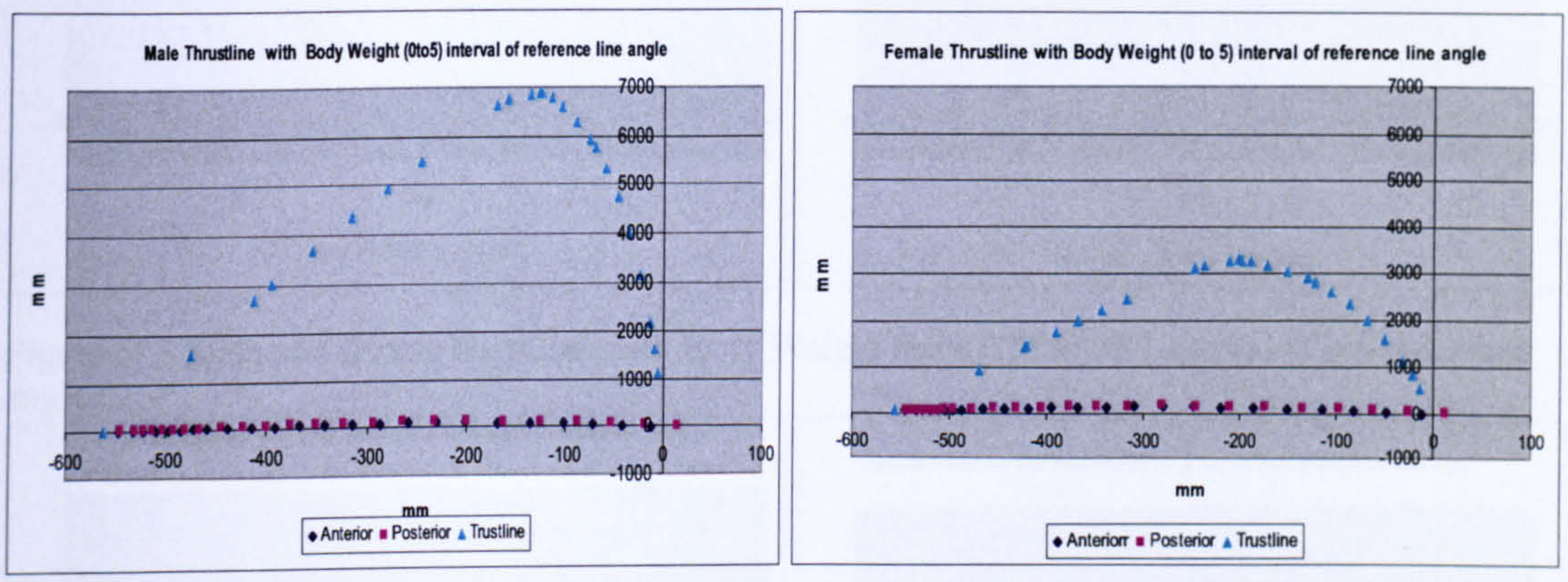


Figure 6- 1 Male and female thrustline with Body Weight force (0° to 5°) interval of reference line angle.

For the next interval of (5° to 10°) of reference line angle, the difference between the instability of the female and male spine is very similar. The peak points of thrustline on y axis are 2086mm and 2037mm for males and females respectively. (Figure 6.2)

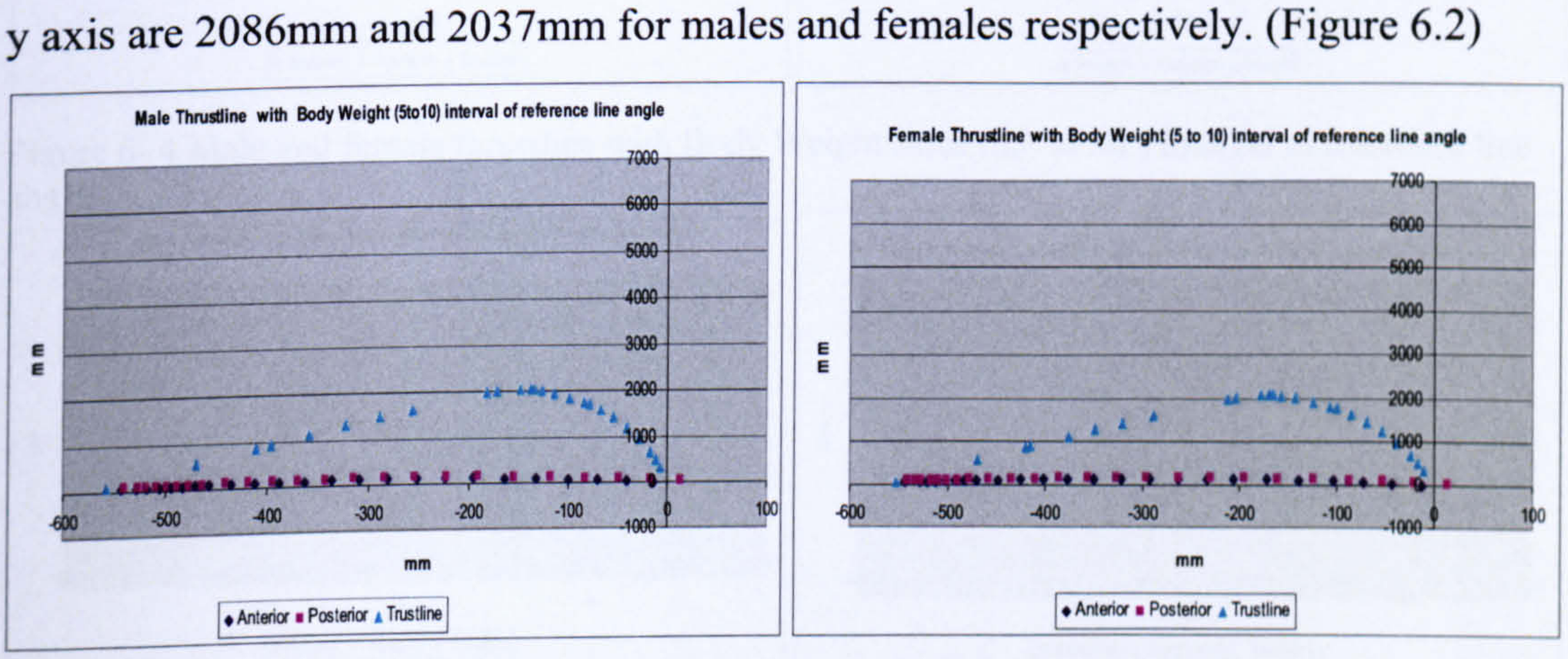


Figure 6- 2 Male and female thrustline with Body Weight force (5° to 10°) interval of reference line angle.

For the rest of the intervals, this trend is similar. The examples of some of the postures are provided below for the intervals of (15° to 20°), (25° to 30°), (40° to 45°) of reference line angle respectively (Figure 6.3, Figure 6.4, and Figure 6.5).

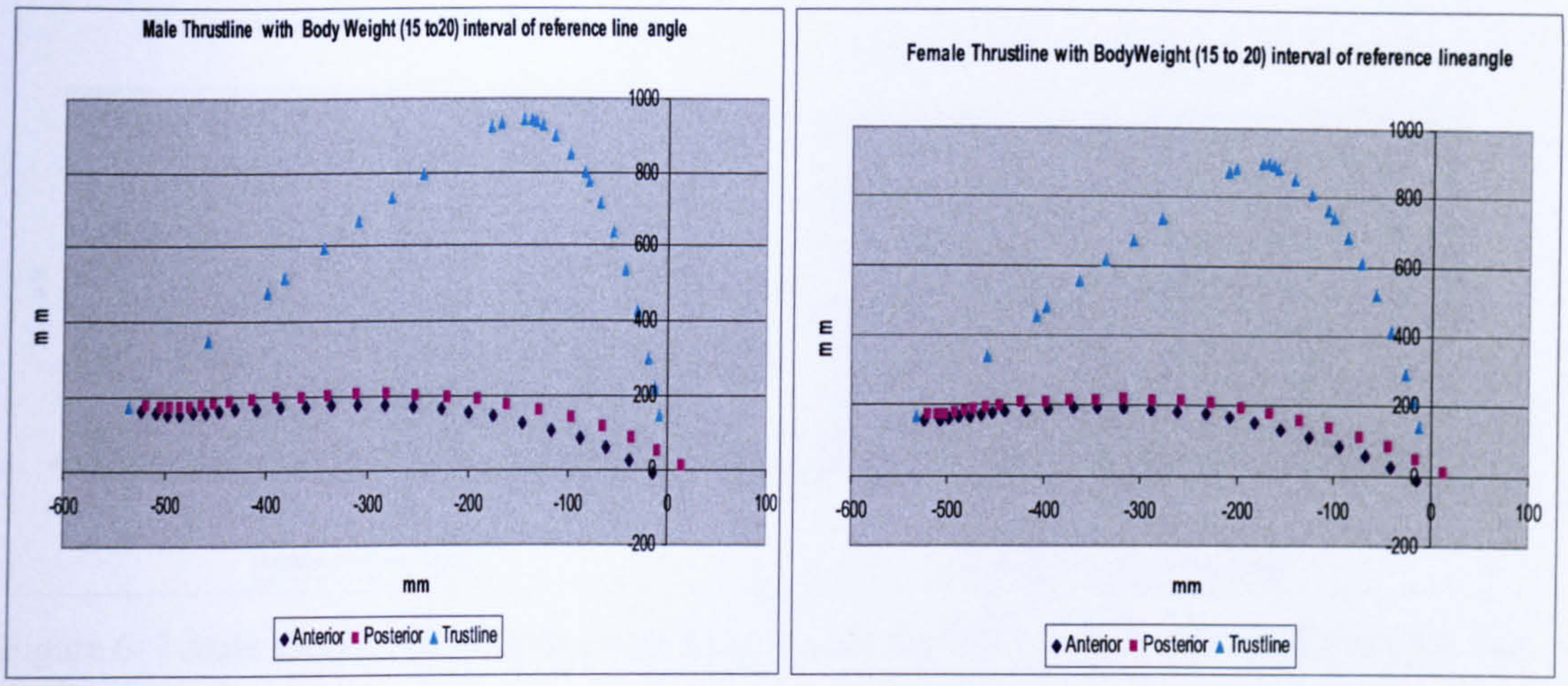


Figure 6- 3 Male and female thrustline with Body Weight force (15° to 20°) interval of reference line angle.

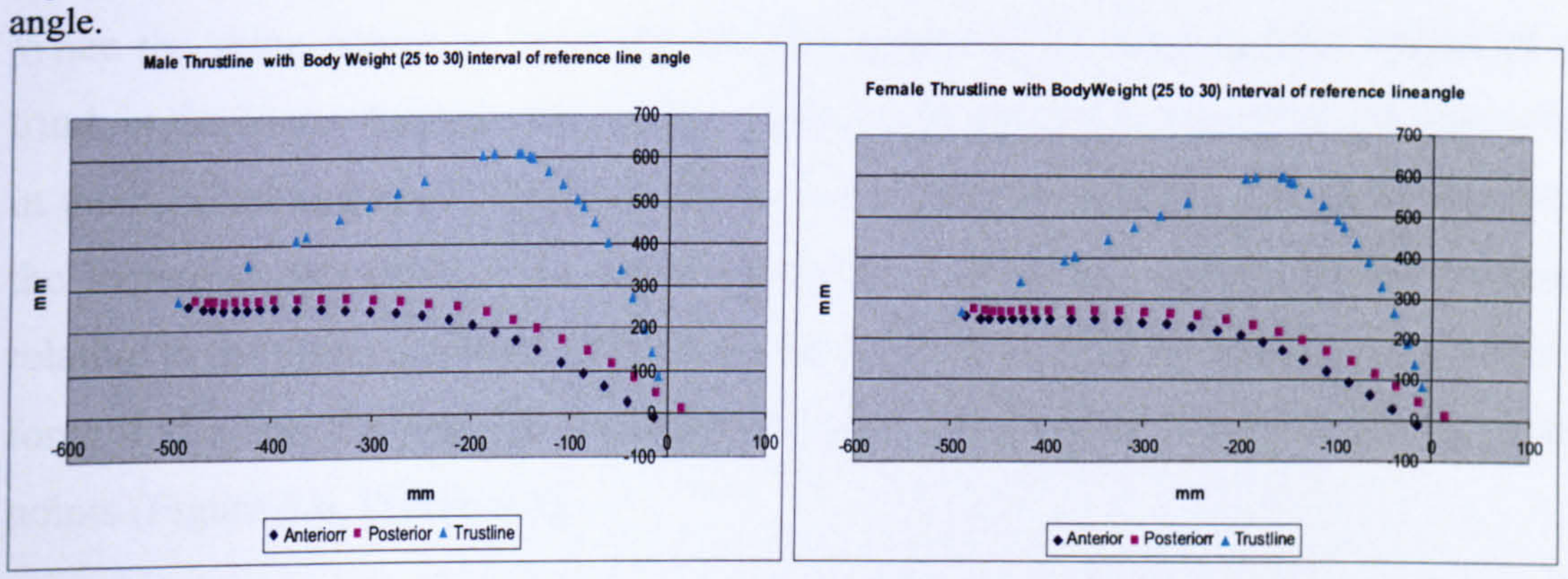


Figure 6- 4 Male and female thrustline with Body Weight force (25° to 30°) interval of reference line angle

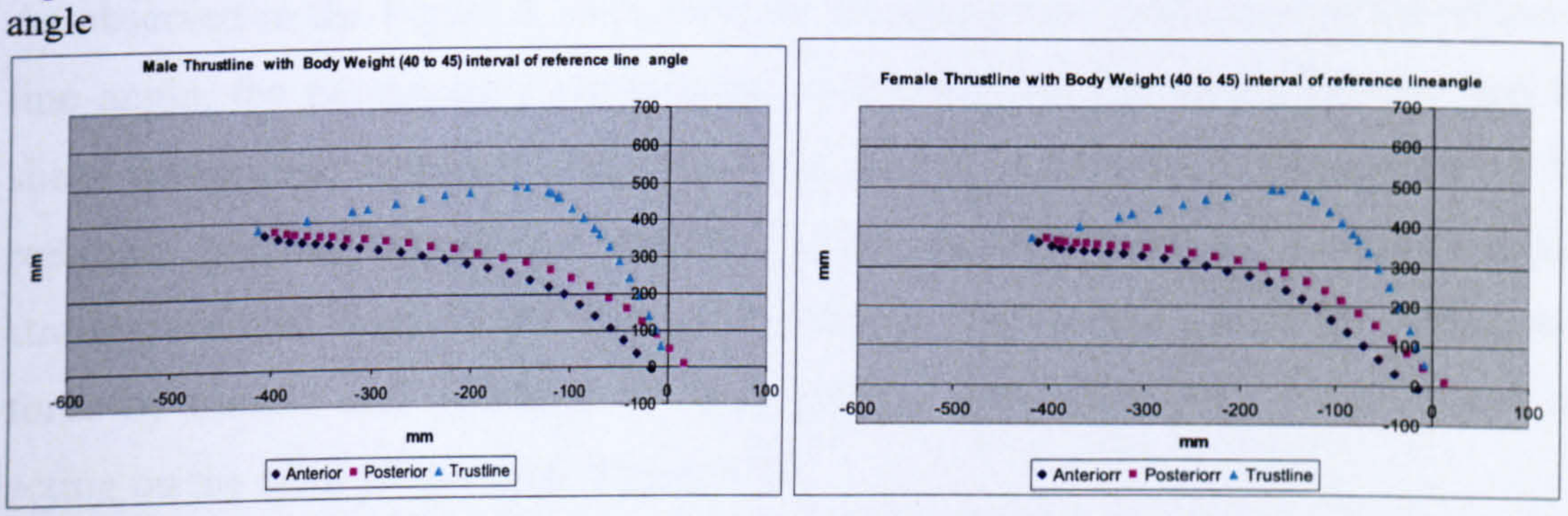


Figure 6- 5 Male and female thrustline with Body Weight force (40° to 45°) interval of reference line angle

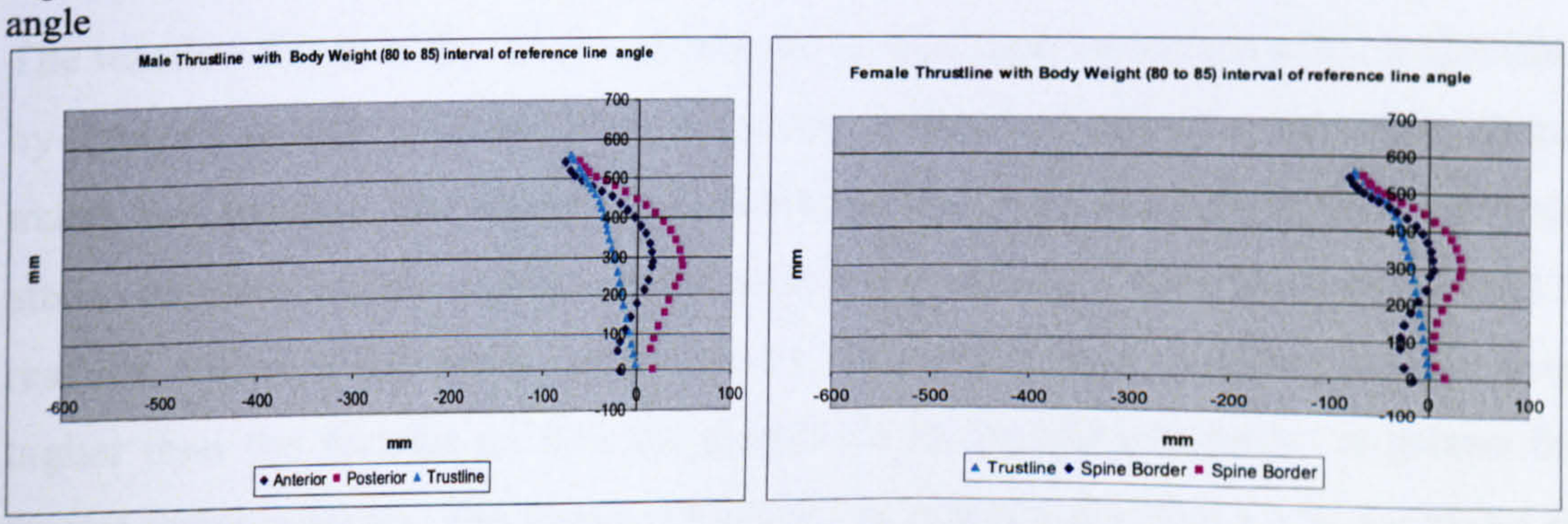


Figure 6- 6 Male and female thrustline with Body Weight force (80° to 85°) interval of reference line angle.

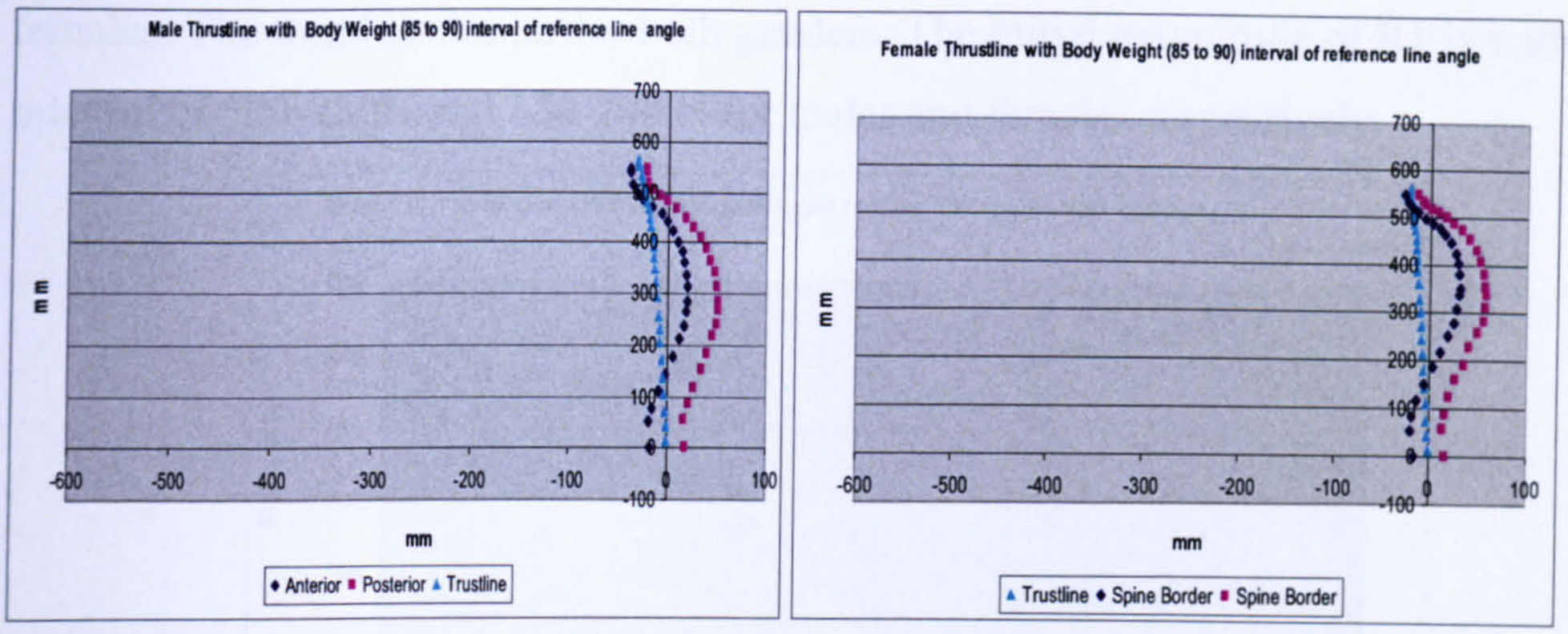


Figure 6- 7 Male and female thrustline with Body Weight force (85° to 90°) interval of reference line angle.

When the spine attains an erect posture, the weight of the head and the weight of the trunk in the lower thoracic and lumbar regions acts anterior to the reference line, while in the cervical and upper thoracic regions, the weight is posterior. For flexed postures, the increased curvature of the spine moves the forces due to body weight posterior relative to the reference line. This affects the moment arm of the parallel component of force and alters the sign of the moments produced by these components about end points (Figure 6.6, Figure 6.7).

As observed in the Figure 6.1-6.7, with the increase of the inclination of the reference line angle, the compressive components of the body weight forces increase and the shear component decreases. This results in less deviation of the thrustline from the reference line. As a result, the instability of the spine decreases as the spine attains a straight posture. Even for the fully erect postures there is still a need for compressive force by muscle and ligaments for both genders when only body weight forces are acting on the spine (Figure 6.6, Figure 6.7).

The reaction forces at the lower end plate of L5 and superior surface of C1 is calculated by the code written in Visual Basic for all the intervals of reference line angle for both males and females. The results show that shear force at L5/S1 decreases as the body attains an erect posture and the compressive force increases; there is a similar trend for reaction forces at the upper surface of C1. The males have an average body weight higher than the females so that the magnitude of the reaction forces is greater than female reaction forces. The Figure 6.8 shows the reaction forces at L5/S1 for males and

females. The trend is similar for both genders. The initial magnitude of R1 is within the interval of 200-250N and 150-200 N for males and females respectively.

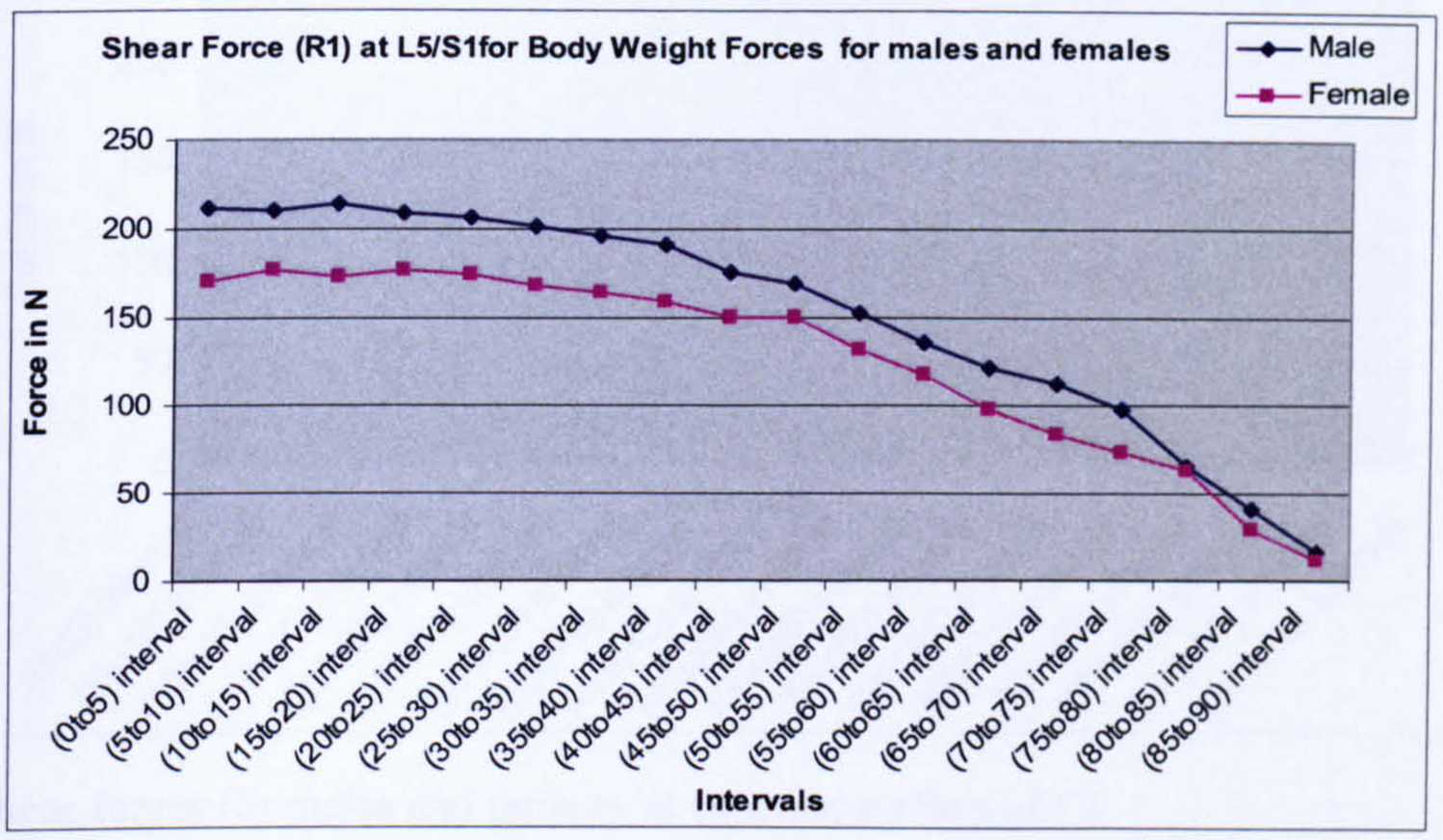


Figure 6- 8 Shear forces for males and females at L5/S1

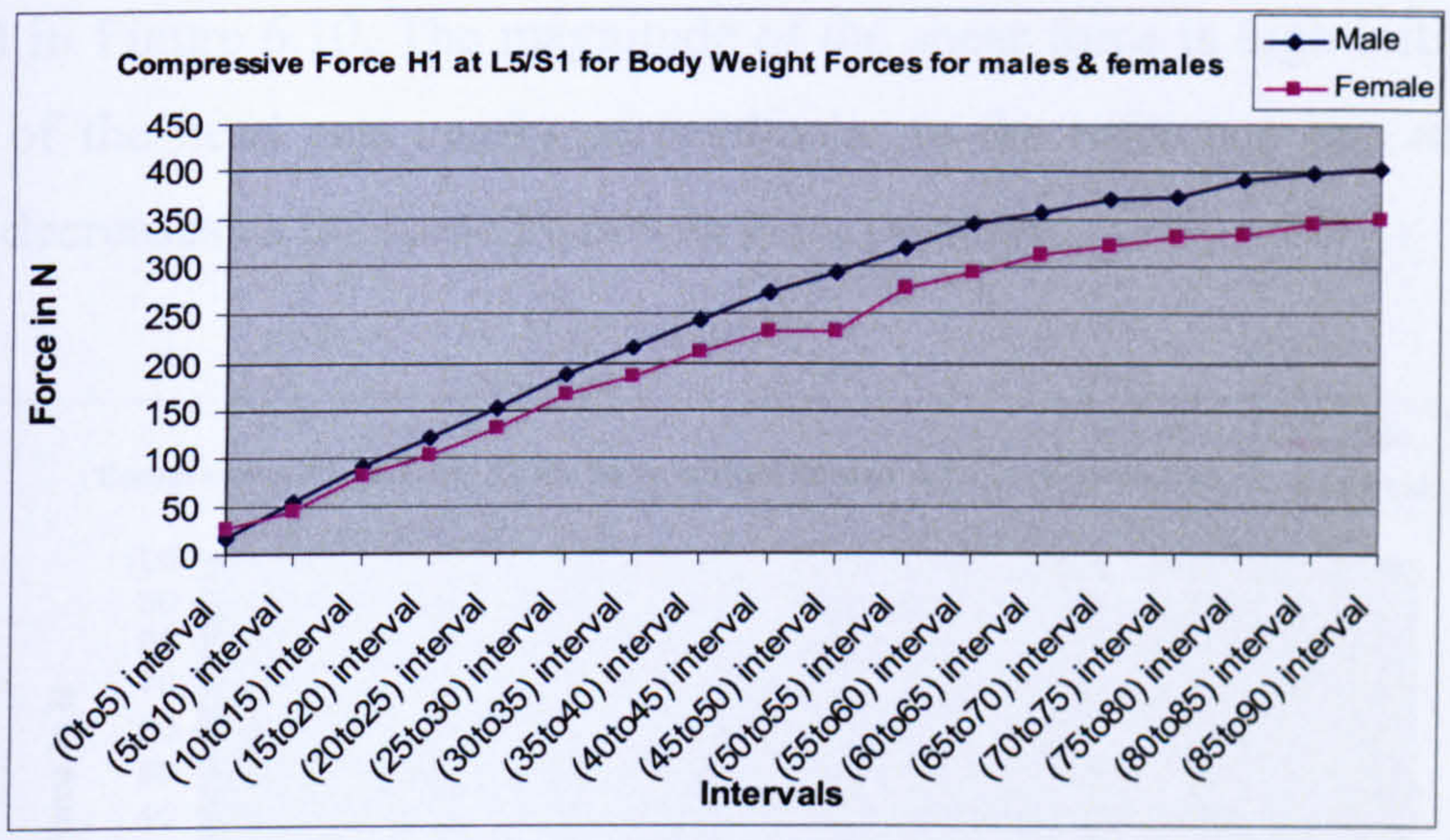


Figure 6- 9 Compressive forces for males and females at L5/S1

The compressive force at L5/S1 increases to the level of 400 N for males and 300 N for females. The difference is due to higher body weight force of males than males. The differences in the postures and the moment arm of the body weight forces with respect to reference line also play role.

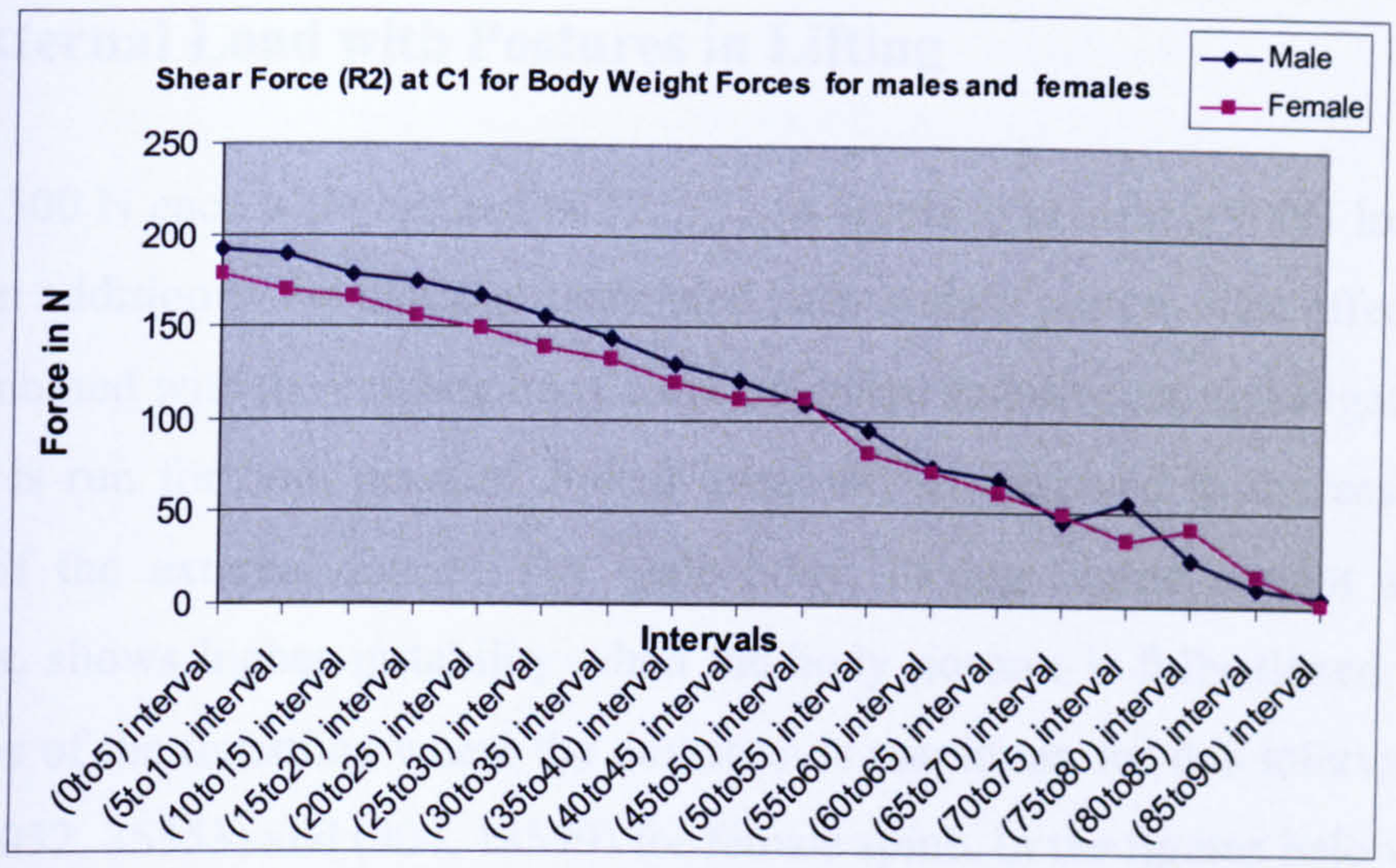


Figure 6- 10 Shear forces for males and females at superior surface of C1

The reaction force at C1 for males is slightly higher than males and decreases gradually as observed in Figure 6.10. The magnitude of the shear force is high initially because the weight of the head acts nearly perpendicular to the reference line and the shear component decreases as the spine attains an erect posture.

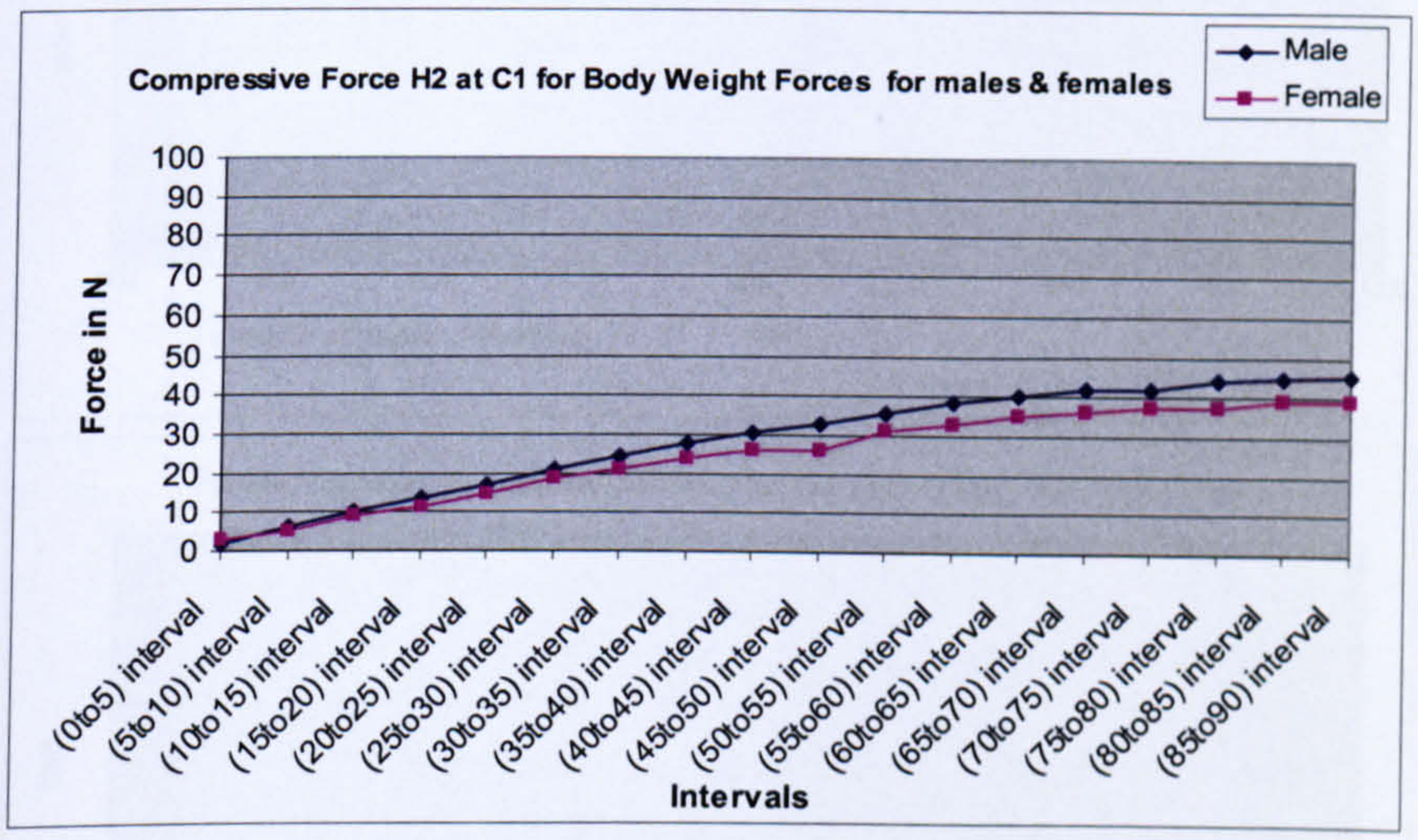


Figure 6- 11 Compressive forces for males and females at superior surface of C1

Compressive force at superior surface of C1 reaches the level of 45 N for males and for females 40 N. This is due to the increasing vertical force component of the weight of the head. The results show that the reaction forces are sensitive to the direction of the shear and compressive forces acting on the spine. With the overall effect of the shear and compressive forces acting on the spine, reaction forces shows the similar trend with the body weight forces acting on the spine.

6.1.2 External Load with Postures in Lifting

Forces of 300 N each were applied to T2, T3, T4 levels to present a 900N load lifted in the arms in addition to the existing distributed body weight pattern. The effects of these forces combined with the existing body force on spinal stability are investigated.

The code is run for both genders. Spinal instability is observed to increase with the addition of the external forces. The male body, having higher weight and height parameters, shows higher instability when the body posture is fully flexed. The peak coordinates of the thrustline where the deviation is maximum for this interval for male spine is (1032, 35553) and (904, 18599) for female spine. In the figures below, it can be observed that male thrustline deviates more when compared to females. This shows that male body is highly sensitive to external loading because of its different anthropometry for fully flexed postures (Figure 6.12).

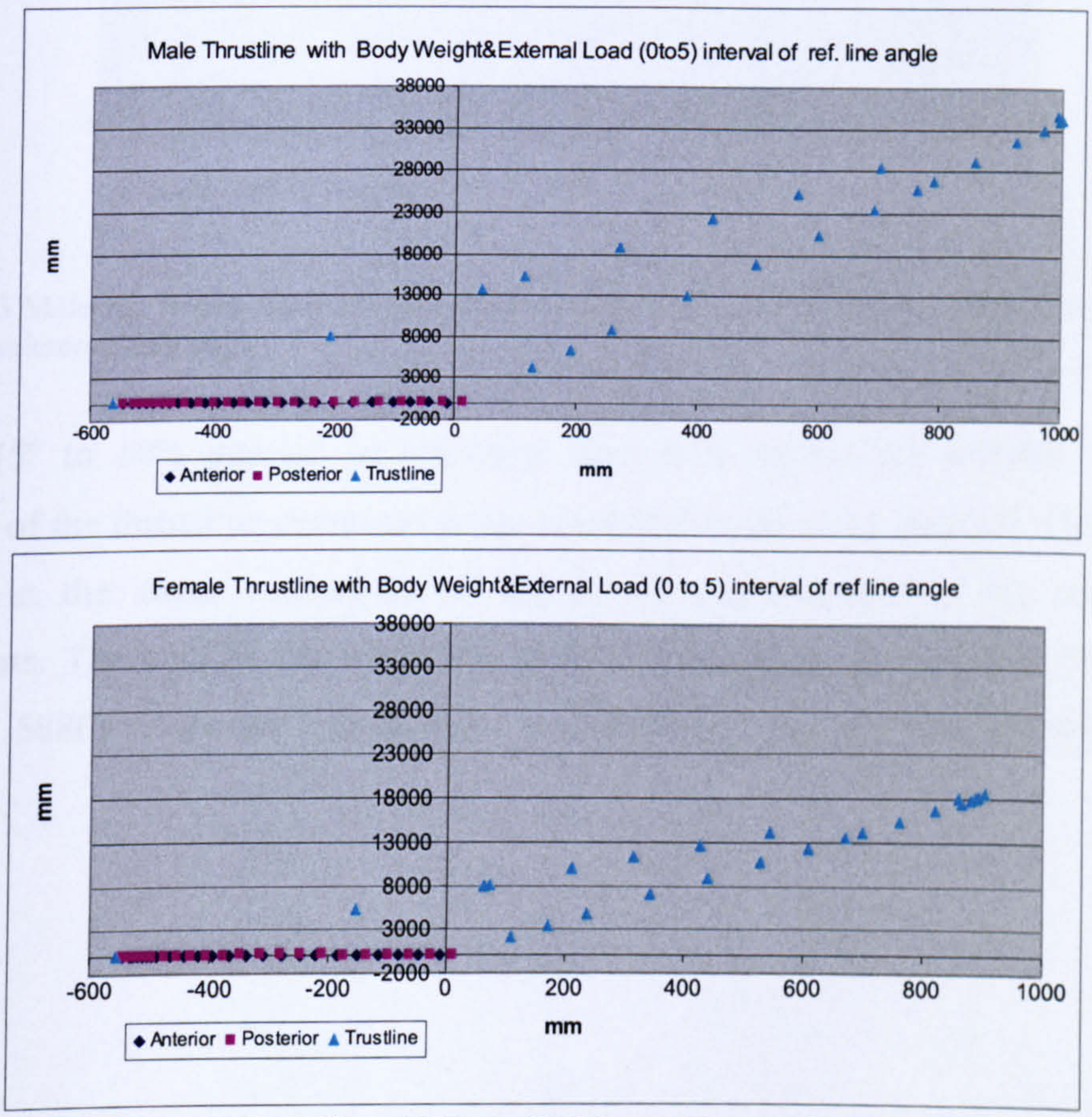
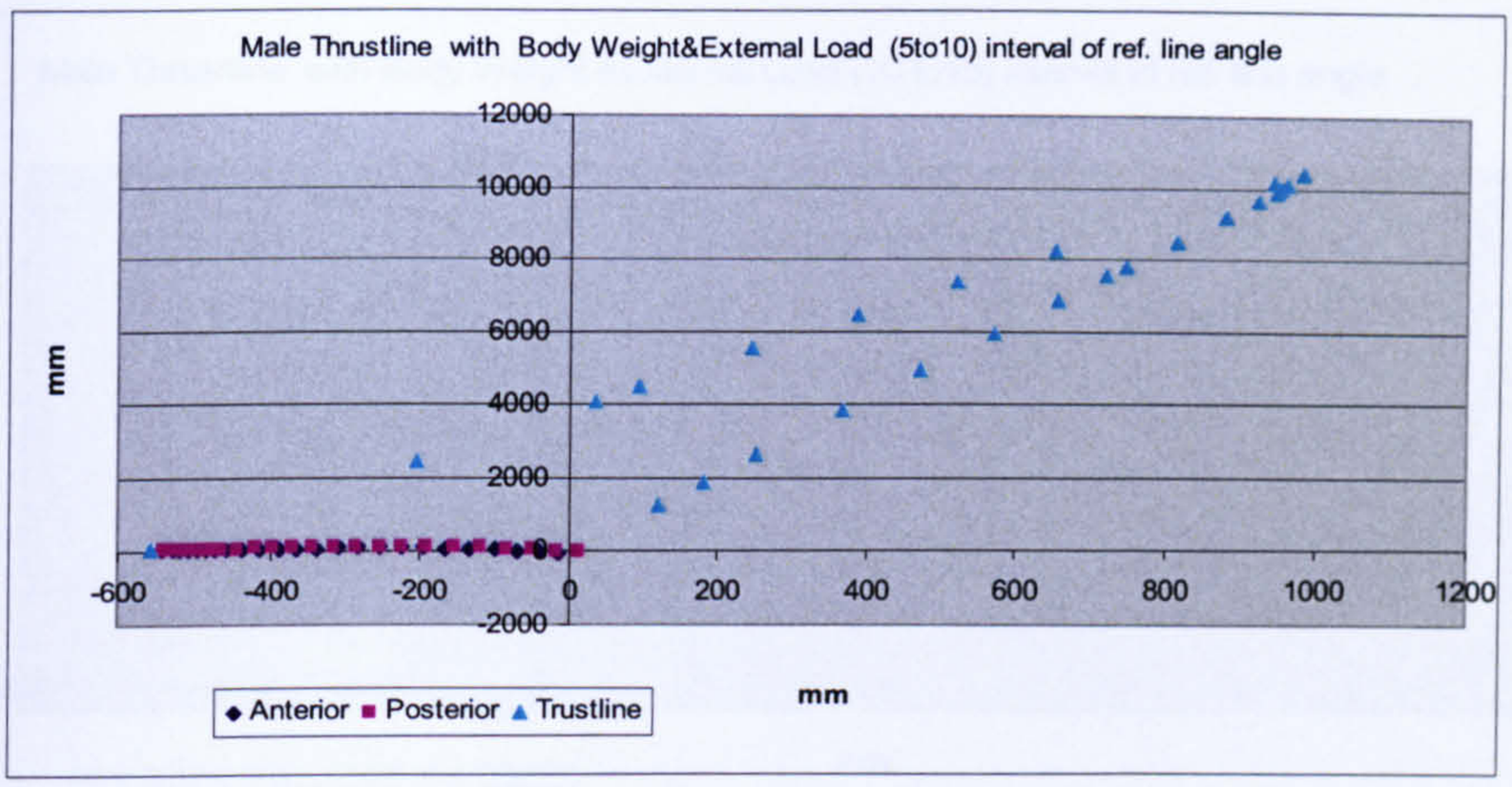


Figure 6- 12 Male and female thrustline with Body Weight and External Load of 900N (0° to 5°) interval of reference line angle.



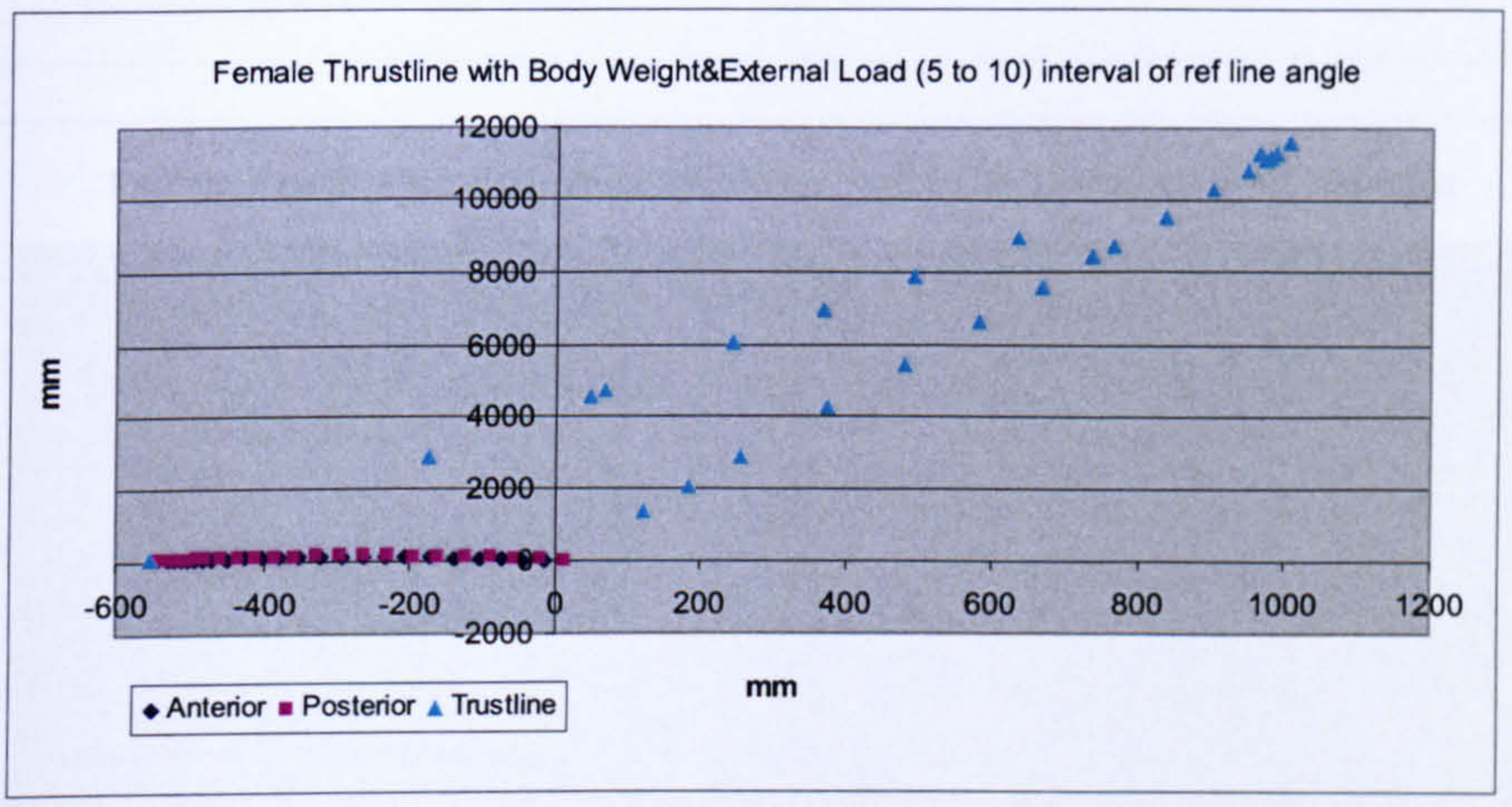
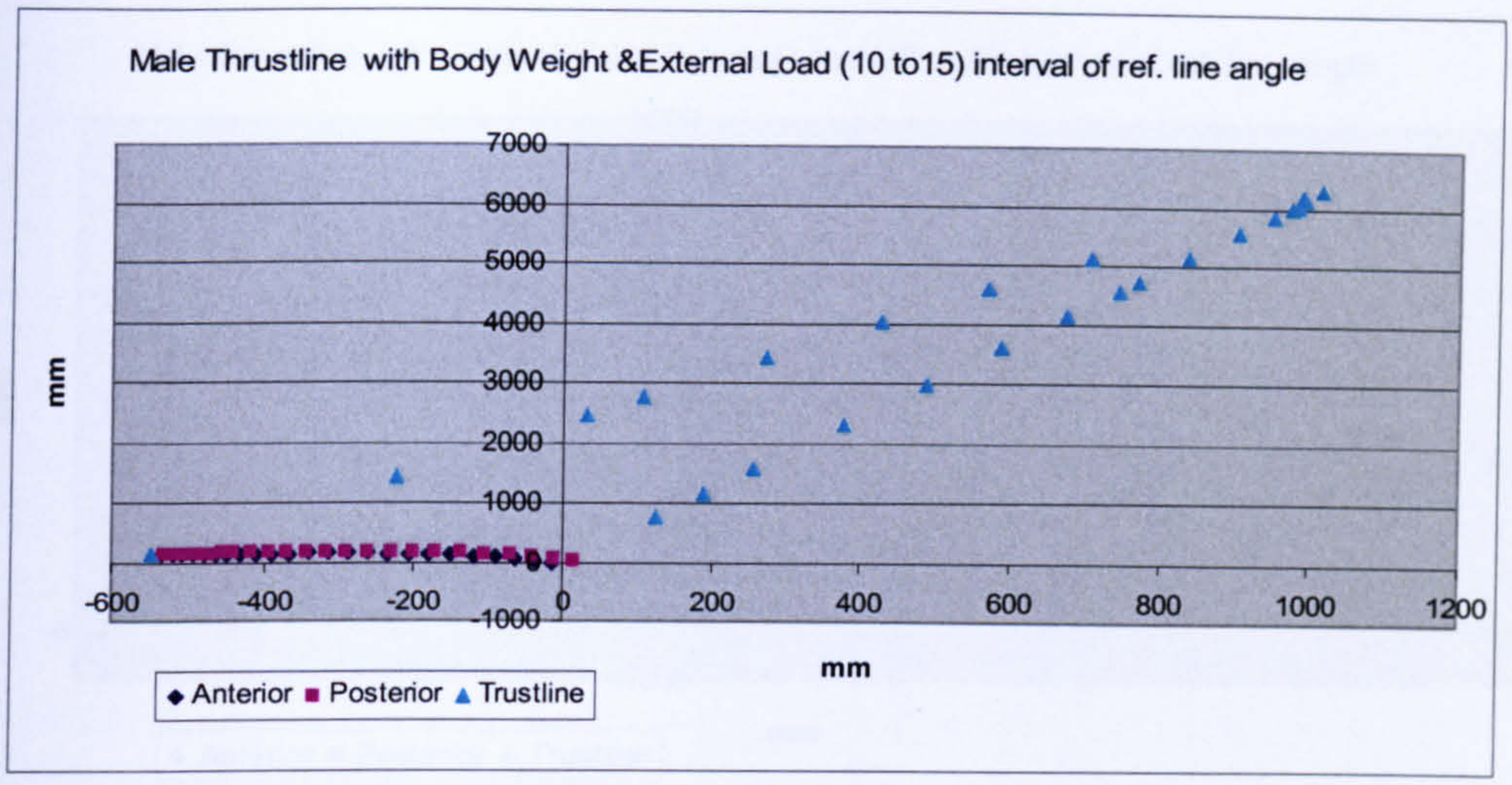


Figure 6- 13 Male and female thrustline with Body Weight and External Load of 900N (5° to 10°) interval of reference line angle.

For the (5° to 10°) interval of reference line, both spines are instable. However, deviation of the thrustline decreases when compared to previous interval. This is due to decrease in the shear component of the forces and increase in the compressive components. The coordinates where the deviation is highest for males is (981, 10360 and (942, 5880) which are less than the coordinates of the previous intervals (Figure 6.13).



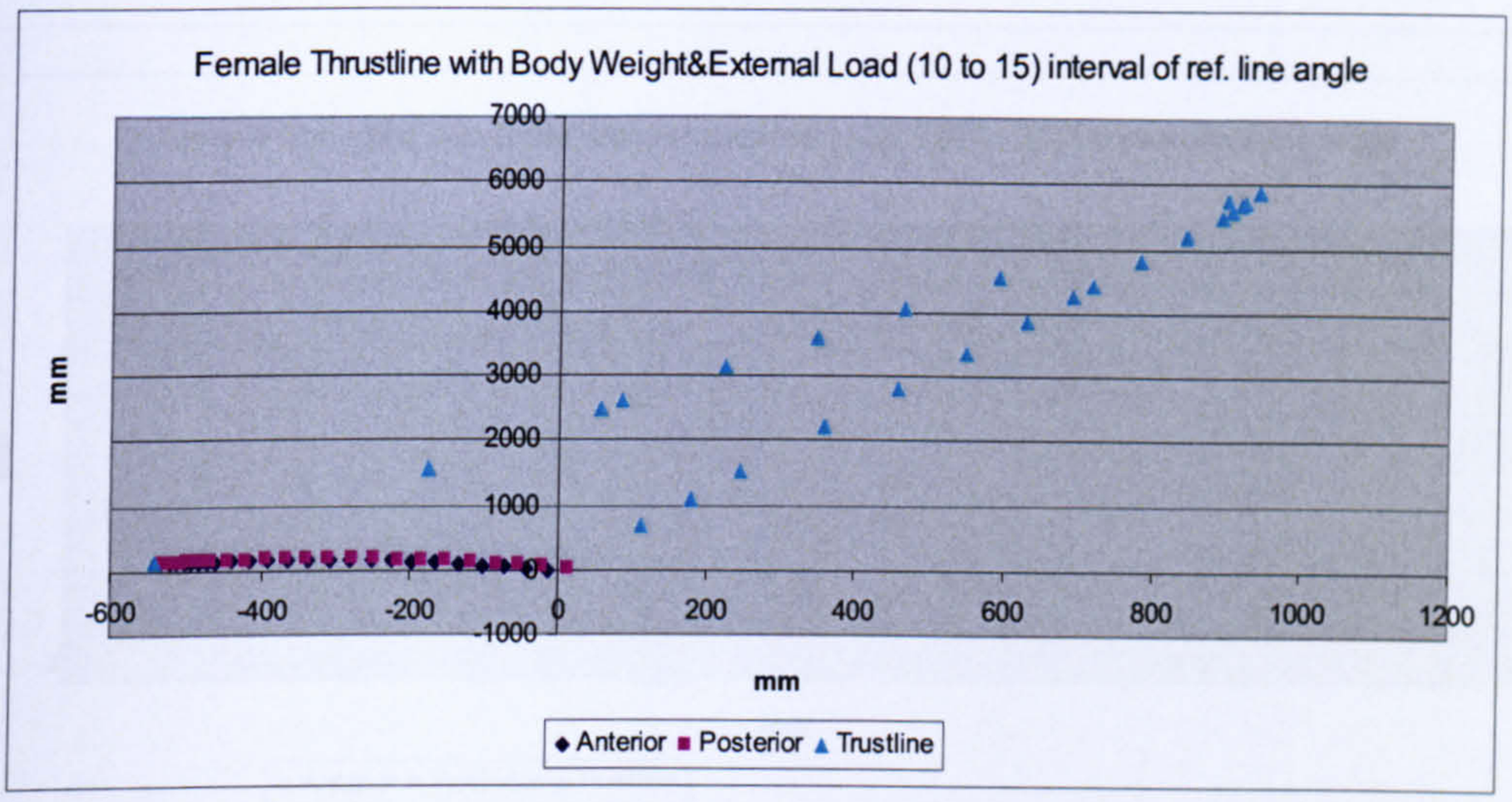
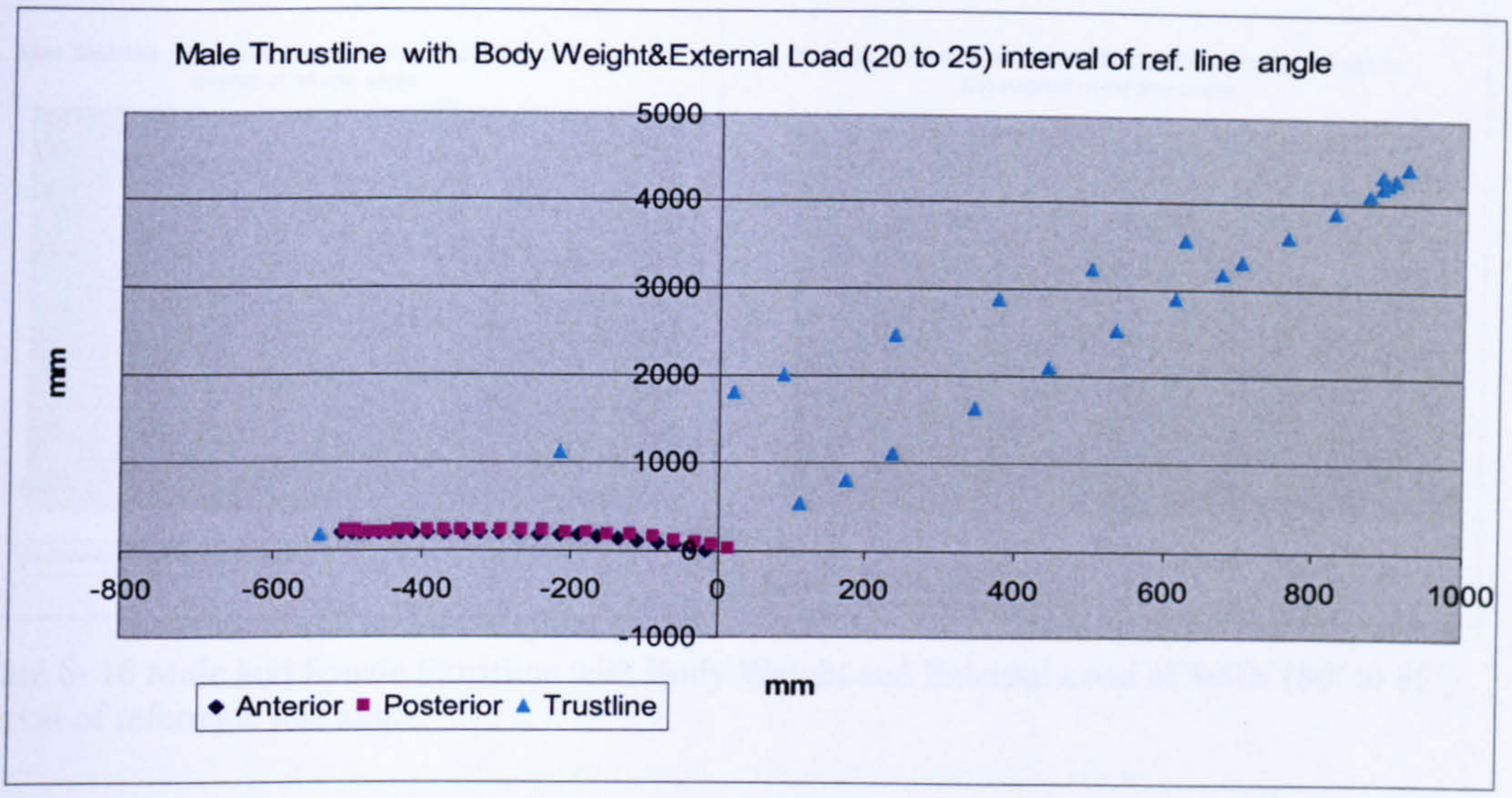


Figure 6- 14 Male and female thrustline with Body Weight and External Load of 900N (10° to 15°) interval of reference line angle.

For (10° to 15°) reference line angle, the peak thrustline coordinates show that the difference between male and female is not much (1016, 6289) and (942, 5881). This shows that as the degree of reference line increases, the spine becomes less sensitive to the differences in loading by the body weight (Figure 6.14).



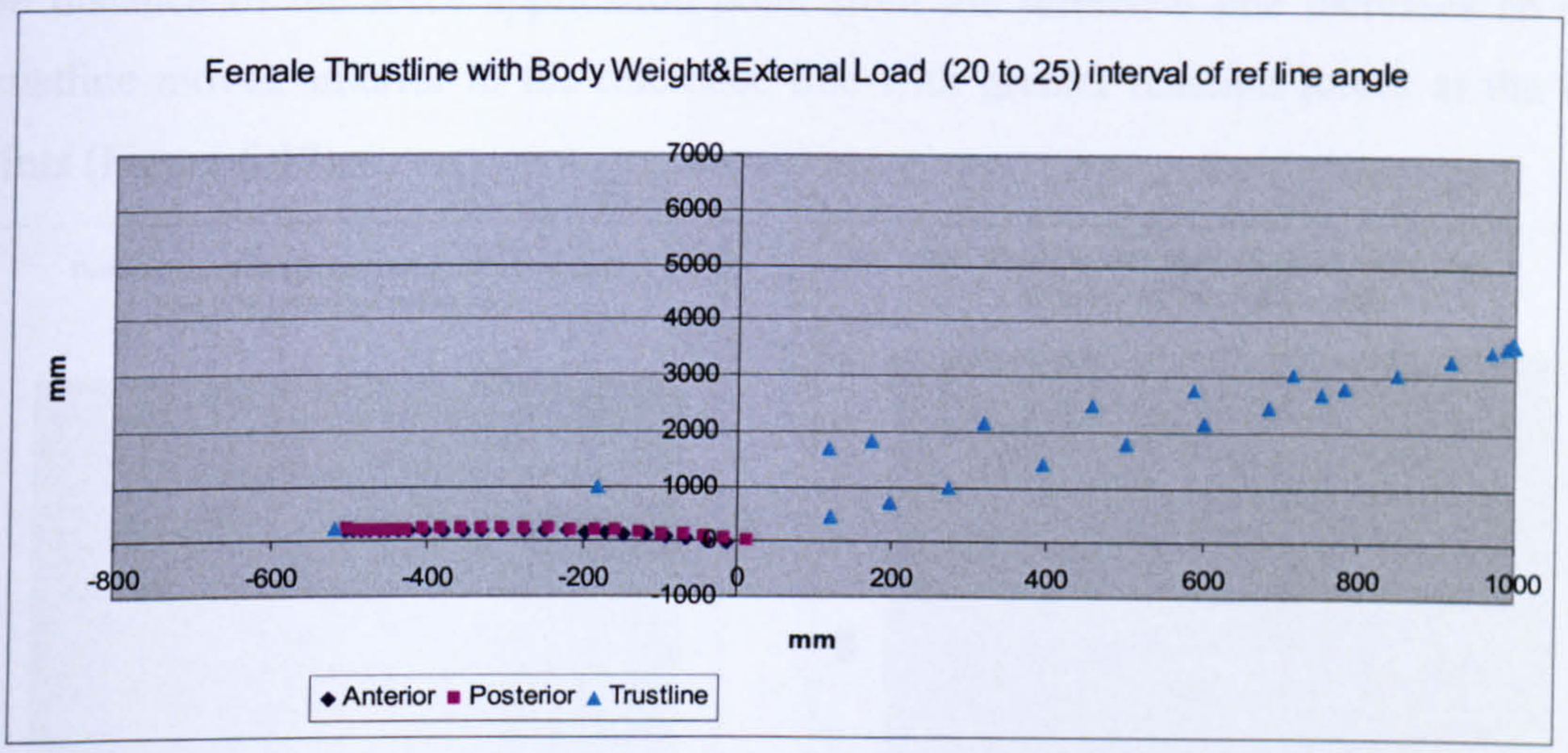


Figure 6- 15 Male and female thrustline with Body Weight and External Load of 900N (20° to 25°) interval of reference line angle.

For the (20° to 25°) reference line interval males have (925, 4407) and females (1033, 3725) (Figure 6.15). For the rest of the intervals deviation of the thrustline follows a similar trend, males have higher instability when compared to the females due to their own body weight when spine is fully flexed. However, for the interval of (80° to 85°) the thrustline curves change the position from posterior to anterior for both females and males (Figure 6.16). The reason for this change is the change in the sign of the reaction forces. The initial positioning of the thrustline depends on the direction of the reaction forces. The application point of external forces moves relative to the reference line for each interval. These effects the moment created by the external forces, thereby affecting the reaction forces. The application point of the external forces moves the thrustline anterior to the reference line in this interval whereas before this interval, application point was posterior to the reference line.

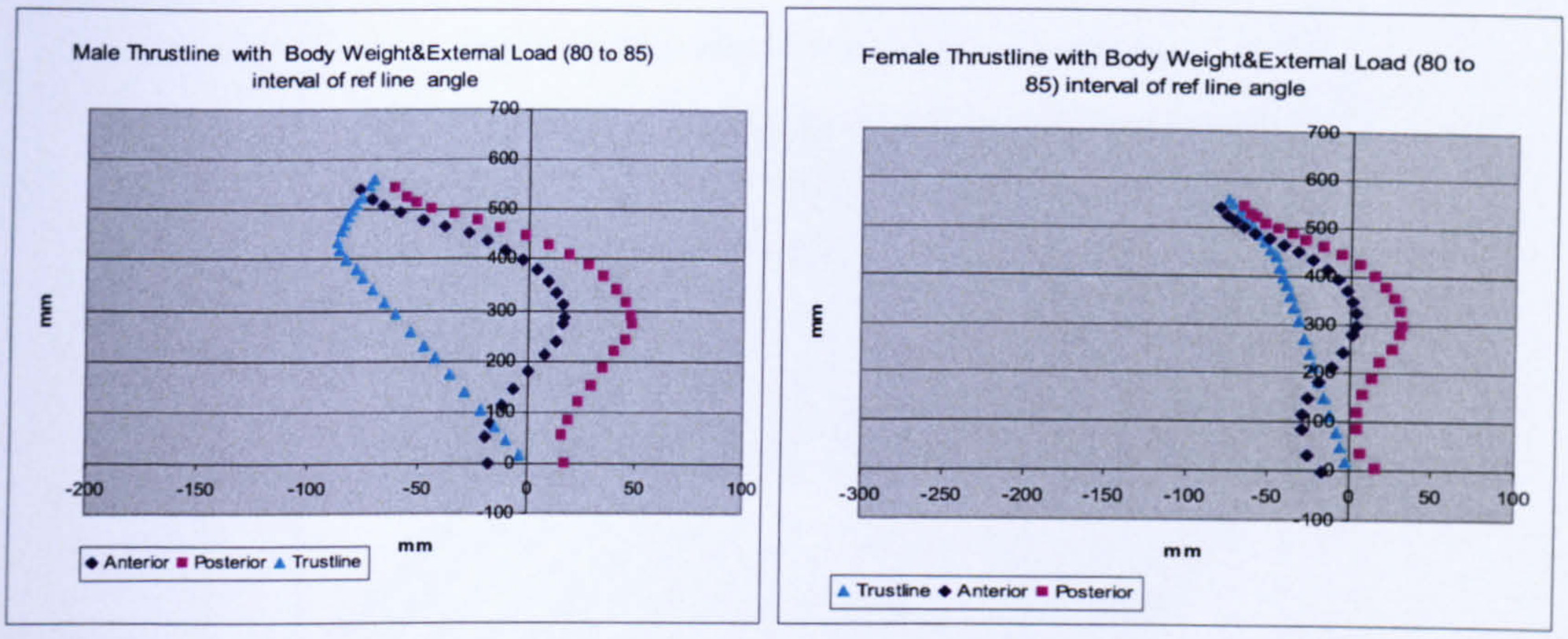


Figure 6- 16 Male and female thrustline with Body Weight and External Load of 900N (80° to 85°) interval of reference line angle.

The distance of the force application point from the reference line increases so that thrustline moves anterior to the reference line with greater reaction forces at the end points (Figure 6.17).

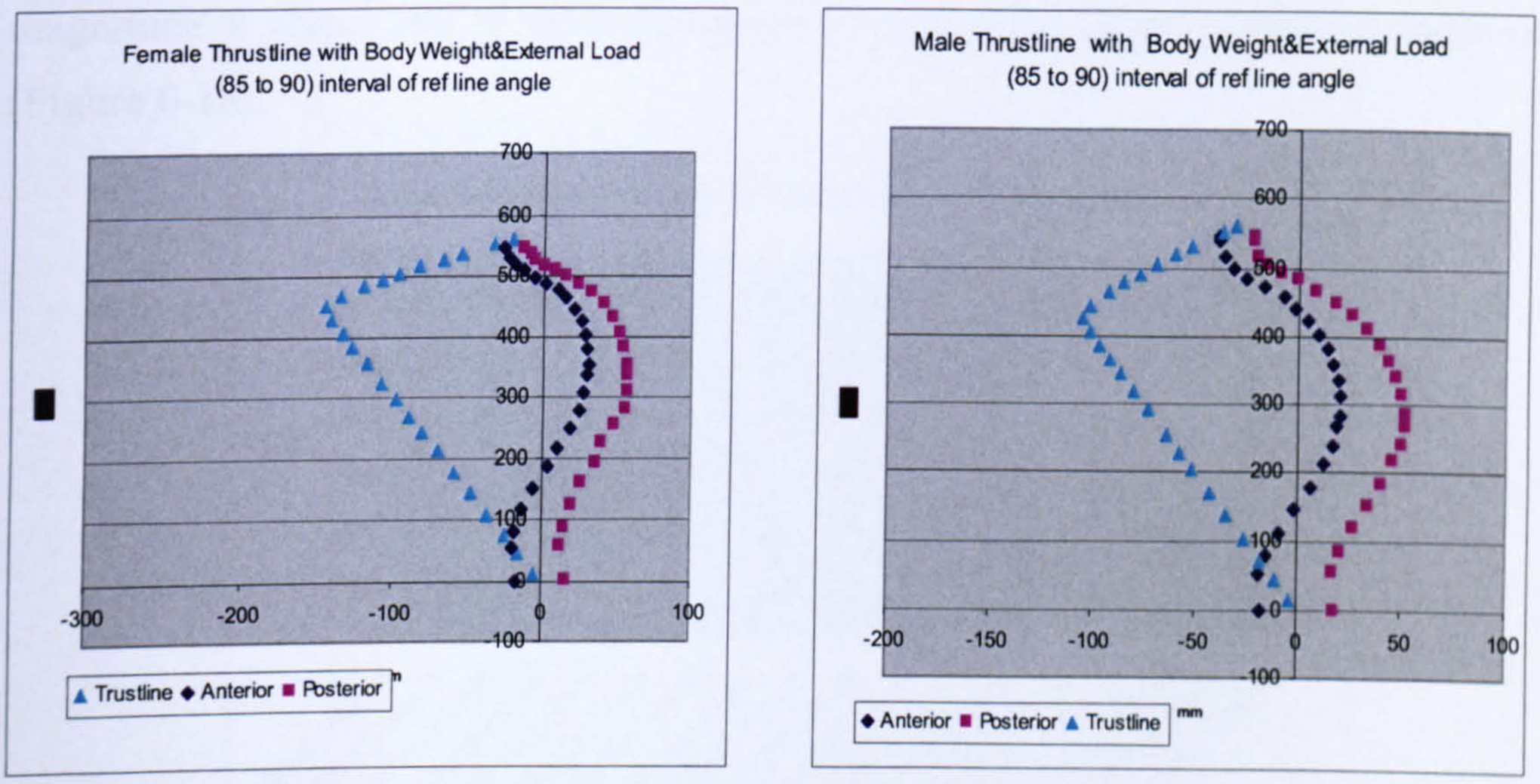


Figure 6- 17 Male and female thrustline with Body Weight and External Load of 900N (85° to 90°) interval of reference line angle.

Reaction forces for the spine are calculated when the external load and the body weight force are acting on the spine. The graphs are drawn for both genders. Similar trend have been observed as with only the body weight forces acting on the spine. However, with the addition of the external load, the magnitude of the reaction forces increases for both compressive and shear forces.

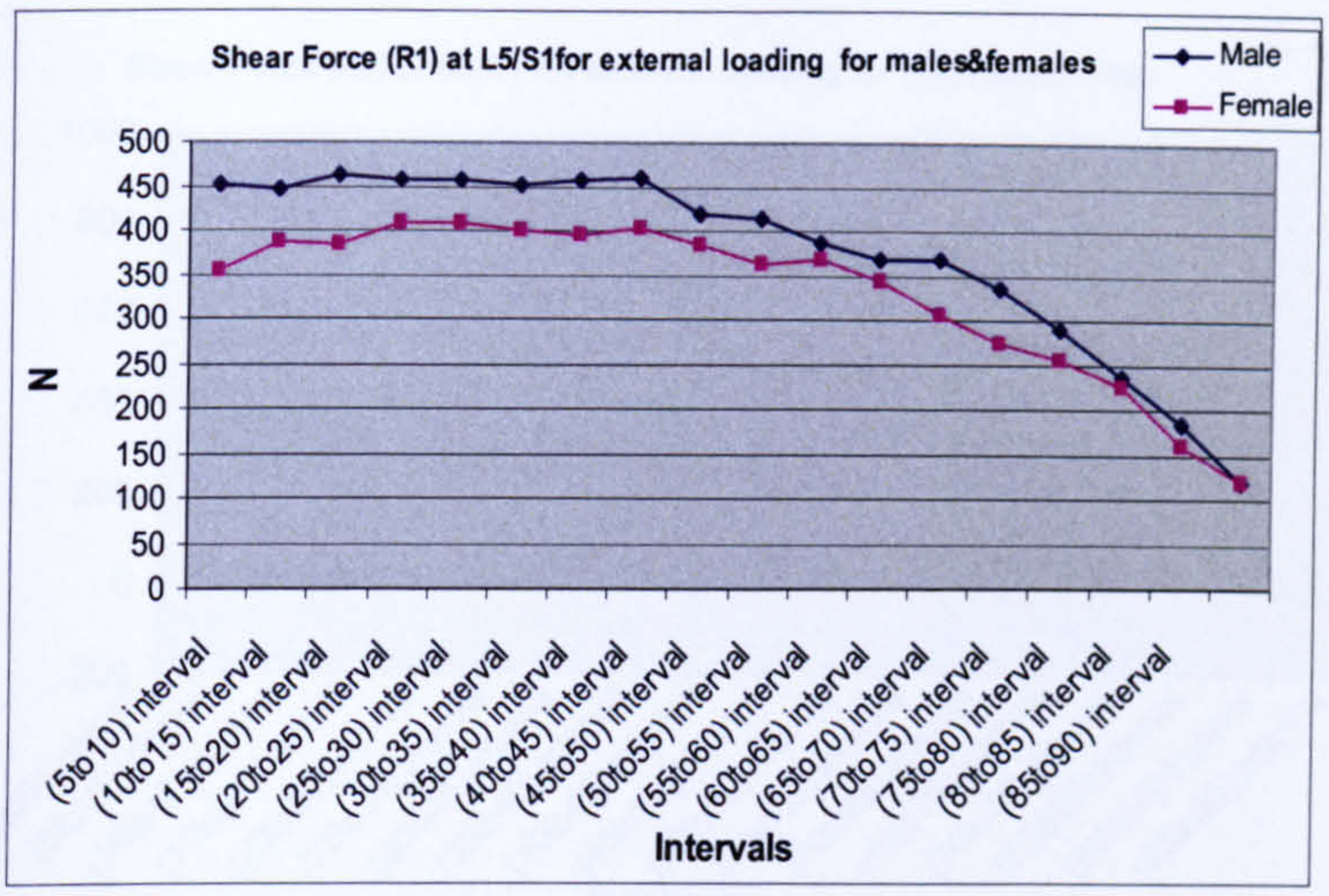


Figure 6- 18 Shear forces for males and females at L5/S1 with external loading

With the addition of external force, the magnitude of shear force increases to the 450-500 N and 350-400 for males and females respectively. The increase in the shear force magnitude is about 200 N when compared to only body weight acting on spine case (Figure 6-18).

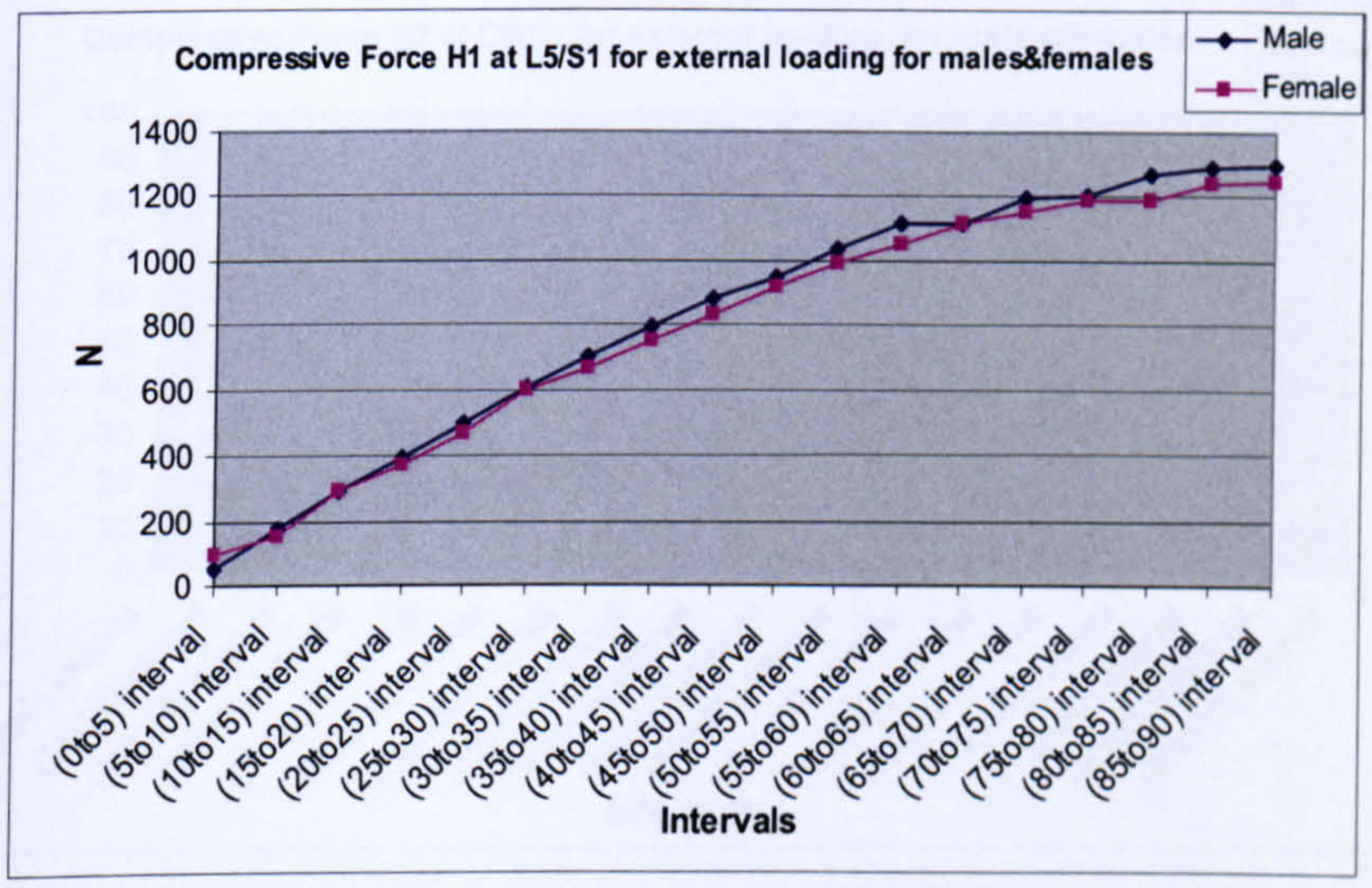


Figure 6- 19 Compressive forces for males and females at L5/S1 with external loading

The magnitude of compressive force acting on spine increases to 1300 N and 1200 N for males and females respectively. The increase in the compressive force is around 900 N when compared to the only body weight forces acting on the spine (Figure 6-19).

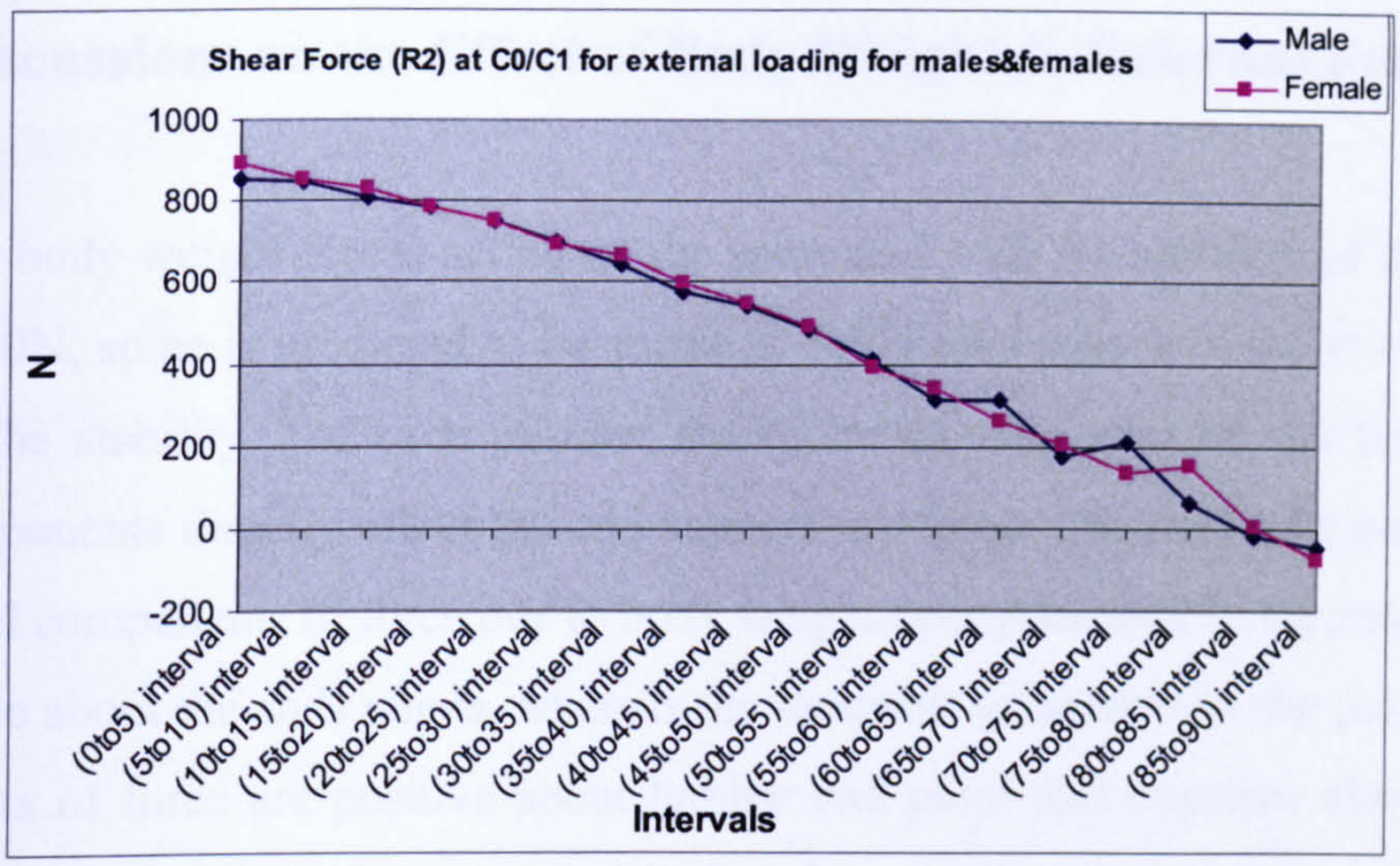


Figure 6- 20 Shear forces for males and females at superior surface of C1 with external loading

The magnitude of shear force acting on the superior surface of C1 increases by more than 600 N when the additional external force is acting on the spine (Figure 6.20).

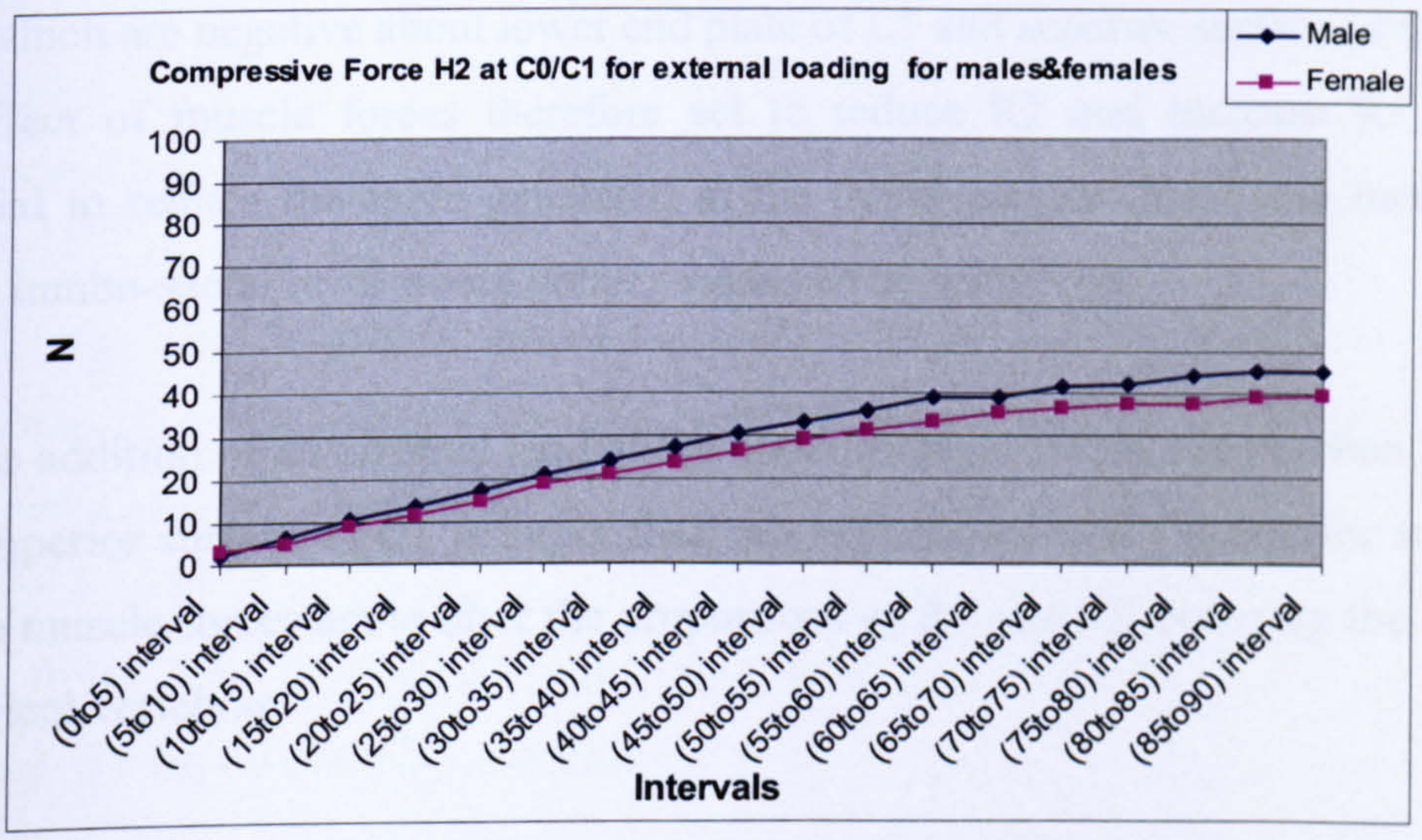


Figure 6- 21 Compressive forces for males and females at superior surface of C1 with external loading.

The point of application of the external force is at T2, T3, T4 levels. They do not cause an increase in the compressive force at the level of C1. The compressive force is applied at superior surface of C1 by the weight of the head only.

6.1.3 Discussions on the Effect of Body Weight & External Forces

With only body weight forces acting on the spine and with the addition of the external load of 900N, spine is predicted to be unstable. Additional muscle force is required for ensuring the stability. For each posture, the moments generated by the body weight force components directly affect the end support reactions. The moments generated by the parallel components of force due to body weight acting anterior to the reference line are positive about the ends points, whereas the moments generated by the perpendicular components of force are positive about lumbar end point and negative about cervical end point. The moments about cervical is therefore reduced due to terms of opposing direction consequently, R1 (shear force at end plate of L5) is less than R2 (Shear force at superior surface of C1).

Muscles acting posterior to the spine generate moments due to parallel components of forces which are negative about lower end plate of L5 and superior surface of C1.
The effect of muscle forces therefore act to reduce R2 and increase R1. This is beneficial to reduce the force generated at the upper cervical level and increase the force at lumbo-sacral level where greater loads can be withstood.

With the addition of an external load at the upper thoracic levels, the reaction force R2 at the superior surface of C1 is larger than the reaction force R1 at inferior surface of L5. The muscle forces act to alter the proportions of R1 and R2, reducing the loads on the cervical vertebrae.

With flexion, the perpendicular components of forces acting on the spine increased and the parallel components decreased. This is accompanied by an increase in both R1 and R2, and a decrease in H1 and H2 for equilibrium. Due to this increase in the perpendicular component of force, a steeper thrustline curve was projected. These effects increased with the application of an external load. Muscle forces are required to oppose the effects of body weight by generating force with perpendicular components in the perpendicular direction or by generating larger parallel components to decrease the proportion of the perpendicular component of the resultant force vectors.

6.2 Grouping of Muscles with Respect to Their Effect on Thrustline

In order to evaluate the effects of each muscle group on spinal stability, the model was run for each muscle group to analyse its effect on thrustline. For this purpose 9 categories were defined.

Category 1: Thrustline moves anterior to the reference line

Category 2: Thrustline moderately flattened

Category 3: Thrustline moderately flattened and localised effect in cervical region

Category 4: Thrustlines flattened by small amount and localised affect in cervical region

Category 5: Thrustline flattened by small amount

Category 6: Negligible effect on overall thrustline

Category 7: Thrustline moderately flattened and localised effect in lumbar region.

Category 8: Thrustline curvature moderately increased.

Category 9: Thrustline curvature significantly increased.

For each interval of reference line angle, a table is formed which shows the category of each muscle group according to the definition above (Appendix4). This table are used to refer when analysing the combined effect of muscle groups on thrustline. There is not much study in literature with the effect of each muscle group on thrustline to refer to in this detail. Without this reference table, it is not possible to decide how each muscle effects the position of thrustline.

Cervical muscles

Rectus capitis posterior major has a localised effect on cervical region starting from the 0 to 20 degrees of reference line angle with a small effect in flattening. This muscle is grouped in the group 4 up to 0-20 degrees of reference line angle with the spine gaining slightly erect postures; thrustline is flattened by small amount resulting classification of this muscle group into category 5.

Rectus capitis posterior minor has similar effects with the rectus capitis posterior major. However, after the 70 degrees of reference line angle the effect of this muscle is slightly reduced and it is classified as category 6.

Obloquies capitis superior in general has the effect of flattening the thrustline by small amount with localized effect in cervical region (Category 4). When the spine attains an erect posture, the effect of this muscle on thrustline becomes negligible (Category 6). The effect of obloquies capitis inferior on thrustline is similar to obliquis capitis superior.

These muscles, RCPMajor, PCPMinor, OCI, and OCS are named as suboccipital muscles and play role in fine tuning movements of the head. It is expect to categorize these muscles within the categories 4, 5 and 6. The effect of these muscles on thrustline is inline with the literature (Kamibayashi and Richmand, 1998).

Longis capitis has the effect of moderately flattening the thrustline and localised effect in the cervical region from 0-5 to 55-60 degrees of reference line angle.. However, in the interval of 60-65, 65-70 this effect is on overall thrustline (category 2). For the intervals of 70-75, 75-80 the effect of muscle reduces and thrustline is affected by small amount (Category 5). For the interval of 80-85 and 85-90 degrees of reference line angle, it is classified as category 8.

Longis capitis , when acting bilaterally flexes the head and neck (Kamibayashi and Richmand, 1998). From the 0 degrees of reference line angle to 70 degrees of reference line angle, longis capitis has a positive effect on thrustline to reduce the curvature and to aligning the curvature nearer to spine. For fully erect postures, the head and the neck is not flexed, this shows that longis capitis might not be needed as it increases the instability. Or it is possible to think that this muscle is not fully activated but with a little percentage.

Longis colli vertical has the moderately flattening the thrustline starting from the 0 to 15 degrees of reference line interval. However, after 15 degrees of reference line angle, the cervical effect is reduced resulting in general flattening effect on thrustline (Category 2) till the interval of 60 to 65 degrees of reference line angle interval. From

the intervals of 60-65 to 75-80, the effect of this muscle on thrustline is small (Category5). For the intervals of 80 to 85 and 85-90, thrustline curvature increases (category 8).

For 0 to 45 degrees of reference line angle, the effect of Longis colli superior oblique flattens by small amount with a localised affect in cervical region. From the angle of 45 to 60 degrees of reference line angle, thrustline is moderately flattened (category 2). For the intervals of 60 to 80 degrees of reference line angle the effect of this muscle is reduced and thrustline is affected by small amount (Category 5). For the intervals of 80-85 and 85-90, thrustline curvature increases classified as category 8.

Longis colli inferior oblique flattens the thrustline for 0 to 30 degrees of reference line angle (Category 2). For 30 to 50 degrees of reference line angle, thrustline is flattened by small amount (Category 5). For the interval of 50 to 70 degrees of reference line angle, the effect is negligible (Category 6). For the intervals of 70 to 90 degrees of reference line angle thrustline curvature is increased (Category 8).

Longis capitis, longis colli vertical, superior and oblique muscles are known as synergist muscles. It is expected that neck and head is not in a flexed posture for the 80-90 degrees of reference line. This is also reflected with the increase of thrustline curvature. However, it is possible to think that these muscles are not fully activated but with a little percentage.

Scalenus anterior flattens the thrustline by small amount with local effect on the cervical region for the intervals of 0-5 and 5-10 degrees of reference line angle (Category4). Starting from the interval of 10-15 to 45-50 degrees of reference line angle, thrustline is moderately flattened (Category 3). From the interval of 50-55 degrees of reference line angle to 85-90 degrees of reference line angle, thrustline is flattened by small amount (Category 5).

Scalenous medius has the effect of flattening moderately with localised effect in cervical region from the intervals 0-5 to 30-35 degrees of reference line angle. From the interval of 35-40 to 40-45 degrees of reference line angle this effect is reduced (Category 4). From 45-50 to 75-80 degrees of reference line angle, thrustline is

flattened by small amount (Category 5). For the interval of 80-85 and 85-90 degrees of reference line angle, thrustline curvature is increased (Category 8).

For the intervals of 0-5 and 5-10 degrees of reference line angle, Scalenus posterior is classified as category 3 because of moderately flattened with a cervical effect. For the interval of 10 to 40 degrees of reference line angle, thrustline is moderately flattened (Category 2). For the intervals of 40 to 70 degrees of reference line angle , Scalenus posterior has little effect on thrùstline (category 5). For the intervals of 70-90 degrees of reference line angle, this muscle is classified in category 8.

Scalenus anterior, medius, posterior muscles are thought to flex the cervical column when contracted symmetrically. These muscles might be considered as activated together.

Longissimus cervicis moderately flattens the thrustline from 0-5 to 45-50 degrees of reference line angle (Category2). For the intervals of 45-50 to 60-65 degrees of reference line angle, longissimus cervicis has small effect on thrustline.65-70 to 85-90 degrees of reference line angle, thrustline curvature is moderately increased.

Longissimus capitis flattens the thrustline moderately (Category2). Spinalis thoracis flattens the thrustline moderately for the intervals of 0-5 to 10-15 degrees of reference line angle. However, the effect of spinalis thoracis is less in the intervals of 15-20 to 85-90 degrees of reference line angle (Category 5). Spinalis cervicis flattens the thrustline moderately from the interval of 0-5 to 30-35 degrees of reference line interval. For the interval of 35-40 to 60-65, spinalis cervicis flattens the thrustline by small amount (Category 5), for the intervals of 65-70 to 85-90, thrustline curvature is moderately increased (Category 8). Iliocostalis cervicis, flattens the thrustline moderately from 0-5 to 35-40 degrees of reference line (Category2), from the interval of 40-45 to 65-70 interval iliocostalis cervicis flattens the thrustline by small amount (Category 5),. From the interval of 70-75 to 85-90 reference line angle, this muscle causes trustline to increase its curvature.

Splenius capitis and Splenius cervicis muscles have the very similar effects on thrustline. Initially, both muscles flattens the thrustline moderately starting from the

interval of 0-5 to 50-55 (Category2). Splenius capitis effects the thrustline with small amount for the intervals of 55-60,60-65, 65-70 and 70-75 degrees of reference line angle, whereas Splenius cervicis, effects the thrustline for the interval of 55-60 moderately (Category2) and has little effect for the interval of 60-65, 65-70, 70-75 degrees of reference line angle. For the intervals of 75-80, 80-85 and 85-90 these muscles increase the curvature of the thrustline (Category 8).

Semispinalis capitis has the size and length which makes itself one of the strongest muscles among the post-vertebral group of neck muscles. It flattens the thrustline starting from the interval of 0-5 to 80-85 degrees of reference line (Category2). For the interval of 85-90 it moves the thrustline anterior to the reference line (Category1)

Semispinalis cervicis flattens the thrustline starting from the interval of 0-5 to 75-80 degrees of reference line angle (Category2). For the intervals of 80-85 degrees of reference line angle, it increases the curvature of the thrustline (Category8).

Semispinalis thoracis moderately flattens the thrustline for starting from the interval of 0-5 to 35-40 degrees of reference line angle (Category2). From the interval of 40-45 to 75-80, it flattens the trustline with some effect on lumbar region (Category7). For the intervals of 80-85 and 85-90 degrees of reference line angle, this muscle increases the curvature of the thrustline (Category 8).

Cervical multifidus flattens the thrustline for the intervals of 0-5 to 75-80 degrees of reference line angle. For the intervals of 80-85 and 85-90, it moves the thrustline anterior to the reference line.

Superficial Back Muscles

Acromiotrap has the effect of flattening the thrustline moderately for the interval of 0-5 to 75-80 degrees of reference line angle (Category2). For the interval of 80-85 and 85-90, it moves the thrustline anterior to the reference line (Category1). Trapezius flattens the thrustline moderately from 0-5 to 40-45 degrees of reference line angle (Category 2). However, as the spine attains more erect posture the effect of this muscle on stability decreases (Category5).

Levator scapulae, flattens the thrustline moderately from the interval of 0-5 to 55-60 degrees of reference line angle. However this effect reduces after this interval until the interval of 80-85 degrees of reference line angle. For the interval of 80-85 and 85-90 degrees of reference line angle, thrustline moves anterior to the reference line (Category1).

Lattissimus dorsi flattens the thrustline moderately until the interval of 55-60 degrees of reference line angle (Category2). However, this effect reduces slight and thrustline is effected slightly (Category5) until the posture of 75-80 degrees of reference line angle. From the interval of 75-80 to 85-90 degrees of reference line angle , thrustline moves anterior to the reference line (Category1)

Quadratus lumborum flattens the thrustline slightly until the interval of 40-45 degrees of reference line angle. However with the spine gaining more erect postures this effect is reduced (Category 6). Psoas muscle increases the curvature of the thrustline for all the postures (Category 8). Rectus abdominis and external increase the curvature of the thrustline for all the postures but its effect is found out to be more than the psoas muscle (Category 9).

Thoracic and lumbar multifidus flattens the thrustline moderately for the intervals of 0-5 to 45-50 degrees of reference line angle (Category 2). From the interval of 45-50 to 75-80 degrees of reference line angle they flatten the thrustline with and effect on lumbar region (Category 7). For the intervals of 80-85 and 85-90 degrees of reference line angle, thrustline moves anterior to the reference line angle (Category 8).

Erector Spinae Muscles

Longissimus thoracis pars thoracis, iliocostalis lumborum pars thoracis, longissimus thoracis pars lumborum and iliocostalis lumborum pars lumborum compose the erector spinae muscles.

Erector spinae muscle group have very similar effects. Iliocostalis lumborum pars thoracis, longissimus thoracis pars lumborum and iliocostalis lumborum pars lumborum flatten the curvature of the spine moderately starting from the interval of 0-5 to 75-80

degrees of reference line and is classified in category 2. However, for the intervals of 80-85 and 85-90, this muscle moves the thrustline anterior to the reference line (Category1). Longissimus thoracis pars thoracis, having 9 fascicles and applying more forces than the others, is slightly different. This muscle has the same effect with the other erector spinae muscles until the interval of 70-75. However, this muscle moves the thrustline anterior to the reference line starting from 75-80 to 85-90 degrees of reference line angle.

6.2.1 Discussions on the Effect of Muscle Groups on Thrustline

Muscle groups which have an attachment to the sacrum or pelvis

Muscle groups which have an attachment to the sacrum or pelvis have the most significant effect on the overall thrustline in addition to the muscle groups which attached to the spine or ribcage. Due to the fixed representation of the pelvis the forces acting at this end were not considered. The boundaries of spine for the application of thrustline theory are upper surface of C1 and lower end plate of L5. The muscles which are attached beyond L5 can not be included as they are outside of the boundaries of the spine by definition. The muscle forces and their consequent moments generated at the spinal attachments are therefore unopposed.

For all lumbar muscle groups, the dominant parallel components of force generate large moments about the end points of the spine. Longissimus thoracis, multifidus, iliocostalis and quadrotus lumborum the parallel components of the force act posterior to the reference line and generate moments which oppose the flexion. The psoas muscle groups act both anterior and posterior to the reference line in the erect posture. Due to the similar moment arms for these anterior and posterior forces, the parallel components of with the greater total magnitude anterior to the reference line generate greater moments. These act with the moments generated by anterior body weight forces, increasing the overall flexion moment.

The greatest moments are generated about cervical end point by the perpendicular components of force for all lumbar muscles except the longissimus thoracis. This is because the forces are mainly applied in the lumbar region with large relative moment

arm relative to the cervical end. For all lumbar muscles, majority of the forces have positive perpendicular forces generating moments opposing to body weigh forces. For internal oblique muscles, due to positive perpendicular components of force, moments are generated acting against the body weight. In contrast external oblique acts with body weight. The parallel force components of the muscles groups which act anterior to the spine increase the flexion moment.

Muscle Groups with Attachment Points within the Boundaries of the Spine

Muscle groups acting above the sacrum and pelvis and below the cervical spine generate pairs of force in opposing directions at their attachment points. Those attaching between the vertebrae and the head generate forces above and below the superior surface of C1. For the muscles which act above the head, the force value with its moment generated is transferred to the superior surface of C1 with the muscle direction remaining same. Those attaching between the vertebrae or between the vertebrae and ribcage generate forces between the superior surface of C1 and lower end plate of L5. Figure 6.22

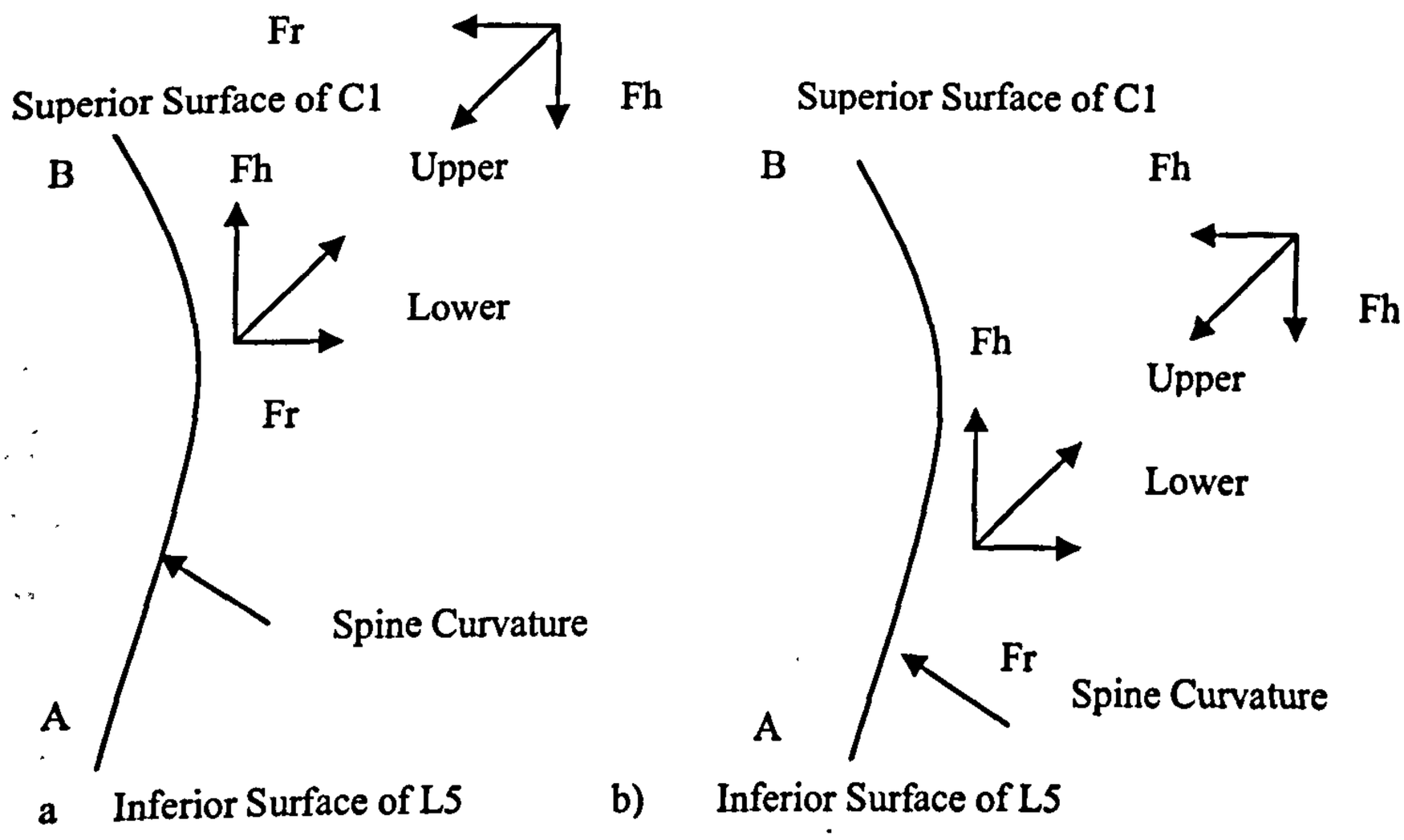


Figure 6- 22 a) Illustration of force pair acting on the spine above and below the superior surface of C1
b) Illustration of force pair acting on the spine between the superior surface of C1 and lower end plate of L5

For muscles with oblique orientation, the attachment points differ in their positioning relative to the reference line. The forces as in Figure 6.22 is positioned further posterior to the reference line, so that the parallel component has a moment arm greater than that at a lower attachment. Despite the forces of equal magnitude, the moment due to

parallel components of force is greater at the upper attachment. For the perpendicular components, when forces act between A and B, equal moments are generated in opposing directions. However, when the upper attachment is above B, the moments generated are in the same direction about B. Therefore despite forces of opposing directions, small differences in moments occur.

The muscle forces generated at the lower attachments act upwards with positive parallel components so that they oppose the effect of body weight and reduce the gradient of the following thrustline sections for erect postures. Positive perpendicular components of force also oppose the effects of body weight, whereas negative perpendicular components act with body weight reducing the effect of the parallel component. The application of a muscle force at the upper attachment opposes the direction of the initial muscle force, but does not counteract the flatting effect on the thrustline. Consequently, the overall depth of the thrustline curve is reduced. Muscles of this type have greater effect with the number of levels spanned.

The forces, acting above the upper surface of C1 which is point B, are incorporated into H2 which affects the direction of the final portion of the thrustline. The forces applied at the lower attachments of the muscles have more significant effect. The forces generated at the lower attachment for semispinalis capitis, longissimus capitis, spinalis capitis have positive perpendicular and parallel components which act against body weight. A change in thrustline direction occurs in the cervical region due to the application of these forces. Application of forces due to semispinalis capitis of large muscles over a number of levels in the thoracic and cervical regions results in considerable flattening of the thrustline.

Forces due to muscles attaching between the head and the upper two vertebral levels also show small localised flattening effects in the cervical region. However their forces are effective only for these end vertebral levels.

For the muscles which are attached between the vertebrae, the ribcage, scapula, clavicle, like acromiotrap, trapezius, levator scapula and latissimus dorsi, the force generated at the lower attachment has negative perpendicular and positive parallel components. These perpendicular components are greater than those due to body

weight in this posture and result in an increase in thrustline curvature in erect postures. The opposing force generated at the upper end with positive perpendicular component opposes this effect indicated by a small reduction in thrustline slope although between these points of attachment a small increase in thrustline occurs.

Flexed postures:

In the Appendix 4, it is shown that the effect of muscle groups changes with the change of reference line angle.

Lumbar muscles

Although the magnitude of the muscle forces applied by the muscle groups have not been changed, the relative proportion of force in perpendicular and parallel directions relative to the reference line is affected. When the spine is flexed, the inclination of the reference line angle changes the muscle line of action accompanying a change in the relative movement of the vertebrae to which they are attached.

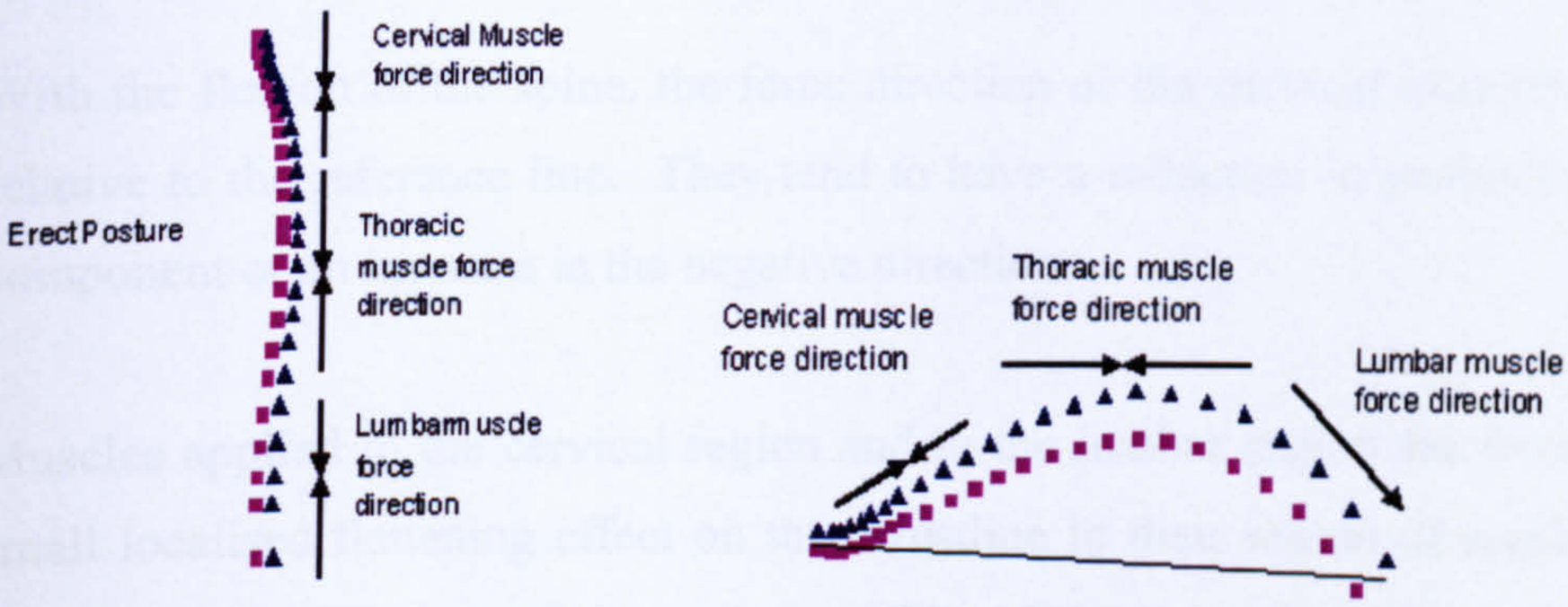


Figure 6- 23 Illustration of an increase in the direction of lumbar and cervical muscle forces in the negative perpendicular direction relative to the reference line due to the flexion.

Figure 6.23 shows the general change in direction of forces in the lumbar regions which accompanies flexion. Muscles attached between the lumbar vertebrae and pelvis follow a direction almost parallel to the reference line in the erect posture. With flexion, the attachment points on the vertebrae are positioned further posterior from the reference line and from the pelvis. Their direction relative to the reference line becomes more oblique. The negative force component is increased. Although the components of the lumbar muscles forces are increased in the negative direction with flexion, the perpendicular components of body weight are also increased. The lumbar muscle forces therefore still oppose the effects of forces due to body weight. But, the effects of the

moments generated by the lumbar muscle forces are reduced with flexion. With flexion, the perpendicular components of force due to body weight increase and the moments generated by lumbar muscle forces have smaller effects.

Abdominal muscles

The internal oblique muscles significantly increase the thrustline curve in the flexed postures. In flexed postures, the perpendicular components of body weight increase in the negative direction. The muscle forces become less effective in opposing the effects of body weight and the overall projection of the thrustline is posterior to the reference line as for body weight. Also the generated moments due to the parallel component of this muscle force contribute to the increase in end support reactions and an increase in thrustline curve.

Cervical muscles

With the flexion of the spine, the force direction of the cervical muscles also changes relative to the reference line. They tend to have a reduction in positive perpendicular component or an increase in the negative direction.

Muscles applied in the cervical region and in the lumbar region are found to result in small localised flattening effect on the thrustline in their region of application. These are considered important for ensuring stability of the spine. In addition to the localised flattening effect, these muscles resulted in an overall decrease in thrustline curve depth. Contraction of these muscles to ensure regional stability may therefore also affect the overall stability of the whole spine. In particular, muscles contracting to ensure equilibrium of the head such as semipinalis capitis, longissimus capitis, can significantly affect the thrustline path.

Lumbar Muscles

The thrustline curve due to bodyweight is increased by the abdominal muscles rectus abdominis and external oblique indicating an increase in the flexion moment on the spinal arch. These muscles are therefore considered to oppose the effects of the extensor muscles in moving the thrustline closer to the spine. Muscles in category 9 had

a considerable affect of increasing the thrustline curvature. Muscles in category two, three, four and seven were significant for their local effects on the thrustline path.

The only way of appreciating contribution of each muscle group to the stability of the spine is considered to categorize the muscles depending on the effects on thrustline. Due to the number of 5 degrees of intervals, 19 different postures are evaluated for stability in terms of effect of muscle forces. With the change of the thrustline curvature at each posture, it is expected that longer muscles do not follow a direct line which connects the insertion and origin points of these muscles. For a more detailed study the change of muscle force application point should be considered. For very long muscles it can be considered that insertion and origin points of the muscles can be in the direction of the peak point of the spinal curvature. However, still, this approach is based on assumptions and not much is known about the direction of muscle forces in a living spine.

In the model, the attachment points of the male and female is changed. This is provided by the scaling of vertebrae size with respect to height of the person. The attachment points of the muscles are defined with respect to the vertebrae corners. When the size of the vertebrae is scaled the attachment point of the muscles are altered automatically.

For the magnitude of the force, PCSA is the main criteria for us. However, there is not much data available in literature for gender differences. 38 muscle groups have been used in this study. There is no study to cover all these muscle groups in terms of gender differences.

In this study we have different postures for females and males. The attachment points of the muscle groups are also scaled according to the body dimensions. The body weight for male data is also different from the female data. This implies that different reaction forces and different thrustlines are expected because of different moment arms and positions of the muscles for each gender posture.

6.3 Muscle groups with body weight forces and external load

The muscle map produced in the previous section and the data from literature as to the role of each muscle group on spine movement have been used as a guideline to decide on muscle groups to have the spine in the most stable condition as possible. Based on this strategy, combinations of possible muscle groups are applied on the spine to align the thrustline which results in the most stable thrustline positioning. To simulate a lifting activity, an external force of 900N is applied to the centre of vertebra T2, T3, and T4. Although the arm muscles and shoulder muscles are expected to distribute this load in a different way, not much is known how these forces and moment values are transferred. For this purpose, based on the other studies in literature, the external load is applied to the centre of the T2, T3 and T4 vertebrae.

The analyses have been conducted for both males and females. Below the results have been supplied for each interval of reference line angle. The muscle groups which are used to apply force for each interval is included in the Appendix5. The code written is flexible enough to include any muscle to check the stability of the spine for any posture. Below the thrustlines which are formed by the combination of muscle forces, external load and body weight force is supplied.

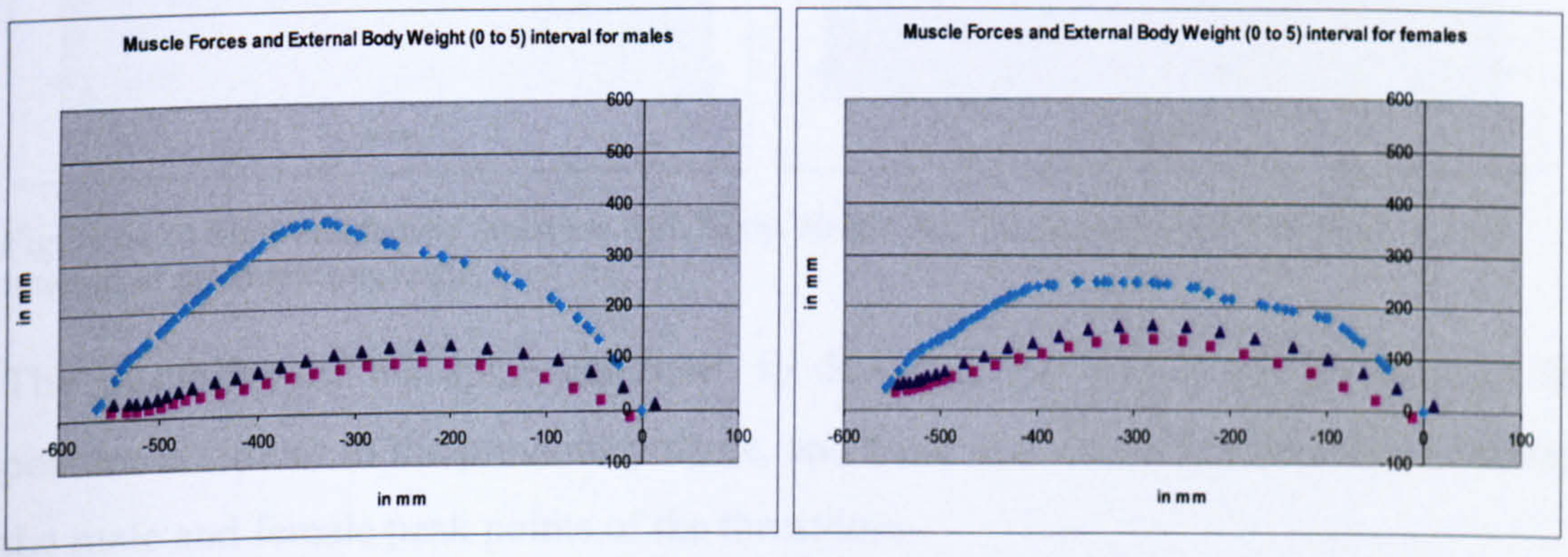


Figure 6- 24 Male and female thrustline with Body Weight and External Load of 900N (0° to 5°) interval of reference line angle.

For the interval of 0-5 degrees of reference line angle, it is observed that spine is unstable. The males have heavy bodyweight which makes the male spine more vulnerable to instability when compared to female spine. In the model ligaments forces have not been applied it is expected that the addition of the ligaments support the spine and increase its stability.

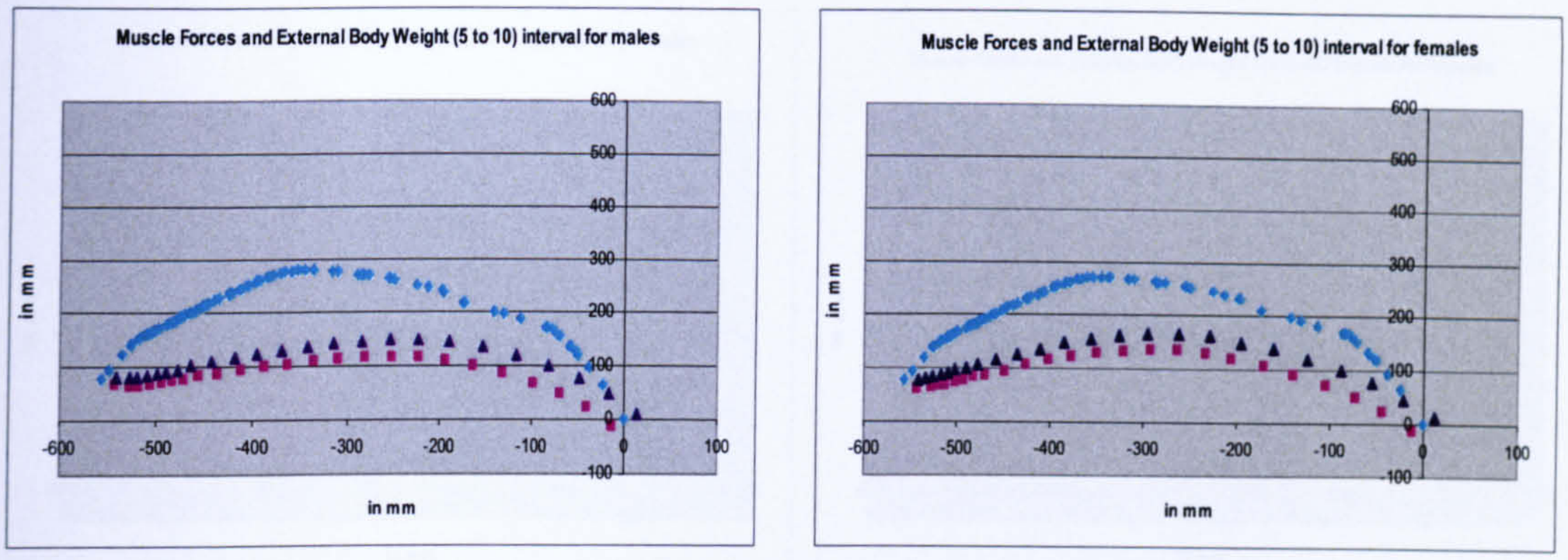


Figure 6- 25 Male and female thrustline with Body Weight and External Load of 900N (5° to 10°) interval of reference line angle.

With the increase of the reference line angle with respect to the horizontal axis, the shear component of the forces decreases when compared to previous posture. The deviation of the thrustline from the spine border decreases. The difference between the male and female thrustline curves is negligible.

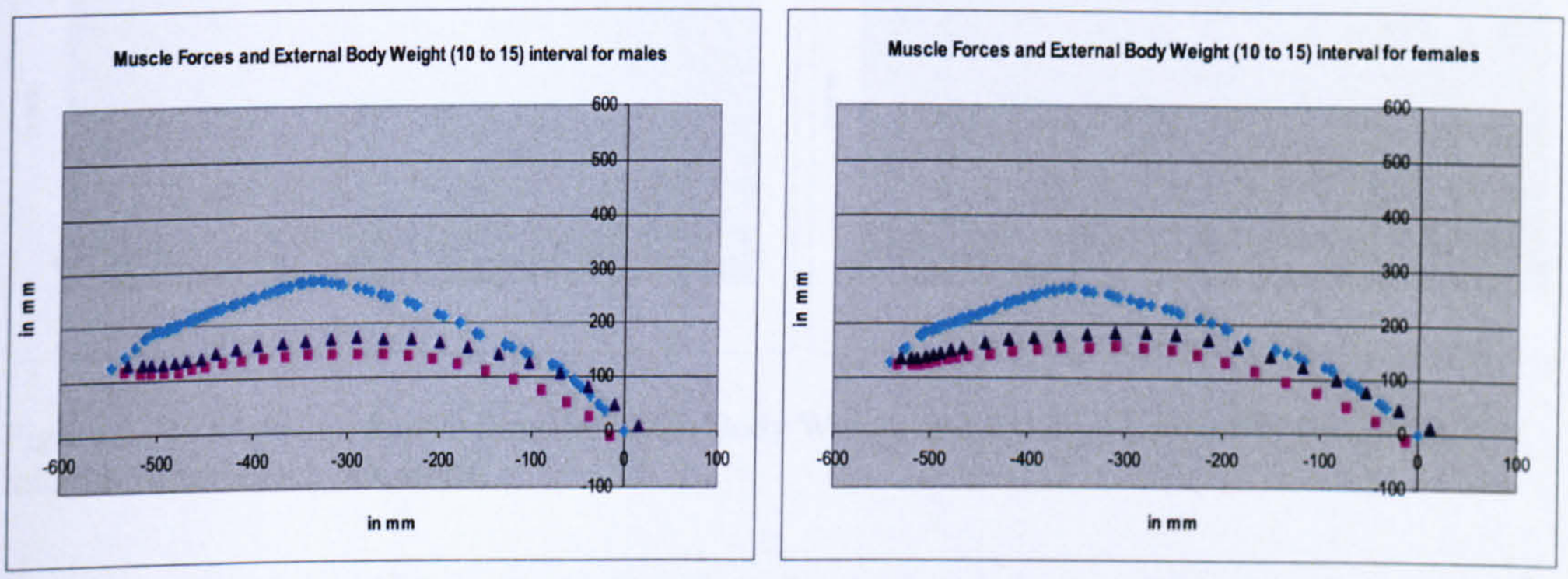


Figure 6- 26 Male and female thrustline with Body Weight and External Load of 900N (10° to 15°) interval of reference line angle.

The instability of the spine continues to decrease, the muscle groups used in this posture is similar to the previous posture, and there is a very slight difference between the male and female peak points of the thrustlines.

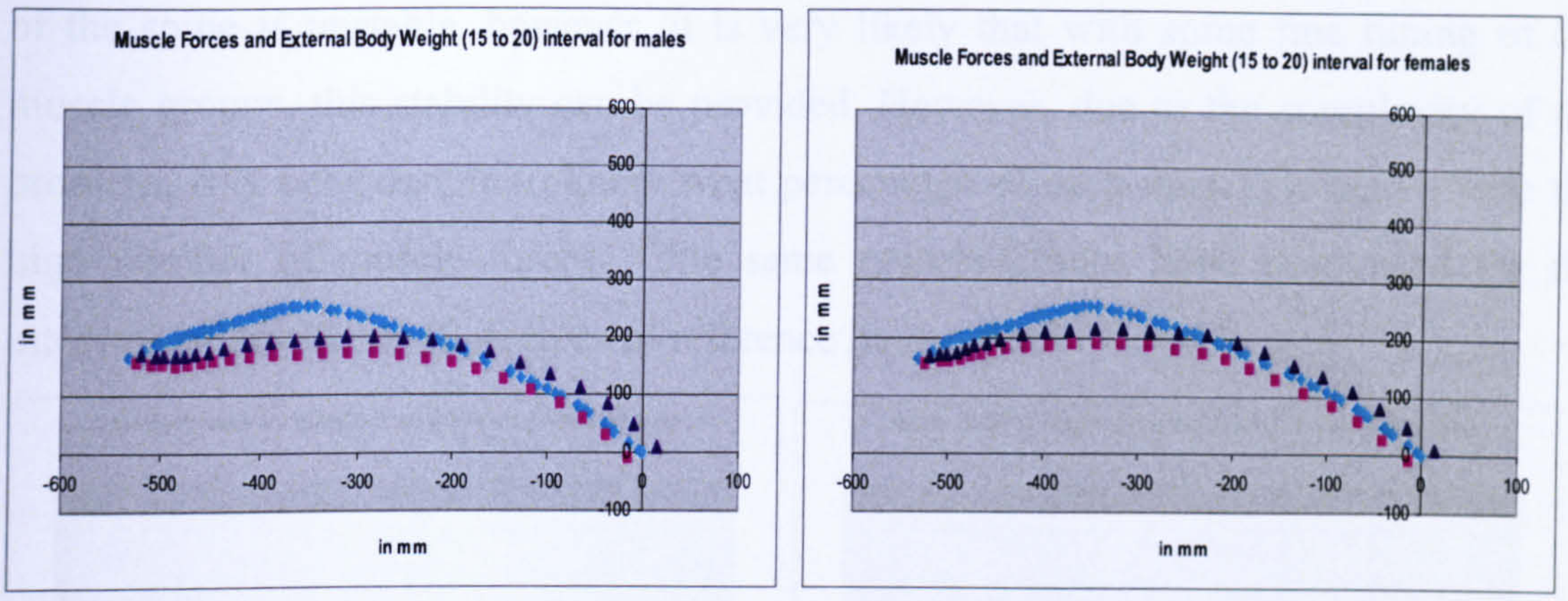


Figure 6- 27 Male and female thrustline with Body Weight and External Load of 900N (15° to 20°) interval of reference line angle.

The instability of the spine is mainly in the thoracic region. But in overall, stability of the spine is improved.

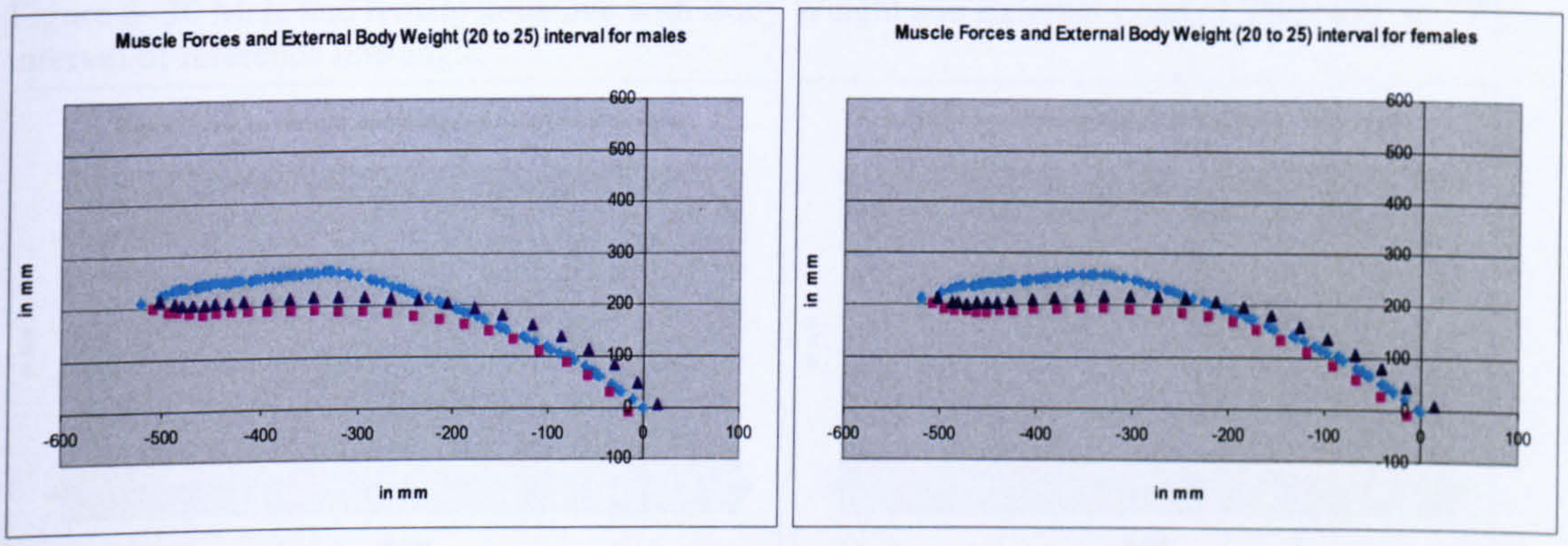


Figure 6- 28 Male and female thrustline with Body Weight and External Load of 900N (20° to 25°) interval of reference line angle.

Instability between the male and female postures does not differ much. Still, stability needs to be improved in the thoracic region.

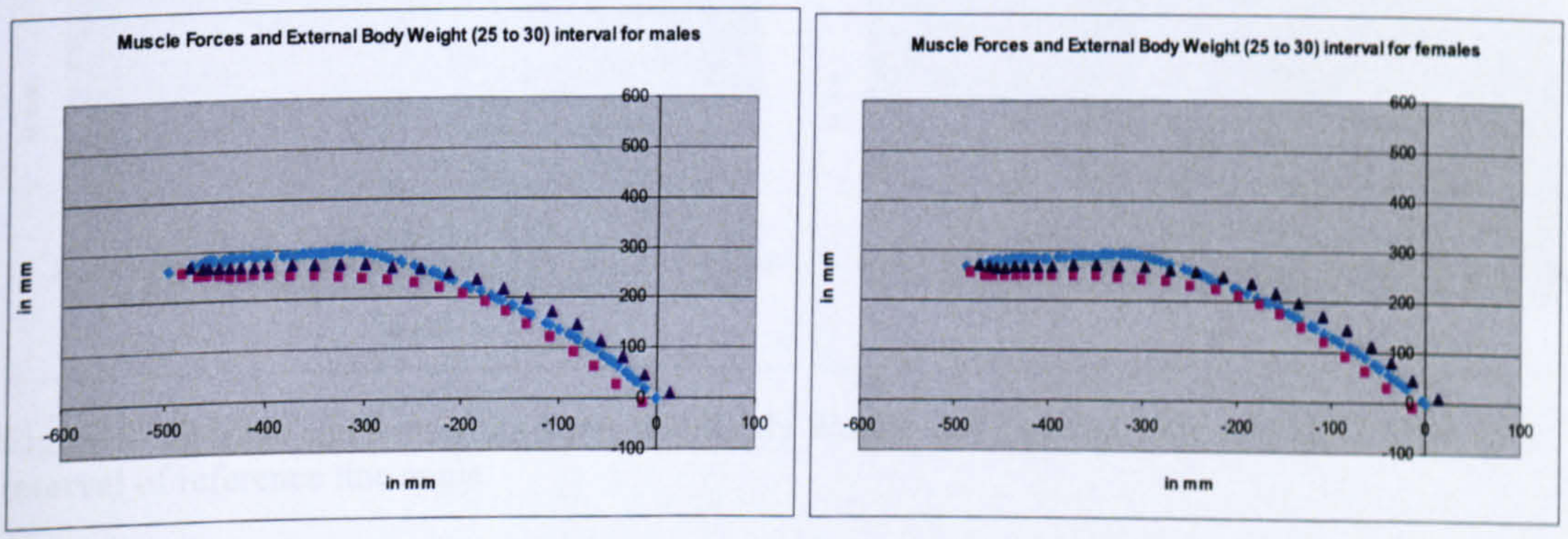


Figure 6- 29 Male and female thrustline with Body Weight and External Load of 900N (25° to 30°) interval of reference line angle.

With the decrease of flexion in the spine posture, compressive forces increase. The requirement for the muscle forces is decreased slightly for this reason. The thoracic part

of the spine is unstable, however, it is very likely that with some fine tuning of the muscle groups, this stability can be provided. However, due to the complexity of the problem, it is not possible to know what percentage of each muscle is active with the high number of muscle forces. The same muscle groups have been used for the intervals of 30-35, 35-40 degrees of reference line angle.

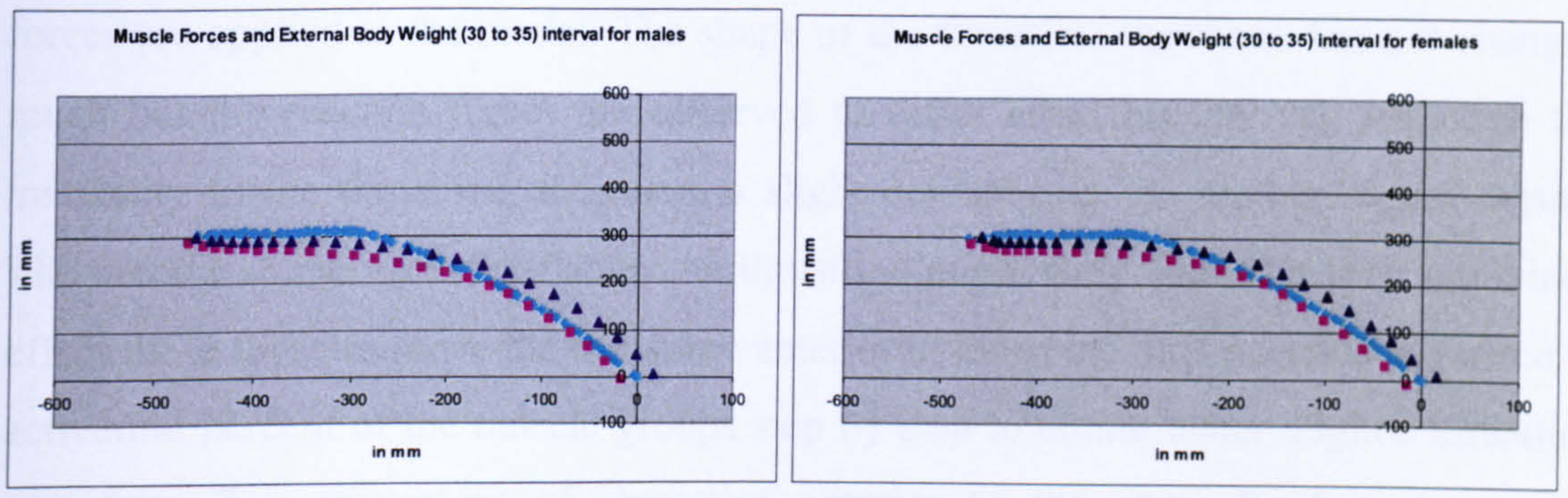


Figure 6- 30 Male and female thrustline with Body Weight and External Load of 900N (30° to 35°) interval of reference line angle.

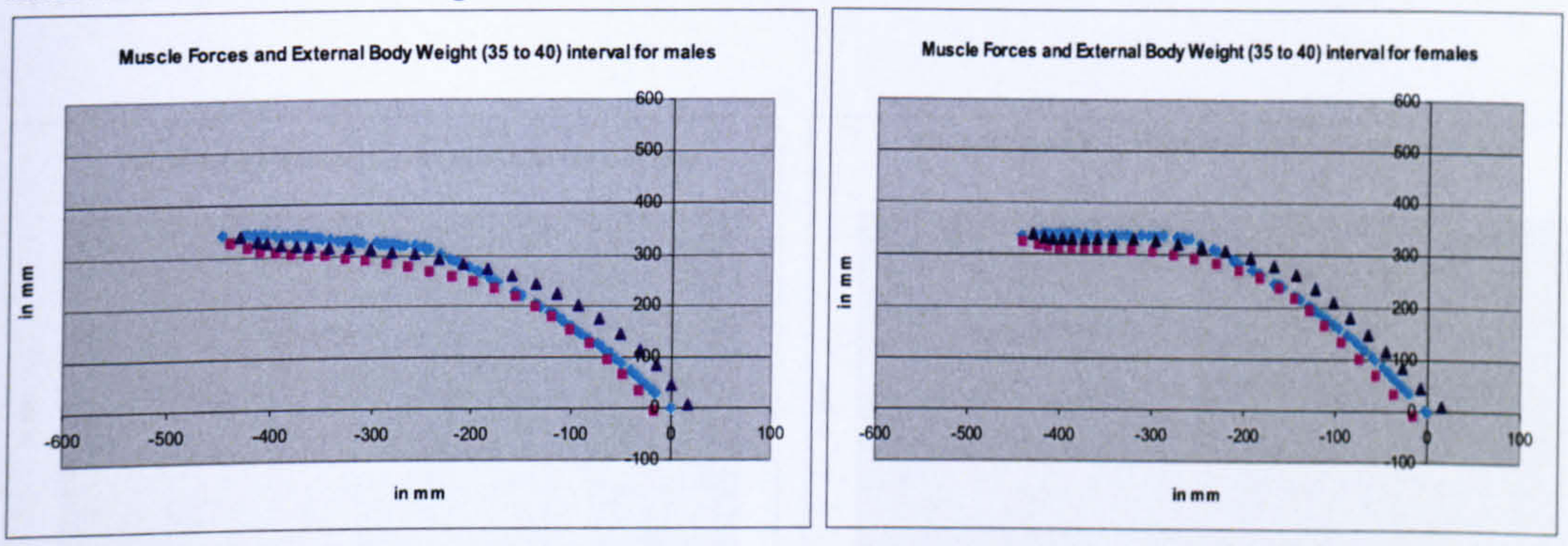


Figure 6- 31 Male and female thrustline with Body Weight and External Load of 900N (35° to 40°) interval of reference line angle.

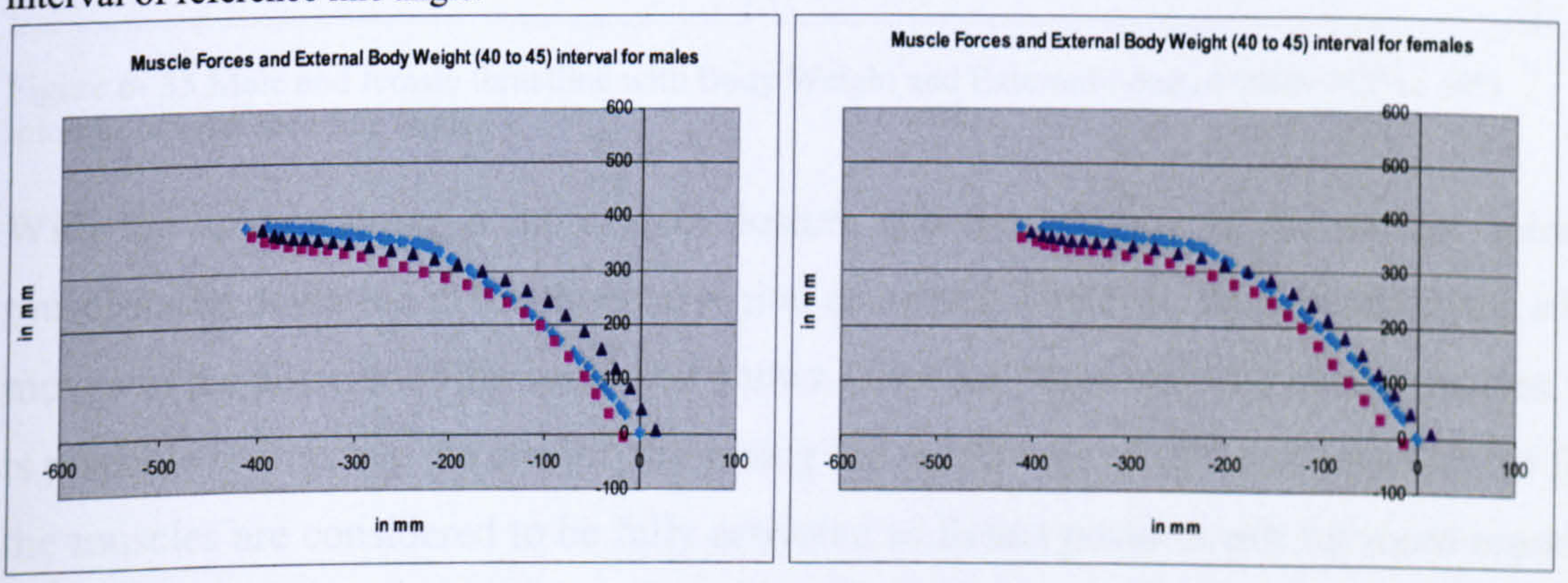


Figure 6- 32 Male and female thrustline with Body Weight and External Load of 900N (40° to 45°) interval of reference line angle.

The erector spinae muscles are considered to be in silence for flexed postures so far. A number of studies have reported minimal activity of the large superficial spinal muscles in the fully flexed posture (Floyd and Silver, 1955, Schultz et al 1985, Andersson et al,

1996). Schultz et al (1985) report that EMG activity measured at the L3/L4 level for this position was less than in the upright standing position and was minimal for both surface and deep erector spinae muscle activity.

After the interval of 35-40 degrees of reference line angle, the erector spinae muscle forces are applied to the model. The shape of the thrustline curvature has not changed much but the reaction forces are observed to differ after this interval. Although the instability in the thrustline decreases, a slight deviation in the lumbar region occurs. The erector spinae muscles flatten the thrustline moderately and with their combined effect these muscles move the thrustline anterior to the spine. It is possible to reduce to activation percent of the muscle groups step by step to obtain better aligned thrustline curvature. The movement of thrustline anterior to the spine borders shows the application of excessive amount of the muscle forces.

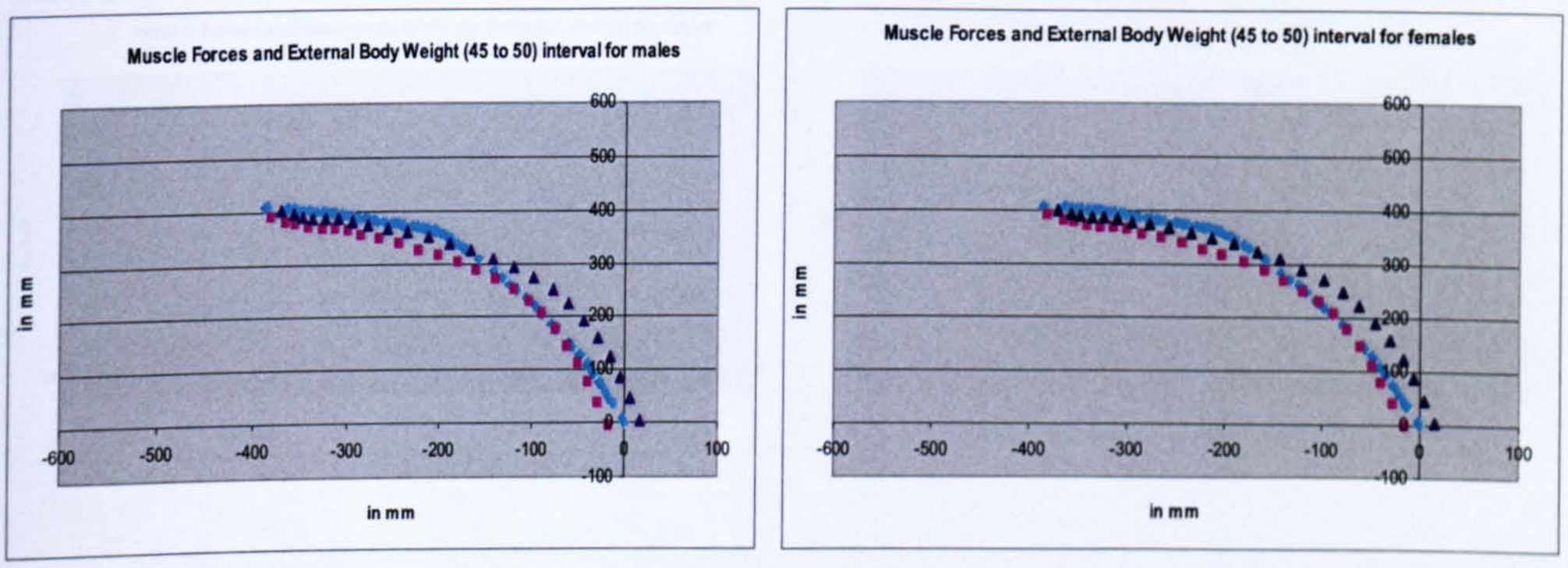


Figure 6- 33 Male and female thrustline with Body Weight and External Load of 900N (45° to 50°) interval of reference line angle.

With the spine gaining a more erect posture and the addition of the erector spinae muscles, the deviation in the thoracic region decreases, however, the lumbar region still moves to the anterior of the spine, this shows excessive force exertion of the muscles. It is possible to improve the stability by tuning the percentage of the muscles used. So far the muscles are considered to be fully activated as flexed postures ask for more muscle force to support the spine due to high shear forces imposed on. When the spine attains an erect posture, the body weight acts to increase the compressive force in the vertical direction and increases the stability with a decreased need for the high muscle forces.

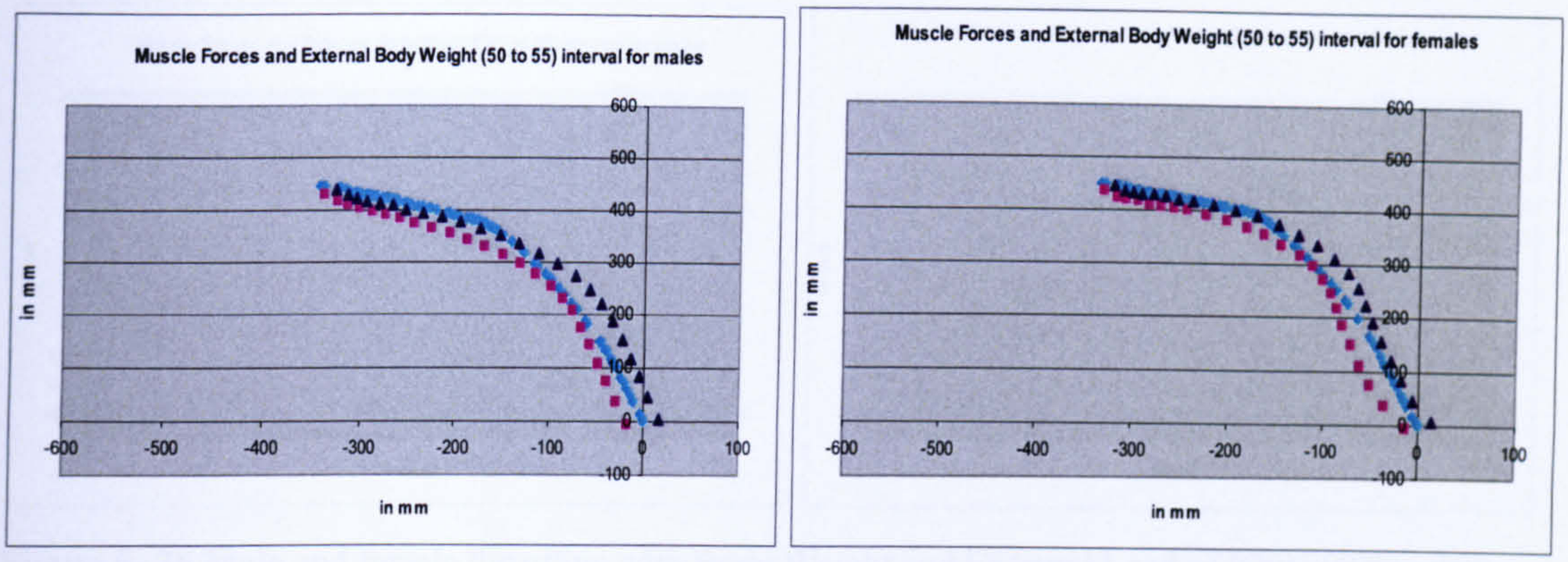


Figure 6- 34 Male and female thrustline with Body Weight and External Load of 900N (50° to 55°) interval of reference line angle.

However, in the interval of 50 to 55 degrees of reference line angle, the erector spinae muscles (4 of them) are activated by 30%. The lumbar portion of the thrustline moves in the spine boundaries.

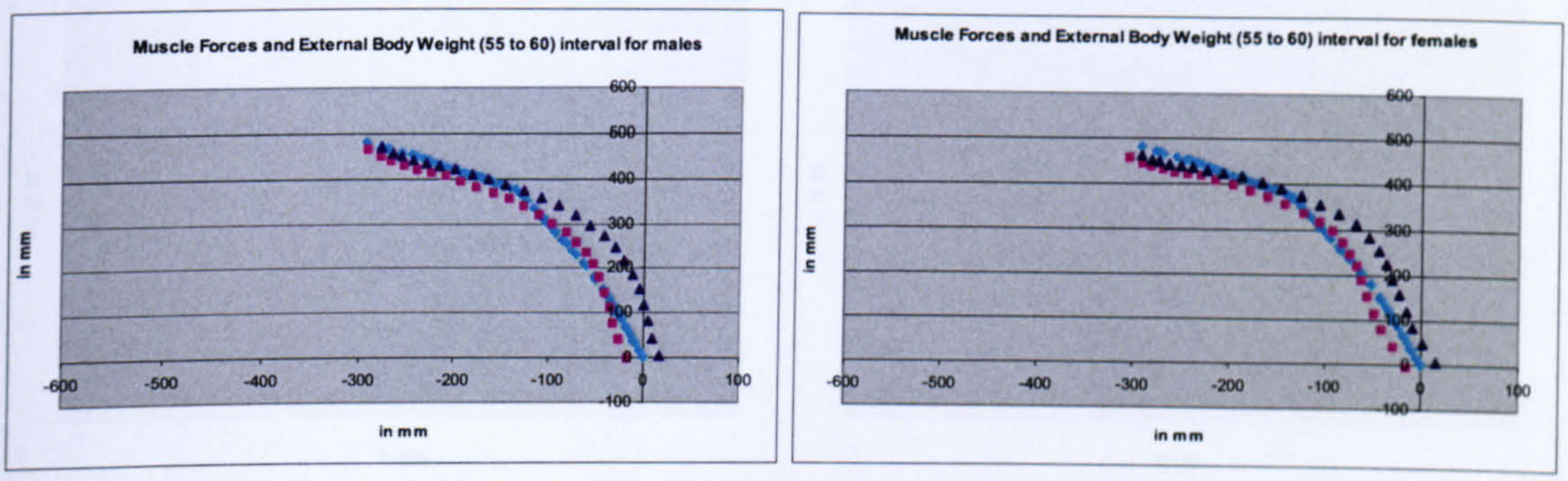


Figure 6- 35 Male and female thrustline with Body Weight and External Load of 900N (55° to 60°) interval of reference line angle.

The upper part of the thoracic spine attains stability, but lower thoracic spine, still needs fine tuning. For more erect postures, it is difficult to find the optimum combination of muscle forces to provide spinal stability. The muscle forces act to force the thrustline anterior to the spine. This is due to overloading of the spine by excessive muscle forces.

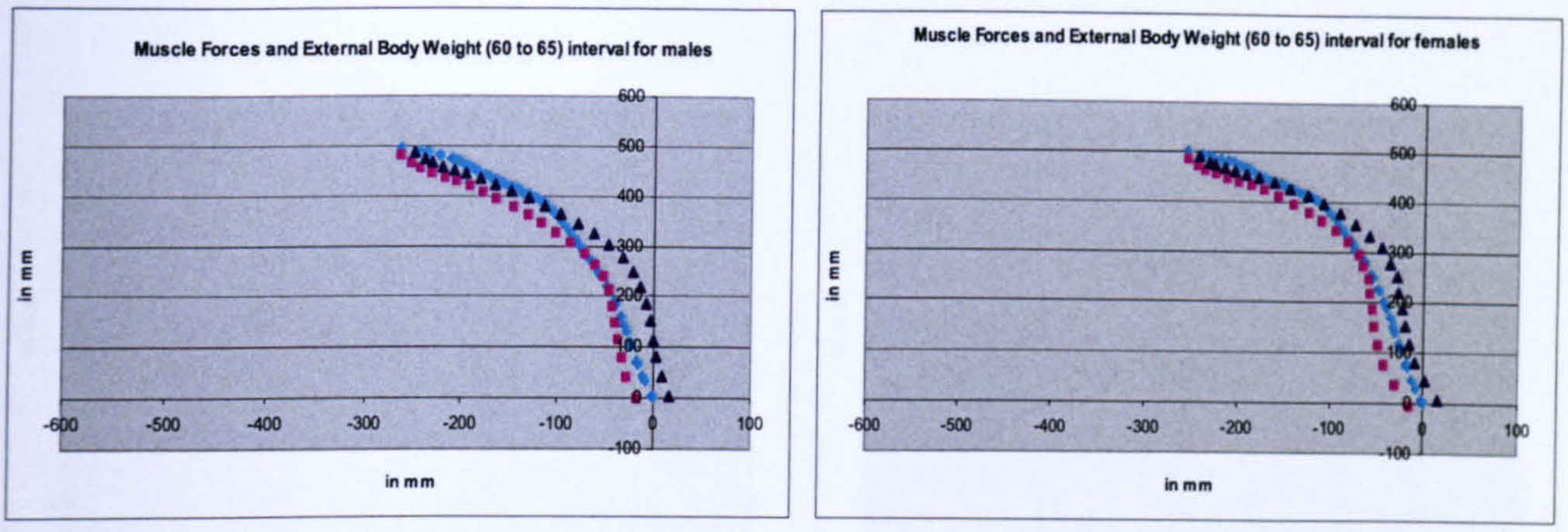


Figure 6- 36 Male and female thrustline with Body Weight and External Load of 900N (60° to 65°) interval of reference line angle.

For the interval of 60 to 65 degrees of reference line angle, there is slight instability in the cervical part. The erector spinae muscle group is activated by 30% based on Grilli (1997).

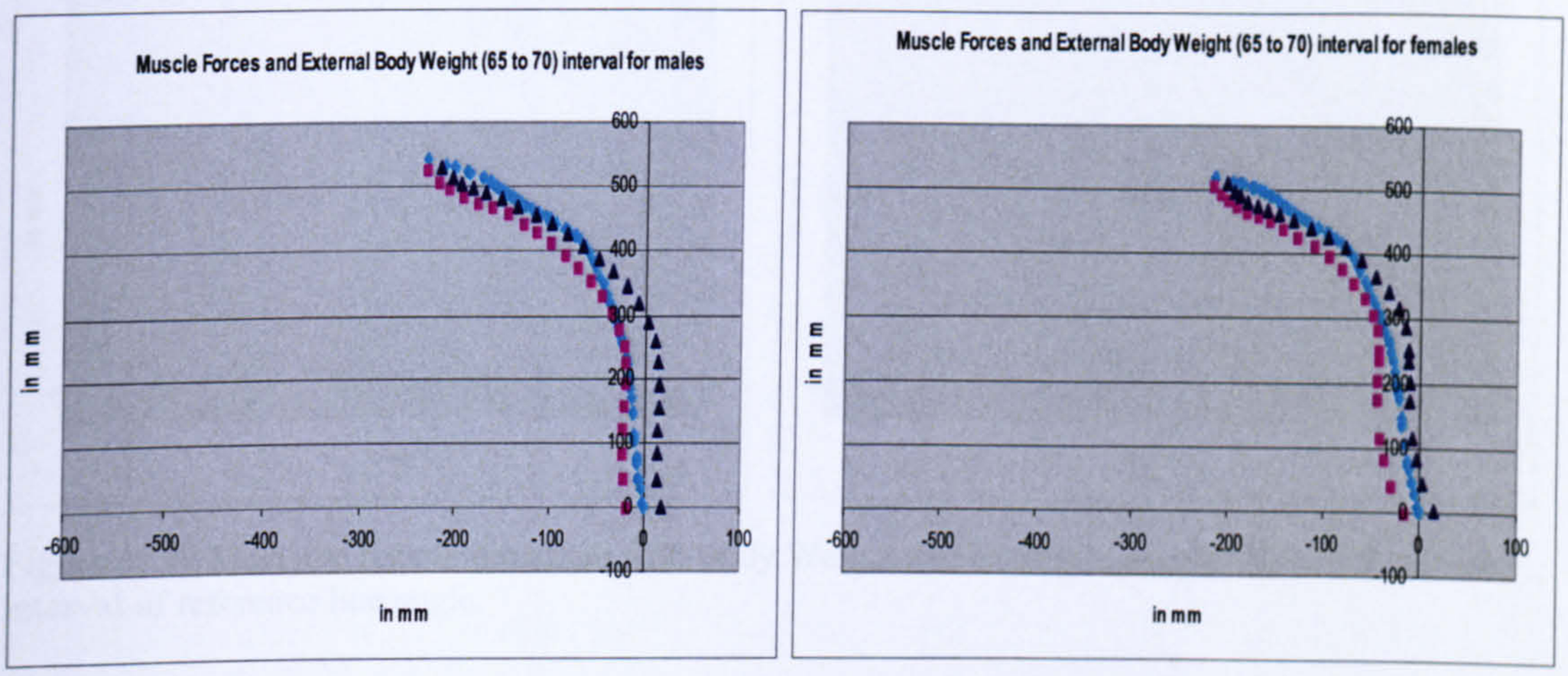


Figure 6- 37 Male and female thrustline with Body Weight and External Load of 900N (65° to 70°) interval of reference line angle.

For the interval of 65 to 70 degrees of reference line angle, the erector spine muscles are activated by 30% based on Grill (1997). The number of the muscle groups to provide spinal stability decreases. The stability in the overall spine improves. The same muscles groups are used for the interval of 70-75 degrees of reference line angle.

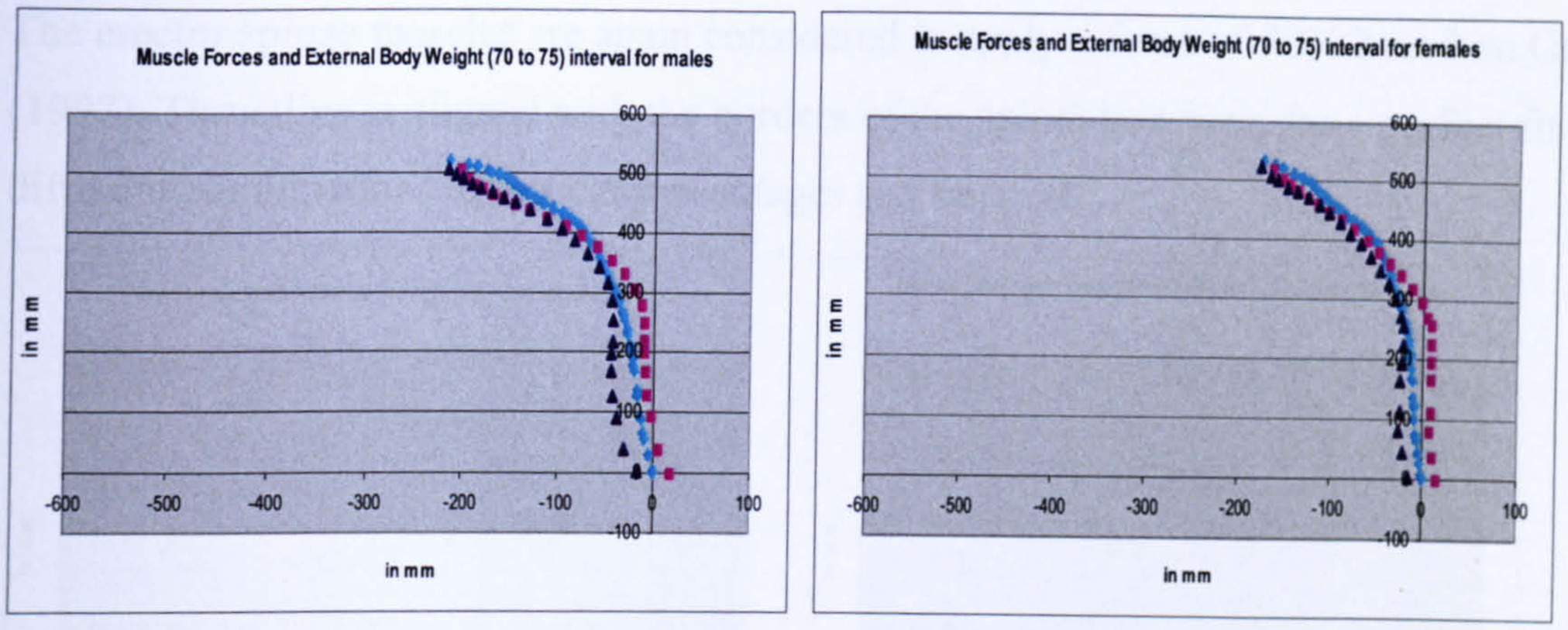


Figure 6- 38 Male and female thrustline with Body Weight and External Load of 900N (70° to 75°) interval of reference line angle.

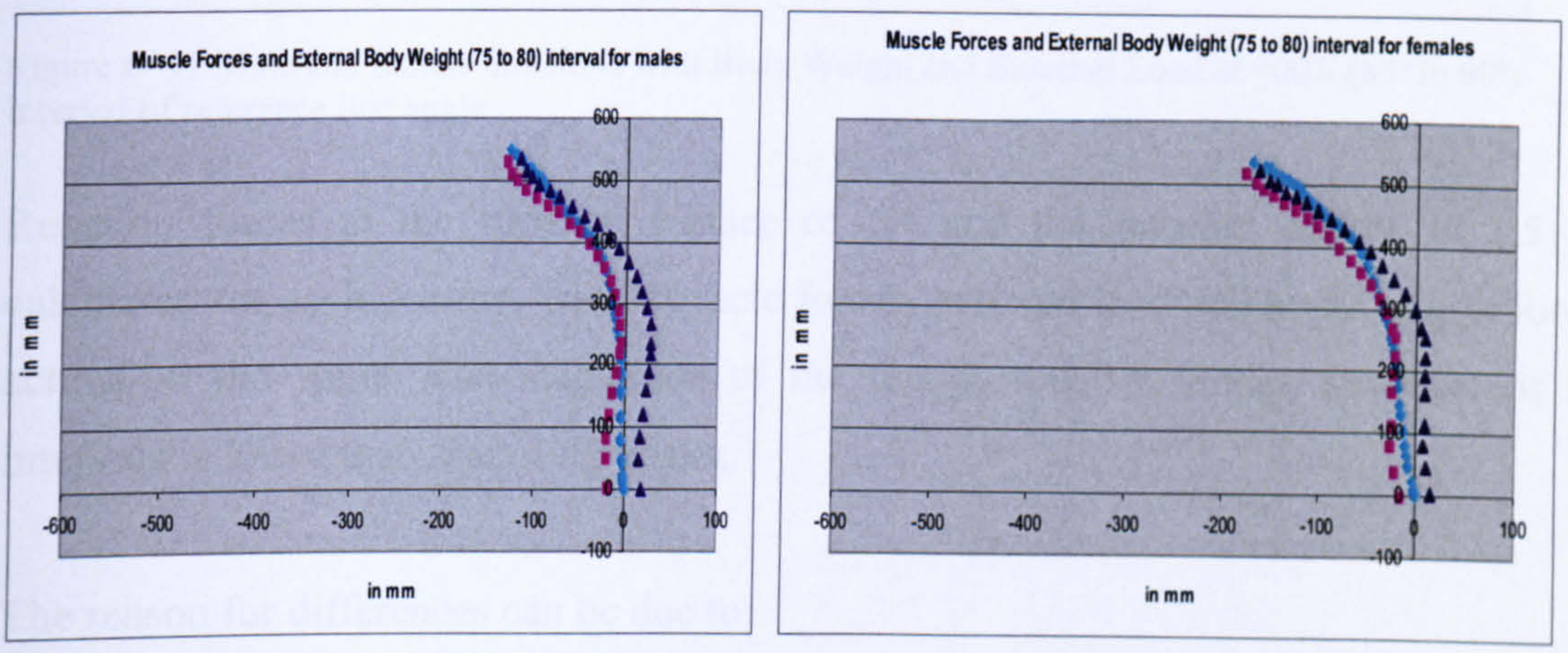


Figure 6- 39 Male and female thrustline with Body Weight and External Load of 900N (75° to 80°) interval of reference line angle.

For the interval of 75-80 degrees of reference line angle, the erector spinae muscles are applied with 30% activation based on Grilli, (1997). Thrustline curvature moves anterior to the spine borders in the mid thoracic region.

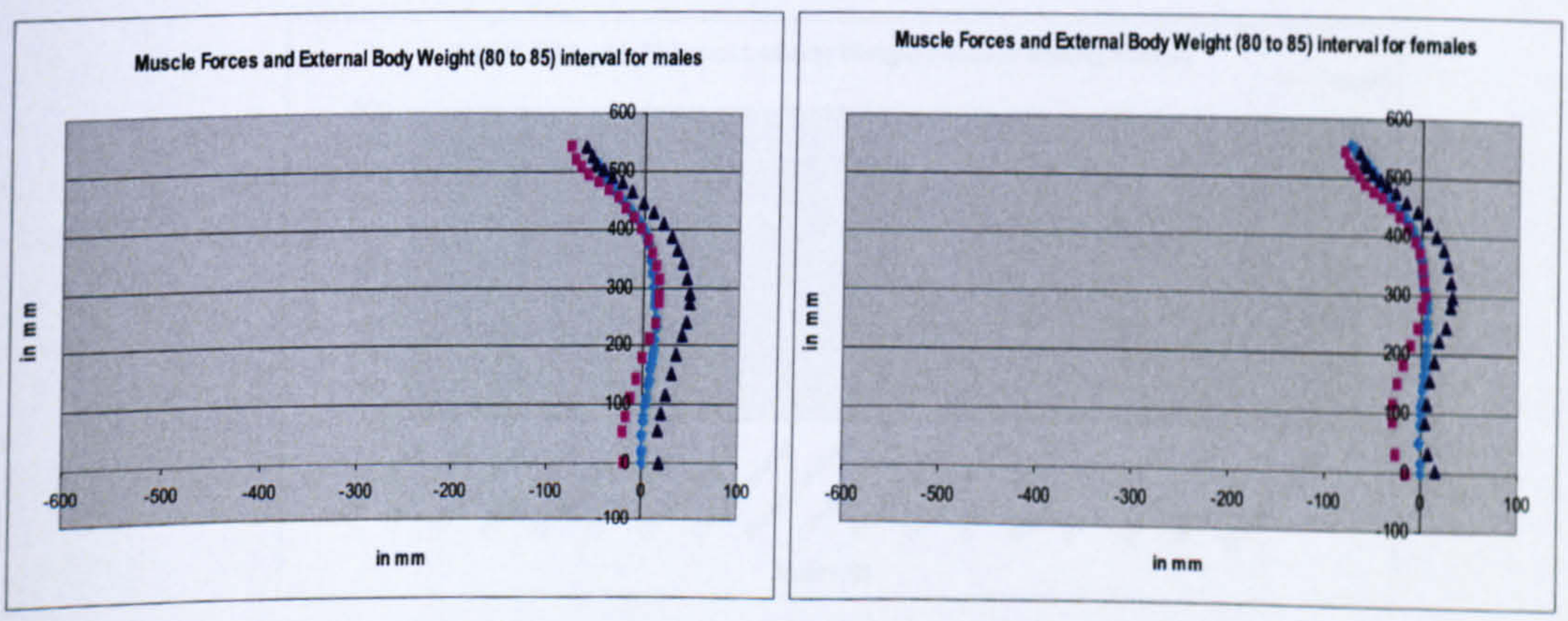


Figure 6- 40 Male and female thrustline with Body Weight and External Load of 900N (80° to 85°) interval of reference line angle.

The erector spinae muscles are again considered to apply a force of 30% based on Grilli (1997). Thrustline is aligned with the borders of the spine; however, for a perfect fit the different combinations of muscle percentages can be tried.

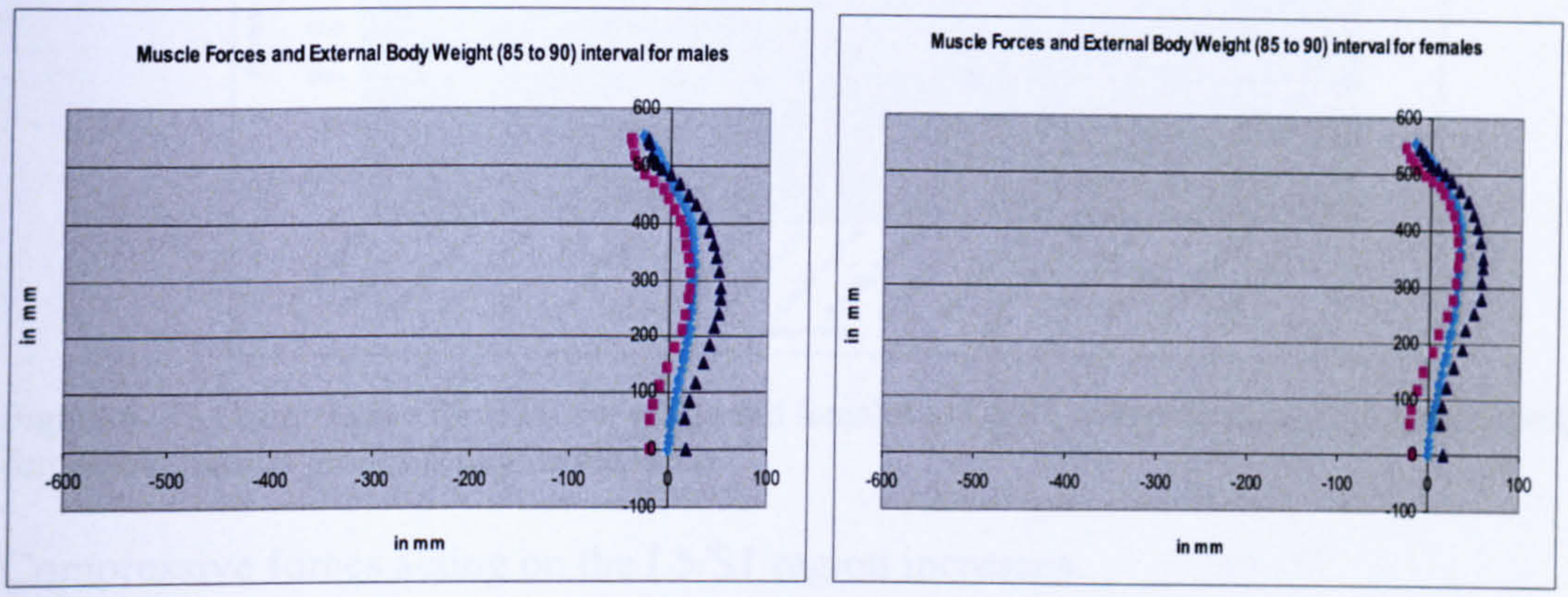


Figure 6- 41 Male and female thrustline with Body Weight and External Load of 900N (85° to 90°) interval of reference line angle.

Reaction forces at the superior surface of C1 and the inferior surface of L5 are calculated for each posture, while muscle forces, external load and body weight forces acting on the spine. The magnitude of the female reaction forces for most of the intervals is lower than that of the males.

The reason for differences can be due to:

Males and females have different postures as explained in chapter 7. Male and female vertebrae dimensions are scaled with respect to the height values. The positioning of the muscle attachments are defined with respect to the vertebrae coordinates. This might result in differences in the length of the moment arm of the muscles. The reaction force when the spine gains an erect posture decreases. This is basically the decrease of shear components of the external forces acting on the spine.

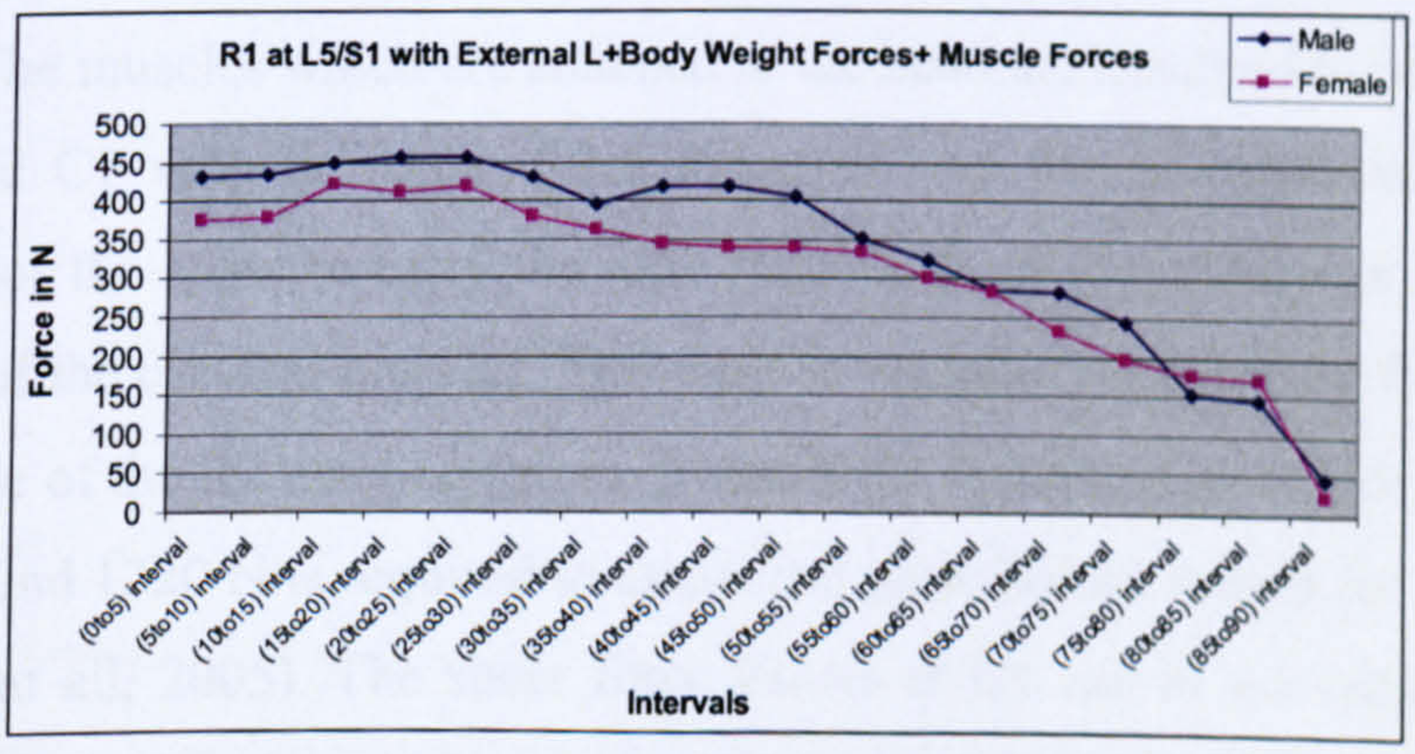


Figure 6- 42 Shear forces for males and females at L5/S1 with external loading, body weight forces and muscle groups acting on the spine.

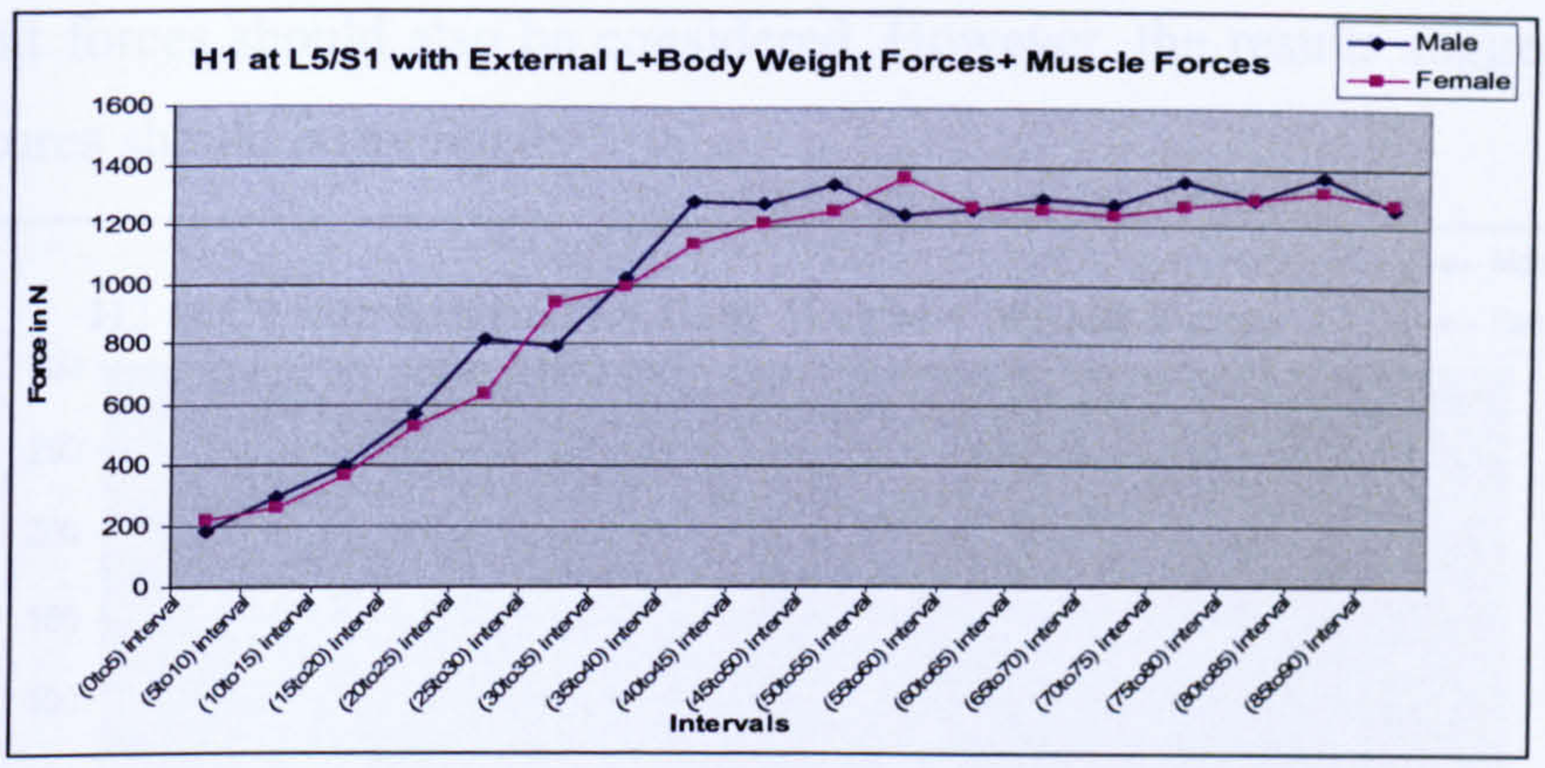


Figure 6- 43 Compressive force H1 for males and females at L5/S1 with external loading, body weight forces and muscle groups acting on the spine.

Compressive forces acting on the L5/S1 region increases.

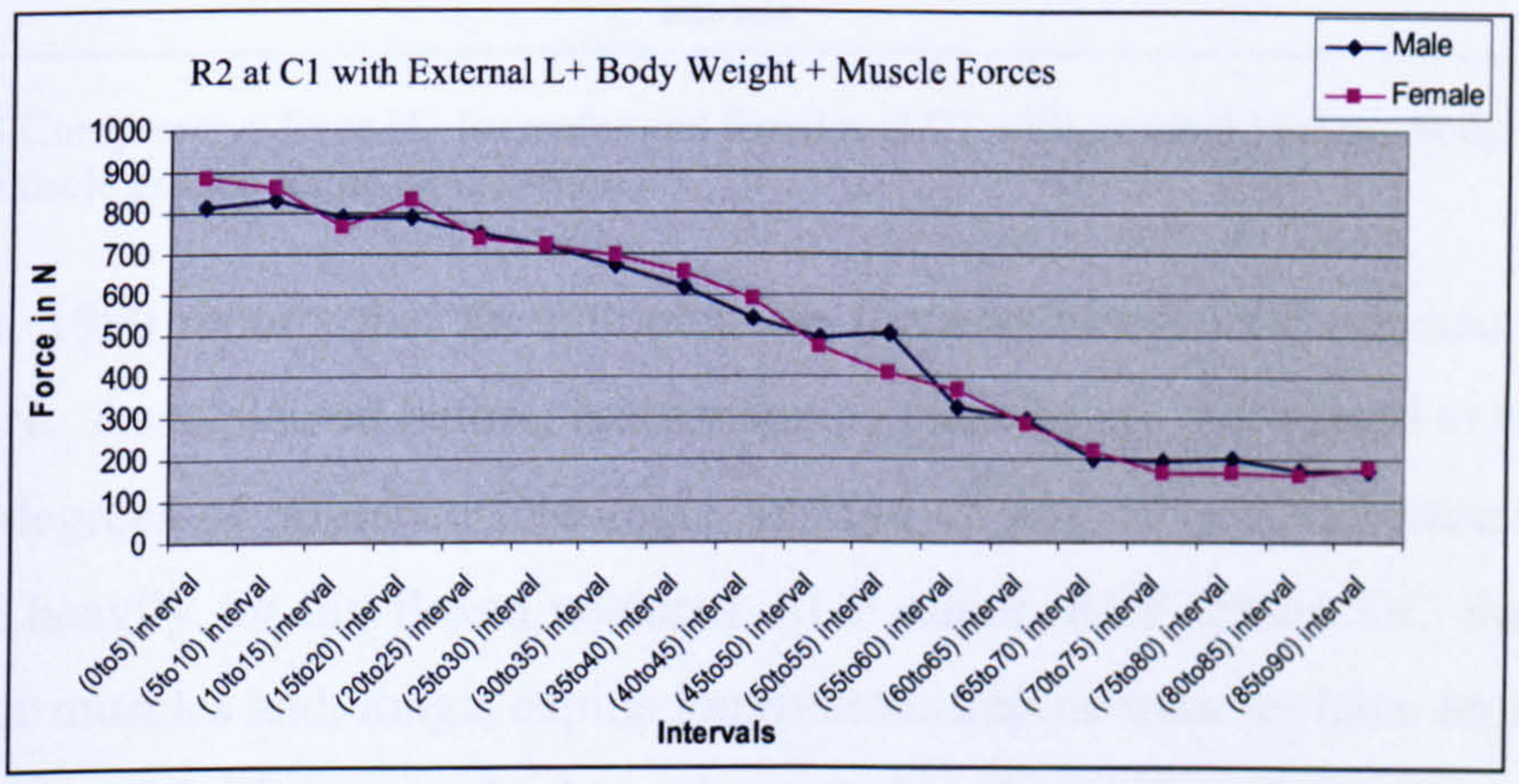


Figure 6- 44 Shear force R2 for males and females at superior surface of C1 with external loading, body weight forces and muscle groups acting on the spine.

When body weight, external load and muscle forces apply force on the spine, the magnitude of the shear force increases at superior surface of C1. Without muscles, it is only the weight of the head which can provide this shear force component as R2 reaction force which is relatively small when compared to the 900N force acting on T2, T3, and T4. The muscles which are attached to the head are assumed to act on the upper surface of the C1 with the same force direction and the moment created by them transferred. For the spine to carry the high magnitude of loads there is a need for the heavy usage of the cervical muscles. The spine is unstable for the fully flexed postures. The magnitude of the R2 reaction forces is also high. An antero-posterior shear force of between 840 and 1220 N is required to cause end plate failure values for cervical spine (Haghpanahi at all, 2005). The shear force values at C1 are in the range of cause of injury to the cervical region. Although the selection of the muscle groups has a role on the stability of the spine, thrustline theory also implies the instability. The addition of

the ligament forces should also be considered. However, the results suggest that fully flexed postures should be avoided.

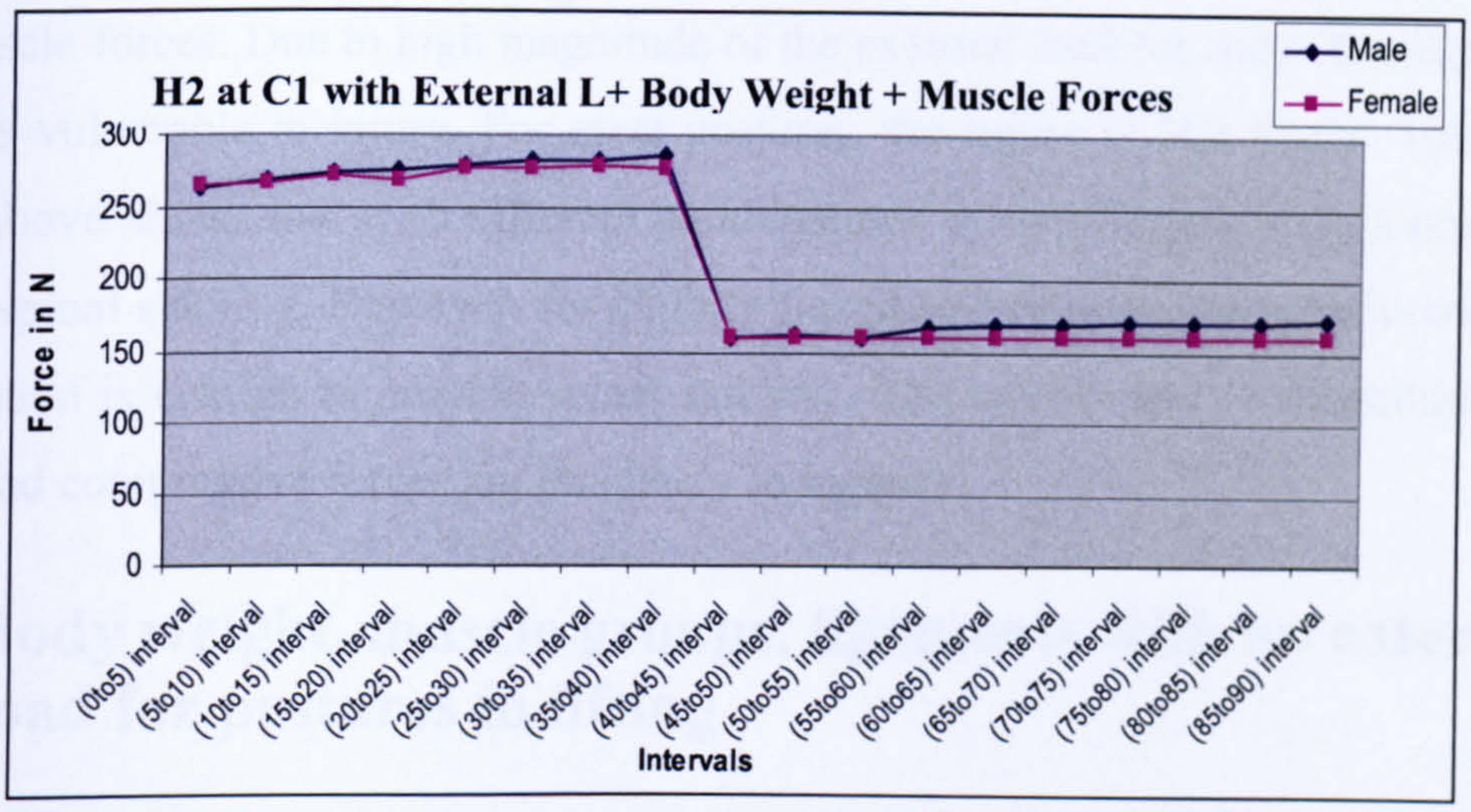


Figure 6- 45 Compressive force H2 for males and females at C1 with external loading, body weight forces and muscle groups acting on the spine.

Goel et al, 1990 reports that the compressive force values for the cervical region are 667N-445N. As explained before, erector spinae muscles are considered to be silent up to the 40 degrees of reference line angle. Instead of this suboccipital muscle muscles were used heavily for the flexed postures. RCP major, RCP minor, OC Superior and OC inferior muscles and, longis capitis longissimus capitis muscles have an attachment to C1 in the model. These muscles have the capacity of applying 178N, 98N, 188 N 246 N, 184 N, 160N force respectively. These muscle forces directly increase the compression force at superior surface of C1 when they are activated with 100%. A reduction in H2 compressive force occurs when the muscle groups which have attachment to the spine are included and the erector spinae muscles are included. The range for a possible injury due to compressive forces at cervical spine starts with 667N according to Goel et al, (1990). This shows that a compressive force failure is not expected at cervical spine. However, for more realistic solutions, percentage approach for the muscle activations can be another approach to check the stability of the spine and failure due to compressive and shear force values.

The muscle groups to check the stability of the spine have been selected depending on the role of the muscles and the table showing the effect of muscles on the thrustline from the previous section. Thrustline theory is based on the ability of the spine to transmit compressive forces. These compressive forces are the body weight forces and

the muscles which are attached to the spine. For fully flexed postures, the body weight forces, the weight of the head act as shear forces. This causes a need for the support of the muscle forces. Due to high magnitude of the external load for fully flexed postures, spine is vulnerable to injury. For erect postures, the injury is less likely. The figures listed above shows that with different combinations of muscle forces, it is possible to obtain spinal stability. However, for slightly flexed and erect postures, reduced muscle contraction is enough to provide spinal stability. The injuries due to magnitude of the shear and compressive forces are less likely to happen.

6.4 Body weight, muscle groups, ligaments with an external load for postures in lifting

In chapter 5, the ligaments to use in the model are introduced. 3 different sets of ligament stiffness functions for the cervical region were formulated. For convenience the stiffness formulas for cervical spine are named as the Yoganandan et al, 2000 data as Group1, Yoganandan et al, 1998 data as Group2, Yoganandan et at, 2001 data as Group 2 cervical ligaments. Ligament force is calculated by subtracting the length of the ligament of the posture under investigation from the length of the ligament of the erect posture. The ligament force values are calculated for each interval. Not much difference is observed between the magnitudes of the force provided by the 3 sets of the ligament groups. For this reason for the cervical ligaments the latest data by Yoganandan et al, 2001 is used in the model. The effect of ligaments on thrustline is inspected and similar table is produced with the muscles. For Lumbar ligaments, only one set of experiment function for PLL, ALL and LF force is used. The magnitudes of force values produced by these ligaments are calculated and provided in Appendix6.

The linear approach where ligament force is calculated by using the direct relation between the failure strain and failure force is observed to apply high loads on spine. For this purpose, a force strain curve for the cervical spine is decided to be for the simulations.

The cervical ligament force data sets were compared with the magnitude of force values at failure by data set of Myklebust et al, (1988). The force produced by the cervical and lumbar ligaments is less than the magnitude of the force which is necessary for them to

fail. Ligaments have very close connection points. This results in reduced effect in their moment creating capability. The reaction forces at superior surface of C1 and the inferior surface of L5 are inspected with the body weight and the ligament forces acting on the spine. The effect of ligament forces on reaction forces is nearly negligible. The path of thrustline is determined by the forces acting on the spine, although the magnitude of the reaction forces is not affected much by the ligament groups, the path of the thrustline is affected.

In order to investigate the effect of ligaments combined with the muscle groups, same muscle groups which were active in the previous section were used with the ligament groups. Unlike muscles, ligaments produce force when they are stretched. For this purpose when spine is concave anteriorly, the posterior part of the spine is stretched and the anterior portion of the spine is compressed. For this purpose for the regions where spine has a convex cervical or lumbar part the posterior longitudinal ligaments are considered to be active.

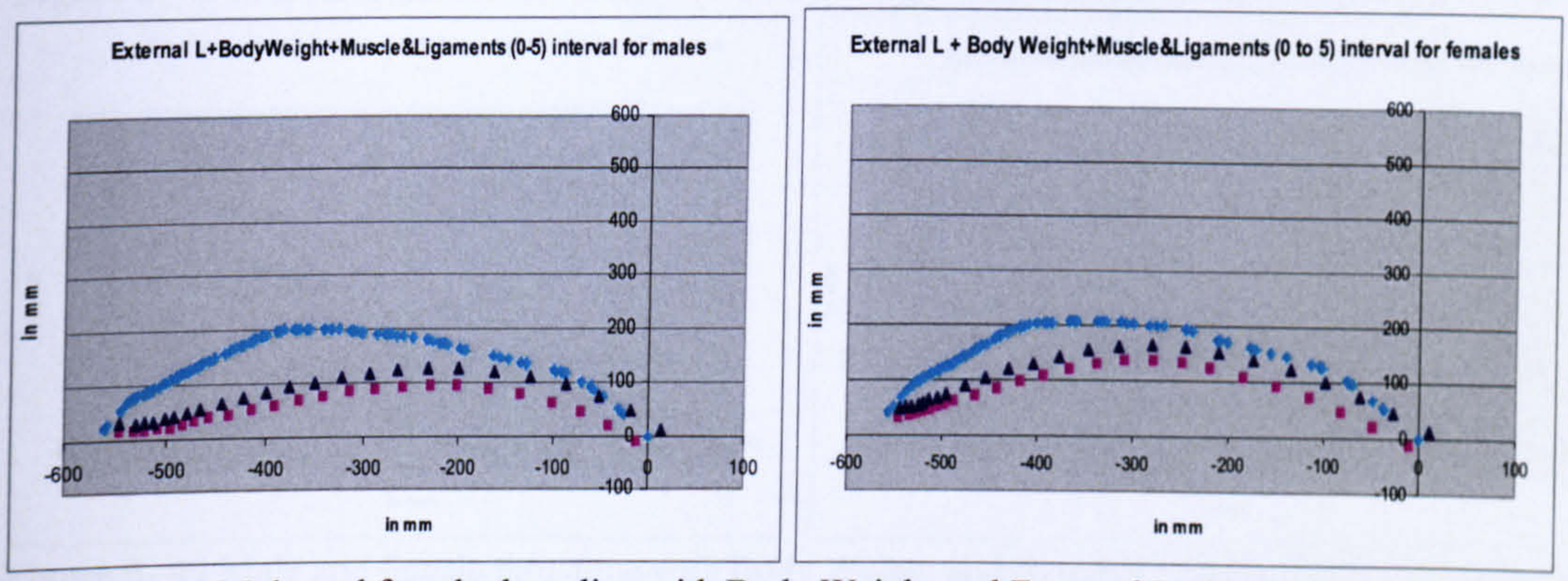


Figure 6- 46 Male and female thrustline with Body Weight and External Load of 900N (0° to 5°)

For the interval of 0 to 5 degrees of reference line angle, the spine is observed to have a fully convex curvature. For this purpose, the posterior longitudinal ligaments are considered to be active. With the addition of the PLL, LF forces at lumbar and cervical spine, the stability of the spine is improved. However, due to large moment arm and the magnitude of the external force applied, instability of the spine persists. The similar case is observed for the interval of 5-10, 10-15, and 15-20 degrees of reference line angle.

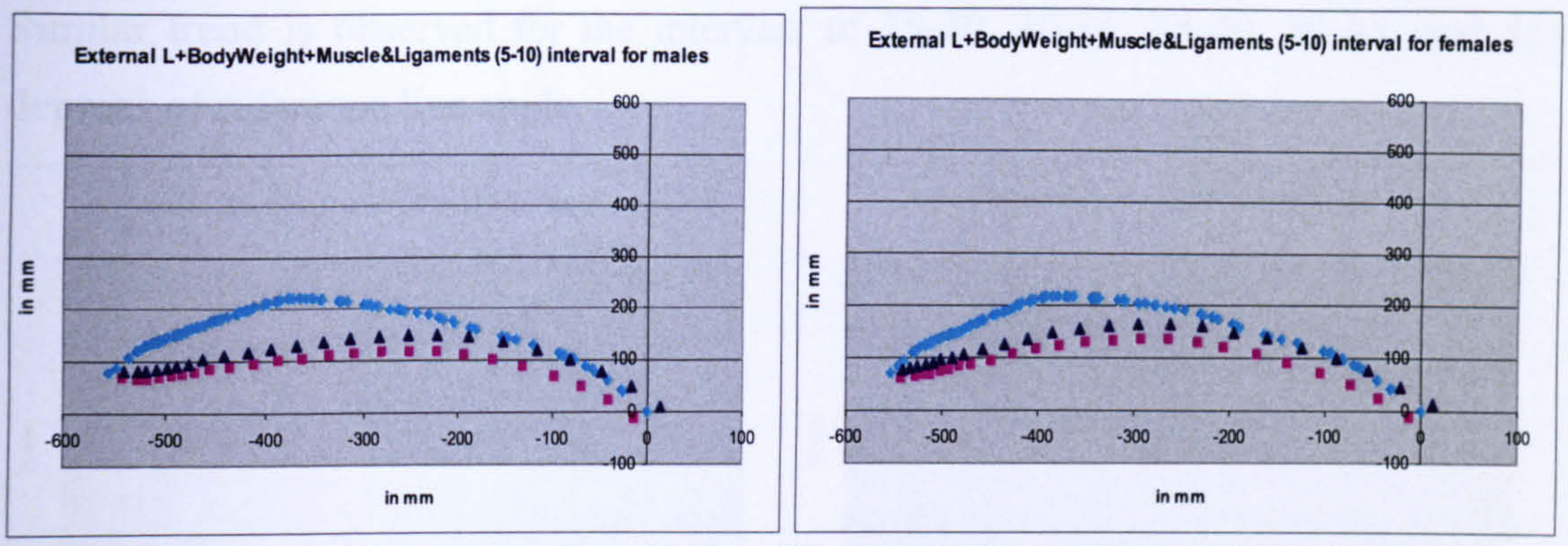


Figure 6- 47 Male and female thrustline with Body Weight and External Load of 900N (5º to 10º)

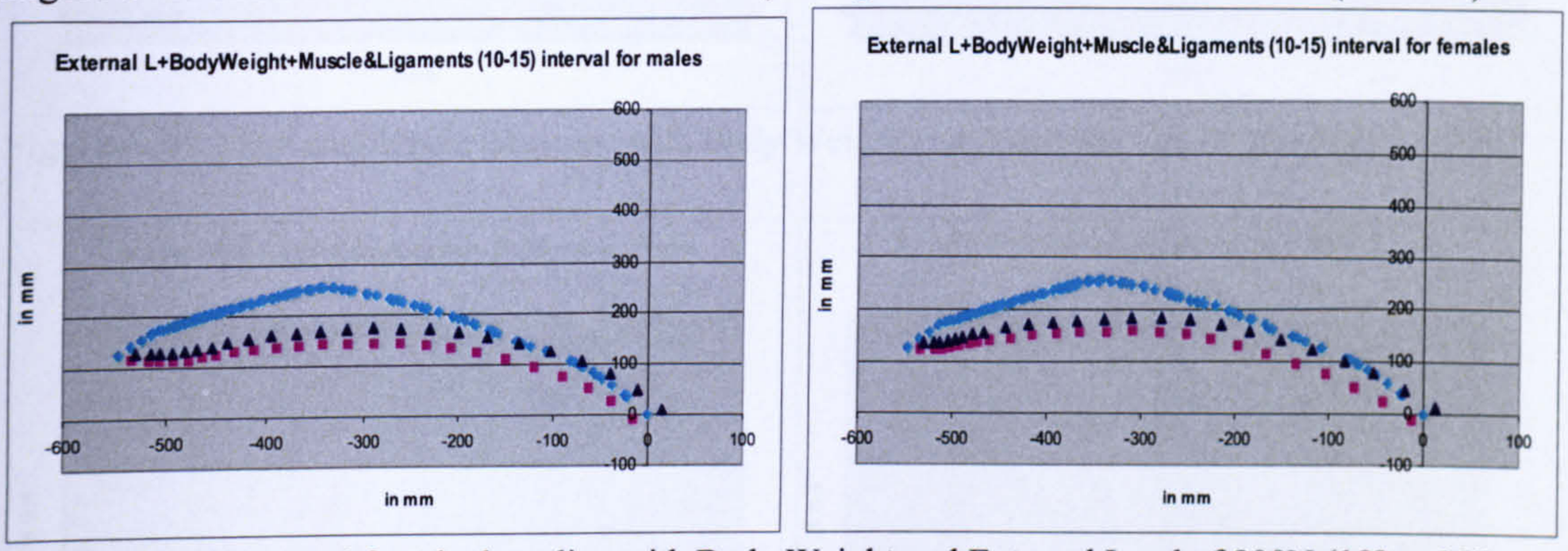


Figure 6- 48 Male and female thrustline with Body Weight and External Load of 900N (10º to 15º)

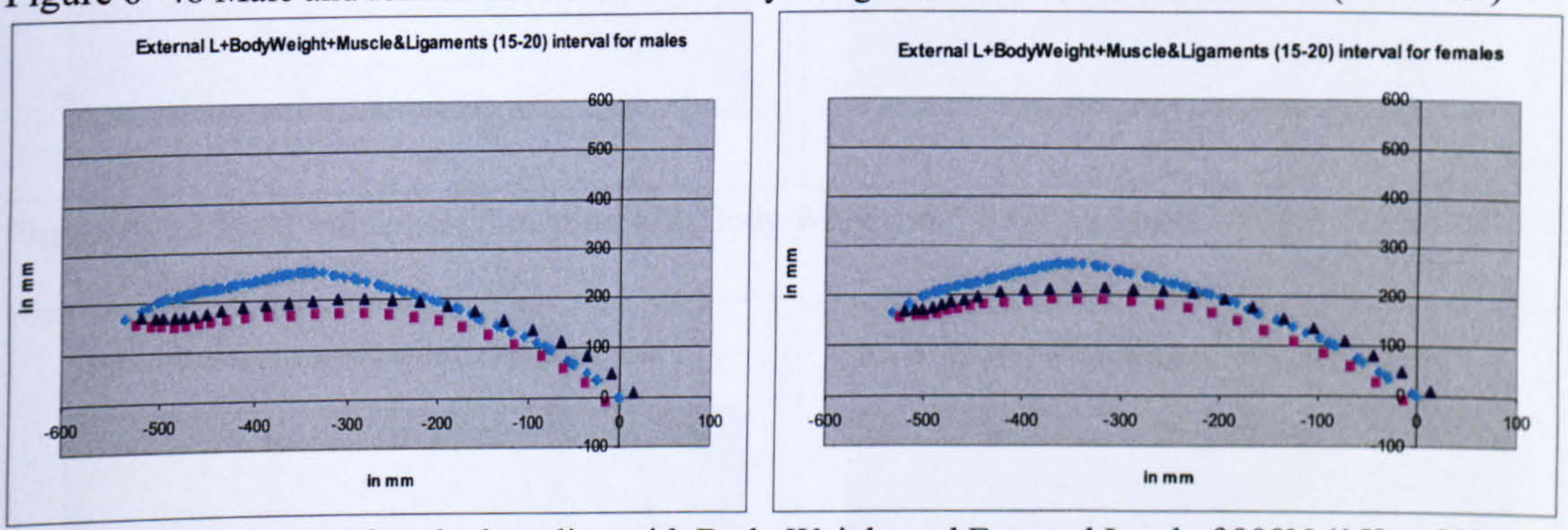


Figure 6- 49 Male and female thrustline with Body Weight and External Load of 900N (15º to 20º)

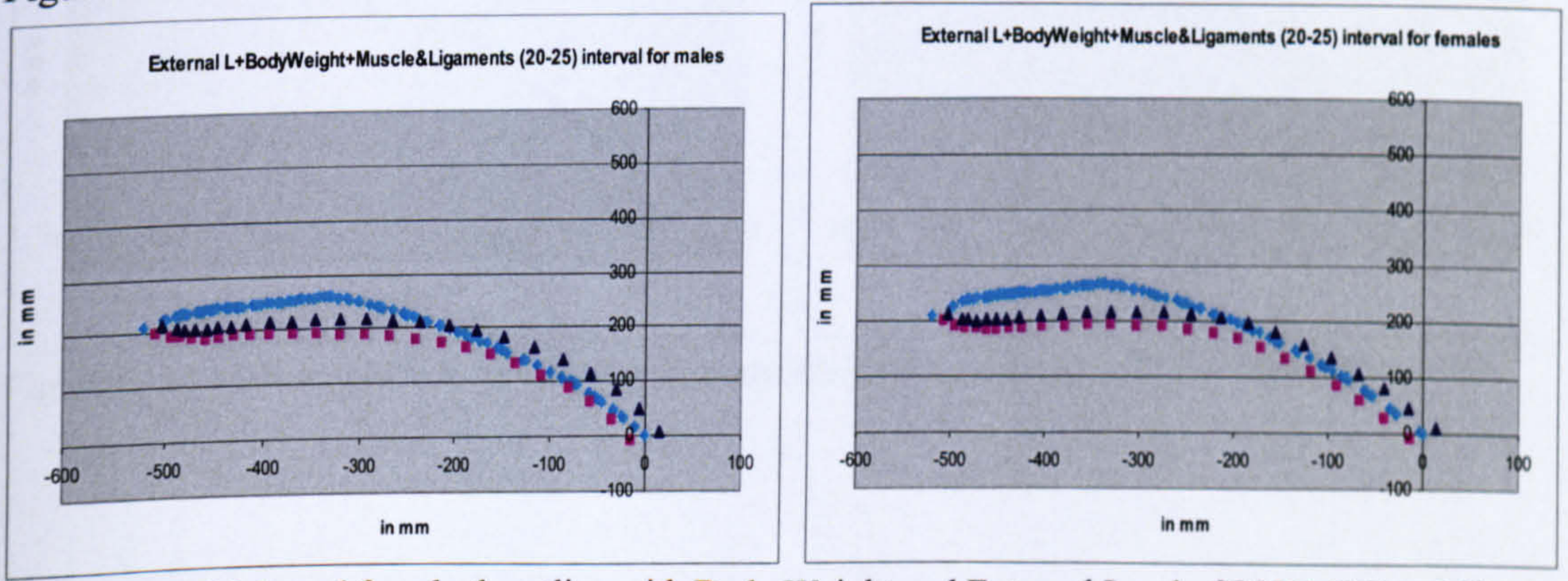


Figure 6- 50 Male and female thrustline with Body Weight and External Load of 900N (20º to 25º)

For the interval of 20-25 degrees of reference line angle, the cervical spine is observed to gain a concave curvature, for this purpose, ALL is assumed to be active. The stability of the spine is observed to be improved when compared to the previous sections.

Similar trend is observed for the intervals of 25-30, 30-35, 35-40, 40-45, and 45-50 degrees of reference line angle.

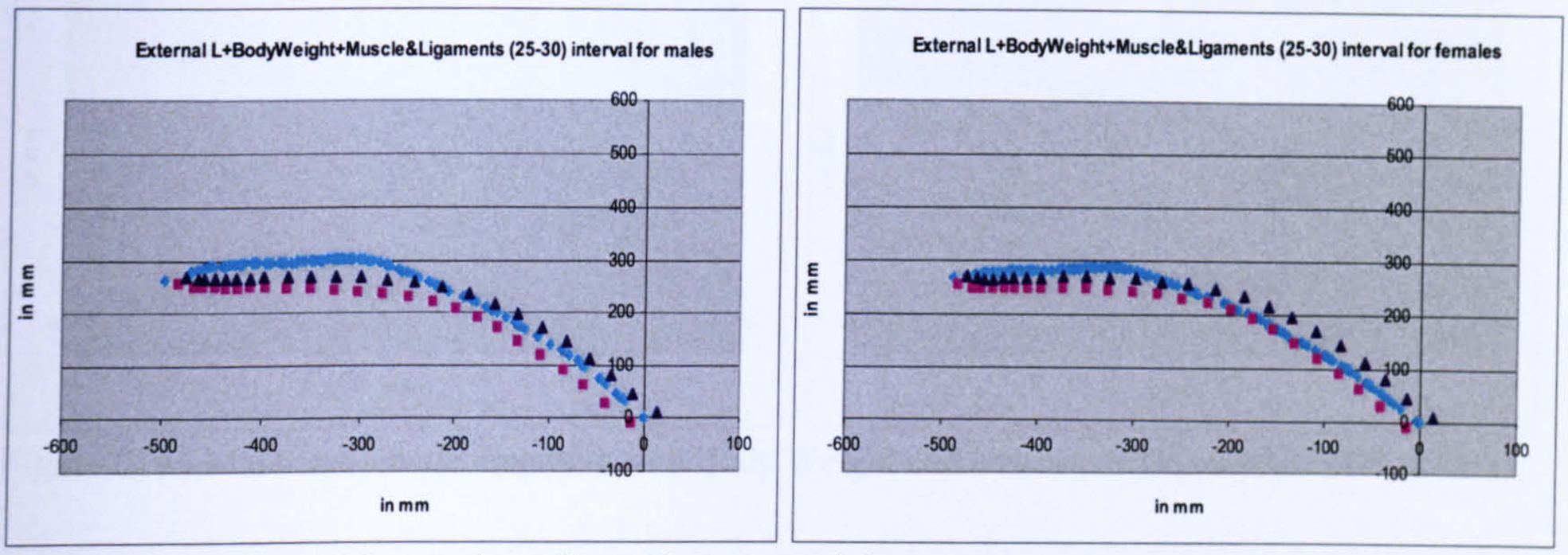


Figure 6- 51 Male and female thrustline with Body Weight and External Load of 900N (25° to 30°)

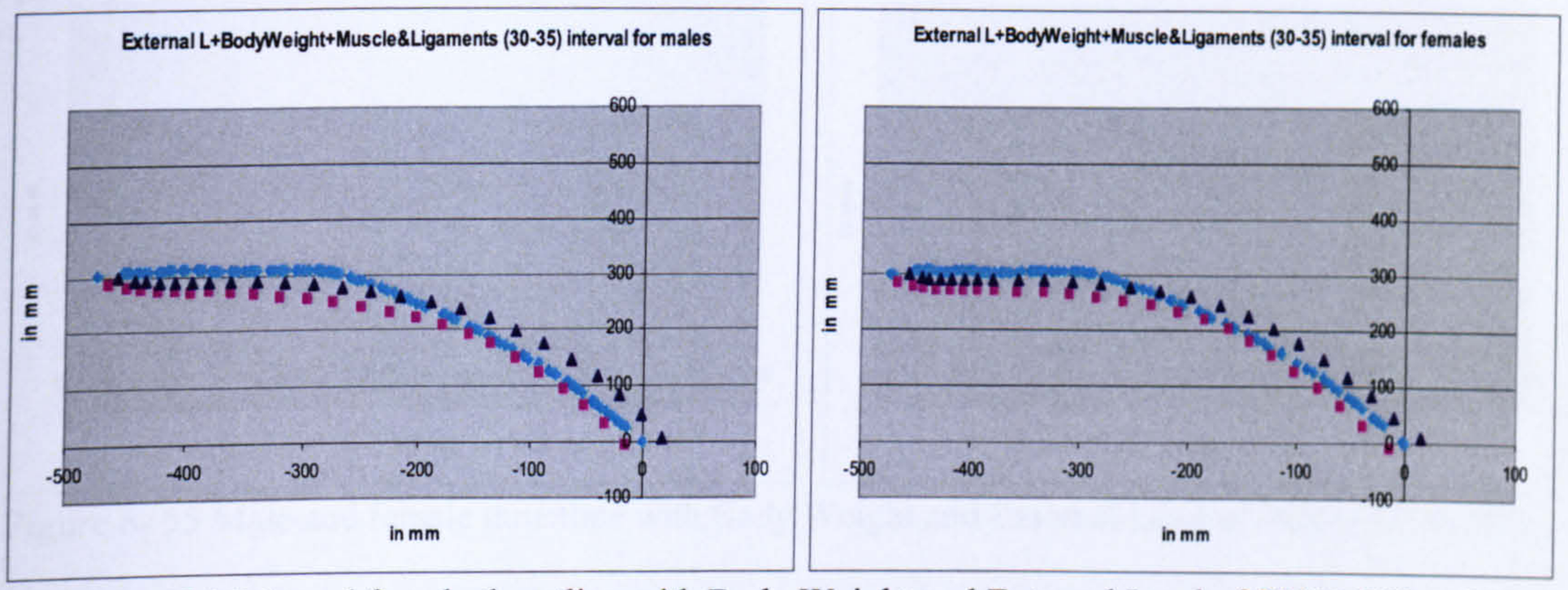


Figure 6- 52 Male and female thrustline with Body Weight and External Load of 900N (30° to 35°)

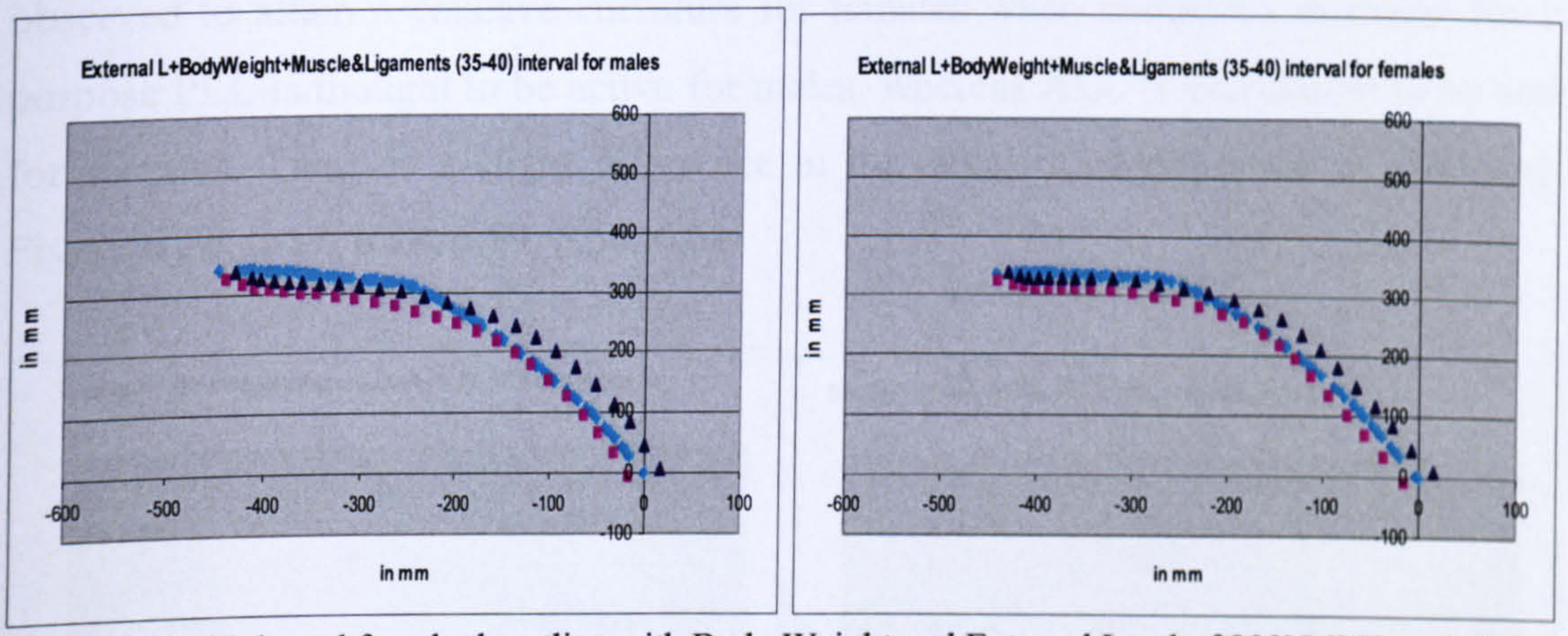


Figure 6- 53 Male and female thrustline with Body Weight and External Load of 900N (35° to 40°)

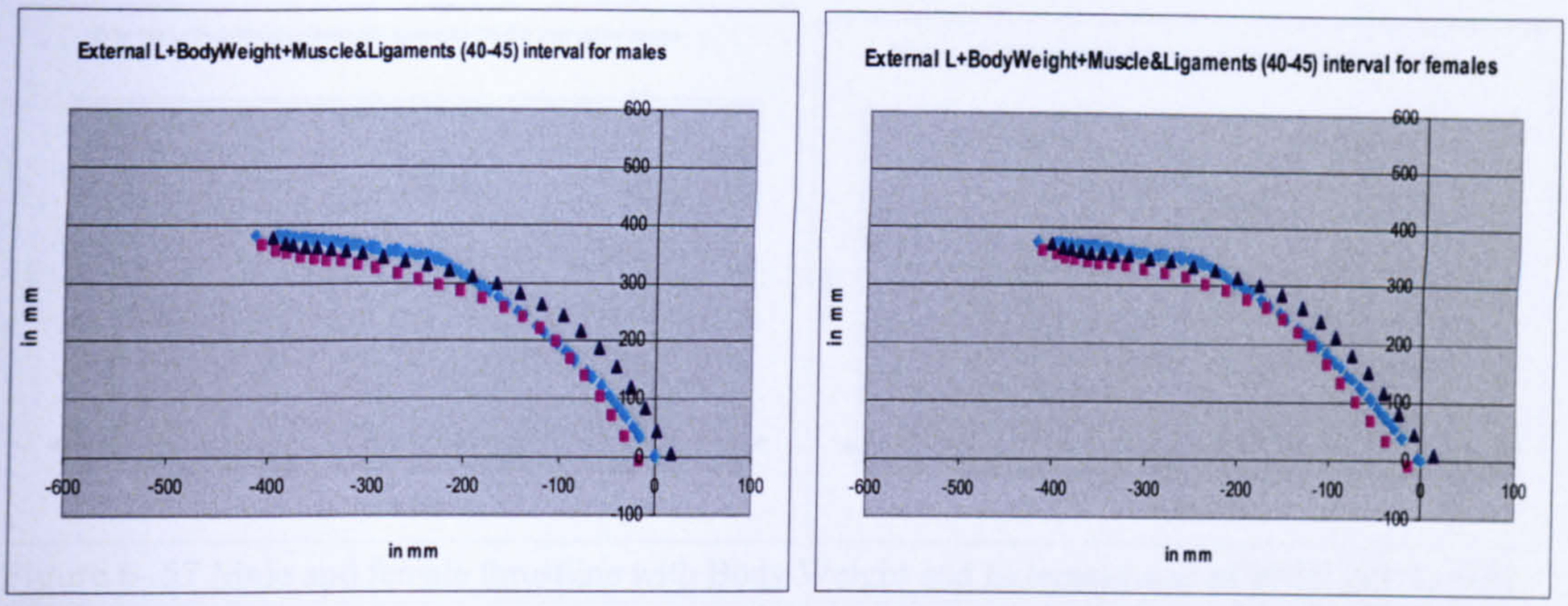


Figure 6- 54 Male and female thrustline with Body Weight and External Load of 900N (40° to 45°)

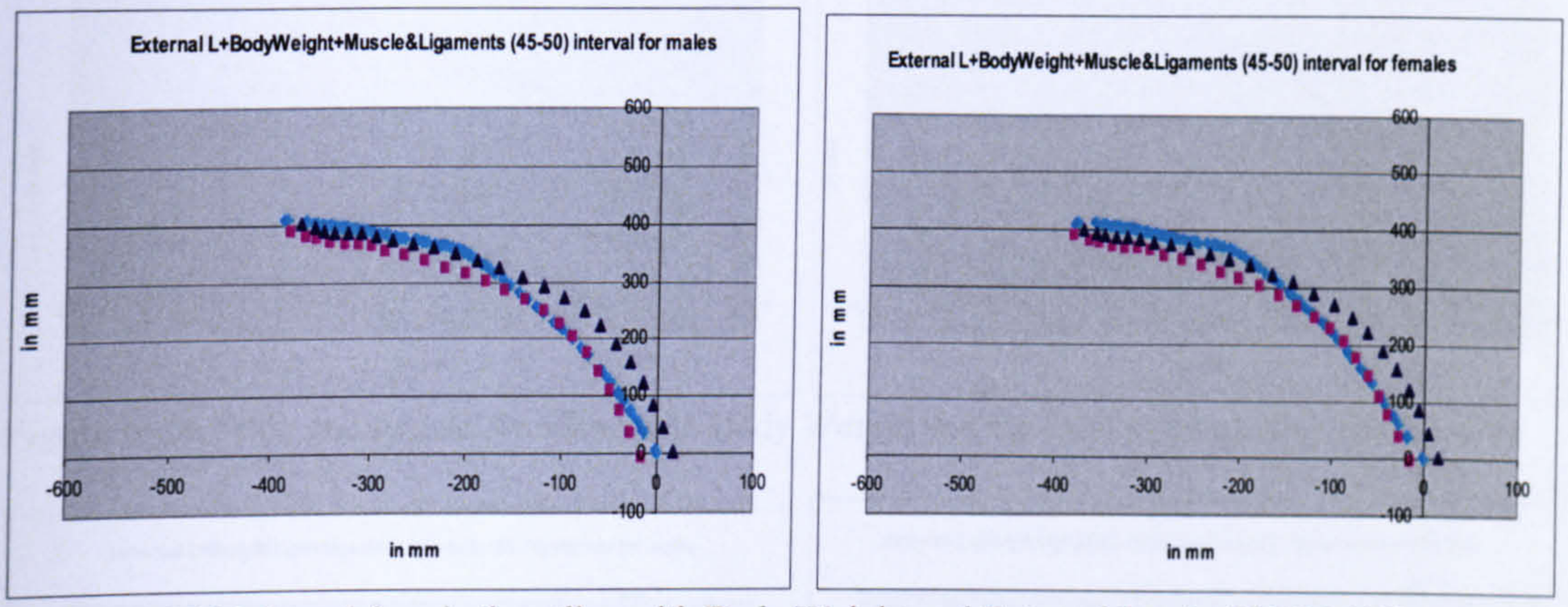


Figure 6- 55 Male and female thrustline with Body Weight and External Load of 900N (45° to 50°)

Starting from the interval of 50-55 degrees of reference line angle, the lumbar region is observed to attain a concave curvature for females when compared to males for this purpose PLL is thought to be active for males, whereas ALL is considered to be active for females. There is a slight difference in the stability of the spine as observed in Figure 6.56, 6.57, 6.58, 6.59, 6.60, 6.61.

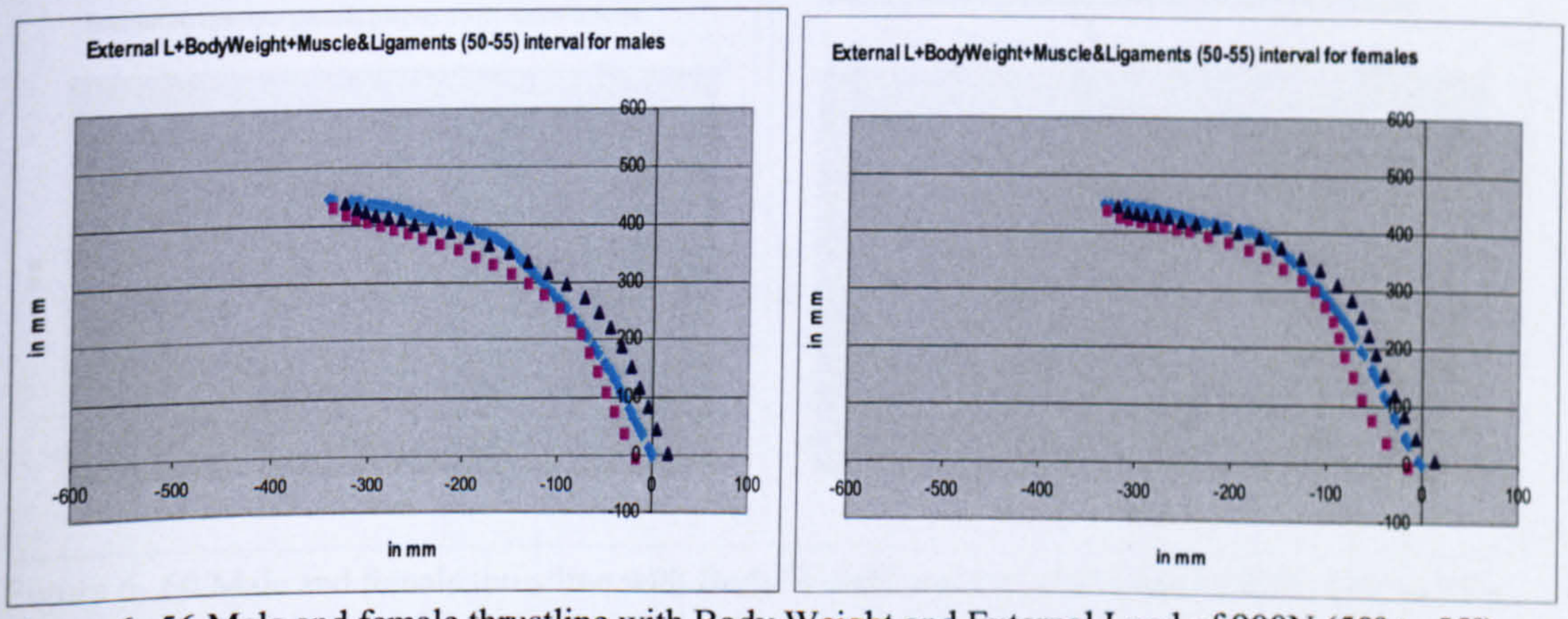


Figure 6- 56 Male and female thrustline with Body Weight and External Load of 900N (50° to 55°)

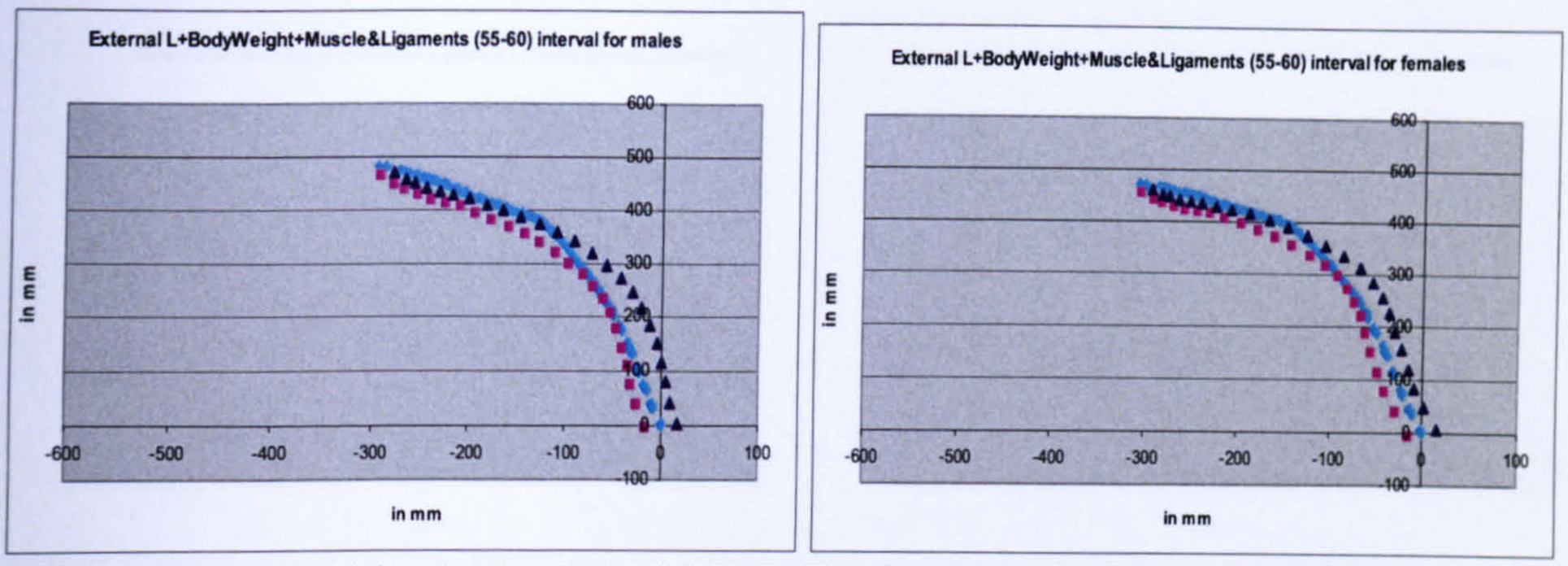


Figure 6- 57 Male and female thrustline with Body Weight and External Load of 900N (55° to 60°)

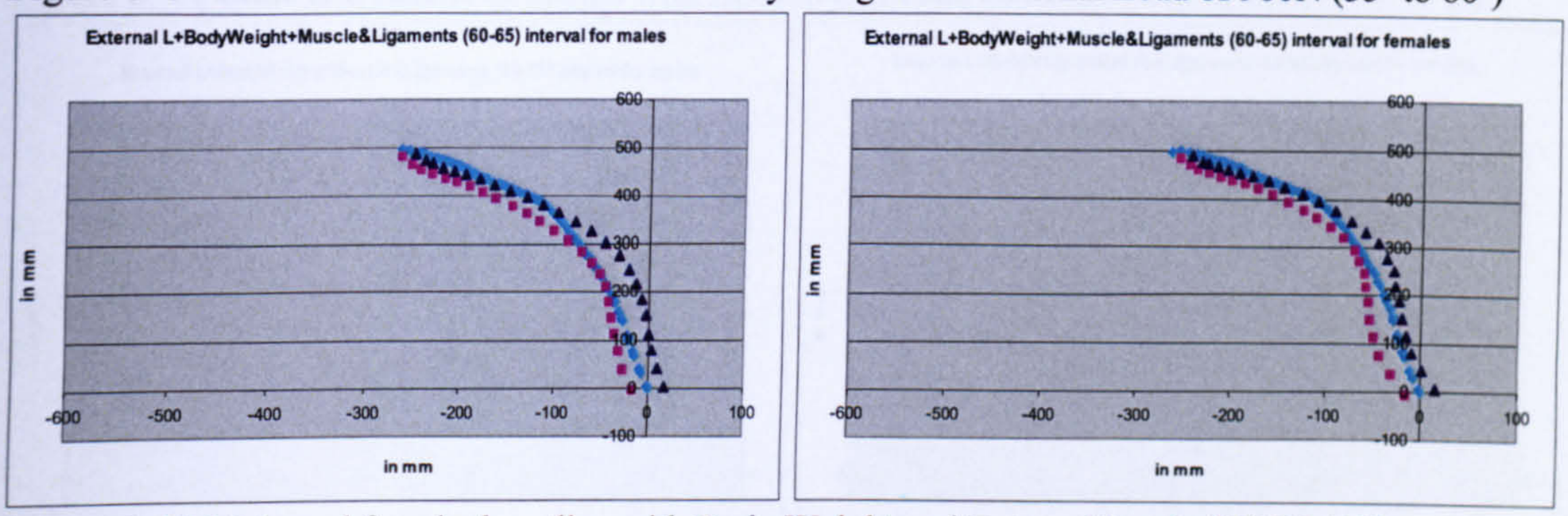


Figure 6- 58 Male and female thrustline with Body Weight and External Load of 900N (60° to 65°)

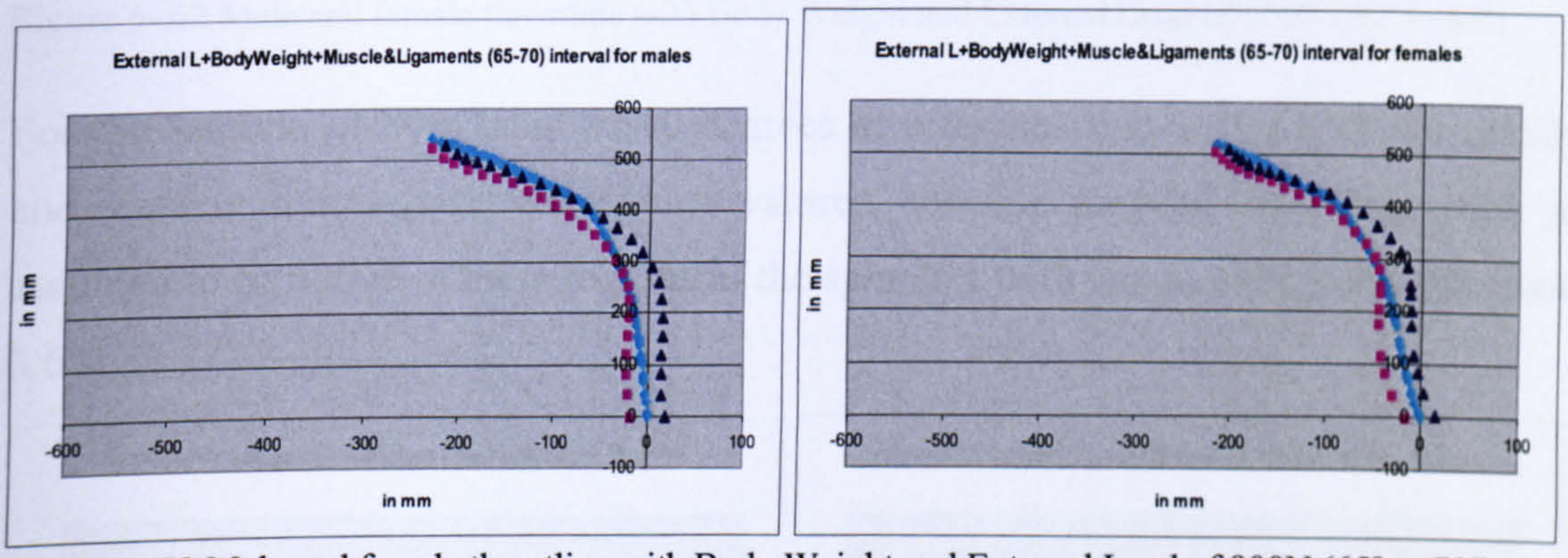


Figure 6- 59 Male and female thrustline with Body Weight and External Load of 900N (65° to 70°)

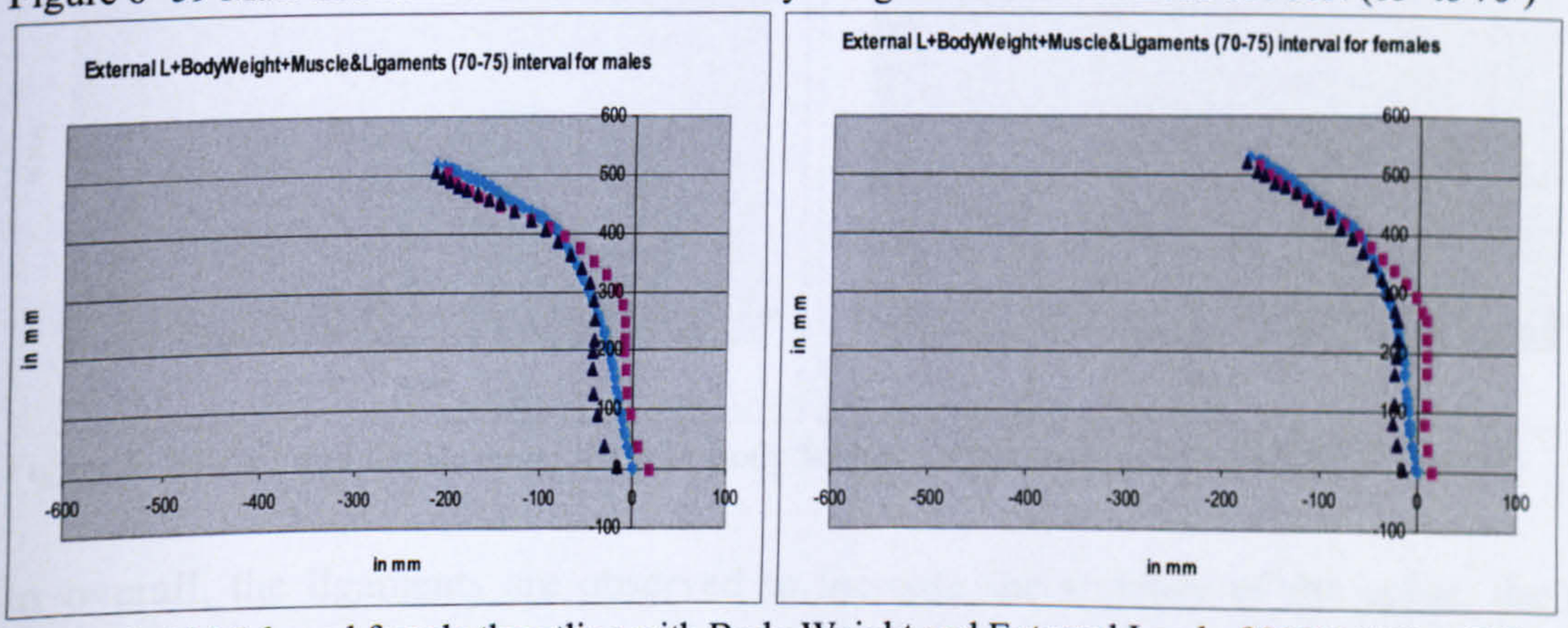


Figure 6- 60 Male and female thrustline with Body Weight and External Load of 900N (70° to 75°)

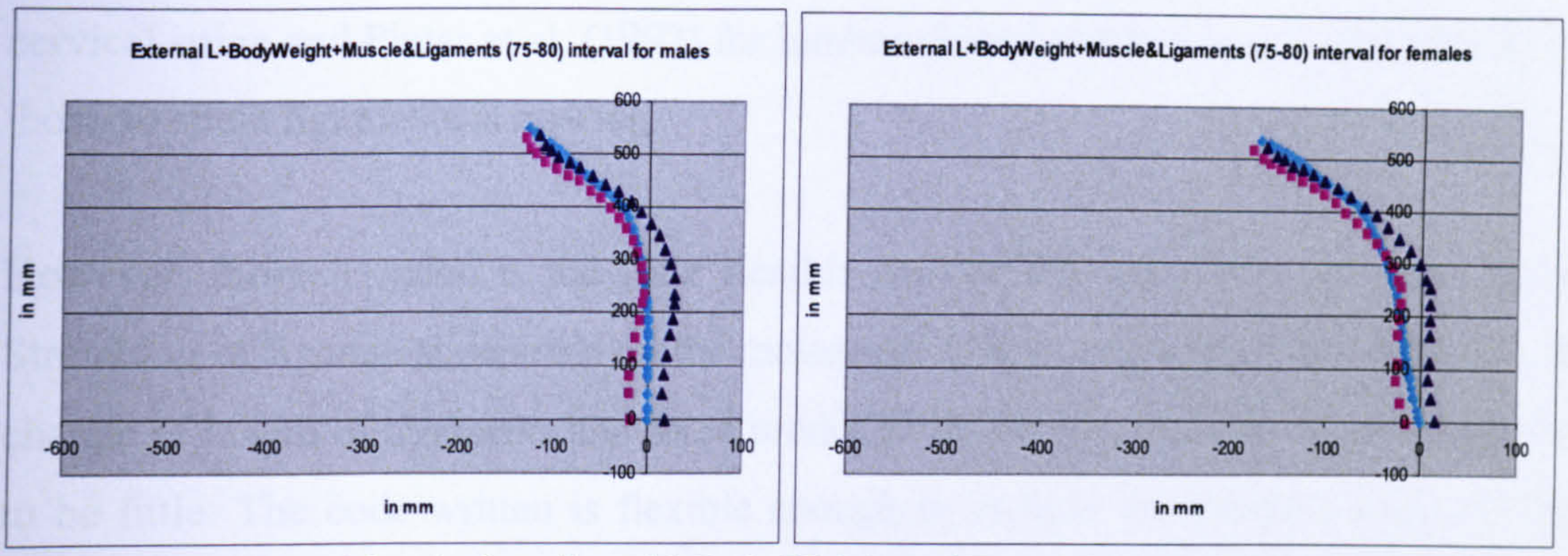


Figure 6- 61 Male and female thrustline with Body Weight and External Load of 900N (75° to 80°)

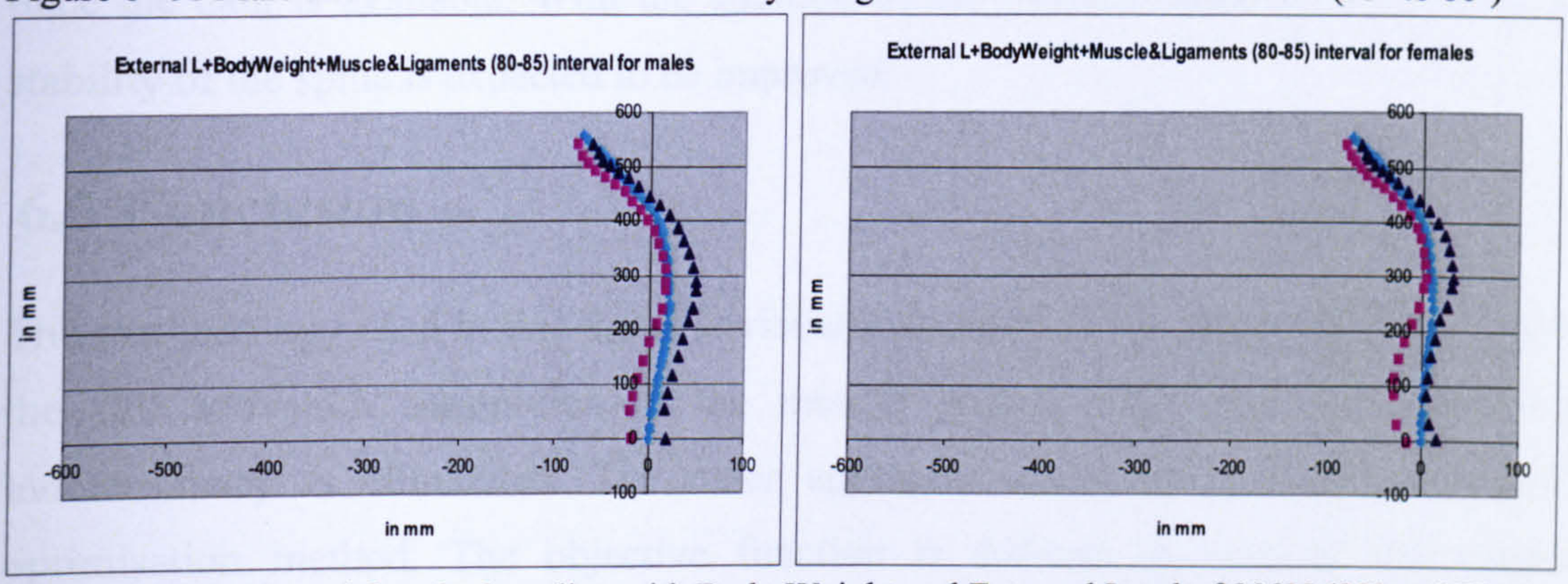


Figure 6- 62 Male and female thrustline with Body Weight and External Load of 900N (80° to 85°)

For the interval of 80-85 and 85-90 degrees of reference line angles both the cervical and lumbar spines have concave curvatures, for this purpose ALL ligaments are assumed to be active in these regions of the spine for both genders (Figure 6.62, Figure 6.63)

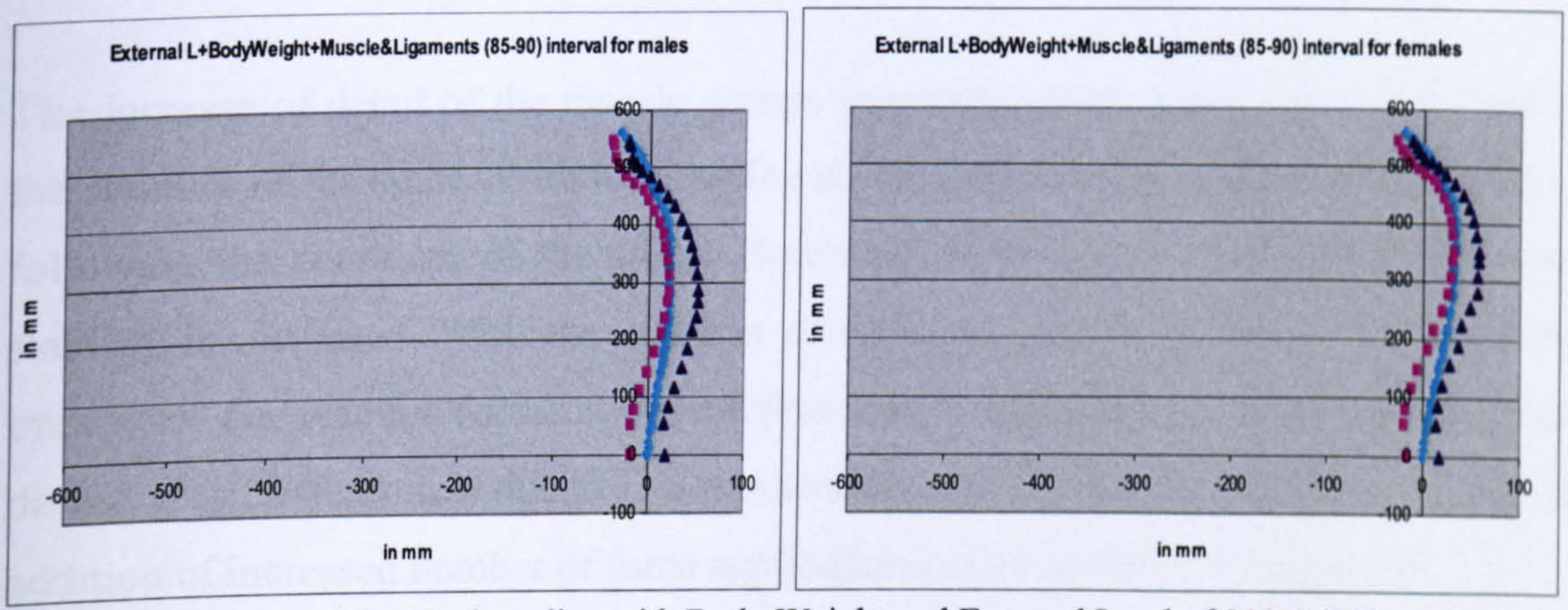


Figure 6- 63Male and female thrustline with Body Weight and External Load of 900N (85° to 90°)

In overall, the ligaments are observed to increase the stability of the spine, the fine tunings with the muscle forces still needs to be improved with the percentage approach. In this model, the stiffness formulas obtained from the Yoganandan et al, (2001) for

cervical spine and Pintar et al, (1992) for lumbar spine have been used. The data on the thoracic spine ligaments is missing.

However, thoracic spine is the least flexible part of the spine with the least ROM. Stretching of ligaments depends on the movement of the vertebrae. For this reason, the change of length of ligaments and force produced by them in thoracic spine is expected to be little. The code written is flexible enough to include the thoracic ligament data once the data is available. With the addition of the thoracic spine ligament data, the stability of the spine is expected to be improved.

6.5 Conclusion

The methodology used in this thesis is visual inspection of the muscle forces based on the full activation assumption of the muscle groups. This way the problem of indeterminacy is eliminated. The other approach would be to implementing the optimisation method. The objective function is defined as keeping the distance minimum between the boundaries of the spine and defining the constraint functions as the physiological limits of the muscle and ligament forces. One of the basic problems for this method would be the results of the optimisation would not reflect the real condition while the experimental subjects lift the object. For this reason, visual inspection method is used.

The increase of detail of the muscle groups improves analysis conducted for checking the stability of the spine. Without muscle groups, thrustline curvature is not capable of following the curvature of the spine. However, when the muscles support the spine stability is increased. With the addition of ligament groups, stability of the spine is improved. The reaction forces at the end points after the addition of the ligament groups do not get affected much due to low moment arm of the ligaments. However, with the addition of increased number of force application points, stability is improved.

CHAPTER 7

7 Evaluation of the Model and Conceptual Designs

The model is compared with the Single Equivalent Muscle Model (SEM). Distributed body weight loading approach is compared with the point force loading where the body weight is applied at only two levels of T2, and T12 for males and females to compare the biofidelity of the distributed body weight approach. Intervertebral joint reaction forces are calculated for the19 intervals of reference line angle. Model structure is explained. Compatibility of the results with the other studies in literature is evaluated. The conceptual design ideas are suggested to improve the stability of the spine.

7.1 Single Equivalent Muscle Model

The common assumption about the lever model is that bending moments produced by lifting a weight in front of the body are directly balanced by a moment generated by the erector spinae muscles. The sum of the forward bending moments produced by the weight of the trunk, plus any extra load being carried is equal to the erector spinae muscle tension multiplied by the perpendicular distance of this muscle from the pivot.
For the single equivalent muscle model (SEM), the perpendicular distance of the muscles from the pivot point which is the centre of inferior surface of L5 in our case, is 5 cm. For this purpose, moment imposed on the lower end plate of the L5 is calculated for the body weight for both genders. The results show that not much difference is observed between males and females. However, males are observed to be imposed on larger moments when compared to females. The magnitude of the moment imposed on spine by the body weight forces is directly related to the magnitude of the body weight and the moment arm of the forces with respect to the pivot point. Males having a higher average body weight are expected to have high moment values on their spine. To calculate the equivalent muscle force with a moment arm of 5 cm, the force which would be imposed on single muscle is calculated. The order of the force value imposed

on single muscle is calculated to be huge for the fully flexed postures. This shows that it is misleading to assume that single equivalent muscle (SEM) is realistic (Hsiang *et al.*, 1997; Brown and Potvin, 2004). The magnitude of the initial force calculated is in the order of 1200-1400 N. It might be possible to divide this force within the number of muscle groups, but it is not possible to estimate which muscle is carrying which percent of the load (Hsiang *et al.*, 1997; Brown and Potvin, 2004).

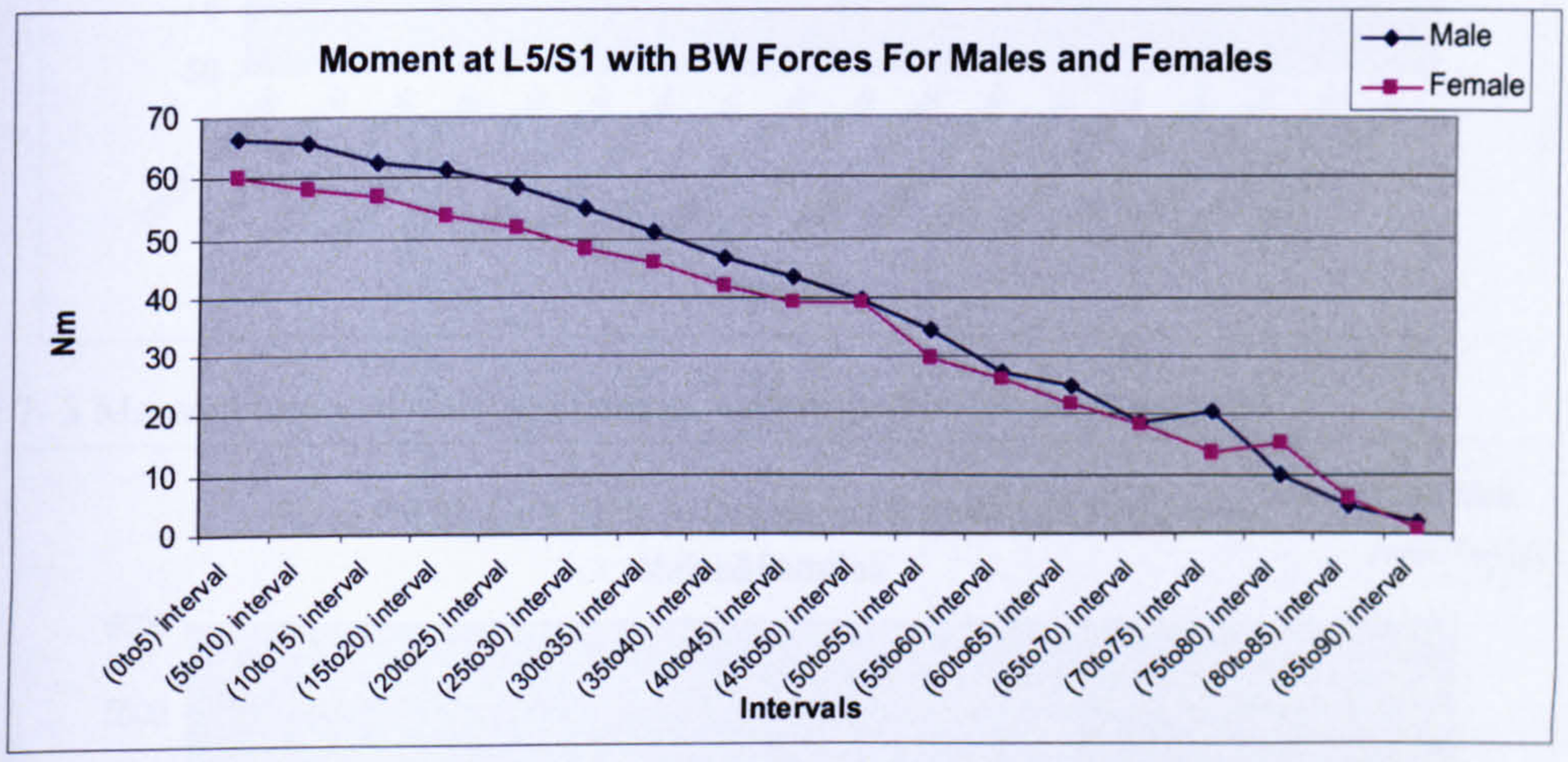


Figure 7- 1Moment imposed male and females with respect to the pivot point L5

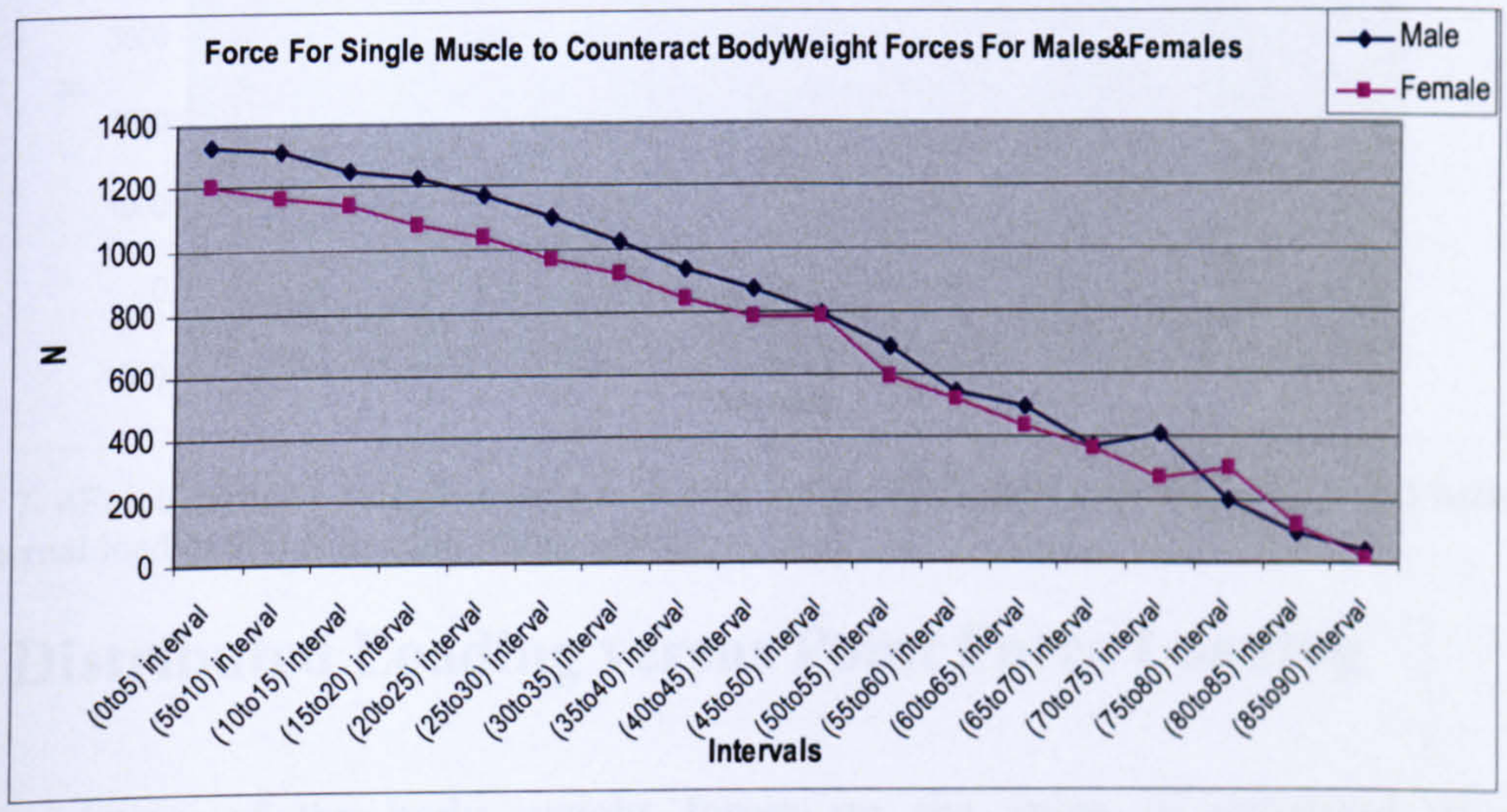


Figure 7- 2 Force carried by single muscle according to the SEM model imposed on male and females for the full lifting activity.

With the addition of the external force acting on the spine, the moment imposed on the pivot point which is the lower end plate of L5 is observed to increase by more than 4 times (Figure 7.3). The magnitude of the moment imposed on female and male is similar. With the moment arm of 5 cm for a single equivalent muscle model, the muscle force is thought to be unrealistic for any single muscle to carry this load.

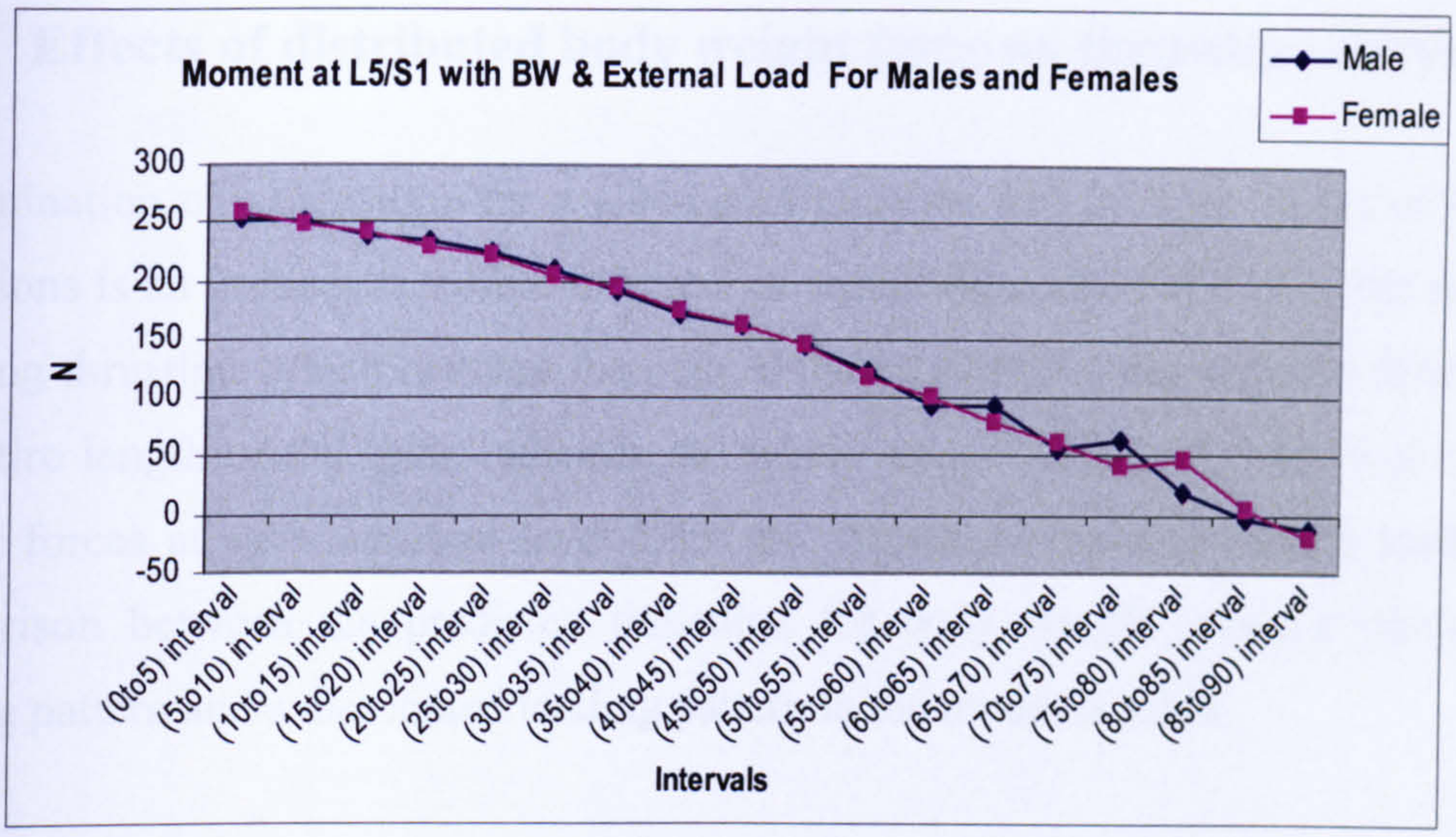


Figure 7- 3 Moment imposed male and females with respect to the pivot point L5

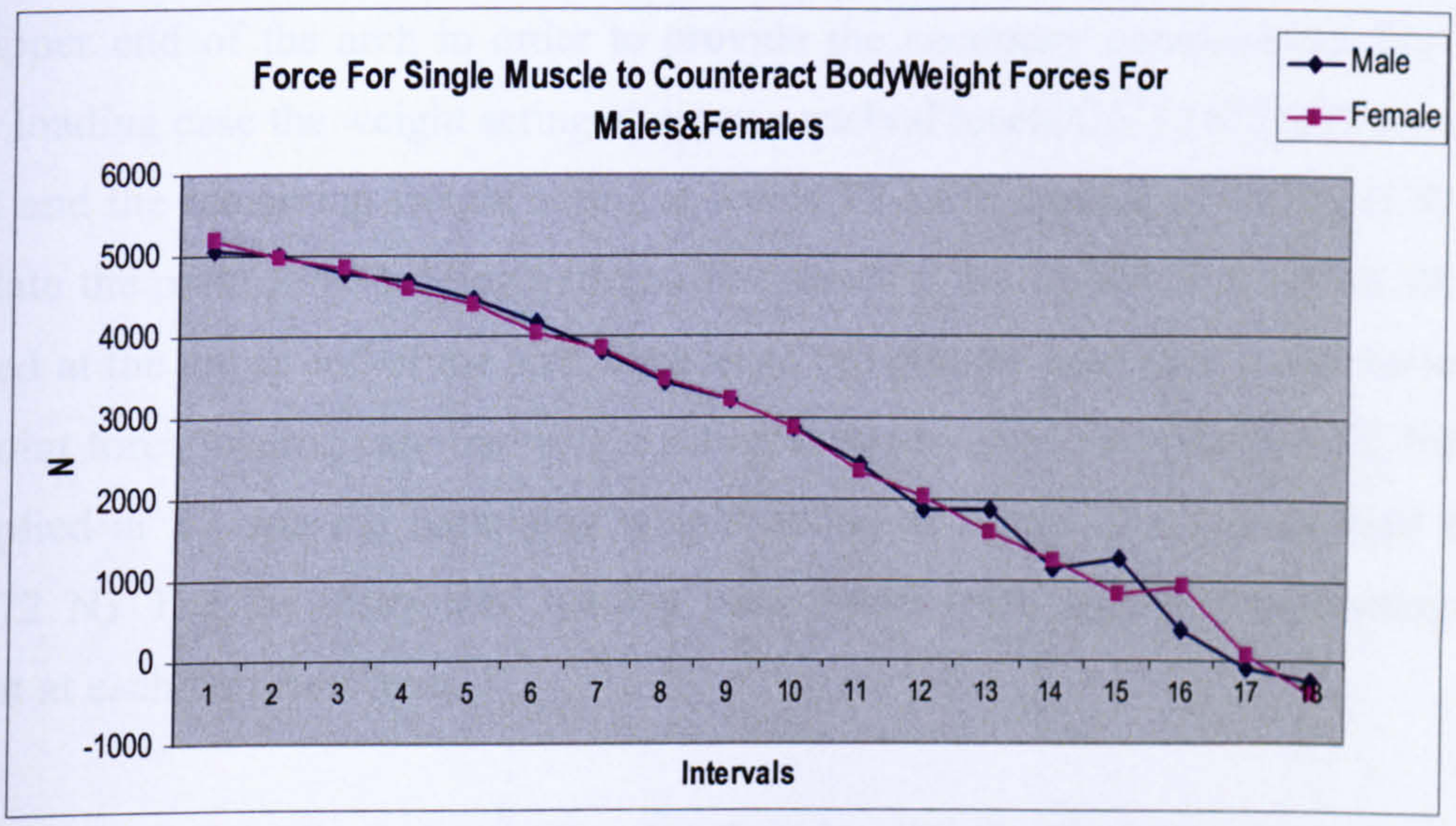


Figure 7- 4Force carried by single muscle according to the SEM model imposed on male and females for the external load of 900 N in a full lifting activity.

7.2 Distributed Loading versus Point Force Loading

Representation of the body weight forces on the spine is simulated as acting incrementally at each vertebral level by using the developed mathematical model for both genders. A comparison is made by applying a point force representing the body weight force at T2 and T12 instead of distributed body weight loading. The stability analysis and intervertebral joint force analysis are conducted for each type of loading to compare the biofidelity of the model.

7.2.1 Effects of distributed body weight force on thrustline curvature

Determination of a thrustline for a given configuration and for a given set of loading conditions is an immediate visible indicator of equilibrium and stability of the spine. A resulting thrustline which matches the path of the vertebral bodies at every level along the entire length of the spine indicates the whole spine stability. Application of body weight forces at each vertebral level helps the thrustline follow a smooth loading. A comparison between the predicted thrustline for body weight using a point force loading pattern and a distributed loading pattern in the model is made.

To present a point force loading, the weight of the head 45.2 N for males is applied at the upper end of the arch in order to provide the necessary compression. For point force loading case the weight acting at upper vertebral levels C1-T2 (75.98N) is applied at T2 and the remaining weight acting at levels T3-L5 is applied at T12 (281.62 N) to simulate the point force loading pattern . For females, the weight of the head 39.1 N is applied at the upper end of the arch in order to provide the necessary compression. For the point force loading case the weight acting at upper vertebral levels C1-T2 (65.75N) is applied at T2 and the remaining weight acting at levels T3-L5 is applied at T12 (243.72 N). For the distributed loading case forces were applied representing body weight at each vertebral level.

The predicted thrustlines due to the distributed and point force loading patterns for bodyweight are compared for the 19 different intervals for both genders. The program is run for 19 times for both genders. It is observed that the collective loading pattern, the predicted thrustline consists of three linear portions which show sharp changes in direction upon application of force. In contrast the distributed loading pattern results in a thrustline with a greater number of smaller linear portions so that the overall path can be approximated by a smooth curve (Figure 7.5, Figure 7.6).

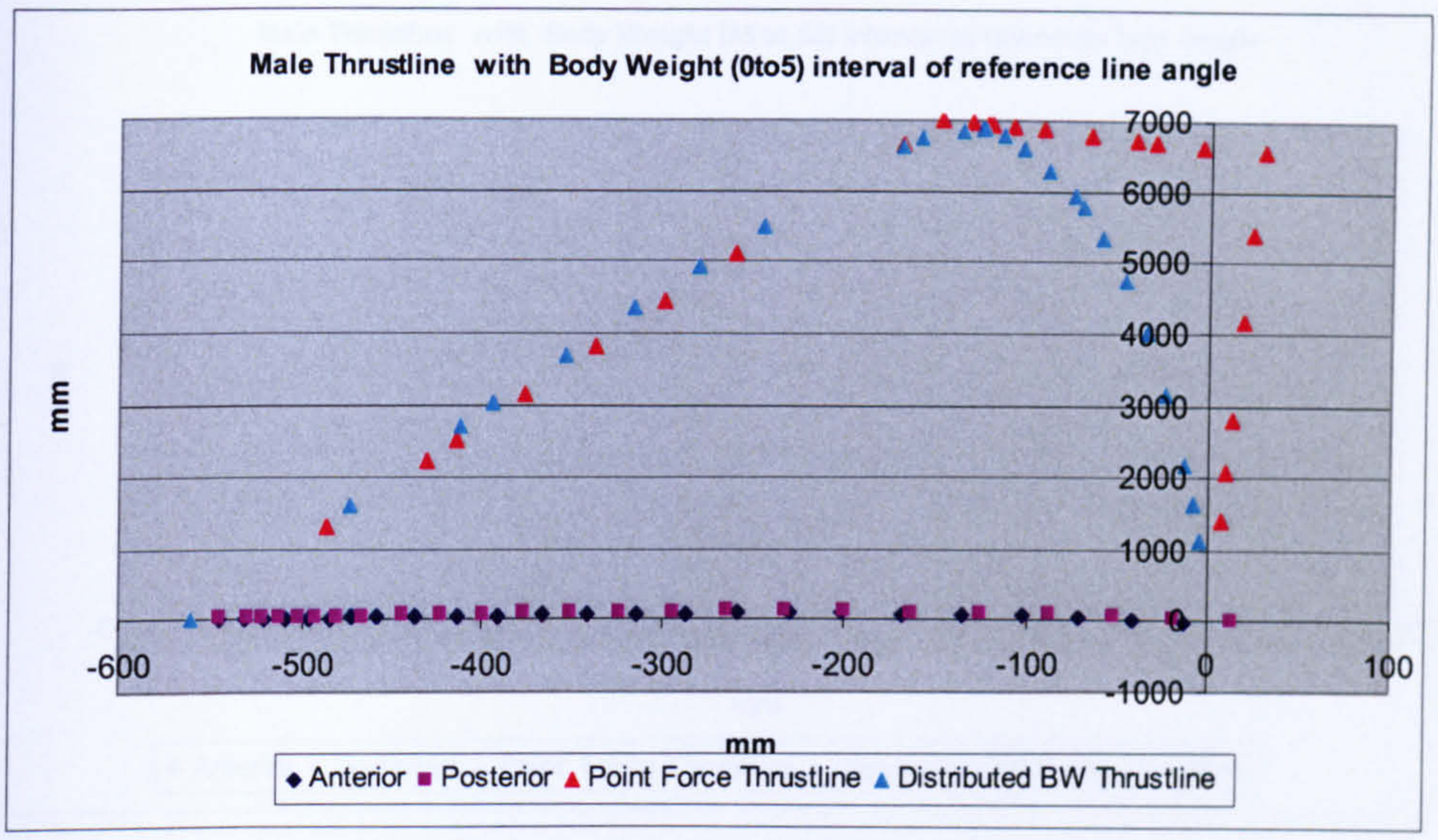


Figure 7- 5Thrustline for males for the interval of 0-5 degrees of reference line angle with distributed body weight force and point force

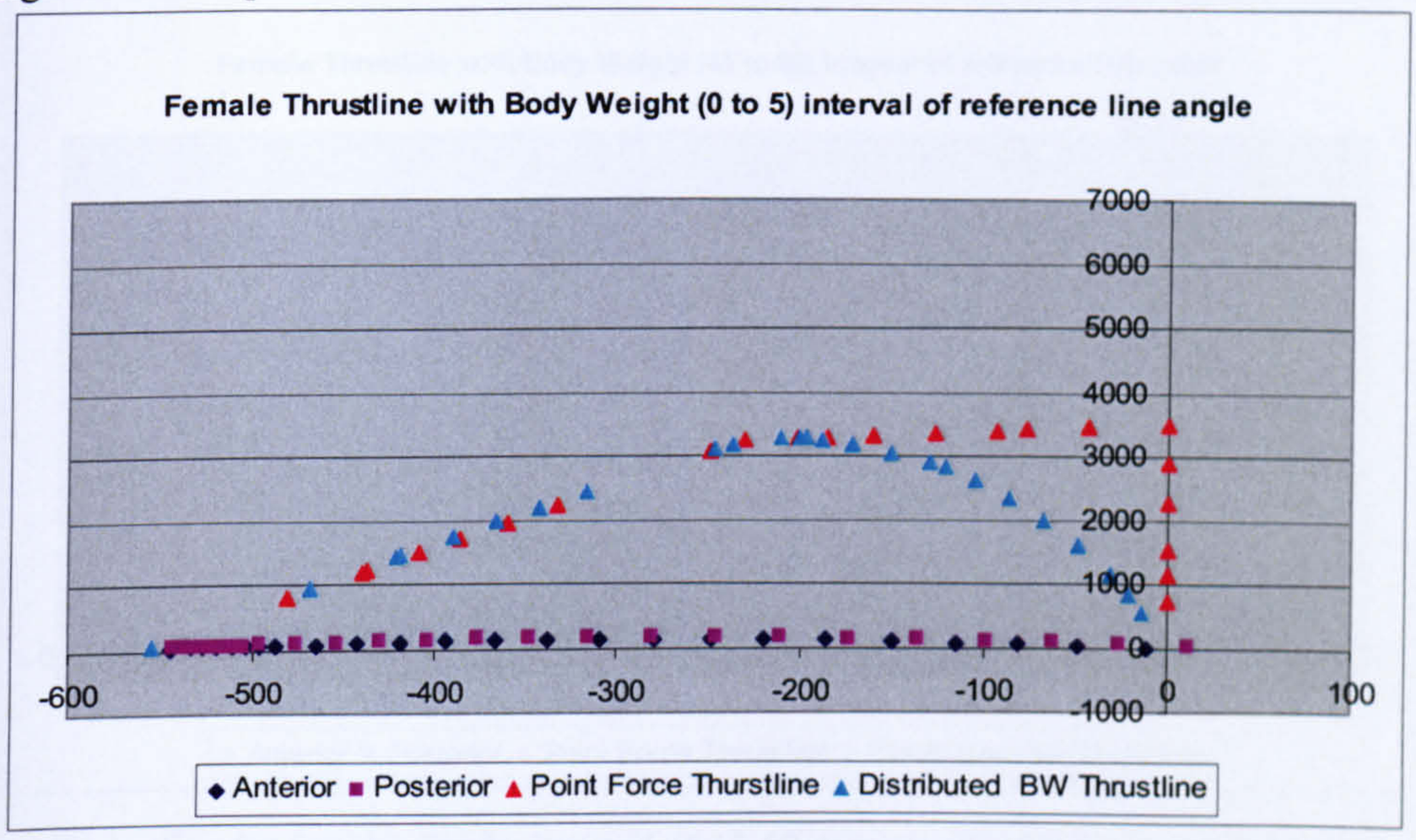


Figure 7- 6 Thrustline for females for the interval of 0-5 degrees of reference line angle with distributed body weight force and point force

The figures above show the differences for males and females with the distributed body weight forces and point force. The contour of the thrustline for 3 point force shows two sharp corners where the forces are applied. The deviation of the thrustline is high. The thrustline is not capable of following the contour of the spine but results in having sharp changes (Figure 7.7, Figure 7.8).

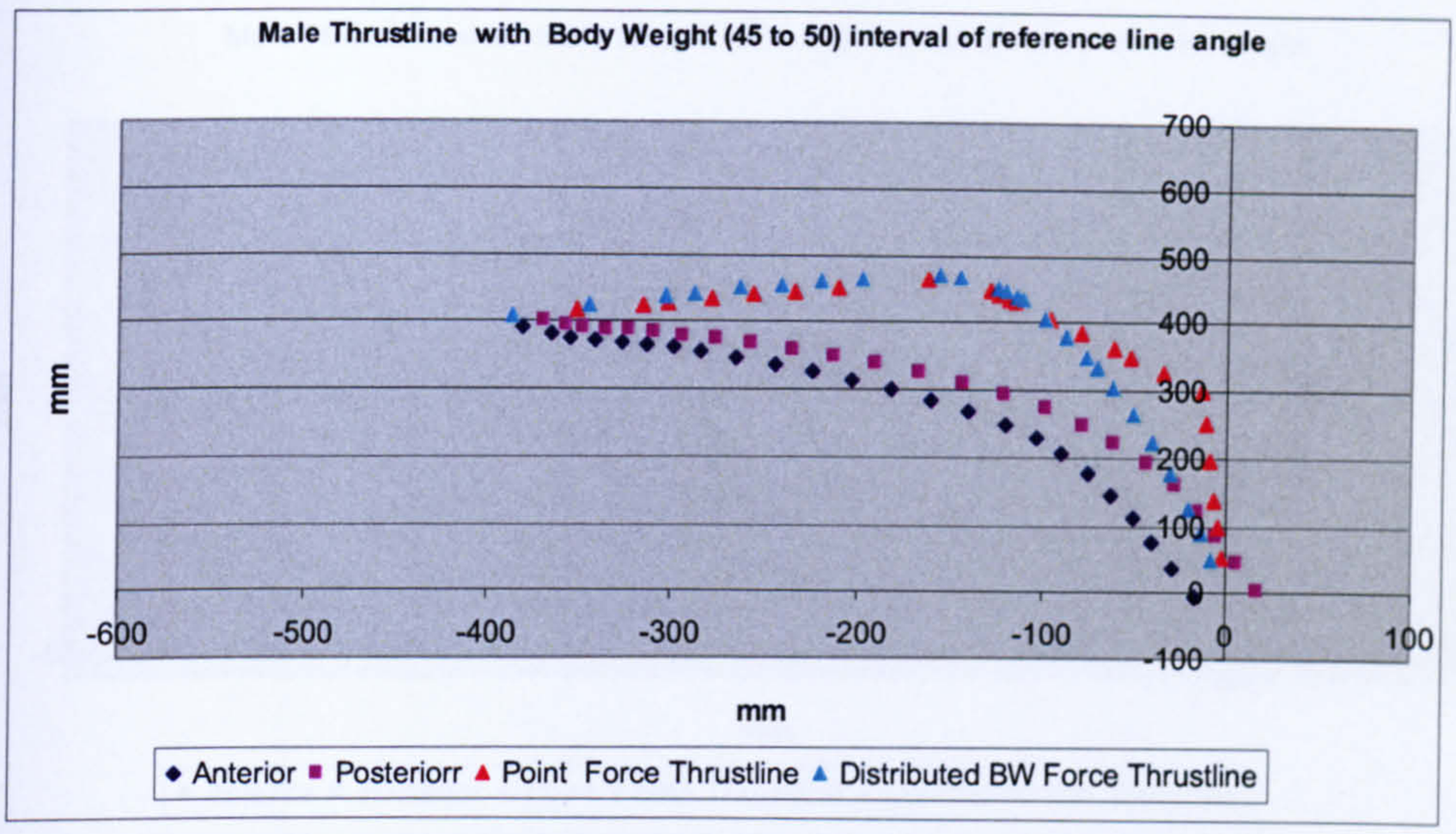


Figure 7- 7Thrustline for males for the interval of 45-50 degrees of reference line angle with distributed body weight force and point force

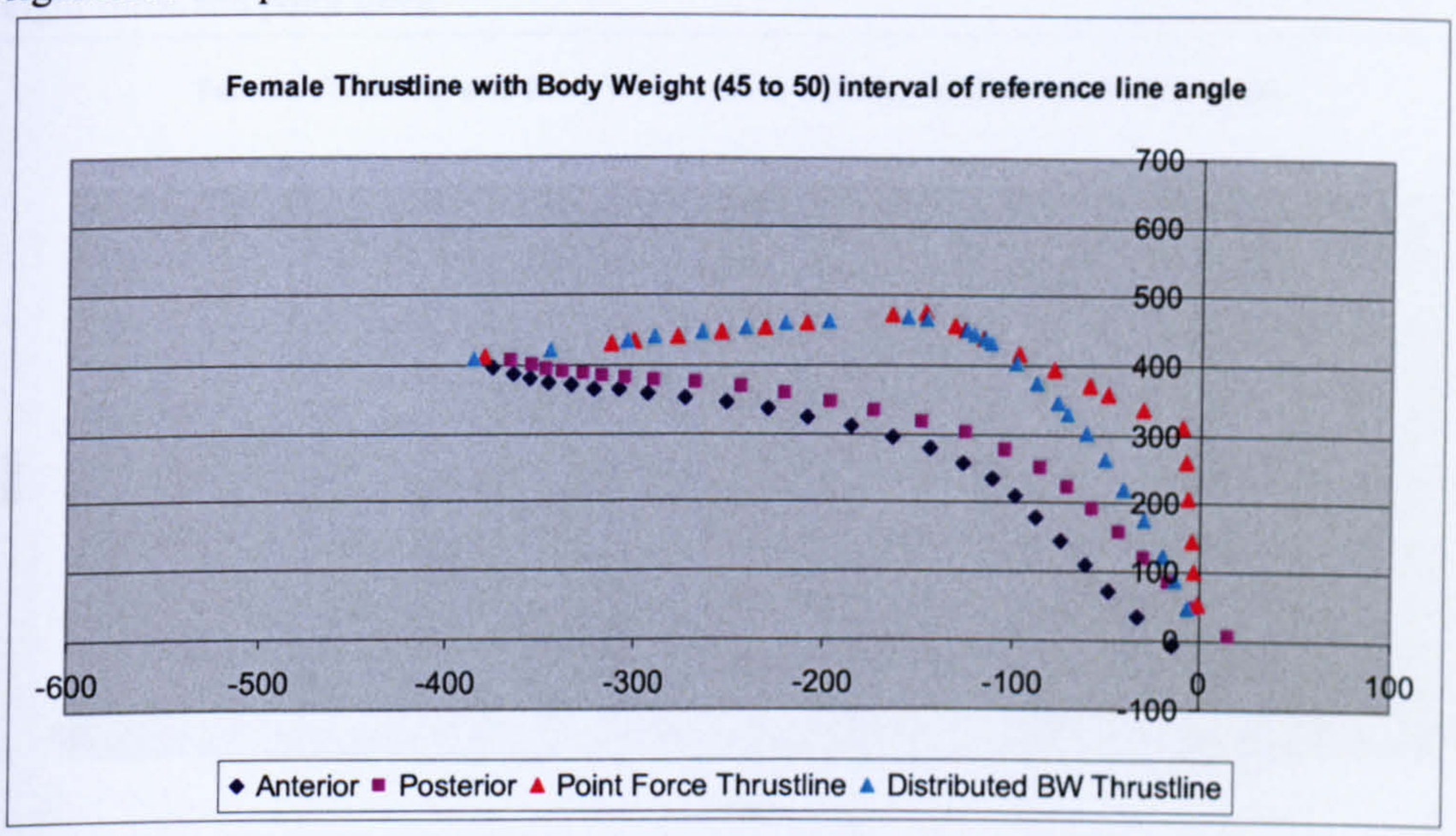


Figure 7- 8 Thrustline for females for the interval of 45-50 degrees of reference line angle with distributed body weight force and point force

For the interval of 85-90 degrees of reference line angle, the difference between two approaches is not as high as in the interval of 45-50 degrees of reference line angle interval. This is due to the position of the applied forces with respect to the reference line. The moment arms of the forces applied get closer to the reference line and the moment they apply has less effect (Figure 7-9, Figure 7-10).

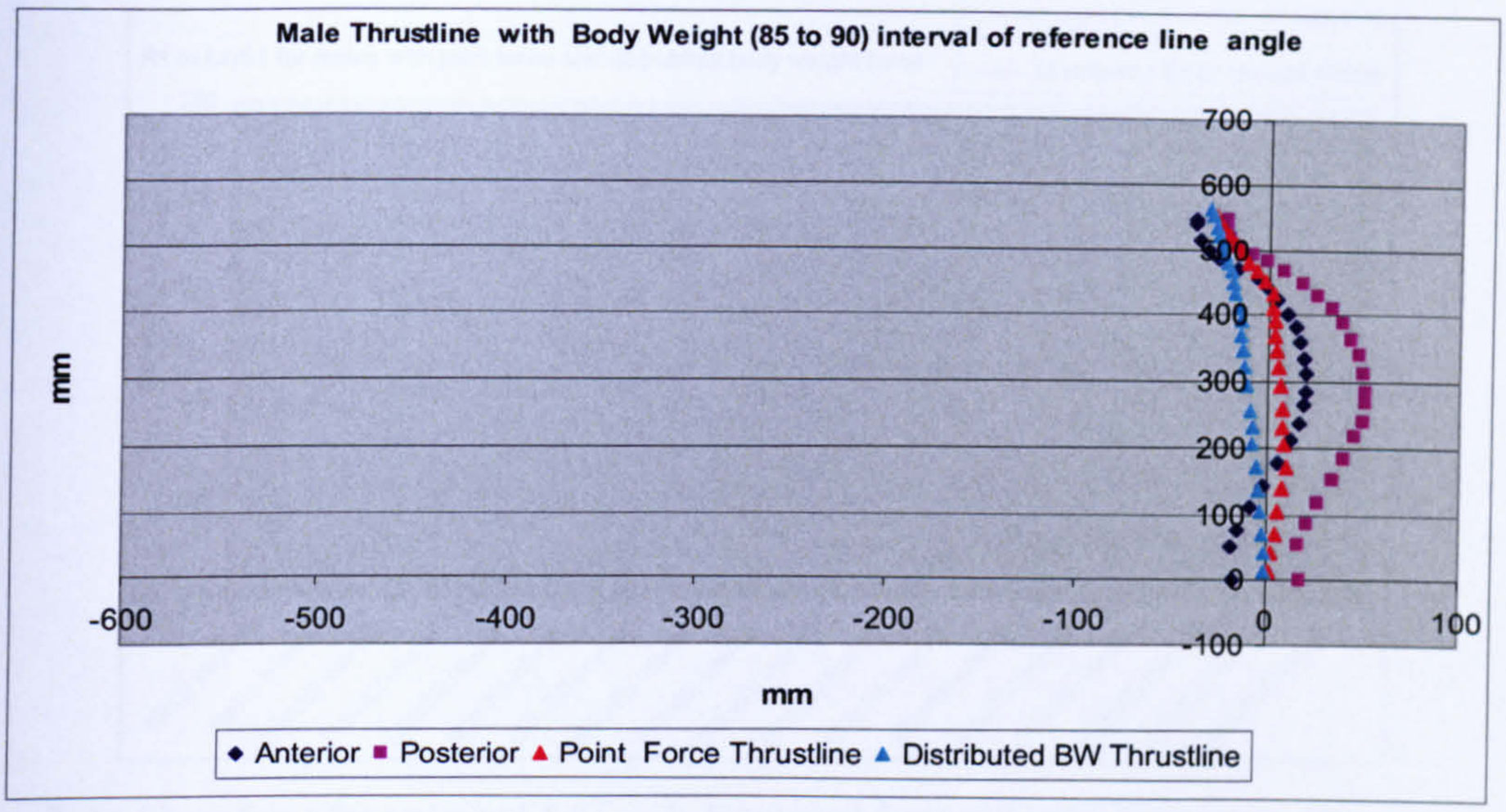


Figure 7- 9 Thrustline for males for the interval of 85-90 degrees of reference line angle with distributed body weight force and point force

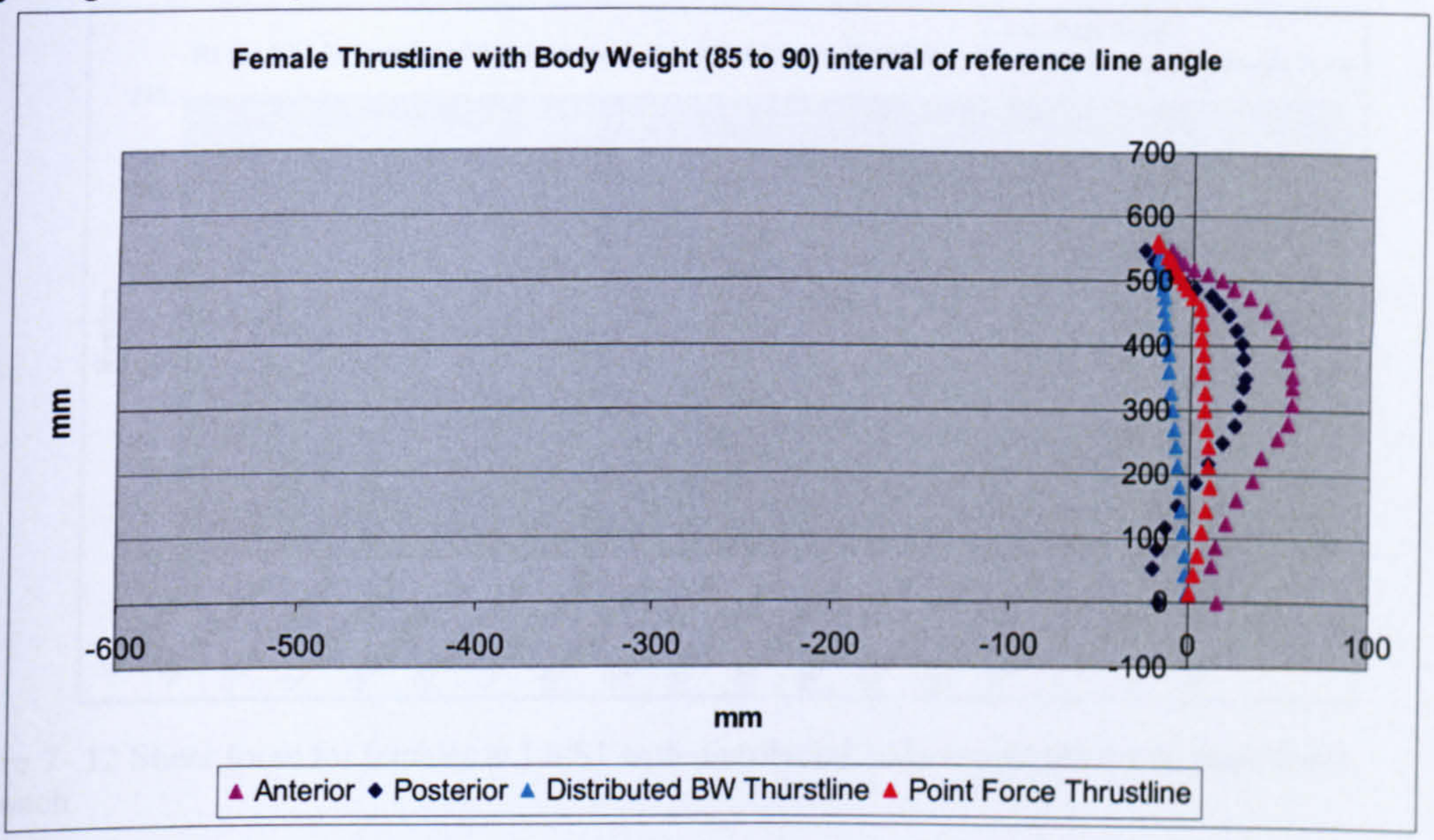


Figure 7- 10 Thrustline for females for the interval of 85-90 degrees of reference line angle with distributed body weight force and point force.

With the distributed body weight approach, it is observed that the exact location of application of body weight forces at each vertebral level let the thrustline follow the counter of the spine. With the point force loading approach, the thrustline curvature is not capable of following the curvature of the spine.

The reaction forces are also compared and not much difference is observed in compression, whereas shear forces differ more when compared to compression forces for both males and females.

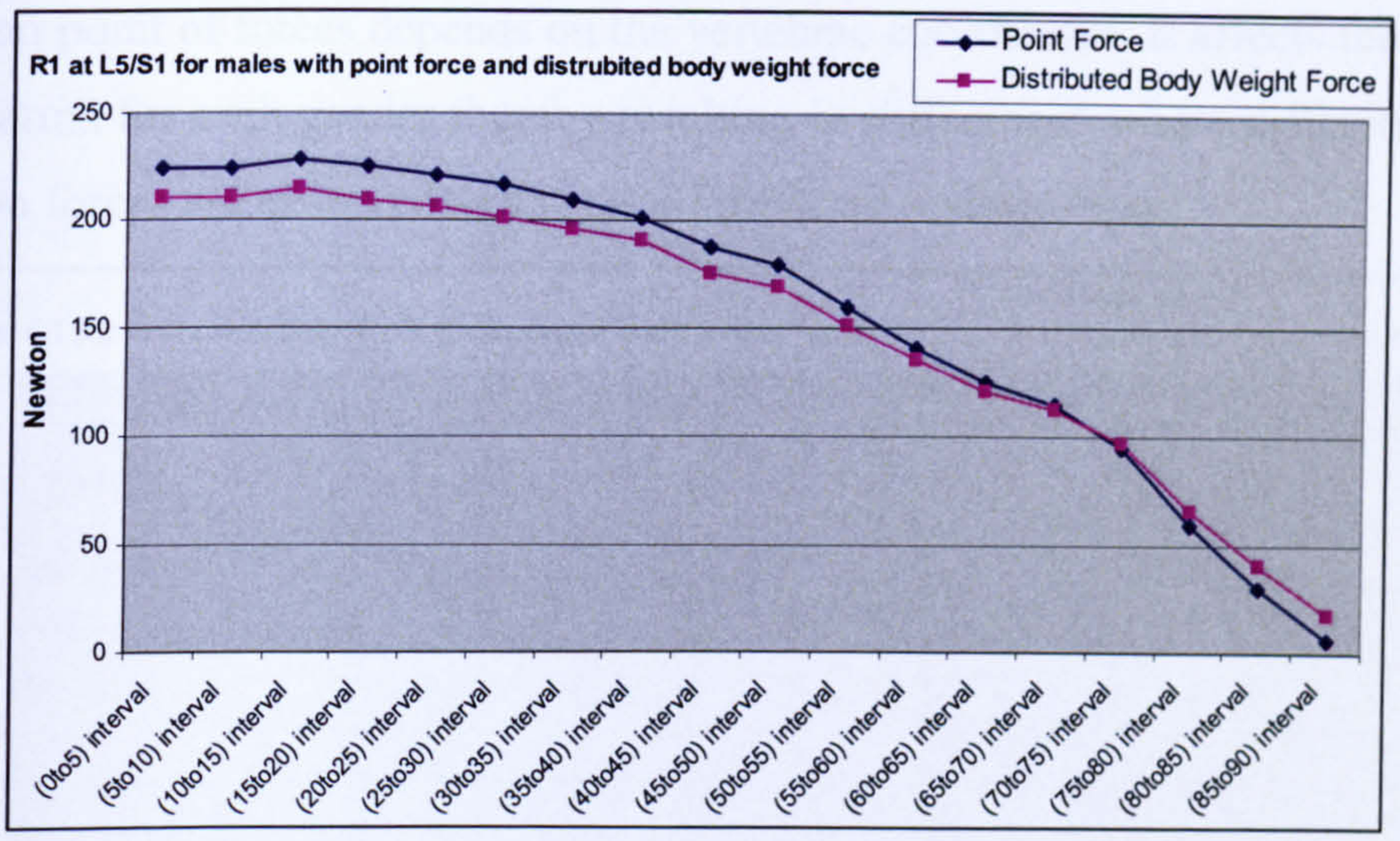


Figure 7- 11 Shear force for males at L5/S1 with distributed force and point force approach.

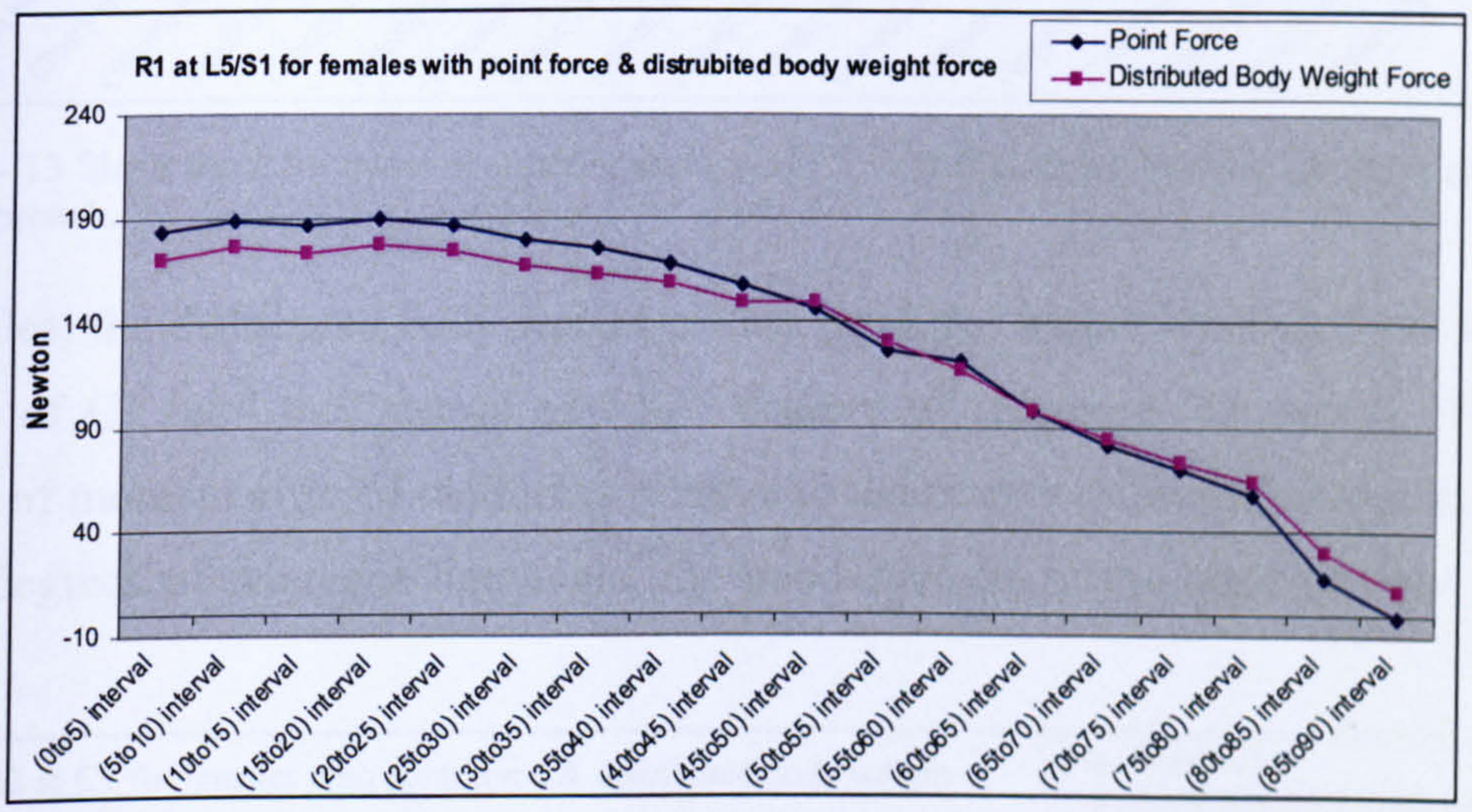


Figure 7- 12 Shear force for females at L5/S1 with distributed bodyweight force and point force approach.

The distributed body weight force approach results in less shear force than the point force approach at L5/S1 level up to the interval of 75 to 80 degrees of reference line angle for males. After this interval the distributed body weight force results in higher shear forces at L5/S1. This is due to the change of moment arm lengths. When the distance of the moment arm is shorter, the difference between the point force approach and distributed body weight becomes less. For females, until the interval of 45 to 50, the point force loading results in higher shear reaction forces due to the longer length of moment arms. For the rest of the intervals the difference between the point force type of loading and distributed body weight loading decreases. For the difference between females and males, the difference between two types of loading is observed at different intervals. This is due to the different vertebrae coordinates of females and males as the

application point of forces depends on the vertebrae coordinates. It affects the length of moment arms for each gender thereby resulting in differences where different patterns in reaction forces are observed as a result of different loading types.

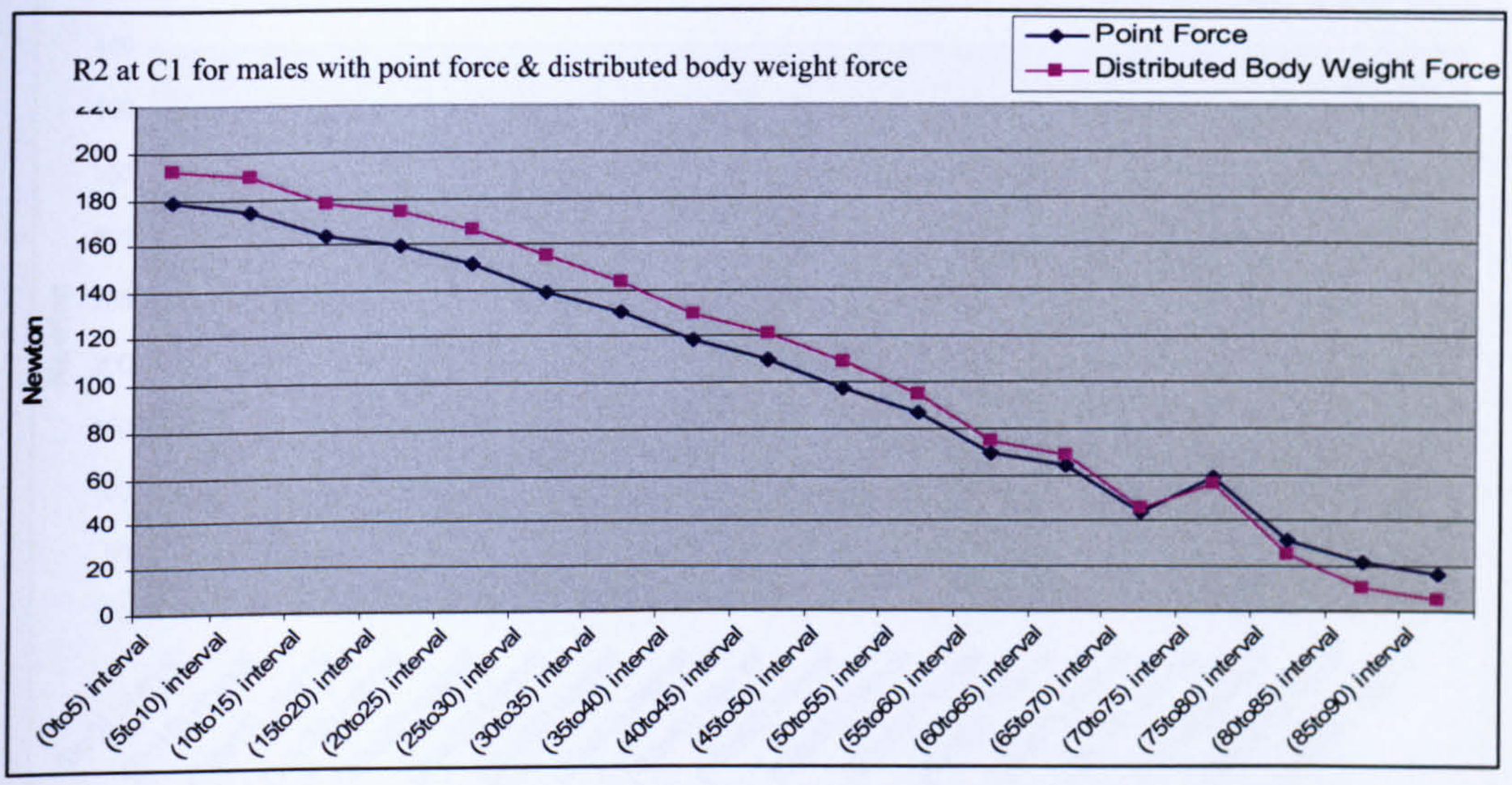


Figure 7- 13 Shear force for males at superior surface of C1 with distributed bodyweight force and point force approach.

For males, the distributed body weight pattern produces higher reaction force superior surface of C1 until the interval of 70-75 degrees of reference line angle. With the change of moment arms of the forces relative to the reference line, after the interval of 70-75 degrees of reference line angle, the trend changes in the opposite way (Figure 7.13).

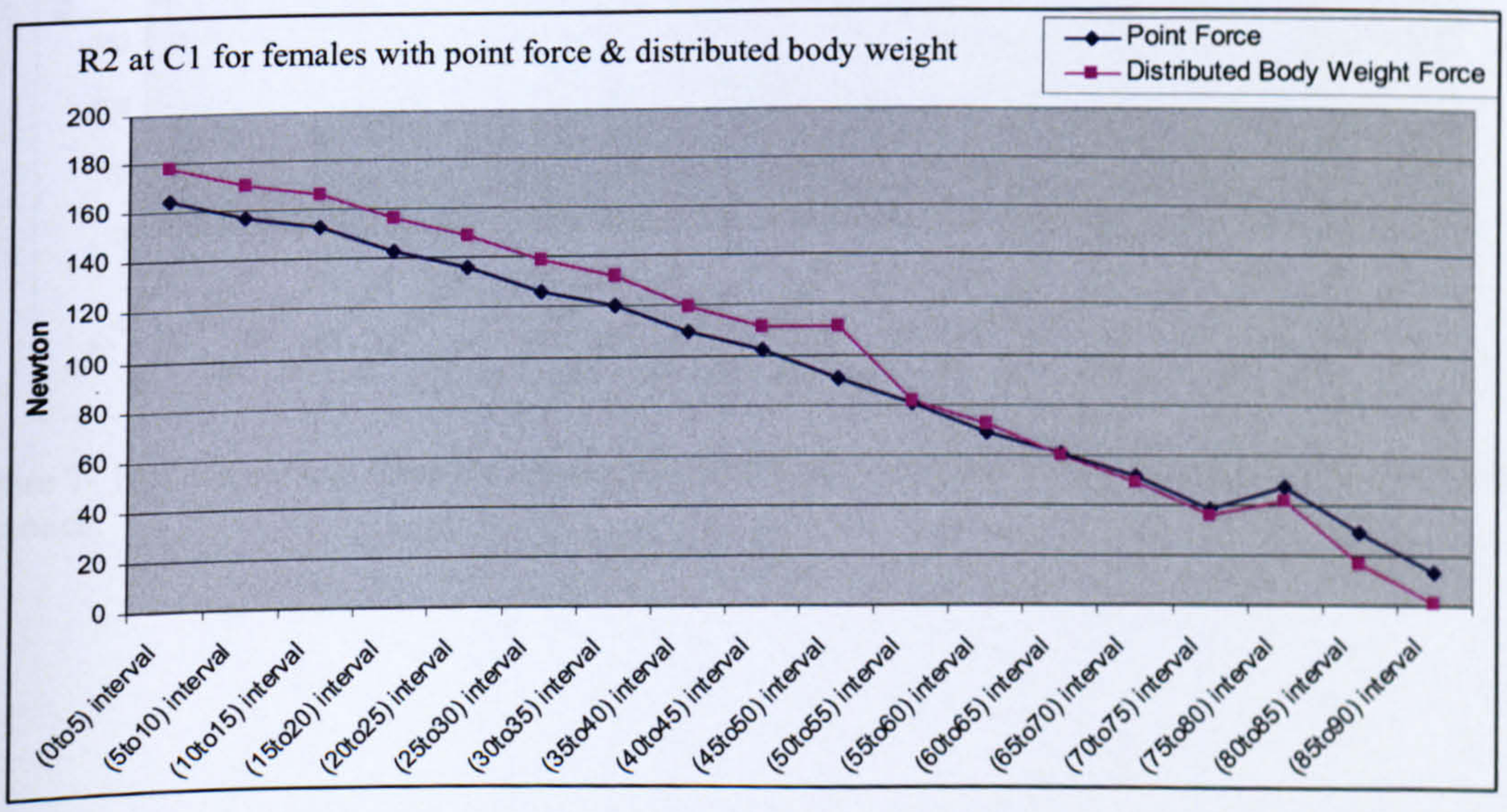


Figure 7- 14 Shear force for females at superior surface of C1 with distributed bodyweight force and point force approach.

For females, a similar trend is observed to males. However, the difference in magnitudes is not as high as the males (Figure 7.14).

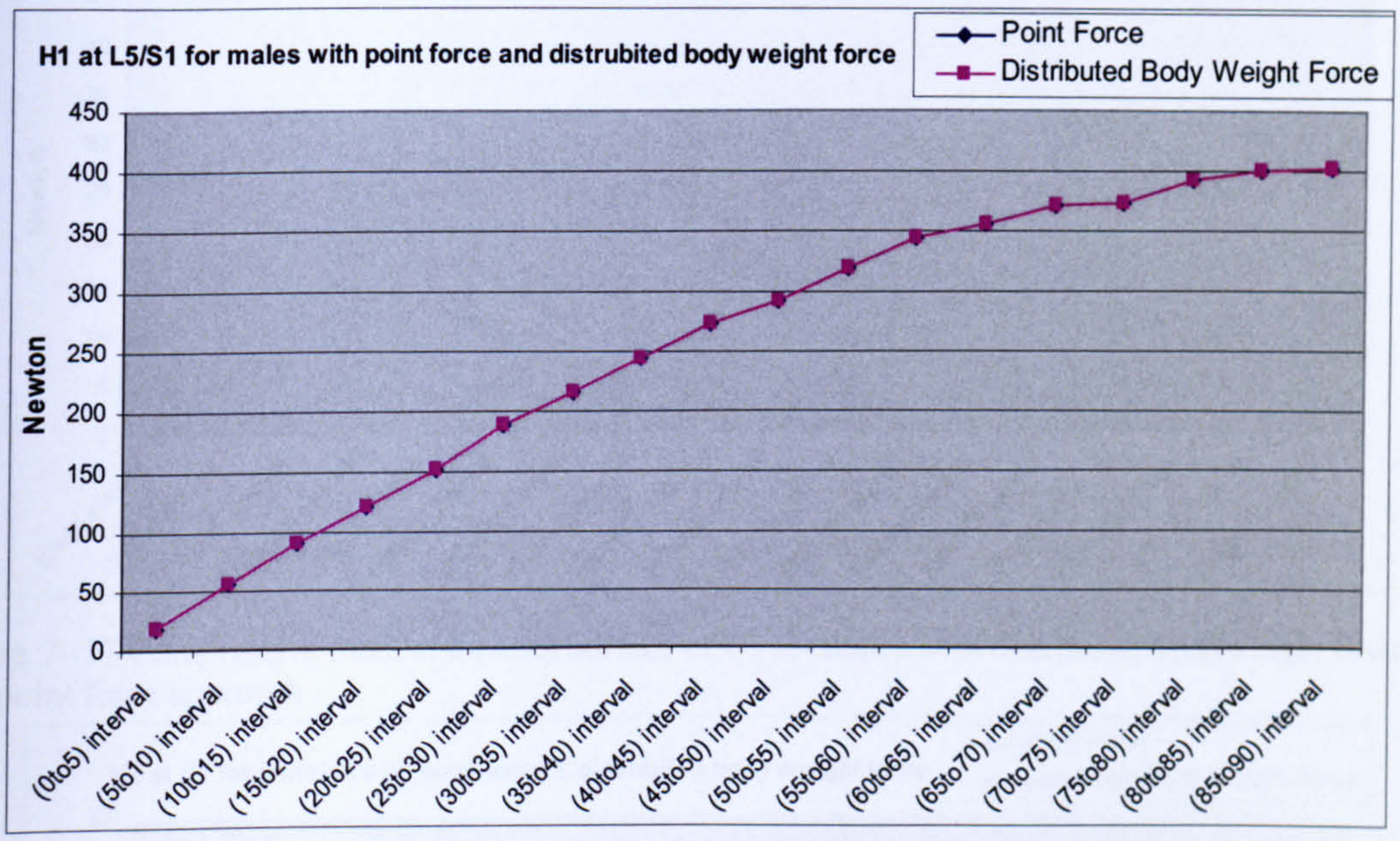


Figure 7- 15 Compressive force for males at L5/S1 with distributed bodyweight force and point force approach.

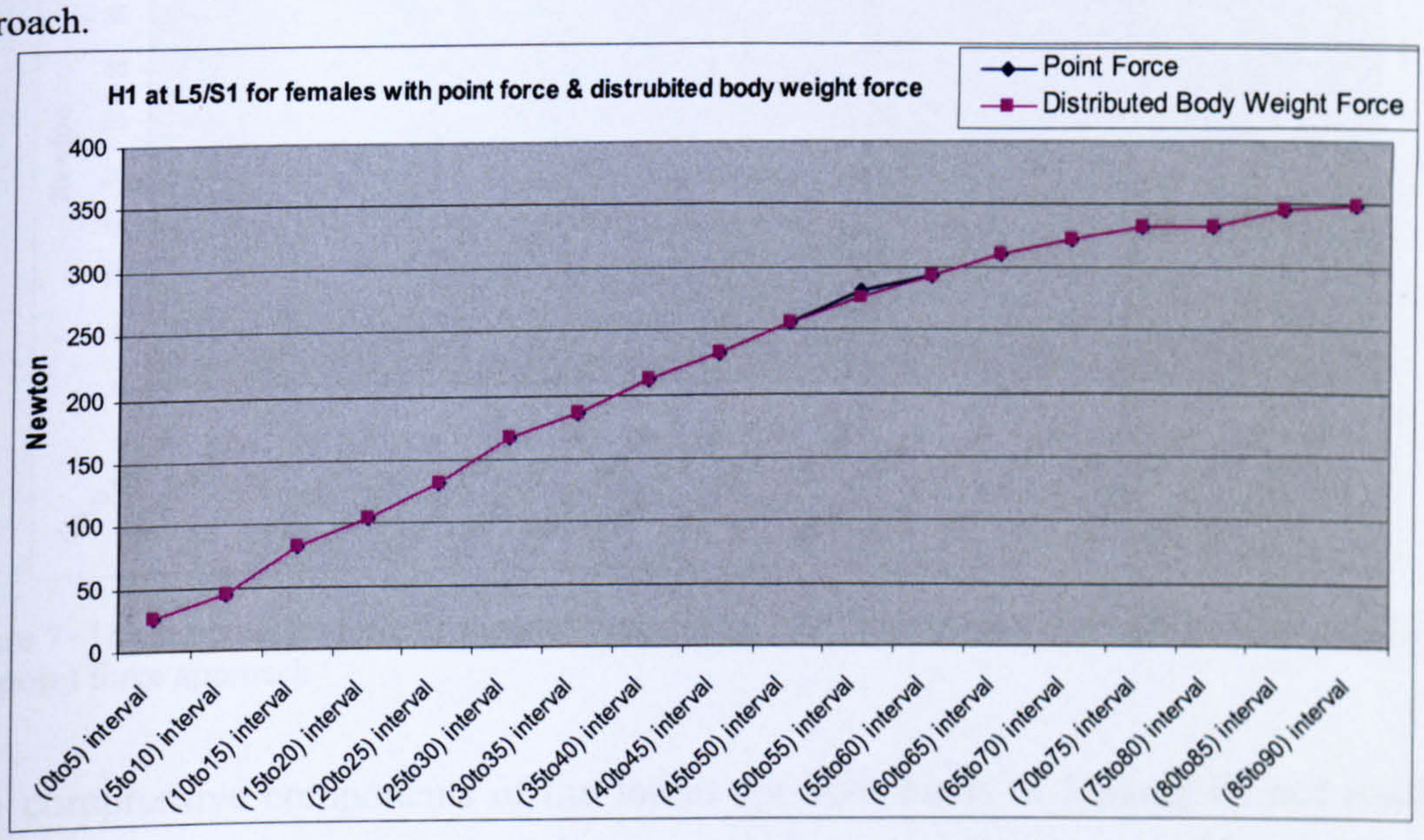


Figure 7- 16 Compressive force for females at L5/S1 with distributed bodyweight force and point force approach.

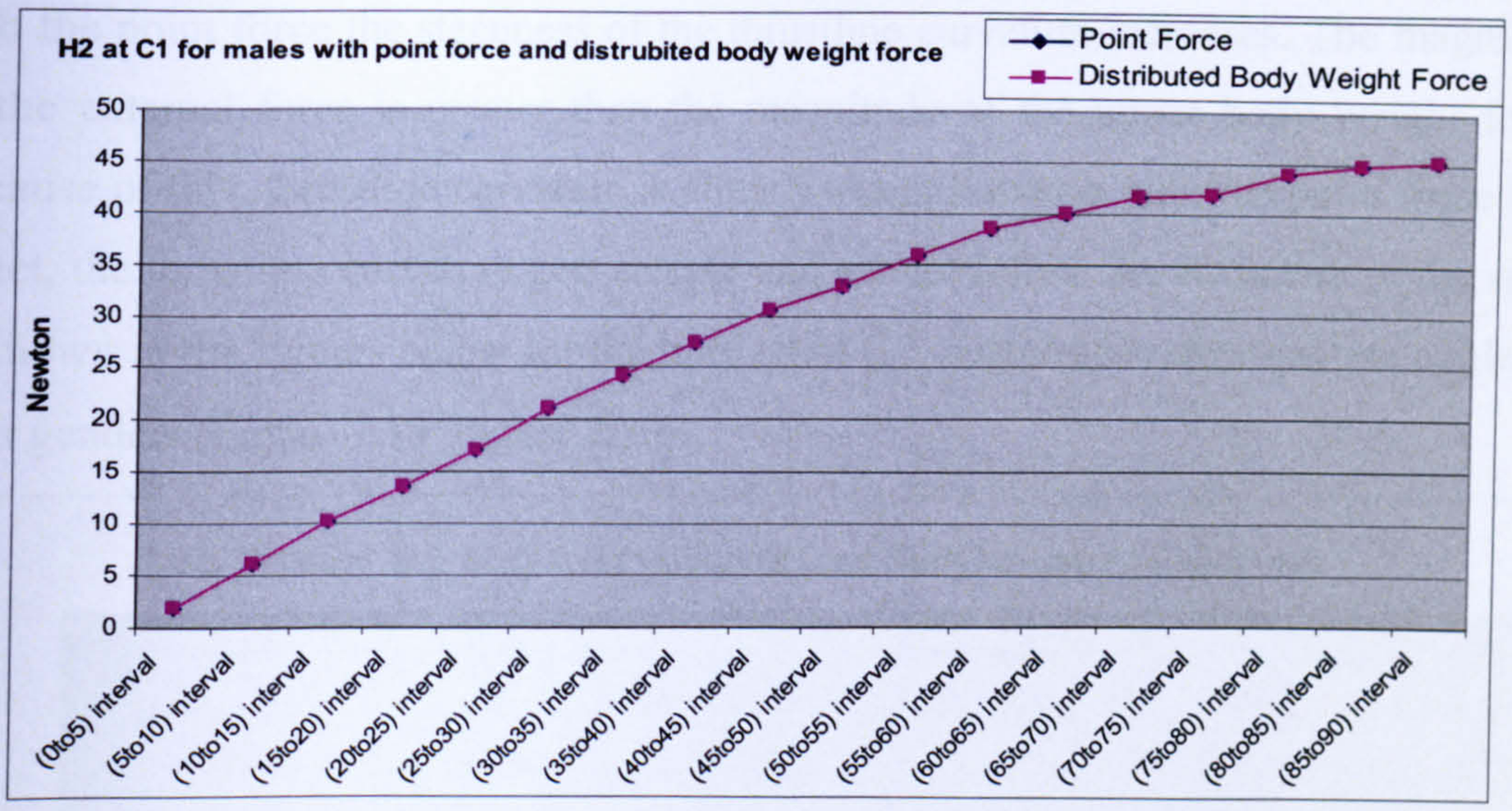


Figure 7- 17 Compressive force at superior surface of C1 for males with distributed bodyweight force and point force approach

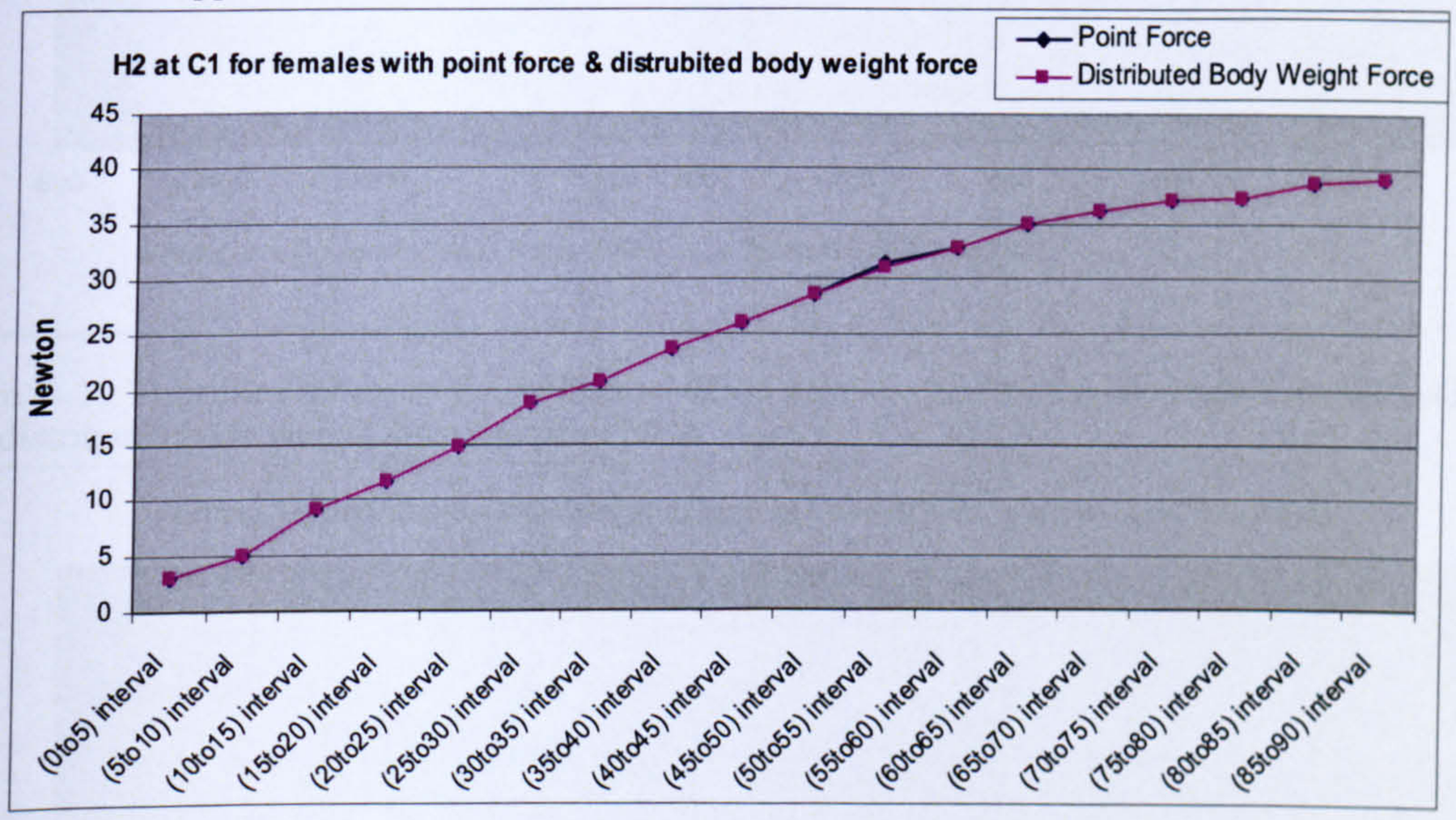


Figure 7- 18 Compressive force at superior surface of C1 for females with distributed bodyweight force and point force approach

The compressive components of the forces for both kinds of loading do not result in any differences for both genders at lower end plate of L5/S1 (Figure 7.15, Figure 7.16) and at superior surface of C1 which means that there is not much difference in the horizontal components of the load with respect to the reference line (Figure 7.17, Figure 7.18). The distance for the parallel components of the loads is small, whereas the positioning of the shear forces differs much along the lengths of the reference line.

By adding 300N load at T2, T3, and T4, both the distributed loading pattern and the point force loading pattern are compared. Application of external load when combined

with the point force the steepness of the thrustline curvature increases. The magnitude of the external force is greater than the magnitude of the upper body weight force. Because of this, thrustline curvature is already steep; however with the point force load effect, the thrustline curvature gets steeper and cannot follow the curvature of the spine as shown in the figures below for the interval of 0-5 degrees of reference line angle for both genders (Figure 7.19, Figure 7.20).

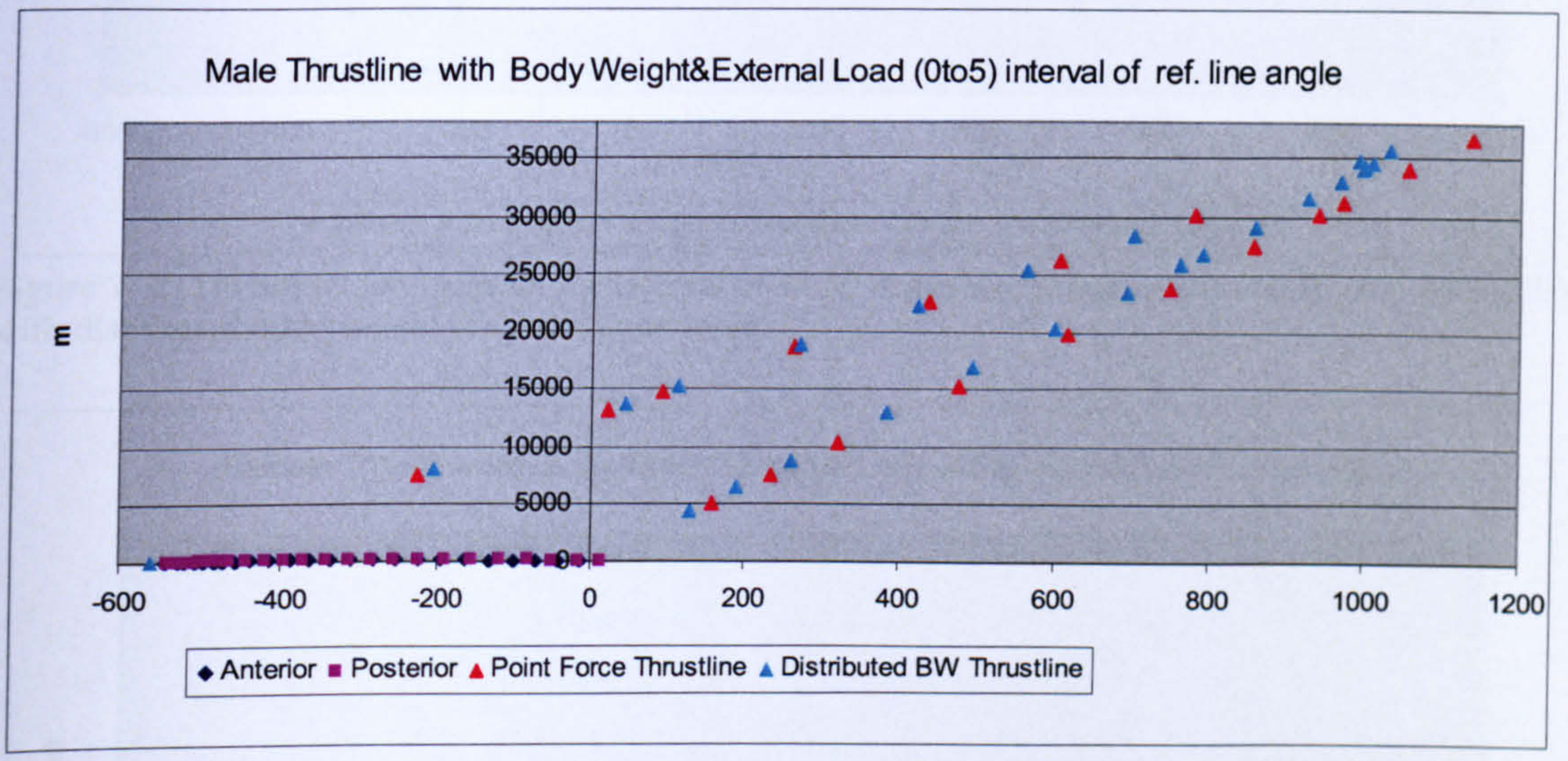


Figure 7- 19 Thrustline for males for the interval of 0-5 degrees of reference line angle external loading with distributed body weight force and point force.

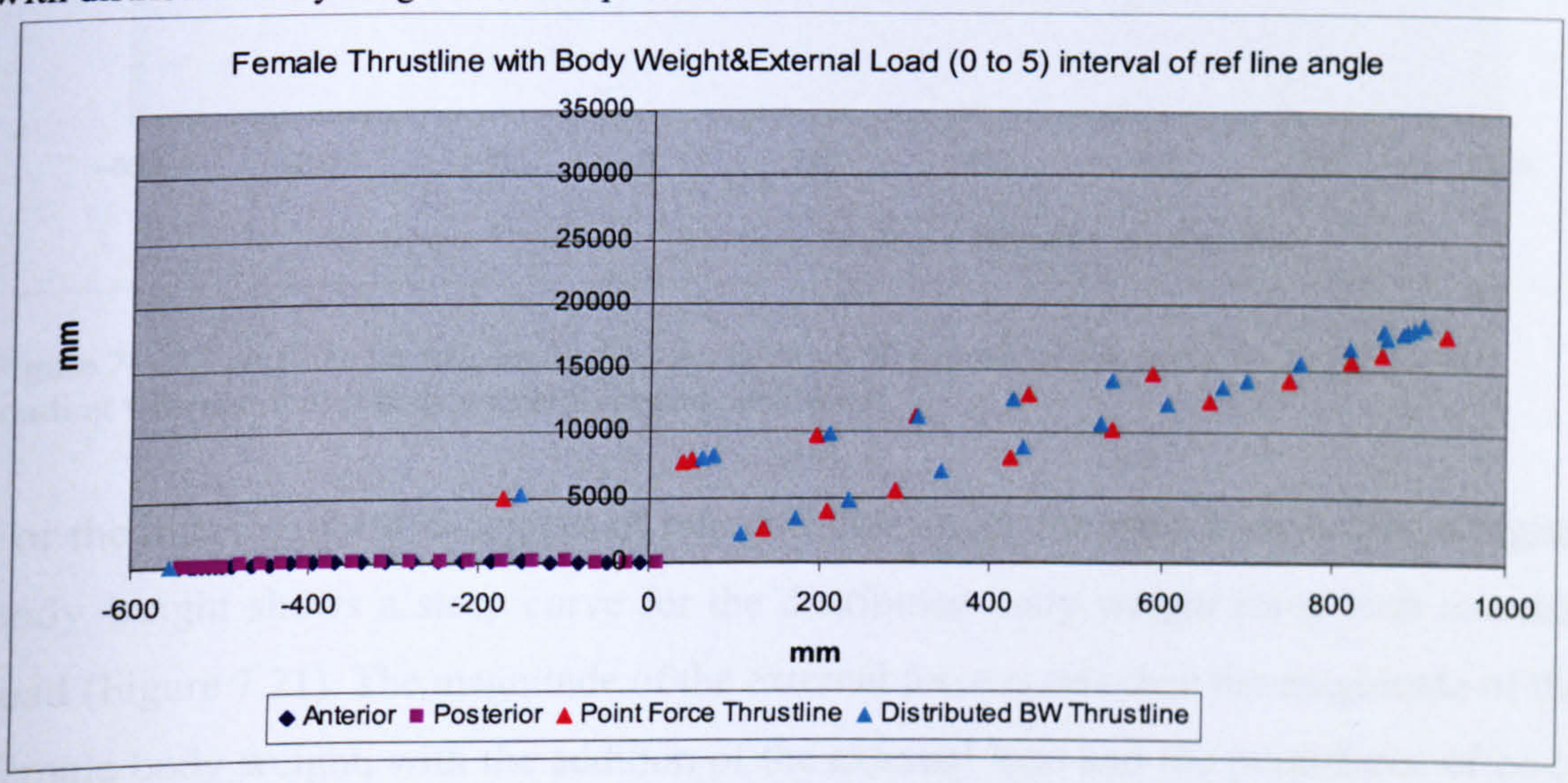


Figure 7- 20 Thrustline for females for the interval of 0-5 degrees of reference line angle external loading with distributed body weight force and point force.

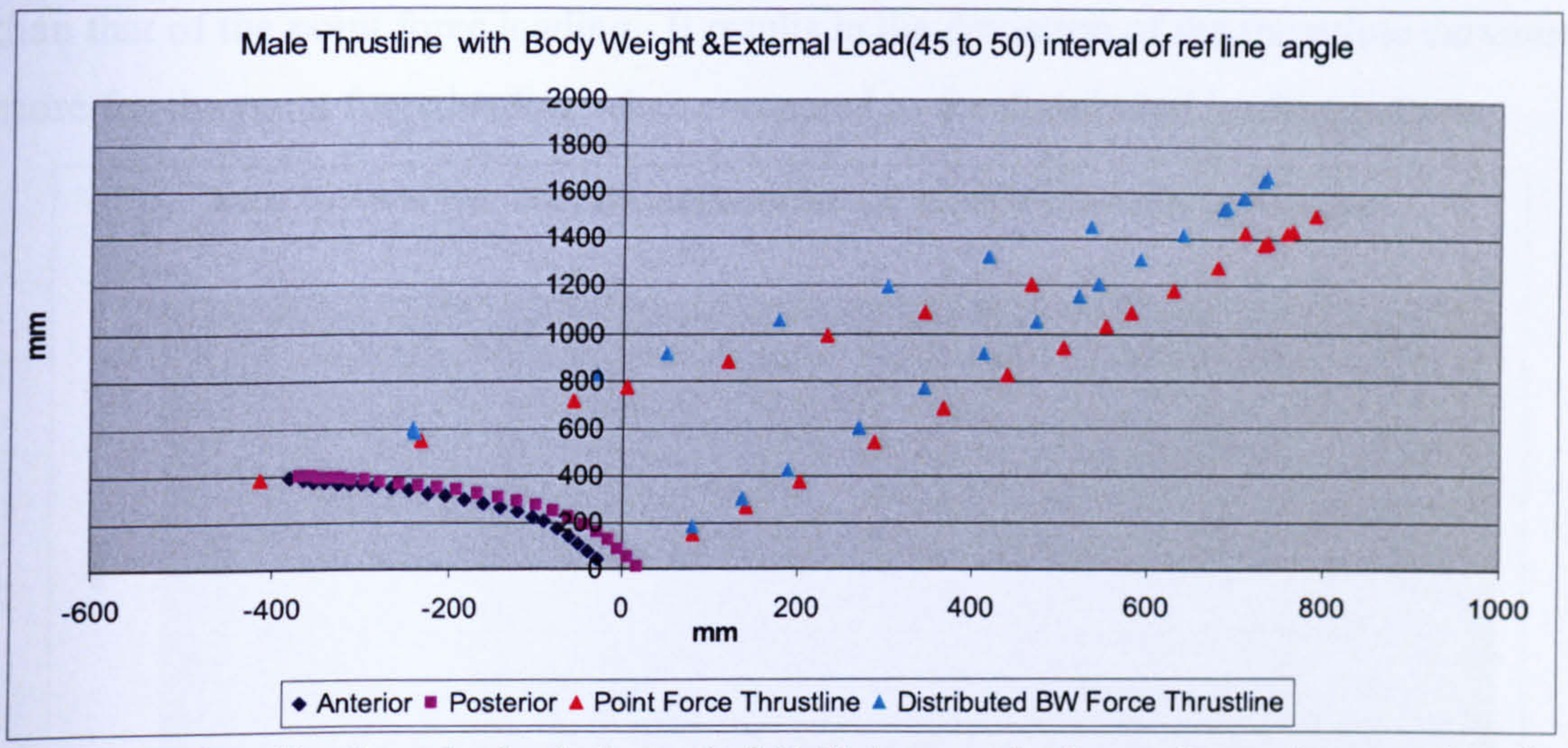


Figure 7- 21Thrustline for males for the interval of 45-50 degrees of reference line angle external loading with distributed body weight force and point force.

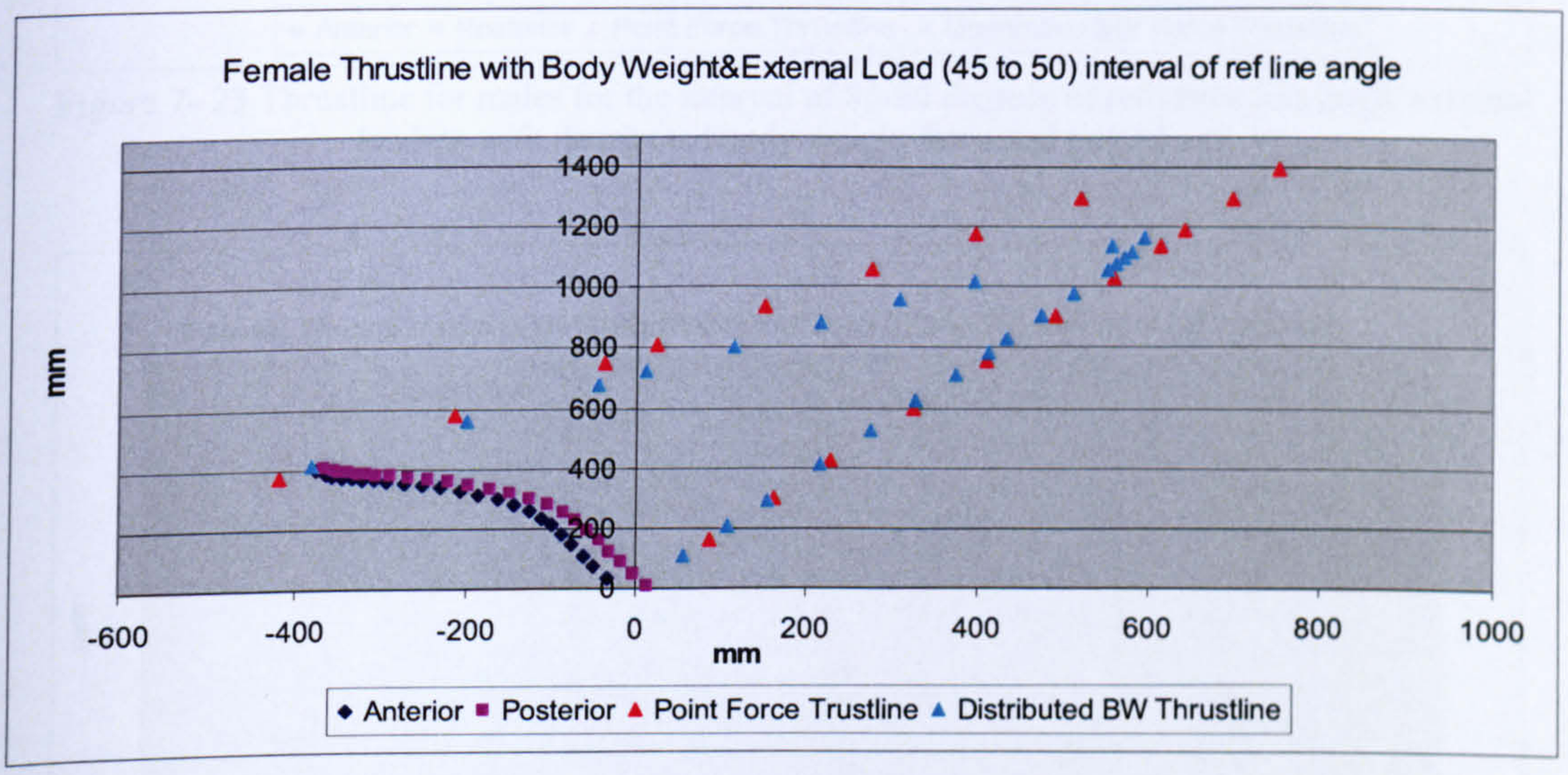


Figure 7- 22 Thrustline for females for the interval of 45-50 degrees of reference line angle external loading with distributed body weight force and point force.

For the interval of 45-50 degrees of reference line angle, the male body having a higher body weight shows a steep curve for the distributed body weight force with external load (Figure 7.21). The magnitude of the external force is less than the magnitude of the female body weight, with the addition of the external load and the point force of body weight force, the steepness of the thrustline increases more when compared to the increase in the thrustline of males (Figure 7.22).

For the interval of 85 to 90 degrees of reference line angle, the difference between the point force loading and distributed loading with the external load is little (Figure 7.23, Figure 7.24). The moment arm of the loads for distributed body weight forces is greater

than that of the point force loading. It results in the deviation of the thrustline curvature more for the point force loading when compared to the distributed loading pattern.

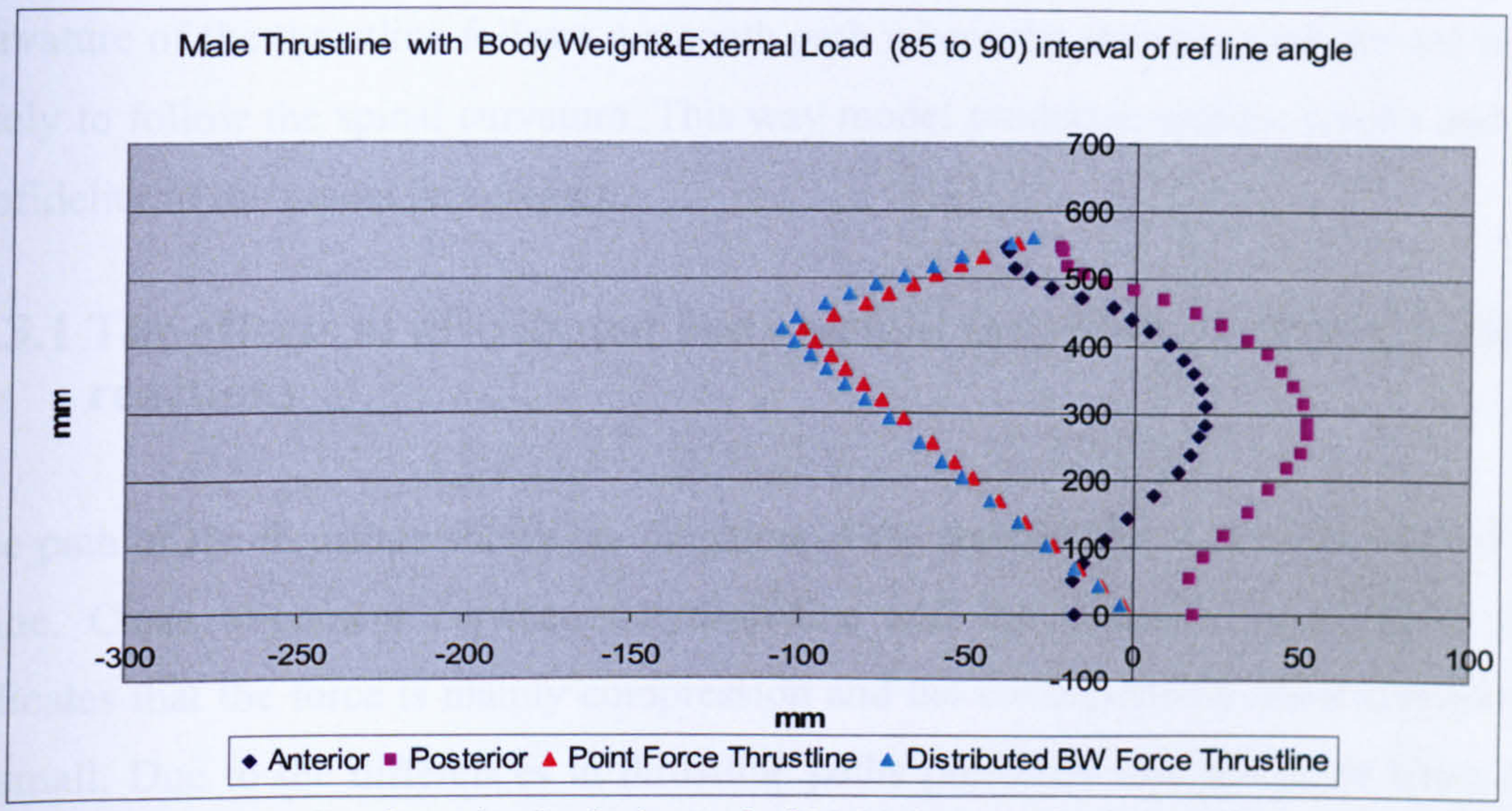


Figure 7- 23 Thrustline for males for the interval of 85-90 degrees of reference line angle external loading with distributed body weight force and point force.

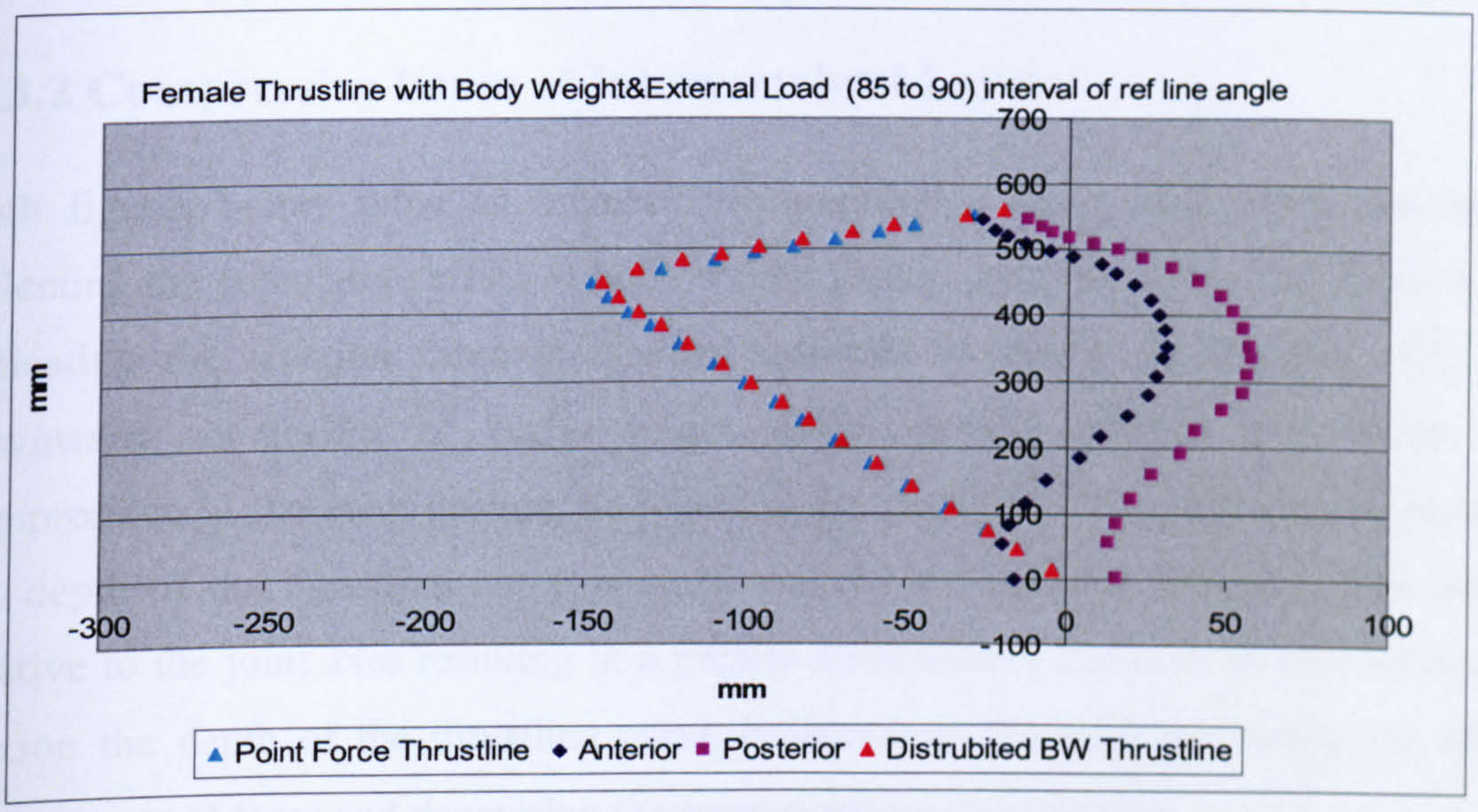


Figure 7- 24 Thrustline for females for the interval of 85-90 degrees of reference line angle external loading with distributed body weight force and point force.

7.3 Discussion

The results show that the point force loading is a poor estimate of the thrustline to check the stability of the spine. The distributed loading approach helps thrustline curvature to change its path along the spine in an incremental way. However, for point force loading sharp changes occur along at the application point of the force due to sudden high loading.

With point force loading approach, the sudden sharp corners of the thrustline might result in evaluating a stable posture as unstable. However, with distributed loading the curvature of the thrustline follows a smooth path where the stability analyses are more likely to follow the spinal curvature. This way model produces realistic results and the biofidelity of the model is increased.

7.3.1 The effects of distributed body weight forces on predicted joint reactions

The path of the thrustline shows the direction of the resultant force at each level of the spine. Close alignment between the thrustline and the vertebral longitudinal axis indicates that the force is mainly compression and the corresponding shear component is small. Due to the differences in thrustline paths predicted with the point force and distributed loading, a comparison between joint reactions predicted for collective and distributed body weight loading patterns is made for both genders for the 19 intervals.

7.3.2 Compressive Force at Intervertebral Level

Both figures below show an increase in compression forces descending the spine reflecting the cumulative effect of body weight forces. Also the values are all positive, indicating the reaction force is directed upwards to satisfy equilibrium with the downward component of body weight. Both loading patterns also show the compression in the erect posture, and least in the flexed posture. In the erect posture, the depth of the thrustline curve is small and the path of the thrustline runs closer relative to the joint axes resulting in a greater compression component. In contrast, in flexion the depth of the thrustline curve is increased. Thereby increasing the shear components of force and decreasing the corresponding compression.

The nature of the compression curves is different for point force and distributed loading. In distributed loading, the transition is smooth along the spine units (Figure 7.25); however with point force loading pattern the loading is sharp (Figure 7.26). For higher loads, this might result in an estimation of an injury, although it is not the case. The distributed loading pattern is more realistic to predict injury for this reason.

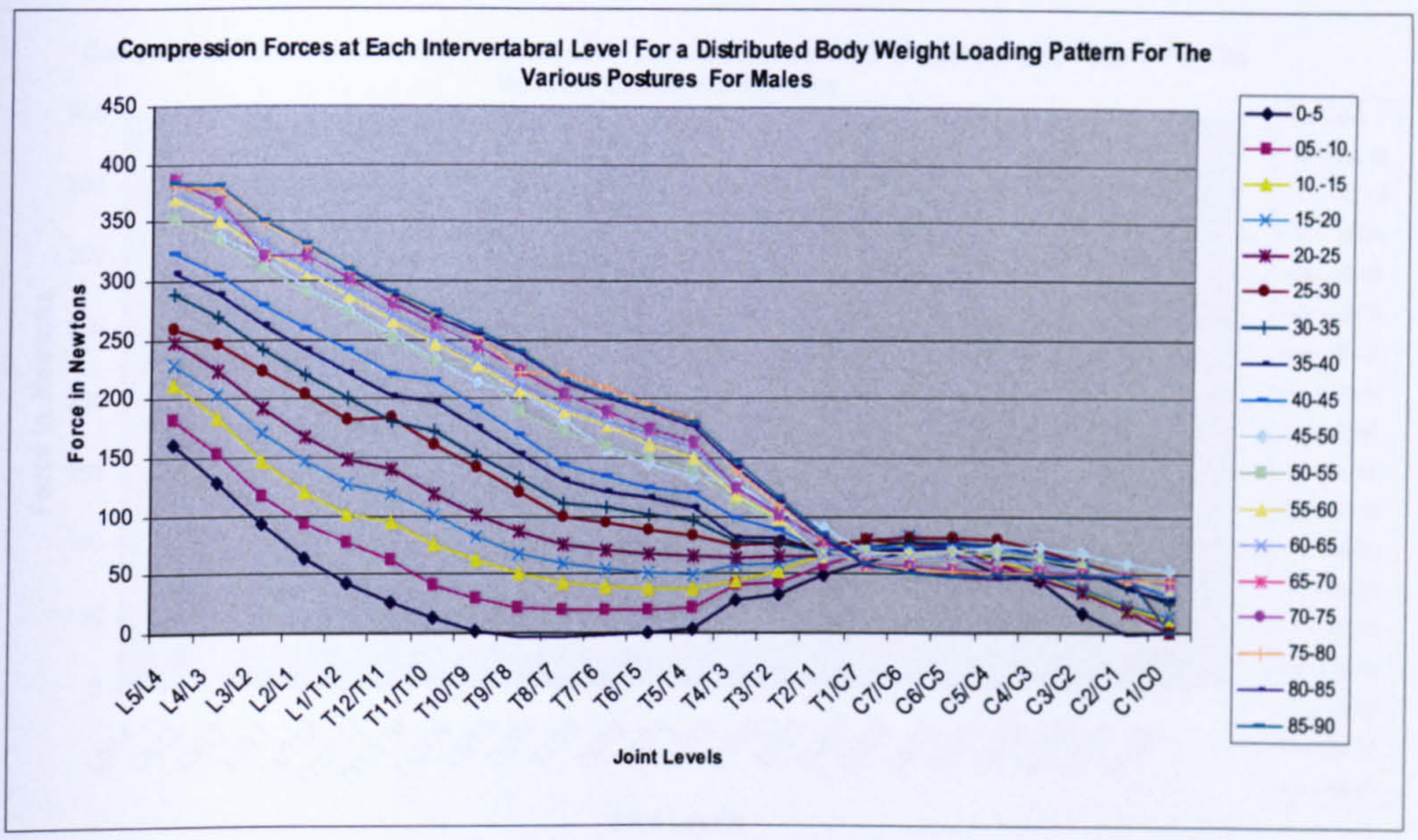


Figure 7- 25 Compression values at each inter-vertebral level for a distributed bodyweight loading pattern for the various postures for males.

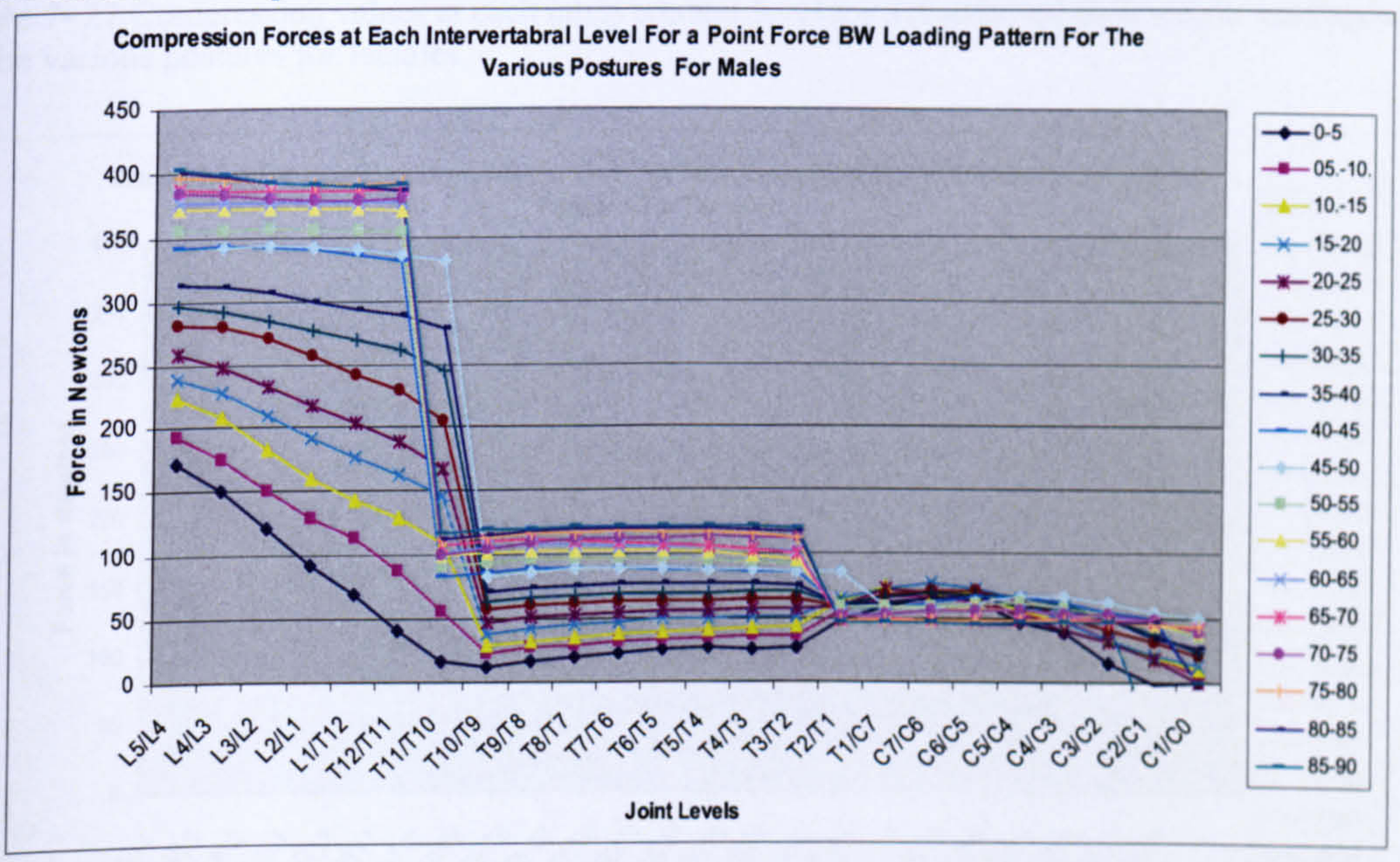


Figure 7- 26 Compression values at each intervertabral level for a point force loading pattern for the various postures for males.

For females, the pattern of the loading is similar with the males. However, the magnitudes of the forces acting on the intervertebral joints are less than the males (Figure 7.27, Figure 7.28).

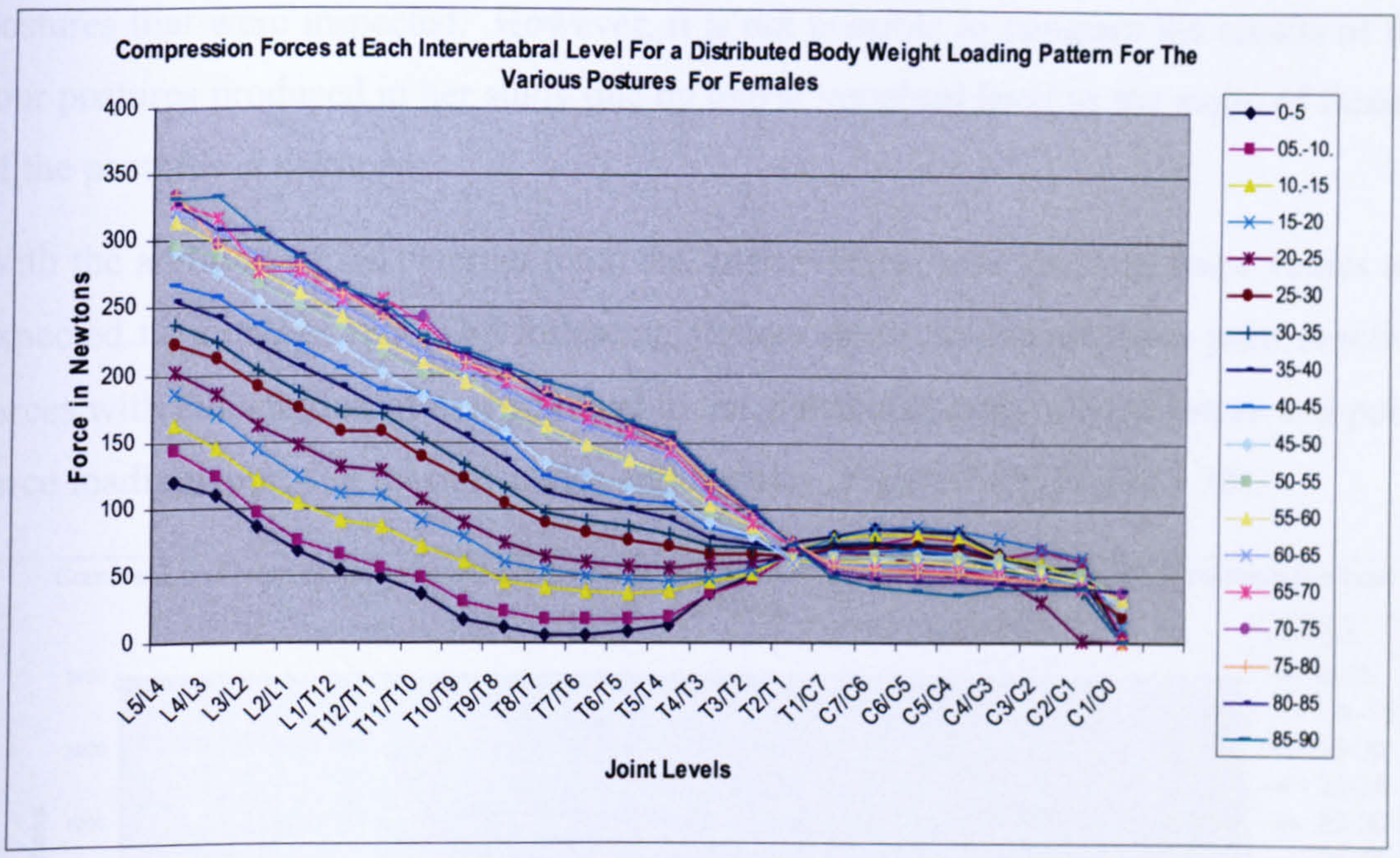


Figure 7- 27 Compression values at each intervertabral level for a distributed bodyweight loading pattern for the various postures for females

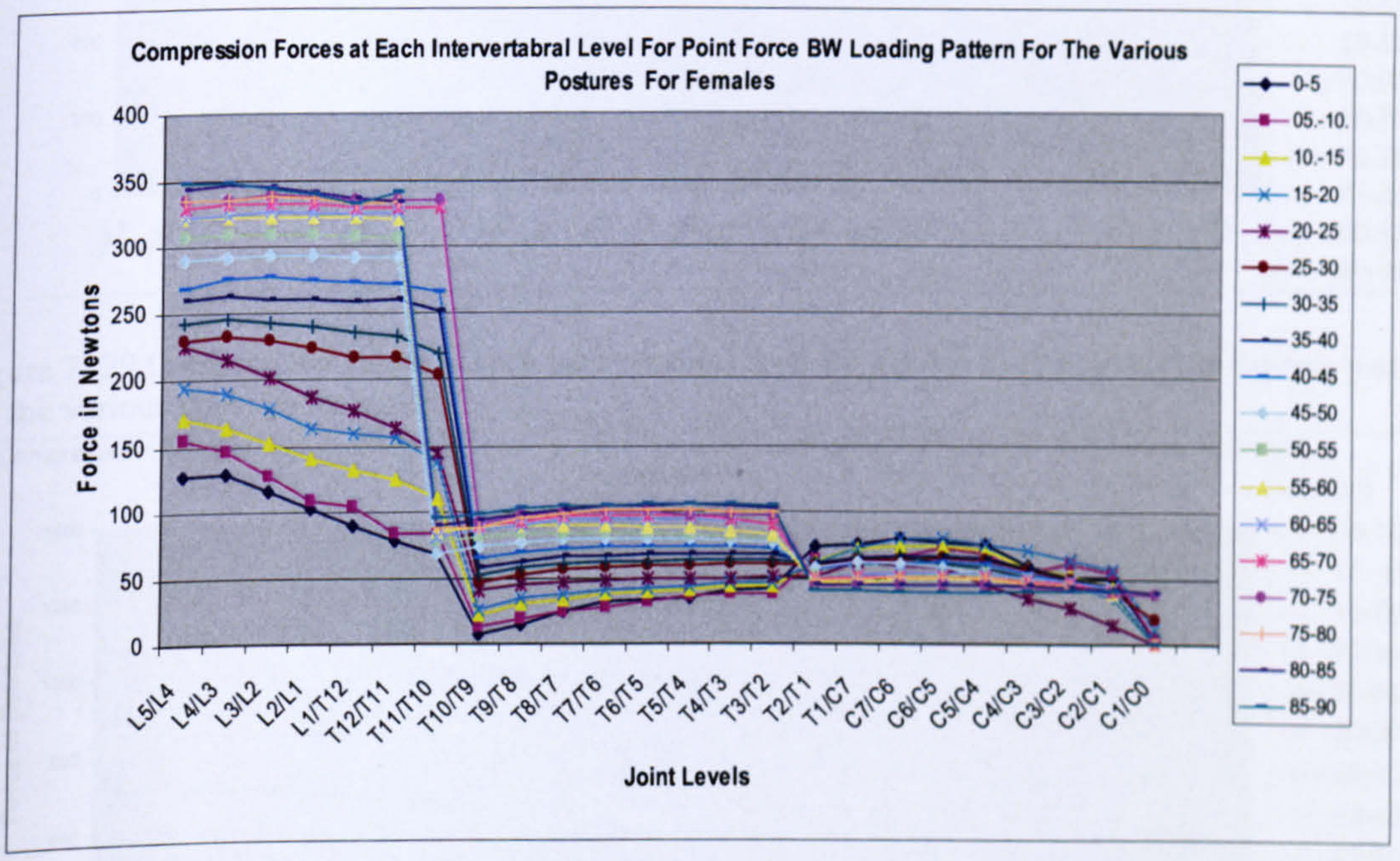


Figure 7- 28 Compression values at each intervertabral level for a point force bodyweight loading pattern for the various postures for females.

Grilli (1997) evaluated joint reaction forces for four different postures starting from fully flexed posture to fully erect posture. However, the results had no gender specific information. The joint reaction forces produced in this thesis show a similar trend with the joint reaction forces calculated in the study of Grilli. The magnitudes of force in her study for compressive forces have the peak value compressive value at L5/L4 with 350N, 330N, 270N, 170 N. Our results are also inline with her study for the similar

postures that were inspected. However, it is not possible to compare the results of the four postures produced in her study one by one at vertebral level as the angle of flexion of the postures is unknown.

With the addition of the external load, the intervertebral joint reaction force values are expected to increase also. The following figures show the compressive joint reaction forces with the addition of external load to the distributed body weight forces and point force loading approach for both males and females (Figure 7.29, Figure 7.30).

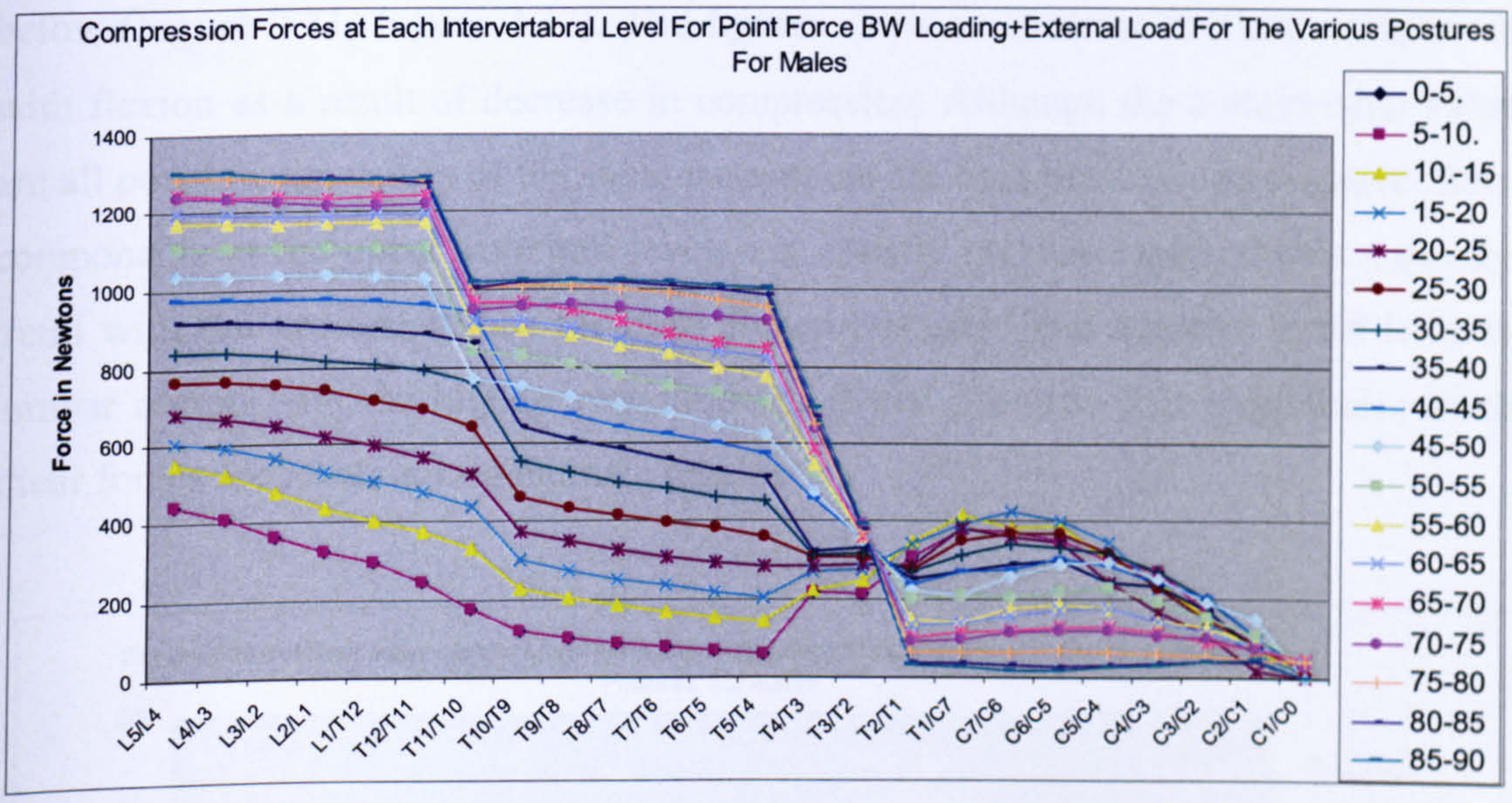


Figure 7- 29 Compression values at each intervertabral level for a point force bodyweight loading pattern for the various postures for males.

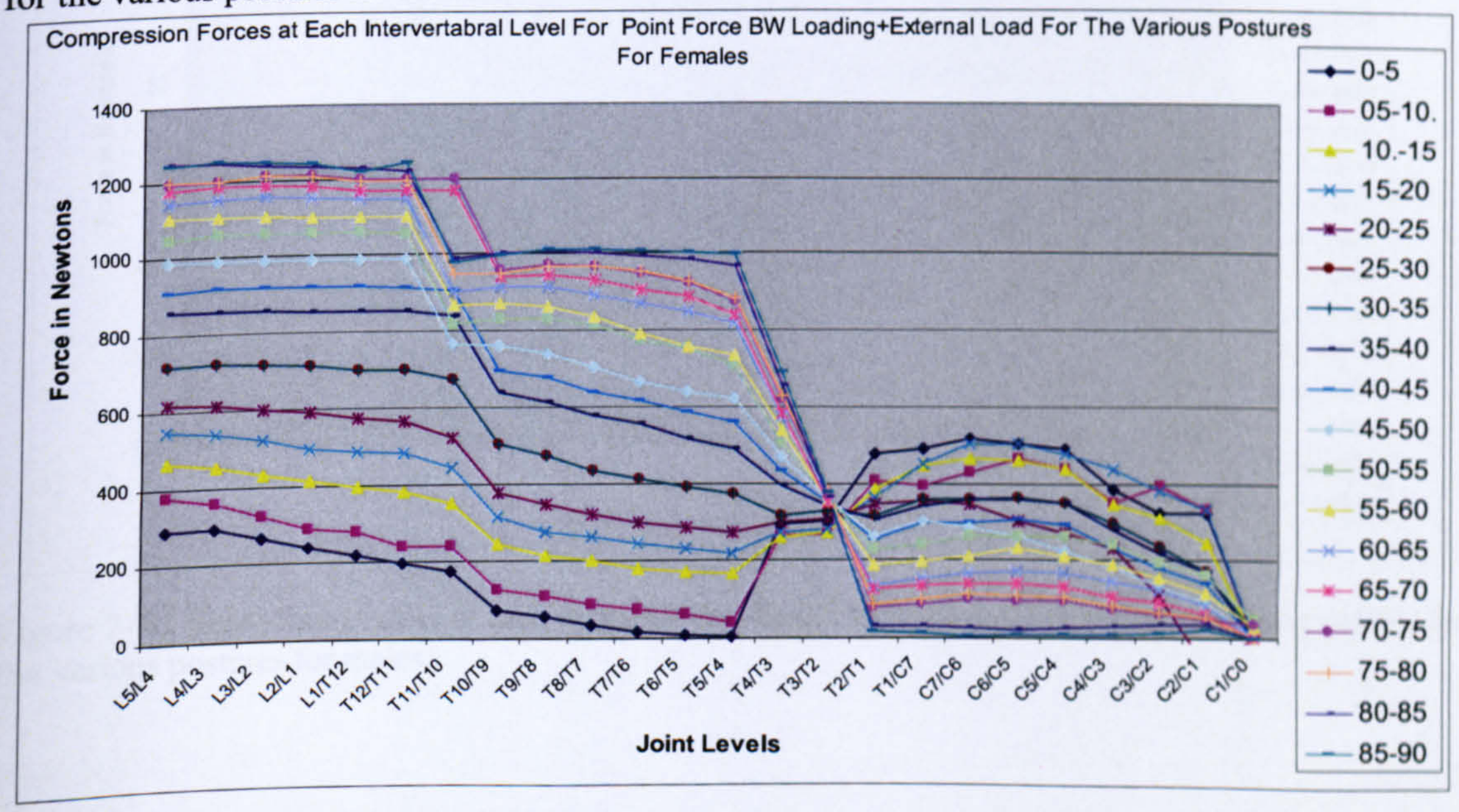


Figure 7- 30 Compression values at each intervertabral level for point force bodyweight loading pattern for the various postures for females.

The pattern of the intervertebral joint reaction forces with point force body weight and external load is similar. For males there is not much difference for the compressive force values of the intervals 0-5 and 5-10 degrees of reference line angle, whereas for females there is little difference in between these two intervals.

7.3.3 Shear Force at Intervertebral Level

The distributed force loading pattern for males and females is provided as in the figures below (Figure 7.31, Figure 7.32). The figures show an increase in shear components with flexion as a result of decrease in compression. Although the compression values are all positive, the values of the shear component are both positive and negative. Shear components at the upper vertebral levels i.e., mostly cervical spine, shows a positive trend with the greatest values for most flexed postures. The negative trend is in the lumbar region with the highest magnitude in flexed postures. The magnitudes of the shear forces are lower at mid thoracic regions.

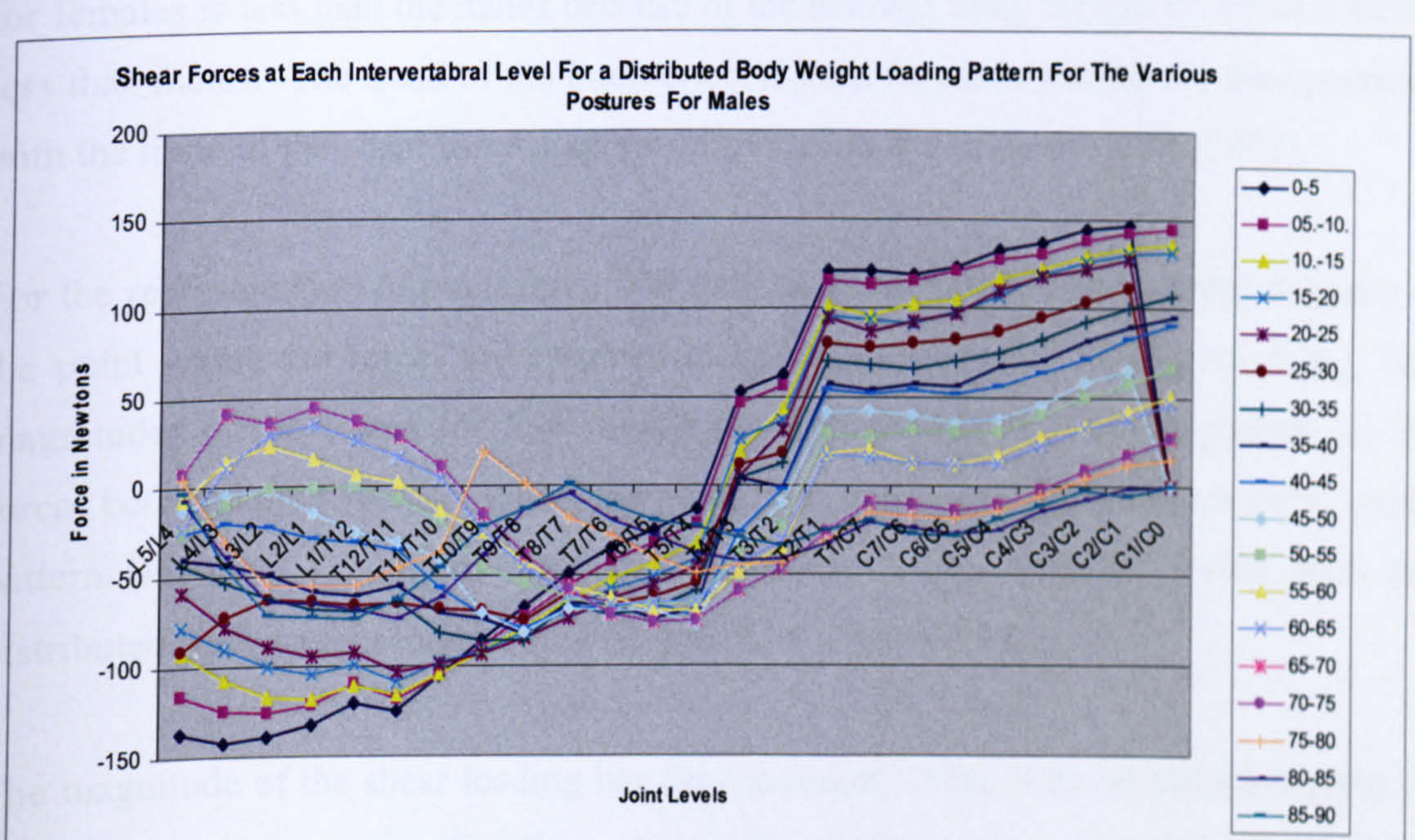


Figure 7- 31 Shear force values at each intervertebral level for distributed bodyweight loading pattern for the various postures for males.

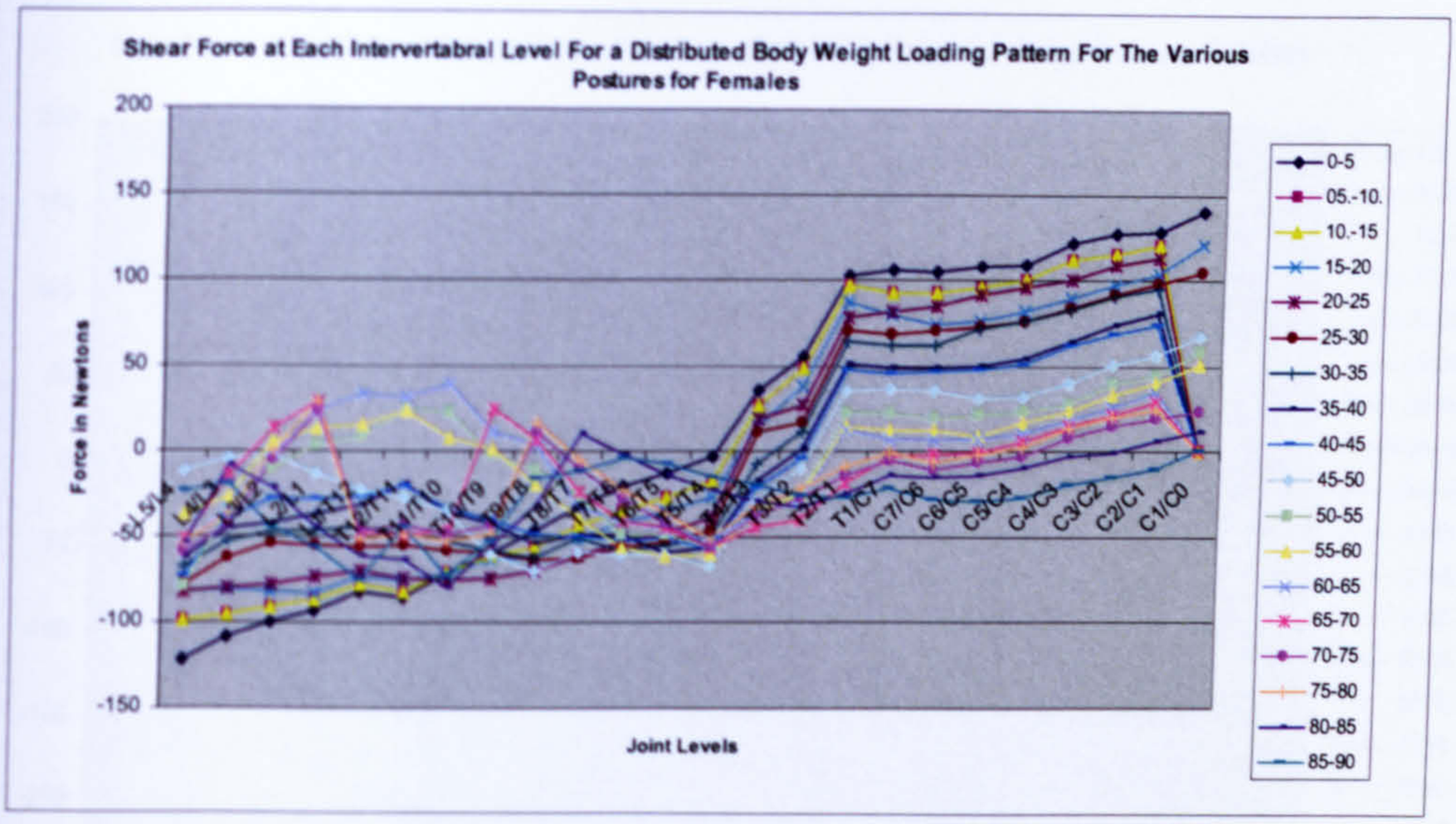


Figure 7- 32 Shear force values at each intervertebral level for a distributed bodyweight loading pattern for the various postures for females.

The figures for females and males show the similar trend for the shear loading for the 19 different reference line angle intervals. However, the magnitude of the shear forces for females is less than the males because of the average body weight of females being less than males. The trend of the intervertebral joint forces is similar for four postures with the trend of the shear force diagrams provided in the study of Grilli (1997).

For the representation of point force BW pattern, shear graphs show abrupt changes at the point where the forces are assumed to be acting (Figure 7.33, Figure 7.34). The magnitudes of the forces for fully flexed postures are higher. The magnitude of the forces between the two cases where the point force loading is applied has a more stable pattern (Figure 7.33, Figure 7.34) in the thoracic region than the forces with the distributed body weight loading case (Figure 7.31, Figure 7.32).

The magnitude of the shear loading has the maximum value at the application point of point force in the negative direction, whereas it was decreasing gradually starting from L5/L4 for fully flexed postures with distributed bodyweight approach. But, the point force BW loading pattern has a peak value for the T10/T9 for the fully flexed postures as shown in the figures below (Figure 7.33, Figure 7.34). The magnitude of the force values for females is slightly less than the males.

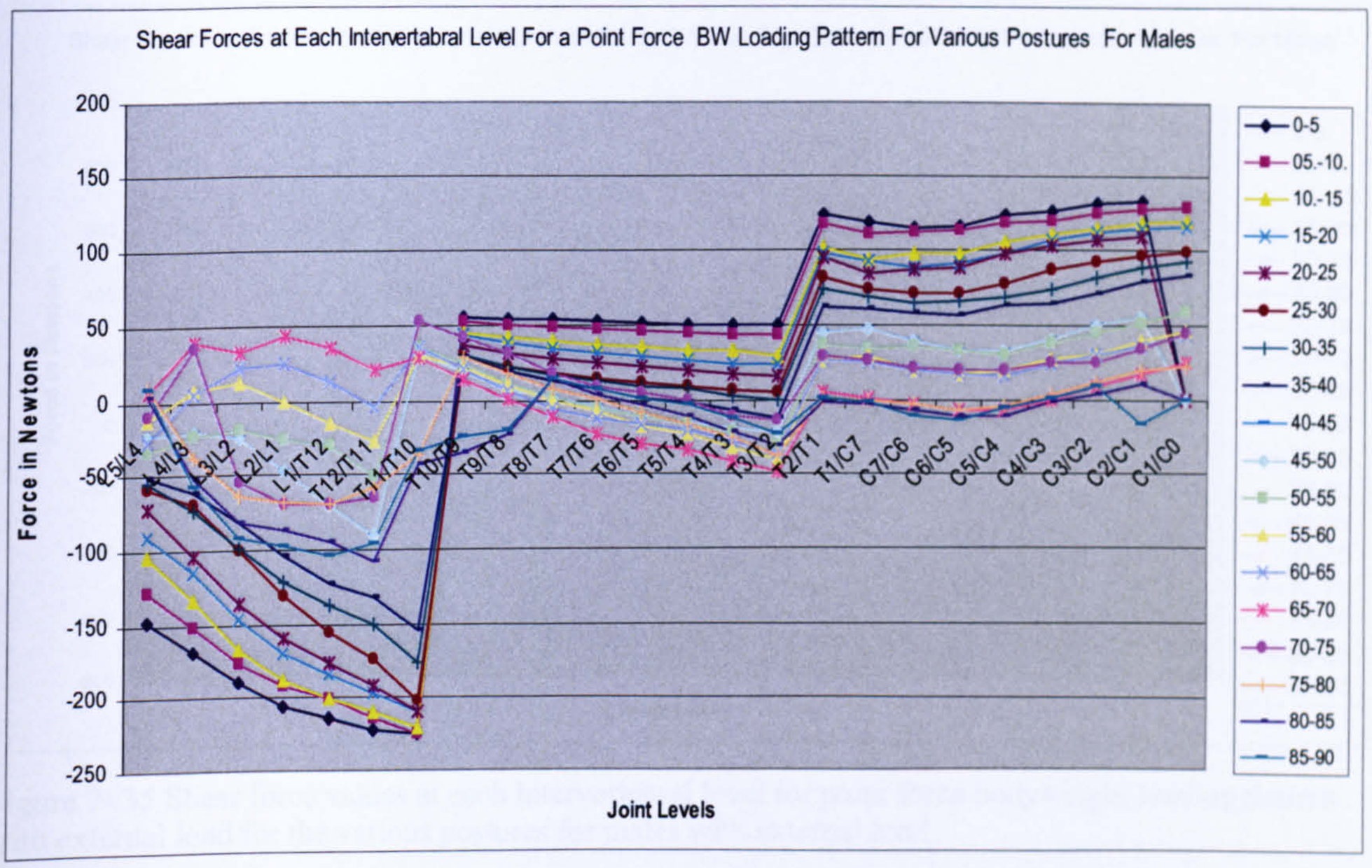


Figure 7- 33 Shear force values at each intervertebral level for a point force bodyweight loading pattern for the various postures for males.

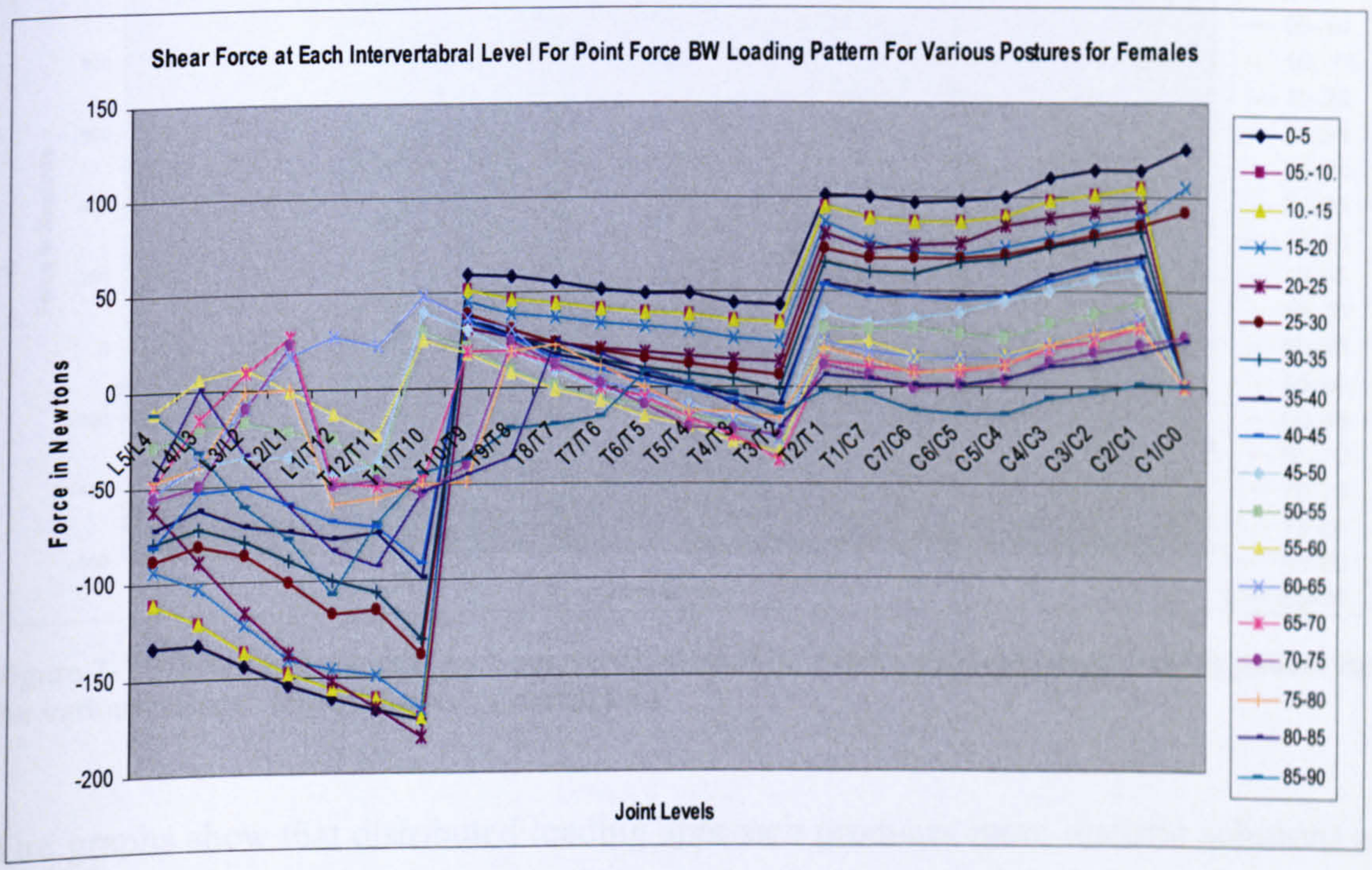


Figure 7- 34 Shear force values at each intervertebral level for a point force bodyweight loading pattern for the various postures for females.

With the addition of the external load to the, case of point force loading, sudden change is observed. The magnitude of the shear forces at the cervical region are observed to increase. Not much difference is observed between the females and males (Figure 7.35, Figure 7.36).

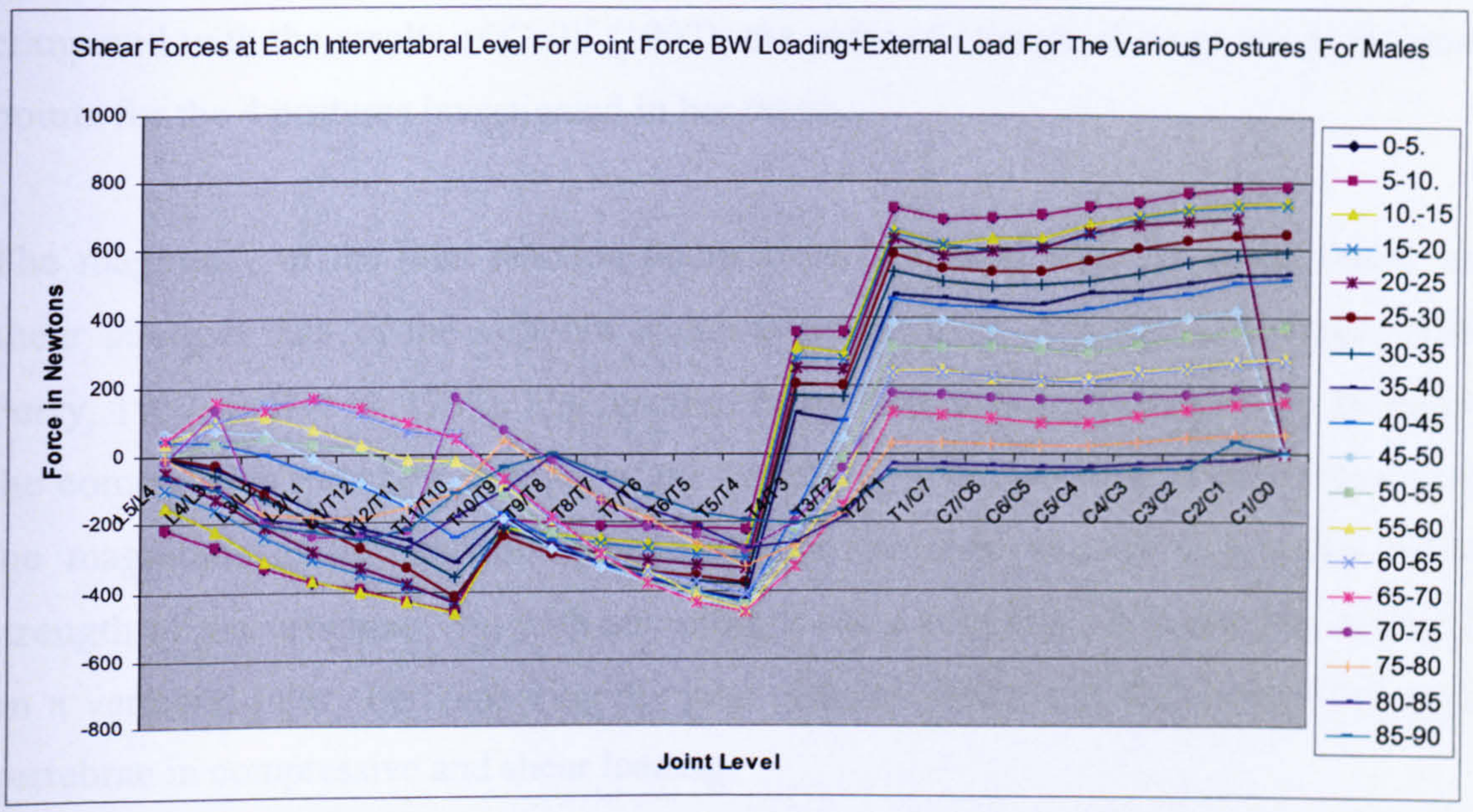


Figure 7- 35 Shear force values at each intervertebral level for point force bodyweight loading pattern with external load for the various postures for males with external load.

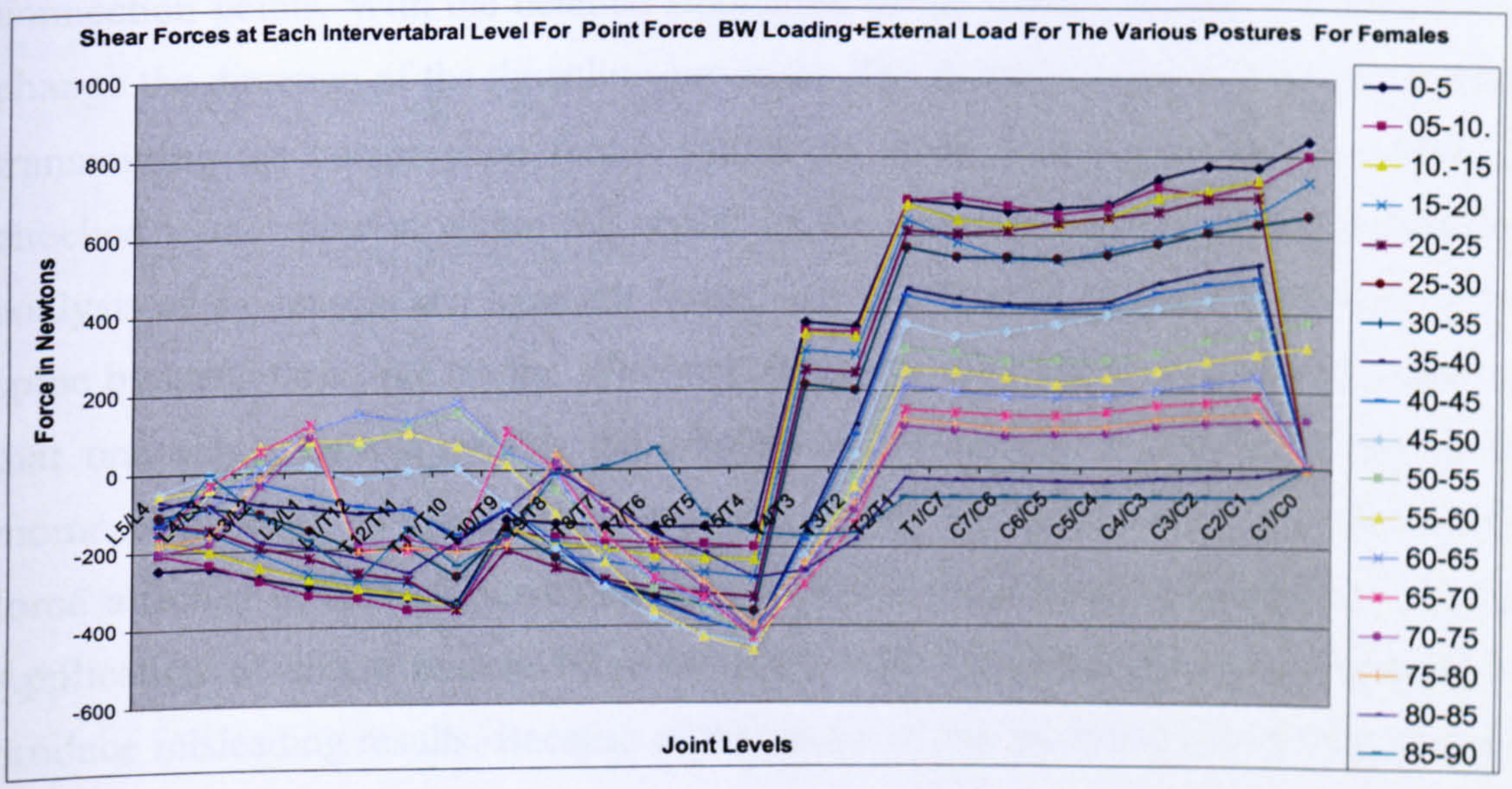


Figure 7- 36Shear force values at each intervertebral level for point force bodyweight loading pattern for the various postures for females with external load.

The graphs show that distributed loading approach produces more realistic solutions as they represent the actual loading on the spine imposed by the body weights. Thrustline changes its direction at the point of application of forces. The distributed body weight forces results in a smooth transition thereby resulting thrustline to follow the spine curvature. This is also reflected in the intervertebral forces. With the point force approach sudden loading is imposed on the intervertebral parts. However, with distributed force approach, transition is observed to be smooth. The results have been

compared with the results of Grilli (1997), the point of change of sings are at the same points for the 4 postures investigated in her thesis.

The magnitude of the joint reaction forces were compared with the compressive and shear strength data of the vertebra which is available in literature (Messerer, 1880, Perry, 1957, Bell et al, 1967). The reaction forces with only body weight are far below the compressive and shear strength of the vertebrae. With the addition of external load, the magnitude of the reaction forces increases but they are still below the failure strength of the vertebrae. But with any other loading condition, it is possible to decide on a vertebral injury by comparing the joint reaction forces and the strength values of vertebrae in compressive and shear loading.

In this thesis, the muscles and ligaments have been simulated in detail in terms of their connection points. With the detailed simulation of the muscle forces, it is possible to change the direction of the thrustline curvature. The thrustline theory is based on spine transmitting the compression forces within the spine boundaries. This condition is checked if the spine is within the region of the spine boundaries. With the detailed analysis of the muscle and ligament forces, it is possible to analyse the stability of the spine by using thrustline theory. Whereas, single muscle force models (SEM), assumes that one single muscle applies the whole force necessary to counteract the spinal moments imposed on spine. With thrustline theory application of one single muscle force attached to spine, causes thrustline to deviate and result in instability already. Application of single muscle force on spine with thrustline theory is expected to produce misleading results. Because of the nature of the thrustline theory, the increase of anatomic detail is appreciated more for thrustline curvature to fit in the spine borders. The results in the previous sections show that thrustline curvature fits in the spine borders except for the fully flexed conditions. In order to avoid from back pain related injuries, fully flexed postures should be avoided.

7.4 Comparison of the Model

7.4.1 Structure

The program is developed in visual basic. From 0 to 90 degrees of reference line angle postures for each gender with 5 degrees of increments have been recorded in excel files. The model is parametric with respect to weight of each person. The vertebrae dimensions are scaled accordingly. Distributed body weight forces are defined to act with an eccentricity to the centre of each vertebra.

The code is developed in Visual Basic to have any number of muscle groups as long as the number of attachment points and the amount of the force provided by the muscle is defined. For ligaments, the coordinates of the erect postures are read from the excel sheets to calculate the strain to be inserted into ligament force calculations. The program sorts all the forces defined along the reference line with respect to their distance. The y coordinate values of the forces applied on the spine are the same with coordinates of the thrustline. For this reason, y coordinates of the forces acting on the spine needs to be sorted in y dimension. The algorithm uses MsFlexGrid option to sort the forces in y direction. This makes the algorithm fast and efficient.

7.4.2 Compatibility of the Results

In the erect posture, the predicted compression at L5/S1 intervertabral joint when supporting the body weight using the distributed loading patterns is 405 N for males and 355 N for females. In the study of Dolan and Adams (1995) in quiet standing this is reported as 500N.

For flexed postures, intra discal pressure was predicted by Schultz et al (1982). For subjects with a trunk flexion angle of 30 degrees with the arms extended with the external load, the intra discal pressure is approximately 1040 KPa at L5. This corresponds to a force of 1736.1N. In this study for the intervals of 65 to 70 degrees of reference line angle and 70 to 75 degrees of reference line angle interval can be compared with the posture that they measured. In this model, for males, 1280 N and for females 1265 N forces is estimated at L5. These values are lower than the value reported by Schultz et al.

While the current model predicts muscle combinations which satisfy stability, they may not represent the actual loading pattern on the spine. The actual loading can be slightly different however, providing stability for one posture is enough to provide the stability; it shows that stability is possible. Precise agreement between in vivo observations and the muscle combinations applied in this model is therefore not expected. However, comparison of in vivo observations and the requirement for force in the model in the erect and the flexed postures provides some validity to the model predictions. For flexed postures, stability has not been observed, for the study of stability by Grilli (1997), the stability for the fully postures have not been observed either.

Comparison with in vivo measurements of intra discal pressure provides some indication of the expected joint reaction for the muscle recruitment patterns applied in the model. Combinations of muscle groups which satisfied stability involved a different numbers of muscle groups for each interval of reference line angle. Although these patterns are not indicative of the actual spinal loading, the predicted joint reactions for the model do not exceed the reported values by Messerer, 1880, Perry, 1957, Bell et al, 1967.

Muscle groups which generate significant extension moments are longissimus thoracis, iliocostalis lumborum, multifidus and semispinalis capitis in the upright posture, whilst psoas he abdominal muscles generates significant flexion moments. This corresponds to their respective roles of extension and flexion described in anatomy textbooks. The superficial lumbar erector spinae muscles longissimus thoracic and iliocostalis lumborum have also been reported to be well positioned to generate significant bending moments on the spine and control overall movement (Aspden, 1992, Bergmark, 1989).

The requirement for muscle force varies with each individual posture, according to the vertebral configuration and the overall direction of the reference line. In the erect posture the amount of the muscle force available is far greater than that required to counter act the flexion moment due other external load and body weight in this posture. The problem is to determine the combination of the forces required local application of small amounts of muscle force in the cervical and lumbar regions. Electromyography activity recorded for in vivo studies during upright standing confirms the inactivity of

the large extensor muscles semispinalis capitis and the erector spinae (Takebe et al, 1974, Floyd and Silver, 1955).

In flexion, the force patterns identified in our model demonstrated the requirement for greater muscle force to be generated. The roles of the main extensor muscles (semispinalis capitis, longissimus thoracis and thoracic iliocostalis) become significant. Under these loading conditions, the effects of an increase in force due to the curved representation of longissimus thoracis and thoracic iliocostalis become evident. In fully flexed postures, with the muscles and ligaments, even the maximum contraction of these muscles is not sufficient to maintain stability. This is inline with observations of Grilli (1997). The observations of Schultz et al, (1985) who reported activation of the back muscles in fully flexed posture when supporting an external load supports the reasoning for the deactivation of erector spinae muscles in fully flexed postures.

A number of studies have reported minimal activity of the large superficial spinal muscles in the fully flexed posture (Floyd and Silver, 1955, Schultz et al 1985, Andersson et al, 1996). Schultz et al (1985) report EMG activity measured at the L3/L4 level for this position was less than in the upright standing position and was minimal for both surface and deep erector spinae muscle activity. Floyd and Silver (1955) suggested in fully flexed postures the ligaments are the dominant forces acting to support the spine, while Adams et al (1980 and Adams and Dolan, 1996) have reported in full flexion the ligaments resist approximately 70% of the bending moment.

The amount of force generated within the ligaments depends on the extent of stretching and hence the extent of spinal flexion. The amount of flatting supplied by the ligaments is increased with the flexed postures and decreases as the spine gains an erect posture. When combined with the intersegmental muscles i.e. multifidus a further flattening effect was observed but this was not sufficient to ensure stability. Additional force is therefore required in this posture, supporting the findings of Anderson et al (1996).

The applied force in our model is assumed to be generated by active contractile elements of the muscles and the passive force generated by stretching of the muscle with flexion is ignored. McGill and Norman (1986) previously estimated the contribution of the lumbar muscle forces due to stretching to the overall extension

moment required for a lifting activity. They reported due to the lifting strategy employed in which subjects' maintained lumbar lordosis, the contribution due to muscle stretching is approximately less than 2%. However, fascicles of longissimus thoracis and thoracic iliocostalis which extend over several layers of the thoracic spine were predicted in this model to be significantly affected by curvature in the flexed postures. The length of these fascicles is therefore likely to be increased by the curvature and the passive components of force may be more significant.

7.5 Discussion

Determination of a thrustline for a given configuration and for a given set of loading conditions is an immediate visible indicator of equilibrium and stability of the spine. The transmission of the compressive force within the spine indicates the stability. Without the muscles, it is not possible to maintain stability in fully flexed postures. Although the stability could have been improved by activating the erector spinae muscles for flexed postures, this was avoided considering the information in literature. The addition of number of muscles showed that stability of the spine is improved.

The thrustline curvature follows a smoother path with the increased number of muscle groups. The external load acting is chosen to be 900 N as to challenge the spinal stability with high loading. Fully flexed postures are not stable with 900N external load. However, the addition of ligaments to the model improves the stability. But still for fully flexed postures, instability persists. For this reason, fully flexed postures should be avoided. Any design which helps to improve spinal stability should eliminate the postures which are fully flexed.

7.6 Conceptual design suggestions for lifting

In the analysis conducted so far it is found out that both for females and males fully flexed spinal postures are considered to result in unstable postures when the external load is applied. This is caused by an increase in shear force values. The thrustline deviates from the spine borders indicating instability.

A case study for a lifting activity in this research is chosen as lifting an object from the boot of the car. It is common for a person to flex their body when they lift an object.

To eliminate the extreme flexed postures, design suggestions which prevent people from bending their spine are made.

Three conceptual design alternatives have been proposed. With the help of these design changes flexion of the spine is reduced. The amount of time that the body interacts with the load is also reduced. As the interaction time with the load decreases, the possibility of getting an injury with less flexed postures decreased.

7.6.1 Conceptual Designs

7.6.1.1 Alternative 1

When a person aims to lift the load from the boot of the car, the first thing is to flex the spine as much as possible to reach the load. To eliminate the flexion of the spine in the vertical direction, it is proposed that the load should travel in the vertical direction towards human body. For this purpose, a scissor lifts have been considered to be mounted in the boots of cars. Scissor lift has two bars attached to each other with a revolute joint on each side of the platform (Figure 7.37). The vertical motion of this table is provided by hydraulic pistons driven by a pump. The height to which the load should travel can be controlled by position sensors

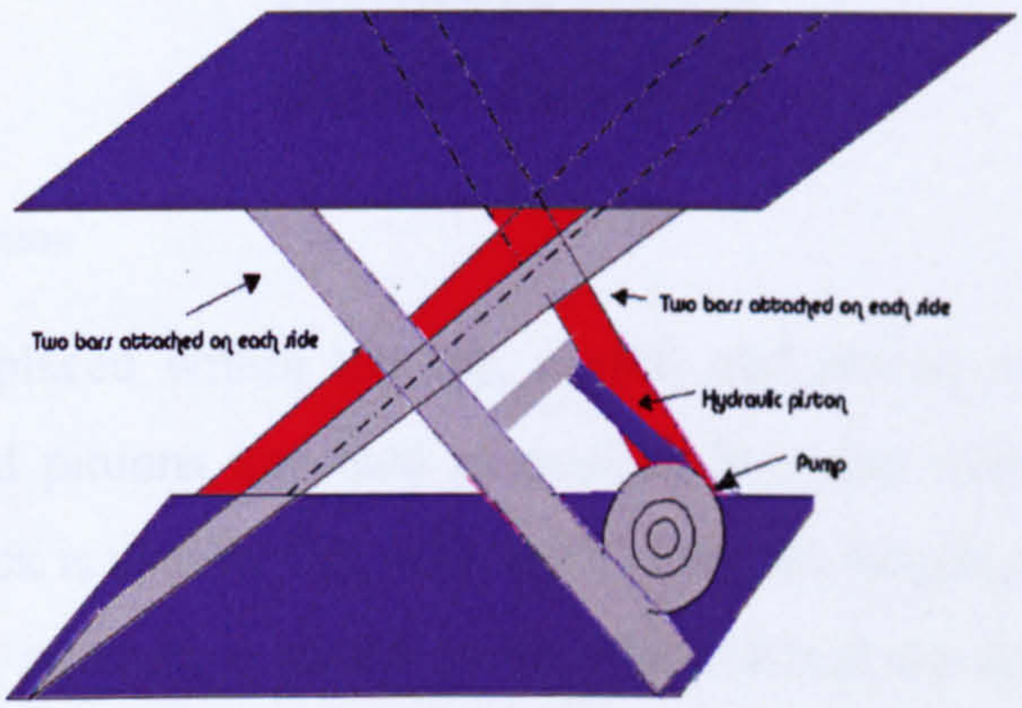


Figure 7- 37 Scissor lift

When the person aims to lift the load from the boot of the car, the boot of the car is opened first. By triggering the scissor lift, the load travels in the upward direction (Figure 7.38) and there is no need to flex the spine to reach the load. It is expected that

this way reduces the postures at which the reference line angle of the spine is within the 0-30 degrees range.

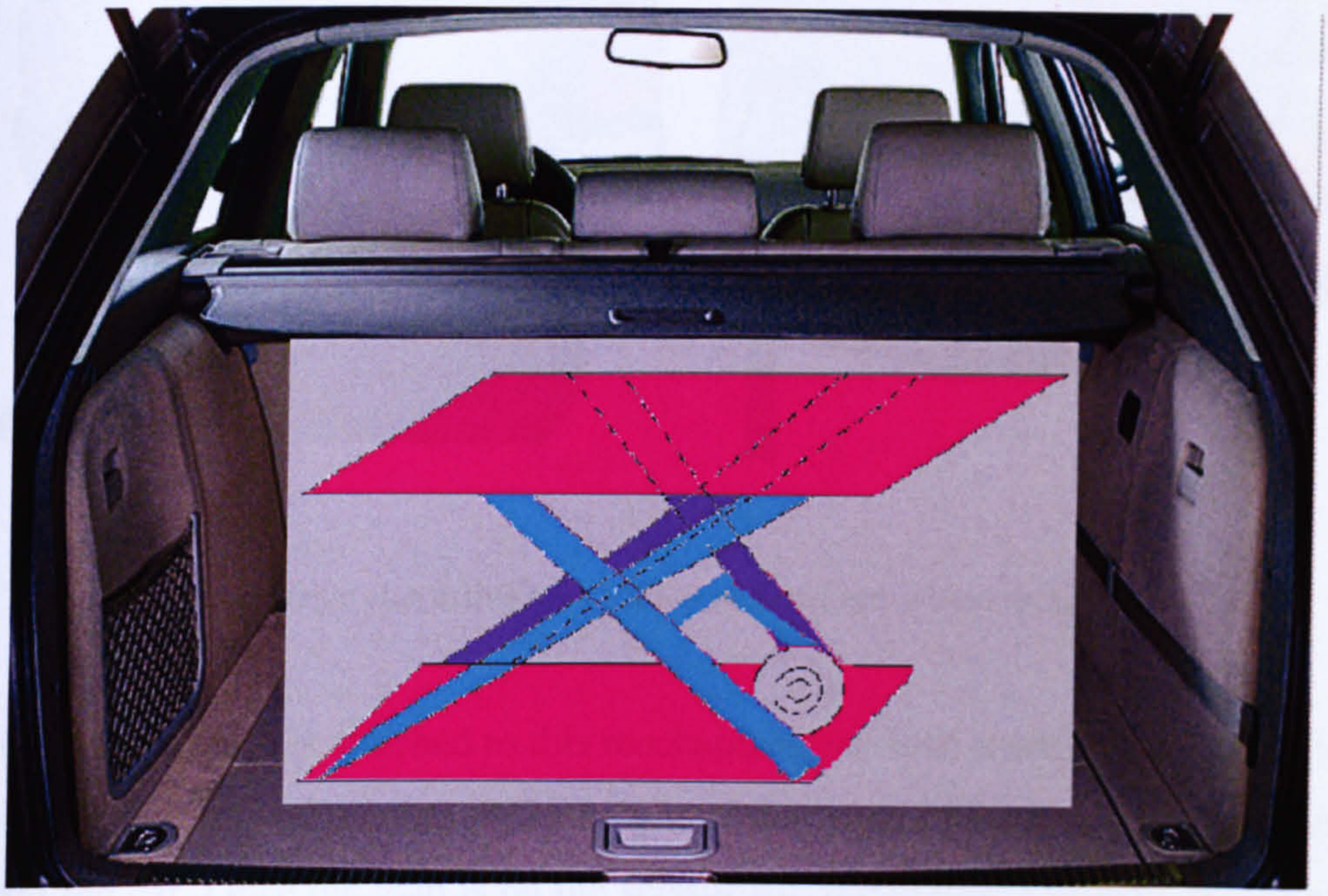


Figure 7- 38 Conceptual design alternative scissor lift mounted in a car boot.

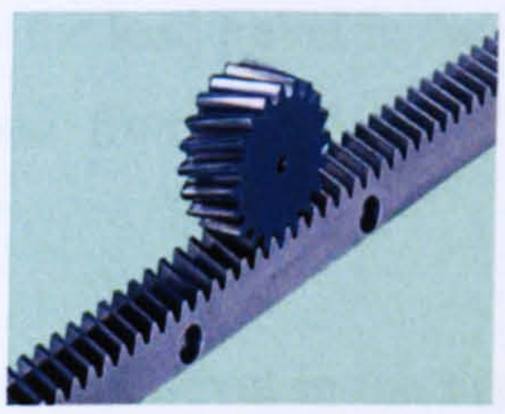


Figure 7- 39 Rack and pinion

For the load to be placed within the car, a rack and pinion mechanism can be an alternative. Rack and pinions are used to convert between rotary and linear motion (Figure 7.39). The rack is usually flat, with teeth along the length and pinion is the gear. Pinion is attached to an electric motor to be driven along the teeth to provide rotary motion around its own axis.

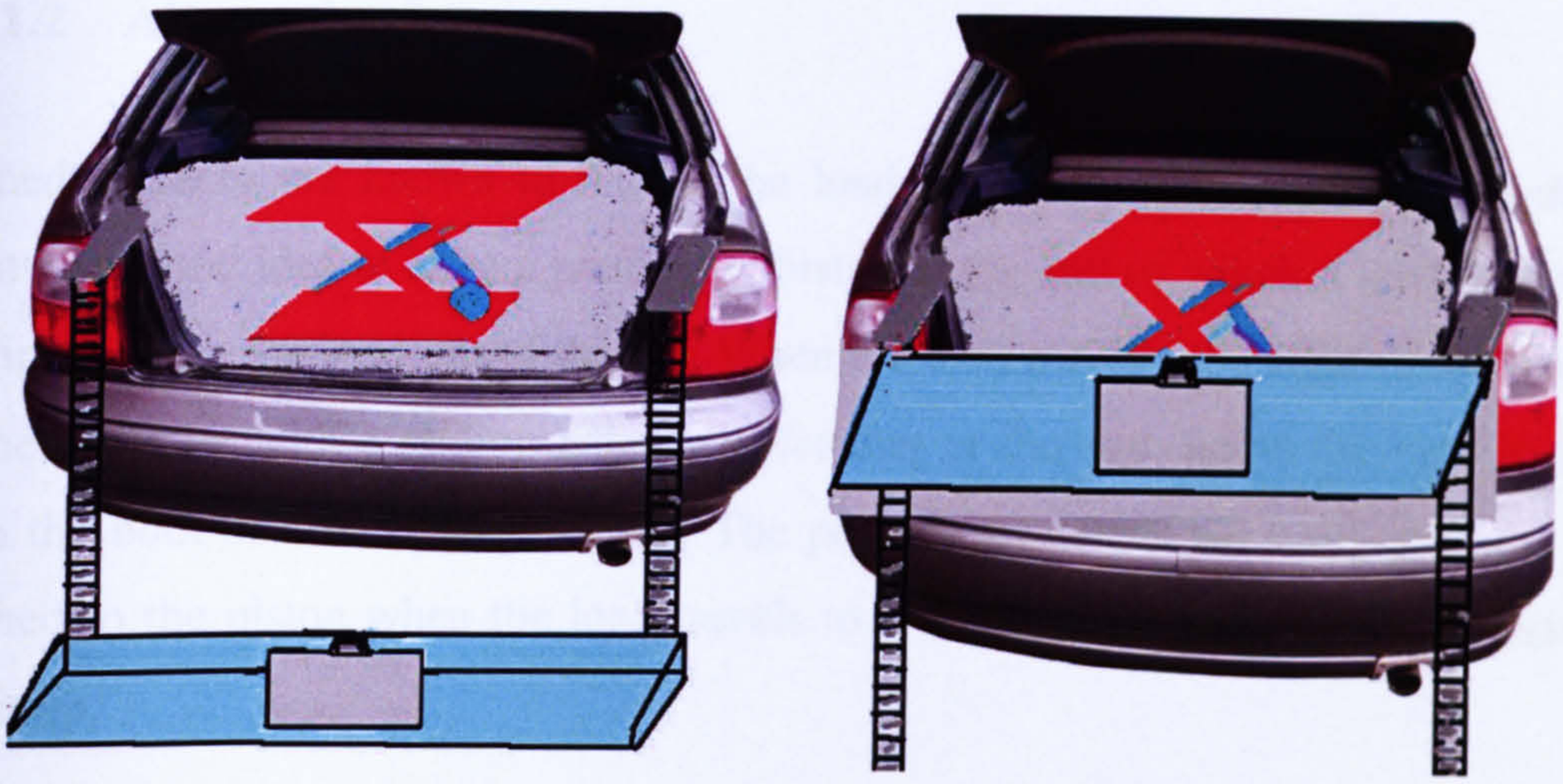


Figure 7- 40 Conceptual design alternative for a load to be lifted into a boot space.

A horizontal platform is attached to this mechanism; the load travels along the height of the boot. When the load reaches to the height of the scissor lift, the person can push the load into the car. Once the load is on the scissor lift, the pressure sensors on the scissor lift sense that the load is on the tray so that the scissor table starts lowering itself.

The first part (scissor lift) moves the load travel in the vertical direction to eliminate the spine flexion for lifting the load from the boot of the car. The first part can be integrated within the car trunk.

The second part however lets the load travel in the vertical direction for the loading of the boot. This is also expected to reduce the interaction of the person with the load and eliminate flexion. The only interaction with the load in this mechanism is the pushing of the load to the car boot which is equivalent to

$$F=\mu.N$$

Where μ is the coefficient of friction and N is the reaction force equivalent to the weight of the load. Usually μ is less than 1 and the resultant force is less than the weight of the load. With this conceptual design alternative, the flexion of the spine and the interaction with the load is reduced.

7.6.1.2 Alternative 2

Inclined surfaces are known to reduce the load. For cars, which have high boots, it might be a good idea to have a pneumatic piston at the end of which a load is attached by clips to push the load out of the car. When the load reaches the edge of the boot, an inclined surface with a sliding belt on it, leaning at the end, helps the load to travel down the boot of the car (Figure 7.2). The person can detach the load from the clips attached to the piston when the load travels to a comfortable position for a person to pick it up.

In this way, the interaction of the load with the person is eliminated. The inclined surface with the conveyor belt on is external to the car and easy to use. The piston system can be integrated within the car as a part of manufacturing. It might be optional to exclude the inclined surface if the height of the car boot eliminates the fully flexed postures. The piston itself helps the load to travel within the boot thereby eliminating the need to reach the load and stretching of the spine.

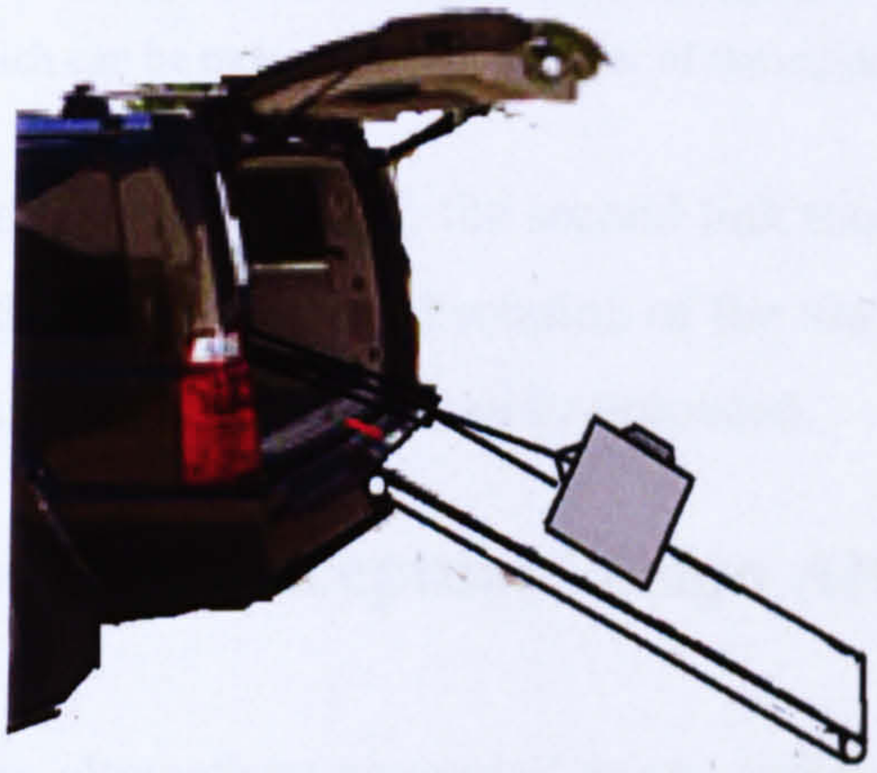


Figure 7- 41 Piston-rope-clips and an inclined surface for cars having a higher boot.

For loading the car boot, reverse motion of the load is expected. The load travels along the inclined surface while the piston retracts itself so that the load is positioned in the car boot.

7.6.1.3 Alternative 3

A lifting arm is attached to the tow bar of the car. After the load is attached to the rope of the arm, first the motor unit winds the rope up so that the load moves upwards along the z axis (Figure 7.3). With the rotation of link1 around the z axis, the load is aligned with the middle section of the car boot. The second motion is to align the load with the car boot by rotation of link 2 around z axis. The rope starts unwinding and stops when the load touches the surface of the car boot with feed back from pressure sensors aligned within the car.

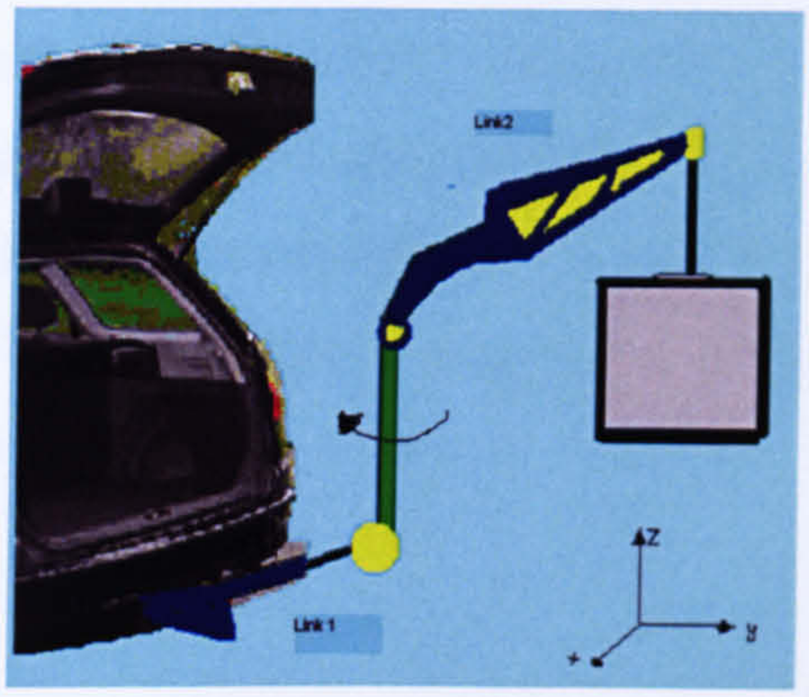


Figure 7- 42 Rotary arm which can be mounted on the tow bar of the car during lifting.

While unloading from the boot of the car, the second link rotates around the z axis and moves the load out of the car. The second rotation of the load, around z axis takes the load into its initial position where the load can be unloaded.

7.7 Evaluation of the Conceptual Design Alternatives

The main criteria for the alternatives suggested are to reduce the flexion of the spine and eliminate the interaction of the load with the people to reduce the loading on the spine. The alternatives are thought to alter the postures of the spine while lifting an object from the boot of a car.

In order to decide which alternative is the best in terms of spinal stability, it is recommended to produce prototypes of the conceptual designs. With these prototypes, the postures of the spine when the person interacts with the load should be recorded by spinal mouse to check the stability in the thrustline model written in VB. With the

available postures, it is possible to check stability by thrustline theory for a person with their spine measurements and anthropometric data known. It is possible to expect some changes in the conceptual designs depending on the result of the experiments with the prototypes and simulation analysis if they still produce unstable postures.

In this research, we mainly focused on lifting an object from the boot of a car. In the alternative design suggestions, however, we still consider the loading of an object into the car boot. But, we do not know much about the postures of the spine while loading the object into the car. The conditions for loading of an object into the car boot are mentioned to complete the full picture for loading and unloading an object. It is still recommended to consider the postures while loading an object into the car boot first, as we investigated in this research for unloading an object from the boot of a car. So that it is possible to know what kind of postures should be avoided by analyzing the postures. The new postures gained by the alternative suggestions for loading the car boot should also be checked for spinal stability.

CHAPTER 9

8 Conclusions and Recommendations

The rationale behind the research described in this thesis was that a mathematical model of the full human spine model which is capable of simulating the lifting postures that could help understanding the injury of mechanism of back pain. The objective of the research is to develop a model that could investigate the spinal stability which can be an indicator of an injury to the spine due to the failure of transmission of compressive forces within the spine. As well as being able to predict the failure of compressive forces for the postures of body during lifting an object from the boot of a car, the soft tissue failure of the ligaments and any structural failure of the vertebral bodies to due to compressive and shear forces can be estimated.

This chapter summarises the development and validation of the full human spine model described in this thesis and reviews the findings of this research.

8.1 Model Development

The mathematical model described in this thesis represents the full human spine for 19 different interval of reference line angle for both genders. Implemented in Visual Basic, the model comprises 24 vertebrae as rigid bodies, in addition to detailed muscle and ligament attachments to the vertebrae. The configuration of vertebrae is based on the experimental measurements of spine curvature of 20 male and 19 female subjects; the space between the rectangular representations of the vertebra represents the discs. The soft tissues of 38 muscle groups presented by force vectors acting on the spine with AL, PL and LF ligaments for the cervical and lumbar regions have been defined.

The code is produced flexible enough to include several muscle and ligament combinations for the understanding of the mechanism of injury due to spinal instability. The model is capable of reflecting the effect of different body weights acting on the spine by entering the weight of the person. With the produced generic male and female

postures according to the experiment results, model is applied to investigate the differences of stability between the male and the females.

The model also calculates the reaction forces at the inferior surface centre of L5 and at the superior surface centre of C1 in addition to calculating moment values acting on the L5/S1 by using the lever theory to compare the differences. The model produces the coordinates of the thrustline curvature, intervertebral joint reaction forces and the calculated ligament forces depending on the elongation of the ligaments according to the selected posture. These data is stored in tabular format in VB forms as an output and can be transferred to Excel for graphical representations of the results.

8.2 Contribution to the knowledge

According to the results of the experiment, males were able to bend more by producing postures which have a reference line angle of -15 to -10 degrees. The produced data shows that the male and female spine has differences especially for the lumbar spine in X axis. This shows that muscles and ligaments have different moment arms for the same interval of reference line angle for both genders.

Detailed information about the position and orientation of each vertebra in a lifting activity is produced starting from 0° to 90° with 5 degrees of increments. It is believed that with the full spine curvature data in at least 10 postures of 39 subjects would be very useful to the researchers investigating lifting activities.

First, the data based on the results of the experiment is used with the body weight forces only. The results show that stability of the spine for fully flexed postures is very sensitive to the body weight forces. Male spine has more instability for flexed postures than female spine.

Thrustline curvature is sensitive to the application point of any force acting on the spine. The number and characteristics of muscle groups affect curvature of the thrustline. With the improved number of muscle groups, the stability of the spine is also improved.

The effect of each muscle and ligament group on thrustline curvature is investigated for each interval and categorized. This table might be referred by other researchers as guideline in investigation of spinal stability in future. The muscles which are force pairs within the spine borders have less effect on spinal stability. The muscles which have attachments out side the borders of the spine have more effect on thrustline curvature as there is no force to oppose. This study reveals that cervical and lumbar muscle groups are necessary for local control of the thrustline. The stability analysis of the flexed postures shows instability at thoracic spine. This also implies that thoracic muscles are important for improving the stability.

The ligaments do not have much affect on reaction forces at the end points of the spine (superior surface of C1 and inferior surface of L5) because of their close attachment points they have small moment arms. The ligaments are modelled by using the stiffness function so the force applied by them depends on the posture and calculated within the program for the selected posture. Ligament failure is checked by comparing the produced force by the ligaments and force necessary for them to fail. Within the current loading conditions, the ligaments are within the safe region without resulting in any failure. However, for any other case, injury due to overstretching of the ligaments during lifting activities can be estimated with the same methodology.

Fully flexed postures are not stable with 900N external load although the addition of ligaments to the model lessens the instability. However, for fully flexed postures, instability persists. For this reason, fully flexed postures are to be avoided. Any design which prevents instability of the spine should avoid fully flexed postures of the spine. Conceptual design ideas are produced mainly for preventing the fully flexed postures.

The model predictions show that combinations of different muscle groups are sufficient to ensure the conditions of stability of the spine for each posture. A number of other possible thrustlines can be obtained with alternative recruitment patterns of muscles in various states of contraction. The existence of at least one thrustline which satisfy stability can be used to indicate the spinal stability.

Consideration of body weight at each vertebral level is viewed necessary to provide a loading pattern which matches the precise curvature of the spine. Point force loading

results in sharp changes in the thrustline curvature. Distributed body weight approach improves the applicability of the theory to the stability checks in a realistic way. With point force loading approach, because of sudden changes in the path of thrustline, it is possible to predict stable postures as unstable because of mismatch of the thrustline curvature and the spine curvature; however with the distributed body weight approach thrustline curvature has a smooth transition from one vertebral level to the other. Distributed body weight approach is considered as more realistic when compared to point force for flexed postures where the moment arms of the forces acting on the spine have high value. For fully erect postures, since the moments arms of the forces acting on the spine is shorter, there is not much difference in between these two approaches.

An external load 900 N is applied to challenge the spine for fully flexed postures for stability checks. Determination of a thrustline for a given configuration and for a given set of loading conditions is an immediate visible indicator of equilibrium and stability of the spine. Without the muscles, it is not possible to maintain stability in fully flexed postures. The muscle groups were chosen for each posture by using the table which was produced to indicate the role of each muscle group on thrustline curvature and the data from the literature. Although the stability could have been improved by activating the erector spinae muscles for flexed postures, this is avoided as the number of studies observed the minimal activity of the large superficial spinal muscles in fully flexed posture.

The results of this research have conformity with the results of Dolan and Adams (1995) for the compression force at L5/S1 in the erect posture, and with Schultz et all(1982) for intra discal pressure with a trunk flexion angle of 30 degrees. The amount of detail and the number of the postures in this study are immense; it is not possible to find a validation result for the intervertebral joint reaction forces for each interval. The intra-discal pressure measurements at each level and at each interval of lifting activity could be compared with the results of this research.

8.3 Future Work

The muscle modelling due to the increased number of the muscle groups focused on only the muscle cross sectional area parameter. However, muscle force length relationship can be implemented into the code written in VB for a more realistic approach. The muscles are assumed to be 100% activate. With the implementation of the optimisation method, different level of activation patterns can be obtained and checked with the experiments where EMG is used as a future work.

In this thesis, the muscle activation patterns in the model are based on the table produced for their effect on thrustline and the information of muscle functions based on the data from anatomy books. With the support of EMG studies, for each interval of lifting activity, the activation pattern of muscles used in the model can be checked and necessary alterations can be made in the muscle recruitment patterns for each interval. However, the results of EMG studies are also questionable due to the problem of cross talking and difficulty in detecting the deep muscle activity patterns.

The conceptual design ideas to prevent from spinal injuries have been suggested by avoiding fully flexed postures. However, the effect of the suggested designs should be investigated. For this reason, using the prototype produced the spinal curvature data during the lifting is collected and spinal stability check is made. With one group of people who do not make use of the suggested design ideas long term back pain study can be conducted and with the other group who make use of the suggested designs can be compared. With this approach, the impact of suggested designs on long term injury prevention can be evaluated.

In the current study the external load carried is assumed to be a direct extension of the weight of the arms and is applied as an additional load at T2, T3 and T4 levels. Flattening of the thrustline curve mainly by lumbar muscle activity is not sufficient to result in stability at the upper levels of the spine in the flexed postures (0 to 30 degrees of reference line angle). As a future study, the way how the load carried by the arms transferred from the shoulders to the spine can be integrated to the current model.

In this study, the differences between male and female postures have been investigated in detail. In addition to this, the model has the fundamental structure to include the female only muscle and ligament data. Once these data are available, female muscle and ligament data can be incorporated into the model. With the inclusion of male and female data separately to the program, the model can be made available for checking the spinal stability of both genders more accurately. With this approach, better understanding of the mechanism of spinal injuries is expected for both genders. The results could be supported with the EMG studies for both genders to confirm if there are differences between the activation patterns of the muscles depending on the posture.

The intervertebral forces are calculated for each posture during the full span of a lifting activity. The shear and compressive force components at intervertebral joints can be used for FEA for further investigations. It is expected to gain detailed knowledge about the soft tissue injuries with the calculated results for 19 different postures and full spine data. The intra-discal pressure measurements are usually based on point measurements in spine. The results of the FEA measurements can be compared with intra-discal pressure measurements for validation purposes.

Thrustline theory is one of the optimum models that can be used for static case of loading of spine in sagittal plane. The program has its structure for muscle and ligaments once the posture data is available, the code can be applied to any other cases i.e., sitting postures for a research which focuses on the spinal injuries related to long term sitting or effect of office furniture on the spinal postures and spinal stability. With the new results produced design changes in office furniture can be suggested. The code written can be implemented with other software's such as Jack or Anybody so that stability approach can be used in those models also.

REFERENCES

Acar, B.S. and Susannah, L.G. (2002a). "Distributed Body Weight Over the Whole Spine For Improved Influence in Spine Modelling". *Computer Methods in Biomechanics and Biomedical Engineering*, 5(1), 81-89

Acar, B.S. and Grilli, S.L. (2002b). "Matching the Force Requirements in Human Spine Modelling. Studies and Monographs." *International Biomechanics Society*, 63, p. 55-61.

Adams, A. and Dolan, P. (1996). "Time Dependent Changes in Lumbar Spine's Resistance to Bending." *Clinical Biomechanics*, 11(4), 194-200.

Adams, M A. and Dolan, P. (1995). "Recent advances in lumbar spinal mechanics and their clinical significance." *Clinical Biomechanics*, 10, 3-19.

Adams, M. A. Green, T. P. and Dolan, P. (1994a). "The strength in anterior bending of lumbar intervertebral discs." *Spine*, 19(19), 2197-203.

Adams, M. A. and Hutton, W.C. (1982). "Prolapsed intervertebral disc. A hyper flexion injury 1981 Volvo Award in Basic Science." *Spine*, 7(3), 184-91.

Adams, M. A., and Hutton, W. C. (1985). "Gradual disc prolapse." *Spine*, 10(6), 524-31.

Adams, M. A., Hutton, W. C., and Stott, J. R. (1980). "The resistance to flexion of the lumbar intervertebral joint." *Spine*, 5(3), 245-53.

Adams, M. A., Mannion, A. F., and Dolan, P.(1999). "Personal risk factors for first-time low back pain." *Spine*, 24(23), 2497-505.

Adams, M. A., Mcnally, D. S., Chinn, H., and Dolan, P. (1994b). "Posture and the compressive strength of the lumbar spine." *Clinical Biomechanics*, 9, 5-14.

Al-Eisa E, Egan D, and R, Wassersug. (2004). "Fluctuating asymmetry and low back pain." *Evolution and Human Behaviour*, 25, 31-37.

Allread, W. G., Marras, W. S. and Parnianpour, M. (1996). "Trunk kinematics of one-handed lifting, and the effects of asymmetry and load weight." *Ergonomics*, 39(2), 322-34.

Anderson, J.A. (1982). "The Thoraco-Lumbar Spine". *Clinics in Rheumatic Diseases*, 8(3), 631-653.

Andersson, E.A., Oddsson, L.I.E., Grundstrom, H., Nilsson, J., and Thorstensson, A. (1996). "EMG activities of the Quadrestus Lumborum and Erector Spinae Muscles During Flexion-Relaxation and other Motor Tasks." *Clinical Biomechanics*, 11(7), 392-400.

Andersson, G.B. (1998). "Epidemiology of Low Back Pain". *Acta Orthopaedica Scandinavica. Supplementum*, 281, 28-31.

Aspden, R.M. (1992). "Review of the Functional Anatomy of the Spine Ligaments and the Lumbar Erector Spine Muscles". *Clinical Anatomy*, 5, 372-387.

Ayoub, M.M. (1992). "Problems and Solutions in Manual Material Handling: The State of the Art". *Ergonomics*, 35(7/8), 713-728.

B. Myklebust, F. Pintar, N. Yoganandan, J.F. Cusick, D. Maiman, Myers, T.J., and Sances, A. (1988). "Tensile strength of spinal ligaments." *Spine*, 13((5)), pp. 526–531.

Baldwin, M. L. (2004). "Reducing the costs of work-related musculoskeletal disorders:targeting strategies to chronic disability cases." *Journal of Electromyography and Kinesiology*, 14, 33-41.

Basmajian, John V. (1921). *Muscles alive: their functions revealed by electromyograph. Editor* De Luca, Carlo J..

Battié, M.C., Videman, T., Gibbons, L.E., Fisher, L.D., Gill, H. and Gill, K. (1995). "Determinants of Lumbar Disc Degeneration". *Spine*, 20(24), 2601-2612.

Bell, G.H., Dunbar, O., Beck, J.S. and Gibb, A. (1967). "Variations in Strength of Vertebrae with Age and Their Relation to Osteoporosis". *Calcified Tissue Research*, 1(1), 75–86.

Belytschko, T.B., Andriacchi, T.P., Schultz, A.B. and Galante, J.O. (1973). "Analog Studies of Forces in the Human Spine: Computational Techniques". *Journal of Biomechanics*, 6(4), 361-371.

Bergmark, A. (1989). "Mechanical Stability of the Human Lumbar Spine". *Acta Orthopaedica Scandinavica. Supplementum*, 60(230), 5-54.

Bogduk, N., Johnson, G. and Spalding, D. (1998). "The Morphology and Biomechanics of Latissimus Dorsi". *Clinical Biomechanics*, 13(6), 377-385.

Bogduk, N., Macintosh, J.E. and Pearcy, M.J. (1992). "A Universal Model of the Lumbar Back Muscles in the Upright Position". *Spine*, 17(8), 897-913.

Bogduk, N., Pearcy, M. and Hadfield, G. (1992c). "Anatomy and Biomechanics of Psoas Major". *Clinical Biomechanics*, 7, 109-119.

Brand, Ra., Pedersen, Dr., and Friederich, Ja. (1986). "The sensitivity of muscle force prediction to changes in physiologic cross-sectional area." *Journal of biomechanics*, 1986(19), 589-596.

Brinckmann, P., Biggemann, M., and Hilweg, D. (1989). "Prediction of the compressive strength of human lumbar vertebrae." *Spine*, 14(6), 606-10.

Brown, S. H., and Potvin, J. R. (2004). "Constraining spine stability levels in an

optimization model leads to the prediction of trunk muscle co-contraction and improved spine compression force estimates." *Journal of Biomechanics*, Article in Press.

Bureau of Labour Statistics. (1999). "Lost-work time injuries and illnesses: Characteristics and resulting time away from work,1997." Department of Labour, Bureau of Labour Statistics, USDL 99-102, Washington, DC: US.

Burgess-Limerick, R. (2003). "Squat, stoop or something in between?" *International Journal of Industrial Ergonomics*, 31, 143-148.

Burnette, C. S., W (1998). "Issues in using Jack human figure modelling software to assess human- vehicle interaction in a driving simulator." Transportation Research Record 1631:1-7.

Burton Ak, and F, Balague. (2006). "European guidelines for prevention in low back pain." *Eur Spine Journal*, 15(2), 136-168.

Buseck, M., Schipplein, O., Andersson, G.B.J, and Andriacchi , T.P. (1988). "Influence of dynamic factors and external loads on the moment at the lumbar spine in lifting." *Spine*, 13, 918-921.

Bush-Joseph, C., Schipplein, O. , Andersson, G.B.J., and Andriacchi , T.P. (1988). " Influence of dynamic factors on the lumbar spine moment in lifting." *Erogonomics*, 31(2), 211-216.

Cady, Ld., Bischoff, D.P., O'connell, E.R., Thomas, P.C., and Allan, J.H.. (1979.). "Strength and fitness and subsequent injuries in fire fighters - Letter to the editor." *JOM*(21), 724-725.

Caine, M. P., Mcconnell, A. K., and Taylor., D. (1996). "Assessment of spinal curvature:an evaluation of the flexicurve and associated means of analysis." *International Journal of Rehabilitation Research*, 19, 271–278.

Case, K., Xiao, D. C. , Acar, B. S. , and Porter, J. M. (1999). "Computer Aided Modelling of the Human Spine." *Proc Instn Mechanical Engineers*, 213(B), 83-86.

Ceran, M.(2006). "Parametric Human Spine Modelling," Loughborough University, Loughborough.

Chaffin, D. (1969). ""A computerized biomechanical model development of and use in studying gross body actions" *Journal of Biomechanics*, 2, 429-441.

Chaffin, D. B., and Page, G. B.(1994). "Postural effects on biomechanical and psychophysical weight-lifting limits." *Ergonomics*, 37(4), 663-76.

Chaffin, D. B., and Park, K.S. (1973). "A longitudinal study of low-back pain associated with occupational weight lifting factors." *American Industrial Hygiene Association Journal*, 34, 513-525.

Chaffin, D.B., and Anderson, G.B.J. (1984). *Occupational Biomechanics*, Newyork,.

Chazal J, Tanguy A, Bourges M, Gaurel G, Escande G, Guillot M, and G, Vanneuville. (1985). "Biomechanical properties of spinal ligaments and a histological study of the supraspinal ligament in traction." *Journal of Biomechanics*, 18(3), 167–176.

Chen, Y-L, and Lee, Y-H. (1997). "A non-invasive protocol for the determination of lumbosacral vertebral angle." *Clinical Biomechanics*, 12, 185–189.

Cholewicki, J. , and Mcgill, S.M. (1992). "Lumbar posterior ligament involvement during extremely heavy lifts estimated from fluoroscopic measurements." *Journal of Biomechanical Engineering*, 25((1)), 17-28.

Cholewicki, J., Mcgill, S. M., and Norman, R. W. (1991). "Lumbar Spine loads during lifting extremely heavy weights." *Medical Science and Sports Exercise*, 23(10), 1179-1186.

Cyron, B. M., and Hutton, W. C. (1978). "The fatigue strength of the lumbar neural

arch in spondylolysis." *Journal of Bone Joint Surgery Br*, 60-B(2), 234-8.

Davis, H. (1994) "Increasing rates of cervical and lumbar spine surgery in the United States, 1979-1990." *Spine*, 19(10), 1117-23; discussion 1123-4.

Davis, K. G., and Marras, W. S. (2000a). "Assessment of the relationship between box weight and trunk kinematics: does a reduction in box weight necessarily correspond to a decrease in spinal loading?" *Human Factors*, 42(2), 195-208.

Davis, K. G., and Marras, W. S. (2000b). "The effects of motion on trunk biomechanics." *Clinical Biomechanics (Bristol, Avon)*, 15(10), 703-17.

Davis, K. G., and Marras, W. S. (2003). "Partitioning the contributing role of Biomechanical, psychosocial, and individual risk factors in the development of spine loads." *Spine Journal*, 3(5), 331-8.

Davis, P. R. (1985). "Intratruncal pressure mechanisms." *Ergonomics*, 28(1), 293-7.

De Looze, M. P., Kingma, I., Thunnissen, W., Van Wijk, M.J., and Toussaint, H. M. (1994). "The evaluation of a practical biomechanical model estimating lumbar moments in occupational activities." *Ergonomics*, 37, 1495-1502.

Delp Md, Bloomfield Sa, Hogan Ha, Suva Lj, and Rt., Turner. (2001). "Alteration in skeletal perfusion with hand limb unloading: a possible mechanism for bone remodeling." A. In Bioastronautics Investigators. Workshop and H. p. Volume ; USRA, eds.

Department for Work and Pensions. (2002) Great Britain.

Department of Health Statistics Division. (1998). "The prevelance of back pain in Great Britain in 1998. London: Government Statistical Service, 1999."

Descarreaux M, Blouin Js, and N., Teasdale. (2003a). "A non-invasive technique for measurement of cervical vertebral angle: report of a preliminary study." *European Spine Journal*, 12(314-329).

Deyo, R.A, and Weinstein, J.N. (2001). " Low Back Pain." *N. Eng Journal of Med*, 344(5), 363-370.

Dolan, P., and A., Adams M. "Forces acting on the lumbar spine." *In Lumbar Spine Disorders: Current concepts, World Scientific*, Singapore.

Dolan, P., and Adams, M. A. (1993). "The relationship between the EMG activity and extensor moment generation in the erector spinae muscles during bending and lifting activities." Journal of Biomechanics . *1993*, 26, 513-522.

Dolan, P., Kingma, I., De Looze, M. P., Van Dieen, J. H., Toussaint, H. M., Baten, C. T., and Adams, M. A. (2001). "An EMG technique for measuring spinal loading during asymmetric lifting." *Clinical Biomechanics (Bristol, Avon)*, 16 Suppl 1, S17-24.

Dolan, P., Mannion, A. F., and Adams, M. A. (1994). "Passive tissues help the back muscles to generate extensor moments during lifting." *Journal of Biomechanics*, 27, 1237-1248.

D'osualdo, Flavio , Schierano, Stefano , and Iannis, Mariarosa. (1997). "Validation of Clinical Measurement of Kyphosis With a Simple Instrument, the Arcometer." *Spine*, 22(4), 408-413.

Drury, C.G., and Pfeil, R.E. (1975). "A task-based model of manual lifting performance." *International Journal of Prod Res*, 13(137-148).

Dysart, M. J., and Woldstad, J. C. (1996). "Posture Prediction For Static Sagittal Plane Lifting ". *Journal of Biomechanics*, 21(10), 1393-1397.

Elaine Thomas, Alan J. Silman, Papageorgiou, Ann C., Macfarlane, Gary J., and Croft.,

Evans, F. G., and Lissner, H. R. (1959). "Biomechanical studies on the lumbar spine and pelvis." *Journal of Bone Joint Surgery*, 41(A), 218–290.

Ferguson, S. A., Marras, W. S., and Waters, T. R. (1992). "Quantification of back motion during asymmetric lifting." *Ergonomics*, 35(7-8), 845-59.

Floyd, W., and Silver, P. (1955). "The function of the erectores spinae muscles in Certain Movements and Postures in Man." *Journal of Physiology*, 129, 184-203.

Frank, Jw, Brooker, As, and Demaio, Se. (1996). "Disability resulting from occupational low back pain. Part II: What do we know about secondary prevention? A review of the scientific evidence on prevention after disability begins." *Spine*, 21, 2908-2917.

Freivalds, A., Chaffin, D. B., Garg, A., and Lee, K. S. (1984). "A dynamic Biomechanical evaluation of lifting maximum acceptable loads." *Journal of Biomechanics*, 17(4), 251-62.

Friberg, O. (1983). "Clinical symptoms and biomechanics of lumbar spine and hip joint in leg length inequality." *Spine*, 8, 634-651.

G.A. Dumas, L. Beaudoin, and G. Drouin. (1987). "In situ mechanical behavior of posterior spinal ligaments in the lumbar region." *Journal of Biomechanics*, 20, 301 310.

Gagnon, D., and Gagnon, M. (1992). "The influence of dynamic factors on triaxial net muscular moments at the L5/S1 joint during asymmetrical lifting and lowering." *J Biomech*, 25(8), 891-901.

Gallagher, S., Hamrick, C. A., Love, A. C., and Marras, W. S. (1994). "Dynamic biomechanical modelling of symmetric and asymmetric lifting tasks in restricted postures." *Ergonomics*, 37(8), 1289-310.

Garg, A., and Moore, J. S. (1992). "Epidemiology of low-back pain in industry." *OccupMed*, 7(4), 593-608.

Genaidy, A.M., Waly, S.M., Khalil, T.M. , and Hidalgo, J. (1993). "Spinal Compression tolerance limits for the design of manual material handling operations in the workplace." *Ergonomics*, 36, 415.

Goel, V. K., Monroe, B. T., Gilbertson, L. G., and Brinckmann, P. (1995). "Interlaminar shear stresses and laminae separation in a disc. Finite element analysis of the L3-L4 motion segment subjected to axial compressive loads." *Spine*, 20(6), 689-98.

Gordon, S. J., Yang, K. H., Mayer, P. J., Mace, A. H., Jr., Kish, V. L., and Radin, E. L.(1991). "Mechanism of disc rupture. A preliminary report." *Spine*, 16(4), 450-6.

Gracovetsky, S. (1986). "Function of the spine." *Journal of Biomedical Engineering*, 8(3), 217-23.

Granata, K. P., and Marras, W. S. (1995a). "An EMG-assisted model of trunk loading during free-dynamic lifting." *Journal of Biomechicanics*, 28(11), 1309-17.

Granata, K. P., and Marras, W. S. (1995b). "The influence of trunk muscle coactivity on dynamic spinal loads." *Spine*, 20(8), 913-9.

Granata, K. P., Marras, W. S., and Davis, K. G. (1999). "Variation in spinal load and trunk dynamics during repeated lifting exertions." *Clinical Biomechanics (Bristol,Avon)*, 14(6),367-75.

Gray, H. (1980). *Grays anatomy.*, Churchill Livingstone.

Grilli, S. L. (1997). "Spinal Modelling to Investigate Postural Loading and Stability," Doctoral (PhD) Thesis, Loughborough, UK.

Gurumoorthy, D., and Twomey, L.T. (2000.). "Morphology of cervical muscles and

Relevance to whiplash. In Frontiers in Whiplash Trauma. In Frontiers in Whiplash Trauma." Clinical and Biomechanical, N. Yoganandan and Pintar, eds., IOS Press,, Amsterdamn., 60-71.

Hagen, K. B., Hallen, J., and Harms-Ringdahl, K. (1993). "Physiological and subjectivere sponses to maximal repetitive lifting employing stoop and squat technique." *European Journal of* Applied *Physiology Occupational Physiology*, 67(4), 291-7.

Hall, H., Mcintosh, G., Wilson, L., and Melles, T. (1998). "Spontaneous onset of back pain." *Clinical Journal of Pain*, 14(2), 129-33.

Hall, S. J. (1985). "Effect of attempted lifting speed on forces and torque exerted on the lumbar spine." *Medicine and Science in Sports and Exercise*, 17, 440-444.

Hansson, T., and Roos, B. (1981). "Microcalluses of the trabeculae in lumbar vertebrae and their relation to the bone mineral content." *Spine*, 6(4), 375-80.

Hart, Erin S. (2005). "Pediatric Orthopaedic Ailments: Scoliosis. Web. Massachusetts General Hospital -." http://www.massgeneral.org/ortho/Scoliosis.htm., ed.

Herrin, G. A., Jaraiedi, M., and Anderson, J. K. (1986). "Prediction of overexertion injuries using biomechanical and psychophysical models." *American Industrial Hygiene Association Journal*, 47(322-330).

Heyman, J. (1982). "The middle-third Rule." The Masonry Arch., Ellis Horwood Ltd,, New York, Brisbane,.

Hindle, R., Pearcy, M., Cross, A. , and Miller, D. (1990). "Three-dimensional Kinematics of the human back." *Clinical Biomechanics*, 5(218-228.).

Hinman, Martha R. (2004). "Comparison of thoracic kyphosis and postural stiffness in younger and older women" *The Spine Journal*, 4, 413–417.

Hsiang, S.M., Brogmus, G.E., and Courtney, T.K. (1997). "Low back pain (LBP) and lifting technique-A review." *International Journal of Industrial Ergonomics*, 19, 59-74.

Hukins, D. W. L., Kirby, M. C., Sikoryn, T. A., Aspden, R. M., and Cox, A. J. (1990). "Comparison of structure, mechanical properties and functions of lumbar spinal ligaments,." *Spine*, 15, 787-795.

IASP, Subcommittee on Taxonomy. (1979). "Pain terms: A list with definitions and notes on usage." *Pain*, 6, 249-252.

J. M. Farnsworth. (2007). "Unpublished PhD thesis, Spine Analysis," Loughborough University, Loughborough.

Jager, M., and Luttmann, A. (1989). "Biomechanical analysis and assessment of lumbar stress during load lifting using a dynamic 19-segment human model." *Ergonomics*, 32(1), 93-112.

Jager, M., and Luttmann, A. (1992). "The load on the lumbar spine during asymmetrical bi-manual materials handling." *Ergonomics*, 35(7-8), 783-805.

Janet E Macintosh, and Nikolai Bogduk. (1987). "The morphology of the lumbar erector spinae." *Spine*, 12, 658-668.

Jensen, M. C., Brant-Zawadzki, M. N., Obuchowski, N., Modic, M. T., Malkasian, D., and Ross, J. S. (1994). "Magnetic resonance imaging of the lumbar spine in people without back pain." *New England Journal of Medicine*, 331(2), 69-73.

John H. Warfel. (1985). *The head, neck, and trunk*, LEA&FEBIGER, Philadelphia.

Johnson, G., Bogduk, N., Nowitzke, A., and House, D. (1994.). " Anatomy and actions of the trapezius muscle." *Clinical Biomechanics*, 9, 44-50.

Jorgensen, M.J., Davis, K. G., Kirking, B.C., Karen, E. K., and Marras, W. S. (1999). "Significance of biomechanical and physiological variables during the determination of maximum acceptable weights of lift." *Ergonomics*, 42(9), 1216-1232.

Jorgensen, M.J., W.M. Marras, and Gupta, P.(2003). "Cross-sectional area of the lumbar back muscles as a function of torso flexion." *Clinical Biomechanics*, 18, 280-6.

Kamibayashi L.K., and Richmond F.J.R. (1998). "Morphometry of human neck muscles." *Spine*, 23((12)), 1314-1323.

Kapandji, I.A. (1974). The Physiology of the Joints, Churchill Livingstone, Edinburgh

Kroemer, K.H.E. (1983). "An isoinertial technique to asses individual lifting capability." Human Factors, 25(5), 493-506.

Kumar, S. (1984). "The physiological cost of three different methods of lifting in sagittal and lateral planes." Ergonomics, 27, 425-433.

Kumar, S. (1994). "Lumbosacral compression in maximal lifting efforts in sagittal plane with varying mechanical disadvantage in isometric and isokinetic modes." Ergonomics, 37(12), 1975-83.

Kumar, S. (1994). "Lumbosacral compression in maximal lifting efforts in sagittal plane with varying mechanical disadvantage in isometric and isokinetic modes." *Ergonomics*, 37(12), 1975-83.

Kumar, S., and Davis, P. R. (1983). "Spinal loading in static and dynamic postures: EMG and intra-abdominal pressure study." *Ergonomics*, 26(9), 913-22.

Kumaresan, S., Yoganandan, N., and Pintar, F. A. (1998). "Finite Element Modeling Approaches of Human Cervical Spine Facet Joint Capsule,." *Journal of Biomechanics*, 31(4), 371-376.

Kumaresan, S., Yoganandan, N., and Pintar, F. A. (1999a). "Biomechanical Responses of Pediatric Cervical Spine Using Nonlinear Finite Element Approach,." *American Society of Mechanical Engineers, Bioengineering Division (Publication) BED, Advances in Bioengineering,*, 42, 143-144.

Kumaresan, S., Yoganandan, N., and Pintar, F. A. (1999b). "Finite Element Modeling of Spinal Ligaments,." *American Society of Mechanical Engineers Bioengineering Division (Publication) BED, Advances in Bioengineering,*, 42, 281-282.

Kumaresan, S., Yoganandan, N., Pintar, F. A. , Maiman, D. J., and Kuppa, S. (2000). "Biomechanical Study of Pediatric Human Cervical Spine: A Finite Element Approach,." *Journal of Biomechanical Engineering, Transactions of the ASME,*, 122(1), 60-71.

Kumaresan, S., Yoganandan, N., Pintar, F. A., Maiman, D. J., and Goel, V. K. (2001). "Contribution of Disc Degeneration to Osteophyte Formation in the Cervical Spine: A Biomechanical Investigation,." *Journal of Orthopaedic Research*, 19, 977-984.

Kumaresan, S., Yoganandan, N., and Pintar, F.A. (1997.). "Methodology to quantify the uncovertebral joint in the human cervical spine." *Journal of Musculoskeletal Research,*, 1, 1-9.

L. Lindback, and K. Kjellberg, (2001). "Gender differences in lifting technique." *Ergonomics*, 44(2), 202-214.

Lavender, S. A., Marras, W. S., and Miller, R.A. (1993). "The development of response strategies in preparation for sudden loading to the torso." *Spine*, 18(14), 2097-2105.

Lavender, S.A., Anderson, G.B.J., Schipplein, O.D., and Fuentes, H.J. (2003). "The effects of initial lifting height, load magnitude, and lifting speed on the peak dynamic L5/S1 moments." *International Journal Of Industrial Ergonomics*, 31, 51-59.

Leboeuf-Yde, C. (2004). "Back pain--individual and genetic factors." *J Electromyogr Kinesiol*, 14(1), 129-33.

Lee, D. (1989). *The pelvic girdle: an approach to the examination and treatment of the lumbo- pelvic-hip region.*, Churchill Livingstone.

Leskinen, T.P.J., Stalhammar, H.R., and Kuorinka, I.A.A. (1983). "A dynamic analysis

of spinal compression with different lifting techniques." *Ergonomics*, 26(6), 595-604.

Lin, C.J., Bernard, T. M., and Ayoub, M.M. (1999). "A biomechanical evaluation of lifting speed using work and moment-related measures." *Ergonomics*, 42(8), 1051 1059.

Liu, Y.K., Njus, G., Buckwalter, J., and Wakona, K. (1983). "Fatigue Response of lumbar intervertebral joints under axial cycling loading." *Spine*, 8, 857-865.

M. Haghpanahi, S. Sohrabi, and A. Gorginzadeh "A Finite Element Model of Second Cervical Vertebra (Axis) to Study Hangman's Fracture." *Biomechanics*, Benidorm, Spain.

Macintosh, Janet E, and Bogduk, Nikolai. (1991). "The attachments of the lumbar erector spinae." *Spine*, 16(7), 783-792.

Mackinnon, S., and Li, J.-C. (1998). "Temporal relationships of load and lumbar spine kinematics during lifting." *International Journal of Industrial Ergonomics*, 22, 359 366.

Mannion, Anne F., Knecht, Katrin, Balaban, Gordana, Dvorak, Jiri, and Grob, Dieter. (2004). "A new skin-surface device for measuring the curvature and global and segmental ranges of motion of the spine: reliability of measurements and comparison with data reviewed from the literature." *European Spine Journal*, 13, 122–136.

Marras, W. S., Ferguson, S. A., Burr, D., Davis, K. G., and Gupta, P. (2004). "Spine loading in patients with low back pain during asymmetric lifting exertions." *Spine Journal*,4(1), 64-75.

Marras, W. S., and Mirka, G. A. (1990). "Muscle activities during asymmetric trunk angular accelerations." *J Orthop Res*, 8(6), 824-32.

Marras, W. S., and Mirka, G. A. (1992). "A comprehensive evaluation of trunk response to asymmetric trunk motion." *Spine*, 17(3), 318-26.

Marras, W. S., and Mirka, G. A. (1993). "Electromyographic studies of the lumbar trunk musculature during the generation of low-level trunk acceleration." *Journal of Orthopedical Research*,11(6), 811-7.

Marras, W. S., and Sommerich, C. M. (1991). "A three-dimensional motion model of loads on the lumbar spine: II. Model validation." *Human Factors*, 33(2), 139-49.

Marras, W.S., and Granata, K.P. (1997). "The development of an EMG assisted model to assess spine loading during whole-body freee -dynamic lifting." *Journal of Electromyography Kinesiology*, 7, 259-68.

Marras, W.S., Jorgensen, M.J., Granata, K.P., and Wiand, B. (2001a). "Female and Male trunk geometry :size and prediction of the spine loading trunk muscles derived from MRI." *Clinical Biomechanics*, 16, 38-46.

Mcgill, S. (2002). *Low Back Disorders Evidence Based Prevention and Rehabilitation.*

Mcgill, S.M. (1997). "The biomechanics of low back injury implications on current practice in industry and the clinic." *Journal of Biomechanics*, 30, 465-475.

Mcgill, SM., and Norman Rw. (1986). "Partitioning of the L4-5 dynamic moment into disc, ligamanetous and muscular components during lifting." *Spine*, 1986(11), 666-678.

Mcgill, SM., and Norman, Rw. (1987). "Effects of an Anatomically Detailed Erector spinae Model on L4/L5 disc compression and shear." *Journal of biomechanics*, 20(6), 591-600.

Mcgill, SM., Santiguida L, and J., Stevens. (1993). "Measurement of the trunk musculature from T5 to L5 using MRI scans of 15 young males corrected for muscle fiber orientation." *Clinical Biomechanics*, 1993(8), 171-178.

McGill, S.M. (1997). "The biomechanics of low back injury implications on current practice in industry and the clinic." *Journal of Biomechanics*, 30, 465-475.

McGill, S.M. (2002). *Low Back Disorders: Evidence-based Prevention and Rehabilitation*, Champaign, IL, USA.

McGill, S.M., and Kippers, V. (1994). "Transfer of loads between lumbar tissues during the flexion-relaxation phenomenon." *Spine*, 19, 2190-2196.

McGill, S.M., and Norman, R.W. (1985). "Dynamically and statically determined low back moments during lifting." *Journal of Biomechanics*, 18(12), 877-885.

Meakin, J. R., Hukins, D. W., and Aspden, R. M. (1996). "Euler buckling as a model for the curvature and flexion of the human lumbar spine." *Proc R Soc Lond Biological Science*, 263(1375), 1383-7.

Melhorn, J. M. (2003). "Work-related musculoskeletal back pain: the many facets." *Spine Journal*, 3(6), 411-6.

Mercer S, and N., Bogduk. (1999). "The ligaments and annulus fibrosus of human adult cervical intervertebral discs." *Spine*, 24(7), 619-26.

Messerer, O. (1880). *Uber Elasticitat und Festigkeit der menschlichen Knochen*, Knochen, . Stuttgart Cotta.

Michel A. Leroux, Karl Zabjek, Genevi`Eve Simard, Johanne Badeaux, Christine Coillard, and Rivard., Charles H. (2000). "A non-invasive anthropometric technique for measuring kyphosis and lordosis: An application for idiopathic scoliosis." *Spine, :*, 25, 1689–1694.

Michel A.Leroux, Karl Zabjek, Genevi`Eve Simard, Johanne Badeaux, Christine Coillard, and Rivard., Charles H. (2000). "A noninvasive anthropometric technique for measuring kyphosis and lordosis: An application for idiopathic scoliosis." *Spine*, 25, 1689–1694,.

Morrissey, S. J., and Liou, Y. H. (1988). "Maximum acceptable weights in load carriage." *Ergonomics*, 31(2), 217-26.

Myklebust, J. B., Pintar, F., Yoganandan, N., Cusick, J. F., Maiman, D., Myers, T. J., and Sances, A. . (1988). "Tensile Strength of Spinal Ligaments." *Spine*, 13(5), 526-531.

N. Yoganandan, F. A. Pintar, and Kumaresan. S. (1998). "Biomechanical Assessment of Human Cervical Spine Ligaments." *Society of Automotive Engineers SAE Paper No.983159.*

N. Yoganandan, Kumaresan, S., and F.A. Pintar. (2000). "Geometric and mechanical properties of human cervical spine ligaments." *Journal of Biomechanical Engineering*, 122, 623–629.

Nachemson, A. L. (1981). "Disc pressure measurements." *Spine*, 6(1), 93-7.

Nachemson, A. and Morris, J. M. (1964). "In Vivo Measurements of Intra-discal Pressure. Discometry, a Method for the Determination of Pressure in the Lower Lumbar Discs." *Journal of Bone Joint Surg Am*, 46, 1077-92.

Narayan Yoganandan, and Pintar, Frank A. (2003). "Biomechanics of human head-neck in rear impacts." *International Journal of Vehicle Design (IJVD)*, Vol. 32(No.1/2,), 1-3.

Narayan Yoganandan, Srirangam Kumaresan, and Pintar, Frank A. (2000). "Biomechanics of the cervical spine Part2. Cervical spine soft tissue responses and biomechanical modelling." *Clinical Biomechanics.*, 16, 1-27.

Narici, M. (1999). "Human skeletal muscle architecture studied in viov by non-invasive imaging techniques: functional significance and applications." *Journal of Electromyography Kinesiology*, 9, 97-103.

NIOSH. (1981). "Work practices guide for manual material lifting. Technical report. DHHS Department of Health and Human Services.(NIOSH)." NIOSH, Cincinnati, OH.

Oliver J, and Middleditch A. (1991). *Functional Anatomy of the Spine*, Butterworth Heinemann, Oxford.

Orne, D. , and Y.K. Liu. (1971). "A Mathematical Model of Spinal Response to Impact." *Journal of Biomechanics,*, 4, p. 44-71.

Palmer Kt, and K, Walsh. (2000). "Back pain in Britain: Comparison of two Prevalence surveys at an interval of 10 years." *BMJ*, 1577-1578.

Panjabi, M. M. (1973). "Three-dimensional mathematical model of the human spine structure." *Journal of Biomechanics*, 6(6), 671-80.

Panjabi, M.M., Goel, V.K., and Takata, K. (1982). "Physiological strains in lumbar spinal ligaments, an in vitro biomechanical study." *Spine*, 7 192–203.

Panjabi, M.M., Takata, K., Goel, V., Federico, D., Oxland, T., Duranceau, J., And Krag, M. (1991). "Thoracic human vertebrae: Quantitative Three-dimensional anatomy." *Spine*, 16((8)), 888-901.

Pearsall, D, and Reid, J. G. (1992). "Line of gravity relative to upright vertebral posture." *Clinical Biomechanics,*, 7, 80-86.

Perry, O. (1957). "Fracture of the vertebral endplate in the lumbar spine." *Acta Orthop Scand.*, 25 (Suppl.) 25-29

Pintar, F.A., Yogonandan, Narayan, Myers, Thomas, Elhagediab, Ali, and Sances, Anthony. (1992) "Biomechanical properties of human lumbar spine ligaments." *Journal of Biomechanics*, 25.(11), 1351-6.

Potvin, J. R., McGill, S. M., and Norman, R. W. (1991). "Trunk muscle and lumbar ligament contributions to dynamic lifts with varying degrees of trunk flexion." *Spine*, 16(9), 1099-107.

Priest, D.T., and Hoggart, B. (2002). "Chronic pain: Mechanisms and treatment." *Current Opinion in Pharmacology*, 2, 310-316.

Rannou, F., Corvol, M., Revel, M., and Poiraudeau, S. (2001). "Disk degeneration and disk herniation: The contribution of mechanical stress." *Joint Bone Spine*, 68(543-546.).

Rasmussen, J., M. Damsgaard, et al. (2002). "Design optimization with respect to ergonomic properties." Structural and Multidisciplinary Optimization 24: 89-97.

Reid, J.G. , and P.A., Costigan. (1985). "Geometry of Adult Rectus Abdominis and Erector Spinae Muscles." *J. Orthopaedic and Sports Physical Therapy*, 5, 278-280.

Rosse C., and Gaddum-Rosse P. (1997). *Textbook of Anatomy*, Philadelphia, New York.

Schipplein, O. D., Reinsel, T. E., Andersson, G. B., and Lavender, S. A. (1995). "The influence of initial horizontal weight placement on the loads at the lumbar spine while lifting." *Spine*, 20(17), 1895-8.

Schipplein, O. D., Trafimow, J. H., Andersson, G. B., and Andriacchi, T. P. (1990). "Relationship between moments at the L5/S1 level, hip and knee joint when lifting." *Journal of Biomechanics*, 23(9), 907-12.

Schultz, A. , and Anderson, G.B.J. (1982). "Loads on the Lumbar Spine: Validation of a Biomechanical Analysis by Measurements of Intra-discal Pressures and Myoelectric Signals." *Journal of Bone and Joint Surgery*, 62(A), 713-720.

Schultz, A. B., and Andersson, G. B. (1981). "Analysis of loads on the lumbar spine." *Spine*, 6(1), 76-82.

Schultz, A. B., Haderspeck, K.A, G., Sinkora, and N., Warwick. D. (1985). "Quantitative Studies of the Flexion-Relation Phenomenon in the Back Muscles." *Journal of Orthopaedic Research*, 3, 189-197.

Scott L. D., Srikanth Suryanarayananb, Wendy M. Murrayc, Jim Uhlirc,, and

Trioloc, Ronald J. (2001). "Architecture of the rectus abdominis, quadratus lumborum, and erector spinae." *Journal of biomechanics*, 34, 371-375.

Shirazi-Adl, A. (1991). "Finite-element evaluation of contact loads on facets of an L2 L3 lumbar segment in complex loads." *Spine*, 16(5), 533-41.

Smedley, J., Egger, P., Cooper, C., and Coggon, D. (1997). "Prospective cohort study of predictors of incident low back pain in nurses." *British Medical Journal*, 314(7089), 1225-1228.

Smeltzer, S.C., and Bare, B.G. (1996). *Brunner and Suddarth's Textbook of Medical and Surgical Nursing.*

Snook, S. H. (1978). "The design of manual handling tasks." *Ergonomics*, 21(2), 963 985.

Snook, S. H., Campanelli, R. A., and Hart, J. W. (1978). "A study of three preventive approaches to low back injury." *Journal of Occupational Medicine*, 20(7), 478-81.

Snook, S. H., and Ciriello, V. M. (1991). "The design of manual handling tasks: revised tables of maximum acceptable weights and forces." *Ergonomics*, 34(9), 1197-213.

Snook, S.H. (1988). "Comparison of different approaches for the prevention of low back pain." *Applied Industrial Hygiene*, 3, 73-78.

Snook, S.H. (2004). "Work related low back pain: secondary intervention." *Journal of Electromyography and Kinesiology*, 14, 153-160.

Sonada, T., and Kyoto J. (1962). "Studies on compression tension and torsion strength of the human vertebral column." Prefect Med. Univ., 659–702.

Spss, I.. (2006). ""SPSS 13." Genre: Statistical analysis (Latest release: 15.0 (Win),."

Stambough, J., Genaidy, A., and Guo, L. (1995). "A mathematical lifting model of the

lumbar spine." *Journal of Spinal Disorders*, 8(4), 264-277.

Stokes, I , and Gardner-Morse, M. (1995). "Lumbar spine maximum efforts and muscle recruitment patterns predicted by a model with multi joint muscles and joint with stiffness." *Journal of Biomechanics,*, 28((2)), 173- 186.

Stokes, I. A. F., and Gardner-Morse, M. (1999). "Quantitative anatomy of the lumbar musculature." *Journal of biomechanics*, 32, 311-316.

Straker, L. (2003). "Evidence to support using squat, semi-squat and stoop techniques to lift low-lying objects." *International Journal of Industrial Ergonomics*, 31, 149-160.

Takashima, T., Singh, S. P., Haderspeck, K.A , and Schultz, A. B. (1979). "A model for Semi-Quantitative Studies of Muscle Actions." *Journal of Biomechanics*, 12, 929-939.

Takebe, E.A., Winters, J.M., and Woo, S. L-Y. (1974). "Multiple Muscle Systems: Biomechanical and Movement Organisations." Appendix, Springer Verlag, New Yorc inc.

Thompson, D. D, and Chaffin, D. B. "Can biomechanically determined stress be Perceived?" *Proceedings of the Human Factors and Ergonomics Society 37th Annual Meeting, 11-15 October,1993*, Seattle., 789-792.

Tillotson, K. Malcolm, and Burton, A. Kim. (1991). "Non-invasive measurement of lumbar sagittal mobility: An assessment of the flexicurve technique." *Spine*, 16, 29–33.

Timoshenko, S.P., and Young, D.H. (1965). *Theory of Structures.* McGraw-Hill Book Company, New York USA.

Toussaint, H. M., De Winter, A. F., De Haas, Y., De Looze, M. P., Van Dieen, J. H., and Kingma, I. (1995). "Flexion relaxation during lifting: implications for torque production by muscle activity and tissue strain at the lumbo-sacral joint." *Journal of Biomech*anics 28(2), 199-210.

Troup, J.D.G., Leskinen, T., Stalhammer, H., and Kuorinka, I. (1983). "A comparison of intra-abdominal pressure increases, hip torque and lumbar vertebral compression in different lifting techniques." *Human Factors*, 25, 517-525.

Tvait, P. , Daggfeldt, K., Hetland, S., and Thorstensson, A. (1994). "Erector spinae lever arm lenght variations with changes in spina l curvature." *Spine*, 19, 199-204.

Van De Graaff K.M., and Fox S.I. (1995). *Concepts of Human Anatomy*, Wm.C Brown Publishers.

Van Der Horst, M.J. (2002). "Human Head Neck Response in Frontal, Lateral and Rear End Impact Loading - modelling and validation.," Technical University of Eindhoven.

Van Dieen, J. H., Creemers, M, Draisma, I., and Toussaint, H. M. (1994). "Repetitive lifting and spinal shrinkage effects of age and lifting technique." *Clinical Biomechanics*, 9, 367-374.

Van Dieen, J. H., Hoozemans, M. J., and Toussaint, H. M. (1999a). "Stoop or squat: a review of biomechanical studies on lifting technique." *Clinical Biomechanics (Bristol, Avon)*, 14(10), 685-96.

Van Dieen, J. H., Hoozemans, M. J., Van Der Beek, A.J., and Mulllender, M. (2002). "Precision of estimates of mean and peak spinal loads in lifting." *Journal of Biomechanics*, 2002, 979-982.

Van Dieen, J. H., and Kingma, I. (1999b). "Total trunk muscle force and spinal compression are lower in asymmetric moments as compared to pure extension moments." *Journal of Biomechanics*, 32, 681-687.

Van Dieen, J. H., Kingma, I., Meijer, R., Hansel, L., and Huiskes, R. (2001). "Stress distribution changes in bovine vertebrae just below the endplate after sustained loading." *Clin Biomech (Bristol, Avon)*, 16 Suppl 1, S135-42.

Van Lopik, D. (2004). "Modelling the human head and neck for the study of

'Whiplash'," Loughborough University, Loughborough.

Vasavada, A.N., Li, S., and Delp, S.L. (1998.). "Influence of muscle morphometry and moment arms on the moment-generating capacity of human neck muscles." *Spine*, 23 (4), 412-422.

Vernon-Roberts, B. (1988). *Disc Pathology and Disease State*, CRC Press, Boca Raton FL.

Videman, T. , Battie, M.C., Gibbons, L.E., Maravilla, K., Kaprio, H. , and Kaprio, J. (2003). "Association between back pain history and lumbar MRI findings." *Spine*, 28(6), 582-588.

Warfel, J.H. (1985.). *The Head, Neck, and Trunk*, Philadelphia.

Waters, T. R., Putz-Anderson, V., Garg, A. , and Fine, L. Z. (1993). "Revised NIOSH Equation for the Design and Evaluation of Manual Lifting Tasks." *Ergonomics*, 36, 749 776.

White, A.A, and Panjabi, M.M. (1979). *Clinical Biomechanics of the Spine.*, Philedelphia, PA.

White, A.A. , and Gordon, S.L. (1982). "Synopsis: Workshop on idiopathic low back pain." *Spine*, 12, 305.

Yamaguchi, G. (1990). J. Winters and W. Savio, eds., Springer-Verlag.

Y-H Lee, W-K Chiou, W-J Chen, M-Y Lee, and Lin., Y-H. (1995). "Predictive model of intersegmental mobility of lumbar spine in the sagittal plane from skin markers." *Clinical Biomechanics*, 10, 413–420.

Yoganandan, N., Pintar, F.A., Maiman, D.J., Cusick, J.F., Sances, and Jr., A., Walsh,. (1996). "Human head-neck biomechanics under axial tension." *Medical Engineering and Physics*, 18(4), 289-294.

Yoganandan, N., Kumaresan, S. , and Pintar, F. A. (2001). "Biomechanics of the cervical spine Part 2. Cervical spine soft tissue responses and biomechanical modeling." *Clinical Biomechanics*, 16, 1-27.

Yoganandan, N., Kumaresan, S., and Pintar, F. A. (2000). "Geometric and Mechanical Properties of Human Cervical Spine Ligaments,." *Journal of Biomedical Engineering*, 122(6), 623-629.

Yoganandan, N., Pintar, F. A., Kumaresan, S., and Elhagediab, A. (1999). "Biomechanical Assessment of Human Cervical Spine Ligaments,." *SAE (Society of Automotive Engineers) Transactions*, 107(6), 2852-2861.

APPENDIX 1

The percentage of body weight at each vertebral slice is embedded within the code. When the user enters the weight value, the code calculates the actual weight at each vertebral segment.

Table A1 Percentage of body weight carried by each vertebral level

Percentage of Body Weight Carried By Each Vertebral Level	
% of Body Weight	Vertebral Level
0.25	L5
0.35	L4
0.26	L3
0.26	L2
0.29	L1
0.26	T12
0.25	T11
0.25	T10
0.20	T9
0.14	T8
0.17	T7
0.15	T6
0.14	T5
0.43	T4
0.38	T3
0.43	T2
0.38	T1
0.05	C7
0.03	C6
0.04	C5
0.03	C4
0.02	C3
0.02	C2
0.02	C1

APPENDIX 2

This table represents a sample for the male's 0 to 5 degrees reference line angle of interval. The first coordinate column is X coordinate, the second column is Y coordinates and in the third column the relative angle orientation of each vertebra is. The forth column represents the radius of the vertebrae whereas the fifth column represents the height of the vertebrae.

Table A2. Coordinate and size values for male's 0 to 5 degrees of reference line angle of interval

Xc	Yc	alpR	R	t
0	0	0	0	0
0.00	0.00	42.61	16.95	23.00
-30.71	33.38	7.61	16.95	24.10
-62.46	59.82	8.91	17.40	23.80
-95.00	79.27	8.56	17.45	24.30
-130.62	93.89	6.17	17.65	23.80
-165.96	104.12	7.76	16.70	22.70
-200.86	109.27	5.95	15.90	21.30
-231.25	110.56	6.99	15.80	20.20
-261.39	108.16	5.56	15.50	19.30
-290.54	102.96	2.30	14.70	18.70
-318.61	96.78	4.11	14.25	18.20
-345.87	88.70	2.84	13.45	17.40
-371.18	79.80	2.11	12.90	16.20
-394.88	70.48	-1.05	12.25	16.20
-418.02	61.86	0.33	11.65	15.70
-440.59	53.31	-2.00	10.80	15.60
-461.79	46.11	4.39	9.85	14.10
-475.98	40.05	4.13	8.40	12.80
-488.15	33.77	-1.67	9.25	10.90
-498.84	28.65	-8.02	8.95	11.00
-510.47	24.97	-3.13	7.95	10.00
-521.54	22.12	-11.30	7.80	9.20
-531.11	21.59	-7.09	7.80	11.30
-545.86	22.61	1.57	7.40	14.90

APPENDIX 3

Muscle attachments to the vertebrae

Each vertebra is assumed to made up from 10 different geometrically non-linear features.

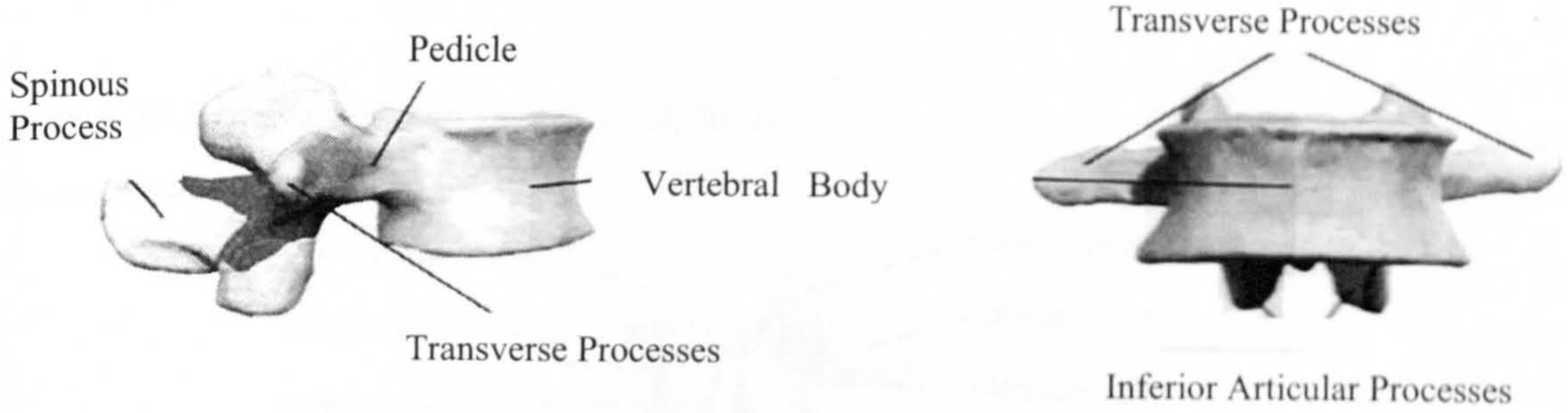


Figure A.3.1 Vertebral Body with front and side views.

1. The main vertebral body
2. Left pedicle
3. Right pedicle
4. Spinal channel
5. Spinous process
6. The left transverse processes
7. The right transverse processes
8. The left superior and inferior facet
9. The right superior and inferior facet

The muscles are attached to one of these physical units. The headings are given with their physical connections to the spine for the muscle groups.

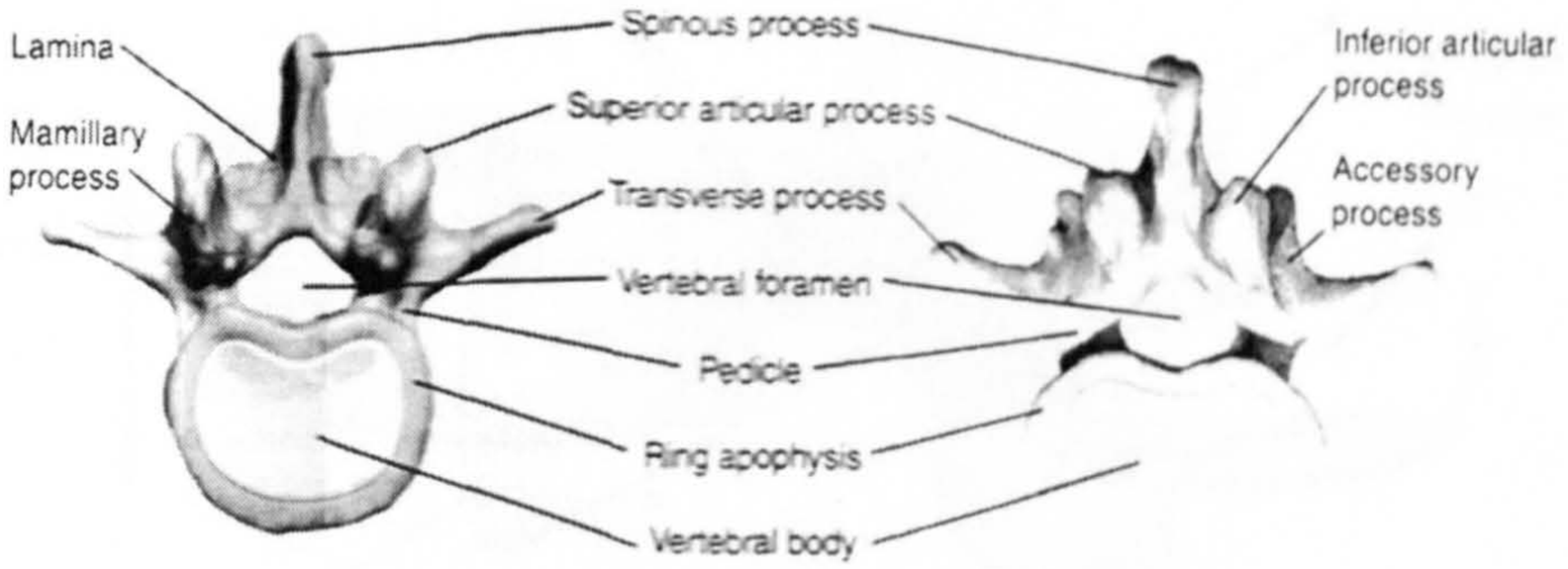


Figure A.3.2 Vertebral body top view (McGill, 2002)

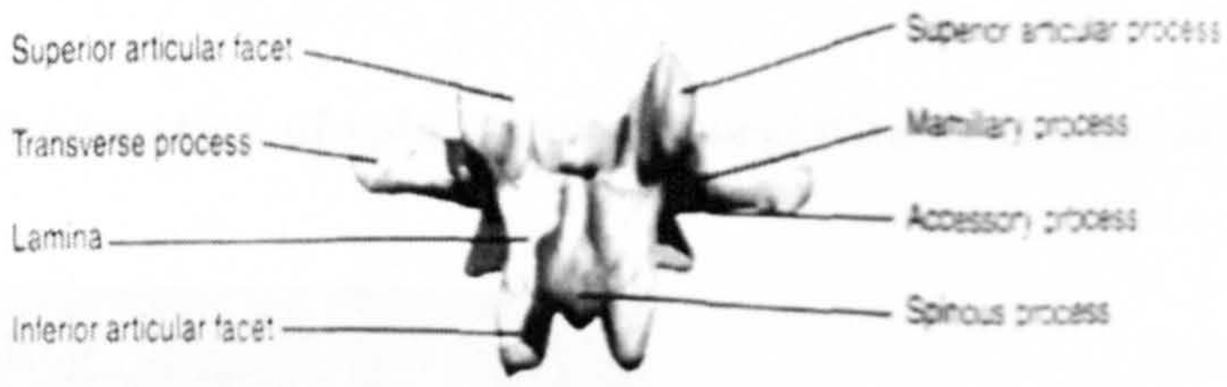


Figure A.3.3 Figure Vertebral body posterior view (McGill, 2002)

Although the point of attachment of each muscle group varies on the surface of the vertebral processes, a single representative point is used for each.

Spinous process (e.g. for interspinalis, spinalis thoracis)
Transverse process (e.g. for longissimus thoracis, intertransverse)
Articular process (e.g. for semispinalis capitis in cervical region)
Mamillary processes (for multifidus in the lumbar region)

Representation of the points of muscle attachment to the vertebrae

The position of each representative point for muscle attachment on the spinous process, transverse process, superior articulating processes, and vertebral lamina is to be calculated. For each vertebral level, an expression defining the x and y co-ordinates of these points relative to the origin of the vertebrae are used.

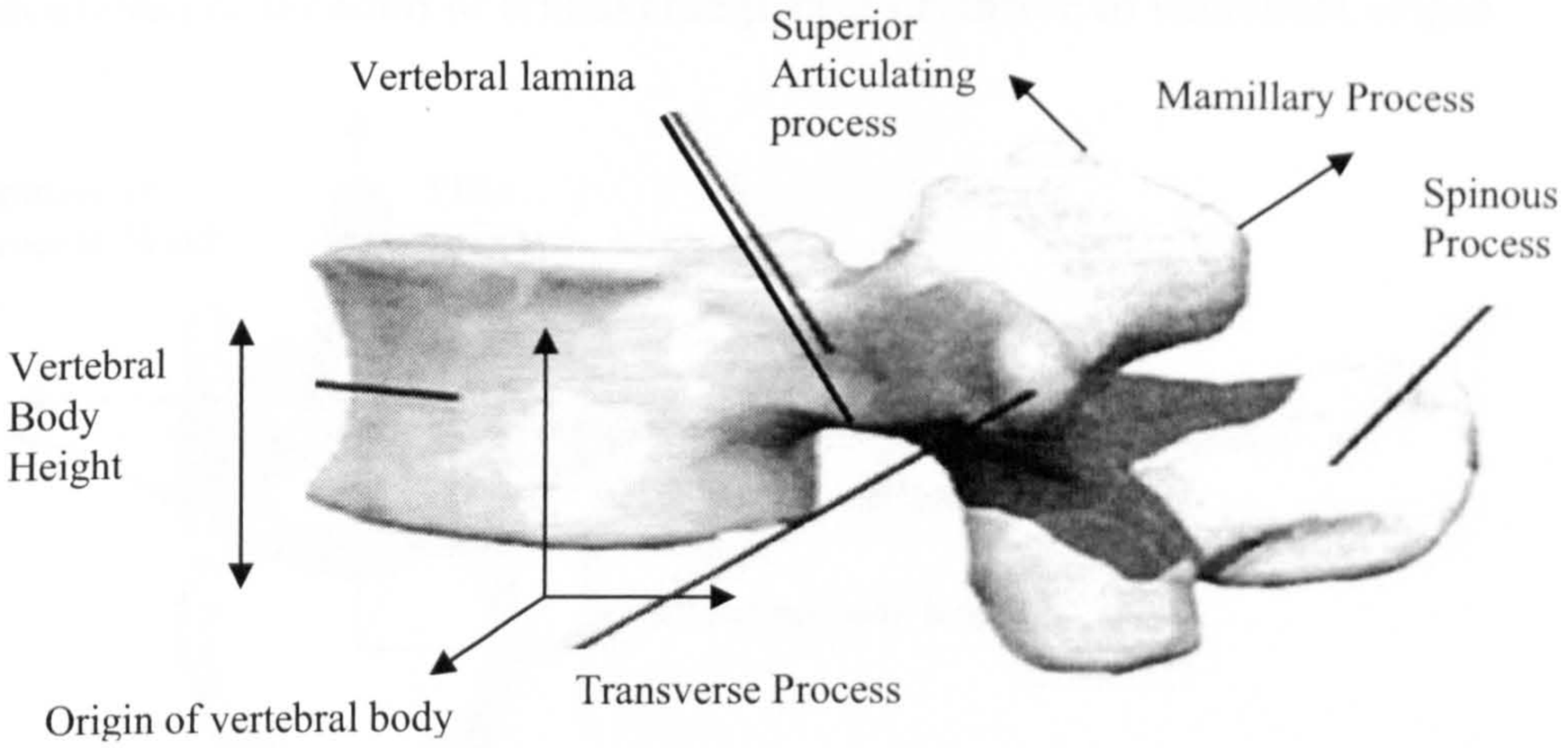


Figure A.3.4 Vertebral connection points (McGill, 2002)

Calculation of the location of spinous process relative to vertebral origin

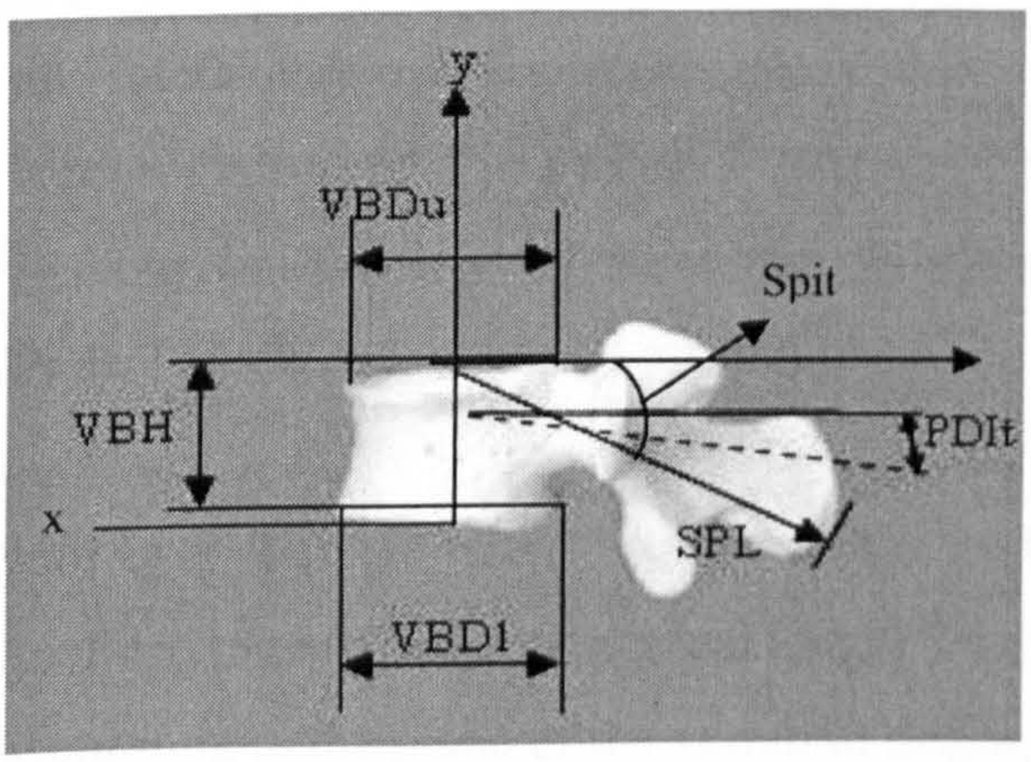


Figure A.3. 5 Sagittal views with the dimensions shown

Below the formulations for each muscle attachment point is provided. The data to be used in the formulations are provided from (Ceran, 2006) for each vertebrae starting from C1 to L5.

The coordinates of the spinal processes can be determined by using the formula below.

X coordinate: spl*cos(spit))

Y coordinate: vbh-spl*sin(spit))

Where;

Vbh: vertebral body height

Spl: length of spinous process

Spit: Angle of spinous process relative to the horizontal

Calculation of location of transverse process relative to vertebral origin

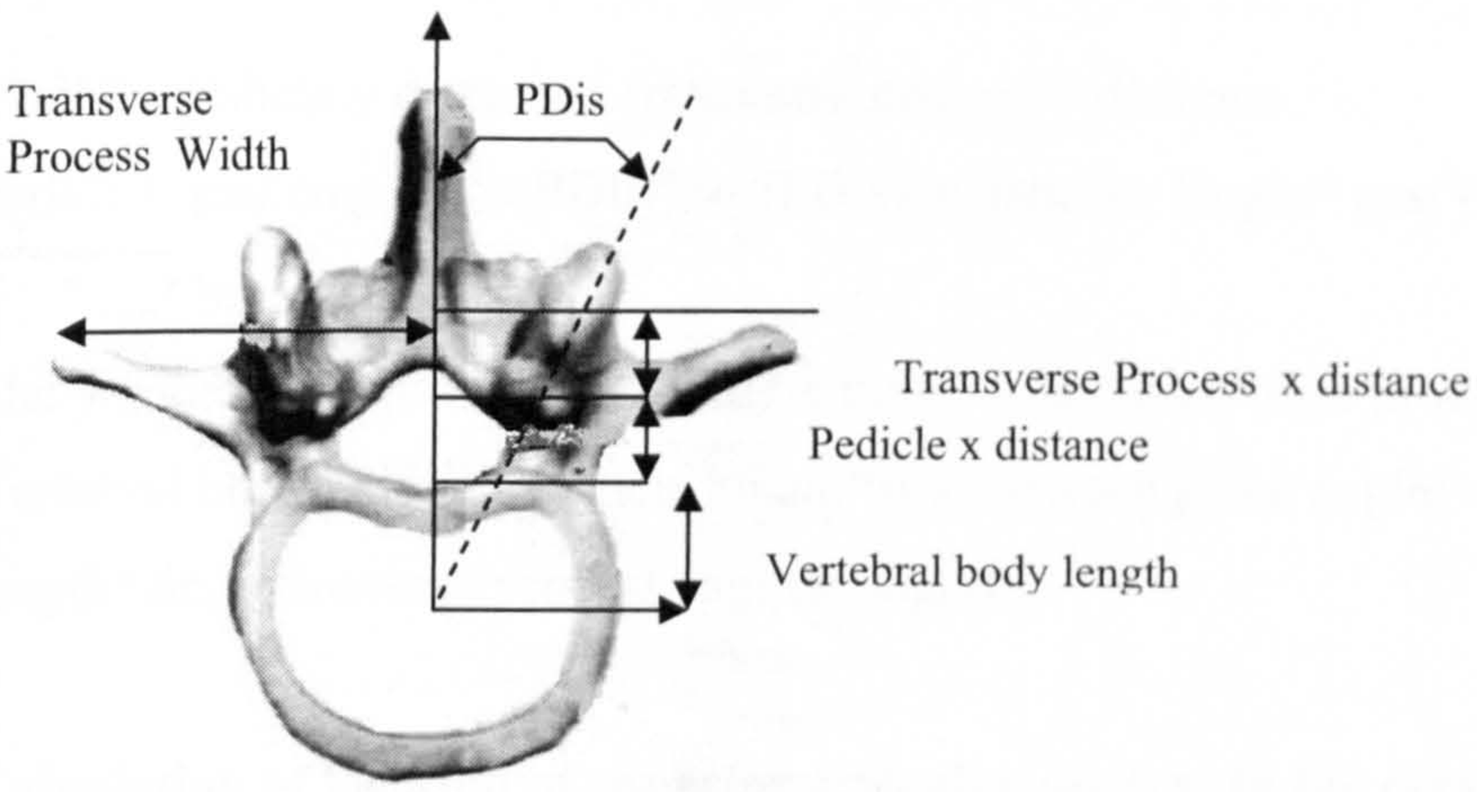


Figure A.3. 6 Sagittal views with top view for transverse process

The position of the representative point on the transverse process in the sagittal plane depends upon dimensions and orientations of both the pedicles and transverse processes and lateral and sagittal planes

Xcoordinate= vbdl/2 + pedicle x distance + transverse process x distance

Pedicle X distance=vbdl/2+inclined plane distance *cos(PDlt)

PDlt: Pedicle inclination in sagittal plane

However, inclined plane distance is affected by the lateral inclination of the pedicles

Inclined plane distance = pedical lenght*cos(pdis)

Returning to the plane of the vertebral origin, the x distance of the end point of the pedicles

Pediclexdistance=vbdl/2+ pedical lenght*cos (PDlt)*cos (PDis)

Y coordinate of the end of the pedicle is unaffected by lateral orientation and is pedicallength*sin(pdit)

Similarly the x coordinate of the transverse process is affected by the orientation in both the sagittal (TDlt) and lateral planes (TDis).

Transverse process = transverse process length *cos (TDlt)*cos (TDis)

Transverse process length= 1/3 of transverse process width

The x coordinate of the representative point on the transverse process is therefore:

Vbdl/2+ pedicle y distance+ transverse process y distance

vbdl/2 + pedlenght*cos(PDlt)*cos(PDis) + trans. pr lenght* cos(TDlt)*cos(TDis)

The y coordinate of the representative point on the transverse process is therefore:

Vertebral body height + Pedicle length*sin(inclined plane angle)+ transverse process length*sin (transverse process sagittal angle)

Calculation of location of superior articular process in the cervical region relative to vertebral origin:

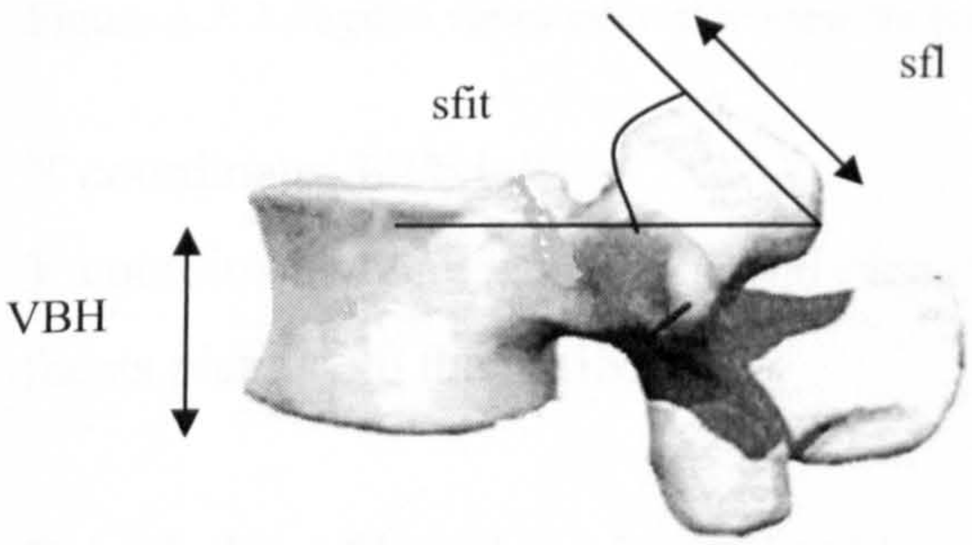


Figure A.3. 7 Sagittal views with top view for transverse process

X coordinate: 1/2*vbdl+ superior articular process length* cos (angle of superior articular process)

Y coordinate: vertebral body height+ superior articular process length * sin (angle of superior articular process).

Calculation of location of mamillary process in the lumbar region relative to vertebral origin 3/2Vbdl

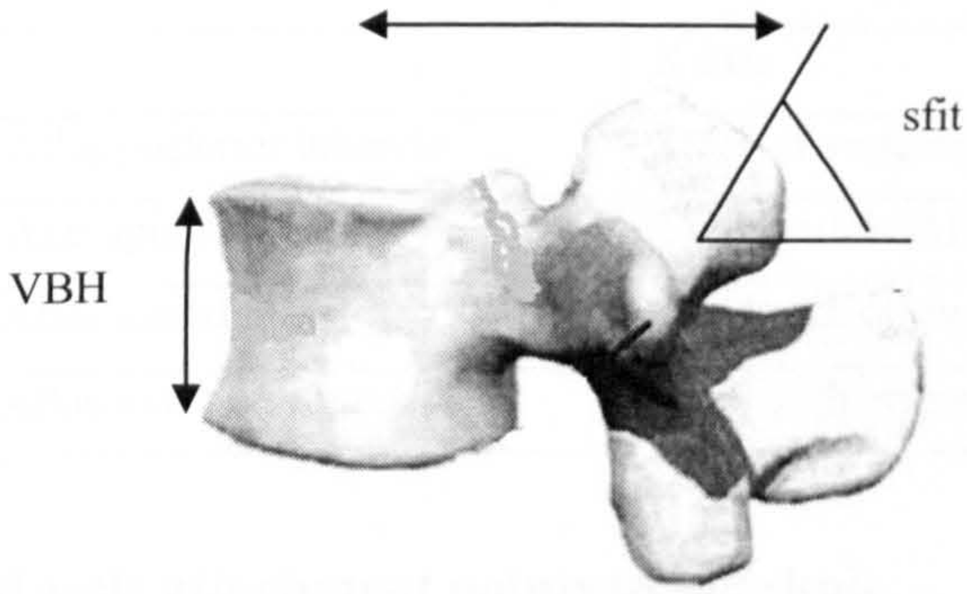


Figure A.3. 8 Sagittal views with side view for mamillary process

X coordinate: 3/2*vbdl

Y coordinate vbheight+1/2*sagittal plane length of the facets*sin(angle of superior facets plane with the horizontal)

Calculation of location of vertebral lamina in the thoracic region relative to vertebral origin

X coordinate: vbdl + spinal channel length

Y coordinate: vbheight/2

Muscle attachments to the head

Points of attachment of the neck muscles require definition of certain points on the skull and on the atlas and axis vertebrae.

Atlas and axis vertebrae:

For certain groups it is necessary to determine representative points of attachment on the atlas and axis. These were:

i) Atlas spinous process:

ii) Atlas transverse process:

iii) Atlas lateral mass:

iv) Atlas posterior tubercles

These were estimated using scaled cross sectional anatomy drawings of Eccleshymer and Shoemaker (1911).

Table A.6.1 Connection points to atlas and axis for suboccipital muscles

Vertebral Feature	Distance from vertebral origin	
	X axis	Y axis
Atlas posterior tubercle	2*5/6 of vertebral body width	Mid vertebral height
Axis spinous process	2*2/3 vertebral body length	Mid vertebral height
Atlas lateral mass	Level with origin	Mid vertebral height
Atlas transverse process	Level with origin	Mid vertebral height

Muscle attachment points to the skull

Illustrations in Gray anatomy were used to identify the relative positions of the muscle points of attachment in vertical plane and the superior surface of that atlas.

Table A.6.2 Calculated x and y coordinates for muscle attachment points to the skull

Muscle Name	X coordinate relative to C1 origin	Y coordinate relative to superior surface of the atlas
Rectus Capitis anterior	-5.57	12.5
Rectus Capitis lateralis	3.52	12.5
Rectus Capitis posterior major	29.66	31.25
Rectus Capitis posterior minor	37.61	31.25
Splenius Capitis	26.25	12.5
Spinalis Capitis	54.66	35.94
Semisplanis Capitis	54.66	40.625
Obliquus Capitis superior	31.93	31.25

APPENDIX 4

Muscle Group\ Interval	(0to5)	(5to10)	(10to15)	(15to20)	(20to25)	(25to30)	(30to35)	(35to40)	(40to45)	(45to50)	(50to55)
rcp major	cat4	cat4	cat4	cat4	cat5	cat5	cat5	cat5	cat5	cat5	cat5
rcp minor	cat4	cat4	cat4	cat4	cat5	cat5	cat5	cat5	cat5	cat5	cat5
OC sup	cat4	cat4	cat4	cat4	cat4	cat4	cat4	cat4	cat4	cat4	cat4
OC inf	cat4	cat4	cat4	cat4	cat4	cat4	cat4	cat4	cat4	cat4	cat4
longis capitis	cat3	cat3	cat3	cat3	cat3	cat3	cat3	cat3	cat3	cat3	cat3
longis colli vertical	cat3	cat3	cat3	cat2	cat2	cat2	cat2	cat2	cat2	cat2	cat2
longis colli superior obl	cat3	cat3	cat3	cat3	cat3	cat3	cat3	cat3	cat3	cat2	cat2
longis colli inferior oblique	cat2	cat2	cat2	cat2	cat2	cat2	cat5	cat5	cat5	cat5	cat6
scalenous ant	cat4	cat4	cat2	cat2	cat2	cat2	cat2	cat2	cat2	cat2	cat5
scalenous medius	cat3	cat3	cat3	cat3	cat3	cat3	cat3	cat4	cat4	cat5	cat5
scalenous post	cat3	cat3	cat2	cat2	cat2	cat2	cat2	cat2	cat5	cat5	cat5
longissumus cervicus	cat2	cat2	cat2	cat2	cat2	cat2	cat2	cat2	cat2	cat5	cat5
longissumus capitis	cat2	cat2	cat2	cat2	cat2	cat2	cat2	cat2	cat2	cat2	cat2
spinalis thoracis	cat2	cat2	cat2	cat5	cat5	cat5	cat5	cat5	cat5	cat5	cat5
spinalis cervicis	cat2	cat2	cat2	cat2	cat2	cat2	cat2	cat5	cat5	cat5	cat5
illiocastalils cercivis	cat2	cat2	cat2	cat2	cat2	cat2	cat2	cat2	cat5	cat5	cat5
illiocostalis lumb. pars thor.	cat2	cat2	cat2	cat2	cat2	cat2	cat2	cat2	cat2	cat2	cat2
longissumus thor. pars thor.	cat2	cat2	cat2	cat2	cat2	cat2	cat2	cat2	cat2	cat2	cat2
illicostalis lumb pars lumb.	cat2	cat2	cat2	cat2	cat2	cat2	cat2	cat2	cat2	cat2	cat2
longissimus thor. pars lumb	cat2	cat2	cat2	cat2	cat2	cat2	cat2	cat2	cat2	cat2	cat2
splenius capitis	cat2	cat2	cat2	cat2	cat2	cat2	cat2	cat2	cat2	cat2	cat2
splenius cervicis	cat2	cat2	cat2	cat2	cat2	cat2	cat2	cat2	cat2	cat2	cat2
semipinalis capitis	cat2	cat2	cat2	cat2	cat2	cat2	cat2	cat2	cat2	cat2	cat2
semispinalis cervicis	cat2	cat2	cat2	cat2	cat2	cat2	cat2	cat2	cat2	cat2	cat2
semispinalis thoracis	cat2	cat2	cat2	cat2	cat2	cat2	cat2	cat2	cat7	cat7	cat7
multifidus cervicis	cat2	cat2	cat2	cat2	cat2	cat2	cat2	cat2	cat2	cat2	cat2
multifidus thoracis	cat2	cat2	cat2	cat2	cat2	cat2	cat2	cat2	cat2	cat2	cat7
multifidus lumbar	cat2	cat2	cat2	cat2	cat2	cat2	cat2	cat2	cat2	cat2	cat7
acromiotrap	cat2	cat2	cat2	cat2	cat2	cat2	cat2	cat2	cat2	cat2	cat2
trapezius	cat2	cat2	cat2	cat2	cat2	cat2	cat2	cat2	cat2	cat5	cat5
levator scapula	cat2	cat2	cat2	cat2	cat2	cat2	cat2	cat2	cat2	cat2	cat2

Muscle Group\ Interval	(0to5)	(5to10)	(10to15)	(15to20)	(20to25)	(25to30)	(30to35)	(35to40)	(40to45)	(45to50)	(50to55)
latissimus dorsi	cat2	cat2	cat2	cat2	cat2	cat2	cat2	cat2	cat2	cat2	cat2
quadrotus lumborum	cat5	cat5	cat5	cat5	cat5	cat5	cat5	cat5	cat5	cat6	cat6
psoas major	cat8	cat8	cat8	cat8	cat8	cat8	cat8	cat8	cat8	cat8	cat8
rectus abdominis	cat9	cat9	cat9	cat9	cat9	cat9	cat9	cat9	cat9	cat9	cat9
internal oblique	cat9	cat9	cat9	cat9	cat9	cat9	cat9	cat9	cat9	cat9	cat9
internal oblique	cat9	cat9	cat9	cat9	cat9	cat9	cat9	cat9	cat9	cat9	cat9
Full ALL	cat2	cat2	cat2	cat2	cat2	cat2	cat2	cat2	cat2	cat2	cat2
Full PLL	cat2	cat2	cat2	cat2	cat2	cat2	cat2	cat2	cat2	cat2	cat5
Full LF	cat2	cat2	cat2	cat2	cat2	cat2	cat2	cat2	cat2	cat2	cat2
Cervical ALL	cat3	cat3	cat3	cat3	cat3	cat5	cat5	cat5	cat5	cat5	cat5
Cervical PLL	cat3	cat3	cat3	cat3	cat3	cat3	cat3	cat5	cat5	cat5	cat5
Cervical LF	cat3	cat3	cat8	cat8	cat8	cat6	cat6	cat6	cat6	cat6	cat6
Lumbar ALL	cat7	cat7	cat7	cat7	cat7	cat7	cat7	cat7	cat7	cat7	cat7
Lumbar PLL	cat7	cat7	cat7	cat7	cat7	cat7	cat7	cat7	cat7	cat7	cat7
Lumbar LF	cat7	cat7	cat7	cat7	cat7	cat7	cat7	catt7	cat7	cat7	cat7

Muscle Group\ Interval	(55to60)	(60to65)	(65to70)	(70to75)	(75to80)	(80to85)	(85to90)
rcp major	cat5	cat5	cat5	cat5	cat5	cat5	cat5
rcp minor	cat5	cat5	cat5	cat6	cat6	cat6	cat6
OC sup	cat4	cat4	cat4	cat6	cat6	cat6	cat6
OC inf	cat4	cat4	cat4	cat6	cat6	cat6	cat6
longis capitis	cat3	cat2	cat2	cat5	cat5	cat8	cat8
longis colli vertical	cat2	cat5	cat5	cat5	cat5	cat8	cat8
longis colli superior obl	cat2	cat5	cat5	cat5	cat5	cat8	cat8
longis colli inferior oblique	cat6	cat6	cat6	cat8	cat8	cat8	cat8
scalenous ant	cat5	cat5	cat5	cat5	cat5	cat8	cat8
scalenous medius	cat5	cat5	cat5	cat5	cat5	cat8	cat8
scalenous post	cat5	cat5	cat5	cat8	cat8	cat8	cat8
longissumus cervicus	cat5	cat5	cat8	cat8	cat8	cat8	cat8
longissumus capitis	cat2	cat2	cat2	cat2	cat2	cat2	cat2
spinalis thoracis	cat5	cat5	cat5	cat5	cat5	cat5	cat5
spinalis cervicis	cat5	cat5	cat8	cat8	cat8	cat8	cat8
illiocastalils cercivis	cat5	cat5	cat8	cat8	cat8	cat8	cat8
illiocostalis lumb. pars thor.	cat2	cat2	cat2	cat2	cat2	cat1	cat1
longissumus thor. pars thor.	cat2	cat2	cat2	cat2	cat1	cat1	cat1
illicostalis lumb pars lumb.	cat2	cat2	cat2	cat2	cat2	cat1	cat1
longissimus thor. pars lumb	cat2	cat2	cat2	cat2	cat2	cat1	cat1
splenius capitis	cat5	cat5	cat5	cat5	cat8	cat8	cat8
splenius cervicis	cat2	cat5	cat5	cat5	cat8	cat8	cat8
semipinalis capitis	cat2	cat2	cat2	cat2	cat2	cat2	cat1
semispinalis cervicis	cat2	cat2	cat2	cat2	cat2	cat8	cat8
semispinalis thoracis	cat7	cat7	cat7	cat7	cat7	cat8	cat8
multifidus cervicis	cat2	cat2	cat2	cat2	cat2	cat8	cat8
multifidus thoracis	cat7	cat7	cat7	cat7	cat7	cat8	cat8
multifidus lumbar	cat7	cat7	cat7	cat7	cat7	cat8	cat8
acromiotrap	cat2	cat2	cat2	cat2	cat2	cat8	cat8
trapezius	cat5	cat5	cat5	cat5	cat5	cat5	cat5
levator scapula	cat2	cat5	cat5	cat5	cat5	cat1	cat1

Muscle Group\ Interval	(55to60)	(60to65)	(65to70)	(70to75)	(75to80)	(80to85)	(85to90)
latissimus dorsi	cat2	cat5	cat5	cat5	cat1	cat1	cat1
quadrotus lumborum	cat6	cat6	cat6	cat6	cat6	cat6	cat6
psoas major	cat8	cat8	cat8	cat8	cat8	cat8	cat8
rectus abdominis	cat9	cat9	cat9	cat9	cat9	cat9	cat9
internal oblique	cat9	cat9	cat9	cat9	cat9	cat9	cat9
internal oblique	cat9	cat9	cat9	cat9	cat9	cat9	cat9
Full ALL	cat2	cat2	cat2	cat2	cat2	cat2	cat6
Full PLL	cat5	cat5	cat5	cat5	cat5	cat5	cat6
Full LF	cat2	cat5	cat5	cat5	cat5	cat5	cat6
Cervical ALL	cat5	cat5	cat5	cat5	cat8	cat8	cat6
Cervical PLL	cat5	cat5	cat5	cat5	cat8	cat8	cat6
Cervical LF	cat6	cat6	cat6	cat6	cat6	cat6	cat6
Lumbar ALL	cat7	cat5	cat5	cat5	cat5	cat5	cat6
Lumbar PLL	cat7	cat5	cat5	cat5	cat5	cat5	cat6
Lumbar LF	cat5	cat5	cat5	cat5	cat5	cat5	cat6

APPENDIX 5

Table A5 Interval of reference angle and the active muscle groups for each interval.

Interval	Muscle Groups
(0° to 5°)	RCP major, RCP minor, OCSup, OCinf, longis capitis, longis colli vertical, longis colli superior oblique, longis colli inferior oblique, scalenous anterior, scalenous medius, scalenous posterior, longissimus cervicis, longissimus capitis, Spinalis cervicis, Splenius capitis, semispinalis capitis, semispinalis cervicis, semispinalis thoracis, internal oblique, external oblique and psoas, trapezius, elevator scapula.
(5° to 10°)	RCP major, RCP minor, OCSup, OCinf, longis capitis, longis colli vertical, longis colli superior oblique, longis colli inferior oblique, scalenous anterior, scalenous medius, scalenous posterior, longissimus cervicis, longissimus capitis, Spinalis cervicis, Splenius capitis, semispinalis capitis, semispinalis cervicis, semispinalis thoracis, internal oblique, external oblique and psoas, trapezius, elevator scapula.
(10° to 15°)	RCP major, RCP minor, OCSup, OCinf, longis capitis, longis colli vertical, longis colli superior oblique, longis colli inferior oblique, scalenous anterior, scalenous medius, scalenous posterior, longissimus cervicis, longissimus capitis, Spinalis cervicis, Splenius capitis, semispinalis capitis, semispinalis cervicis, semispinalis thoracis, internal oblique, external oblique and psoas, trapezius, elevator scapula, cervical, thoracic and lumbar multifidus.
(15° to 20°)	RCP major, RCP minor, OCSup, OCinf, longis capitis, longis colli vertical, longis colli superior oblique, longis colli inferior oblique, scalenous anterior, scalenous medius, scalenous posterior, longissimus cervicis, longissimus capitis, Spinalis cervicis, Splenius capitis, semispinalis capitis, semispinalis cervicis, semispinalis thoracis, internal oblique, external oblique and psoas, trapezius, elevator scapula, cervical, thoracic and lumbar multifidus.
(20° to 25°)	RCP major, RCP minor, longis capitis, longis colli vertical, longis colli superior oblique, longis colli inferior oblique, scalenous anterior, scalenous medius, scalenous posterior, longissimus cervicis, longissimus capitis, Spinalis cervicis, Splenius capitis, semispinalis capitis, semispinalis cervicis, semispinalis thoracis,psoas, trapezius, elevator scapula, cervical, thoracic and lumbar multifidus
(25° to 30°)	RCP major, RCP minor, longis capitis, longis colli vertical, longis colli superior oblique, longis colli inferior oblique, scalenous anterior, scalenous medius, scalenous posterior, longissimus cervicis, longissimus capitis, Spinalis cervicis, Splenius capitis, semispinalis capitis, semispinalis cervicis, semispinalis thoracis,psoas, trapezius, elevator scapula, cervical and thoracic multifidus.

(30° to 35°)	RCP major, RCP minor, longis capitis, longis colli vertical, longis colli superior oblique, longis colli inferior oblique, scalenous anterior, scalenous medius, scalenous posterior, longissimus cervicis, longissimus capitis, Spinalis cervicis, Splenius capitis, semispinalis capitis, semispinalis cervicis, semispinalis thoracis, psoas, trapezius, elevator scapula, cervical and thoracic multifidus
(35° to 40°)	RCP major, RCP minor, longis capitis, longis colli vertical, longis colli superior oblique, longis colli inferior oblique, scalenous anterior, scalenous medius, scalenous posterior, longissimus cervicis, longissimus capitis, Spinalis cervicis, Splenius capitis, semispinalis capitis, semispinalis cervicis, semispinalis thoracis,psoas, trapezius, elevator scapula, cervical and thoracic multifidus
(40° to 45°)	RCP major, RCP minor, longis capitis, longis colli vertical, longis colli superior oblique, longis colli inferior oblique, scalenous anterior, scalenous medius, scalenous posterior, longissimus cervicis, longissimus capitis, Spinalis cervicis, Splenius capitis, semispinalis capitis, semispinalis cervicis, semispinalis thoracis, internal oblique, external oblique and psoas, trapezius, elevator scapula, illiocostalis lumborum pars lumbar multifidus, longissimus thoracis pars lumborum
(45° to 50°)	longis colli vertical, longis colli superior oblique, longis colli inferior oblique, scalenous anterior, scalenous medius, scalenous posterior, longissimus cervicis, longissimus capitis, Spinalis cervicis, Splenius capitis, semispinalis capitis, semispinalis cervicis, semispinalis thoracis, internal oblique, external oblique and psoas, trapezius, elevator scapula, iliocostalis cervicis, illiocostalis lumborum pars lumbar, illiocostalis lumborum pars thoracis, longissimus thoracis pars lumborum, longissimus thoracis pars thoracis
(50° to 55°)	longis colli vertical, longis colli superior oblique, longis colli inferior oblique, scalenous anterior, scalenous medius, scalenous posterior, longissimus cervicis, longissimus capitis, Spinalis cervicis, Splenius capitis, semispinalis capitis, semispinalis cervicis, semispinalis thoracis, internal oblique, external oblique and psoas, trapezius, elevator scapula, iliocostalis cervicis, illiocostalis lumborum pars lumbar, illiocostalis lumborum pars thoracis, longissimus thoracis pars lumborum, longissimus thoracis pars thoracis
(55° to 60°)	scalenous anterior scalenous medius scalenous posterior longissimus cervices longissimus capitis, spinalis thoracis, spinalis cervicis, iliocostalis cervicis, illiocostalis lumborum pars lumbar, illiocostalis lumborum pars thoracis, longissimus thoracis pars lumborum, longissimus thoracis pars thoracis, multifidus cervicis, multifidus thoracis, multifidus lumbar, spinalis thoracis, spinalis cervicis muscles
(60° to 65°)	scalenous anterior scalenous medius scalenous posterior longissumus cervicus longissumus capitis, spinalis thoracis, spinalis cervicis, iliocostalils cervicis, illicostalis lumbarum pars lumbar, illicostalis lumborum pars thoracis, longissimus thoracis pars lumborum, longissimus thoracis pars thoracis, multifidus cervicis, multifidus thoracis, , splenius capitis, splenius cervicis, semipinalis capitis, semispinalis cervicis, semispinalis thoracis

(65° to 70°)	longis colli vertical, longis colli superior oblique, longis colli inferior oblique, illicostalis lumbarum pars lumbar, illicostalis lumborum pars thoracis, longissimus thoracis pars lumborum, longissimus thoracis pars thoracis, splenius capitis, splenius cervicis, semispinalis cervicis, semispinalis thoracis, multifidus cervicis, multifidus thoracis.
(70° to 75°)	longis colli vertical, longis colli superior oblique, longis colli inferior oblique, illicostalis lumbarum pars lumbar, illicostalis lumborum pars thoracis, longissimus thoracis pars lumborum, longissimus thoracis pars thoracis, splenius capitis, splenius cervicis, semispinalis cervicis, semispinalis thoracis, multifidus cervicis, multifidus thoracis.
(75° to 80°)	illicostalis lumb pars lumb, longissimus thor. pars lumb, splenius cervicis semipinalis capitis, semispinalis cervicis, semispinalis thoracis, multifidus cervicis, multifidus thoracis.
(80 to 85)	longis colli vertical longis colli superior obl longis colli inferior oblique scalenous ant scalenous medius scalenous post longissumus cervicus longissumus capitis spinalis thoracis spinalis cervicis illiocastalils cercivis splenius cervicis semipinalis capitis splenius capitis
(85 to 90)	scalenous ant scalenous medius scalenous post longissumus cervicus longissumus capitis spinalis thoracis spinalis cervicis illiocastalils cercivis, splenius cervicis semipinalis capitis semispinalis cervicis semispinalis thoracis multifidus thoracis splenius capitis splenius capitis multifidus cervicis latissimus dorsi levator scapula muscles

APPENDIX 6

The force magnitude by the lumbar ALL, PLL and LF are provided on the graphs below for all the intervals. For ALL, the peak force is observed at L4/L3 and L3/L2 regions. The PLL force in general tends to increase for the upper lumbar regions. The force supplied by ALL is greater than PLL and LF. The LF has peak value at L5/L4 and decreases at L4/L3 and L3/L2 and has a tendency to increase at T12/L1.

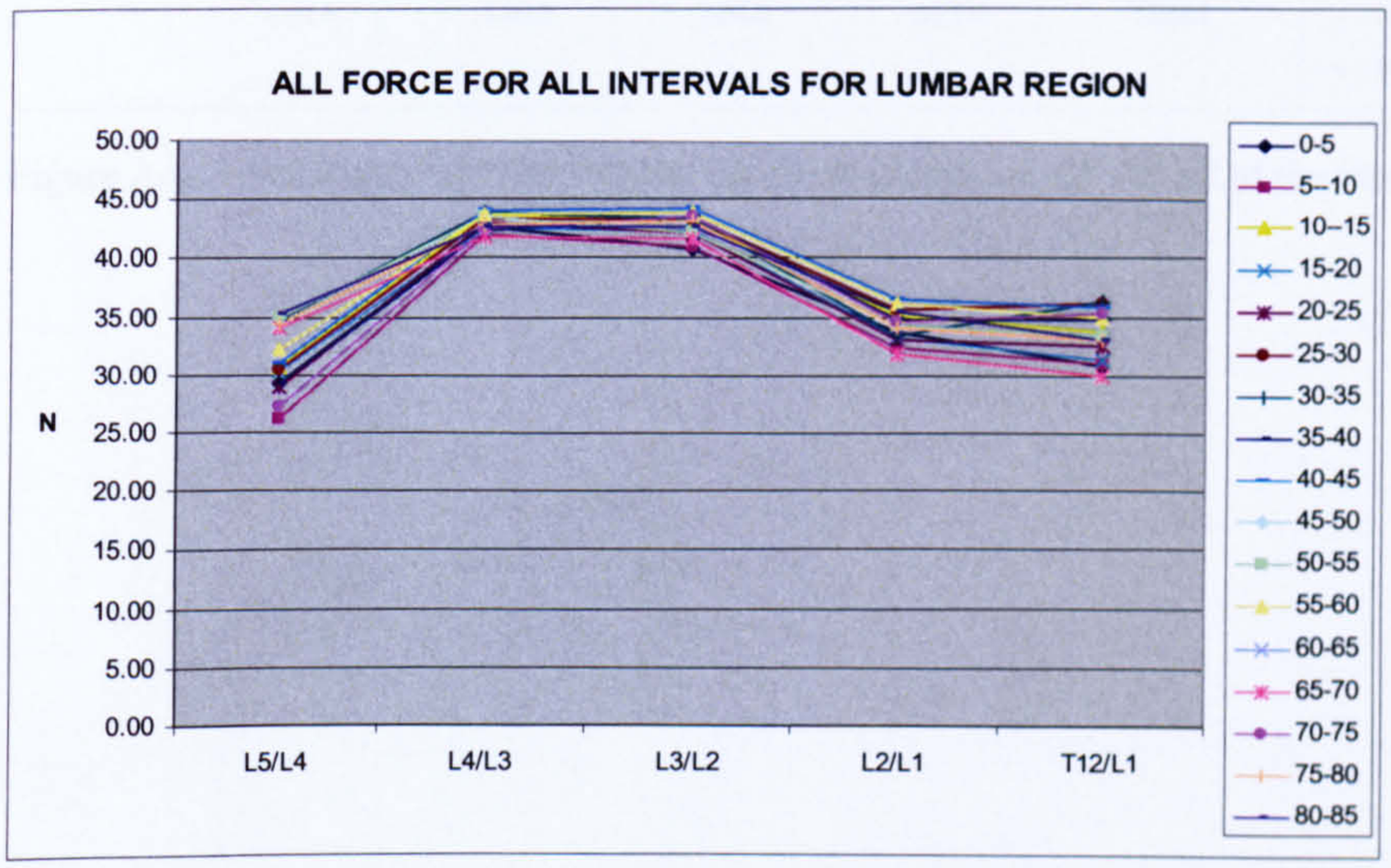


Figure A.6.1 Force provided by lumbar ligament groups of ALL for all of the intervals.

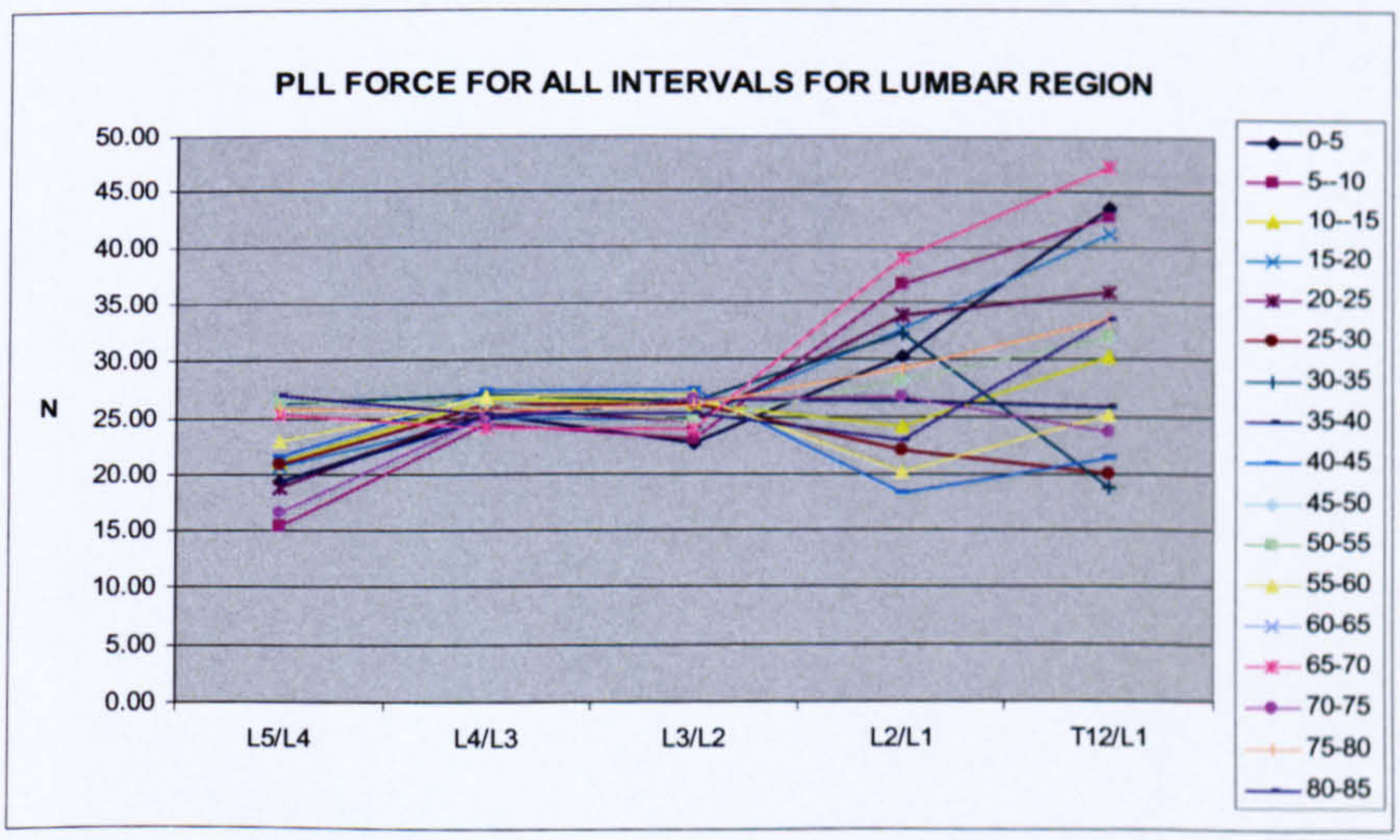


Figure A.6.2 Force provided by lumbar ligament groups of PLL for all of the intervals.

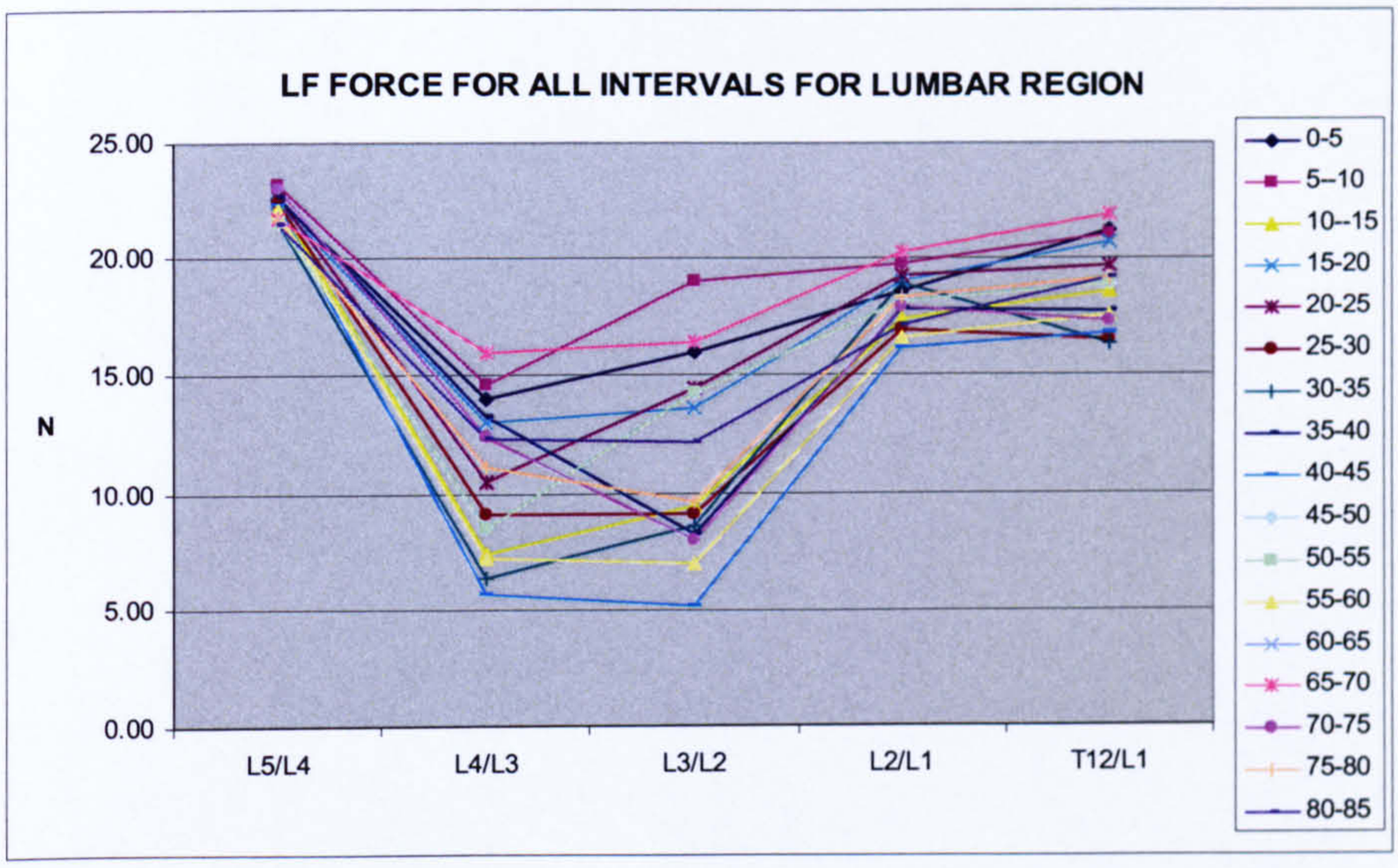


Figure A.6. 3 Force provided by lumbar ligament groups of, LF for all of the intervals.